Characterisation of *Plasmodium* proteins playing critical roles in mosquito midgut infection and malaria transmission

Maria Giorgalli

Department of Life Sciences
Faculty of Natural Sciences
Imperial College London

A thesis submitted in accordance with the requirements of Imperial College London for the degree of Doctor of Philosophy

DECLARATION OF OWN WORK

I certify that this thesis and the research to which it refers is the product of my own work and that any ideas or quotations from the work of other people, published or otherwise, are fully acknowledged in accordance with standard referencing practices and with scientific collaborators clearly listed.

ABSTRACT

Malaria parasites undergo dramatic losses during their gametocyte-to-ookinete-to-oocyst developmental transition. This PhD thesis primarily aimed to use the Signature Tagged Mutagenesis (STM) methodology to simultaneously phenotype pools of individually tagged *P. berghei* mutants, of genes previously found to be highly upregulated during the gametocyte-to-ookinete-to-oocyst developmental transition stages and possibly involved in mosquito-parasite interactions. Although the first pool of mutants acted as a proof-of-concept experiment, it revealed three novel *Plasmodium* genes with essential functions during the parasite ookinete-to-oocyst-to-sporozoite transition. Specifically, AQP2 is essential for sporozoite formation in the developing oocyst, N38 is important for the gametocyte-to-ookinete developmental transition and N350 is critical for ookinete motility prior to midgut invasion

The mosquito complement-like system is responsible for the greatest parasite population bottleneck observed during the ookinete-to-oocyst developmental transition, which also coincides with the ookinete traversal through the mosquito midgut epithelium. Therefore, this PhD also aimed to shed light on the molecular mechanisms mediated by the mosquito innate immune system to clear the *Plasmodium* parasites and thus regulate the infection outcome. Several *P. berghei* genes have been identified to play an essential role in the parasite protection from the mosquito complement responses including *c01*, *PIMMS43*, *P47* and *c57*. Knockout of any of these genes leads to ookinete elimination by the mosquito complement-like reactions upon reaching the basal sub-epithelial space, unless silencing key factors of the mosquito complement system. Based on these findings, it was further suggested that (i) either all of these genes have essential functions in parasite immune evasion, or (ii) their loss-of-function bears a fitness cost that exceeds a certain threshold required for parasites to endure the mosquito complement responses. Serial mouse-to-mosquito-to-mouse transmission cycles followed by allele quantification revealed that the mosquito complement system is responsible for instantly removing 99% of the introduced in the population knockout alleles.

This study offers new perspectives for further understanding the mosquito-parasite interactions leading to malaria transmission.

DEDICATION

Στην οικογένεια μου. . που είναι πάντα στο πλευρό μου

Στους δασκάλους μου. . που μου έμαθαν από το Α στο Ω

Στους φίλους μου. . που γέλασα, έκλαψα, παραπονέθηκα κι ακόμα μ' αγαπάνε!

ACKNOWLEDGEMENTS

Many people have contributed to the completion of this thesis and are deserving of my sincere thanks. I would first like to thank Dr. Dina Vlachou for project supervision and day-to-day discussions. Equally, Prof. George K. Christophides for his scientific guidance and advices throughout my studies as well as for teaching me scientific rigor and sharing his enthusiasm for science. I am grateful for the all the opportunities conducting research under their guidance has given me.

Several others in the lab provided help, mostly in the form of thousands of mosquitoes, for which I am much obliged. In approximate chronological order: Claudia Wyer, Faye Rodgers and Lara Selles-Vidal. I am also thankful to Kasia Sala, Fiona Angrisano, Andrew Blagborough, Sofia Tapanelli, Kathrin Witmer and Fabio Fisher for technical assistance and mouse work advice. I am especially thankful to Ana-Rita Gomes for all her experimental support, training and guidance during my first steps in the lab as well as in thesis writing. Also, many thanks to Valerie C. Ukegbu for trainig, sharing unpublished data and for providing some of the mutant *P. berghei* lines.

A thank you also goes out to Konstantinos Koussis, Andrew Blagborough, David Ellis and Claudia Wyer for replying to my unstoppable grammar-related questions during writing and for helping me turn my eccentric Greek into what you are about to read. I thank my past and current colleagues; Tibebu Habtewold, Mathilde Gendrin, Sarah Kelly, Andre Pitaluga, Melina Campos, Bob MacCallum, Astrid Hoermann, George Avraam, Giannis Kirmintzoglou and Louisa Rona for stimulating discussions, for making me realise that the road is still long and for being next to me as friends and family. A huge thank you also goes to Chryssa Taxiarchi, Nikos Trasanides, Ioanna Bechlivanidi, Kyros Kyrou, Georgia Adamou, Zaphiris Tsisios and 'The Greek Society' for the countless hours of discussion, for pushing me out of my day-to-day routine and for comforting me with any kind of despair. Last but not least, a huge thank you goes to my family and friends in Cyprus for never getting tired listening to my 'nonsense theories', for offering support in everything I decided to do and for being patient with my absence. From now on, I promise to get back to your calls within a week time.

I am also grateful to my PhD advisors; Dr. Jean Langhorne (Crick) for her constructive and helpful comments during our discussions and Prof. Jake Baum (ICL) for his sensible advices, guidance and great support upon completion of my thesis.

FUNDING

Funding for this project was provided by the Wellcome Trust Project Grant 093587/Z/10/Z to Prof. George Christophides and Dr. Dina Vlachou, and the Wellcome Trust Senior Investigator Award 107983/Z/15/Z to Prof. George Christophides.

TABLE OF CONTENTS

LIST OF FIGURES

LIST OF TABLES

CHAPTER 2

CHAPTER 3

LIST OF APPENDICIES

PUBLICATIONS

Giorgalli, M., Vlachou, D., Christophides, G. K. (2019) Characterisation of the impact of the mosquito complement-like response on shaping the transmitted malaria parasite populations. *in preparation.*

Ukegbu, C. V.*, **Giorgalli, M.***, Tapanelli, S., Rona L., Jaye, A., Wyer, C., Angrisano, F., Blagborough, A., Christophides, G. K., Vlachou, D. (2020) *Plasmodium PIMMS43* is required for ookinete evasion of the mosquito complement-like response and sporogonic development in the oocyst. *Proc Natl Acad Sci USA*. 117, 7363-7373.

Ukegbu, C. V., **Giorgalli, M.**, Ramirez, J. L., Yassine, H., Taxiarchi, C., Barillas-Mury, C., Christophides, G. K. and Vlachou, D. (2017) *Plasmodium berghei P47* protects ookinetes from the mosquito complement -like system. *Sci Rep*. 7, 6026-6037.

ABBREVIATIONS

AA	Amino Acid
AB	Antibody
ABS	Asexual Blood Stages
ACT	Artemisinin Combination Therapy
*Ag*STAT-A	*Anopheles gambiae* STAT-A
*Ag*STAT-B	*Anopheles gambiae* STAT-B
AMP	Antimicrobial Peptides
ANKA	Anvers/Kasapa
ANOVA	Analysis of Variance
APL1C	*Anopheles Plasmodium*-responsive Leucine-rich repeat protein C
APN1	Aminopeptidase 1
APO	Apolipophorin
Arg-tRNA	Arginyl-tRNA Synthetase
AT	Adenine-Thymine
ATP	Adenosine Triphosphate
BF	Bright Field
BL	Basal Lamina
bp	Base Pair
BSA	Bovine Serum Albumin
C3	Complement protein 3
c57 BL/6	c57 Black 6
CelTos	Cell-Traversal protein for Ookinetes and Sporozoites
CDPK	Calcium Dependent Protein Kinase
cDNA	Complementary DNA
CF11	Cellulose Fiber powder 11
CLB	Coelenterazine Loading Buffer
CLIP	Clip-domain Serine Proteases
CLIPA2	Clip-domain Serine Protease 2
CLIPA5	Clip-domain Serine Protease 5
CLIPA7	Clip-domain Serine Protease 7
CM	Complete Medium
CRISPR	Clustered Regularly Interspaced Short Palindromic Repeats
CSA	Chondroitin sulfate A

CSP	Circumsporozoite Protein
CTL	C-Type Lectin
CTL4	C-Type Lectin 4
CTLMA2	C-Type Lectin Mannose-binding A2
CTRP	Circumsporozoite protein and TRAP-Related Protein
Δc01	*P. berghei* knockout parasite line for *c01*
Δc43	*P. berghei* knockout parasite line for *c43*
ΔP47	*P. berghei* knockout parasite line for *P47*
Δc57	*P. berghei* knockout parasite line for *c57*
ΔP48/45	*P. berghei* knockout parasite line for *P48/45*
ΔPIMMS2	*P. berghei* knockout parasite line for *PIMMS2*
ΔAQP2	*P. berghei* knockout parasite line for *AQP2*
ΔN38	*P. berghei* knockout parasite line for *N38*
ΔN350	*P. berghei* knockout parasite line for *N350*
Δmap2	*P. berghei* knockout parasite line for *map2*
Δhap2	*P. berghei* knockout parasite line for *hap2*
Δnek4	*P. berghei* knockout parasite line for *nek4*
DAPI	4',6-diamidino-2-phenylindole
dH_20	Distilled Water
DIC	Differential Interference Contrast
DNA	Deoxyribonucleic Acid
DsRNA	Double-Stranded RNA
Dscam	Down Syndrome Cell Adhesion Molecule Gene
d-ssu	d small subunit
EBP	Enolase Binding Protein
ECL	Enhanced Chemiluminescence
ECM	Experimental Cerebral Malaria
EDTA	Ethylene Diamine Tetraacetic Acid
EEF	Eukaryotic Elongation Factor
EGF	Epidermal Growth Factor
EST	Expressed Sequence Tag
F-actin	Filamentous actin
FACS	Fluorescence-Activated Cell Sorting
FBS	Foetal Bovine Serum
FCS	Foetal Calf Serum

FH	Human Complement Factors
FREP	Fibrinogen-Related Proteins
FWD	Forward
g	Grams
Gc	Gametocyte
gDNA	Genomic DNA
GFP	Green Fluorescent Protein
GNBP	Gram-Negative Binding Proteins
GPI	Glycosyl Phosphatidyl Inositol
Hepes	4-(2-HydroxyEthyl)-1-Piperazine Ethane Sulfonic acid
HCL	Hydrochloric Acid
HDF	Haemocyte Differentiation Factor
*h*DHFR/yFCU	Human DHFR (*h*dhfr) and Yeast FCU
HEG	Homing Gene Drives
HPX2	Haeme Peroxidase 2
HRP	Horseradish Peroxidase
IFA	Immunofluorescence Assay
IgG	Immunoglobin G
IM	Intramuscular
Imd	Immune Deficiency
IMPer	Immune-Modulatory Peroxidase
INT	Integration
IP	Intraperitoneal
IPTG	Isopropyl-1-Thio-β-d-g-Galactopyranoside
IRS	Indoor Residual Spraying
ITN	Insecticide Treated Nets
JAK/STAT	Janus Kinase-Signal Transducers and Activators of Transcription
JNK	c-Jun N-terminal Kinase
KD	Knock–Down
kDa	Kilodalton
KO	Knockout
LAP	LCCL/lectin adhesive- like protein
LB	Luria broth
LPS	Lipopolysaccharides
LRIM	Leucine-Rich Immune Molecule

LRIM1	Leucine-Rich Immune Molecule 1
LITAF	Lipopolysaccharide-Induced Tumor Apoptosis Factor
LYSC1	Lysozyme c-1
mAb	Monoclonal Antibody
Map2	Mitogen-activated protein kinase
MG	Midgut
MIN	Minute
MISFIT	Male-Inherited Sporulation Factor Important for Transmission
ml	Millilitre
mM	Millimolar
MMP1	Matrix metalloprotease 1
mRNA	Messenger RNA
MTOC	Microtubule Organising Centre
MW	Molecular Weight
ng	Nanogram
NGS	Next Generation Sequencing
Nek4	NIMA related kinase 4
NF-κB	Nuclear Factor Kappa-light-chain-enhancer of activated B cells
NGP	Non-Gametocyte Producing
NIMA	Never In Mitosis/Aspergillus
nL	Nanolitre
NLS	Nuclear Localisation Signal
NO	Nitric Oxide
NOS	Nitric Oxide Synthase
NOX5	NADPH Oxidase 5
NTSbl	Non-Triton Soluble fraction
Ooc	Oocyst
Ook	Ookinetes
ORF	Open Reading Frame
p	Probability
PAGE	Polyacrylamide Gel Electrophoresis
PAMPs	Pathogen Associated Molecular Patterns
PBF	Post Blood Feeding
PBS	Phosphate-Buffered Saline
PBS-PI	PBS/Protease-Inhibitors

PCR	Polymerase Chain Reaction
PEV	Pre-erythrocytic vaccines
*Pf*EMP	*P. falciparum* Erythrocyte Membrane Protein
PH	Phenylhydrazinium Chloride
PGN	Peptidoglycans
PGRP	Peptidoglycan Recognition Proteins
PI	Protease Inhibitors
PIMMS2	*Plasmodium* Invasion of Mosquito Midgut Screen candidate 2
PIMMS43	*Plasmodium* Invasion of Mosquito Midgut Screen candidate 43
PM	Peritrophic Matrix
PPKL	Protein Phosphatase with Kelch-Like domains
PPO	Prophenoloxidase
PO	Phenoloxidase
PRR	Protein Recognition Receptor
PVDF	Polyvinylidene Difluoride
qRT-PCR	Quantitative Real-Time Reverse Transcription PCR
RBC	Red Blood Cell
REV	Reverse
RNA	Ribonucleic Acid
RNAi	RNA-interference
RPMI	Roswell Park Memorial Institute
RT-PCR	Reverse-Transcription PCR
Sbl	Soluble fraction
SDS	Sodium Dodecyl Sulphate
Serpin	Serine protease inhibitor
SG	Salivary Gland
SOAP	Secreted Ookinete Adhesive Protein
SP	Signal Peptide
SPH	Serine Protease Homologs
Spz	Sporozoite
STAT	Signal Transducer and Activator of Transcription
StDev	Standard Deviation
SUB	Subtilisin
T	Temperature
Tm	Melting Temperature

TBA	Transmission Blocking Activity
TBV	Transmission Blocking Vaccines
TBE	Tris/Borate/EDTA
TEP	Thioester-Containing Protein
*Tg*DHFR-TS	*T. gondii* Dihydrofolate Reductase-Thymidylate Synthase
TM	Transmembrane Domain
TNF	Tumor Necrosis Factor
TSbl	Triton Soluble fraction
TRAP	Thrombospondin-Related Adhesive Protein
TRI	Transmission Reducing Immunity
tRNA	transferRNA
TUB	Tubulin
u(µ)g	Microgram
u(µ)L	Microlitre
u(µ)M	Micromolar
USD	United States Dollar
UTR	Untranslated Region
WASP	Wiskott–Aldrich Syndrome Protein
WARP	Willebrand factor A domain-Related Protein
WB	Western Blot
WHO	World Health Organisation
WT	Wild-Type
XA	Xanthurenic Acid

CHAPTER 1. GENERAL INTRODUCTION

1.1 Malaria: An ancient disease and a contemporary global health problem

1.1.1 Historical aspects and milestone discoveries

> *''The belief is growing on me that the disease is*
> *communicated by the bite of the mosquito.*
> *She always injects a small quantity of fluid with her bite*
> *what if the parasites get into the system in this manner''*
> Ronald Ross (1857 – 1932)

Malaria is an ancient disease; as far back as 2700 B.C., the Chinese Canon of Medicine Nei Ching discussed malaria like symptoms and the relationship between fevers and enlarged spleens (Oaks *et al.*, 1991). Its typical clinical manifestations of extremely high fever, often following a distinctive every-other or every-third-day pattern, accompanied by rigor, common malaise and severe anaemia (White, 2008) has also been well documented in a series of writings from the ancient Homer, Aristotle, Plato, Socrates, Horace, Tacitus, Carus, Varro, Chaucer, Pepys to the most recent Shakespeare plays (Bruce-Chwatt *et al*., 1988).

The Greek physician Hippocrates was the first to make a connection between the proximity of stagnant bodies of water and the occurrence of fevers in the local population. The Romans also related marshes with fever and pioneered early efforts at swamp drainage. Appropriately, the role of standing bodies of water and marshes in causing fevers was described by the Italians as “mal'aria” (bad air) beginning in the mid-sixteenth century (Oaks *et al.*, 1991), and the term entered the English language as “malaria” some 200 years later.

Many scientists made considerable but futile efforts to isolate the causative agent from water and soil samples collected from malarial areas. It would take until 1897, when a British officer in the Indian Medical Service, Ronald Ross, was able to demonstrate that the malaria parasite could be transmitted from infected patients to mosquitoes necessitating a sporogonic cycle (the time interval during which the parasite developed in the mosquito) (Ross, 1897). Parallel work led by Giovanni Battista Grassi, established that only specific strains of Anopheline infected mosquitoes could transmit the disease to a healthy individual and indicated for the first time the complete

sporogonic cycle of *Plasmodium falciparum*, *Plasmodium vivax* and *Plasmodium malariae* in *Anopheles* mosquitoes (Grassi, 1898).

Based on this knowledge, we now know that malaria is a mosquito-borne disease, transmitted by female *Anopheline* mosquitoes and caused by parasites of the genus *Plasmodium*. The five *Plasmodium* species causing malaria to humans are *P. falciparum* (originally named *Oscillaria malariae* by Laveran 1880 but renamed by William H. Welch in 1889), *P. vivax*, *P. malariae* (both described in 1890 by G. B. Grassi and R. R. Filett), *Plasmodium malariae* (Collins *et al.*, 2012) and *Plasmodium ovale* (reported in 1922 by Stephens), with *P. falciparum* being the most prevalent and fatal. *P malariae*, which has the primate *Macaca fascicularis* as its natural vertebrate host, has been only recently deemed as the fifth human malaria parasite (White, 2008) since human infections have been reported in South-East Asia (Singh & Daneshvar, 2013). Certain animals are also susceptible to malaria, such as murine rodents (infected by *Plasmodium berghei, Plasmodium chabaudi, Plasmodium vinckei* and *Plasmodium yoelii*) and chicken (infected by *Plasmodium gallinaceum*), providing useful models for laboratory studies of the human malaria.

About 40 Anopheline species, of the approximately 430 species identified to date, play a pivotal role in malaria transmission with *Anopheles gambiae* being the major malaria vector in Africa (WHO. Malaria 2015; 2016). *Anophelines* that can transmit malaria are found in malaria-endemic areas as well as in areas where malaria has been previously eliminated. The latter areas are thus constantly at risk of reviving the disease.

1.1.2 Current burdens of malaria

The latest figure from the World Health Organisation (WHO) estimates an annual malaria caseload of 228 million cases worldwide with the majority of them occurring in the WHO African Region, where temperature and rainfall levels are most suitable for the development of the malaria-causing parasites in *Anopheles* mosquitoes (WHO. Malaria 2019). In 2018, there were an estimated 405 000 deaths from malaria globally, out of which 61% were recorded in African children under the age of 5 years. The most virulent of the human malaria *Plasmodium* species in the sub-Saharan Africa is *P. falciparum*, whereas *P. vivax* is responsible for most of the malaria cases outside Africa, especially in the Asia-Pacific region (WHO. Malaria 2019). Pregnant women are also of higher risk and sensitivity since malaria poses a great risk of premature delivery, low birth-weight and infant mortality (Miller & Greenwood, 2002).

Poverty is mostly found in the tropical and subtropical zones and specifically within the geographical regions that malaria plagues and malaria-related mortality is high. Thus, malaria associated morbidity poses an enormous barrier to socioeconomic growth by provoking high health care costs, decreased productivity due to time taken off from school or work, massive population movements and reduction in the foreign trade and investments. It is, therefore, not surprising that malaria-endemic countries are not only poorer than non-malaria endemic areas, but they also have lower rates of economic growth (Sachs & Malaney, 2002; Onwujekwe *et al.*, 2009). In some countries with severe malaria burden, the disease is responsible for as much as 40% of public health expenditure and 30% to 50% of inpatient admissions (WHO. Malaria 2019).

The incidence rate of malaria decreased globally between 2010 and 2018, from 71 to 57 cases per 1000 population at risk. This reduction has stood at the same levels since 2014 (WHO. Malaria 2019), possibly indicating an increasing disease burden. Experts have attributed this to several causes including population movements, changing agricultural practices, deforestation and more speculatively, long-term climate changes. Millions of people currently do not have access to malaria commodities (such as antimalarial drugs, insecticides and diagnostic supplies) and thousands of malaria cases remain unrecorded indicating that current worldwide disease control measures are still insufficient. Furthermore, the increasing development of resistance to drugs and insecticides makes their use insufficient and instead, results in faster growing caseloads. With a rapidly growing population in regions with high malaria transmission, it has been estimated that in the absence of effective intervention strategies the number of malaria cases will double over the next 20 years (WHO. Malaria 2019).

1.1.3 Overview of the malaria lifecycle

The malaria lifecycle constitutes one of the most complicated lifecycles of any organism and constitutes of a series of intracellular replication events alternated by extracellular migration and invasion patterns; a motif that seems to be conserved between all *Plasmodium* species infecting their vertebrate hosts. The parasite requires both a vertebrate host and an invertebrate vector to complete its developmental cycle (Greenwood *et al.*, 2008) (**Figure 1.1**). Interestingly, the duration of the specific events during the malaria infection development within the vertebrate host and mosquito vector can vary based on the parasite strain, vertebrate host and mosquito vector species combination, as well as on temperature and geographic distribution.

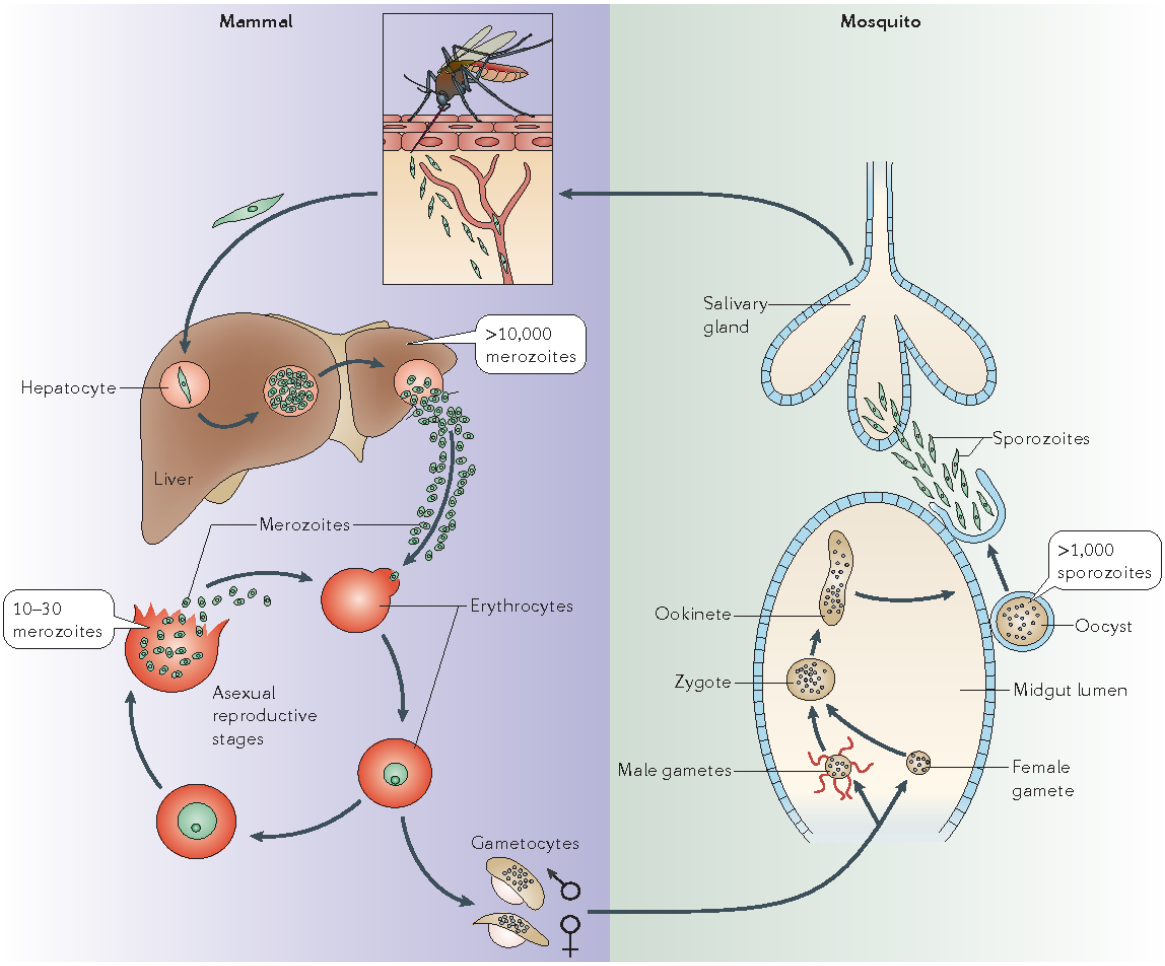

Figure 1.1. The lifecycle of malaria parasites. The *Plasmodium* lifecycle in the vertebrate host starts when mosquito derived sporozoites enter the bloodstream during a bloodmeal and sequester within the liver until subsequent invasion of hepatocytes in order to form exoerythrocytic schizonts. Over a period of 2-10 days asexual replication within the schizonts creates merozoites, which - following schizont rupture - are released into the bloodstream. Following many cycles within the red blood cells (RBCs), sexual forms (called gametocytes) are produced. Development of *Plasmodium* in the mosquito begins with the ingestion of a bloodmeal containing gametocytes, which after fusion form zygotes that later develop into motile ookinetes. Following ookinete invasion of the mosquito midgut epithelium, extracellular oocysts are formed to produce sporozoites. Upon oocyst rupture, sporozoites are released, circulate in the haemolymph and upon maturation they finally colonise the mosquito salivary glands, rendering the mosquito infective. Figure was adapted from (Menard *et al.*, 2013) and permission for its republishing can be found in **Appendix 1**.

The malaria parasite enters its vertebrate host by the passive transfer of infective sporozoites from an infected female *Anopheles* mosquito during uptake of a

bloodmeal. Sporozoites present in the mosquito saliva travel through the dermis and reach the blood stream, from where they can subsequently migrate to the liver (Frischknecht *et al.*, 2004; Xu *et al.*, 2010; Frischknecht *et al.*, 2017). The sporozoites actively enter the liver through the Kupffer cells where they migrate through several hepatocytes, until they eventually arrest intracellularly and develop into the exoerythrocytic schizonts (Pradel *et al*., 2001). After an incubation period of about 10 days, the schizonts rupture releasing several thousand merozoites that exit the liver cells and re-enter the bloodstream. It is worth mentioning that in the case of *P. vivax* and *P. ovale,* sporozoites may not follow the reproduction step and stay dormant (hypnozoites) in the liver; they may be activated after a long time and enter the blood stream as merozoites after weeks, months or even years. Each merozoite enters a RBC by an active process and transforms into the young ring stage. This will soon mature into the trophozoite from which the blood stage schizont will derive. Within 24 hours, schizonts rupture in order to release a new set of merozoites into the bloodstream and the asexual cycle continues (Cowman *et al.*, 2006). This asexual blood stage (ABS) cycles of invasion and replication can continue for several parasite generations and are associated to the pathology of the disease (Matuschewski, 2006). Specifically, clinical symptoms occur in synchrony with the continuous rupture of the infected erythrocytes and the release of erythrocyte and parasite debris such as the malarial pigment haemozoin and glycophosphatidylinositol, combination also known as the 'malaria toxin' (Schofield *et al.*, 1993; Clark *et al.*, 2003). Importantly, a subset of trophozoites exits these asexual cycles and develop into the sexual forms, the male and female gametocytes (Bannister & Mitchell, 2003).

In general, parasites within a vertebrate must keep a balance between forming replicating asexual-stage parasites that maintain the infection and producing enough non-proliferative gametocytes in order to ensure transmission (Schneider *et al.*, 2018). The factors that govern gametocytogenesis are poorly defined (Alano, 2007), whereas the rate of gametocytogenesis is variable and influenced by genetic factors as well as environmental stimuli, suggesting that an interplay between pathogen and host factors influences gametocyte commitment (Josling *et al.*, 2018). It has been found that a transcription factor of the ApiAP2 family termed *Pfap2-g* is the conserved master regulator of sexual conversion in all *Plasmodium* species (Kafsack *et al.*, 2014; Sinha *et al.*, 2014; Zhang *et al.*, 2017). The current model states that in asexual parasites, the *ap2-g* gene is silenced by epigenetic mechanisms that involve heterochromatin at

this locus. Activation of the gene, which in *P. falciparum* requires displacement of the heterochromatin protein 1 (HP1) in a process that depends on the gametocyte development 1 protein (GDV1) (Filarsky *et al.*, 2018), results in sexual commitment. Several downstream regulators including the transcriptional repressor *ap2-g2* (Sinha *et al.*, 2014; Yuda *et al.*, 2015), contribute to the subsequent steps of sexual differentiation including whether the parasite will become a male or female gametocyte. The mechanism underlying this differentiation is poorly understood (Tadesse *et al.*, 2019) and the female to male sex ratio is highly variable, but across Plasmodia a female bias is generally observed. Nevertheless, both male and female gametocytes are arrested in a G0 state within the PV of their host RBC and activated once ingested by a female *Anopheles* mosquito (Sinden, 1998).

Inside the mosquito midgut lumen, in response to certain environmental factors such as a drop in the temperature and pH (Billker *et al.*, 1997) and mosquito specific factors such as xanthurenic acid (Billker *et al.*, 1998), *Plasmodium* male and female gametocytes soon emerge from the RBCs and mature to form gametes that later fuse to form diploid zygotes. These zygotes eventually differentiate into the motile invasive ookinetes. These extracellular ookinetes then migrate out of the blood bolus, traverse the midgut epithelium and transform into vegetative oocysts in the subepithelial space between the midgut epithelium and the basal lamina. Cytological studies have shown that following fertilisation, the genetic organisation of the parasite is returned to a haploid state (Janse *et al.*, 1986), however it was later found that this is due to a two-step meiotic division which results in the production of four haploid genomes in the ookinetes (4N) (Sinden *et al.*, 1991). Indeed, it was experimentally confirmed that each oocyst has the potential to contain four discrete and potentially recombinant genotypes, mainly due to recombination events occurring during the meiotic divisions (Ranford-Cartwright *et al.*, 1991). Inside the oocysts several mitotic endoreplications occur over a period of approximately 1-2 weeks, as it undergoes sporogony to produce thousands of haploid sporozoites. Due to the rapid growth, oocysts impose a high nutritional demand from their mosquito host in addition to the transcriptomic changes that further support the development and maturation of the oocyst capsule (Rono *et al.*, 2010). Once oocysts are fully matured, sporozoites are released into the mosquito haemocoel in order to later invade the lumen of the salivary glands. The salivary gland sporozoites are now ready for infection into a vertebrate host, once the mosquito uptakes its next bloodmeal (Bannister & Mitchell, 2003; Sinden, 2015).

1.1.4 The pathogenic basis of malaria

The developmental cycle of *Plasmodium* parasites spans across both a vertebrate host and a mosquito vector, with the pathogenesis caused being closely related with its lifecycle in the former. The liver stage infection is completely asymptomatic and all malaria associated pathology stems from the Asexual Blood Stage (ABS) cycle of invasion and replication (Matuschewski, 2006). The invasion of the RBCs by malaria parasites, particularly *P. falciparum* (Langreth *et al.*, 1985), results in progressive and dramatic structural, biochemical and mechanical modifications of the RBCs making malaria a potentially multisystem disease, as every organ of the body is reached by the blood. Initial manifestations of the disease are similar to flu-like symptoms such as headache, fever, joint pain and vomiting. As the disease progresses, patients might also suffer from more severe symptoms such as anaemia, haemoglobin in the urine, retinal damage and convulsions (Beare *et al.*, 2006). Regularly, some patients progress into severe malaria when infected with *P. falciparum* parasites. The other human malaria species typically cause febrile but nonfatal disease (Pasvol, 2005).

Several factors have been associated with *P. falciparum* increased virulence and pathogenicity to its human host; nevertheless, a great deal is yet to be uncovered (Pasvol, 2001; Kaestli *et al.,* 2006; Brazier *et al.*, 2017). One of the factors found to be important for its increased virulence, compared to any of the other human malaria parasites, is related with its ability to cytoadhere (Bignami *et al.*, 1890; Sherman *et al.*, 2003) using a variety of ligand-receptor combinations (Olszewski *et al.*, 2009). Furthermore, it is able to invade not only young immature RBCs (reticulocytes) - like *P. vivax* - but also more mature forms of RBCs. Both these factors greatly contribute to the tendency of *P. falciparum* to create higher parasitaemia levels resulting in worse clinical manifestations and in many occasions death (Miller & Greenwood, 2002).

As previously mentioned, the enhanced pathogenicity of *P. falciparum* is associated with its ability to cytoadhere and sequester to the endothelium of multiple capillaries and venules, by modifying the surface of the infected RBCs. As a result, gametocytes cytoadhere primarily in the bone marrow whereas trophozoites and schizonts cytoadhere to the vascular epithelium of the heart, lungs, subcutaneous tissues and liver, as well as to the brain and placental endothelium often leading to cerebral and placental malaria (Weatherall *et al.*, 2002). Therefore, as immature ring-forms circulate in the host blood stream, their removal from the circulation as they pass through the

spleen or their oxidative damage as they pass through the lungs is prevented (Jenkins *et al.*, 2007; Zougbete *et al.*, 2011).

The ability of the infected RBCs to adhere to the vascular epithelium is largely facilitated by a single parasite encoded protein which is localised on the surface of the infected RBCs and consists of multiple adhesion domains; the *P. falciparum* erythrocyte membrane protein 1 (*Pf*EMP1). *Pf*EMP1 also binds to the complement receptor-1 resulting in clustering of unparasitised RBCs around parasitised ones (rosetting), contributing also to microvascular obstruction effects. *Pf*EMP1 is encoded by the multigene var family comprising of about 60 members, which are subject to clonal antigenic variation (Baruch *et al.*, 1995) thus enabling the parasite to evade the host immune response and establish chronic malaria infections (Warimwe *et al.*, 2009; Tembo *et al.*, 2014). Numerous receptors for *P. falciparum* cytoadhesion have been identified including CD36, the intercellular adhesion molecule 1 (ICAM-1) and the endothelial protein C receptor (EPCR) (Rowe *et al.*, 2009; Turner *et al.*, 2013) from which the ICAM-1 and the EPCR candidate receptors were found to be responsible for the deadly complications of cerebral malaria (Avril *et al.*, 2016).

Parasite adhesion interactions include binding to endothelial cells (cytoadherence), rosetting exclusively with non-infected erythrocytes and platelet-mediated clumping of infected erythrocytes. However, the exact mechanism underlying parasite ability to adhere and/or sequester and how this links to the clinical pathology is poorly understood. It has been once suggested that damage to the host endothelium and organs may be caused by obstruction to the blood flow and localised or systemic production of pro-inflammatory cytokines (Heddini, 2002; Dunst *et al.*, 2017) such as the tumor necrosis factor (TNF). Specifically, TNF seems to be involved in the host immunological responses in initiating diverse cellular responses ranging from proliferation to activation of apoptosis. Inhibitors of TNF production were also found to be associated with the reduced ability of the *Plasmodium*-infected RBCs cytoadherence (Wassmer *et al.*, 2006; Chakravorty *et al.*, 2008; Bubik *et al.*, 2012).

1.1.5 Clinical manifestations and diagnosis

The clinical manifestations and outcomes of any malaria infection are determined by a combination of parasite, host and socio-geographical factors. However, the exact contribution and precise role of each factor often remains unclear.

In the vertebrate host, liver stage infection is completely asymptomatic where all malaria associated pathology results from the repetitive ABS cycles of invasion and replication (Matuschewski, 2006). Uncomplicated malaria is usually associated with non-specific symptoms of fever, headache, sweats, chills, rigors and joint pain (Bell & Winstanley, 2004). Symptoms of severe malaria can vary depending on patient factors such as age, genetic background, pregnancy, previous exposure (as influenced by endemic transmission rates) as well as parasite drug-susceptibility and poor clinical management of previous uncomplicated malaria (Miller & Greenwood, 2002). Patients with severe malaria typically present symptoms ranging from cerebral malaria (manifested as an unrousable coma, with children often displaying vomiting and convulsions), severe anaemia, metabolic acidosis, respiratory difficulties, renal failure and coagulation failure (WHO. Malaria 2000; Pasvol, 2005).

Apart from clinical findings, microscopic examination of thick (unified drop of blood) and thin (methanol-fixed monolayer) blood smears remain the gold standard in malaria diagnosis (Pasvol, 2005). For use in clinical diagnosis and epidemiological studies, the highly sensitive and user-friendly quantitative Real-Time Reverse Transcription PCR (qRT-PCR) technique is also a relevant tool. More recently, antigen capture tests have been also developed (Craig *et al.*, 2002). Rapid diagnostic tests (RDT) were later introduced into the clinical management of malaria and since then, more than one million RDTs are used every year in various health facilities in countries affected by malaria (Chandler *et al.*, 2010). Although microscopy is currently the gold standard for malaria diagnosis, RDT is not meant to replace it but rather to complement the information that comes with it (Wongsrichanalai *et al.*, 2007). It is important, though, to first identify and express the diagnostic needs of the endemic regions and then develop adequate diagnostic methods.

1.2 Malaria control and obstacles to eradication

Malaria has not always been a disease of the poorest regions of the world. However, the world-wide malaria eradication campaign launched by the WHO after the end of the Second World War saw the successful eradication of malaria from many temperate zone countries (including the U.S., former Soviet Union and the Mediterranean), as a result of mainly financial development and public health measures in the developed world. A significant reduction in disease burden was also achieved in some tropical regions (foremost parts of South East Asia, South America and India, and some fewer

African nations) (Mabaso *et al.*, 2004). Despite the dramatic reduction in malaria cases originally observed, the campaign foundered due to the emergence of regimen-resistant *Plasmodium* parasites and *Anopheles* mosquitoes.

Malaria differs from many other infectious diseases in that the parasite lifecycle is dependent upon both its vertebrate host and mosquito vector, hence impairing definite control or complete eradication of the disease. This complex host-vector relationship of the disease adds a layer of complexity to its management, but also opens up an additional window for new global therapeutic and control strategies. Malaria control measures can be broadly divided into five categories, out of which three are vector control strategies (Bruce-Chwatt, 1987):

i. Elimination of parasites from the human host.
ii. Mosquito-host contact reduction.
iii. Destruction of adult vector mosquitoes.
iv. Elimination of vector mosquito breeding sites or elimination of mosquito larvae.
v. Genetic control of mosquitoes.

1.2.1 Addressing the vertebrate host

1.2.1.1 Anti-malarial drugs

Anti-malarial drugs have found widespread use in both treatment and prevention strategies. The latter has been widely established in the form of prophylactic treatment for travellers but also for residents of endemic areas and high risk individuals i.e. pregnant women, foremost as Intermittent Presumptive Therapy (IPT) (White, 2008). Anti-malarial drugs can be broadly classified by their parasite subcellular and biochemical targets: food vacuole (haem-detoxification), cytoplasm (folate synthesis), mitochondrion (electron transport chain) and the chloroplast-like organelle, the apicoplast (protein synthesis) (Greenwood *et al.*, 2008).

Main regimens include quinolines, antifolates, artemisinin and primaquine; all acting in a wide range of parasite metabolic processes. For example, quinolines, quinine and the artificially synthetised substance chloroquine are hypothesised to both eliminate mature trophozoites and inhibit haemoglobin detoxification (Egan & Kaschula, 2007). On the other hand, pyrimethamine interfere with the parasite folate synthesis pathway and therefore inhibit nucleic acid synthesis (Hyde, 2007) while the natural compound extracted from the shrub *Artemesia annua*, artemisimin, has been found to be implicated in the interference of protein transport and processing and, mitochondrial

function (Wang *et al.*, 2010). It has been previously shown that artemisinin is active against both ABS and sexual stage gametocytes and hence, it is considered to be a largely revolutionary anti-malaria drug (Golenser *et al.*, 2006; White, 2008). Primaquine, by causing oxidative damage to the cell, is currently the number one transmission blocking drug recommended for use by the WHO (Hill *et al.*, 2014).

Despite the continued efforts for developing new antimalarial drugs, malaria chemotherapy is plagued by two significant problems, lack of new drugs and resistance of *P. falciparum* and *P. vivax* against existing drugs. Unlike bacteria, *Plasmodium spp.* are eukaryotes and can acquire or lose polygenic resistance mechanisms during meiosis. Resistance to several drugs arises readily because single point mutations confer resistance and per-parasite mutation frequencies are high (Hamilton *et al*., 2017). For example, mutations in *Pfmdr1* (*P. falciparum* multi drug resistance) and *Pfcrt* (*P. falciparum* chloroquine resistance transporter) genes (Mita *et al.*, 2009), associated with transporter membrane proteins, are attributable for resistance to quinoline. Similarly, progressive acquisition of mutations in the dihydrofolate reductase (*dhfr*) or dihydropterate synthetase (*dhps*) genes (Mita *et al.*, 2009) is responsible for the development of resistance to antifolate derived drugs. Further studies suggest that *Plasmodium* can evade antimalarial drugs in hematopoietic tissues, eventually developing resistance (Lee *et al.*, 2018).

During the last decade, different types of artemisinin combination therapy (ACT) are recommended as first-line treatment for all *P. falciparum* malaria in endemic countries (White, 2008). However, artemisinin-resistant *P. falciparum* parasites have been reported in Southeast Asia over the last two decades (Ashley *et al.*, 2014) and although no cases of resistance have been reported in developed countries, its potential emergence is still a major concern. Specifically, in 2014, a molecular marker for artemisinin resistance was reported after identifying single point mutations in the "propeller" region of the *P. falciparum kelch* protein gene on chromosome 13 (*Pfkelch13*) in Cambodian provinces (Ariey *et al*., 2014) as well as throughout the mainland of Southeast Asia (Ashley *et al.*, 2014). Later, a novel *Pfkelch13* gene polymorphism was identified, also associated with artemisinin resistance in Eastern India (Das *et al.*, 2018). Thus, the increasing identification of artemisinin-resistant isolates together with new mutations and increasing combination therapy failures raise alarms for urgent malaria long-term control and where possible, elimination.

1.2.1.2 Vaccines

Malaria vaccines could be one of the most cost-effective and yet difficult interventions to reduce the enormous burden of malaria in the poorest countries of the world, hence no effective malaria vaccine is currently available. There are a number of leads emerging, with three conceivable vaccine strategies:

i. Pre-erythrocytic, liver stage vaccines.
ii. Erythrocytic, blood stage vaccines.
iii. Transmission blocking, mosquito stage vaccines.

Vaccines are likely to have different or indeed combine mechanisms of action, each one protecting in different ways and against different parasite stages. A liver stage vaccine would reduce the chances of a person becoming infected, whereas an ABS vaccine would reduce disease severity and risk of death during infection. A transmission blocking vaccine (TBV) on the other hand targets the sexual stages of the parasite while in the mosquito vector (Matuschewski, 2006).

It is worth noting that these vaccines might not be able to confer total immunity, but nonetheless, may still act to reduce parasite load and decreasing morbidity and mortality (Matuschewski, 2006; Matuschewski & Mueller, 2007). Pre-erythrocytic liver stage vaccines target both the sporozoites and the hepatocytes invaded by them, whereas anti-sporozoite inhibitory antibodies are able to impair parasite motility or migration towards hepatocytes. However, in such attempts, it is imperative to take into consideration that one single sporozoite by transforming into an exoerythrocytic schizont can later generate thousands of merozoites that can ultimately lead to a massive parasite load in the blood stream of the mammalian host (Matuschewski, 2006). Protective immunity by injection of irradiated, live attenuated sporozoites has been achieved in both rodent models (Nussenzweig *et al.*, 1967) as well as human volunteers (Hoffman *et al.*, 2002).

Nevertheless, safety and practical concerns including selection of resistant strains, instability, varying efficiency, lack of high-throughput production, preservation and distribution hamper a broad use of application (Matuschewski, 2006). Previous efforts in injecting genetic live attenuated sporozoites has proven to elicit protracted sterile protection and overcome the above concern (Mueller *et al.*, 2005; van Dijk *et al.*, 2005), however future experimental and clinical evidence was inadequate. A more cost effective solution lies during the last decades in vaccines such as RTS,S (Alonso *et*

al., 2004, 2005) and *Pf*SPZ (Nussenzweig *et al.*, 1967; Rieckmann *et al.*, 1974; Lyke *et al.*, 2017) which have, so far, shown promising results. Encouragingly, the GlaxoSmithKline Biomedicals RTS,S/ AS01A vaccine, specific for the carboxy-terminal segment of the *P. falciparum* circumsporozoite (CS) protein, is the first vaccine candidate to advance this far; having completed Phase III clinical testing and is now being used for the immunisation of 360 000 children in Ghana, Kenya and Malawi (Adepoju, 2019). The irradiated whole sporozoite *Pf*SPZ vaccine, made by Sanaria, has been demonstrated to be safe, well tolerated and had promising protection against malaria when administered intravenously. Large-scale pilots of the *Pf*SPZ vaccine are also ongoing in Mali, Gabon, Tanzania, and Guinea including also several hundreds of thousands of infants (Epstein *et al.*, 2011, 2017; Seder *et al.*, 2013; RTS,S Clinical Trials Partnership, 2014; 2015; Ishizuka *et al.*, 2016; Regules *et al.*, 2016; WHO. Malaria 2017, 2018). Additionally, immunity against VAR_2CSA, a member of the *P. falciparum* erythrocyte membrane protein 1 family that has been shown to specifically bind to the chemical compound which *P. falciparum* parasites use in order to sequester in the placenta tissue, chondroitin sulfate A (CSA), may offer protection against placental malaria (Fried & Duffy, 2015).

The milestones for erythrocytic blood stage vaccine development include antibody-mediated inhibition of merozoites and cytoadhesion by infected erythrocytes. These approaches aim to reduce asexual parasite load as well as to accelerate the immunological memories of naive individuals, compromising disease severity (Matuschewski & Mueller, 2007). Clinical trials targeting hepatocytic development and invasion ability of merozoites have commenced with promising results (Druilhe *et al.*, 2005). Nevertheless, the polymorphic nature of merozoite antigens that does not allow establishment of long term immune memory against any of the merozoite surface protein members remains a long term obstacle (Matuschewski, 2006). Targeting the parasite cytoadherence ability, by simply generating antibodies against *Pf*EMP1, represents another choice (Avril *et al.*, 2006; Beeson *et al*, 2013; Bull & Abdi, 2016; Hviid *et al.*, 2018). Attempts to develop a blood stage vaccine have also focused on two highly polymorphic *P. falciparum* blood stage proteins; the apical membrane antigen 1 (AMA1) and merozoite surface protein 1 (MSP1) as antigens (Malkin *et al.*, 2008; Douglas *et al.*, 2011). AMA1 is needed for the successful interaction between erythrocytes and merozoites, whereas the exact function of MSP1 has not been yet revealed though it has been shown to be essential for parasite viability.

1.2.1.3 Transmission blocking vaccines (TBV) and targets

TBVs target the parasite sexual stages and their use could prevent the spread of malaria through the community. In contrast to classical vaccines, the TBV approach does not directly protect the immunised individual from contracting the disease. Instead it is a community-based intervention, indirectly protecting individuals in the vaccinated community by reducing the number of infection carrying vectors (Dinglasan & Jacobs-Lorena, 2008). The use of a TBV is also believed to greatly prolong the useful life of other malaria vaccine components and anti-malarial drugs, even those that target other developmental stages of the parasite, by preventing the spread of parasites that become resistant to these vaccines (Carter *et al.*, 2000).

The principle of TBV is based on the vaccination of either infected or non-infected individuals with sexual or mosquito-stage parasite proteins, using the human adaptive immune response to generate antibodies that are subsequently transferred to the mosquito midgut during uptake of a bloodmeal (Dinglasan & Jacobs-Lorena, 2008). The antibodies are targeted so to bind the parasite within the mosquito midgut and thus facilitate antibody (and in some cases complement) mediated killing or alternatively, interfere with parasite protein function thereby blocking development and abolishing transmission (Allan, 2007; Doumbo *et al.*, 2018). Importantly, it has been previously demonstrated that use of transmission-blocking interventions alone can force elimination in a closed lab vertebrate population (Blagborough *et al.*, 2013b).

Since TBV mediated parasite killing is well defined (neutralising antibody or complement-mediated killing through antibodies), simple mosquito membrane feeding assays where gametocytes are fed in presence of immunised sera, provides a powerful way of assessing efficacy *ex vivo* without putting immunised individuals at risk of infection. Furthermore, malaria transmission is a localised event, with mosquito dispersal ranges within a few hundred to a thousand meters. This has the advantage that a relatively small, localised vaccination cohort would give rise to a significant reduction in local transmission rates. In addition, TBV implementation may prevent the spread of drug and vaccine resistance by inhibiting transmission of resistant parasite populations, thereby prolonging the life-span of other important malaria control tools (Carter, 2001). More promisingly, the use of anti-malarial pre-erythrocytic vaccines (PEV) and TBV vaccines together has been shown to boost their effectiveness. Specifically, it has been demonstrated that co-administration of anti-sporozoite and

anti-transmission interventions act synergistically, enhancing PEV efficacy across a range of TBV doses and transmission intensities (Sherrard-Smith *et al.*, 2018).

The genes encoding *Pfs48/45*, *Pfs230* and *Pfs25* in *P. falciparum* as well as *Pvs25* in *P. vivax,* are the major candidates for clinical development of TBVs already in the past three decades (Hisaeda *et al.*, 2000, Carter, 2001; Tomas *et al.*, 2001; Pradel, 2007; Saxena *et al.*, 2007; Bousema & Drakeley, 2011; Nunes *et al.*, 2014). These genes fall into two different groups in terms of their expression pattern: pre- or post-fertilisation (Saxena *et al.*, 2007). Since parasites antibody-mediated killing occurs up to several hours after a mosquito bloodmeal (Sinder, 1982; Aikawa *et al.*, 1984), targeting these proteins in the mosquito midgut could efficiently eliminate parasite survival before infection establishment.

Antibodies against the gametocyte expressed proteins *Pf*s48/45 and *Pf*s230 successfully block transmission by killing the parasite upon entry into the midgut lumen, when the proteins become exposed on the gamete surface as a result of gametocyte activation. During the past years, significant progress in the development of a *Pf*s48/45 or *Pf*s230 based TBV has been hampered mainly due to the difficulties in expressing the proteins *in vitro* whilst retaining a conformation which confers the correct immunogenicity (Allan, 2007; Williamson, 2003). However, a new study shows that antibodies against all protein fragments containing the CM domain 1 of the *Pf*s230 protein display strong inhibitions (Tachibana *et al.*, 2019), encouraging future research. In contrast, *Pf*s25 and *Pf*s28 are exclusively displayed on the parasite surface following gametocytes activation upon entry into the mosquito midgut, while no presence within the vertebrate host, apart from low level expression of *Pfs25* in early gametogenesis, has been indicated (Vermeulen *et al.*, 1985). This confers an advantage over blood stage expressed vaccine candidates - due to the absence of selective pressure in the vertebrate host - *Pfs25* and *Pfs28* display minimal polymorphisms, and immunity is thereby not strain-specific (Saxena *et al.*, 2007). A major drawback of *Pf*s25 and *Pf*s28 is the extremely high concentration of antibody required in order to completely block transmission (Allan, 2007; Doumbo *et al.*, 2018).

Recent work from Canepa *et al.* showed that antibodies targeting a 52 amino acid (aa) region of Pfs47, a *P. falciparum* gene expressed on the surface of female gametocytes, confer a strong (78–99%) transmission blocking activity (TBA). This has

been proven to be due to the high affinity of the antibody with the surface protein leading to fertilisation inhibition and thus, ookinete formation (Canepa *et al.*, 2018).

Ookinete-secreted proteins have been identified as targets of TB immunity including chitinase 1, von Willebrand factor-A domain-related protein (WARP), thrombospondin-related anonymous protein-related protein (TRAP), membrane-attack ookinete protein (MAOP), secreted ookinete adhesive protein (SOAP), and cell-traversal protein for ookinetes and sporozoites (CelTOS) (Dessens *et al.*, 2003; Kariu *et al.*, 2006).

Significant progress has been made since the malaria community first considered TBV as an effective tool for eradicating malaria, however there are still a lot of drawbacks to be overcome. The major stumbling blocks for all candidate proteins tested so far include the expression of appropriately folded target proteins and their downstream purification, the insufficient induction of sustained functional blocking antibody titres by candidate vaccines in humans, and the validation of a number of bioassays as a transmission blocking antibody (TBA) correlate in the field (reviewed in Nunes *et al.*, 2014). Currently, many more gametocyte or ookinete proteins are under investigation for their transmission blocking potential (Coehlo *et al.*, 2017; Drapel *et al.*, 2018; Acquah *et al.*, 2019). In addition, it is possible to envisage the use of mosquito protein targets to raise TBA. These mosquito-derived targets may be those directly binding to the parasite surface or alternatively, may be essential parasite-interaction partners so that when access to these proteins is blocked, parasite development is inhibited (Dinglasan & Jacobs-Lorena, 2008). In any case, the historical success of vector control highlights the importance of studying transmission and vector-host interactions in order to assist the development of successful malaria control methods.

1.2.1.4 Naturally acquired transmission-blocking immunity

The induction of transmission-blocking immunity as a potential tool in malarial control was first demonstrated in the avian malaria parasite *P. gallinaceum* in the 50's and 70's where the infectivity of gametocytes was shown to be reduced due to the prior immunisation of their avian hosts with inactivated gametocytes (Huff *et al*., 1958; Gwadz *et al*., 1976; Carter *et al*., 1976). Further experiments aiming at identifying the targets of this transmission-reducing immunity revealed three candidate antigens; Pfs25, Pfs230 and Pfs48/45 (Rener *et al*., 1983; Vermeulen *et al*., 1985) which were later shown to be sexual stage proteins that have no function in gametocyte development but are essential for gamete fertilisation or post-fertilisation development

in the mosquito (Sauerwein *et al*., 2015). The identification of these proteins was later confirmed by the detection of specific antibodies against them, in the sera of individuals living in malaria-endemic areas (Graves *et al*., 1988; Drakeley *et al*., 2006; Bousema *et al*., 2006; Jones *et al*., 2015; Stone *et al*., 2018; Ouédraogo *et al*., 2018) indicating that such parasite pre-fertilisation antigens are immune targets. In field-based mosquito-feeding assays the possibility and rate of mosquito infection are significantly lower for individuals that were found to be reactive to either the Pfs48/45 or Pfs230 proteins (Stone *et al*., 2018). This also explains why the majority of the circulating gametocytes are destroyed by the host immune system prior to mosquito transmission (Ouédraogo *et al*., 2011; Stone *et al*., 2016; Stone *et al*., 2018).

Today, it is widely accepted that naturally acquired immunity to *falciparum* malaria protects millions of people that have been repeatedly exposed to *Plasmodium falciparum* infection, from severe disease and death (Ouédraogo *et al*., 2018). In fact, children in high-transmission areas are often resistant to severe malarial disease by the time they reach puberty, although infection itself is not completely prohibited (Drakeley *et al*., 2006; Bousema *et al*., 2007). Transmission-reducing immunity (TRI) is therefore based on the identification of naturally acquired antibodies against blood stage gametocytes that have not yet been taken up by mosquitoes, in response to proteins of their surface (Mendis *et al*., 1987). The way that this works is based on the fact that when these gametocytes die, they release intracellular proteins/antigens into the host circulation. Among these, are also proteins produced by gametocytes which are crucial for the extracellular parasite development in the mosquito midgut (Alano *et al*., 1991; Sinden *et al*., 2010). These antigens are then processed and presented by resident presenting cells which following immune responses elicitation, can cause substantial or complete blockade of parasite development in the mosquito. When these human antibodies are then taken up by a mosquito, they inhibit fertilisation of malarial male and female gametes within the mosquito bloodmeal (e.g. anti-P230, P48/45, HAP2) or interact with the parasite post-fertilisation, in the mosquito gut (e.g. anti-APN-1, P25 and P28) (Sinden, 2017).

While TBVs do not protect against clinical disease, they aim to reduce parasite density in the mosquito to levels that cannot support further transmission (Matuschewski, 2006; Matuschewski & Mueller, 2007). The feasibility of a TBV has been demonstrated in multiple species, with a wide range of target antigens, expression systems and

delivery methods assessed and examined. Despite this, the practical development and use of a TBV within the field also requires a range of fundamental additional research. So far, the naturally acquired immunity to *P. falciparum* TBV candidates has been adequately characterised (Bousema *et al*., 2007; Ouedraogo *et al*., 2011) and TBVs for *P. falciparum* are currently in pre-clinical and clinical trials. However, *P. vivax* TBV candidates are less advanced.

1.2.2 Addressing the invertebrate host

1.2.2.1 Host-mosquito contact reduction and destruction of adult mosquitoes

The use of bed nets as a protection against malaria was suggested by Ronald Ross in 1910, due to the nocturnal feeding pattern of most *Anopheline* vector species (Pates & Curtis, 2004). Nowadays, insecticides are deployed primarily against adult mosquitoes through indoor residual spraying (IRS) and insecticide treated nets (ITNs); with 57 % of the at-risk population estimated to have access to an ITN (WHO. Malaria 2019). Whilst there are four classes of insecticide available, only pyrethroids are licensed for use on ITNs. Pyrethroids are ion channel toxins prolonging neuronal excitation, and their use as treatment method results in a lower risk of mosquitoes entering the net through any gaps or biting through the net. Exposure to lethal insecticides also significantly impairs mosquito survival, with fewer female mosquitoes surviving until an age at which infective sporozoites are formed, thus providing protection to the wider community (Curtis *et al.*, 1999; Curtis *et al.*, 2007).

Resistance to at least one insecticide has been reported in 73 endemic countries that regularly submit monitoring data. Similarly, 75% of the countries monitoring pyrethroid resistance have reported resistance (WHO. Malaria 2019). In addition, the loss of natural malaria immunity, acquired as a result of living in high transmission areas, may be compromised by ITN campaigns (Pates & Curtis, 2004; Curtis *et al.*, 2007). Indeed, it is not clear whether the current tools alone are capable of completely eliminating malaria in high transmission settings (Mendis *et al.*, 2009).

1.2.2.2 Destruction of adult vector mosquitoes

The implementation of large scale IRS using dichlorodiphenyltrichloroethane (DDT) formed the cornerstone of the WHO Global Malaria Eradication campaign launched in 1955, which in conjunction with chloroquine saw the disappearance of malaria from many temperate and tropical low-transmission zones (Sadasivaiah *et al.*, 2007). However, malaria eradication was not achieved in high-transmission tropical zones

due to the DDT-resistance emerged by the early 1960s and the negative publicity regarding environmental concerns and poorly substantiated human health hazard links (Mabaso *et al.*, 2004; Rogan & Chen, 2005).

IRS works on the basis of an endophilic feeding pattern of many anopheline females. Following uptake of a bloodmeal, the female mosquito seeks out a resting place within the dwelling. Coating the walls of human and animal dwellings with a low concentration of DDT causes the female mosquito to be exposed to a lethal dose of insecticide during her resting period. Therefore, IRS leads to a significant reduction in the number of females that survive until the time of sporozoite-development and a reduction of total mosquito population numbers (Bruce-Chwatt, 1987).

1.2.2.3 Destruction of mosquito breeding sites and larvicidal methods

Prior to the introduction of DDT, environmental engineering resulting in draining breeding grounds of water and larvicidal methods such as spreading oil onto the surface of breeding pools were the main methods for controlling mosquito vector populations. In addition to that, biological larvicidal methods such as introduction of larvivorous fish and trials with pathogenic fungi, bacteria and nematodes were conducted with varying success. However, the emergence of insecticide resistance has led to a renewed interest in larvicidal based control methods (Ngufor *et al.*, 2014), with scientists now seeking to better understand of the regional differences in ecology, population dynamics and mosquito behaviour (Pates & Curtis, 2004).

1.2.2.4 Genetic control of mosquitoes

The current burden of malaria that exceeds the capabilities of existing or planned infrastructure in addition to the emerging spread of insecticides and drugs resistance, threaten to reduce the efficacy of front-line interventions currently available for malaria eradication such that even maintaining the current levels of disease transmission is expected to cost significantly more in the coming years (WHO. Malaria 2019). As a result, scientists are increasingly focusing on the genetic manipulation of mosquitoes with the ultimate aim to reduce the harmful impact of vector populations through the dissemination of desirable traits by mating or inheritance. Two approaches are currently under investigation for transgenic mosquitoes; those with a reduced capacity for spreading human disease and those with a reduced capacity for reproducing, known as population replacement and population suppression, respectively.

The release of insects carrying a Dominant Lethal (RIDL) gene is an approach whereby male mosquitoes of a strain homozygous for a dominant lethal transgene are released, so that following mating with WT females of the natural population no viable offspring are produced (Thomas *et al.*, 2000). Development of this technique for *Aedes aegypti* is now advanced to field trials (de Valdez *et al.*, 2011; Carvalho *et al.*, 2015) and is also under investigation for the Asian vector *Anopheles stephensi* (Marinotti *et al.*, 2013). Another method for the genetic manipulation of mosquitoes is the use of self-sustaining genetic technologies that make use of selfish genetic elements known as homing endonuclease genes (HEGs) (Windbichler *et al.*, 2007). HEGs are able to increase their frequency in a population by duplicating their DNA sequence in a process known as homing. The homing endonuclease is encoded within its own recognition sequence such that chromosomes containing the HEG cannot be cleaved, but chromosomes lacking it are targeted for DNA cleavage. Following homologous recombination and repair of the broken chromosome, the HEG is copied into the targeted chromosome and HEG heterozygosity results in homozygosity. In sexually reproducing organisms, this ensures that the inheritance of the HEG is strongly biased which makes them great candidates to use in gene drive systems (Burt *et al.*, 2003).

The use of previous HEG technologies (TALEN, ZFN) was quickly followed by the development of Clustered Regularly Interspaced Short Palindromic Repeats (CRISPR) - a family of DNA sequences found within the genomes of prokaryotic organisms such as bacteria and archaea - and CRISPR associated proteins (Cas) (CRISPR/Cas or CRISPR) (Jinek *et al.*, 2012). This system is based upon an endonuclease, called Cas9, directed to its genomic target by a short guide RNA that can be easily modified to target almost any area in the genome. It constitutes the most recent revolutionary discovery and was immediately adapted to mosquitoes. Hammond *et al.* developed a CRISPR-Cas9 based gene drive mechanism in order to disrupt a recessive female fertility gene. This mutation was transmissible to progeny rates of up to 99.6 % (Hammond *et al.*, 2016), expediting in this way the development of a gene drive mechanism able to suppress mosquito populations to levels that do not allow continuation of malaria transmission. Most recently, the use of a CRISPR-Cas9 gene drive construct targeting *doublesex*, a gene that controls differentiation of the two sexes, resulted in a remarkably rapid spread within caged mosquitoes and a 100% population crash of *A. gambiae* mosquitoes (Kyrou *et al.*, 2018).

There are increasing efforts in using gene drive technologies for replacement methods since the introduction of native or synthetic transgenes that render the mosquito resistant to parasite establishment when overexpressed, raises hopes for malaria eradication. Many such genes have been already described and demonstrated to be effective at reducing *Plasmodium* infection load including immune effectors (Moreira *et al.*, 2002; Abraham *et al.*, 2005; Yoshida *et al.*, 2007; Isaacs *et al.*, 2011; Meredith *et al.*, 2011), signal transducers (Corby-Harris *et al.*, 2010; Dong *et al.*, 2011) and mosquito receptor binding peptides (Ito *et al.*, 2002). However, these genes might have varied effects on mosquito fitness and would likely need to be combined with a gene drive mechanism in order to be stably introduced into a population.

Rather than introducing a transgene into the mosquito genome, an alternative approach involves launching transgenes via the genome of a microbial symbiont known as paratransgenesis (Wilke & Marrelli, 2015). This approach has two important advantages: first, genetic manipulation of bacteria is technically more straightforward than mosquitoes and secondly bacteria species are likely able to colonise multiple host species. The potential of this technology has been demonstrated using *Escherichia coli* (Yoshida *et al.*, 2001; Riehle *et al.*, 2008) and more recently is being developed for microorganisms that naturally occur as part of the mosquito gut microbiota (Bisi & Lampe, 2011; Fang *et al.*, 2011; Wang *et al.*, 2012). *Asaia* seems to consist a strong paratransgenesis candidate since it has been found to colonise multiple mosquito species (Favia *et al.*, 2007; Crotti *et al.*, 2009; Damiani *et al.*, 2010; Minard *et al.*, 2013; de Freece *et al.*, 2014), it does not colonise human populations (Epis *et al.*, 2012), it is present in mosquito tissues(i.e. midgut and salivary glands) associated with *Plasmodium* development (Favia *et al.*, 2007; Damiani *et al.*, 2010) and can successfully express multiple anti-*Plasmodium* factors (Bongio & Lampe, 2015). The latter also applies for bacteria of the *Serratia* strain AS1, which have been successfully modified so as to express multiple *Anopheles* antimicrobial peptides (AMPs) (Wang *et al.*, 2017). Wolbachia, a genus of intracellular maternally inherited bacteria, naturally infects about 40% of all arthropod species (Zug & Hammerstein, 2012) and can be used as a biological control agent for two reasons: it can be reproductively manipulative and it can affect its host's ability to transmit pathogens via effects on longevity and resistance (Bourtzis *et al.*, 2014). Finally, several bacterial genera that are common components of the anopheline gut microbiota such as *Acinetobacter*, *Comamonas spp.*, *Pantoea spp.* and *Pseudomonas spp.* have been identified as

having the potential to reduce vector competence via effects on mosquito longevity, immune induction and direct parasite killing (Bando *et al.*, 2013; Bahia *et al.*, 2014).

1.3 Parasite development in the mosquito

The *Plasmodium* lifecycle in the mosquito vector can be additionally subdivided into three phases: (i) parasite sexual development and fertilisation, taking place in the mosquito midgut lumen, (ii) ookinete-to-oocyst transition, which coincides with ookinete traversal through the mosquito midgut epithelium and, (iii) parasite mature sporogonic development and transmission to the vertebrate host, following sporozoites movement to the mosquito salivary glands.

1.3.1 Parasite sexual development and fertilisation

Sexual development is essential for the successful completion of the malaria transmission cycle as with all other apicomplexa (Smith *et al.*, 2002). In *Plasmodium*, the sexual phase of development is already initiated in the infected vertebrate host, when a subset of ABS parasites escapes the continuous cycle of RBC invasion and replication and commit to the production of either male or female gametocytes (Bruce *et al.*, 1990). The timing of sexual differentiation seems to differ between species varying from 10 days in *P. falciparum* to 28 hours in *P. berghei* (Waters & Janse, 2004).

Little is known about the molecules that trigger or regulate sexual commitment in *Plasmodium*. The GDV1, a perinuclear *P. falciparum* protein, was firstly identified to play a key role in gametocytogenesis (Eksi *et al.*, 2012). Later, Sinha *et al.* identified AP2-G in both *P. falciparum* and *P. berghei* as the master regulator of gametocytogenesis. AP2-G is a member of the apiAP2 transcription factor family and it was found to control the switch between the asexual and sexual development (Sinha *et al.*, 2014). The authors also proposed that an unknown yet environmental trigger acts to release the *ap2-g* locus into a euchromatic state, which facilitates its transcriptional activation and expression in all the daughter merozoites. As a consequence, all merozoites deriving from a single sexually committed schizont are pre-determined to develop into all male or female gametocytes (Silvestrini *et al.*, 2000). The HP1 and histone deacetylase 2 (HDA2) also act as epigenetic regulators of sexual commitment by controlling *ap2-g* expression further suggesting that gametocytogenesis is under epigenetic control (Brancucci *et al.*, 2014; Coleman *et al.*, 2014). Additionally, GDV1 evicts HP1 from H3K9me3 sites in the parasite genome thereby depressing *ap2-g* expression and inducing gametocytogenesis (Filarsky *et al.*,

2018). It has been also shown that multiple environmental stimuli such as high parasitaemia, depletion of fresh RBC, TNFα levels and antibodies, intra and inter specific competition and the presence of chloroquine increase the rate of gametocyte differentiation *in vitro* (Bruce *et al.*, 1990; Buckling *et al.*, 1999; Talman *et al.*, 2004)

During maturation in its vertebrate host, a gametocyte remains enclosed within the erythrocyte parasitophorous vacuole (PV) and obtains nutrients through digestion of haemoglobulin and importation of its extracellular environment. As development proceeds, male and female gametocytes become morphologically distinct and start to exhibit an increasingly different metabolic profile when compared to asexual parasites (Lang-Unnasch & Murphy, 2002). Gametocytes are sexually dimorphic; the male being terminally differentiated while the female endures and undergoes further development after fertilisation (Sinden, 1998).

Once gametocytes gain access to the mosquito midgut following uptake within the bloodmeal from an infected vertebrate host, they get exposed to an increase in the pH (Billker *et al*., 2000) and xanthurenic acid levels (XA), and a drop in the temperature (Billker *et al.*, 1997; Billker *et al.*, 1998; Arai *et al.*, 2004). As a result, a signal transduction cascade is initiated resulting in the release of calcium into the cytoplasm of the gametocytes, triggering their maturation into gametes (Billker *et al.*, 2004; Kawamoto *et al.*, 1990). Additionally, the parasite PV and RBC membranes break and the activated gametocytes are released into the mosquito midgut (de Koning-Ward *et al.*, 2008; Sinden, 1998; Sinden, 1982). The *P. berghei* and *P*. *falciparum* PPLP2 has an important function in egress of the gametocyte from the host cell, as a mutant lacking the protein is trapped inside the RBC (Deligianni *et al.*, 2013; Wirth *et al.*, 2014). Interestingly, the *P. berghei* subtilisin-like SUB1 protein, previously known to facilitate *Plasmodium* egress from the host hepatocytes (Withers-Martinez *et al.*, 2012; Tawk *et al.*, 2013; Olivieri *et al.*, 2015; Pino *et al.*, 2017), seems to also be involved in male gamete egress in the mosquito midgut lumen (Pace *et al.*, 2019). Following the completion of three rounds of DNA replication, male gamete maturation culminates with the release of eight motile haploid flagellated microgametes (Janse *et al.*, 1986; Sinden, 1998). A paternally inherited formin, misfit, has been suggested to play a putative role in the regulation of mitotic spindle formation during male gametogenesis. Specifically, its disruption results in microneme defects and altered transcriptional profiles of putative cell cycle regulators (Bushell *et al.*, 2009). Unlike male

gametogenesis, the activated female macrogamete does not undergo DNA replication. Instead, osmophilic bodies facilitate its emergence through the RBCs (Sinden, 1998). Intriguingly, macrogamete maturation is associated with the translation of a subset of translationally repressed mRNA transcripts including the P25/28 surface protein (Sidén-Kiamos *et al.*, 2000). In *P. berghei*, the P25/P28 complex can be detected soon after activation and by the time of zygote and ookinete development, it can be abundantly found on the surface (Mair *et al.*, 2006).

During fertilisation, fusion of the macrogamete and microgamete plasma membrane occurs, with the male nucleus and its axoneme entering the macrogamete cytoplasm (Sinden & Hartley, 1985). The ability of *P. berghei* microgametes to fuse with the macrogamete is governed by a male-specific microgamete surface protein encoded by the conserved male sterility gene *hap2* (Liu *et al.*, 2008). HAP2 is also considered as a potential target for anti-malarial TBV (Blagborough *et al.*, 2009; Angrisano *et al.*, 2017). Adhesion during the initial stages of fertilisation has been also suggested to be governed by gamete surface molecules of the 6-cys repeat motif family: P47, P230 and P48/45. *P. falciparum* and *P. berghei* mutants lacking the gamete surface molecule P48/45 produce infertile female gametes (van Dijk *et al.*, 2001; Khan *et al.*, 2005; van Dijk *et al.*, 2010). The *P. falciparum* P230 protein has been shown to play an essential role in interactions of the male gametes with RBCs resulting in exflagellation impairment (Eksi *et al.*, 2006), a phenotype that is not shared by its *P. berghei* orthologue (van Dijk *et al.*, 2010). *P. falciparum* male gametes lacking expression of *P230p*, a paralog of *P230* which is exclusively expressed in male gametocytes, are also unable to attach to RBCs *in vitro* (Marin-Mogollon *et al.*, 2018). Lastly, the *P. berghei* female gametocyte specific P47 protein was found to have a crucial role in both *in vivo* and *in vitro* fertilisation (van Dijk *et al.*, 2010; Ukegbu *et al.*, 2017b). Thus, these molecules may be involved in male-female recognition, adhesion, or presentation of accessory molecules necessary for fertilisation.

1.3.2 Zygote and ookinete maturation

The male and female derived nuclei fuse shortly after fertilisation (Aikawa *et al.*, 1984) resulting in a diploid zygote which eventually matures into the tetraploid motile ookinete. The latter process is a result of meiosis which occurs in the absence of nuclear division or cytokinesis (Sinden & Hartley, 1985) and, it is associated with an increase of the genome value to that of tetraploid (Janse *et al.*, 1986). DNA replication

during this meiotic event is regulated by the female-specific expression of two NIMA (never in mitosis/Aspergillus) related kinases, *nek2* and *nek4* (Khan *et al.*, 2005; Reininger *et al.*, 2005). The initially spherical zygote gradually elongates by a growing apical protrusion and within the next 12-24 hours it transforms into the crescent-shaped motile ookinete. The *P. berghei* male mdv-1 gene appears to significantly contribute to zygote development, since upon gametocyte activation it has been found to mobilise to the leading edge of this very apical protrusion in the retort stage (Lal *et al.*, 2009a). Ookinete elongation is associated with the generation of an extensive network of subpellicular microtubules lining the inside of the ookinete, as well as the formation of their associated Microtubule Organising Centre (MTOC). In parallel, anterior secretory organelles known as micronemes are synthetised (Canning & Sinden, 1973). Ookinete maturation is accompanied by *de novo* protein synthesis, from transcripts that are translationally either repressed in the female gametocyte or newly produced in the ookinete (Hall *et al.*, 2005; Mair *et al.*, 2006). Ukegbu *et al.* have revealed that the zygote/early ookinete stage solely expresses maternal reporters which derives from either maternal mRNA inheritance or *de novo* transcription of the maternal allele. Their respective paternal alleles were shown to be silenced at this stage and re-expressed during ookinete midgut epithelium traversal. It is believed that this re-transcription and re-expression pattern is under epigenetic regulation (Ukegbu *et al.*, 2015). Together these events are necessary to facilitate the motility and invasive ability required for the ookinete to escape the hostile environment of the midgut blood bolus and traverse the mosquito midgut epithelium.

1.3.3 Ookinete motility and binding to midgut epithelial cells

Plasmodium ookinetes are polarised banana-shaped cells that share similarities with other stages of the *Plasmodium* lifecycle, as well as of other apicomplexa. They develop inside the mosquito midgut lumen from the round zygote, over a period of about 15–18 hours and via an intermediate stage called the retort. After the establishment of apical polarity in the zygote, microtubules, and the inner membrane complex (IMC) are slowly increasing in length to eventually form the crescent shaped ookinete. As an actomyosin motor, the IMC provides the force for *Plasmodium* motility and invasion. The IMC links to the apical complex including the MTOC centre, the collar, and the multiple micronemes. Micronemes represent the ookinete's specialised secretory organelles that are responsible for releasing both secreted and membrane-anchored proteins (Lal *et al.*, 2009b), while they have been shown to be also important

in both *Toxoplasma* and *Plasmodium* host cell invasion (Dubremetz *et al.*, 1998; Carruthers *et al.*, 2010; Dubois & Soldati-Favre, 2019). Specifically, they are released upon cell invasion and attract proteins known to be involved in apicomplexa cell invasion such as the CS and TRAP-Related Protein (CTRP) (Dessens *et al.*, 1999) and the secreted *Plasmodium* Perforin-like proteins (PPLP) (Kadota *et al.*, 2004).

Development to the motile ookinete allows the parasite to escape from the tightly packed and digestive environment of the blood bolus, by crossing the sturdy peritrophic matrix (PM) and then invading the gut epithelium. The success of each of these activities may depend on the degree of the biochemical and physical barriers in the mosquito and the ability of the ookinete to overcome these barriers. The main obstacles an ookinete needs to face include the density of the blood bolus, the PM thickness, the proteolytic activities taking place in the gut lumen and the mosquito immune responses triggered following its recognition. Additionally, ookinete motility and ability to secrete specific chitinases as well as to survive the active digestive enzymes of the blood bolus and recognition/invasion of the midgut epithelium all play crucial roles in the transformation into oocyst (reviewed in Whitten *et al*, 2006).

In apicomplexa, the molecular machineries required for motility and invasion are tightly linked. Its strict conservation is mirrored by the fact that all three zoite stages (merozoite, ookinete and sporozoite) of the parasite that engage in cell invasion are dependent on apical discharge of secretory vesicles to ensure successful motility and invasion (Baum *et al.*, 2006). This was further highlighted by the study of a TRAP protein family, members of which are found along the surface of all three invasive stages. Characteristically, targeted disruption of any of its members in the respective parasite developmental stage renders *Plasmodium* immotile and unable to invade the midgut epithelium in the case of the ookinete (CTRP-ookinete surface protein) (Dessens *et al.*, 1999; Yuda *et al.*, 1999), the salivary glands in the case of the sporozoite (TRAP) (Sultan *et al.*, 1997; Kappe *et al.*, 1999) or respectively the RBC for merozoites (MTRAP) (Baum *et al.*, 2006). Interestingly, a transmission-blocking small molecule (VS1) is found to disrupt ookinete invasion of the mosquito midgut through its interaction with the micronemal protein CTRP (Mathias *et al.*, 2013). Other genes identified to be critical for ookinete motility include the Calcium Dependent Protein Kinase-3 (CDPK3) (Ishinoe *et al.*, 2006; Sidén-Kiamos *et al.*, 2006), the cyclic GMP (GCbeta) (Hirai *et al.*, 2006; Moon *et al.*, 2009), the membrane skeletal proteins

IMC1b-h (Tremp *et al.*, 2008; Volkmann *et al.*, 2012) and the protein phosphatase with Kelch-like domains (PPKL) (Guttery *et al.*, 2012; Philip *et al.*, 2012).

The first barrier encountered by the invading ookinete is the chitin-rich PM, coating the apical side of the midgut epithelium, which ookinetes overcome by expressing chitinase-1 (CHIT1) (Dessens *et al.*, 2001). This process is fundamental before ookinetes entrance in the polarised columnar midgut epithelial cells (Zieler & Dvorak, 2000). After crossing the PM ookinetes must establish specific molecular interactions with the midgut epithelial cells, which will later facilitate their penetration. Evidence indicates that the initial interaction of the ookinetes with the midgut epithelium occurs through the classic route of receptor-ligand interaction (Zieler *et al.*, 1999; Ghosh *et al.*, 2001; Rodríguez *et al.*, 2007; Vega-Rodríguez *et al.*, 2014). The surface protein *Pvs*25 of *P. vivax* ookinetes was initially shown to interact with calreticulin, located on the midgut apical surface of the malaria vector *A. albimanus* (Rodríguez *et al.*, 2007). A phage display peptide library screen identified SM1 as a peptide that binds to the mosquito midgut epithelium and inhibits ookinete invasion (Ghosh *et al.*, 2001). SM1 was characterised as a mimotope of an ookinete surface enolase which presumably competes for binding to a putative midgut receptor (Ghosh & Jacobs-Lorena, 2011; Ghosh *et al*., 2011). The interaction of SM1 with the enolase-binding protein (EBP), a receptor located on the luminal side of the mosquito midgut epithelium, is suggested to mediate ookinete invasion (Ghosh & Jacobs-Lorena, 2011; Vega-Rodriguez *et al.*, 2014). The same authors suggest that *Plasmodium* ookinetes invade the mosquito midgut by at least two alternative pathways: one dependent on and the other independent of the EBP-SM1 interaction. Oligosaccharides (such as glycans and lectins) coating the microvilli of the apical side of the mosquito midgut epithelium are also essential for *P. falciparum*, *P. berghei* and *P. gallinaceum* ookinetes to successfully complete midgut invasion (Zieler *et al.*, 1999, 2000; Dinglasan *et al.*, 2003; 2007). Notably, inhibition of *A. gambiae* glycosaminoglycan chain synthesis reduces midgut chondroitin sulphate levels and leads to significantly reduced *P. falciparum* ookinete midgut invasion (Dinglasan *et al.*, 2007). Modification of midgut epithelial cell membranes lipid content has also been associated with impairment of midgut invasion (Zieler *et al.*, 2001; Moreira *et al.*, 2002).

A number of *Plasmodium* surface or secreted proteins are known to mediate the invasion process including members of the conserved *pplp* family. *P. berghei*

ookinetes express two genes of the *pplp* gene family: *pplp*3 and *pplp*5 (Kadota *et al.*, 2004; Kaiser *et al.*, 2004; Raibaud *et al.*, 2006; Ecker *et al.*, 2007). PPLP3 is located to the micronemes supporting the secretion of other conserved PPLPs during parasite cell invasion (Kadota *et al.*, 2004; Kaiser *et al.*, 2004). Ookinetes lacking expression of *pplp3* or pplp5 are able to attach to the midgut epithelium but are unable to enter the cytoplasm indicating that PPLP3 and PPLP5 are essential during membrane disruption and ookinete midgut invasion (Kadota *et al.*, 2004; Ecker *et al.*, 2007). *P. falciparum pplp4* was found to be expressed in female gametocytes and ookinetes while its knockout (KO) leads to accumulation of ookinetes in the mosquito midgut lumen. These findings suggest an essential role of the gene just before midgut invasion (Wirth *et al.*, 2015). In addition, the major ookinete surface proteins P25 and P28 seem to play a crucial role in both ookinete development and midgut invasion. Even though targeted disruption of either of the two genes leads to no significant phenotype - indicating their functionally redundant nature - ookinetes lacking both *P25* and *P28* display increased sensitivity to proteases in the mosquito midgut, significant defects in traversing the midgut epithelium and reduced ability to transform into oocysts (Tomas *et al.*, 2001). Of note, the P25/P28 proteins encode three or four epidermal growth factor (EGF) domains, probably facilitating receptor-ligand interactions (Tomas *et al.*, 2001). Furthermore, the WARP (Yuda *et al.*, 2001), the secreted ookinete adhesive protein (SOAP) (Dessens *et al.*, 2003), the putative secreted ookinete proteins PSOP2, PSOP7 and PSOP9 (Ecker *et al.*, 2008) have been also identified as key molecules during ookinete midgut invasion. Additionally, several mosquito surface proteins such as aminopeptidase 1 (APN1) (Dinglasan *et al.*, 2007), the annexin-like proteins (Kotsyfakis *et al.*, 2005), carboxypeptidase B (Lavazec *et al.*, 2007) and the croquemort scavenger receptor homolog (González-Lázaro *et al.*, 2009) have been shown to be involved in this process, but the molecular mechanisms underlying their specific interactions are still unknown.

1.3.4 Ookinete traversal through the mosquito midgut epithelium

During parasite traversal of the mosquito midgut epithelium, a series of complex interactions take place between the parasites and the mosquito midgut epithelium. Secretion of the subtilisin-like protease PSUB2 into the cytoplasm of the invaded cells and its localisation in close association with the actin aggregates was detected by fluorescence microscopy (Han *et al.*, 2000). PSUB2 facilitates parasite migration through the invaded cells by either direct proteolytic cleavage of the actin cytoskeleton

or activation of other factors involved in the actin polymerisation. The *Plasmodium* invasion of mosquito midgut screen candidate 2 (PIMMS2), a recently identified *P. berghei* protein with structural similarities to subtilisin-like proteins, is also an ookinete-specific protein found to be involved in parasite traversal of the mosquito midgut epithelium. Parasites lacking PIMMS2 fail to form oocysts, leading to malaria transmission blockade (Ukegbu *et al.*, 2017a). Navigation across the cytoplasm of the invaded midgut epithelial cells is mediated by a protein termed Cell-Traversal protein for Ookinetes and Sporozoites (CelTos). In *P. berghei*, Δ*celtos* ookinetes are motile and able to successfully disrupt the midgut epithelial barrier in order to enter the cell lumen (Kariu *et al.*, 2006). The P25/P28 proteins, located on the surface of female gametocytes, zygotes and ookinetes, also play an important role in ookinete survival during traversal through the mosquito midgut. As previously mentioned, concomitant KO of these genes lead to a significant reduction in the parasite ability to traverse the midgut epithelium and transform into oocysts (Tomas *et al.*, 2001).

As the *P. berghei* ookinete traverses the mosquito midgut epithelium, it invades multiple epithelial cells before it reaches the sub-epithelial space and transforms into the oocyst. As ookinetes move from the apical to the basal side of the midgut epithelium, they use a predominant intracellular route (Vlachou *et al.*, 2004) during which the ookinete glides on the cell membranes including those forming the basal labyrinth. During this journey, the ookinete uses three discrete types of motility: stationary rotation, translocational spiralling (rotational motility in conjunction with directional changes and translocation) and straight-segment motility (Vlachou *et al.*, 2004). Additionally, it has been shown that most ookinetes choose to traverse sequentially several neighbouring cells before finally reaching the basal lamina (Han *et al.*, 2000; Vlachou *et al.*, 2006b). Following ookinete invasion, the damaged invaded cells project towards the midgut lumen and suffer various characteristic changes including induction of nitric oxide synthase (NOS) expression, a substantial loss of microvilli, acquirement of an abnormal nuclear morphology preceding genomic DNA (gDNA) fragmentation and radical reorganisation of their actin cytoskeleton. All these changes lead to a subsequent death of the invaded cells through apoptosis (Han *et al.*, 2000; Zieler & Dvorak, 2000; Vlachou *et al.*, 2004). However, the epithelial damage inflicted is repaired by an actin purse-string-mediated restitution mechanism which allows the epithelium to expel the apoptotic cells without losing its integrity thus guaranteeing mosquito survival (Han *et al.*, 2000). A hood of lamellipodial origin,

provided by the neighbouring epithelial cells, cover the ookinete during its egress from the epithelium and constitutes an additional healing mechanism which facilitates the restoration of the epithelial barrier (Vlachou *et al.*, 2004). The same hood was also found to be associated with ookinetes killing through lysis. Silencing of WASP, a promoter of actin filament nucleation which is colocalised with the formed hood, results in increased oocyst numbers (Schlegelmilch & Vlachou, 2013).

1.3.5 Ookinete-to-oocyst transformation

The ookinete traverses and exits the mosquito midgut epithelial cell until it reaches the sub-epithelial space, where it encounters the basal lamina and transforms into the oocyst. It has been suggested that actual contact of the ookinete with structural elements of the basal lamina, consisting of laminin, collagen IV, entactin and perlecan, acts as a trigger for the ookinete to oocyst transformation (Weathersby, 1952). Data for the latter hypothesis come from studies confirming the formation of oocysts on the basal lamina of the Malpighian tubules and the fat body when ookinetes are injected directly in the haemocoel (Weathersby, 1954). Laminin may indeed play a crucial role in oocyst formation considering that P25 and P28 (Arrighi & Hurd, 2002; Vlachou *et al.*, 2001), SOAP (Dessens *et al.*, 2003) and CTRP (Mahairaki *et al.*, 2005) have been shown to bear mosquito laminin binding capacity, while their silencing results in oocysts reduction (Arrighi, 2005). DNA replication, chromosome segregation and nuclear division occur in the motile ookinete upon reaching the basal lamina of the midgut epithelium, where it rounds up and transforms into the sessile oocyst. Adequate environmental concentration of bicarbonate and other nutrients such as amino acids and sugars, also act as a trigger to ensure completion of the oocyst development (Carter *et al.*, 2007). However, the exact role of the interaction between the basal-lamina and the ookinete is still to be elucidated. Some believe that whilst important, it is not essential; in the absence of any basal lamina components, Carter *et al.* have reported successful *in vitro* oocyst formation (Carter *et al.*, 2007).

Morphologically, the ookinete loses its characteristic subpellicular microtubules, apical complex and pellicle upon transformation to oocyst (Canning & Sinden, 1973). A female gametocyte and ookinete specific protein, PPKL, is shown to have an essential function during ookinete differentiation in affecting the apical end integrity, collar and pellicle morphology and microtubule linkage to the IMC, all crucial for the ookinete shape differentiation and its development into an oocyst. Deleting this gene produces

ookinetes whose shape is abnormal, resulting in non-motile parasites that are unable to penetrate the mosquito gut wall (Guttery *et al.*, 2012). An intermediate form, the transforming ookinete (took), has been described during the ookinete-to-oocyst transformation where a hump is formed at the convex outer side of the crescent-shaped ookinete and the protrusions (former apical and posterior tips) are gradually absorbed, to round up to the sessile oocyst. In parallel, the ookinete double-membrane pellicle is sequentially replaced by the single-membrane plasmalemma of the oocyst (Carter *et al.*, 2007) which is surrounded by a proteinaceous capsule (Sinden & Strong, 1978; Vanderberg & Rhodin, 1967), later ensuring the oocyst survival and maturation.

During their journey towards oocyst formation, some ookinetes once outside the midgut epithelial cells, are detected and labelled by mosquito immune factors and subsequently targeted for instant destruction by a variety of innate immune responses (Blandin *et al.*, 2002; Osta *et al.*, 2004b; Vlachou *et al.*, 2006; Sinden *et al.*, 2007). These events are responsible for a dramatic parasite population bottleneck as major parasite losses are observed during this stage, in some cases leading to refractoriness to the parasite and hence transmission abolishment. These interaction features largely determine the success of the infection and the competence of the mosquito as an intermediate vector (reviewed in Whitten *et al.*, 2006).

1.3.6 Parasite sporogonic development and transmission to the vertebrate host

Despite its sessile nature, oocyst development is dynamic and with clear morphological differences between early and mature oocysts. With time, the developing oocyst becomes encased in a proteinaceous capsule, which surrounds its plasmalemma (Sinden & Strong, 1978; Vanderberg & Rhodin, 1967). As development progresses, the oocyst nucleus starts to enlarge and becomes digitated as it undergoes multiple rounds of endomitosis (Sinden & Strong, 1978). It is from this large polyploid nucleus that the haploid sporozoite nuclei originate. In parallel to genome replication, the plasmalemma invaginates so to form vacuolated structures known as sporoblasts. At the onset of sporozoite formation, nuclear divisions occur simultaneous to sporozoites budding off from the sporoblasts resulting in the mature oocyst which contains thousands of haploid sporozoites ready to be released in the mosquito haemolymph (**Figure 1.2**) (Sinden & Strong, 1978; Vanderberg & Rhodin, 1967).

Despite the comprehensive understanding of *Plasmodium* sporogonic development at an ultrastructural level, the molecular machinery that underpins this process is largely

unknown. Few proteins have been identified so far, with a distinctive role in the sporulation process. The best characterised proteins known to be essential for sporozoite formation is the circumsporozoite surface protein (CSP), which is found to be conserved across plasmodia. In the maturing oocyst, CSP is distributed to the plasmalemma, which lines the inner capsule surface. As sporogony proceeds, CSP is mobilised into the developing sporoblasts and subsequently localises to the outer surface of the sporoblast plasma membrane. It remains associated with the surface of the budding sporozoites and becomes the main surface protein of haemocoel and salivary gland sporozoites, distributed uniformly over the sporozoite surface (Nagasawa *et al.*, 1987). Its KO leads to disruption of the cytokinetic events occurring in the developing oocyst and abolishment of sporozoite formation (Ménard *et al.*, 1997). A membrane skeleton component, the inner membrane complex protein (IMC1α), is also involved in *P. berghei* sporozoite development. Specifically, its targeted disruption generates sporozoites of abnormal shape, which further display reduced motility and infectivity (Khater *et al.*, 2004).

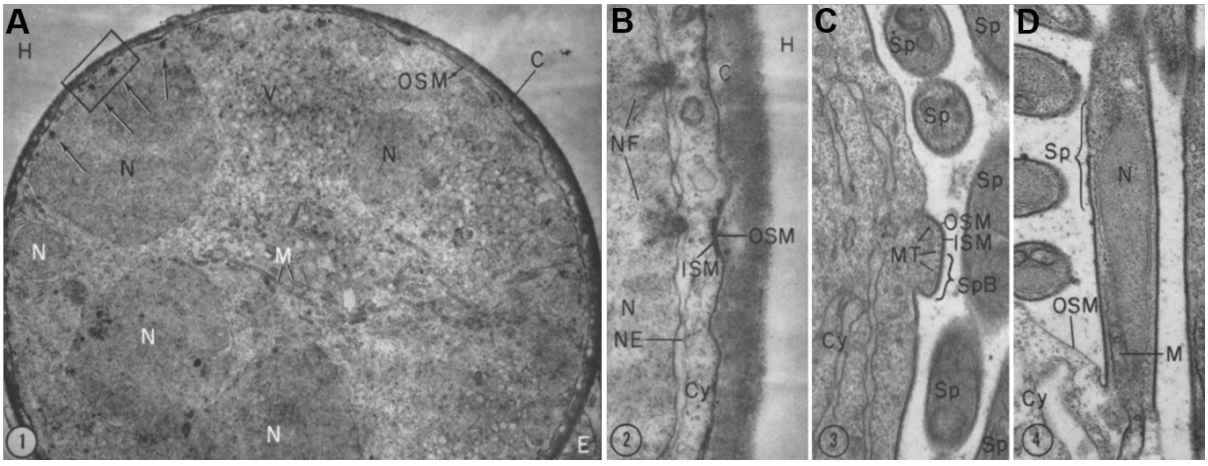

Figure 1.2 Electron microscopy images showing *P. berghei* oocyst development in *Anopheles quadrimaculatus.* (A) Micrograph of a developing oocyst attached to the midgut epithelium and while projecting into the mosquito haemolymph (H). The oocyst is covered by a thick capsule (C) where, underneath, the outer sporoblastoid membrane (OSM) surrounds the sporoblastoid body. The cytoplasm of the sporoblastoid body contains mitochondria (M), circular vesicles (V) and a nucleus (N). Since the oocyst is mature, the nucleus has moved close to the periphery and has become flattened on one side. The flattened side of this nucleus shows condensed nuclear material (arrows) which in **(B)** are seen to consist of nuclear fibers (NF). Additionally, some portions of the new membrane, the inner sporoblastoid membrane

(ISM), have formed just under the outer sporoblastoid membrane. Seen in high magnification are the nucleus, nuclear envelope (NE), cytoplasm of the sporoblastoid body (Cy), oocyst capsule and mosquito haemolymph. **(C)** A sporozoite bud (SpB) and a row of microtubules (MT) have formed as the result of the OSM and ISM membranes evagination. Sporozoites (Sp) which have already budded off from the sporoblastoid body are also visible. **(D)** Further elongation of the sporozoite bud produces a sporozoite (Sp). Figure adapted from (Vanderberg & Rhodin, 1967).

Oocyst development requires the parasite to persist for a minimum of 10-14 days in the hostile, rich in immune factors environment of the mosquito haemocoel. To do so, oocysts are protected by a capsule or cyst wall. The *P. berghei* Cap380 (Srinivasan *et al.*, 2008) and Cap93 (Sasaki *et al.*, 2017) proteins have been identified to be abundantly expressed within the oocyst capsule. Deletion of *Cap380* in *P. berghei* results in sporozoite differentiation interruption (Srinivasan *et al.*, 2008). *P. falciparum* Cap380 is also abundantly found on the oocyst capsule surface (Itsara *et al.*, 2018) but its function still remains elusive. The recently identified *P. berghei* Cap93 protein, secreted from the sporoblasts within the lining of the oocyst capsule and localised to the interior membrane of the capsule, seems to also play a role in sporoblast and sporozoite development. In its absence, the oocyst capsule appears to have low electron density (Sasaki *et al.*, 2017). Additionally, the mosquito-derived laminin is found on the outer surface and within the capsule structure (Nacer *et al.*, 2008). It has been proposed that while the ookinete becomes coated in laminin during its passage through the midgut epithelium and during its transformation into the oocyst, it continuously incorporates laminin into its capsule which possible masks the oocyst from mosquito immune responses (Arrighi, 2005; Nacer *et al.*, 2008). The mosquito proteins matrix metalloprotease 1 (MMP1) and lysozyme c-1 (LYSC1) are also incorporated into the oocyst capsule (Srinivasan *et al.*, 2008; Goulielmaki *et al.*, 2014).

Female gamete specific inherited members of the *P. berghei* limulus clotting factor C, Coch-5b2 and LgII (LCCL) / lectin adhesive-like protein (*Pb*LAP) family and *Pb*LAP1-6 (Claudianos *et al.*, 2002; Trueman *et al.*, 2006; Raine *et al.*, 2007) have also been found to play a role in sporozoite development. Intriguingly, their targeted disruption

leads to defective sporulation even though their protein expression appears to peak during gametocyte stages (Claudianos *et al*., 2002; Pradel et al., 2004; Trueman *et al*., 2006; Raine *et al*., 2007; Ecker *et al*., 2008; Scholz *et al*., 2008). Similarly, absence of the *asp* and *sop13*, two ookinete specific genes, leads to oocysts that largely fail to sporulate and thus display a degenerative morphology (Ecker *et al.*, 2008).

In order for the sporozoites to migrate to the mosquito salivary glands, they must be released into the haemocoel. Sporozoite excystment is an active process (Sinden, 1974) but the motility requirements have not been formally shown. Several proteins including egress cysteine protease 1 (ECP1) and a positively charged region of CSP, seem to function in sporozoite egress indicating an active participation by the sporozoites (Aly & Matuschewski, 2005; Wang *et al.*, 2005). It has been also shown that the interaction between two proteins, the oocyst rupture proteins 1 (ORP1) and 2 (ORP2) leads to destabilisation of the capsule structure needed for sporozoite escape (Currà *et al.*, 2016; Sidén-Kiamos *et al.*, 2018). The thrombospondin-repeat containing sporozoite-specific protein named thrombospondin-related protein 1 (TRP1) seems to also be important for oocyst egress and salivary gland invasion (Klug & Frischknecht, 2017). Following their egress, sporozoites need to actively migrate through the haemocoel in order to enter the salivary glands. In the haemocoel, sporozoites are passively transported by the movement of the mosquito haemolymph and although they are carried throughout the mosquito open circulatory system, they appear to preferentially recognise and invade the salivary glands (Douglas *et al.*, 2015).

The last stage of the parasite lifecycle in its mosquito vector consists of the translocation of the haemolymph sporozoites into the salivary gland lumen, a process that largely depends on the parasite and mosquito vector combination. One can compare the sporozoite invasion of the salivary gland epithelium to the ookinete midgut wall penetration; several characteristics including sporozoite motility and its invasive ability, suggest the existence of a conserved underlying mechanism shared by the invasive stages of *Plasmodium*. Additionally, similar to ookinetes midgut invasion, sporozoites salivary gland invasion also poses a natural bottleneck in parasite development since sporozoites that fail to invade the salivary glands epithelial cells are rapidly eliminated by the mosquito immune responses (Hillyer *et al.*, 2007). However, unlike ookinetes, sporozoites are not harmful to the cells they enter since no apoptosis of the invaded epithelial cells has been observed (Pimenta *et al.*, 1994).

Sporozoite motility is governed by multiple genes including *csp* (Tewari *et al.*, 2002), *trap* (Sultan *et al.*, 1997; Kappe *et al.*, 1999; Munter *et al.*, 2009), *g2* (López *et al.*, 2003; Tremp *et al.*, 2013) and the alveolin *IMC1a* (Khater *et al.*, 2004). Similar to ookinete midgut epithelium invasion, sporozoite invasion of the salivary glands is thought to be mediated by specific ligand-receptor interactions that might as well be shared (Ghosh *et al.*, 2009). For example, the *A. gambiae* salivary protein saglin has been identified to inhibit the invasive ability of sporozoites (Okulate *et al.*, 2007) in addition to the sporozoite protein, MAEBL, member of the erythrocyte binding ligand (EBL) family, which was also found to be required at this stage (Saenz *et al.*, 2008).

The passive transfer of the infective sporozoites from the mosquito salivary gland lumen, during a bloodmeal, to its next host completes the *Plasmodium* transmission cycle. Nevertheless, the sporozoites need to undergo significant developmental changes in order to achieve invasion of the vertebrate cells, in this case hepatocytes. This process is reflected in the differential gene regulation as well as protein expression between oocyst and salivary gland sporozoites (Matuschewski *et al.*, 2002; Lasonder *et al.*, 2008; Mikolajczak *et al.*, 2008).

1.3.7 The *Plasmodium* bottleneck

The parasite population undergoes dramatic losses during development in the *Anopheles* vector, and this is known as the *Plasmodium* bottleneck hypothesis. During the last decade, studies on the development of two model malaria parasites (*P. berghei;* rodent parasite and *P. gallinaceum;* avian parasite) in three mosquito species (*A. gambiae, A. stephensi* and *Ae. aegypti)* identified three developmental bottlenecks (Sinden *et al.*, 2007). *Plasmodium* population dynamics studies revealed that the parasite losses in the mosquito are density dependent and they can be most markedly observed during the gametocyte-to-ookinete developmental stage and at the ookinete-to-oocyst and oocyst sporozoites-to-salivary gland sporozoites transition stages (Sinden *et al.*, 2007). The greatest population bottleneck occurs during the ookinete-to-oocyst transition which coincides with the ookinete traversal of the mosquito midgut epithelium (Blandin *et al.*, 2004; Osta *et al.*, 2004b; Vlachou *et al.*, 2006) (**Figure 1.3**). Due to the lowest observed abundance of *Plasmodium* parasites during midgut stages, they constitute prime targets for malaria transmission blocking interventions.

There is evidence that the mosquito can sense the presence of malaria parasites shortly after the bloodmeal ingestion, but it appears that the primary midgut immune

responses are triggered only in response to ookinete invasion (Vlachou *et al.*, 2005). Transcriptional analysis of *A. gambiae* midgut responses occurring during ookinete traversal of the midgut epithelium has revealed several mosquito genes related to innate immunity responses and, intracellular and local epithelial responses that either promote or antagonise the parasite development in the mosquito. Actin-cytoskeleton and microtubule-cytoskeleton remodelling is a major response of the mosquito midgut epithelium to ookinete penetration, whereas other responses encompass components of innate immunity, extracellular-matrix remodelling and apoptosis. Combined transcriptional and reverse-genetic analysis further identified effector molecules of mosquito immunity responsible for parasite survival (Vlachou *et al.*, 2005).

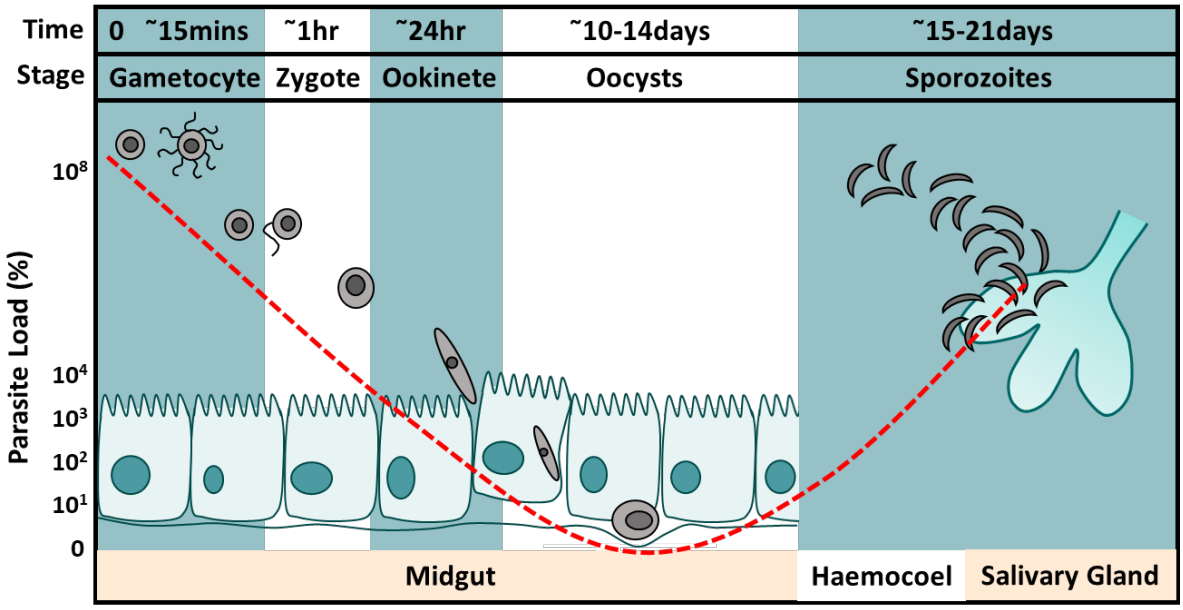

Figure 1.3. *P. berghei* population dynamics during its development in *A. gambiae*. The greatest parasite losses occur during the gametocyte-to-ookinete, ookinete-to-oocyst and oocyst sporozoite-to-salivary gland sporozoite transition stages. The lowest population density takes place at the midgut oocyst stage, whereas a rapid expansion in the parasite numbers can be observed when thousands of sporozoites are released from each oocyst on their way to the salivary glands. In laboratory conditions, of approximately 1000 ookinetes, the average number that survive through this stage and develop into oocysts is about 20 (red dashed line).

It has been estimated that over 80% of the formed ookinetes cannot make it through the oocyst stage. This has been shown to be partly associated with the human complement activity which remains active in the mosquito midgut (Lensen *et al.*, 1997), the transmission blocking antibodies and cytokines ingested during the mosquito

bloodmeal from individuals in endemic areas that have been repeatedly exposed to the malaria parasites (Sinden, 2010; Sutherland, 2009), the mosquito intestinal microbial flora which is able to modulate vectorial capacity of *Anopheles* through the innate immune system (Dong *et al.*, 2009; Meister *et al.*, 2009) and most effectively, with the mosquito innate immune responses occurring after ookinetes exit the midgut epithelial cells (Blandin *et al.*, 2004; Osta *et al.*, 2004b; Vlachou *et al.*, 2006).

1.4 The Mosquito Immune System

1.4.1 Overview of *A. gambiae* innate immune defence mechanisms

There are two main compartments in the mosquito: the nominally sterile haemocoel which houses the fat body, the main metabolic and the major immune organ of the insect, and the gut which is open to the environment, receives and digests blood and sugar meals, and houses the microbiota. Immunosurveillance blood cells, known as haemocytes, circulate within the haemocoel. Both compartments are vulnerable to infection; the former either via cuticular damage or pathogen penetration through the gut epithelium, and the latter via microbe ingestion. However, as in all metazoans, mosquitoes are equipped to fight off invading microbes by using an array of defence mechanisms collectively referred as the immune system. The evolutionary ancestral innate immune system, which insects have exclusively developed, is the organism inherited primary line of defence and as such, it depends on a given number of humoral and cellular system immune molecules that already exist in the organism.

The innate immune system recognises non-self from self through the binding of Pathogen Associated Molecular Patterns (PAMPs) to a limited number of receptors called Pattern Recognition Receptors (PRRs), resulting in an intracellular or extracellular signalling cascade. These PRRs are specialised in recognising invariant molecules that are either on the surface of or are shed by microorganisms (Janeway & Medzhitov, 2002). The family of PRRs in the *Anopheles* species includes thioester containing proteins (TEPs), Gram-negative binding proteins (GNBPs), fibrinogen-related proteins (FREPs), peptidoglycan recognition proteins (PGRPs) and immunoglobulin superfamily proteins (reviewed in Clayton *et al.*, 2014; Smith *et al.*, 2014; Povelones *et al.*, 2016). Also, within the class of PRRs in *A. gambiae* are the splice variants of the *A. gambiae* Down syndrome cell adhesion molecule gene (*AgDscam*), which has been shown to protect mosquitoes against challenge with either *P. berghei* or *P. falciparum* (Dong *et al.*, 2006; 2012). On the other hand,

microbial PAMPs include molecules such as peptidoglycans (PGN) and b-1,3-glucans, as well as Glycosyl Phosphatidyl Inositol (GPI) anchors (Teixeira *et al.*, 2002).

The main intracellular signalling cascades involved in the mosquito innate immune defences are the Toll, Imd (Immune deficiency) and JAK/STAT (Janus kinase/signal transducers and activators of transcription pathways). These pathways result in transcriptional responses that directly or indirectly lead to pathogen killing via the production of AMPs, nitric oxide (NO) or reactive oxygen species (ROS), or in the activation of the host tolerance mechanisms. The extracellular signalling cascades, by contrast, result in the killing of the pathogen at the place that it previously triggered the respective pathway. In all cases, the outcome for the pathogen is one of three methods of killing: lysis, melanisation or phagocytosis (**Figure 1.4**).

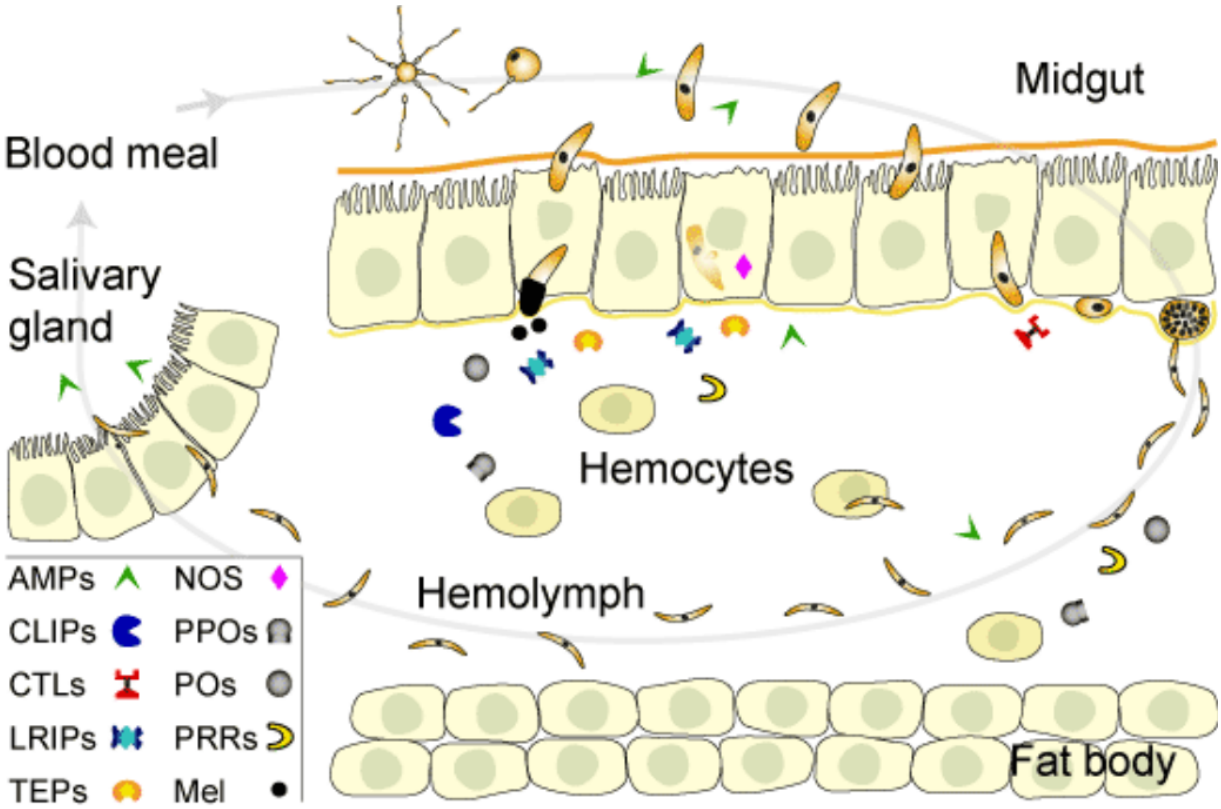

Figure 1.4. Interactions of the *Plasmodium* parasite with the *A. gambiae* innate immune system during its development in the mosquito. Schematic diagram of the *Plasmodium* mosquito stages, also highlighting the multiple sites of parasite killing by components of the mosquito innate immune system. All those components result from transcriptional responses of the Toll, Imd and JAK/STAT immune pathways. The intracellular signalling cascades of the mosquito immune responses against *Plasmodium* infection, occur in both compartments: midgut and haemocoel, the latter

also including the fat body. Figure was adapted from (Osta *et al.*, 2004b) and permission for its republishing can be found in **Appendix 2**.

Circulating haemocytes are important contributors to the haemolymph immune responses (Lavine & Strand, 2002). They are thought to participate in pathogen recognition, mediate fat body production of AMPs, mediate and coordinate the mosquito systemic immune responses including phagocytosis and encapsulation and, are responsible for the production and subsequent secretion of soluble humoral factors such as complement-like proteins and components of proteolytic cascades that control melanisation (Lavine & Strand, 2002; Bartholomay *et al.*, 2007; Strand, 2008b). The Toll, the JAK/STAT and the Jun-N-terminal kinase (JNK) cascades are essential for haemocyte differentiation, with the Toll pathway is essential for the subsequent activation of the complement-like immune responses following *Plasmodium* or other microbial infections (Ramirez *et al.*, 2014). Haemocyte differentiation is also essential for the release of the Haemocyte Differentiation Factor (HDF), found to be directly involved in the expansion of the granulocyte population of challenged *A. gambiae* mosquitoes and eventually to the induction of enhanced innate immune responses against *Plasmodium* infections (Ramirez *et al.*, 2014).

1.4.2 Anti-*Plasmodium* immunity pathways

Microarray analyses identified several mosquito-derived molecules that exhibit both anti-plasmodial and anti-bacterial activity (Dong *et al.*, 2006). This suggests that after an infectious bloodmeal, the mosquitoes use besides the direct anti-plasmodial immune responses, also the anti-bacterial immune responses that are initiated through increased multiplication of bacteria after the bloodmeal, to fight against *Plasmodium* infection. This therefore makes the bacterial midgut flora an important regulator of the permissiveness of *Anopheles* to *Plasmodium* parasites (Dong *et al.*, 2006; 2009).

The major signalling pathways shown to directly contribute to *Anopheles* anti-*Plasmodium* defence mechanisms are the Toll, Imd, JAK/STAT and JNK pathways (Meister *et al.*, 2005; Dong *et al.*, 2009; Meister *et al.*, 2009; Cirimotich *et al.*, 2010). Considerable insight into these innate immune pathways has been gathered from studies previously conducted in *Drosophila* i.e. the Imd and Toll pathways were identified upon the sequencing of the *A. gambiae* genome (Holt *et al.*, 2002) by comparison to their homologous pathways in *Drosophila melanogaster.* Both these pathways seem to mediate antiplasmodial immune responses that target the ookinete

stage of the parasite (Garver *et al.*, 2006; Frolet *et al.*, 2006; Garver *et al.*, 2012), while the JAK/STAT pathway limits parasites at the oocyst stage, called the late phase of immunity (Gupta *et al.*, 2009). It is suggested that all these pathways are eliminating *Plasmodium* parasites by triggering complex killing cascades on their surface.

After a bloodmeal, midgut bacterial levels and hence the bacterial elicitors of the immune system, increase dramatically. These responses lead to activation of the NF-κB signalling pathways, Toll and Imd (Dong *et al.*, 2009; Meister *et al.*, 2009). Recognition of PAMPs from different classes of microbial pathogens followed by the subsequent translocation of the NF-κB transcription factor REL2 into the cell nucleus, ultimately leads to the transcriptional activation of immune effector genes such as AMPs (defensins, cecropins, attacin and gambicin which are known to act against Gram-negative bacteria, Gram-positive bacteria, yeast, fungi, and *Plasmodium*), complement-like proteins and components of the melanisation cascades. These resulting immune responses are largely responsible for the parasite losses observed in the midgut lumen and, despite the fact that direct parasite recognition by the Imd and Toll pathways are shown (Garver *et al.*, 2012), the mechanisms involved in this recognition are yet unknown. *Rel1* and *Rel2* are known to be negatively regulated by Cactus and Caspar, respectively (Clayton *et al.*, 2014; Belachew *et al.*, 2018).

Little is known about the role of JAK/STAT in mosquitoes, however, in *Drosophila,* this pathway is involved in a variety of developmental processes such as stem cell maintenance, eye development and the expression of pair-rule genes involved in embryonic segmentation (reviewed in Arbouzova & Zeidler, 2006). It has been shown that this pathway is initiated by the binding of the cytokine ligand Unpaired (UPD) to the transmembrane receptor DOME, which then leads to the nuclear translocation of STAT and the transcriptional activation of multiple immune effector genes (Agaisse & Perrimon, 2004). In *A. gambiae*, the JAK/STAT pathway has been shown to be implicated in the antibacterial, antiviral and antiplasmodial defence mechanisms (Barillas-Mury *et al.*, 1999; Gupta *et al.*, 2009). There are two *STAT* genes in *A. gambiae* (*STAT1*/*AgSTAT-B* and *STAT2*/*AgSTAT-A*) (Christophides *et al.*, 2004; Meister *et al.*, 2004) which have been shown to mediate the transcriptional activation of NOS (Gupta *et al.*, 2009). As previously mentioned, NOS can be induced in response to *Plasmodium* infection and leads to high levels of reactive NO, thereby diminishing parasite development. Silencing of the STAT genes increases mature

oocyst development in *P. berghei* and *P. falciparum* infected mosquitoes, further suggesting that the JAK/STAT pathway also mediates the late phase of immunity against the oocyst stage of the parasite (Gupta *et al.*, 2009). Furthermore, work from Bahia *et al.* showed implementation of the JAK/STAT pathway in the early stages of *A. aquasalis* infection with *P. vivax* (Bahia *et al.*, 2011).

When ookinetes invade the midgut epithelium, activation of the JNK pathway triggers a nitration reaction with two important outcomes: apoptosis of the invaded cells and marking of ookinetes for destruction by the mosquito complement-like system. Specifically, JNK signalling is required for mosquito midgut cells to induce expression of two enzymes, the haeme peroxidase 2 (HPX2) and the NADPH oxidase 5 (NOX5), known to be involved in the epithelial nitration in response to parasite invasion (Oliveira *et al.*, 2012). These reactions modify the parasite surface and activate the mosquito complement system, finally leading to parasite lysis. Thus, silencing of the JNK signalling enhances *Plasmodium* infection (Jaramillo *et al.*, 2010; Garver *et al.*, 2013). Same work showed that JNK signalling is important for the regulation of *TEP1* and *FBN9* basal levels of expression; two components of the complement system that are produced by haemocytes and secreted into the haemocoel (Garver *et al.*, 2013).

While the Toll, Imd and JAK/STAT are the best characterised pathways, so far, other pathways have also been shown to play key roles in antiplasmodial immunity such as the insulin/insulin growth factor-1 signalling (IIS) pathway. It has been shown that the activation of the IIS pathway increases *A. stephensi* susceptibility to *P. falciparum* infections, and may even alter a form of NF-κB dependent immunity (Luckhart & Riehle, 2007; Drexler *et al.*, 2012; Pakpour *et al.*, 2012).

1.4.3 Anti-*Plasmodium* defence mechanisms

The past years have witnessed great progress in understanding both the mosquito innate immune responses and the variety of putative immune effectors implicated in the defence mechanisms triggered against *Plasmodium* infection. The responses taking place in the epithelial cells and haemocoel, especially those of the complement-like system, as well as immune reactions that occur earlier in the mosquito midgut lumen seem to be the major players of such defences (Blandin *et al.*, 2004; Fraiture *et al.*, 2009; Povelones *et al.*, 2009; Habtewold *et al.*, 2017).

1.4.3.1 The “Time Bomb” Theory

Midgut invasion by the *Plasmodium* ookinete does not leave the mosquito unharmed. Actually, the invading ookinetes inflict irreversible damage on the mosquito midgut epithelial cells including NOS expression upregulation, microvilli reduction, increased DNA fragmentation and possession of abnormally shaped nuclei and a remodelled actin cytoskeleton. This damage is extensive and irreversible resulting in cell apoptosis and subsequent expulsion of the degenerated cell (Han *et al.*, 2000; Zieler & Dvorak, 2000; Vlachou *et al.*, 2004). In addition to causing cellular damage and eliciting molecular responses, the ookinetes also shed the P28 surface protein and *Pb*SUB2 protease (Han *et al.*, 2000; Danielli *et al.*, 2005) which possibly help in their motility as they glide across the epithelium. The defence response of elevated NOS expression (and consequent NO generation) and the initiation of the cell apoptosis and protrusion create an altogether hostile environment for the traversing ookinete. According to the “Time Bomb” theory (**Figure 1.5**), a model firstly described for the cellular and molecular responses of the *Anopheles* midgut epithelium in response to *P. berghei* ookinete invasion (Han *et al.*, 2000; Han & Barillas-Mury, 2002), there is a very delicate relationship between the speed at which the parasite crosses the epithelial cell, the toxic nitrate environment of the midgut epithelial cell and how long the cell can sustain these changes and possibly other possible defence responses as it undergoes cell death, which is critical for determining the invasion outcome.

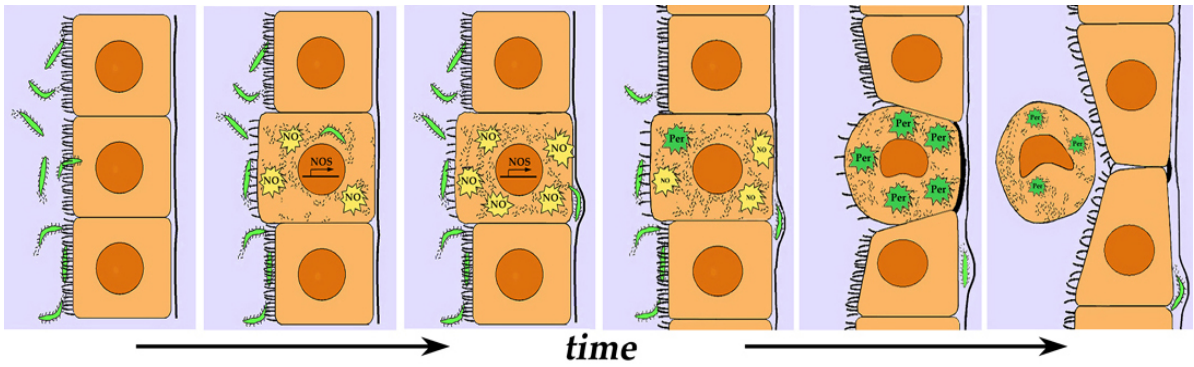

Figure 1.5. Time Bomb Model of *Plasmodium* ookinete midgut invasion. *Plasmodium* invasion triggers the induction of NOS and an inducible midgut peroxidase (Kumar *et al.*, 2004) thus creating a highly nitrated environment within the invaded cells. Subsequently, these damaged cells undergo apoptosis and budding-off into the mosquito midgut lumen. The surrounding area undergoes multiple cellular responses to seal the invaded area including neighbouring cells becoming elongated

and extending lamellipodia towards the protruding cell. Due to the hostile environment, ookinetes move fast between cells in order to reach the basal lamina and differentiate into oocysts. Figure was adapted from, (Han *et al*., 2000) and permission for its republishing can be found in **Appendix 3**.

While the majority of studies have been conducted in *A. stephensi*, NOS expression is also known to be elevated in *A. gambiae* after *P. berghei* infection (Dimopoulos *et al.*, 1998; Luckhart *et al.*, 2002). Biochemical studies in *A. gambiae* revealed nitration in *Plasmodium*-invaded midgut cells to occur as a two-step process in which the induction of NOS expression is followed by peroxidase activity (Kumar *et al.*, 2004; Kumar & Barillas-Mury, 2005). A more recent work identified HPX2 and NOX5 as mediators of nitration in the *A. gambiae* midgut epithelium and demonstrated that epithelial nitration and TEP1-mediated lysis work sequentially to target *Plasmodium* ookinetes (Oliveira *et al.*, 2012). Additionally, the authors propose that nitration of ookinetes in the midgut promotes the subsequent activation of the mosquito complement system, suggesting a potential link between the humoral and cellular antiplasmodial immune responses taking place in *A. gambiae*.

Actin-based cytoplasmic protrusions originated from the *A. gambiae* basal part of the invaded epithelial cells were shown to surround the ookinetes right after their traversal, and in this way contribute to their death via an unknown yet mechanism (Vlachou *et al.*, 2005). KO of *wasp*, a gene regulator of the actin cytoskeleton reorganisation, showed an increase on the number of *P. berghei* oocysts formed in the midguts of *A. gambiae* mosquitoes (Schlegelmilch & Vlachou, 2013) suggesting that the observed actin-rich cytoplasmic protrusions might also constitute a form of cellular defence mechanism against parasite invasion. Indeed, the antagonistic effect of WASP against parasites is linked to a significant reduction of the actin–based cytoplasmic protrusions as observed in midgut microscopic sections (Schlegelmilch & Vlachou, 2013).

A wound-healing response mechanism to dead or dying ookinetes has been argued to be in conflict with the “Time Bomb” theory (Shiao *et al.*, 2006). In this study, the authors claim that while the majority of *P. berghei* ookinetes are killed in the extracellular space in the *A. gambiae* mosquitoes, dead or dying ookinetes are surrounded by a polymerised actin zone formed at the basal layer of the adjacent midgut epithelial cells. Thus, the critical point whether a parasite will survive takes place after it traverses the midgut wall, at the haemolymph-bathed epithelial space.

1.4.3.2 The mosquito complement system

It has been previously shown that following ookinete invasion of the mosquito midgut epithelium and subsequent activation of the JNK pathway (Oliveira *et al.*, 2012; Garver *et al.*, 2013), nitration responses are induced within the midgut epithelial cells which are then responsible for prompting complement-like related reactions (Garver *et al.*, 2013). The latter is the most critical of all immune responses since it is responsible for the greatest population bottleneck that *Plasmodium* parasites and other bacterial and fungal pathogens undergo (Blandin *et al.*, 2004; Fraiture *et al.*, 2008; Povelones *et al.*, 2009; Povelones *et al.*, 2011), as well as the central focus of this project.

The mosquito complement-like system is a network of haemolymph-circulating proteins of which the thioester-containing protein 1 (TEP1) was found to be the key player. TEP1 is a structural and functional homologue of the human complement factor 3 (C3) and it has been shown to play a major role in the elimination of the parasite by either lysis and/or melanisation (Levashina *et al.*, 2001) (**Figure 1.6**). TEP1 function is promoted after its direct binding on the ookinete surface, provided that the latter have successfully egressed through the mosquito midgut epithelium (Blandin *et al.*, 2004). Briefly, its binding initiates the assembly of an innate immune complex which based on the exact molecular composition instantly promotes parasite death (Blandin *et al.*, 2004; Fraiture *et al.*, 2009; Povelones *et al.*, 2009; Povelones *et al.*, 2011). This binding, similar to C3, is mediated through its highly polymorphic thioester motif (Fraiture *et al.*, 2009). TEP1-positive ookinetes are either dead or in the killing process, as evidenced by their irregular morphology, loss of nuclear stain and the presence of bubble-like projections from their surface. Actin-mediated cellular responses of the ookinete-invaded cells also assist during TEP1-mediated killing (Schlegelmilch & Vlachou, 2013; Shiao *et al.*, 2006), however, the exact order of the events and the underlying mechanism triggering TEP1 localisation on the invading ookinetes is not yet clear. TEP1 is upregulated 24 hours after ingestion of either *P. berghei* or *P. falciparum* infected blood, due to the upregulation of the mucosal immunity in the midgut lumen including the Imd and JNK signalling pathways (Dong *et al.*, 2006; Garver *et al.*, 2009; Garver *et al.*, 2013) as well as from the haemozoin presented in the ingested blood (Khan *et al.*, 2016). Importantly, mosquitoes are capable of triggering TEP1-upregulation by just sensing infected blood constituents in the absence of invading ookinetes (Dong *et al.*, 2006). Additionally, TEP1-upregulation is

highly associated with the microbiota amplification following mosquito blood feed (Dong *et al.*, 2006, 2011; Blandin *et al.*, 2008; Garver *et al.*,2009; Garver *et al.*, 2012).

TEP1 can be found in the haemolymph in two forms: the inactivated full-length soluble precursor ($TEP1_F$) and the activated proteolytically cleaved protein ($TEP1_{CUT}$) (Le, Williams *et al.*, 2012). Given that the protease cleavage site is likely to adopt several extended conformations, it is hypothesised that it might be targeted by diverse proteases (Baxter *et al.*, 2007). The identity of the protease(s) that perform this cleavage though is not yet known. Candidate proteases belonging to the family of CLIP-domain serine proteases have been silenced individually without affecting the amount of $TEP1_{CUT}$ formation. This suggests that either CLIPs function redundantly for TEP1 processing or another class of proteases performs this function. However, a protease capable of processing $TEP1_F$ exists in the haemolymph as injection of $TEP1_F$ into mosquitoes led to the rapid appearance of $TEP1_{CUT}$ (Fraiture *et al.*, 2009).

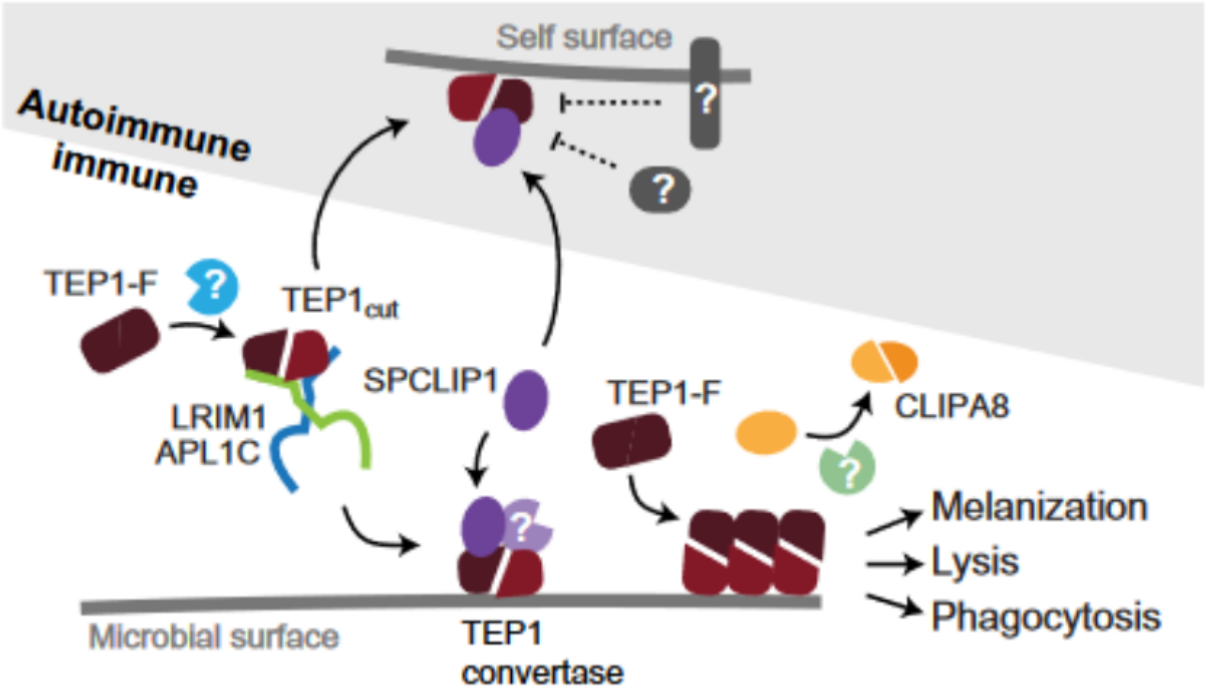

Figure 1.6 Schematic model of *A. gambiae* complement-like pathway. Schematic model of *A. gambiae* complement pathway. Black arrows indicate known interactions or proteolytic reactions. Hypothesised components or interactions are indicated with a question mark or dashed line, respectively. Activating events are indicated with arrows. Inhibitory events are shown with a flat line. Mosquito complement components that are not yet placed within this model but whose function is known to be depended on TEP1 (CTL4/CTLMA2, CLIPA2), or highly expected to be depended on TEP1

based on their RNA interference (RNAi) phenotypes (CLIPB14, CLIPB15, CLIPB8 and CLIPA7) are not shown. Figure was adapted and simplified from (Povelones *et al.*, 2016) and permission for its republishing can be found in **Appendix 4**.

Following $TEP1_F$ maturation cleavage, two members of the Leucine-Rich Immune Molecule (LRIM) family - the Leucine-Rich Immune Molecule 1 (LRIM1) and the *Anopheles Plasmodium* responsive Leucine-rich repeat protein 1C (APL1C) - circulating in the haemolymph as a disulphide bonded dimer, act as a scaffold keeping $TEP1_{CUT}$ in an active state (Fraiture *et al.*, 2009; Povelones *et al.*, 2009; 2011). Additionally, this complex prevents $TEP1_{CUT}$ from binding elsewhere apart to the microbial surface while it prevents its autoimmune reaction with components of the haemolymph and surrounding tissues (Blandin *et al.*, 2004; Fraiture *et al.*, 2009; Povelones *et al.*, 2009). The C-terminal coiled-coil domain of the LRIM1/APL1C complex is sufficient to stabilise the $TEP1_{CUT}$ product in the solution, but cleaved forms of the disulphide-stabilised $TEP1_{CUT}$ have not been shown to interact with the LRIM1/APL1C complex. This implies that the formation of the $TEP1_{CUT}$/LRIM1/APL1C complex is dependent on the same conformational change that induces the precipitation of the $TEP1_{CUT}$ (Williams *et al.*, 2019). Together these factors establish the core of the complement-like pathway, which is pivotal for the antiplasmodial defence mechanisms (Fraiture *et al.*, 2009). Silencing any of these factors results in an increased *Plasmodium* oocyst load (Blandin *et al.*, 2004; Osta *et al.*, 2004a).

The mechanics of the complement-like pathway are under continuing investigation, with positive and negative regulators continuously being identified (Povelones *et al.*, 2013; Yassine *et al.*, 2014). For example, CLIPA2, a serine protease homologue, seems to act as a negative regulator of the mosquito complement amplification. Its knockdown leads to an enhanced consumption of the $TEP1_{CUT}$ haemolymph reservoir and subsequent increased resistance to *Plasmodium* infections (Yassine *et al.*, 2014; Kamareddine *et al.*, 2016). Additionally, SPCLIP1, a non-catalytic CLIP-domain serine protease was found to be localised on the surface of *P. berghei* ookinetes and promote rapid accumulation of the TEP1 complement-like protein. However, activation of the mosquito complement-like pathway by the LRIM1/APL1C/$TEP1_{CUT}$ complex is a separate event, occurring upstream of the SPCLIP1-dependent complement amplification process (Povelones *et al.*, 2013). Moreover, mosquito Lipophorins play an important role in regulating mosquito complement during systemic infections. Apart

from their function during lipid transportation, ApoII/I (Lipophorin) silencing in *A. gambiae* leads to upregulation of *TEP1* expression followed by a subsequent reduction of *P. berghei* and *P. falciparum* oocyst numbers (Mendes *et al.*, 2008; Kamareddine *et al.*, 2016). Thus, guided by the LRIM1 and APL1C proteins, TEP1 and several other molecules accompanied by their seemingly inactive homologues bind to the ookinetes as soon as they appear on the basal sub-epithelial space orchestrating their lysis and/or melanisation (Povelones *et al.*, 2013; Yassine *et al.*, 2014).

The role of the complement-like responses against *P. falciparum* infection has so far been unclear, with one field study supporting no effect of LRIM1-silencing in the development of *P. falciparum* parasites (Cohuet *et al.*, 2006) and another laboratory study suggesting that APL1C may be replaced by a paralogue, APL1A, in order to fight *P. falciparum* infection (Mitri *et al.*, 2009). However, TEP1 itself appears to be active against human malaria parasites (Dong *et al.*, 2006; Garver *et al.*, 2009). Remarkably, it has been shown that *P. falciparum* found a way to evade the mosquito complement-like responses by suppressing midgut nitration (Molina-Cruz *et al.*, 2013).

Several members of the FREP gene family, specifically FBN8, FBN9 and FBN39 have also been proved to be critical components of the *A. gambiae* complement-like system and thus exhibit anti-*Plasmodium* activities. FBN39 regulates mosquito resistance to *P. falciparum*, whereas FBN8 and FBN9 provide resistance to both *P. falciparum* and to *P. berghei* (Dimopoulos *et al.*, 2002a, 2002b; Dong *et al.*, 2006; 2009).

1.4.3.3 Haemocyte-mediated defences

Blood cells known as haemocytes exist in the insect open circulatory system and play a key role in the innate immune responses against pathogens. These cells function in defence against pathogens either directly through phagocytosis or indirectly through secretion of effectors such as AMPs, complement-like proteins, and effectors of the melanisation response (Strand, 2008a). The haemocoel of *A. gambiae* female adults contains three haemocyte sub-types: granulocytes, oenocytoids, and prohaemocytes. Granulocytes have been shown to function in phagocytosis, oenocytoids are known to play a role during melanisation and prohaemocytes are hypothesised to serve as hematopoietic progenitors (Castillo *et al.*, 2006). Transcriptomic profiling of adult female *A. gambiae* haemocytes following bacteria and *Plasmodium* infection revealed pathogen-specific signatures of gene regulation and expression (Baton *et al.*, 2009). In addition to transcriptomic profiles, the number of circulating haemocytes in adult

mosquitoes significantly changes in response to blood feeding and infection as well as age and physiological state of the mosquito (Hillyer *et al.*, 2005; Rodrigues *et al.*, 2010; Castillo *et al.*, 2011; Coggins *et al.*, 2012; Bryant & Michel, 2014).

AMPs are small, cationic peptides, typically 33-46 amino acids that are key factors in fighting off infections in insects (Bulet *et al.*, 1999; Meister *et al.*, 2000). Apart from haemocytes, they can also be synthetised by the fat body and epithelia. The *A. gambiae* genome encodes four families of AMP: four cecropins, four defensins, one attacin and one gambicin (Waterhouse *et al.*, 2007). Cecropins have broad spectrum of activity against both Gram types of bacteria, filamentous fungi, yeast, viruses, *Leishmania* and *P. berghei* (Vizioli *et al.*, 2000; Kim *et al.*, 2009; Luplertlop *et al.*, 2011), where gambicin, a mosquito specific AMP, is active against both Gram types of bacteria, fungi and *P. berghei* ookinetes (Vizioli *et al.*, 2002). Defensins seem to be more specific in their activity killing Gram-positive bacteria and filamentous fungi but with no effect on yeast, Gram-negative bacteria or *Plasmodium* parasites (Vizioli *et al.*, 2001; Blandin *et al.*, 2002). The *A. gambiae* genome also encodes eight C-type lysozymes that act by hydrolysing peptidoglycan molecules. LYSC1, in addition to its antibacterial role, appears to also facilitate *Plasmodium* development and has been shown to bind both *P. falciparum* and *P. berghei* oocysts *in vivo* (Kajla *et al.*, 2011).

The differentiation of haemocytes has been shown to be involved in *A. gambiae* innate immune memory. While the innate immune system is unable to establish memory in a fashion similar to the adaptive immune system, memory-like responses termed immune priming have been described in insects as well as in other invertebrates (Moret & Siva-Jothy, 2003; Schmid-Hempel, 2004; Sadd & Schmid-Hempel, 2006; Pham *et al.*, 2007; Roth *et al.*, 2009). Recent work has demonstrated that mosquitoes with untreated midgut microbiota population, display an immune priming mechanism when infected with *Plasmodium* parasites at the time of ookinete midgut invasion. In effect, this enhanced antibacterial immunity indirectly reduces *Plasmodium* parasite survival upon reinfection (Rodrigues *et al.*, 2010). Evokin and lipoxin, both released by haemocytes into the haemolymph upon infection, have been also recently identified as mediators of haemocyte differentiation and immune priming (Ramirez *et al.*, 2015).

1.4.3.4 Melanisation in the anti-*Plasmodium* responses

A separate subpopulation of haemocytes, the oenocytoids, produce the enzymes involved in melanisation; the deposition of melanin and cross-linked proteins on the

surface of a pathogen, causing its death by either asphyxiation or accumulation of toxic effectors inside the melanin-capsule (Gotz *et al.*, 1986). In general, insect melanisation is essential for several physiological processes including cuticle hardening and egg darkening. The rate-limiting step in melanisation is the conversion of tyrosine to melanin precursors, catalysed by phenoloxidases (PO). POs exist in a zymogen form, ProPOs, where a proteolytic cleavage cascade activated upon pathogen recognition results in their activation. This cascade is thought to involve PRRs, CLIP serine proteases and serine protease inhibitors (Yassine & Osta, 2010).

Considerable interest in melanisation was raised after the observation that the L3-5 laboratory strain of *A. gambiae* that was selected for *Plasmodium* refractoriness, kills ookinetes by melanisation (Collins *et al.*, 1986). It was later found that this genetically selected *A. gambiae* strain is refractory to the rodent parasite *P. berghei* through melanotic encapsulation at the ookinete stage, but it can support infection with the African human parasite *P. falciparum (*Dong *et al.*, 2006*)*. Today we know that two genetically selected *A. gambiae* strains exist; the refractory (R) and the susceptible (S) strains, that can efficiently or not, respectively, block *Plasmodium* development in the midgut via melanisation. However, it has since transpired that non-selected laboratory strains and wild caught mosquitoes rarely melanise ookinetes and indeed that melanisation may only be a relevant response in allopatric mosquito-parasite species combinations (Michel *et al.*, 2006; Schwartz & Koella, 2009). This would be also in agreement with what has been shown with regards to the different transcription profiling of *P. berghei* and *P. falciparum* as well as the different effect they have on the *Anopheles* innate immune responses (Dong *et al.*, 2006; Simoes *et al.*, 2017).

The melanisation process is highly regulated by haemolymph components including serine protease inhibitors or serpins (SRPNs) that block the activation of PO (reviewed in Barillas-Mury, 2007). The complex of two C-type lectins (CTLs), CTL4 and CTLMA2, has also been found to directly bind to the ookinete surface and regulate the switching status between lysis and melanisation (Osta *et al.*, 2004a; Volz *et al.*, 2006). CTL4 activity depends on the presence of TEP1 on the ookinete surface and thus, knockdown of TEP1 results in the same phenotype as knocking down CTL4 (G. K. Christophides personal communication, unpublished). Other factors found to negatively control melanisation and thus promote parasite killing by lysis include the CLIPA2, CLIPA5, CLIPA7 and CLIPA14. Co-silencing of CLIPA2 and CLIPA14 results

in an increased melanisation-mediated killing of ookinetes as well as haemolymph PO activity (Nakhleh *et al.*, 2017). Two CLIPBs; CLIPB14 and CLIPB15, are also involved in the killing of *Plasmodium* ookinetes via melanisation and participate in the defence against Gram-negative bacteria (Volz *et al.*, 2005). CLIPB3, B4, B8 and B17 promote ookinete invasion (Volz *et al.*, 2006; Barillas-Mury, 2007), whereas silencing of SRPN2 increases melanisation and reduces the ability of *P. berghei* ookinetes to traverse the midgut epithelium (Michel *et al.*, 2005). A study has demonstrated that CLIPB9 acts as a PPO-activating proteinase that is inhibited by SRPN2 (An *et al.*, 2011). Another SRPN; SRPN6, was found to mediate the defence against malaria parasites and bacteria. Particularly, *SRPN6* expression is induced upon infection with both rodent and human malaria parasites, specifically in midgut cells invaded by ookinetes and in surrounding haemocytes. Silencing of *SRPN6* in *A. gambiae* has demonstrated that its role in parasite clearance is to inhibit melanisation in order to promote parasite lysis (Abraham *et al.*, 2005). Additionally, silencing of *SRPN6* reduces sporozoite numbers in the salivary glands (Pinto *et al.*, 2008). Lastly, silencing of *Rel2* and *PGRP-LC* leads to an increased melanisation activity against *Plasmodium* parasites in the mosquito midgut suggesting that the Imd pathway is a negative regulator of the melanisation response in the mosquito (Meister *et al.*, 2005; 2009; Frolet *et al.*, 2006).

TEP1 is also involved in *Plasmodium* melanisation since RNAi-mediated silencing of *TEP1* in R females results in a reduced load of melanised *P. berghei* ookinetes, thereby increasing the mosquito permissiveness to malaria infection. However, *TEP1*-silencing in S mosquitoes increases the parasite numbers (Blandin *et al.*, 2004).

1.4.3.5 *Anopheles* late-phase immunity against *Plasmodium* development

The broadly accepted view is that once oocysts mature and modify their surface, they are largely “hidden” and unaffected by the mosquito immune system. However, it was shown that following successful development into an oocyst, the parasite faces another line of immune responses known as the late phase of immunity (Smith *et al.*, 2015). The JAK/STAT pathway has been suggested to mediate this late phase of immunity against the malaria parasite through both STAT genes, *AgSTAT-A* and *AgSTAT-B*. It has been shown that silencing of *Ag*STAT-A reduces the number of early *Plasmodium* oocysts in the midgut, but nevertheless enhances the overall infection by increasing oocyst survival. Silencing of SOCS, a STAT suppressor, has the opposite effect; it reduces *Plasmodium* infection by increasing NOS expression. Thus, chemical

inhibition of mosquito NOS activity after oocyst formation increases oocyst survival (Smith *et al.*, 2015). LITAF-like3 (LL3), an LPS-induced TNFα transcription factor, seems to be also implicated in this late phase of immunity. It is induced in the midgut cells during ookinete invasion of the mosquito midgut epithelium and it was found not to limit ookinete invasion, but to enhance subsequent oocyst survival. Knocking down LL3 results in an increased oocyst load (Smith *et al.*, 2012).

In conclusion, both the LL3 and JAK/STAT pathways are believed to be regulators of the haemocyte differentiation. They are induced following *Plasmodium* invasion and affect oocysts survival by reducing the number of those that complete maturation through a yet not fully understood mechanism (Smith *et al.*, 2015). The elucidation of killing mechanisms that target the oocyst stage is particularly attractive to control disease transmission, as *Plasmodium* parasites require several days to complete this stage and the number of parasites is at its lowest inside the vector.

1.4.4 *Plasmodium* evasion of mosquito complement

Genetic engineering of malaria parasites, primarily *P. berghei*, has been instrumental in studying the early steps of mosquito infection and in analysing components of the complement-like pathway. However, the strong RNA-interference (RNAi) phenotypes exhibited by the key complement pathway components LRIM1, CTL4 and CTLMA2 using *P. berghei* infections were not observed when *P. falciparum* field isolates were first used to infect mosquitoes (Cohuet *et al.*, 2006). Initially, this raised concerns as to the *Plasmodium* species-specificity of mosquito immune reactions and questioned the appropriateness of using *P. berghei* as a model malaria parasite. An alternative interpretation of these data is that the human malaria parasites, which actually coevolved with *A. gambiae* mosquitoes, are able to evade the mosquito complement responses, whereas rodent parasites, which are not naturally transmitted by *A. gambiae*, are not. In this context, the human parasites may utilise specific molecules that allow them to actively avoid complement-mediated killing. In support to this hypothesis and following the application of the same experimental approach but using different *P. falciparum* and *A. gambiae* strains combinations, it was shown that TEP1 protected mosquitoes from being infected by both the rodent and human malaria parasites (Dong *et al.*, 2006). Furthermore, silencing other key-molecules of the mosquito complement pathway such as LRIM1, APL1C or SPCLIP1 resulted in an increased *P. falciparum* infection (Molina-Cruz *et al.*, 2012; 2013; Garver *et al.*, 2012;

Mitri *et al.*, 2015). However, it remained unclear for years whether the mosquito immune system behaves differently in the presence of different parasite species.

The molecular basis of complement evasion is not yet fully understood, however recent reverse genetics experiments have shed some light on this important question. Two different isolates of *P. falciparum* were found to have different phenotypes after infecting the refractory L3-5 strain of African *A. gambiae* mosquitoes; the Brazilian isolate was strongly attacked and melanised immediately after mosquito midgut traversal, whereas the African isolate made it to the oocyst stage (Molina-Cruz *et al.*, 2013). Interestingly, a single locus, *Pf*s47, was found to act as the determinant factor of whether parasites death was due to melanisation or not. *Pf*s47 haplotype was later found to protect the parasite only from the complement-mediated responses of its sympatric mosquito vector but left it vulnerable to that of the allopatric mosquito vector. This was termed the “lock-and-key theory” of malaria globalization, where *Pf*s47 acts as the “key” that enables the parasite to “turn off” the mosquito detection system by interacting with a specific mosquito receptor protein, the “lock”. Interestingly, different haplotypes of this key exist and the parasite every time needs to have the right “key” for the “lock” of a given mosquito species to survive, continue to be transmitted, and become established in a new region (Molina-Cruz *et al.*, 2015).

It was later shown that parasites expressing a *Pfs47* haplotype compatible with a given mosquito vector are able to disrupt the JNK signalling cascade triggered by the invaded midgut epithelial cell, and in this way to prevent an effective nitration response that would otherwise lead to their TEP1-mediated killing (Molina-Cruz *et al.*, 2013; Ramphul *et al.*, 2015). The fact that *P. falciparum* evolved the capacity to evade mosquito immunity suggests that these responses are an important barrier to transmission. The *P. falciparum* gametocyte surface protein P47 has been an intense target of study due to its potential as a TBV target (van Schaijk *et al.*, 2006).

This function of *P. falciparum* P47 is shared by its *P. berghei* rodent orthologue *Pb*P47 (Ukegbu *et al.*, 2017b). *P. berghei P47* is expressed on the surface of both female gametocytes and ookinetes and it has been shown to play a role in *in vitro* (van Dijk *et al.*, 2010) and *in vivo* (Ukegbu *et al.*, 2017b) fertilisation, as well as in protecting ookinetes from the mosquito complement-like responses (Ukegbu *et al.*, 2017b). *ΔPbP47* ookinetes traverse the midgut epithelium but are eliminated soon after exposure to haemolymph proteins of the complement-like system. Whilst the former

function is important, yet non-essential *in vivo,* the latter is essential since its disruption completely abolishes transmission (Ukegbu *et al.*, 2017b).

Human complement factors (FH) are also able to influence the initial stages of *Plasmodium* infections inside the mosquito vector. Gametes found a way to escape the attacks from the human complement factor inside the mosquito midgut lumen by expressing on their surface a specific FH receptor known as glideosome-associated protein 50 (GAP50) (Dinko *et al*., 2016). Additionally, the expression of the immune-modulatory peroxidase (*IMPer*) helps the parasite evade the complement-like system by suppressing the activation of NOS (Crompton *et al*., 2014).

1.5 Reverse genetic analysis in *A. gambiae* by RNA interference (RNAi)

The functional characterisation of specific genes implemented in antipathogen defence strategies and the unravelling of the regulatory pathways in which they are involved has been largely investigated in *A. gambiae* mosquitoes, by targeted gene silencing via injection of long double-stranded RNA (dsRNA) (Blandin *et al.*, 2004). In adult mosquitoes, RNAi is efficient in tissues that are invaded by the parasites and in immune-related tissues including the midgut, haemocytes, fat body and salivary glands (Blandin *et al.*, 2002; Blandin *et al.*, 2004; Boisson *et al.*, 2006). The typical experimental strategy couples the multiple functional genomics approaches with the microinjection of dsRNA into the thorax of adult mosquitoes, followed by challenge with malaria parasites or other pathogens and, subsequent examination of the mosquitoes in order to evaluate the resulting phenotype (i.e. mosquito survival rate, infection prevalence/intensity, melanisation etc). An extended RNAi method additionally allows silencing of specific alleles of a given gene in a heterozygous context (Lamacchia *et al.*, 2013) thus, allowing the comparison of the different alleles contribution to a phenotype, even when in the same genetic background.

For example *LRIM1*, *CTL4* and *CTLMA2* were initially reported in an *A. gambiae* functional genomics analysis (Christophides *et al.*, 2002) and were characterised using the RNAi technology, as important complement components with crucial role in *Plasmodium* infection (Osta *et al.*, 2004a). *LRIM1*-silencing leads to a substantial increase in the oocyst load while the two C-type lectins, *CTL4* and *CTLMA2*, when silenced alone lead to killing of almost all parasites via melanisation but when silenced in combination with *LRIM1* lead to an *LRIM1*-silencing phenotype indicating the hierarchy of events. Similarly, *TEP1*-silencing leads to a phenotype that is almost

identical to that of *LRIM1*-silencing (Blandin *et al.*, 2004). Other genes have been identified using similar strategies such as *WASP*, whose silencing partly abolishes the ookinete actin-rich hood and causes a great increase in the oocyst numbers (Vlachou *et al.*, 2005), and *lipophorin ApoII/I* complex whose silencing leads to a drastic decrease of both *P. berghei* and *P. falciparum* oocyst numbers as well as disruption of the mosquito egg development (Mendes *et al.*, 2008). In summary, targeted gene silencing coupled with other functional genomic approaches provides an increasing understanding of the mosquito biology and its molecular interactions with pathogens.

1.6 *P. berghei*: A rodent malaria transmission model

The establishment of a continuous *in vitro* culturing of *P. falciparum* (Trager & Jensen, 1976) has been pivotal for our understanding of malaria. Its use has been fundamental to the ongoing dissection of the molecular mechanisms that underpin basic parasite biology as well as in studies of direct clinical relevance. However, work with the human pathogen *P. falciparum* is restricted by its risk to human health and the fact that there is not any non-primate animal model compatible with it (Herrera *et al.*, 2002). Hence, the strict legal and practical constraints associated with primate research together with the ethical and safety related restrictions regarding human clinical trials, have led to the utilisation of other *Plasmodium* model organisms (reviewed in Craig *et al.*, 2012).

Malaria studies, already since the 1950s, have been using animal models to understand the pathogenesis of the disease (Basir *et al.*, 2012; de Oca *et al.*, 2013; Taniguchi *et al.*, 2015) as well as the parasite biology, immune regulation and disease molecular and cellular processes. Moreover, these models have been used for preclinical testing of various drugs and vaccines (Leitner *et al.*, 2010; Goodman *et al.*, 2013). An appealing feature regarding the use of mouse malaria models is that there are four lab-adapted West African species of murine malaria native to the thicket rat; *P. berghei*, *P. chabaudi*, *P. yoelii* and *P. vinckei* (Carlton *et al.*, 2001) as well as various strains, each displaying different biological characteristics and pathogenicity (Doolan, 2002). Infections caused by parasites such as *P. berghei* and some strains of *P. vinckei* (*P. vinckei vinckei*), *P. yoelii* (*P. yoelii YM*, *P. yoelii XL*) and *P. chabaudi* (*P. chabaudi CB*) cause lethal infections in mice, whereas infections with some strains of *P. yoelii* (*P. yoelii 17XNL*), *P. chabaudi* (*P. chabaudi chabaudi AS*, *P. chabaudi adami*) and *P. vinckei* (*P. vinckei petteri*) are cleared after the initial acute parasitaemia (Doolan, 2002). In contrast to *P. berghei* which rapidly causes fatal murine malaria in

most mouse strains, *P. chabaudi* is able to establish persistent non-lethal murine malaria thereby offering an opportunity to study drug resistance and antigenic variation (Phillips *et al.*, 1997; Carlton *et al.*, 2001), while *P. yoelii* is extensively used for exploratory vaccine studies (Doolan *et al.*, 1998). Additionally, *P. berghei* infects both mature RBC and reticulocytes and in c57BL/6 and CBA/T6 mice is used to investigate the pathogenesis of experimental cerebral malaria (Doolan, 2002). Apart from studies related to *Plasmodium* biology and pathogenesis in the vertebrate host, rodent malaria parasites have been key in investigations of the genetic and molecular interactions between *Plasmodium* and its *Anopheles* mosquito vectors.

Due to the ease of breeding and handling, rodent model systems dominate non-human malaria research today. *P. berghei* is an excellent malaria transmission model system which provides efficient and reliable murine and mosquito malaria infections, while it allows scientists to handle and manipulate malaria infected mosquitoes in the absence of risk of human infection (Sinden, 1996). In contrast to *P. falciparum*, various mosquito stages of *P. berghei* can be cultivated *in vitro* and purified (Janse & Waters, 1995; Waters & Janse, 2004). Rodent malaria parasites are also more amenable to genetic modifications than *P. falciparum*. In fact today, it takes as little as two weeks to obtain a clonal population of *P. berghei* transgenic parasites, while for the human parasites it takes three-to-four weeks using the CRISPR-Cas9 system (Ghorbal *et al.*, 2014) to at least two months when using more traditional methods (van Dijk *et al.*, 1995; Wu *et al.*, 1996). Additionally, the availability of fluorescent rodent parasite lines and transgenic mice permits exploration of specific host parasite interactions that are not yet widely available for studies using the human malaria parasites (Amino *et al.*, 2007). Only recently, Marin-Mogollon *et al.* have reported the generation of transgenic *P. falciparum* line that expresses *mCherry* and *luciferase* during the gametocytes, ookinetes, oocysts, sporozoites and liver stages (Marin-Mogollon *et al.*, 2019).

In the wild, the only known natural vector of *P. berghei* is *A. dureni* (Boëte, 2005). Most *Anopheles* species for which established laboratory colonies exist are part or completely refractory to *P. berghei* infection, whereas the species which provides the most efficient experimental transmission is *A. stephensi* (Sinden, 1996). Some species of the *A. gambiae* complex are also susceptible to *P. berghei* infection, although to a much lesser degree. However, since *A. gambiae* is the principal vector of malaria in Africa, the study of *A. gambiae* malaria transmission using *P. berghei* is highly valued.

1.7 *Plasmodium* genetics and genomics

1.7.1 Genome sequencing: A gateway to new discoveries

As whole organism genome sequencing became possible, malaria research entered a new era. Today, the full genome sequences are available for the two human malaria parasites *P. falciparum* (Gardner *et al.*, 2002) and *P. vivax* (Carlton *et al.*, 2008). Several of the malaria model organisms have also been sequenced, with full genome sequences existing for the rodent malaria parasites *P. berghei* (Hall *et al.*, 2005), *P. yoelii* (Carlton *et al.*, 2002) and *P. chabaudi* (Janssen *et al.*, 2001; Otto *et al.*, 2014; Brugat *et al.*, 2017; Lin *et al.*, 2018) as well as for the simian and human malaria parasite *P. malariae* (Pain *et al.*, 2008). Of a great advantage, the release of the mosquito vector and human host full genome sequences (Venter *et al.*, 2001; McPherson *et al.*, 2001; Holt *et al.*, 2002), encourages further investigations in understanding their genetic and molecular interaction networks.

The *P. falciparum* nuclear genome is composed of 22.8 Mbp distributed among 14 chromosomes, and contains about 5,268 genes (Waters & Janse, 2004). Similarly, the *P. berghei* genome bears 23 Mbp on 14 chromosomes and around 5,864 genes (Waters & Janse, 2004). In common with *P. falciparum* which exhibits an 81% AT bias, the *P. berghei* genome is also characterised by an extreme AT-richness while about 90% on average of the total length of genes accounts for introns and intergenic regions (Carlton *et al.*, 2002; Gardner *et al.*, 2002; Waters & Janse, 2004).

Malaria parasites are obligate sexual organisms and thus can undergo meiosis and associated recombination, providing the ability to perform genetic crosses (Walliker *et al.*, 1987) and linkage analysis. The chloroquine resistance gene is a striking example of such ability (Wang *et al.*, 2005). Genome-wide *in silico* analysis of chloroquine-resistant parasites has brought deep insights into the parasite biology including their ability to infer homology searches to other organisms, predict protein domain function and identify novel regulatory pathways. Other examples include metabolic maps (Ginsburg, 2006), regulatory kinases (Ward *et al.*, 2004) or protein localisation patterns (Marti *et al.*, 2004). Moreover, genome-wide surveys have been conducted both at the transcriptome and proteome level and have been critical for the characterisation of *Plasmodium* gene regulation during development in the human host and mosquito vector. Parasite processes were examined by investigating the gene stage specific expression (Young *et al.*, 2005; Patankar *et al.*, 2013; Broadbent *et al.*, 2015),

interaction networks (Lacount *et al.*, 2005), organellar proteomics (Sam-Yellowe *et al.*, 2004), antigenic (Doolan *et al.*, 2003) or metabolic profiling (Daily *et al.*, 2007) and drug treatment dynamics (Prieto *et al.*, 2008, Prieto *et al.*, 2014).

1.7.2 Reverse genetics roadblocks in *P. berghei*

Our understanding of the molecular mechanisms underlying *Plasmodium* development has been hindered by the fact that only a small number of genes has been experimentally characterised by using either forward or reverse genetic approaches. Forward genetics aims at the identification of genes responsible for a particular phenotype by performing techniques such as transposon mutagenesis, a technology that has been widely used both in *P. berghei* (Sakamoto *et al.*, 2005) and in *P. falciparum* (Ikadai *et al.*, 2013). Reverse genetics involves alteration or disruption of a specific gene in order to enable the study of its biological function.

Reverse genetics is the favored approach for analysing parasite gene functions. Usually it comprises three main stages: assembly of the targeting vector, transfection of the parasites and phenotypic analysis of the mutants. Stable transfection technologies became available for *Plasmodium* parasites in the late 1990's (Goonewardene *et al.*, 1993; van Dijk *et al.*, 1995; Wu *et al.*, 1996; van der Wel *et al.*, 1997) and within the next years efficient protocols were developed especially for *P. berghei*, the most genetically tractable of the malaria parasites (Janse *et al.*, 2006b). A key step of this protocol is the use of the non-viral nucleofector technology (Janse *et al*., 2006b), crucial due to the intracellular lifecycle of the parasite and the fact that its genetic material is enclosed within four membranes including the RBCs membrane, the parasitophorous vacuolar membrane (PVM), the parasite membrane and lastly, the nuclear envelope. Other difficulties encountered during *Plasmodium* genetic manipulation includes the high AT-content in their DNA and the fact their genome is unstable in *E. coli* (Carlton *et al.*, 2002; Gardner *et al.*, 2002). The limited number of selection markers has also been a limiting factor for developing an efficient transfection protocol, especially for *P. berghei* studies where drug toxicity for the animals can be an issue. Currently, the *human dhfr* (*hdhfr*) (de Koning-Ward *et al.*, 2000) and *Toxoplasma dhfr* (*dhfr-ts*) (de Koning-Ward *et al.*, 2002; Carvalho & Ménard, 2005) genes are used to select mutants with pyrimethamine, a drug that inhibits parasite DNA synthesis when provided in the mouse drinking water. Protocols for isolating isogenic populations of *P. berghei* mutants without the need of *in vivo*

cloning are now available and include sorting by flow cytometry of green fluorescent protein (*GFP*)- or cyan fluorescent protein (*CFP*)-expressing transgenic parasites (Janse *et al.*, 2006a; Kenthirapalan *et al.*, 2012).

1.7.3 The PlasmoGEM project and genetic screens by barcode counting

Plasmodium genomes encode around 5,400 genes and are organised in fourteen chromosomes. It has been estimated that more than 60% of those encoding proteins have poor or no homology to other known eukaryotes, rendering gene function studies difficult. To facilitate the functional analysis of all *Plasmodium* genes, the Malaria Program at the Wellcome Trust Sanger Institute has developed the *Plasmodium* genetic modification (PlasmoGEM) project, which focuses on the generation of a global resource of efficient *P. berghei* genetic modification vectors. Currently, this library has 9,946 clones and targets about ˜91% of characterised and non-characterised *P. berghei* genes. *P. chabaudi* library clones are also underway, with more than 80% of the rest annotated gene models already covered. As these vectors are generated from library clones, they contain homology arms that are several kb long as opposed to the traditional 0.4-1 kb. Additionally, these vectors are not circular and thus are not kept in the cytoplasm as episomes. This approach has enhanced the transfection efficiency and reproducibility as well as it has greatly reduced the time necessary for generating large numbers of targeting vectors.

Phenotypic analysis of mutant parasites is the most laborious stage, especially when *in vivo* infection models are required. Different methods have been previously suggested for the simultaneous screen of multiple mutant parasites, however, each mutant had to be still screened individually making all these methods unattractive to be used. Only recently, Gomes *et al.* suggested a method to perform phenotypic analysis of large numbers of *P. berghei* mutants by adapting the Signature tagged mutagenesis (STM) (Gomes *et al.*, 2015). STM was extensively used in the past for bacterial pathogens, in order to perform parallel phenotypic analysis of pools of individually barcoded mutants (Hensel *et al.*, 1995; Mazurkiewicz *et al.*, 2006; Langridge *et al.*, 2009). However, this was not feasible for malaria parasites as such pools could not be produced at the time.

The greatest advantage of the STM technology is the ability to identify each mutant within a pool, by the presence of a signature tag or barcode (a unique short DNA sequence) introduced into the microorganism genome upon integration of the

modulated targeting vector. STM screens have been designed in many ways, reflecting the diversity of genetic systems for different taxa. Common to all is a workflow that starts with the mutagenesis step i.e. generation of the barcoded mutants, which is followed by the propagation of these mutants in pools and finally identification and quantification of the mutants through their barcode. This method enables quantitative analysis of complex pools, based on the frequency at which a specific barcode is detected in the sequencing data. The quantitative analysis later informs us about the abundance of a given mutant within the pool (Smith *et al.*, 2009).

The STM methodology opens the possibility for establishing large-scale reverse genetic screens in order to uncover the multiple areas of *Plasmodium* biology. For this reason, each KO vector produced by the PlasmoGEM project is designed to carry a 10-11bp gene-specific barcode which is flanked by constant primer annealing sites. These barcodes when carried by each mutant can be then quantified by Next Generation Sequencing (NGS) (Smith *et al.*, 2009) thus, enabling the calculation of the relative growth rate for each mutant within the pool and how it changes during infection progression. The specific length of the barcode permits that enough sequences could be generated in order to cover the entire *Plasmodium* genome. Interestingly, it is now possible to produce pools of over 50 mutants in a single mouse, that could also be used to later infect the mosquito vectors.

1.8 Aims and Objectives

The mosquito midgut stages of malaria parasites are crucial for establishing an infection in the insect vector and to thus ensure further spread of the pathogen. This is mainly due to the fact that the parasite population experiences dramatic bottleneck effects, largely caused by the mosquito innate immune reactions encountered immediately after ookinetes traverse their midgut epithelium (Clayton *et al.*, 2014; Povelones *et al.*, 2016). The aim of my PhD project was to primarily identify and characterise new *Plasmodium* genes that are essential for parasites to establish successful infection in the mosquito midgut and then, to scrutinise the molecular basis of the mosquito innate immune responses to *Plasmodium* infection by first characterising genes for which preliminary evidence suggested to be crucial during midgut stages development and parasite evasion of the mosquito immune responses.

In vivo transcriptional profiling studies previously carried out using both *P. berghei* and field *P. falciparum* populations in infected *A. gambiae* and/or *Anopheles arabiensis*

mosquitoes (Akinosoglou *et al.*, 2015) revealed hundreds of *Plasmodium* genes, highly upregulated during the parasite gametocyte-to-ookinete-to-oocyst developmental transition. Upregulation of a gene at any of these critical time points suggests either a developmental role of the gene during parasite development within the mosquito vector or facilitation of essential interactions between the parasite and the mosquito microenvironment. Of those, genes that appeared to be conserved between the different *Plasmodium* species and encoded surface or secreted proteins were selected for further characterisation as well as to investigate their essentiality in mosquito-parasite interactions. These genes include *P47*, a gene previously found to be important during *in vitro* fertilisation of *P. berghei* parasites (van Dijk *et al*., 2010) and protection of *P. falciparum* ookinetes from reactions of the mosquito innate immune system (Molina-Cruz *et al.*, 2013; Ramphul *et al.*, 2015) as well as the *Plasmodium* invasion of mosquito midgut screen candidate 43 (*PIMMS43*, referred to as *c43*), a gene for which preliminary evidence indicated to facilitate parasite mosquito immune evasion and oocysts sporogonic development (Ukegbu *et al*., 2020). Two genes that were also selected for further characterisation were the *c01* and *c57,* for which preliminary data suggested to be essential in parasite transmission (unpublished data, with the permission of Dr. Valerie Ukegbu, Imperial College London). At the same time, of special concern was to further narrow down the long list of genes found to be highly upregulated during the mosquito midgut stages of malaria parasites by adapting a high-throughput reverse genetics screening approach. To further investigate this, various mutants were simultaneously assessed for their ability to establish infection in the *Anopheles* mosquito vector.

Whether parasites surviving the mosquito immune attacks are selected as the most fit to continue disease transmission or whether parasite elimination is stochastic, has been a question for many years. For example, one could imagine that the immunity-mediated bottleneck acts as a filter for parasites that are unable to complete their lifecycle. By shielding themselves with specific proteins, *Plasmodium* parasites could secure fitness levels that exceed a basic survival threshold and are therefore not eliminated by the mosquito responses. In agreement with that, some of these proteins are thought to contribute to *Plasmodium* immune evasion or endurance in the hostile environment triggered by the mosquito vector.

Based on these concepts, the specific objectives of this project were set as follows:

1. Identification of new genes with important roles in parasite development in the mosquito vector by using a high-throughput reverse genetics screening approach,
2. Detailed characterisation of *P. berghei c01*, *c43*, *P47* and *c57,*
3. Characterisation of the genetic and molecular impact of *Plasmodium* immunity mediated bottleneck observed in the mosquito midgut, and
4. Investigation of the current model that specific parasite proteins facilitate parasite immune evasion and specifically from reactions of the complement system.

CHAPTER 2. MATERIALS AND METHODS

2.1 Bioinformatics

2.1.1 *Plasmodium spp.* sequence retrieval and domain prediction

Plasmodium protein and DNA sequences were primarily retrieved from PlasmoDB (http://plasmodb.org/plasmo/) (Bahl *et al.*, 2003). Nucleotide and protein BLAST searches were conducted using the BLASTN and BLASTP tools available through PlasmoDB and NCBI (http://www.ncbi.nlm.nih.gov/ blast/). Confirmation of signal peptide and transmembrane predictions were performed using SignalP Server v.3.0 (Bendtsen *et al.*, 2004). Functional and structural domain predictions were confirmed and updated by InterproScan (Quevillon *et al.*, 2005) and the web portal Phyre2 (Kelley *et al.*, 2015). AQP2 protein feature visualisation was carried-out using the Protter web application (Omasits *et al.*, 2014).

Multiple sequence alignments were conducted using ClustalW (Thompson *et al.*, 2003) and visualised by Bioedit Sequence Alignment Editor v.7.0.5.3 (Hall, 1999).

2.1.2 AQP2 phylogenetic analysis

AQP2 proteins were aligned separately using the profile alignment feature implemented in ClustalW. In total, 58 aquaporin genes from different species (*P. berghei, P. falciparum, P. vivax, P. yoelii, P. malariae, Trypanosoma brucei, Toxoplasma gondii, Pseudomonas, Mus musculus, Arabidopsis thaliana, E. coli, Homo sapiens, A. gambiae* and *Anopheles coluzzii*) were individually added to the combined alignment. The phylogenetic tree was built based on this final alignment using Mega X (Kumar *et al.*, 2018) and the ClustalW's Neighbor-Joining algorithm (Saitou & Nei, 1987).

2.2 Parasite maintenance, cultivation and purification

2.2.1 Ethics statement

All animal procedures were reviewed and approved by the Imperial College Animal Welfare and Ethical Review Body and carried out in accordance with the Animal Scientific Procedures Act 1986. Protocols demanding *P. berghei* infections of mice as well as mosquito infections through blood feeding on *Plasmodium*-infected mice were performed under the UK Home Office License PPL70/8788. Human RBCs were provided by the National Blood Service of the United Kingdom National Health Service and were previously collected from healthy donors upon their written consent.

2.2.2 *P. falciparum* standard membrane feeding assays (SMFAs)

SMFA were carried out as described previously (Ponnudurai *et al*., 1982; Ponnudurai *et al*., 1989). Briefly, day 14, stage V gametocyte cultures were pooled in a pre-warmed falcon tube containing 20% (v/v) of uninfected serum-free *h*RBCs and 50% (v/v) heat-inactivated human serum. The α-*Pfc*43 antibodies were added to the gametocytaemic blood mix to final antibody concentrations of 50, 125 and 250 µg/mL, in a 300 µL final volume. This was immediately transferred to pre-warmed glass feeders, which were previously kept at 37°C. Blood fed mosquitoes were maintained at 27°C, 70% humidity and 12/12 hours light/dark cycle. At day-7 post blood feeding (pbf) midguts were dissected and infection intensity and prevalence were recorded. Experimental procedures were assisted by Dr. Sofia Tapanelli.

2.2.3 Parasite strains

The *P. berghei* lines used throughout this project are listed in **Table 2.1**. Briefly, disruption of all genes was carried out by double crossover homologous recombination in either the ANKA *507m6cl1*, here termed as the *c507* line, or ANKA *1804cl1* reference (parental) lines. For the generation of the *Δc43*, *ΔP47*, *Δc01*, *Δc57*, *ΔP48/48* and *ΔPIMMS2* mutant lines, the upstream and downstream homology regions as well as the open reading frame (ORF) of the gene were amplified by a polymerase chain reaction (PCR) from *P. berghei* gDNA and cloned into the pBS-*Tg*DHFR/*Ts* vector in which polylinker sites flank a *T. gondii* dihydrofolate reductase/thymidylate synthase gene (*Tg*DHFR/*Ts*) pyrimethamine resistance cassette (Dessens *et al.*, 1999). Transfection of the linearised constructs, selection of the transgenic parasites and clonal selection was carried out as previously described (Janse *et al.*, 2006b). Subsequently, gDNA from the KO parasites was analysed by PCR to confirm correct positioning of the insertion in the parasite genome and complete lack of the WT locus.

Specifically, for the generation of *ΔAQP2*, *ΔN38*, *ΔN350*, *AQP2-3HA*, *N38-3HA* and *N350-3HA* transgenic parasites, the *P. berghei* ANKA *c507* reference line was used. The expression of *eGFP* is under control of the *eef-1a* promoter and the expression cassette was introduced into the genome by homologous crossover into the type D small subunit (*dssu*) ribosomal RNA locus of *P. berghei*. This *c507* clone was selected in the absence of a drug resistance marker by the use of flow-cytometry (Janse *et al.*, 2006a) and therefore, allows for subsequent modification of the wild-type (WT) locus by the use of the *Tg*DHFR/*Ts* pyrimethamine selection system. Consequently, it also

allows for the generation of transgenic parasites in a GFP background, assisting phenotypic analysis. The transfectant vectors used were obtained from the PlasmoGEM resource (Schwach *et al.*, 2015).

Table 2.1. *P. berghei* parasite lines. Column 2 includes the reference (background) line used for the generation of the mutant line. Mutant parasite lines generated on the *c507* reference line constitutively express *GFP*, whereas mutant parasite lines generated on the 1804cl1 reference line constitutively express mCherry.

***P. berghei* parasite line**	**Reference line**
c507 (RMgm7) (MR4; Janse *et al.*, 2006a)	ANKA strain (Taxon ID: 5823)
1804cl1 (RMgm928) (Burda *et al.*, 2015)	ANKA strain (Taxon ID: 5823)
2.34 (RMgm4155) (MR4; Fang *et al.*, 2017)	ANKA strain (Taxon ID: 5823)
ΔAQP2	ANKA *c507*
AQP2-3HA	ANKA *c507*
ΔN38	ANKA *c507*
N38-3HA	ANKA *c507*
ΔN350	ANKA *c507*
N350-3HA	ANKA *c507*
Δc43 (Ukegbu *et al.*, 2020)	ANKA *c507*
Δc43 (Ukegbu *et al.*, 2020)	ANKA *1804cl1*
ΔP47 765acl1 (RMgm347; van Dijk *et al.*, 2010)	ANKA *c507*
ΔP47 (PbGEM-343204) (Gomes *et al*., unpublished)	ANKA *1804cl1*
Δc01 (Ukegbu *et al.*, unpublished)	ANKA *c507*
Δc57 (Ukegbu *et al*., unpublished)	ANKA *c507*
ΔP48/45 764acl1 (RMgm346) (Janse *et al.*, 2006b)	ANKA *c507*
ΔPIMMS2 (Ukegbu *et al.*, 2017a)	ANKA *c507*

2.2.4 *P. berghei* maintenance

The *P. berghei* parasite lines were maintained in CD1 mice (Charles River Laboratories International Inc., UK) as previously described (Sinden, 1996). Parasitaemia was monitored by the counting of blood stage parasites in air dried, methanol fixed, and Giemsa (Sigma) stained thin tail-blood smears. Giemsa solution was prepared by a 1:5 dilution in distilled water (dH_20) and staining was performed for 15 min at room temperature. Mice were infected by intraperitoneal (IP) injection of 100-200 µL *P. berghei* infected blood. For infections where a high parasitaemia/ gametocytaemia was desirable, reticulocyte proliferation was stimulated by IP injection of phenylhydrazinium chloride (PH) (6 mg/mL stock (Sigma) solution in Phosphate Buffer Saline (PBS); 10X stock solution of 0.2 M phosphate, 1.5 M NaCl,

pH 7.4), 2-3 days prior to *P. berghei* infection. Infected blood for passage or experimental use was collected by cardiac puncture (syringe with 15 U heparin per mL of blood, Sigma) at day 3-4 of infection, from terminally anaesthetised mice (intramuscular injection (IM) of 0.05 mL/10g body weight of Rompun (2% stock solution, Bayer), Ketastet (100 mg/mL ketamine, Fort Dodge Animal Health Ltd. and Phosphate Buffer Saline (PBS, Sigma) prepared to a ratio of 1:2:3).

Parasite stocks were maintained at -80^{o}C in 90% (v/v) Alsever's solution (Sigma) and 10% (v/v) glycerol, prepared with infected blood at 1:2 ratio of blood to freezing solution. Upon thawing the stocks were immediately injected into mice.

2.2.5 *P. falciparum* maintenance and culturing

P. falciparum maintenance and culturing was performed as previously described (Haynes *et al.*, 1976). Briefly, human RBCs (*h*RBCs) (UK National Blood Service) were used for the maintenance of ABS and gametocyte culture of the *P. falciparum* NF54 strain. *Pf*NF54 culture was maintained in complete medium (CM) composed of RPMI-1640 (Sigma), 0.05 g/L Hypoxanthine, 0.3 mg/L L-glutamine powder-(Sigma) and 10% sterile human serum (Interstate Blood Bank Inc.). Set up of *Pf*NF54 asexual culture was performed in T25 cm^2 flasks containing a final volume of 500 µL of A+ or O+ concentrated red blood cells (*c*RBCs; NC15 research grade, NHS Blood and Transplant, UK) and 10 mL of CM, kept at 37°C incubation and regularly supplemented with the "malaria gas" (constituted by 3% O_2, 5% CO_2 and 92% N_2). Gametocyte cultures were initiated by diluting the continuous asexual culture of 4-6% early ring stages in prewarmed (37 °C) 10 mL of CM, supplemented with 500 µL *c*RBC to a final concentration of young merozoites of 1–1.5%. Upon fumigation with the $O_2/CO_2/N_2$ gas mixture for 15 sec, the culture flask was immediately placed in a 37 °C incubator, ensuring daily exchange of around 75% of the CM per flask. During CM replacement, the old medium was carefully aspirated without disturbing the infected RBC layer at the bottom of the flask and fresh CM was gently added. Parasitaemia was assessed daily by Giemsa stained blood smears, whereas gametocytaemia and density of viable mature stage V gametocytes were assessed at day-14 post induction by testing the *in vitro* exflagellation rate of male gametocytes.

2.2.6 Purification of *P. berghei* mixed blood stage parasites

White blood cells were removed from infected blood by passing over CF11 columns (Whatman) (Venkatesan *et al*., 2012). The purified blood was collected after elution

with PBS. Parasites were pelleted by centrifugation at 1500 g for 10 min prior to 30 min incubation in ice-cold 0.17M NH_4Cl to facilitate RBCs lysis (Martin *et al*., 1974). Parasites were pelleted by 10 min centrifugation at 1500 g, supernatant was removed, and pellet was washed in PBS. Samples were then stored at -20°C for western blot analysis or at -80°C for qRT-PCR and reverse transcriptase PCR (RT-PCR) analysis.

2.2.7 *P. berghei* gametocyte purification

For preparation of pure viable gametocytes, Nycodenz (Life Technologies) density gradient purification was used as previously described (Billker *et al.*, 2004). Briefly, infected blood was collected from terminally anaesthetised mice with a parasitaemia of >10% and diluted in 5 mL Coelenterazine Loading Buffer (CLB) (20 mM Hepes, 20 mM Glucose, 4 mM Sodium bicarbonate, 1 mM EDTA; Sigma). Following passage over CF-11 columns pre-calibrated with CLB (elution in 5 mL CLB), the blood was pelleted at 500 g for 5 min at room temperature. The resulting pellets were resuspended in 3 mL of their own supernatant and loaded onto a 5 mL 48% Nycodenz gradient cushion (52% CLB (v/v) and 48% (v/v) Nycodenz; Nycodenz made up in Nycodenz buffer (5.0 mM Tris, 3.0 mM KCl, 0.3 mM EDTA Na_2Ca, pH 7.2; Sigma)). Following low acceleration and deceleration centrifugation at 1000 g for 10 min at room temperature, purified gametocytes were collected from the gradient interface and washed in CLB twice. Gametocytes were then either collected immediately (non-activated) or activated by incubation in ookinete culture medium at 19°C for 30-45 min, until exflagellation was observed. A small sub-fraction of the pellet was mixed with 1 µL of PBS and smeared onto glass slides prior to methanol fixation and Giemsa staining, followed by microscopic observation in order to check the quality of the preparation. Samples were then stored at -20°C for western blot analysis, at -80°C for qRT-PCR, RT-PCR or directly prepared for performing immunofluorescence assays.

2.2.8 *P. berghei* ookinete *in vitro* cultivation

About 1mL of infected mouse blood was collected from terminally anaesthetised mice with a parasitaemia of >10%. Exflagellation was also checked, with an expected rate of 5-8 exflagellation centres per field (400X). The blood was transferred to a tissue culture flask immediately after collection, containing 30 mL of 80% (v/v) RPMI1640 ookinete culture medium enriched with 25 mM Hepes (Sigma), 2 mM L-glutamine (Sigma), 0.2% (w/v) sodium bicarbonate (Sigma), 50 U/mL penicillin, 0.05 mg/mL streptomycin (Pen/Strep solution; Gibco), 50 mg/77mL hypoxanthine (Sigma), 100 uM

xanthurenic acid (pH 7.4, Aldridge), and 20% (v/v) foetal bovine serum (FBS, Gibco). Cultures were incubated for 22-24 hours at 19ºC, to let ookinetes form and mature.

2.2.9 *P. berghei* zygote and ookinete purification

Ookinete purification was facilitated by using Dynabeads® Protein G (Fisher Scientific) coated with an anti-P28 mouse monoclonal antibody (13.1), as previously described (Sidén-Kiamos *et al.*, 2000). All washing and separation steps were conducted using a magnetic separation rack (Magna Rack™, Invitrogen). Briefly, 13.1 coated Dynabeads were prepared by washing the beads twice in PBS prior to incubation with the 13.1 antibody (dilution 1/50 in PBS) for 30 min at room temperature on a rotating rack. Unbound antibody was washed off using PBS, and the P28-conjugated Dynabeads were resuspended in PBS (equivalent to the volume of storage buffer in which the aliquoted beads were originally kept) and stored at 4ºC, until further use.

Ookinete cultures, 22-24 hours post setup, were pelleted by centrifugation at 500 g for 10 min, at room temperature. The resulting pellet was resuspended in 10 mL of their own supernatant prior to addition of 10 µL coated beads per ookinete culture, followed by 20–30 min incubation on a rotating rack at room temperature. Following 3 min incubation on the Magna Rack™, the supernatant was collected. The ookinetes bound to the beads were washed twice with 5-10 mL of ookinete medium. Purified ookinetes were pooled and pelleted at 500 g for 5 min. Quality control by Giemsa-staining and sample storage were performed as for purified gametocyte preparations.

2.3 Mosquito maintenance, infections and microinjection

2.3.1 Mosquito maintenance

The mosquito strains used were N'gousso (*A. coluzzii*, previously M form *A. gambiae*) and *A. stephensi* SDA500 (supplied by Mark Tunnincliff). Mosquito rearing was carried out under standard conditions previously described (Richman *et al*., 1996). Briefly, the mosquito colony was maintained at 28°C with 80% relative humidity and 12/12 hours light/dark cycle. Adult female mosquitoes were given human blood (membrane feeding) twice a week, for egg production. Eggs were collected on a filter paper, sterilised with 1% bleach (v/v), washed with distilled water and put in 1% (w/v) NaCl in dH_2O solution, until hatched. The aquatic stages of mosquitoes were maintained in dH_2O and given 1.8 g of food pellet (TetraMin Baby, Tetra) daily. Adult mosquitoes were fed with cotton balls soaked with autoclaved 10% fructose (w/v) solution.

2.3.2 *P. berghei* mosquito infections

Adult or dsRNA-injected *A. coluzzii* females were infected with *P. berghei* by direct feed on anaesthetised mice with parasitaemia of 5–7% and gametocytaemia of 1-3%. Naïve adult mosquitoes were 3-5 days old at the day of blood feeding, whereas the dsRNA-injected mosquitoes were injected at the age of 0-2 days old and blood fed when they reached the age of 3-5 days old i.e. blood feeding was carried out at day-3 post injection. Prior to mosquito feeding, exflagellation was checked with an expected rate of 2–3 exflagellation centres per field. Mosquitoes were allowed to feed for 15-30 min in the dark at 19^{o}C, and unfed females were removed 48 hours after blood feed.

2.3.3 *P. berghei* SMFAs

SMFA was carried out as previously described (Blagborough & Sinden, 2009). Briefly, female *A. stephensi* mosquitoes were starved for 24 hours prior to feeding on *P. berghei* infected blood. For each feed, 350 µL of *P. berghei 2.34* ANKA WT infected blood containing asexual parasite and gametocyte stages with a parasitaemia of 5-6% and gametocytaemia of 2-3% was mixed with 150 µL of PBS containing either α-*Pb*c43 or the isotopic monoclonal UPC10 (negative control) (Sigma) antibodies to yield final antibody concentrations of 50, 100 and 250 µg/mL. Blood fed mosquitoes were maintained at 21°C, 70% humidity and 12/12 hours light/dark cycle. At day-10 pbf, mosquito midguts were dissected, and oocyst intensity and prevalence were recorded using fluorescent microscopy. Experimental procedures were performed by Dr. Andrew Blagborough and Dr. Fiona Angrisano.

2.3.4 Ookinete haemocoel microinjection

Ookinetes from culture volumes equivalent of 11.6x10^{5} ookinetes (800 ookinetes in 69nL ookinete medium injected per mosquito) were pelleted by centrifugation at 500 g for 5 min at room temperature. The resulting pellets were resuspended in 100 µL (adjusted depending on haematocrit volume) ookinete medium. 69 nL of the ookinete suspensions were injected directly into the haemocoel through the thorax of 1-day old *A. coluzzii* mosquitoes using glass capillary needles and the Nanoject II microinjection system (Drummond Scientific Company).

2.3.5 Microinjection of dsRNA for RNAi-mediated mosquito gene silencing

Complementary DNA (cDNA) was prepared from total RNA, previously extracted from whole adult *A. coluzzii* mosquitoes, and was used to produce *CTL4*, *LRIM1* and *TEP1* dsRNA using gene-specific PCR primers with a T7 promoter sequence, as previously

reported (Osta *et al.*, 2004a; Habtewold *et al.*, 2008; Garver *et al.*, 2012; Smith *et al.*, 2012) (**Table 2.2**). The different dsRNAs were generated using the TranscriptAid T7 High Yield Transcription Kit (ThermoFisher), according to manufacturer's instructions. Following quantitative and qualitative analysis of the produced dsRNA, 69 nL of 3 µg/mL of purified dsRNA (QIAGEN RNAeasy spin column kit) was injected into the thorax of 1–2 days old *A. coluzzii* mosquitoes using glass capillary needles and the Nanoject II microinjector (Drummond Scientific). Injected mosquitoes were left in standard maintenance conditions to recover, and 3 days afterwards were infected with *P. berghei* by direct feeds on infected anaesthetised mice (Blandin *et al.*, 2002).

Table 2.2. T7 primer sequences used for dsRNA mediated gene silencing via RNAi in *A. coluzzii.* Forward (FWD), Reverse (REV)

Primer Name	Primer Sequence
T7 LacZ FWD	AGAATCCGACGGGTTGTTACT
T7 LacZ REV	CACCACGCTCATCGATAATTT
T7 LRIM1 FWD	AATATCTATCTCGCGAACAATAA
T7 LRIM1 REV	TGGCACGGTACACTCTTCC
T7 TEP1 FWD	GGAAATACCGGAGGACACGG
T7 TEP1 REV	TGGGTGCTACCTTAAAGCGTCTG
T7 REL1 FWD	TCCCCGACTGCTTTGTTACC
T7 REL1 REV	CAGGGTACAGCTTCCCCAAG
T7 REL2 FWD	CCGCTACCAGTCGGAGATGCAC
T7 REL2 REV	CTCCACCCGGTACGCCCGGAAG
T7 CTL4 FWD	AAGACTGACACGATCGCAGAAA
T7 CTL4 REV	CCTGTCCGGCGATCAAACTA
T7 LITAF FWD	ATGACTACCATCATAGTGACGAACCC
T7 LITAF REV	TTACACCATTATTAAATAAATAACACAACTTGAGATG

The T7 promoter adaptor sequence (TAATACGACTCACTATAGGG) was added as an extension at the 5' untranslated region (UTR) of both the FWD and REV primers.

2.4 Mosquito tissue harvesting and sample processing

2.4.1 Mosquito midgut dissections

P. berghei or *P. falciparum* infected *A. coluzzii* or *A. stephensi* mosquito midguts were dissected in PBS or in PBS supplemented with 1% (v/v) NaN_3, respectively, under a dissection microscope by gently pulling apart the abdomen from the thorax and removing the carcass, foregut, ovaries and Malphigian tubules. Midguts were subsequently processed for counting of oocysts/sporozoites/melanised ookinetes, imaging or RNA/protein extraction accordingly.

2.4.2 Harvest of *Plasmodium* infected midguts for transcriptional analysis

About 30 midguts or salivary glands were isolated from *P. berghei* or *P. falciparum* infected *A. coluzzii* mosquitoes at discrete time points, each corresponding to a distinct stage of parasite development inside the mosquito vector. Prior to tissue collection, infection establishment was confirmed through observation of the tissue under a light microscope. The time points investigated for *P. berghei* were 1-3 hours (mixed asexual and sexual blood stages), 22-26 hours (invading ookinetes), 10 days (mid-mature oocyst), 15 days (mature oocyst-sporozoite release) and 21 days (salivary gland sporozoites) pbf. The time points investigated for *P. falciparum* were; 1 hours (mixed asexual and sexual blood stages), 24 hours (invading ookinetes), 10 days (mature oocyst-sporozoite release) and 16 days (salivary gland sporozoites) pbf. The dissections were performed on ice and the tissues were stored at -80ºC (**Figure 2.1**).

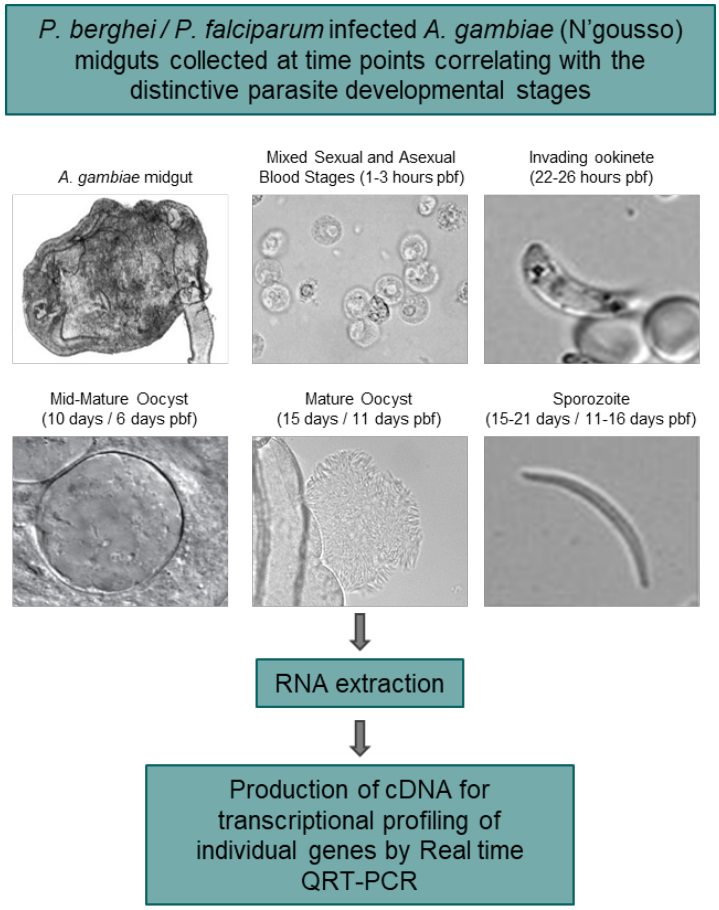

Figure 2.1. Experimental design for RT-PCR and qRT-PCR sample preparation. *P. berghei* or *P. falciparum* infected *A. coluzzii* midguts or salivary glands were dissected at 1 hour, 24 hours, day-10, day-15 and day-21 pbf, and at 1 hour, 24 hours, day-6, day-11 and day-16 pbf, respectively. All samples were processed for RNA extraction prior to reverse transcription and transcriptional profiling.

2.4.3 Total RNA extraction

Immediately upon thawing, tissue and cell sampling was immersed in Trizol reagent (Life Technologies) so that the sample volume did not exceed 10% of the Trizol reagent volume and was then mechanically homogenised under RNAse free conditions. About 30 midguts or salivary glands and 10 whole mosquitoes (after decapitation and removal of legs and wings) were isolated from *P. berghei* or *P. falciparum* infected *A. coluzzii* mosquitoes at discrete time points, as previously described. The integrity of the extracted RNA was assessed by 1.2% (w/v) agarose gel electrophoresis, using Tris/Borate/EDTA (TBE) buffer (Sambrook and Russell, 2001) and denaturing loading buffer (QIAGEN). The RNA concentration was measured using the NanoDrop ND-1000 Spectrophotometer (ThermoScientific). Samples were stored at -80^{o}C upon further use.

2.4.4 Isolation of haemolymph

Haemolymph isolation of *P. berghei* infected mosquitoes was performed as previously described (Povelones *et al.*, 2009). Mosquitoes were briefly anaesthetised using carbon dioxide and placed in groups of 10-20 ventral side up on a clean glass plate chilled on a bed of ice. The proboscis was cut using fine scissors and pressure was applied to the lateral aspects of the thorax forcing a drop of haemolymph to be expelled from the cut proboscis. The haemolymph drop from each mosquito was collected directly into a pipette tip filled with 5 µL of denaturing, non-reducing Laemmli sample buffer (BioRad) and transferred to an Eppendorf tube. After the entire group was collected the final sample volume was adjusted to 1 µL/mosquito. Haemolymph collected from 20-30 mosquitoes was loaded in each lane of a western blot gel.

2.4.5 Gametocyte and ookinete membrane fractionation

About 4x10^{7} purified *in vitro* generated ookinetes were pelleted at 500 g for 5 min and washed twice in PBS containing 10 µg/mL (1X) Protease Inhibitors (PI) (cOmplete EDTA free, Roche). The pellet was resuspended in 200 µL of 5 mM Tris·HCl-PBS-PI (pH 7.4) buffer, mechanically homogenised for 1 min and stored at -80^{o}C until frozen, in order to cause hypotonic lysis to the parasites and release of the protein soluble fraction. Immediately upon thawing, the sample was centrifuged at 8000 g for 1 min, at 4^{o}C and the resulting supernatant containing proteins included in the cytoplasm of the parasite, was placed on ice. The pellet was, later, washed twice with 100 µL PBS/PI. The membrane soluble fraction was extracted in 200 µL 1% Triton X100/5

mM Tris·HCl/PBS/PI on ice for 20 min with occasional mixing. Following extraction, the sample was subjected to centrifugation at 8000 g for 15 min, at 4°C and the resulting supernatant containing membrane proteins, hydrophobic proteins associated with the membrane and proteins that interact with membrane proteins, was collected and placed on ice. The resulting pellet was washed twice with PBS-PI prior to extraction in 200 µL of 4% Sodium Dodecyl Sulphate (SDS)/5 mM Tris·HCl/PBS/PI buffer for 10 min at room temperature. After centrifugation at 8000 g for 5 min, at 4°C the resulting supernatant containing the Triton insoluble proteins of the membrane, was collected and placed on ice. Laemmli buffer (BioRad) was added to all samples used for further western blot analysis.

2.4.6 Protein sample preparation for western blot analysis

About 0.5-1.0 mg of whole cell lysates were prepared by suspending $4x10^7$ purified parasites or 10-15 midgut tissues or 20-30 µL of mosquito haemolymph collected from 20-30 mosquitoes in 150 µL, 200 µL and 20-30 µL RIPA whole cell lysis buffer (Sigma), respectively, supplemented with 10 µg/mL (1X) PI. Following centrifugation for 15 min at 10000 g and 4°C, the supernatant was mixed with Laemmli buffer. Protein samples were boiled under non-reducing or reducing (+ 3-5% v/v 2-mercapthoethanol) conditions at 95°C for 10 min, prior to storage at -80°C.

2.4.7 Genomic DNA isolation

P. berghei gDNA was prepared from 200 µL samples of mixed blood stage parasites (parasitaemia 5-7%) using the DNeasy Blood and Tissue kit (QIAGEN), according to manufacturer's instructions. The gDNA in the end, was eluted in 30 µL water.

2.5 Generation of transgenic parasites

The *ΔAQP2*, *AQP2-3HA*, *ΔN38*, *N38-3HA*, *ΔN350* and *N350-3HA* transgenic parasite lines were generated based on the transfection protocol of (Janse *et al.*, 2006b).

2.5.1 Preparation of DNA for transfections

The PlasmoGEM vectors were prepared for transfection using the Qiagen HiSpeed Plasmid Midi Kit (100 mL cultures grown over-night in 50 µg/mL ampicillin LB medium). All constructs were then linearised prior to transfection by single restriction enzyme digests using NotI (NEB) in order to release the disruption cassette (upstream homology region– *Tg*DHFR/*Ts*-downstream homology region). Linear constructs were purified by ethanol precipitation (J. Sambrook, 2001) and 3-5 µg of DNA in a volume of 5-10 µL molecular biology water was used for each transfection.

2.5.2 Schizont cultivation

Blood was collected on day 1-2 of infection (parasitaemia less than 5%) from three anaesthetised CD1 mice, previously infected with *P. berghei* ANKA *c507* (mechanical passage number <2) parasites to serve as a source of blood stage parasites. At the time of blood collection, the majority of the parasites (80-90%) were at the early trophozoite (ring) stage. The blood was then transferred to a T25 culture flask including 120 mL of 75% (v/v) schizont culture medium RPMI1640 pH 7.2 (RPMI1640, 24 mM L-glutamine, 25 mM HEPES, 0.2% (w/v) NaHCO3 (Gibco), 50 U/mL penicillin, 50 µg/mL streptomycin) and 25% (v/v) FBS. The culture was gassed with 5%CO2, 5% O2 and 90% N2 and incubated overnight shaking gently at 37°C.

2.5.3 Purification of viable schizonts

Following 22-26 hours of cell culturing and prior to starting transfections, the schizont maturation and quantity was assessed on a Giemsa stained smear of the culture. If large mature schizonts were not readily detectable, culturing was continued for at least 2 more hours until re-assessment of their morphology. The schizont culture content was pelleted at 180 g for 15 mins and schizonts were purified on a 15.2% (v/v) Nycodenz/PBS density upon centrifugation for 30 min at 300 g. Those accumulated at the interface between the resulting two layers were collected, washed in 20 mL culture medium and centrifuged again at 300 g for 8 min. The pellet was re-suspended in schizont culture media, split into 1 mL aliquots and spun down for 1 min at 200 g.

2.5.4 AMAXA transfection procedure

Following schizonts purification, the pelleted cells were re-suspended in 100 µL of AMAXA supplemented nucleobuffer (AMAXA) containing about 5 µg of the DNA (in less than 10 µL per transfection) which is to be transfected. The DNA/buffer/parasite solution was transferred to an electroporation cuvette (AMAXA) and electroporation was performed according to manufacturer's instructions (Protocol U33; AMAXA). 150 µL of uninfected mouse blood (obtained from a PH treated mouse on day 2-3 after treatment; 125 mg/kg body weight) was added to the electroporated parasites. The parasites were incubated at 37ºC for 20-25 min in order to allow invasion of merozoites into the erythrocytes and, prior to injection of the suspension (IP) into a new mouse.

2.5.5 Pyrimethamine-based selection of transgenic parasites

One round of selection of pyrimethamine-resistant parasites were performed by administration of 0.07 mg/pyrimethamine (Sigma) in the drinking water.

2.5.6 Limited dilution cloning of transgenic parasites

Transgenic parasite populations were obtained by limited dilution cloning as previously described (Waters *et al.*, 1997). Briefly, blood stage parasites were enumerated in stained tail blood smears from infected mice and diluted in RPMI medium to a final concentration of 20 parasites/mL, prior to IP injection (200 µL) into CD1 mice.

2.5.7 Genotypic analysis of transfected blood stage populations

P. berghei gDNA was prepared from infected mouse blood prior to genotypic analysis. To determine whether parasites surviving the drug selection carried integrated disruption constructs, diagnostic PCRs were performed in order to confirm that parasites encompassed the modified locus and that no contamination with the WT locus is present. The specific primers pairs are indicated in **Table 2.3**.

2.6 Generation of transgenic parasite pools and Illumina sequencing

Protocols were optimised based on protocols previously reported in (Gomes *et al.*, 2015; Bushell *et al*., 2017). Generation of the transgenic parasite pools was carried out by Dr. Ana-Rita Gomes at the Wellcome Sanger Institute, whereas mosquito infections and tissue collection were carried out at Imperial College London.

2.6.1 PlasmoGEM vectors preparation and parasite transfection

To generate pools of mutants for phenotyping by barcode counting, equal amounts of each vector were combined, and the mixture was digested with NotI in order to release the targeting vectors from the bacterial vector arms. A total of 5-8 µL of the digested vector mix, typically containing 100 ng of DNA for each vector, was used per transfection. Experiments with single vectors used 2 µg of *Not*I-restricted DNA per transfection. *Plasmo*GEM identification numbers for vectors used in this study are listed in **Appendix 5**. Transfections were done by electroporation of purified schizonts as described (Janse *et al*., 2006b), with the following modifications; parasites for the schizont culture were from female Wistar rats (200–250 g) (Harlan, UK), to achieve maximal transfection efficiency, and were cultured for 21 hours before schizonts were isolated on a 55% Nycodenz/PBS cushion. Isolated schizonts were then washed in complete media and electroporated using the 4D Nucleofector System (Lonza) in 16-well strips according to the pulse program FI-115. Following, the transfection cocktail with the manipulated parasites were inoculated into Balb/C inbred mice and monitored daily from day-5 post infection onwards, upon observation of blood stage parasites.

Table 2.3. Genotypic analysis primers of *P. berghei* transgenic lines	
Primer Name	**Primer Sequence**
Pb AQP2 KO QCR1	TCAACAATGCCCTTGCCTCA
Pb AQP2 KO QCR2	TCATTCTACGCTTTATTAACTCA
Pb AQP2 KO GT	TTGTGTTAGCTCTCTTGCCT
Pb N38 KO QCR1	TGAATGAACCTATCCCCTGCGT
Pb N38 KO QCR2	TCCCCACCTTTTCCTTCCCT
Pb N38 KO GT	ATTGCACGTTGAATATGCCA
Pb N350 yFCU KO FWD	AAGTGTTCTCGGTCGTGGTC
Pb N350 yFCU KO REV	ACACCCAGAGGTACTGATGGA
Pb N350 hDHFR KO FWD	AGGAAGCCATGAATCACCCAG
Pb N350 WTin KO FWD	CATGATGAAATGCTACAAAAATTTA
Pb N350 WTin KO REV	CCTGAGCAAAACCCAAAAGGATCCA
Pb N350 WTout KO FWD	TGCAATTGTTGGGGCCTTTT
Pb N350 WTout KO REV	TGCTTGTTGAGGTACTTGTGGA
Pb AQP2 TAG GOI/3HA FWD	CATATGGATACCGCGGCAAG
Pb AQP2 TAG GOI/3HA REV	GGATTGGGCCATATGCTGGA
Pb AQP2 TAG hDHFR FWD	CAGCGACGATGCAGTTTAGC
Pb AQP2 TAG hDHFR REV	TGGATCAGCTTGTGCGACAT
Pb AQP2 TAG WT FWD	TGACAAGAAAAAGGTGGCAT
Pb AQP2 TAG WT REV	TGGATCAGCTTGTGCGACAT
Pb AQP2 TAG up/3HA FWD	CATATGGATACCGCGGCAAG
Pb AQP2 TAG up/3HA REV	TGCGATGATTATATGTGCATAAGGA
Pb N38 TAG GT	TCCCCACCTTTTCCTTCCCT
Pb N38 TAG QCR1	GGCTACATCCTCTGTTTGGGAAGTGG
Pb N38 TAG QCR2	ACCAGCACTCGGAATTGCCA
Pb N350 TAG GOI/3HA FWD	CAGGAACATCTTTAAGGGTATGCT
Pb N350 TAG GOI/3HA REV	AAACGGGGCCCTTATGC
Pb N350 TAG hDHFR FWD	TCCATCAGTACCTCTGGGTGT
Pb N350 TAG hDHFR REV	CAGCGACGATGCAGTTTAGC
Pb N350 TAG WT FWD	TCCATCAGTACCTCTGGGTGT
Pb N350 TAG WT REV	TGAGCTTGAAAACAAAACGGCA
Pb N350 TAG up/3HA FWD	GCTGTCAAAGCATGGGCATT
Pb N350 TAG up/3HA REV	AAAACGGGGCCCTTATGC
GW2	CTTTGGTGACAGATACTA
GW1	CATACTAGCCATTTTATGTG
Pb c01 INT FWD	GGATGTATTCCTATAACTATGTG
Pb c01 WT REV	CTCCTTGTATGTTGCTGCTGG
Pb c43 INT FWD	GATCGAAATAATTTTGAATAAG
Pb c43 WT REV	GTACTACTTCACCTGTATTACCAG
Pb P47 INT FWD	ATACAGTAACGCAACGTCG
Pb P47 WT REV	CGCCTAGGCTAGGAAGATGATATTTTTAATTCC
Pb P47red KO FWD	CTTTCCCGACGTCGTTCCG

Pb c57 INT FWD	GATGTCTAGCTA ATTTGGGAATTAGTG
Pb c57 WT REV	GCATTATCTCTATC TTCATAATTTG
Pb P48/45 INT FWD	GGGTATAATATTGCTTAAGCTTAG
Pb P48/45 WT REV	CAAACAAGTAAGGGTATTTTTGATC
Pb PIMMS2 INT FWD	AGCGTCTAGTAGTTTGAGCTAGCTA
Pb PIMMS2 WT REV	GCAATATCAGCGTCATCAGAA
TgDHFR-Ts 5'UTR REV	GATGTGTTATGTGATTAATTCATACAC
Pb c43 WT FWD	GGATCCTTTGGATTGGTCTTTTCCCATAAAG
Pf c43 INT REV	TCCTCTCCGTGACGTTGGCCATCATCTTTG
Pb c43 WT FWD	GGATCCTTTGGATTGGTCTTTTCCCATAAAG
Pb c43 WT REV	GTACTACTTCACCTGTATTACCAG

Gene-specific forward (Integration; INT) primers situated upstream of the target site for homologous recombination, in combination with the WT for the knocked-out gene or *Tg*DHFR reverse primers, were used. Forward (FWD), Reverse (REV). For genotyping the transgenic lines generated using the PlasmoGEM vectors, the GT primer together with the primer GW2 or GW1 and the QCR2 primers together with the primer GW2, were used. To detect the WT locus, the QCR1 and QCR2 primers were used. The PlasmoGEM provided GW, QCR1, QCR2 and GT primers were not conclusive for N350, so custom primers were designed for detection of the integrated construct; specific for the integrated drug selection cassettes yFCU and *h*DHFR, the WT homology region present in both WT and the partial KO mutant line (WTin) and the segment of the wild type gene replaced in the KO line (WTout).

2.6.2 Genotyping

To verify vector integration by diagnostic PCR on parasite gDNA, target gene-specific primers were designed to map to the chromosomal region just outside of the short homology arm of the vector (**Table 2.4**) and paired with a primer annealing to the *h*DHFR/yFCU cassette within it. Vector designs, primer, and barcode sequences can be also viewed in a searchable database at http://plasmogem.sanger.ac.uk.

2.6.3 gDNA extraction from infected *A. coluzzii* mosquito tissues

Following *A. coluzzii* mosquito infections, infected midguts and salivary glands were dissected at day-15 and day-21 pbf. gDNA was then extracted using a phenol/chloroform method. Briefly, mosquito tissue was lysed in a lysis buffer (1% v/v TritonX-100, 50 mM Tris-HCl pH 8.0, 150 mM NaCl, 1X PI) supplemented with 20 mg/mL Proteinase K for 1 hour at 37°C, prior to chloroform/phenol extraction. Following centrifugation at 10000 g for 10 min at 4°C, gDNA was washed twice with 70% (v/v) ethanol. The pellet was air-dried and finally resuspended in 20-30 µL water.

Table 2.4. Primer sequences specific for the PlasmoGEM barcoded mutants. Genotyping primer (GT), Generic primer (GW1 or GW2)

.Primer Name	Primer Sequence
PBANKA_111920 GT	TGTGCACGTGCGTTAGTGGGA
PBANKA_145770 GT	TCACGCCGTTTGATCAGGTT
PBANKA_135960 GT	AGCTTTTGAGAGCCAATCACGT
PBANKA_011110 GT	TGGCTGCGCATAACGTTCCA
PBANKA_030610 GT	GGACACGCACGTACAGGGCC
PBANKA_110760 GT	ACTGCTCGAATACCCCAAGTCCCA
PBANKA_100220 GT	TGCATAAACCCGAAGTGTGCA
PBANKA_135970 GT	AGAAAAGGGACACACACGGCA
PBANKA_100210 GT	TGCCCACTAGTCGGATTTTTGGT
PBANKA_030600 GT	AGGAACAATATGGCTGTTCAATGCC
PBANKA_080810 GT	AGCGTAATGAGGCAGTGAAGGT
PBANKA_100260 GT	CCTCGTTTTCCGTTGTGCTTCCA
PBANKA_142590 GT	TTTGTGCACGCAGATGCATT
PBANKA_081070 GT	TGCCTCTTCCTATGAGACTGA
PBANKA_083040 GT	TCCTGATCCATACCGTGAAATCG
PBANKA_103780 GT	TTTCCCACTGCGTACCCTTT
PBANKA_110690 GT	AGTGTGTGTTTGCATGCTCGA
PBANKA_122540 GT	AGCCCCTGAATCGCCACAAGA
PBANKA_135380 GT	CGACCCCCTATCTAGCGACCCA
PBANKA_060390 GT	ACCTTCCTGGGTCGCGGAAA
PBANKA_072090 GT	TGTTGCATGTGGGGATTACCA
PBANKA_133810 GT	ATTGCACGTTGAATATGCCA
PBANKA_091910 GT	TGCAGCTTTGACATTTGCAGA
PBANKA_142710 GT	TTGTGTTAGCTCTCTTGCCT
PBANKA_114540 GT	TCGATGGGTTGCTACGCTTCGT
PBANKA_134980 GT	TGGGTAGGGGAAATTGTCTTACCCA
PBANKA_041350 GT	ACAGCTGCAAAAATGGAGACGCA
PBANKA_100240-tag GT	ACAAAACTCGAAACACCGAAGA
PBANKA_145120-tag GT	TGCACAATTCTACATGAGCATGTCA
PBANKA_051490-tag GT	AGGATTCCGTGAATGATCCCCCA
PBANKA_030600-tag GT	AGGAACAATATGGCTGTTCAATGCC
PBANKA_041040-tag GT	ACATTCACCCCCTTTGTGTT
GW1	CATACTAGCCATTTTATGTG
GW2	CTTTGGTGACAGATACTA

2.6.4 PCR-based library preparation and barcode sequencing

To amplify all the barcodes from the extracted gDNA samples, 50-100 ng of each DNA sample served as template for a PCR reaction using Advantage 2 Taq polymerase (Clontech) with the primers arg00444 and arg00445 (Gomes *et al*., 2015) (1× 95°C/5 min denaturation, 35 × 95°C/30 s, 55°C/20 sec, 68°C/8 sec, 1 × 10 min at 68°C), which bind to the constant annealing sites flanking each barcode. The reactions occurred in

25 µl, under the following conditions: 0.4 µM of arg00444 and arg00445, 2.5mM of each dNTP, 1X Advantage 2 Buffer (Mg^{2+}), 0.5 U of Taq polymerase. The 167 bp amplicon was further extended in a second PCR reaction using oligonucleotides that in their 5′ extensions introduce Illumina adaptors and sample-specific barcodes. Therefore, with the second PCR reaction universal adapter sequences and sample-specific index tags are added to the previously amplified barcodes (**Figure 2.2**).

For sample-specific indexing, 5 µL of the first amplicon served as a template for further ten amplification cycles (1 × 95°C/2 min, 10 × 95°C/30 sec, 68°C/15 sec, 1 × 5 min, 68°C) using one generic oligonucleotide and one of a set of sample-specific indexing oligonucleotide. A total of 100 ng of each sequencing library was pooled and quality control by quantitative PCR was performed in order to validate the presence of the sequencing adaptors. Due to low complexity, PCR amplicon libraries had to be diluted to 4 nM before loading the flow cell of a MiSeq instrument (Illumina). Libraries were then sequenced using MiSeq Reagent Kit v2 (300 cycle) from Illumina (MS-102-2002).

Using a Perl script previously developed by Frank Schwach (Schwach *et al.*, 2015), barcode sequences were extracted from the sequencer output, counted and the relative abundance of each barcode within the pool was determined. Each barcode abundance in midgut oocyst and salivary gland sporozoites samples were calculated by dividing the number of counts for the specific barcode with the total number of barcode counts in the sample. Any mutant with an abundance of less than 0.1% in the input sample was discarded from subsequent analysis (and abundances recalculated for remaining mutants) (Bushell *et al.*, 2017).

Statistical significance was calculated for each barcode against the normal-growth reference vectors using a two-tailed *t*-test (unequal variance, p values adjusted according to the false discovery rate method) (Gomes *et al.*, 2015).

Figure 2.2. PCR-based library preparation method. Two rounds of PCR ensure both barcode amplification from the gDNA samples and addition of the barcode-specific Illumina adaptors required for sequencing. The index tag added following the second PCR is barcode specific therefore, allowing individual quantification.

2.7 Phenotypic analysis of mutant parasite lines

2.7.1 Exflagellation assays

Exflagellation assays were performed by mixing equal parts of parasite infected tail blood with ookinete culture medium. Following 10 min incubation at room temperature, exflagellation was observed at 400X magnification in a standard haemocytometer (Hausser Scientific, USA). The number of exflagellation centres and total number of RBC were counted (proportion of exflagellating male gametocytes) and were directly compared to the total male gametocytaemia (total proportion of male gametocytes) as determined by Giemsa stained tail-blood smears, processed at the same time.

2.7.2 Mosquito midgut sample preparations for enumeration and imaging

Following dissection, midguts were fixed in 4% formaldehyde (v/v) (16% methanol free, Polysciences Inc.) for 20 - 45 min at room temperature and washed three times for 10 min each in PBS, prior to mounting in Vectashield® (VectorLabs) on glass slides under sealed coverslips. Slides were stored in the dark at 4ºC until processing. *GFP*-expressing oocysts had to be visualised in less than a week, since dissected.

2.7.3 Ookinete enumeration

2.7.3.1 Ookinete imaging

In vitro cultured ookinetes or midgut invading ookinetes were mounted on a microscope slide and covered by a Vaseline-sealed cover slip prior to imaging.

2.7.3.2 Gametocyte-to-ookinete conversion assay

For *in vitro* assays, 100 µL of a 22-24 hours *in vitro* ookinete culture was pelleted, washed in PBS and resuspended in RPMI 1640 (Sigma). For *in vivo* assays, the blood bolus of 10 mosquitoes at 17-18 hours pbf was pelleted, washed in PBS and resuspended in RPMI 1640. The suspension was incubated with a Cy3-labeled P28 (13.1) monoclonal antibody (1:50 dilution) for 20 min on ice. Conversion rates were calculated as the percentage of P28-positive ookinetes to the total number of P28-positive macrogametes and ookinetes.

2.7.3.3 Ookinete invasion assays

To determine the number of ookinetes invading *A. coluzzii* midgut epithelium, infected midguts were dissected at 24-25 hours pbf and the blood bolus was washed off prior to fixation of the midgut epithelium alone in 4% formaldehyde/PBS for 45 min, at room temperature. Following three 10 min washes in PBS, midguts were blocked and permeabilised in 1% Bovine Serum Albumin (BSA) (Sigma), 0.2% Triton X100 in PBS (pH 7.4) for 2 hours at room temperature. Staining of the ookinetes was based on the detection of P28; an ookinete-surface protein of *P. berghei* (Sidén-Kiamos *et al.*, 2000). P28 was detected using a Cy3-labeled anti-P28 mouse monoclonal antibody (13.1) at 1:1000 dilution, diluted in 1% BSA-0.2% Triton X100 in PBS buffer (pH 7.4). Following overnight incubation at 4^{o}C in the dark, midgut tissues were mounted in ProLong antifade mounting medium (ThermoFisher Scientific) prior to DAPI staining at 1:1000 dilution in PBS for 5 min, at room temperature. Visualisation of the ookinetes was performed using fluorescence microscope at X200 magnification.

An alternative protocol of ookinete invasion assay is by determining the number of melanised ookinetes formed, following *CTL4*-silencing (Ecker *et al.*, 2008). *CTL4*-silencing leads to melanisation of ookinetes at the midgut sub-epithelial space upon epithelium traversal thus, providing a powerful mean to enumerate ookinetes that traversed the midgut wall. *CTL4*-silenced mosquitoes were infected with *P. berghei*, at day-3 post dsRNA-silencing. At day-4 or day-7 pbf following midgut dissections, melanised parasites were visualised and enumerated using light microscopy.

2.7.4 Oocysts enumeration and size analysis

2.7.4.1 Oocysts imaging and enumeration

P. berghei infected midguts were obtained from *A. stephensi* or *A. coluzzii* mosquitoes at 3-15 days post infection. Mosquito midguts were fixed in 4% (v/v)

paraformaldehyde/PBS (ThermoFisher) for 30-45 min prior to a 10 min wash in PBS and mounted on microscopy slides with Vectashield (Thermofisher). Oocysts were then enumerated at X100 (fluorescence microscopy; *Pbc507* GFP reference lines). Counting was conducted with the aim of using a minimum of 30 mosquito midguts per parasite genotype or mosquito immune background per replicate. Imaging was performed at X100 and X630 magnification using light and fluorescence microscopy.

P. falciparum infected *A. coluzzii* midguts, prior to fixation in 4% (v/v) paraformaldehyde/ PBS, were stained with 0.5% (v/v) mercurochrome/PBS for 10 min and washed twice in PBS for 30 min. Guts were then mounted on glass slides in 80% glycerol and examined under a light microscope (X200) for oocyst presence.

2.7.4.2 Oocyst size measurements

Oocyst size was measured from fluorescence microscopy images of previously fixed infected mosquito midguts, captured at X100 magnification. Images were then imported to ImageJ 1.38x (http://rsbweb.nih.gov/ij/), converted to 32-bit binary images and oocyst size was measured in arbitrary units using the Analyse Particles tool.

2.7.5 Midgut and salivary gland sporozoites enumeration

Midgut and salivary gland sporozoite numbers were calculated from homogenates of *P. berghei* infected *A. coluzzii* midguts or salivary glands, assayed in three batches of ten to fifteen at day-15 and day-21 pbf, respectively. Dissected midguts or salivary glands were immediately transferred to a 0.1 mL tissue homogenizer (Jencons England, VWR) using a Hamilton syringe (Hamilton Company Ltd.), mechanically homogenised and loaded onto a FastRead-102 counting slide (Immune Systems Ltd.). The final volume was carefully measured using a Hamilton syringe, followed by the calculation of the total number of sporozoites per ten to fifteen mosquitoes using a compound light microscope at X400 magnification.

2.7.6 Transmission to mice

Sporozoite infectivity was assayed by bite-back experiments, where 25-30 *P. berghei* infected mosquitoes (at day-21 pbf) were allowed to feed on anaesthetised c57BL/6 or Balb/C mice for 15-20 min. The mice were then allowed to recover and parasitaemia was monitored on day 5, 7, 10 and 14 following the receipt of potentially infective sporozoites. Infected mice were immediately culled upon detection of blood stage parasites on Giemsa stained tail blood smears, or if remaining uninfected, at the endpoint of the experiment (day-14). Directly after blood collection, gDNA was

extracted and genotypic analysis was performed in order to confirm at first successful transfection and following dilution cloning, that complete replacement of the WT with the modified locus has taken place in the parasite genome.

2.7.7 Genetic crosses

Genetic crosses between different transgenic KO parasite strains were carried out by infecting mice with the different combinations of KO parasite lines. To monitor that the parasitaemia/gametocytaemia is similar between the two lines, similar number of infected RBCs were inoculated in each mouse. *A. coluzzii* mosquitoes were then infected by directly feeding on mice harbouring mixed infections.

2.8 qRT-PCR and RT-PCR analysis

2.8.1 DNeasy treatment and cDNA synthesis

About 1 µg of total RNA was treated with 2 U Turbo^{TM} DNase (Ambion Inc.) for 45 min at 37^{o}C, to remove residual gDNA contamination. Treatment and subsequent DNAse inactivation was performed according to manufacturer's instructions. Subsequently, reverse transcription of total DNase-treated mRNA was obtained for each sample (PrimeScript RT Kit, Takara). The reactions occurred in 20 µl, under the following conditions: 1µg DNase-treated mRNA, 1X PrimeScript Buffer, 25 pM Oligo dT Primer, 200 pM Random 6mers, 1 µL PrimeScript RT Enzyme Mix and incubated for 15 min at 37°C and 5 sec at 85^{o}C. For each reverse transcription reaction, a non-RT and a non-template control reaction was always produced in parallel for each sample, separately. cDNA samples were stored at -20°C, until further processing.

2.8.2 Gene expression analysis by qRT-PCR

qRT-PCR was carried out using 7500 Fast Real-Time PCR System and SYBR Green PCR Mastermix (Applied Biosystems). All reactions were run in triplicates and the final transcriptional profile was generated from the average of three biological experiments. Expression ratios were calculated using primer efficiencies that were determined by amplification of serially diluted targets and transcriptional profiles were presented with values for all time points, calibrated against the time point with the lowest expression level. Two negative controls were used: an RNA-control, to control for environmental contamination, and a reverse transcriptase-control, to control for gDNA contamination (except where the target was DNA). For the analysis, all *P. berghei* gene specific transcript levels were normalised against *eef1-α* driven *eGFP* expression, whereas the *P. falciparum* gene specific transcript levels were normalised against that of *arginine-*

tRNA ligase (*tARG*) (PF3D7_1218600) (Neveu *et al*., 2018). Finally, the *A. coluzzii* ribosomal protein encoding gene S7 (AGAP010592) was used to normalise the transcript levels of specific genes. Expression ratios were calculated as follows:

$$\text{Expression Ratio} = \frac{\text{Primer efficiency } (eGFP, tARG, S7)^{\,\text{Ct}(eGFP,\, tARG,\, S7)}}{\text{Primer efficiency target gene}^{\,\text{Ct(target gene)}}}$$

2.8.3 Gene expression analysis by semi-quantitative RT-PCR

Total RNA and cDNA from purified parasites or mosquito midgut and salivary gland tissues were prepared as described above. Semi-quantitative RT-PCR was performed using the GoTaq Green DNA polymerase master mix (Promega). Gene specific RT-PCR primers were manually designed with a Tm of 55-58^{o}C and an amplicon length of 0.6-1.0 Kb (**Table 2.5**). Semi-quantitative RT-PCR products were then analysed using standard gel electrophoresis run with TBE buffer (Sambrook and Russell, 2001).

Table 2.5. Primer sequences for RT-PCR. Forward (FWD), Reverse (REV)

Primer Name	Primer Sequence
Pb P28 FWD	AATGCACAGGTACAGGAGAAACTAAAT
Pb P28 REV	CACACTCATAATGTTTTCCAGTCAATT
Pb CTRP FWD	AGAGAAGAAGATTGCCCAACAG
Pb CTRP REV	ATCGGATCATTTGCATCGATAAC
Pb GFP	CCTGTCCTTTTACCAGACAACCA
Pb GFP	GGTCTCTCTTTTCGTTGGGATCT
Pb AQP2 FWD	ATGCAAAATATGCGATAAAGGCA
Pb AQP2 REV	TCATCGATGTCTTTCGTGAGT
Pb N38 FWD	CGCAGGGGATAGGTTCATTCA
Pb N38 REV	CCCAAACAGAGGATGTAGCCA
Pb N350 FWD	ACGTGTACAGTTAGGATGGGGT
Pb N350 REV	AAATGGTGTTAGGCGCAGAT
Pb c01 FWD	TCGCTTTATTGTTTACCATAGCATCC
Pb c01 REV	TGTATGTTGCTGCTGGATTTTGTT
Pb c43 FWD	ATACGGGAATCCATCAACCA
Pb c43 REV	ACTTCAAACGACCCTTGTGC
Pb P47 FWD	TCAGATTATATTGCCTTGGTATGC
Pb P47 REV	AGTGAACCTACTTGTGTACTACG
Pb c57 FWD	GCAGGCTGTTTCGTATGTTGTATT
Pb c57 REV	TGTCTTTAAAAGCTTGTGCCCATT
*Pf s*16 FWD	GGTGCCTCTCTTCATGCTGT
Pf s16 REV	CTCCTTCGTCTCCTTCATCTGT
Pf s25 FWD	GCGAAAGTTACCGTGGATACTG
Pf s25 REV	ACTCCAGTTTTAACAGGATTGCT
Pf CTRP FWD	TGGAGTGGTATTGCCACCAG
Pf CTRP REV	ATTCGGTTCCACTGCAAGGT
Pf CSP FWD	TGGACAAGGTCACAATATGCCA
Pf CSP REV	ACGACATTAAACACACTGGAACA
Pf AQP2 FWD	TTTGGTGGTATCGTTGCCAGT
Pf AQP2 REV	AGCATTTTGCTTTGCGCTGT
Pf N38 FWD	TTTCCCAAGGGAATACACAAAGGT
Pf N38 REV	CCACTTCCCAAACTGCCGAT
Pf N350 FWD	TGAGGAAGGATGAATCTGAGATGA
Pf N350 REV	TGTGGACACAATAATCGACACG
Pf c01 FWD	CCGTTTCGTTGTATTATGTCCCA
Pf c01 REV	AAGACTTTGCTTAAACGACTGGA
Pf c43 FWD	GCAGACAACGGAATTCACAACA
Pf c43 REV	CCCGTTCTTTGTTCACTGGC
Pf P47 FWD	CTGTGATTTTAAATTCAAC
Pf P47 REV	ACAGCGCACACAAATTAGA
Pf c57 FWD	TGCACATACATCCGCAAAGT
Pf c57 REV	TGCACATAAGCGTCTAAAGGGT
*Pf Pb(f)*c43 FWD	GTTGATATAAAACAAGATGATTTTACTAATGG
*Pf Pb(f)*c43 REV	GAAATATTTTATACTAGAATATATGGAAGAACCAAACAT

2.8.4 Quantification of parasites KO and WT alleles using gDNA pools

For quantifying the abundance of the *c01*, *c43*, *P47*, *c57*, *P48/45* and *PIMMS2* KO and WT alleles (Chapter 4), *Plasmodium* gDNA was extracted from blood stage parasites (see above) and qRT-PCR was performed using SYBR Green PCR Mastermix (Applied Biosystems), as previously described. Primers were designed using the web-interface of Primer-BLAST (NCBI) according to the following specifications: primer length 20bp, GC-content 40-80%, Tm 58-60^{o}C and amplicon length of 80-200 bp. Gene specific primers are listed in **Table 2.6** and **2.7**.

2.9 *Pb*c43 and *Pb*P47 protein expression for antibody serum purification

Pbc43 and *PbP47* genes were engineered to contain codons allowing optimal expression in *E. coli. Pbc43* and *PbP47* fragments lacking the signal peptide and the C-terminal hydrophobic domain were PCR amplified and cloned by infusion cloning into the NotI site of the pET-32b plasmid, that carries N-terminal hexahistidine and thioredoxin tags (Novagen). Cloning work was carried out by Dr. Hassan Yassine (pET-32b: *Pb*P47-SP/TM) and Dr. Valerie Ukegbu (pET-32b: *Pb*c43-SP/TM).

For protein expression and purification, transfected shuffle T7 *E. coli* cells (NEB) were grown at 30 °C until OD reached 0.6-0.8 at 600nm, induced with 1mM isopropyl-1-thio-β-d-galactopyranoside (IPTG) at 19 °C for 16 hours on a platform rocker, collected by centrifugation, lysed using Bugbuster-Lysonase (Novagen) and supplemented with a protease inhibitors cocktail (cOmplete EDTA-free, Roche). Cell debris was removed by centrifugation at 8000 g for 10 min. The insoluble fusion proteins, both for *Pb*c43 and *Pb*P47, were extracted from inclusion bodies using the inclusion body solubilisation reagent (ThermoScientific), purified by cobalt affinity chromatography using TALON metal affinity resins (Clontech) under denaturing conditions in 8 M Urea in PBS (pH 7.4) and eluted using 250 mM imidazole in PBS (pH 7.4). Protein refolding was achieved by stepwise decrease of Urea concentrations in PBS. Protein samples were analysed by SDS-PAGE and western blots to determine purity. The purified proteins were subsequently used to purify polyclonal antibodies from pooled sera of two immunised rabbits (Eurogentec) using the AminoLink® Plus Couplin Resin Kit (ThermoScientific) according to manufacturer's instructions. Protein expression and purification was carried out using protocols previously developed by Dr. Hassan Yassine and Dr. Valerie Ukegbu, as described in (Ukegbu *et al.*, 2017b; 2020).

Table 2.6. Primer sequences for qRT-PCR. Forward (FWD), Reverse (REV)

Primer Name	Primer Sequence	Optimal Primer Concentration
Pb P28 FWD	AATGCACAGGTACAGGAGAAACTAAAT	500nM
Pb P28 REV	CACACTCATAATGTTTTCCAGTCAATT	500nM
Pb CTRP FWD	GGTGATAGTAGTGAAGGTTTTGG	500nM
Pb CTRP REV	TTCCATATTAGAGTTATGTGGTG	500nM
Pb CSP FWD	GAATTCGTTAAACAGATCAGGGATAGTA	500nM
Pb CSP REV	TTATACCAGAACCACATGTTACGTTACA	500nM
Pb GFP	CCTGTCCTTTTACCAGACAACCA	400nM
Pb GFP	GGTCTCTCTTTTCGTTGGGATCT	400nM
Pb Tub FWD	TTTTGCCTAGAACACGGAATCC	400nM
Pb Tub REV	ATCATCACCACCTGCCACAA	400nM
Pb AQP2 FWD	TGAGGCAAGGGCATTGTTGA	500nM
Pb AQP2 REV	TGGTAACTTCATCCTCTTCCCT	500nM
Pb N38 FWD	TACCGAGGCGGAATGCAAAA	500nM
Pb N38 REV	ACAGGCACATAGAACAGCCAT	500nM
Pb N350 FWD	AGGCTGGCAATCTTGTAACCA	500nM
Pb N350 REV	TGGGGTGAAAGCATTCTACAAG	500nM
Pb c01 FWD	ATTTTAATGGAACAGAAAATGCAGCC	500nM
Pb c01 REV	GAATAATCTCCTTGTATGTTGCTGCT	500nM
Pb c43 FWD	TTGAATTAGCACAAGGGTCGTTTGAA	500nM
Pb c43 REV	CTTCTTTAGCTGGGGTATTATCGTGC	500nM
Pb P47 FWD	ATCTGAAGACAGCGCACACA	500nM
Pb P47 REV	AGCTCGCGTTTTGTTTTGGA	500nM
Pb c57 FWD	GTGGAAATAAAGGCGATGCACAAAAT	500nM
Pb c57 REV	TGGTTATGGTACTATGTGCTGTTGGT	500nM
Pf ARG-tRNA FWD	AAGAGATGCATGTTGGTCATTT	500nM
Pf ARG-tRNA REV	GAGTACCCCAATCACCTACA	500nM
Pf AQP2 FWD	AGCATTTGCCGCAACTTTCC	500nM
Pf AQP2 REV	GCGCTGTTTTTATCTATTAACGGT	500nM
Pf N38 FWD	TGAACGAAGATACCACAGATTCCA	500nM
Pf N38 REV	TGTCCGGCTTTAATTTAGCGAC	500nM
Pf N350 FWD	AGAACCAGCAAAAGGACACAA	500nM
Pf N350 REV	TGTTGACAGAGAATGGTGGATGT	500nM
Ag S7 FWD	GTGCGCGAGTTGGAGAAGA	400nM
Ag S7 REV	ATCGGTTTGGGCAGAATGC	400nM
Ag SRPN6 FWD	CTTTGAAACCGATGGCACCC	500nM
Ag SRPN6 REV	ATTGTCCGGGGTTAGTGCAG	500nM
Ag LRIM1 FWD	AAGTTGACCGGCCAGAATGAGGAAG	500nM
Ag LRIM1 REV	GGCAGATCCTCGCAGCAGTACG	500nM
Ag APL1C FWD	GCTTCACTTTTTGGCGCT	500nM
Ag APL1C REV	CAGGCTGAGTTGAGACAGGA	500nM
Ag TEP1 FWD	AAAGCTAGCAATTTGTTGCGTCA	500nM
Ag TEP1 REV	TTCTCCCACACACCAAACGAA	500nM

Table 2.7. qRT-PCR primer sequences used for quantifying the abundance of the *P. berghei* c01, c43, P47, c57, P48/45 and PIMMS2 WT and KO alleles. Forward (FWD), Reverse (REV)

Primer Name	Primer Sequence	Optimal Primer Concentration
c01 KO FWD2	CGCTTTATTGTTTACCATAGCATCC	500nM
c01 KO 5UTR	GATGTGTTATGTGATTAATTCATACAC	500nM
c01 WT FWD	ATTTTAATGGAACAGAAAATGCAGCC	400nM
c01 WT REV	GAATAATCTCCTTGTATGTTGCTGCT	400nM
c43 KO FWD2	CTTAAAGGAATTTGTTATTGTTATTTTG	500nM
c43 KO REV2	CCAACTCAATTTAATAGATGTGTTATG	500nM
c43 WT FWD	TTGAATTAGCACAAGGGTCGTTTGAA	400nM
c43 WT REV	CTTCTTTAGCTGGGGTATTATCGTGC	400nM
P47 KO FWD2	CGACTATGAGCATATGGAAAAGG	400nM
P47 KO 5UTR	GATGTGTTATGTGATTAATTCATACAC	400nM
P47 WT FWD	TAGCAATGTTGGTGGCATTG	400nM
P47 WT REV	CTCTACCTATATGAACAGTGCA	400nM
c57 KO FWD2	CAAGCTGCTAATAGACACCTTAATA	500nM
c57 KO REV2	CATACACAAACATACAAAAATAAACAC	500nM
c57 WT FWD	GTGGAAATAAAGGCGATGCACAAAAT	400nM
c57 WT REV	TGGTTATGGTACTATGTGCTGTTGGT	400nM
P48/45 KO FWD	GTGAAAGGATTATTCAAATATCGCCAT	500nM
P48/45 KO REV	TTATTGTTGACCTGCAGGCATG	500nM
P48/45 WT FWD	TCCACCGAAGGAATTCATAA	400nM
P48/4 WT REV	TTTTGGGTCATCCTGTTTAGG	400nM
PIMMS2 KO FWD2	GCGTTGATGATAATATGTTTCAAAGGG	400nM
PIMMS2 KO 5UTR	GATGTGTTATGTGATTAATTCATACAC	400nM
PIMMS2 WT FWD	GATGTAACACCGAATGAGTCCA	400nM
PIMMS2 WT REV	CAGAACCACCTTCGTCACAATA	400nM
GFP FWD	CCTGTCCTTTTACCAGACAACCA	400nM
GFP REV	GGTCTCTCTTTTCGTTGGGATCT	400nM

2.10 Immunodetection methodology

2.10.1 Western blot analysis

All parasite samples were boiled for 5 min at 95^{o}C in Laemmli buffer in order to confirm protein denaturation. Multiple incubation times were tested for detecting *P. berghei* c43. For obtaining reducing conditions, +3-5% (v/v) 2-mercapthoethanol was added to the sample buffer prior to boiling. Samples under both reducing and non-reducing conditions were analysed. Subsequently, proteins were separated using a 4–20% gradient polyacrylamide gel electrophoresis (Mini-PROTEAN® TGX™ Precast Protein Gels, BioRad), according to methods previously described (Sambrook and Russell, 2001). Following semi-dry transfer at constant voltage (25 V) (Trans-Blot Turbo Transfer System, BioRad) to a polyvinylidene difluoride (PVDF) membrane (Trans-

Blot Turbo RTA Mini PVDF Transfer Kit, BioRad), membranes were blocked in 3% (w/v) semi skimmed milk powder (Sigma) in PBS/ Tween20 (0.05% v/v) (Sigma) buffer for 2 hours in room temperature. All secondary and primary antibodies (**Table 2.8**) were diluted in 3% milk PBS/Tween20 (0.05% v/v), except for the rabbit anti-HA antibody, which was diluted in 5% PBS/Tween20 (0.05% v/v).

Table 2.8. Primary and secondary antibodies used during western blot and immunofluorescence assays. Columns 2 & 3 indicate the dilution of the different antibodies in the blocking buffer

Primary Antibodies	**WB**	**IFAs**
monoclonal mouse a-*Pb*P28 (13.1; MR4)	1:5000	1:1000
polyclonal rabbit a-*Pbc*43 (Ukegbu *et al.*, 2020)	1:300	1:200
polyclonal rabbit a-*Pb*P47 (Ukegbu *et al.*, 2017b)	1:100	1:200
monoclonal mouse a-*Pb*CSP (3D11; MR4)	N/A	1:500
polyclonal goat a-GFP (Rockland Chemicals)	1:500	N/A
monoclonal rabbit a-HA (C29F4) (Cell Signalling)	1:300	N/A
rabbit antiserum a-*Pf*s16 (MR4)	1:400	1:200
monoclonal mouse a-*Pf*s25 (4B7; MR4)	1:250	1:300
monoclonal mouse a-*Pf*CSP (2A10; MR4)	1:300	1:200
polyclonal rabbit a-*Pf*c43 FL (Ukegbu *et al.*, 2020)	1:500	1:500
polyclonal rabbit a-*Pf*c43 P2 (Ukegbu *et al.*, 2020)	1:500	1:300
polyclonal rabbit a-TEP1 (Blandin *et al.*, 2004)	1:300	1:300
polyclonal rabbit a-LRIM1 (Povelones *et al.*, 2009)	1:500	N/A
polyclonal rabbit a-SRPN3 (Povelones *et al.*, 2009)	1:500	N/A
polyclonal rabbit a-SRPN6 (Abraham *et al.*, 2005)	N/A	1:400
Secondary Antibodies		
goat a-rabbit HRP (ThermoScientific)	1:10000	N/A
goat a-mouse HRP (Promega)	1:10000	N/A
donkey a-goat HRP (ThermoScientific)	1:10000	N/A
ALEXA FLUOR 647 goat a-rabbit 488 (LifeTechnologies)	N/A	1:1000
ALEXA FLUOR 647 goat a-rabbit 568 (LifeTechnologies)	N/A	1:1000
ALEXA FLUOR 568 goat a-mouse 568 (LifeTechnologies)	N/A	1:1000
ALEXA FLUOR 568 goat a-mouse 488 (LifeTechnologies)	N/A	1:1000

Primary antibodies were incubated on a rocker at 4ºC over-night. Incubation with the a-P28 monoclonal antibody was carried out for 2 hours, at room temperature. Secondary antibodies were incubated for 1 hour on a rocker, at room temperature.

Membranes were washed with 0.05% PBS-Tween20 (v/v) three times for 10 min each, between primary and secondary antibody incubation and following secondary antibody incubation. Blots were then developed by enhanced chemiluminescence (ECL) using the ECL Plus Western Blotting Detection Reagents (GE Healthcare), in which the membrane was soaked for 5 min prior to imaging analysis.

2.10.2 Immunofluorescence assay (IFA)

For immunofluorescence (IFAs) assays on purified ookinetes and midgut and salivary gland sporozoites, parasites were re-suspended after collection in RPMI:FCS (1:1), smeared onto glass slides and air-dried prior to fixation in 4% formaldehyde/PBS (16% stock solution; Sigma) for 30 min at room temperature. For IFAs on ookinete invaded *A. coluzzii* midgut epithelium, infected midguts were dissected at 24-25 hours pbf and the blood bolus was removed prior to fixation in 4% formaldehyde/PBS for 45 min, at room temperature. Following three 10 min washes in PBS, midguts and purified ookinetes and sporozoites were blocked and permeabilised in 1% Bovine Serum Albumin (BSA) (Sigma), 0.2% Triton X100 in PBS (pH 7.4) for 2 hours at room temperature. All secondary and primary antibodies (**Table 2.8**) were diluted in 1% BSA/0.2% TritonX100/PBS at 4ºC over-night. When non-Triton-treated samples were needed, samples were blocked in 1% BSA/PBS for 2 hours at room temperature with no Triton addition in any of the buffers used. Primary antibodies were incubated on a rocker at 4ºC over-night. Secondary antibodies were incubated for 2 hours at room temperature in the dark. In case of double staining with the a-P28 antibody, staining was performed for 1 hour at room temperature following overnight incubation with the primary antibodies. Secondary antibodies were added simultaneously, for 2 hours at room temperature in the dark. For actin staining, tissues were incubated with a conjugated phalloidin dye (Invitrogen) for 20 minutes. After staining, cells or tissues were mounted in ProLong antifade mounting medium (ThermoScientific) prior to DAPI (Roche) staining at 1 µg/mL in PBS for 5 min, at room temperature.

2.11 Microscopy

2.11.1 Light and fluorescence microscopy

Parasites were imaged using a Leica DMT fluorescence microscope and images captured using a Zeiss AxioCam HR camera coupled to Zeiss Axiovision40 version 4.6.1.0 software. Post-processing of images was performed using ImageJ x.38.

2.11.2 Confocal microscopy

Images were acquired using a Leica SP5 MP confocal laser-scanning microscope and visualised using ImageJ x 38. Ookinete and sporozoite images were processed by deconvolution using the Huygens software, prior to visualisation. The confocal microscope used, belongs to the "The Facility for Imaging by Light Microscopy (FILM)'' at Imperial College London, which is funded by the Wellcome Trust and BBSRC.

2.12 Statistical analysis

qRT-PCR expression data (including *eGFP*, *tARG* and *S7* analysis) was analysed by one-way Analysis Of Variance (ANOVA) test on a linear mixed effect regression model. Statistical analyses for exflagellation, gametocyte-to-ookinete conversion, TEP1-binding and motility assays was performed using a two-tailed, unpaired Student's t-test. The unpaired Student's t-test was also used to determine statistical significance in the midgut and salivary gland sporozoite load between different mutant parasite lines and/or different mosquito immune backgrounds. The Mann-Whitney U-test was used to determine the statistical significance of oocysts, melanised or invading ookinete load. The infection prevalence was analysed using the Fisher's exact test. For each experimental setup, 2-3 individual biological replicates (i.e. parallel measurements of biologically distinct mosquito and mouse batches) were carried out and the median or mean value is presented based on their distribution pattern (D'Agostino and Pearson Normality test).

Before pooling replicates, the elements (infection intensity, infection prevalence, fold change between the control and the under examination factor for each replicate) were assessed for homogeneity with respect to the parameters estimated. Additionally, equal numbers of infected tissues from the independent biological replicates were pooled for each group. Previous studies that aimed to investigate the relationship between the *Plasmodium* gametocyte density and the levels of mosquito infection suggested that data pooling from at least two individual biological replicates, that each is consisted from a minimum of 25 distinct *Anopheles* midguts, are sufficient to fully or accurately describe the expected outcome with regards to the parasite load in the midgut or salivary gland tissues (Da *et al*., 2014).

CHAPTER 3. HIGH-THROUGHPUT REVERSE GENETIC SCREENING IN *P. BERGHEI* AND PHENOTYPIC ANALYSIS OF GENES CRITICAL FOR ITS DEVELOPMENT IN *A. COLUZZII* MOSQUITOES

3.1 Introduction

Genome-wide collection of mutants or genetic modification vectors have greatly facilitated the discovery of gene functions in various model organisms (Winzeler *et al.*, 1999; Sarov *et al.*, 2006; Skarnes *et al.*, 2011; Ni *et al.*, 2011). On the contrary, efforts to scale up reverse genetics in malaria parasites have suffered from a combination of low rates of homologous recombination and a high content of adenine and thymine (A+T) nucleotides rendering *Plasmodium* DNA difficult to engineer in *E. coli*.

To accelerate the parallel functional analysis of several *P. berghei* genes, Gomes *et al.* have taken advantage of the PlasmoGEM vector properties and by introducing gene specific molecular barcodes in each of the vectors, they managed to develop a high-throughput screen approach (Gomes *et al.*, 2015). This STM approach was initially adapted in order to simultaneously screen thousands of *P. berghei* mutants in a pooled approach and efficiently identify genes essential for blood stage development (Gomes *et al.*, 2015; Bushell *et al.*, 2017). The >2,900 genome modification vectors generated during this study now exist as a resource accessible to the malaria community thus allowing researchers to pursue high-throughput reverse genetics screens under different experimental settings.

Due to the availability of these tools, the first aim of this project was to use the STM and barseq technologies to screen for gene essentiality during parasite development in the mosquito vector, at scale. Such approach has the potential to enhance our understanding of the *P. berghei* gametocyte-to-ookinete-to-oocyst-to-sporozoite developmental transition and its molecular interactions with the mosquito vector. KO mutants within the pool which demonstrated phenotype other than the WT i.e. found to undergo significant losses during their development, were chosen to generate single transgenic parasite lines. Preliminary data on the characterisation of these lines and indications about the genes function are also presented in this chapter.

Conceptualisation of the STM high-throughput reverse genetic screen was carried out by Dr. Dina Vlachou and Prof. George K. Christophides, while Dr. Ana-Rita Gomes performed the initial experiments regarding the generation of the pools with the

barcoded mutants and investigation of their stability during blood stages development. Subsequent mosquito infections, tissue sampling, gDNA extraction and barcode PCR amplification were performed by Dr. Ana-Rita Gomes and myself. Part of the experiments that aimed at characterising the three novel genes revealed with the STM-bar-Seq experiment were performed together with Alexander Bailey and Tanguy Rene Balthazar Besson who provided technical assistance as part of their MRes project in the host laboratory, under my supervision. Specifically, Alexander Bailey assisted in the bioinformatic analysis of the three genes and in generating the KO lines, while Tanguy Rene Balthazar Besson assisted in generating the tagged parasite lines, in analysing the different clonal populations of the mutant KO lines and in investigating the expression pattern of *AQP2*, *N38* and *N350*.

For the sake of concept completion, I am providing here some specifications regarding the design of the *P. berghei* STM-bar-Seq experiment which were determined following the initial experimental procedures that Dr. Ana-Rita Gomes carried out:

- Typically, mosquito stages studies are performed using the vector *A*. *stephensi*. However, since one of the main research focuses in our lab is to also understand the link between the dramatic losses the parasite population undergoes in the mosquito vector and the mosquito innate immune responses mounted following *Plasmodium* infection, we chose to use *A. coluzzii* mosquitoes (previously *A. gambiae* M form). Besides, *A. gambiae* is the primary mosquito vector for malaria transmission in Africa and has been previously used widely for characterising the mosquito innate immunity.
- Co-transfection of multiple PlasmoGEM vectors in the same electroporation reaction can lead to the reproducible generation of complex pools of barcoded *P. berghei* mutants, each carrying a single gene deletion (Gomes *et al.*, 2015). As such, barcoded PlasmoGEM vectors were used to produce six pools of *P. berghei* mutants, each containing about ˜30 transgenic lines. Since the first aim was to establish the aforesaid method for the *P. berghei* / *A. coluzzii* system, the first pool was mainly comprised of KO vectors for genes that had been previously investigated as well as epitope tagging vectors which following homologous recombination do not impose any fitness cost. In this manner, comparison between the resulting and the defined phenotype would allow validation of the suggested method.
- Similar to what has been previously performed for other organisms (Winzeler *et al*., 1999), the proposed STM-like experiment for investigating *P. berghei* genes

essentiality during parasite development in the mosquito vector was designed to start with (1) the mutagenesis step i.e. generation of barcoded mutants, which was followed by (2) the propagation of these mutants in pools, and finally included (3) the identification and quantification of the abundance of the mutants after propagation through their attached barcode. Thus, transfection of barcoded PlasmoGEM vector pools (mutagenesis step) was used to generate multiple pools of *P. berghei* mutants that after being expanded in a single mouse, were used to infect adult *A. coluzzii* mosquitoes (propagation step). Lastly, the identification and abundance of each mutant was validated using sequencing techniques (identification step) (**Figure 3.1**).

- Double integration events if existent, are extremely rare and undetectable (Gomes *et al.*, 2015). Given that the *Plasmodium* genome is haploid during blood stage development, each mutant parasite genome carries only a single barcode. When ingested inside the mosquito gut, the haploid gametes fuse to produce the diploid zygotes. However, the cross-fertilisation events between different mutants within the same pool that have been modified on separate loci would lead to heterozygosity. In other words, mutant parasites could be rescued by the WT allele which would be carried by a different mutant within the same pool, a state not tractable by the current readout of the screen. To bypass this obstacle, single sex screening was carried out by generating the pool of mutants on the male sterile genetic background reference line Δ*hap2.* In order to later permit successful mosquito infection, the *Δhap2* pool had to be crossed with the female deficient line Δ*nek4,* which was otherwise WT for all the bait genes. Because though, the paternal allele (supplied by the female deficient line) is silenced throughout the parasite zygotic development (Ukegbu *et al.*, 2015), the resulting zygotes are expected to be homozygous for the barcoded KO alleles which are carried by the female parasites of the *Δhap2* pool. If the pool was to be generated using any WT background reference line, it would mean that both male and female gametes could potentially carry a KO locus for any of the bait genes. Following fertilisation, the KO allele carried by the male gamete would have been rescued by the WT allele of the specific locus carried by the female gamete. However, following transcriptional activation of the paternal mRNA at a later stage, the KO allele initially carried by the male gamete could potentially have a drastic effect on the parasite fitness. Therefore, when monitored at later developmental stages, this change in the transcriptome would not be tractable and therefore specific phenotypes would not be detected and assigned to specific genes. Therefore, under this optimised

experimental set-up, the intermediate heterozygous status would allow us to study the essentiality of the genes beyond gametocyte and zygote development. Two reference *P. berghei* lines were chosen; the ANKA strain (clone 2.34) used as WT control and the male deficient line Δ*hap2* (von Besser *et al.*, 2006; Liu *et al.*, 2008).

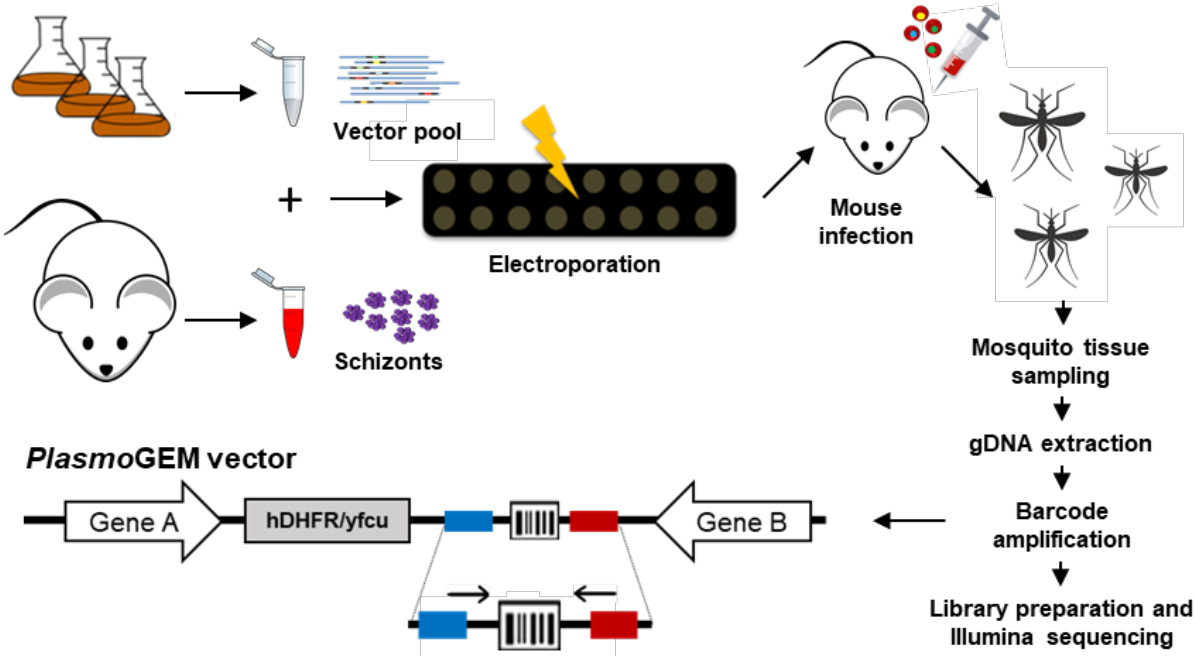

Figure 3.1. Proposed experimental design of the *P. berghei* STM-Bar-seq experiments. PlasmoGEM targeting vectors were used to co-transfect *Plasmodium* schizonts using the Amaxa system, prior to injection of the resulting barcoded mutants into mice. Since all PlasmoGEM vectors contain the *h*DHFR-yFCU marker, mutant parasites were selected under pyrimethamine drug pressure. Once parasitaemia developed in the mice-recipients and the presence of barcoded mutants was confirmed by genotypic PCR and barcode sequencing, mosquito infections were performed. Mosquito tissues were collected and following gDNA extraction, quantification of the barcoded mutants was carried out via Illumina sequencing. Figure adapted from (Gomes *et al.*, 2015) and modified to meet the needs of this chapter.

3.2 Results

3.2.1 Parallel phenotyping of *P. berghei* mutants in *A. coluzzii* mosquitoes

To examine whether the generation of the pool of barcoded mutants enables a high-throughput reverse genetic screen of *Plasmodium* genes during *A. coluzzii* infection,

mosquitoes were allowed to blood-feed on mice infected with the previously described parasite pool prior to mosquito tissue harvest, gDNA extraction and barcode sequencing. Mosquito midguts were collected at day-12 pbf in order to capture the *Plasmodium* sporulated oocyst stage, whereas mosquito salivary glands were collected at day-21 pbf to guarantee capture of the parasite at its mature sporozoite stage prior to inoculation into the next mammalian host. The pools of barcoded mutants in both the *2.34* ANKA WT and Δ*hap2* backgrounds were used to infect *A. coluzzii* mosquitoes. Regarding the pool generated in the WT background, where fertilisation between the mutant gametes is expected to result in the genetic complementation of the KO locus, no reduction in the mutants' barcode abundance was anticipated. This could therefore be used as the threshold line for comparing the abundance of the barcoded mutants in the Δ*hap2* background pool.

In addition to barcode sequencing and in order to confirm the correct integration of all vectors whose barcode was detected following *A. coluzzii* infection, gDNA was extracted from infected midgut tissues at 1 hour post infection and qRT-PCR analysis was performed. For genotyping by long-range PCR, a specific genotyping (GT) primer for each barcoded mutant (annealing at least 200 bp up- or downstream of homology region) together with the generic primer GW2 or GW1 (annealing within the vector resistance cassette) (**Table 2.4**) were used. The presence of all mutant barcoded parasites as detected by barcode sequencing, was confirmed (**Figure 3.2**).

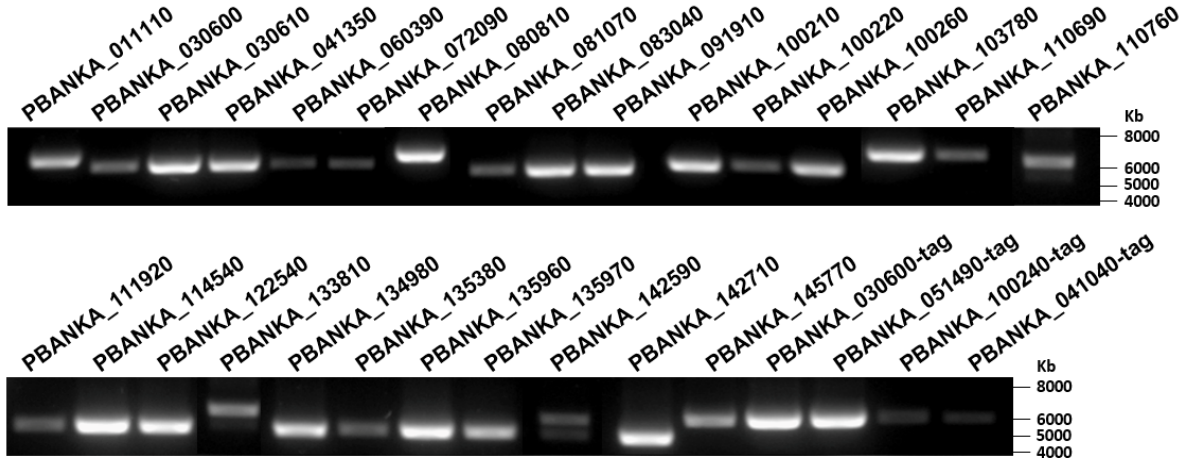

Figure 3.2. PCR confirmation of mosquito infection with all barcoded mutant parasites. PCR products across the predicted integration sites, supporting genomic integration of all vectors detected by barcode sequencing. The gDNA sample used was extracted from *A. coluzzii* midguts, at day-12 post infection with the mutant

barcoded pools of both Δ*Pbhap2* and *2.34* ANKA WT background reference lines. Corresponding agarose gel image of two sets of experiments. gDNA extracted from non-infected *A. coluzzii* mosquitoes as well as from *P. berghei 2.34* ANKA WT infected mosquitoes at day-12 pbf were used to check primers specificity.

Following sequence quantification analysis of each barcode, we can briefly point out that mutant parasites of the WT background do not display noteworthy changes between blood and mosquito stages. As a matter of fact, the proportional dynamics seem to be equally distributed between the mixed blood stages, the mosquito midgut oocyst stage, and the mosquito salivary gland sporozoite stage (**Figure 3.3, A**) i.e. each barcode has a relative abundance of about 33% at each stage. On the other hand, some transgenic parasites of the Δ*Pbhap2* background pool exhibited varying dynamics, especially from the asexual blood stages to mosquito oocyst transition (**Figure 3.3, B**). Taken together, these data confirm that generation of a mutant parasite pool using the WT background line would not be able to inform us on the pure phenotype following gene deletion. As previously mentioned, this comes as a result of genetic complementation at the KO locus following gamete fertilisation.

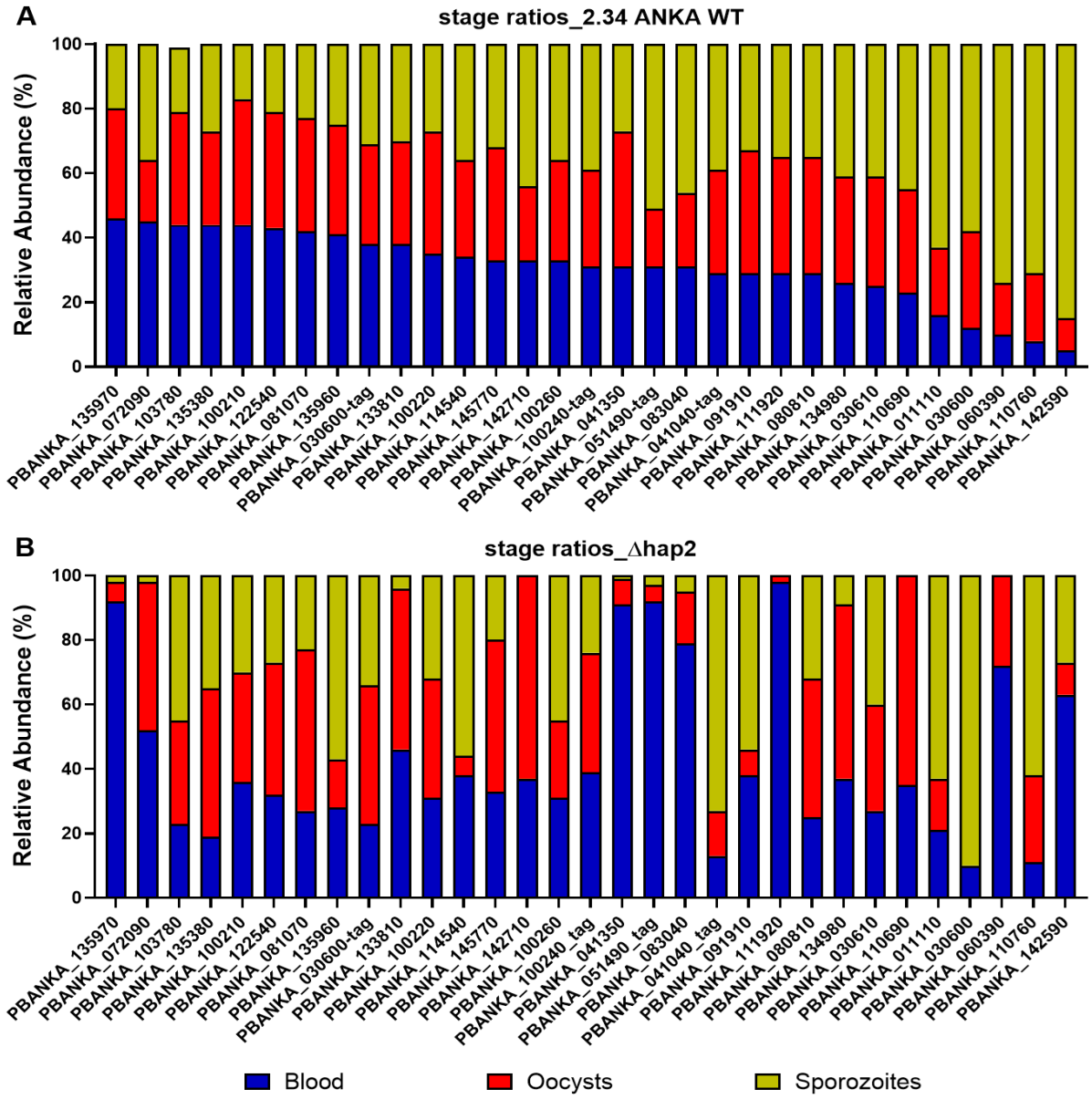

Figure 3.3. Stage dynamics of the barcoded mutant parasite populations in the pool. The inferred proportion of each barcoded mutant in the total parasite load is shown, corresponding vertically to different *Plasmodium* developmental stages. The abundance of each barcoded mutant at each developmental stage is plotted as a percentage of the total number of parasites at that specific developmental stage and in each background. The average relative abundance value of each barcode was calculated based on a total of four biological replicates using both pools of the *2.34* ANKA WT **(A)** and Δ*Pbhap2* **(B)** backgrounds. Each colour represents different parasite developmental stages (blue, MBS; red, midgut oocyst stage; yellow; salivary gland sporozoite stage). Experimental procedures were performed together with Dr. Ana-Rita Gomes, while data analysis was carried out solely by Dr. Ana-Rita Gomes. Data are reproduced here with the permission of Dr. Ana-Rita Gomes.

The graph in **Figure 3.4** illustrates the relative abundance value of each barcoded mutant in the *2.34* ANKA WT or Δ*hap2* background during oocyst (**Figure 3.4, A**) and salivary gland sporozoite (**Figure 3.4, B**) development. The abundance of each allele was determined based on the total number of barcode counts within the population at the oocyst and salivary gland sporozoite stages, without taking into consideration the total number of alleles that were expected to be present in the homozygous or heterozygous state of the parasite (as a result of the cross-fertilisation events). Note that losses following co-infection with the Δ*Pbnek4* line were by passed by all mutants of the Δ*hap2* background pool except *ΔPBANKA_030600 (ΔP230p)* during the fertilisation bottleneck. Since copies of its KO barcode were not identified in the oocyst or sporozoite population, this gene has been excluded in the corresponding figure. Interestingly, the *ΔP230p* mutant in the *2.34* ANKA WT background as well as the one carrying the tagged version of this gene were able to establish successful infection, suggesting a possible interaction between *hap2* and P230p prior to oocyst development. Additionally, the three barcoded mutants *ΔPBANKA_111920* (*Δc43*), *ΔPBANKA_114540* and *ΔPBANKA_135970* (*ΔP47*) of the Δ*hap2* background showed lower oocyst abundance (8-fold, >100-fold and 12-fold reduction, respectively) when compared to the WT control background pool. This phenotype could either be due to fertilisation defects in the KO female gametocytes (van Dijk *et al.*, 2010; Ukegbu *et al.*, 2017b), which could not be overcome by the transcriptionally silenced males of the Δ*Pbnek4* line following fertilisation, or to the impairment of heterozygous ookinetes in their ability to successfully invade and traverse the mosquito midgut epithelium. However, since these mutant parasites are double KO for both *hap2* and the targeting gene of interest, such a phenotype might be further linked to the unfavourable interaction of the two proteins. Nonetheless, it has been already shown that *Δc43* (Ukegbu *et al.*, 2020) and *ΔP47* (Ukegbu *et al.*, 2017b) ookinetes are eliminated immediately after ookinete midgut traversal and before oocyst formation.

As expected, the reduced abundance of some genes during oocyst development was also maintained at the salivary gland sporozoite stage. In addition, parasites lacking expression of *PBANKA_060390* (*HADO*) or *PBANKA_083040* (*g2*) - two genes previously shown to be associated with ookinete motility (Akinosoglou *et al.*, 2015) and morphology (Tremp *et al.*, 2013), respectively - seem to have suffered dramatic losses at the sporozoite stage when in the Δ*Pbhap2* background compared to the WT. In fact, the decreased abundance of the *ΔG2* parasites is possibly due to the previous

reduction that had taken place at the oocyst stage. However, due to inconsistent differences between the individual replicates, no statistical significance was detected at first. Surprisingly, mutant parasites lacking expression of *soap* seem to have higher survival rates when generated in the Δ*hap2* background compared to the WT control but these results do not agree with the current literature showing SOAP to be critical for ookinete midgut invasion and oocyst development (Dessens *et al.*, 2003). Lastly, c43 has been shown to be important during oocyst sporulation (Ukegbu *et al.*, 2020) explaining the dramatic reduction observed in the sporozoite population of the Δ*hap2* background compared to the WT control.

Apart from *ΔPBANKA_041350 (N350*), whose abundance was already significantly reduced (p=0.0238) at the midgut oocyst compared to the blood stages, all other mutant parasites underwent dramatic losses during the oocyst-to-salivary gland sporozoite transition. More specifically, the abundance of the *ΔPBANKA_133810* (*N38*), *ΔPBANKA_1427100* (*ΔAQP2*), *ΔPBANKA_110690* and *ΔPBANKA_072090* mutant parasites of the Δ*hap2* background pool was reduced at the sporozoite stage by 40.0%, 99.9%, 85.3% and 60.0% respectively, revealing a potential function of these proteins during either oocyst sporulation, sporozoite maturation and motility or sporozoite salivary gland invasion. More striking and despite the fact that the *ΔPBANKA_110690* or *ΔPBANKA_142710* (*ΔAQP2*) mutant parasites showed a healthy phenotype at the oocyst stage i.e. relative abundance values of the KO mutants within the Δ*hap2* background pool similar to those determined within the WT background pool, they were almost eliminated at the salivary gland sporozoite stage. These data suggest an essential function of these genes beyond oocyst development, probably during either sporozoite formation and further maturation or invasion of the salivary glands. As previously mentioned, *ΔPBANKA_041350* (*N350*) mutant parasites suffered dramatic losses prior to oocyst and sporozoite formation which resulted in a population of less than halved size compared to that ingested. This reduction also continued at the salivary gland sporozoite stage therefore, further validating the previous bottleneck observed.

The relative abundance of three out of the four tagged parasites, which are otherwise WT and were used as controls, were very similar among them and within the pools of the different genetic backgrounds. Additionally, their relative fitness during midgut oocyst-to-salivary gland sporozoite developmental transition was centred around the

value one, confirming successful parasite development up to the sporozoite stage and also validity of the barseq analysis methodology. However, the average abundance of the attenuated PBANKA_051490·(P28)-tagged mutant at the oocyst stage was significantly lower (p=0.0275) in the Δ*hap2* background. It has been shown that P28 is essential for ookinete to oocyst development (Tomas *et al*., 2001) and thus, conformational disorders of the protein when jointly expressed with the HA-tag could result in a decrease on the mutant parasites abundance at the oocyst stage. However, these oocysts might have produced more sporozoites, due to less nutrient competition, and thus the initial drop observed is recovered at the sporozoite stage.

The results illustrated in **Figure 3.3** compared to those in **Figure 3.4** give us further information about the growth rate of the individual mutants, starting from blood-to-oocyst-to-salivary gland sporozoite transition i.e. the barcode abundance at each developmental stage is shown as the percentage of the total number of barcodes counted for the specific mutant at all the developmental stages that have been examined. For example, the barcode abundance of the *ΔPBANKA_133810* parasites in the WT background pool was calculated to be 0.286 during blood stages development, 0.247 at the oocyst stage and 0.244 at the salivary gland sporozoite stage. The same transgenic parasite in the *Δhap2* background pool appeared with an abundance value of 0.375 during blood stages development, 0.391 at the oocyst stage and 0.038 at the salivary gland sporozoite stage. Therefore, in **Figure 3.3**, the percentage of KO parasite abundance inside the WT background pool is shown to be shared between the three developmental stages (37.2%, 32.1%, 31.7% respectively) indicating that the gene disruption did not cause any fitness cost to the parasite, whereas a gradual decrease on the relative abundance of the same mutant within the *Δhap2* background pool is observed from mixed blood stages-to-oocyst-to-salivary gland sporozoite developmental transition (48.7%, 50.8%, 5.0% respectively). In **Figure 3.4** the abundance of the KO parasite within the WT background pool is higher compared to the abundance of the KO parasite in the *Δhap2* background as well as it remains constant between the two stages. The abundance of the same mutant in the *Δhap2* pool seems to have dropped only at the salivary gland sporozoite stage.

The outcome from this first attempt establishes the STM methodology as a tool to phenotypically characterise large numbers of *P. berghei* mutants during mosquito stages, in parallel. The fact that we were able to observe a clear phenotype only for

the Δ*hap2* background pool, whereas mutants belonging to the WT background pool showed an invariable relative fitness around ˜1, consist a proof that the strategic plan followed can lead to significant and consistent outcomes. Indeed, female mutant parasites of the Δ*hap2* reference line which lack an additional for their development important gene, following fertilisation with Δ*nek4* male parasites whose transcriptome is silent during zygote-to-ookinete transition, did not manage to overcome developmental or mosquito-derived obstacles and thus, suffered huge losses.

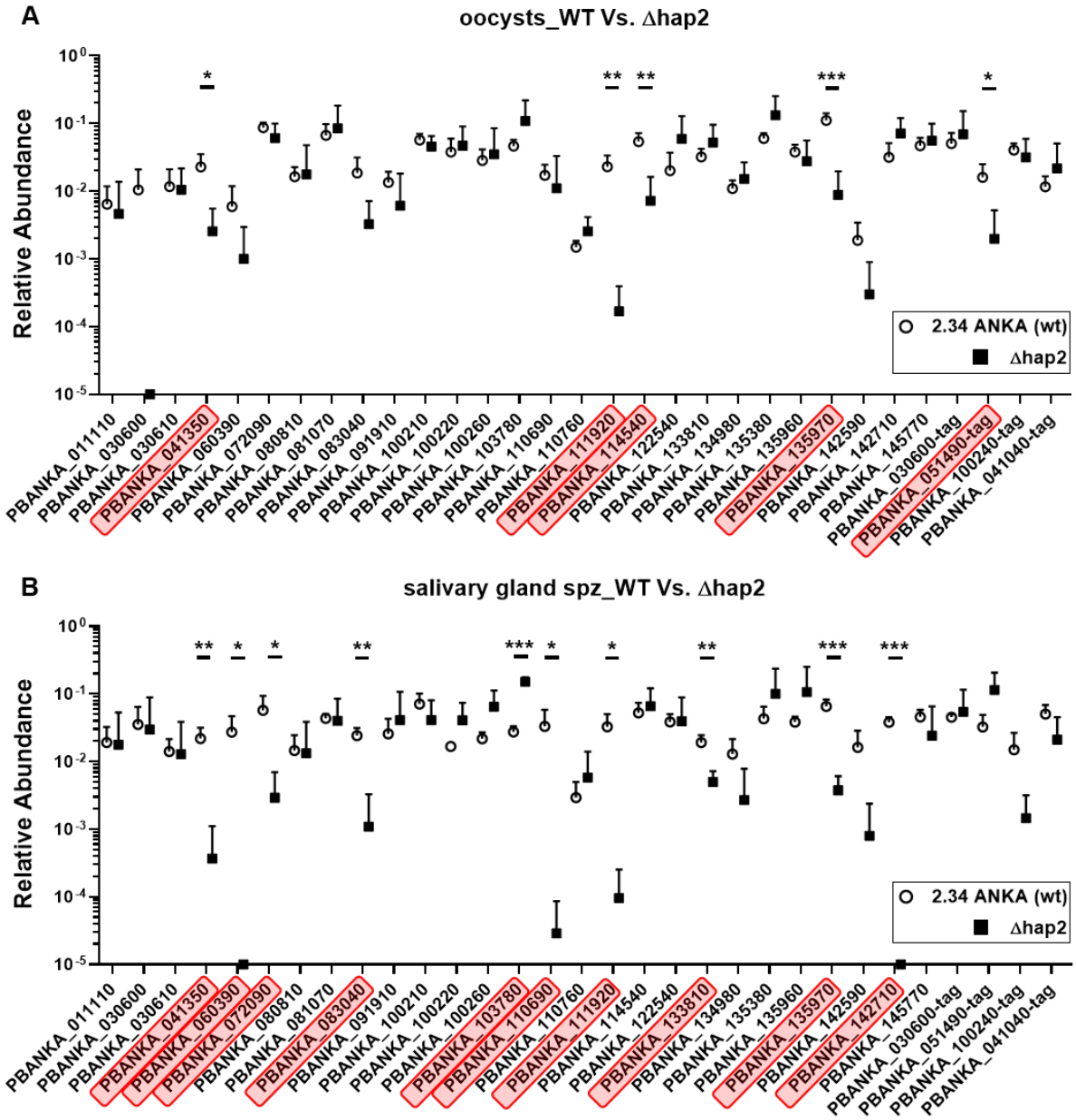

Figure 3.4. Relative abundance of mutant parasites during their development in the mosquito vector, as determined by barcode sequencing. Average relative abundance (y-axis) of the barcoded mutants (x-axis) within the *P. berghei* Δ*hap2* and

2.34 ANKA WT background pools, during parasite development in *A. coluzzii* mosquitoes. Graph **(A)** illustrates, individually, the barcoded mutants relative abundance as captured at the oocyst stage at day-12 pbf, whereas graph **(B)** shows their corresponding abundance at the sporozoite stage as captured at day-21 pbf. Each relative abundance value refers to the average of four individual biological replicates, where error bars show standard error from the mean. Statistical significance was determined using a non-parametric t-test, applied between abundance values calculated for each complex pool of the different background reference line. Red boxes point to those mutants that showed a statistically significant reduction or induction between the *2.34* ANKA (WT) and Δ*hap2* background pools. Experimental design and performance were carried-out by Dr. Ana-Rita Gomes and myself, whereas data analysis was performed solely by Dr. Ana-Rita Gomes. Data are reproduced here with the permission of Dr. Ana-Rita Gomes.

3.2.2 Barcode counting reveals three gamete-specific genes

The results generated by the screen identified three novel genes that are likely to be important for parasite development in the mosquito vector, PBANKA_142710 (*AQP2*), PBANKA_133810 (*N38*) and PBANKA_041350 (*N350*). Specifically, the abundance of the *AQP2* and *N38* KO mutants appeared to undergo extreme reduction at the sporozoite stage, whereas *N350* KO mutants suffered dramatic losses prior to oocyst formation and development, which eventually contributed to the low sporozoite numbers. These results are further supported from previous work that aimed to identify genes highly transcribed during gametogenesis. By performing microarray transcriptional analysis of *A. coluzzii* midguts at 1 hour post infection with the *2.34* ANKA WT and 2.33 ANKA (non-gametocyte producer; NGP) parasite lines, the aforementioned study aimed at identifying *Plasmodium* genes that are highly transcribed during gametogenesis i.e. genes that passed the threshold set based on the values previously determined for the NGP line. Specifically, *AQP2*, *N38* and *N350* transcription levels showed a 3-fold, 10-fold and 3-fold increase at 1 hour pbf, respectively (unpublished data, with the permission of Dr. Valerie Ukegbu, Imperial College London). Therefore, all three genes are upregulated during gametogenesis and are associated with defects occurring either at the ookinete or sporozoite stages. In other words, all these data strongly suggest a function of AQP2, N38 and N350 proteins during parasite development in *Anopheles* mosquitoes.

Henceforward, I went on to further investigate these three novel *P. berghei* genes by (1) performing bioinformatic analysis of their amino acid sequences, (2) generating single KO lines and examining their phenotypic and functional characteristics following *A. coluzzii* infection, and (3) generating tagged-parasites lines in order to investigate their protein expression and localisation.

3.2.3 Phylogenetic and structural analysis of aquaporin 2

Whilst *P. berghei* and *P. falciparum AQP1* (*Pf*AQP1) has been well characterised (Hansen *et al.*, 2002; Promeneur *et al.*, 2007; Hedfalk *et al.*, 2008; Promeneur *et al.*, 2018), there is very little research regarding the *AQP2* gene in these species. The predicted *P. berghei AQP2* (*PbAQP2*) gene consists of a single exon of 1788bp and encodes a medium size (70kDa) putative aquaporin. It contains seven putative membrane-spanning domains (I-VII) separated by six connecting loops (A-F). The aquaporin-like domain of *Pb*AQP2 spans across its C-terminus region and contains five putative transmembrane domains separated by four connecting loops (C-G). In *Pf*AQP1, the NPA (Asn-Pro-Ala) and NPM (Asn-Pro-Met) canonical motifs that outline the pore are found in loops B and E, respectively. In *Pb*AQP2, the corresponding loops where the two canonical motifs can be found are C and F, respectively (**Figure 3.5**).

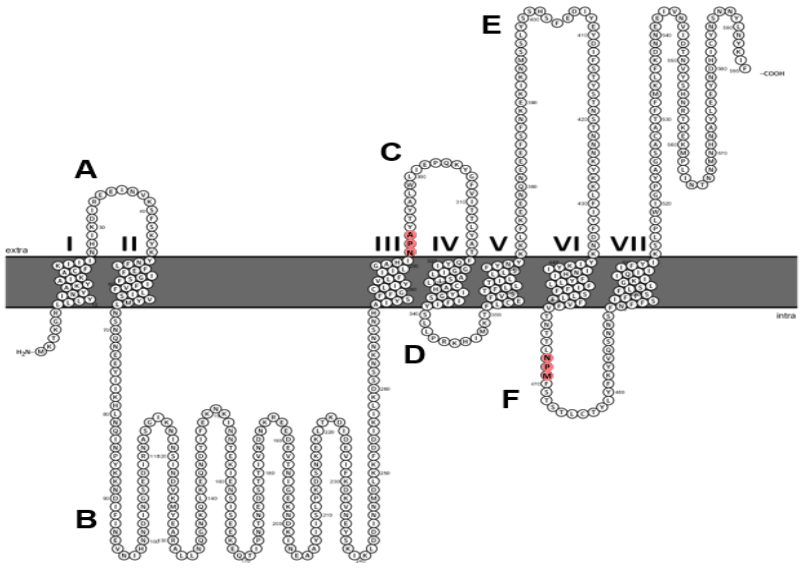

Figure 3.5. Predicted membrane topology of *Pb*AQP2. The putative transmembrane domains were assigned by hydrophobicity analysis using Protter (Omasits *et al.*, 2014), an interactive protein feature visualisation software designed based on the TEXtopo package. Intra- and extracellular loops are labelled alphabetically. The predicted transmembrane domains are also enumerated. NPA and NPM motifs are indicated in loops C and F, respectively.

*Pb*AQP2 orthologues are present in all sequenced *Plasmodia spp.* It is similar in transcript and protein length to its orthologous *P. yoelii* (*Py*AQP2) and *P. falciparum* AQP2 (*Pf*AQP2), whereas the human malaria parasite *P. vivax* (*Pv*AQP2) and the simian malaria parasite *P. malariae* (*Pk*AQP2) orthologues are slightly longer. Additional *in silico* sequence analysis revealed that *Pb*AQP2 amino-acid sequence is highly conserved among *Plasmodium* orthologues, sharing a 93.11% amino acid sequence similarity with *Py*AQP2, 59.82% similarity with *Pf*AQP2*,* 59.76% similarity with *Pv*AQP2 and 61.57% similarity with *Pk*AQP2*.* The fact that the *Pb*AQP2 and *Py*AQP2 pores are encoded by five transmembrane domains (TM), compared to *Pf*AQP2, *Pv*AQP2 and *Pk*AQP2 which are encoded by six such domains, seem to be associated with their higher sequence homology. Additionally, the high amino acid sequence conservation seems to exist close to the C-terminus of the protein, mapping with the predicted aquaporin-like region (**Appendix 6**). This high level of sequence conservation between *Plasmodium spp.* AQP2 possibly points to similar functions.

Compared to aquaporins of other species with a typical range of 200-300 amino acids, all *Plasmodium AQP2* genes are unusually long at about 600-650 amino acids. Other significant differences spotted include their unique variable N-terminal region, their highly conserved regions on their C-terminus as well as around their pore forming motifs. Interestingly, much of the aforementioned extra length of the *AQP2* gene in *Plasmodia spp.* is towards the N-terminus of the protein (**Figure 3.6**). The only other aquaporin of those studied with this extra sequence is the *T. gondii* AQP2 (*Tg*AQP2), however, there is no consensus between species; *Pb*AQP2 and *Tg*AQP2 share 16.67% amino acid sequence similarity, whereas *Pf*AQP2 and *Tg*AQP2 share 33.33% sequence similarity. The C-terminus sequence between *Plasmodia spp.* AQP2 with aquaporins from other organisms is highly conserved. However, in contrast to the canonical NPA (Asn-Pro-Ala) motifs in most aquaporins, some of the *Plasmodium spp.* AQP2 (not *Pb*AQP2) have NLA (Asn-Leu-Ala) and NLM (Asn-Leu-Met) in those positions of the pore forming loops. A similar alteration on the motif sequence has been also observed for the *Plasmodia spp.* AQP1 protein, where the motifs NLA (Asn-Leu-Ala) and NLS (Asn-Leu-Ser) have been identified instead. Despite the differences, all motifs retain the most important structural domains of the pore forming loops and are thought to play a crucial role in the water-selective permeation of the aquaporin water channels (Murata *et al.*, 2000; Hub *et al.*, 2008).

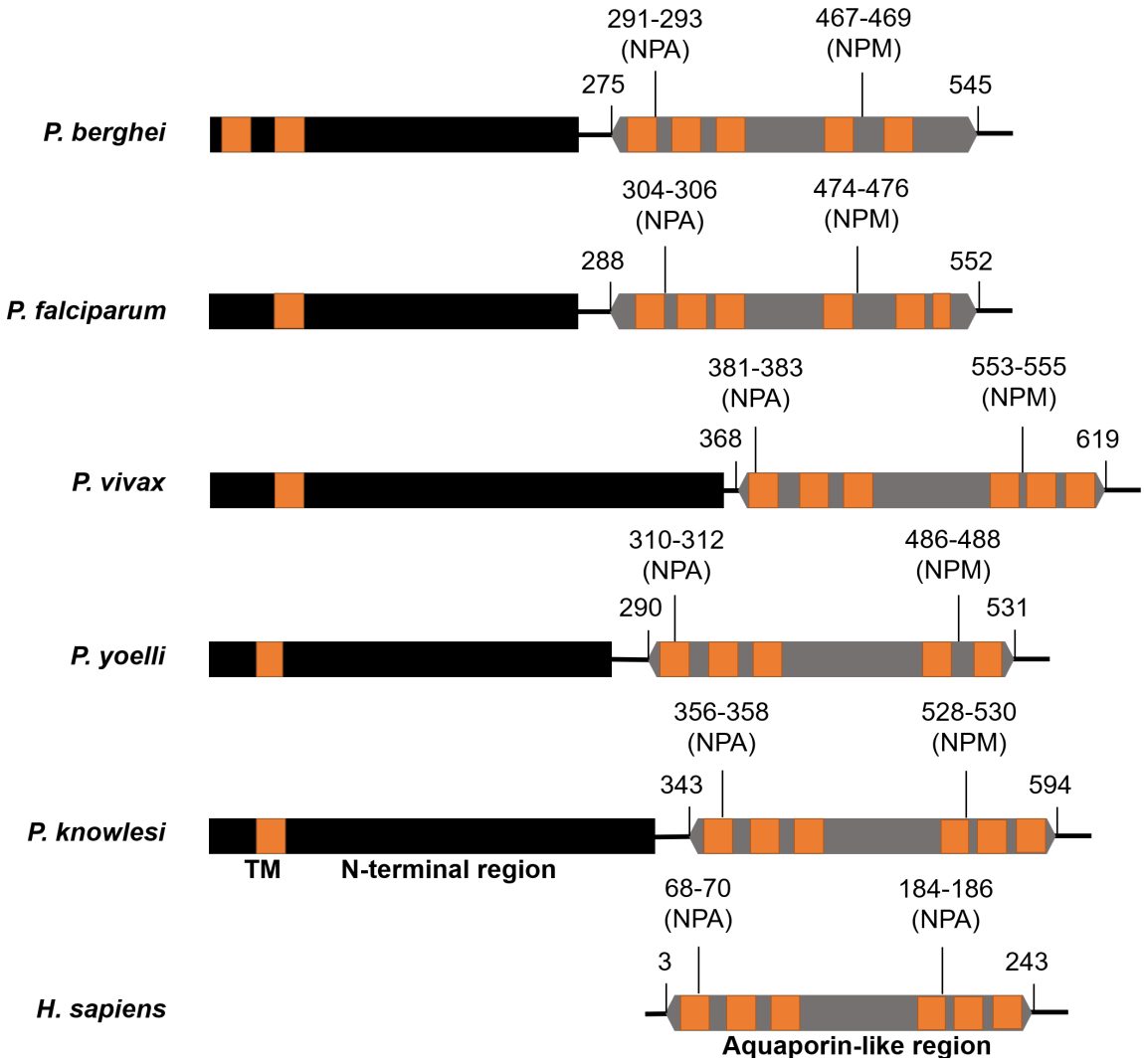

Figure 3.6. Domain architecture of the *Plasmodia spp*. and *H. sapiens* AQP2 orthologous proteins. The schematic protein models of *Plasmodium* and *H. sapiens* AQP2 were generated by *in silico* sequence analysis which revealed that all *Plasmodium* orthologues encode an aquaporin-like domain in their conserved C-terminal position. The predicted transmembrane domain (TM; orange), N-terminal region (black) and C-terminal extension (grey), corresponding to the aquaporin-like region, are shown. The two conserved repeats, each with a pore-forming loop containing a signature Asn-Pro-Ala (NPA) and Asn-Pro-Met (NPM) motives, are also shown. To note, the aquaporin-like domain of the *H. sapiens* AQP2 spans across the full length of the protein and the protein has two conserved NPA motifs. The length of each gene is proportional to its size. Figure has been adapted and amended accordingly from the MRes thesis of Alexander Bailey (2019).

Further *in silico* analysis and structural homology modelling of both *Pb*AQP2 and *Pf*AQP2 proteins, using Phyre2 (Kelley *et al.*, 2015), revealed high conservation with

other known aquaporins. Specifically, a high correlation with 99.5% confidence for *Pb*AQP2 and 99.6% confidence for *Pf*AQP2 was found with the *Pichia pastoris* aquaporin (Aqy1) and the human aquaporin 5 (*h*AQP5) (99.3% confidence for *Pb*AQP2 and 99.4% confidence for *Pf*AQP2, respectively). These, however, only cover 29% of the amino acid sequences towards the C-terminus. Interestingly, protein sequence alignment of all *Plasmodia spp.* N-terminal region indicated a weak conservation across 70% of the domain, probably justifying the fact that a predicted homologue structure with a known function for this domain could not be identified. Only for the *Pf*AQP2 N-terminal region, Phyre2 showed a significant structural homology with the yeast ATPase subunits; with 82.1% confidence for *Saccharomyces cerevisiae* vacuolar proton ATPase subunit b and 81.8% confidence for catalytic subunit a. Thereby, whether this region has retained a conserved function between species or not, it appears to be unclear. Nevertheless, the corresponding aquaporin-like region is thought to predominate for the main function of the protein.

In order to better understand the relationship between *Pb*AQP2 and its different orthologues, a phylogenetic analysis of sixty-nine aquaporin sequences from *P. berghei*, *P. falciparum*, *T. brucei*, *T. gondii*, *S. cerevisiae, P. pastoris*, *Pseudomonas spp.*, *Aspergillus spp.*, *M. musculus*, *A. thaliana*, *E. coli, A. coluzzii, A. gambiae* and *H. sapiens* was performed using at first ClustalW (Sievers *et al.*, 2011) for sequence alignment, and later MEGA X (Kumar *et al.*, 2018) for evolutionary analysis (**Figure 3.7**). The dendrogram produced, demonstrated a weak sequence conservation of *Plasmodium spp.* AQP2 with most of the other aquaporins in the tree, with *S. cerevisiae* Aqy2 and *T. gondii* AQP1 being the most closely related in terms of genetic distance. Similar principal component analysis indicated that the *P. berghei* AQP2 amino acid sequence is significantly conserved to the other rodent malaria parasite *P. yoelii* AQP2 and then, *P. falciparum* AQP2. However, *Pb*AQP2 appears to be at a much closer distance as well as to share a direct ancestor with *P. yoelii* AQP2. Surprisingly, AQP2 proteins show a low degree of similarity with any of the *Plasmodium spp.*, *Toxoplasma spp., Aspergillus spp., Saccharomyces spp.* AQP1 genes. Other aquaporins that have also been found to be in great distance are the *H. sapiens* AQP11 and *H. sapiens* AQP12; also in agreement with what has been previously shown by (Calvanese *et al.*, 2013).

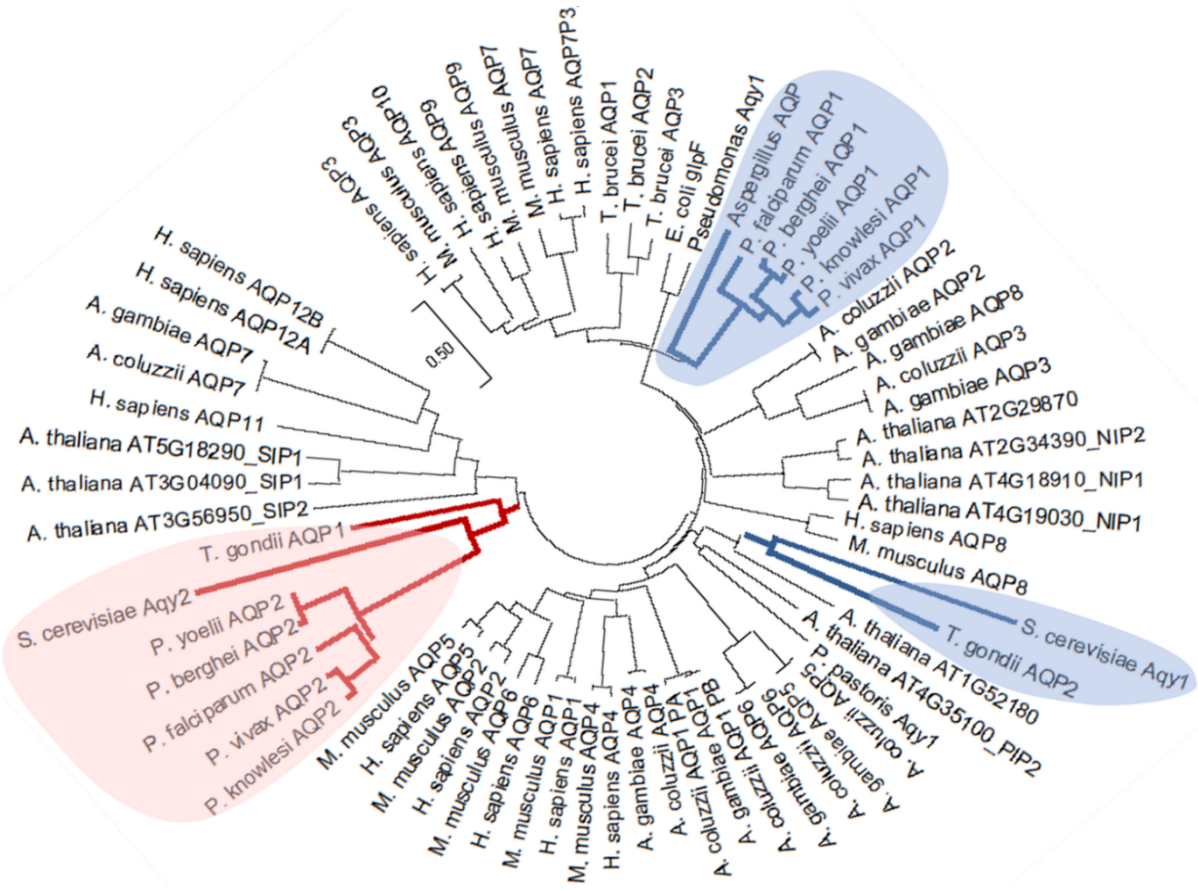

Figure 3.7. Phylogenetic analysis of AQP2 proteins. The evolutionary history was inferred using the Neighbor-Joining method (Saitou & Nei, 1987). The tree is drawn to scale, with branch lengths in the same units as those of the evolutionary distances used to infer the phylogenetic tree. The evolutionary distances were computed using the Poisson correction method (Zuckerland *et al.*, 2014). This analysis involved 69 amino acid sequences from *P. berghei*, *P. falciparum*, *T. brucei*, *T. gondii*, *S. cerevisiae, Pichia Pastoris*, *Pseudomonas spp.*, *Aspergillus spp.*, *M. musculus*, *A. thaliana*, *E. coli, A. coluzzii, A. gambiae* and *H. sapiens*. Evolutionary analyses were conducted in MEGA X (Kumar *et al.*, 2018).

3.2.4 Structural analysis of *P. berghei* N38 and N350

P. berghei N38 (*PbN38*) encodes a small 263 amino acid protein (30.4kDa) sharing structural similarities with the Alphavirus E2 glycoprotein, as revealed by both manual annotation and three-dimensional (3D) homology modelling. Compellingly, twelve potential introns have been identified opening up the possibility of the existence of *N38* spliced variants. An N-terminal signal peptide (amino acids 1-23) and three C-terminal transmembrane domains (amino acids 4-26; 187-209; and 224-243) are also predicted for the protein (**Figure 3.8, A**). None of the three transmembrane domains do not

contain signals for attachment of a GPI lipid anchor, as predicted by the PredGPI software. The deduced protein is conserved among *Plasmodia spp.* with 96%, 76%, 76%, and 74% identity to *P. yoelii* PY17X, *P. falciparum* 3D7, *P. vivax* PVX, *P. malariae* PKH N38 proteins, respectively (**Appendix 7**). Phylogenetic analysis of *Pb*N38 indicated a weak correlation with sequences from other organisms, probably suggesting a unique role of this gene among the different *Plasmodia spp.*

P. berghei N350 (*PbN350*) encodes a large (1037 amino acids: 122kDa) putative transmembrane domain protein, with orthologues in all *Plasmodia spp.* It is predicted to have fourteen transmembrane domains across its N- and C-terminal sides (amino acids 66-88; 108-130; 242-261; 271-293; 312-334; 344-366; 424-446; 746-763; 768-786; 801-823; 830-852; 862-881; 943-965 and 980-1002) (**Figure 3.8, B**). Protein alignment showed a moderate 86%, 62%, 53%, and 56% identity to *P. yoelii* PY17X, *P. falciparum* 3D7, *P. vivax* PVX, *P. malariae* PKH, respectively (**Appendix 8**). Interestingly, these conserved regions match with the N- and C-terminal sides where the predicted transmembrane domains of the protein are mapped. Homology 3D modelling analysis revealed that N350 encodes a protein transporter that share structural similarities with the human dopamine transporter. However, sequence alignment revealed poor conservation. Phylogenetic analysis did not show significant orthologues of *Plasmodium* N350 with other organisms.

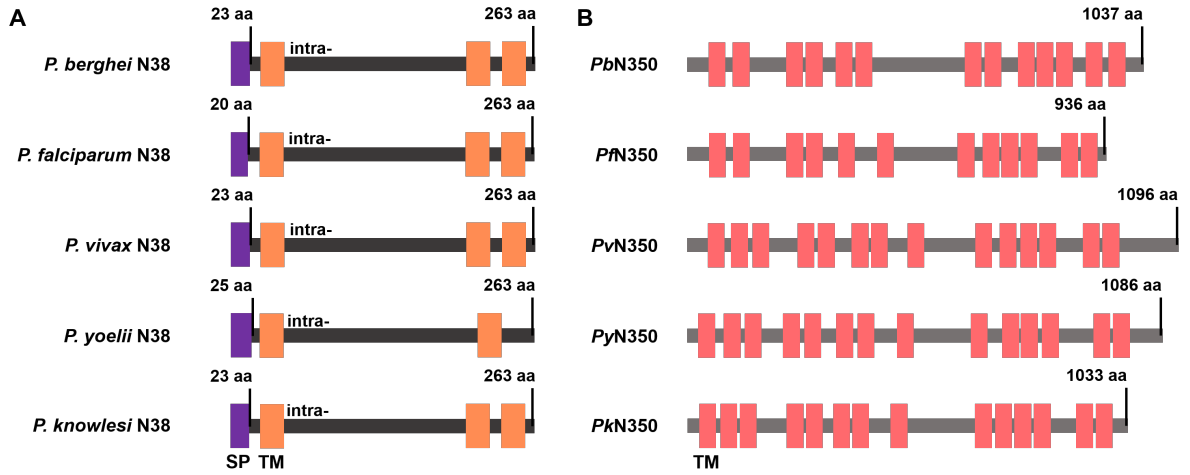

Figure 3.8. Domain architecture of the *Plasmodia spp* N38 and N350 proteins. The schematic protein models of *Plasmodium* N38 **(A)** and N350 **(B)** were generated by *in silico* sequence analysis of their amino acid sequences. The predicted signal peptide (SP), transmembrane domain (TM) and intracellular domain (intra-), are shown. The length of each figure is proportional to the gene size. Figure has been adapted and modified accordingly from the MRes thesis of Alexander Bailey (2019).

3.2.5 Developmental profiling of *P. berghei* and *P. falciparum AQP2*, *N38*, and *N350* transcriptional activity

DNA microarray profiling of *A. coluzzii* midguts infected with the *P. berghei 2.34* ANKA (WT) or the non-gametocyte producing 2.33 ANKA (NGP) parasite lines, revealed *AQP2*, *N38* and *N350* to be highly transcribed at the gametocyte stages (unpublished data, with the permission of Dr. Valerie Ukegbu, Imperial College London). To investigate further their importance during parasite development in the mosquito vector, the transcriptional activity of all three genes in both *P. berghei* and *P. falciparum* isolates was examined *in vivo* and *in vitro* by qRT-PCR and RT-PCR (**Figure 3.9**). In these assays, the *P. berghei* line ANKA *c507* (WT) that constitutively expresses *GFP* as well as the ANKA 2.33 NGP were used as gametocyte positive and negative controls, respectively. The *P. falciparum* NF54 strain was also used to explore the transcriptional profile of the *PfAQP2*, *PfN38* and *PfN350* orthologues.

In the qRT-PCR-based transcriptional survey of *PbAQP2*, *PbN38* and *PbN350,* their associated transcripts were present already during uptake of an infected bloodmeal and reached their peak at the time of gametocyte activation and later on, ookinete midgut invasion (24 hours). In further agreement with that, high transcription levels were also identified in purified *in vitro* ookinete and gametocyte populations. However, at day-10 post infection, *PbN38* and *PbN350* transcripts were no longer detectable suggesting a unique role during gamete fertilisation and ookinete development. *PbAQP2* transcripts reappeared in mosquito salivary glands, indicative of gene re-expression during the sporozoite stage. Statistical significance for qRT-PCR data of *AQP2* at 5dpi shows that the difference between the WT and KO line is non-significant ($p=0.1933$) and thus, the relative abundance value of the *AQP2* transcripts at this stage appear as false positive. A possible explanation for this might be related with the appearance of new transcripts at this time-point (that did not exist before), to which the PCR-primers use as a template and unspecifically bind. All *P. falciparum* orthologues, similarly to *P. berghei*, displayed a prolonged peak of transcript between one hour and 24 hours post infection, after which transcript levels were steadily declining until day-16 post infection, at which point no detectable transcript was present for any of the genes. These data show a potential role of *PfAQP2*, *PfN38* and *PfN350* in the early stages of infection. The transcription pattern of *AQP2* appears to vary between *P. berghei* and *P. falciparum,* where transcription was upregulated in salivary gland sporozoites only for the *P. berghei* orthologue. Purified gametocytes

also displayed high transcription levels of the genes, further supporting the strong signal identified at 1 hour post infection (**Figure 3.9, A**).

A follow-up qRT-PCR analysis was performed in order to examine whether *PbAQP2*, *PbN38* and *PbN350* have distinct transcription differences between male and female gametocytes. To do so, samples from female and male gametocytes of the 8.20 *P. berghei* parasite line (Janse *et al.*, 2006a), previously separated by Fluorescence-Activated Cell Sorting (FACS) based on their mCherry and GFP fluorescence, respectively, was used. Surprisingly, all three genes appeared to have higher transcription levels in the female compared to the male gametocytes (**Figure 3.9, B**), suggesting a female-specific nature. These findings are also in agreement with previous work which compared the transcriptomic pattern of female and male gametocytes (Yeoh *et al.*, 2017).

Consistently with the qRT-PCR data, the RT-PCR based analysis showed that *PbAQP2*, *PbN38* and *PbN350* are predominantly transcribed in both purified gametocytes and ookinetes. These data suggest that transcript signals obtained *in vivo* at 24 hours post infection are likely to not be solely derived from residual gametocyte remained transcripts but also, from *de novo* transcription of the genes in ookinetes. Weak transcript signals were also observed in pure ABS samples (derived from the NGP *Pb*2.33 ANKA line). In agreement to the qRT-PCR results, *PbAQP2* transcripts were absent during sporozoite development in the midgut oocysts but re-appeared at 21dpbf, a time that coincides with sporozoites movement towards the salivary glands. To validate these data, the RT-PCR analysis confirmed lack of *AQP2*, *N38* and *N350* transcripts in the *ΔAQP2*, *ΔN38* and *ΔN350* parasite lines, respectively. As also reported by the qRT-PCR, *PfAQP2*, *PfN38* and *PfN350* are abundantly transcribed at the gametocyte stages. However, since purified *in vitro* ookinetes cannot be obtained for *P. falciparum*, examination of whether the signal obtained *in vivo* at 24 hours post infection is associated with ookinetes *de novo* transcription or with residual gametocyte derived transcripts could not be obtained (**Figure 3.9, C**).

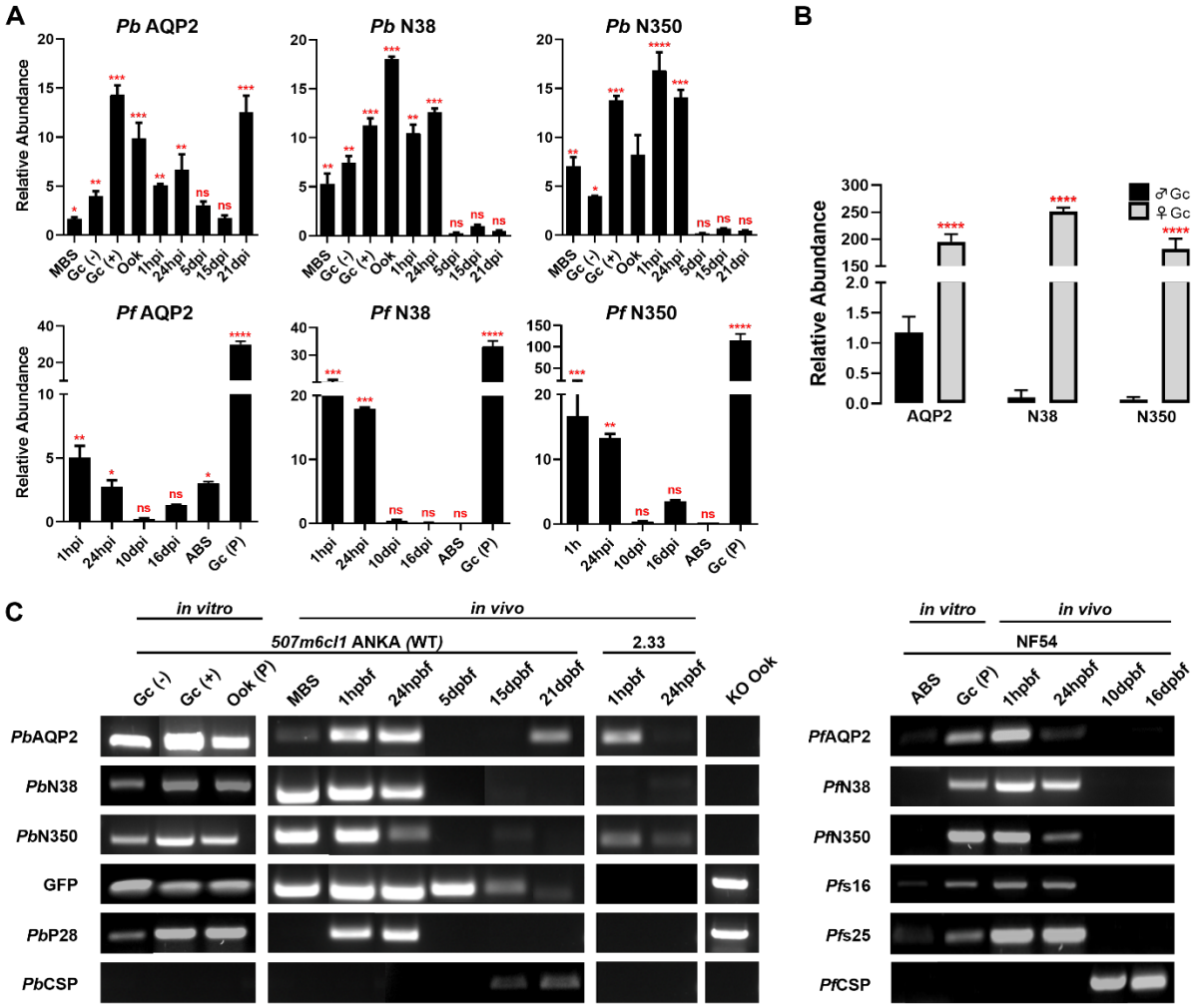

Figure 3.9. *P. berghei* and *P. falciparum AQP2*, *N38* and *N350* transcription profiles. (A) Relative abundance of *AQP2*, *N38* and *N350* transcripts during *P. berghei* and *P. falciparum in vitro* and *in vivo* developmental stages, as determined by qRT-PCR. The *P. berghei* ANKA *c507* (WT) and *P. falciparum* NF54 parasite lines were used, where normalisation was carried out against the constitutively expressed e*GFP* and *tARG* genes, respectively. *In vivo* samples were collected following dissections of *A. coluzzii* mosquito midguts and salivary glands. Each bar is the average of two biological replicates and error bars show SEM. Statistical significance was calculated using one-way ANOVA test between samples of WT and KO-infected (data not shown) mosquito tissues collected at the same time-point. Genes encoding the constitutively expressed e*GFP* and *tARG* ligase served as housekeeping genes for *P. berghei* and *P. falciparum*, respectively. Their expression pattern can be found in (**Appendix 9**). MBS; Mixed Blood Stages, Gc (-); Inactivated Gametocytes, Gc (+); Activated Gametocytes, Ook; Ookinetes, hpi; hours post infection, dpi; days post infection, ABS; Asexual Blood Stages. **(B)** Relative abundance of *P. berghei AQP2*,

N38 and *N350* genes in female and male gametocytes, as determined by qRT-PCR. The *P. berghei 820cl1m1* parasite line was used for harvesting blood stages gametocytes, prior to FACS-sorting and activation. Male gametocytes are GFP-fluorescent, whereas female gametocytes are mCherry fluorescent. Normalisation was carried out against the constitutively expressed *tubulin*. The average expression and standard errors of two independent biological replicates are shown. Statistical significance was calculated using one-way ANOVA test between male and female gametocyte populations for each gene. **(C)** RT-PCR analysis of the expression of *P. berghei* and *P. falciparum AQP2*, *N38* and *N350* transcripts in MBS, gametocytes, *in vitro* ookinetes and various *A. coluzzii* mosquito stages. The *P. berghei* constitutively expressed *GFP*, the gametocyte and ookinete-specific gene *P28* and the sporozoite-specific gene *csp* served as loading and stage specific controls, respectively. The *P. falciparum* gametocyte and ookinete-specific genes *Pfs16* and *Pfs25* as well as the sporozoite-specific gene *csp* served as stage specific controls. cDNA samples from *P. berghei ΔAQP2*, *ΔN38* and *ΔN350* ookinetes were used as negative controls for the primers specificity. MBS; Mixed Blood Stages, Gc (-); Non-activated Gametocytes, Gc (+); Activated Gametocytes, Ook (P); *in vitro* Purified Ookinetes, hpi; hours post infection, dpi; days post infection, ABS; Asexual Blood Stages.

3.2.6 Generation of loss of function mutants by targeted gene disruption

To study the biological role of AQP2, N38 and N350, *P. berghei* parasites in which the *Pb*AQP2, *Pb*N38, or *Pb*N350 loci were disrupted, have been generated using KO vectors from the PlasmoGEM resource (PbGEM-321755 for *ΔAQP2*; PbGEM-252084 for *ΔN38*; and PbGEM-121274 for *ΔN350*). The *P. berghei* ANKA *c507* line, that constitutively expresses *GFP,* was used as the reference line for the generation of these mutants. Following linearisation of the vectors and electroporation into *P. berghei* mature schizonts (immature blood stage forms of the parasites which are known to be susceptible to electroporation), double homologous recombination between the linear gene-targeting cassette and the WT locus was expected to take place in order to ensure integration of the resistance cassette and deletion of the respective WT gene locus. Potential transgenic parasites were later isolated following one round of pyrimethamine selection (**Figure 3.10, A**).

To determine whether the introduced plasmids were integrated into the parasite genome, gDNA of the WT and the cloned transfectant parasite were analysed by PCR.

Two pairs of integration-specific primers (GT+GW1/GW2; GW2+QCR2) and one pair specific for the WT locus (QCR1+QCR2) were used, according to the PlasmoGEM instructions (Schwach *et al.*, 2015) (**Table 2.3**). The first two sets of primers gave PCR products of expected size when used to analyse the *PbAQP2*, *PbN38* and *PbN350* null parasites gDNA, while no such bands were detected when used to analyse the WT gDNA. Similarly, the third set of primers was positive for the WT gDNA, whereas no signal was detected for the KO parasite lines, indicating successful replacement of the WT locus with the *h*DHFR/yFCU cassette (**Figure 3.10, B**).

Following drug and diagnostic selection of integrations, mutant parasite populations were not pure i.e. simultaneous detection of parasite populations that had successfully integrated the PlasmoGEM constructs into their genome and parasite populations that did not. To obtain clonal populations, successive dilutions of this mixed population (limited dilution cloning) was performed under pyrimethamine treatment. Following mouse infection establishment, successful isolation of clonal mutant populations was verified by PCR where a clear lack of WT genome indicated success. Two (VI, VII) clean KO clones for the *Pb*AQP2 KO locus, three (I, VII, VIII) clones of the *Pb*N38 KO locus and three (IV, V, VI) clones for the *Pb*N350 KO locus were rendered, in which the KO locus but not the WT locus could be detected by PCR (**Figure 3.10, C**). From these, one clone per transgenic line was selected for further characterisation.

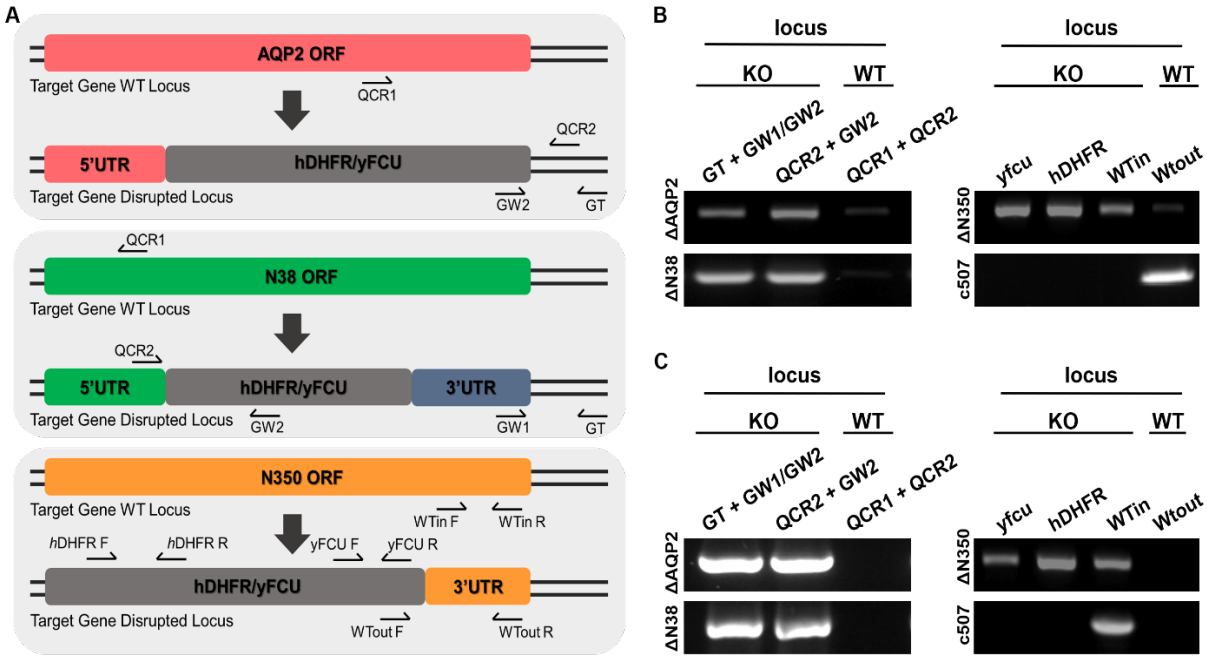

Figure 3.10. Generation of *P berghei AQP2*, *N38* and *N350* KO mutant parasite lines. (A) Schematic representation of the gene targeted disruption of *P. berghei*

AQP2 (top), *N38* (middle) and *N350* (bottom). The gene segment replaced by the *h*DHFR/yFCU selection marker (grey), as a result of the homologous recombination between the disruption vector and the WT locus, is denoted for each candidate as well as the positioning of the primer pairs used for the PCR genotypic analysis. The pyrimethamine resistance cassette is flanked by homology regions encoding a short length of the target gene and/or flanking genome sequence at both ends, to ensure correct orientation of the insert. **(B-C)** Genotypic analysis of the transfectant populations. gDNA was extracted from parasites that survived one round of pyrimethamine selection (B) and later, from those who established an infection following dilution cloning (C) and genotyped by diagnostic PCR. Bands represent presence of integration or WT locus as amplified by specific pairs of primers. The signal initially observed for the WT locus, indicates mixed WT/KO parasite population. However, these WT parasites that had survived the first drug selection possibly through episomal contamination, were completely eliminated following dilution cloning. Successful isolation of the clonal KO populations is demonstrated by the detection of the KO locus in all clonal populations, which lack their respective WT locus. The combination of the GT/GW1, GW2/QCR2 primers maps the integration site following homologous recombination, whereas the QCR1/QCR2 primer combination detects only the WT form of the gene. The PlasmoGEM provided GW, QCR1, QCR2 and GT primers were not conclusive for N350, so custom primers were designed for detection of the integrated construct; specific for the integrated drug selection cassettes (yFCU and *h*DHFR), the WT homology region present in both WT and the partial KO mutant line (WTin) and the segment of the WT gene replaced in the KO line (WTout). gDNA from the *c507* (WT) parasite line was used as a positive control. Images are representative for all clonal populations isolated following dilution cloning. All primer combinations are also shown in the schematic representations above.

3.2.7 Phenotypic characterisation of *P. berghei* parasites lines lacking expression of *AQP2, N38* and *N350*

3.2.7.1 ΔAQP2, *ΔN38* and *ΔN350* blood stage growth

Plasmodium asexual development and gametocytogenesis in the mammalian host is a prerequisite for its subsequent development in the mosquito vector. In order to investigate the asexual and sexual blood stage growth ability of *ΔAQP2*, *ΔN38* and *ΔN350* parasites, mice were infected with the respective mutant parasite lines (using

equivalent passage number among lines and injecting the same number of infected RBCs in each mouse) and quantitative data were collected periodically. Specifically, growth of asexual and sexual blood stages was monitored from Giemsa-stained tail blood smears at day-1, 2, 3 and 4 post infected blood inoculation. As expected, both asexual and sexual blood stage growth rates for all mutants were comparable to those determined for the *c507* (WT) *P. berghei* line (**Figure 3.11, A**), suggesting that all three genes are not involved during parasite blood stages development. These data also point to the fact that even if traits of *AQP2* and *N350* transcripts were identified in blood stage parasites, it is possible that further expression does not take place.

3.2.7.2 *ΔAQP2*, *ΔN38* and *ΔN350* gametocyte development

Successful gametogenesis in the mosquito midgut lumen is crucial for the subsequent fertilisation and *Plasmodium* infection establishment. It has been previously shown that all three genes are specifically transcribed in female gametocytes, hence they are not expected to be associated with male gametocyte developmental defects. However, in order to assess whether mutant male gametogenesis occurs normally or it is impaired, mutant male gametocytes were allowed to be activated until exflagellation was observed. Exflagellating centres were then counted for each parasite line. The *c507* (WT) line was used as a positive control. As expected, all mutant male gametocytes exflagellated both at a rate and induction time comparable to that of the WT (**Figure 3.11, B**). Since quantitative data of macrogametes activation cannot be obtained, morphological observations of the KO macrogametes based on the abundance and localisation of the P28-surface protein would enable us to identify potential abnormalities of the KO female gametes. Similarly, all macrogametes lacking expression of the *AQP2*, *N38* and *N350* genes did not exhibit a morphology that was different from that of WT parasites (**Figure 3.11, C**).

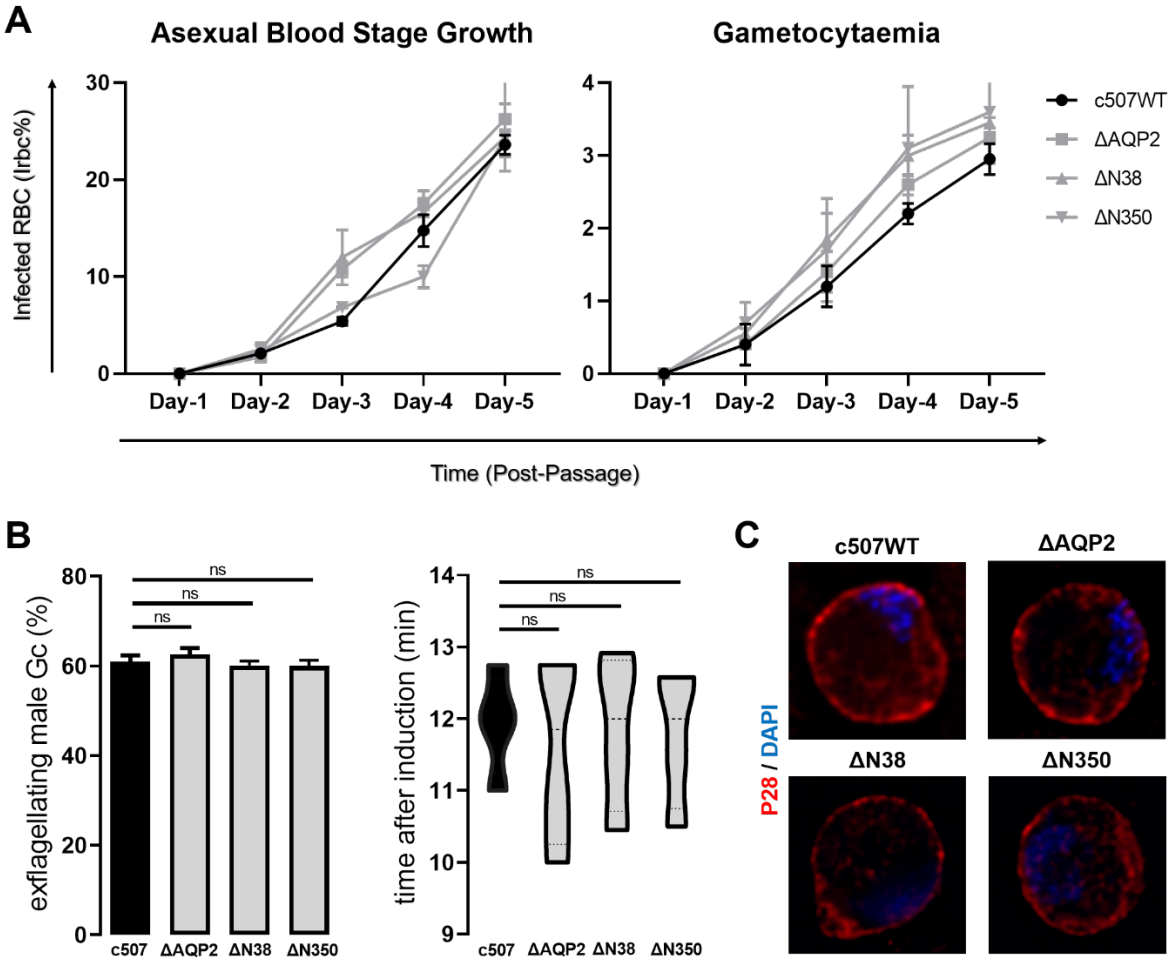

Figure 3.11. *ΔAQP2*, *ΔN38* and *ΔN350* blood stages growth and gametocyte development. (A) ABS growth and gametocyte production of the *Δ*AQP2, *ΔN38* and *ΔN350* mutant parasite lines at day-1, day-2, day-3, day-4 and day-5 post infection. The *P. berghei c507* (WT) line was used as positive control. Mice were infected with the same number of parasite-infected RBCs and each group was consisted from five to six CD1 mice. Data are presented as mean with SEM. Data derived from two individual biological replicates. **(B)** *Δ*AQP2, *ΔN38* and *ΔN350 P. berghei* male gametocytes exflagellation rates, following activation at 21^{0}C. The time at which the first exflagellation centre was observed has also been recorded and presented here. Data derived from two individual biological replicates and statistical significance was determined using the two-tailed, unpaired Student's *t*-test. Error bars indicate standard error of the mean. The *P. berghei c507* (WT) line was used as positive control. **(C)** Fluorescence microscopy images of *ΔAQP2*, *ΔN38*, *ΔN350* and WT female gametocytes stained with an antibody against their P28 surface protein (red) and DNA (blue), while in the *A. coluzzii* midgut lumen 15 min post mosquito blood feeding. Images were taken at x630 magnification. Scale bar is 5 μm.

3.2.7.3 *ΔAQP2*, *ΔN38* and *ΔN350* ookinete formation, development and traversal through *A. coluzzii* mosquito midgut epithelium

Since all three genes exhibit a female specific pattern and no developmental defects have been so far shown to be associated with *ΔAQP2*, *ΔN38* and *ΔN350* macrogamete and microgamete formation, a potential function of these genes prior to mosquito midgut invasion, presumably in fertilisation, was hypothesised. To investigate this, the gametocyte-to-ookinete conversion rate of *ΔAQP2*, *ΔN38* and *ΔN350* parasites both *in vivo* and *in vitro* were measured. Mosquito infection with the *P. berghei* ANKA *c507* (WT) line served as a positive control.

A significant 2.3-fold difference ($p<0.0001$) in the *in vivo* gametocyte-to-ookinete conversion rate was observed between the *ΔN38* and WT parasites, ranging from 70% to 83% (average 74%) in WT and 17% to 34% (average 32%) in *ΔN38* parasites. The *ΔAQP2* and *ΔN350* mutant parasites exhibited conversion rates comparable to that of the WT, ranging from 70% to 83% (average 74%) in WT, 68% to 76% (average 72%) in *ΔAQP2* and 62% to 81% (average 72%) in *ΔN350* during *in vivo* mosquito infections. These data suggest that none of these two genes are essential for gamete fertilisation and/or ookinete development. Staining against the P28 surface protein (Paton *et al.*, 1993) showed that all mutant ookinetes exhibit similar distribution to that of WT, suggesting normal ookinete morphology **(Figure 3.12, A; Table 3.1**).

The *in vitro* gametocyte-to-ookinete rate of ΔN38 parasites was substantially reduced by a 2-fold difference when compared to the WT, ranging from 64% to 70% (average 66%) in WT and 30% to 37% (average 33%) in *ΔN38* parasites in a total of two biological replicates. Nevertheless, the *ΔAQP2* and *ΔN350* gametocyte-to-ookinete conversion rates were comparable to the WT ranging from 64% to 70% (average 66%) in WT, 60% to 70% (average 65%) in *ΔAQP2* and 60% to 70% (average 66%) in *ΔN350* parasites following *in vitro* cultivation. In both cases the ookinete conversion ratios were consistently slightly lower than that of the WT however, these differences were never statistically significant ($p=1067$ and $p=9343$, respectively). (**Figure 3.12, B; Table 3.1**). Therefore, the process of gametocyte-to-ookinete conversion was not influenced by the absence of *AQP2* and *N350* and therefore resulted in the production of similar numbers of ookinetes to the WT. An impaired ookinete formation seems to accompany the *ΔN38* parasite line suggesting an important, not yet essential, role of this gene during gametocyte fertilisation and/or subsequent ookinete formation.

To investigate whether the *ΔAQP2*, *ΔN38* and *ΔN350* lines are associated with developmental defects before, during or immediately after the midgut epithelium traversal, ookinete load of the mutant and WT (control) parasite lines in the midguts of infected *A. coluzzii* was determined. Mosquito midguts were dissected at 25-26 hours pbf, a time that coincides with ookinete midgut epithelium traversal, and ookinetes were visualised after staining with an antibody against their P28 surface protein. Staining with the SRPN6 antibody was also performed in order to confirm invasion of the observed ookinetes in the midgut epithelium cells. *A. coluzzii* SRPN6 is drastically and transiently upregulated during malaria parasite invasion of the midgut (Abraham *et al.*, 2005) and is now widely used as an invasion marker in immunofluorescence assays and mosquito-parasite interaction assays. *ΔAQP2* and *ΔN38* ookinetes, similarly to the *c507* (WT), can be found in close proximity or within SRPN6-positive cells suggesting a successful invasion of the midgut epithelium (**Figure 3.12, D**). The corresponding median number of WT, *ΔAQP2* and *ΔN38* invading ookinetes was 198, 168 and 62, respectively (**Figure 3.12, C; Table 3.2**). The reduced number of invading ookinetes displayed for *ΔN38* compared to the WT and *ΔAQP2* is believed to be due to its impaired gametocyte-to-ookinete conversion rate, as previously observed. Surprisingly, out of 32 mosquito midguts infected with the *ΔN350* ookinetes, none of them appeared to have any SRPN6-positive cells, also explaining the null number of P28-stained ookinetes found inside the mosquito midgut epithelial cells.

To confirm previous observations and to investigate further whether ookinetes initially found to invade the mosquito midgut epithelium are also able to traverse and reach its basal side, infection of *CTL4*-silenced mosquitoes with the mutant parasite lines was performed. WT parasite infections were also used as control to confirm sufficient efficiency of *CTL4*-knockdown. CTL4 is a key regulator of ookinete elimination following attack by the complement-like system, promoting parasite lysis as opposed to melanisation (Osta *et al.*, 2004a). Therefore, *CTL4*-silencing leads to melanisation of ookinetes at the midgut sub-epithelial space upon epithelium traversal providing a powerful means to visualise and enumerate ookinetes that successfully traverse the midgut epithelium (Ecker *et al.*, 2008). The median number of *ΔAQP2* melanised ookinetes was comparable to that of the *c507* (WT), indicating that *ΔAQP2* ookinetes successfully traverse the midgut epithelium. As expected, the number of *ΔN38* melanised ookinetes was substantially reduced by 3.25-fold difference when compared to the WT, again possibly due to their gametocyte-to-ookinete reduced

conversion rates. It is worth mentioning that the number of *ΔAQP2* and *ΔN38* melanised ookinetes that infected the same batch of *CTL4*-silenced mosquitoes was similar to the number of P28-positive ookinetes counted for each line during the previous invasion assay, further validating both the phenotypes observed and the methods performed. However, the median number of melanised *ΔN350* ookinetes found was zero indicating that the ability of *ΔN350* ookinetes to reach the midgut sub-epithelial space was significantly reduced ($p<0.0001$) compared to WT parasites. No melanised ookinetes were observed in the midguts of infected ds*LacZ*-injected control *A. coluzzii* mosquitoes (**Figure 3.12, E**; **Table 3.3**).

3.2.7.4 *ΔN350* ookinetes gliding motility

The current data indicate that *ΔAQP2* and *ΔN38* ookinetes, despite the reduced gametocyte-to-ookinete conversion rates observed for the latter, are able to successfully enter and later traverse the mosquito midgut epithelial cells. On the other hand, *ΔN350* gametocytes, even if they have comparable gametocyte-to-ookinete conversion rates to the WT, their ability to establish successful infection in the mosquito midgut epithelium is significantly compromised ($p<0.0001$). This phenotype might be due to three distinct reasons; (i) ookinetes lacking expression of *N350* are immotile and thus unable to cross the midgut lumen in order to reach the epithelium, (ii) *ΔN350* ookinetes are unable to cross the midgut peritrophic matrix, or (iii) in the absence of N350, ookinetes do not manage to gain access in the midgut epithelium due to protein-protein interaction impairments.

The invasion defective phenotype of *ΔN350* ookinetes was next investigated. Considering that the ookinete invasion machinery is linked to its motility (Baum *et al.*, 2006), motility defects of *ΔN350* ookinetes were assessed by monitoring their Matrigel *in vitro* translocation speed. Matrigel mimics the viscosity of the mosquito midgut lumen environment therefore, allowing the direct comparison of ookinetes movement under both *in vivo* and *in vitro* conditions. *ΔN350* mutant and WT ookinetes exhibited significant variation ($p<0.0001$) as to their gliding motile behaviour; the average velocity of WT and *ΔN350* ookinetes is 7.37 ± 1.57 (N = 55) and 1.64 ± 0.69 μm/min (N = 68), respectively. Additionally, while WT ookinetes display distinct modes of motility; stationary rotation, translocational spiralling and straight-segment motility (Vlachou *et al.*, 2004), *ΔN350* mutant ookinetes only go through a semicircle route within the same time frame (**Figure 3.12, F**). Therefore, this assay establishes that

ΔN350 ookinetes display motility defects that later affect their ability to invade the mosquito midgut epithelium and eventually, establish infection in the midgut.

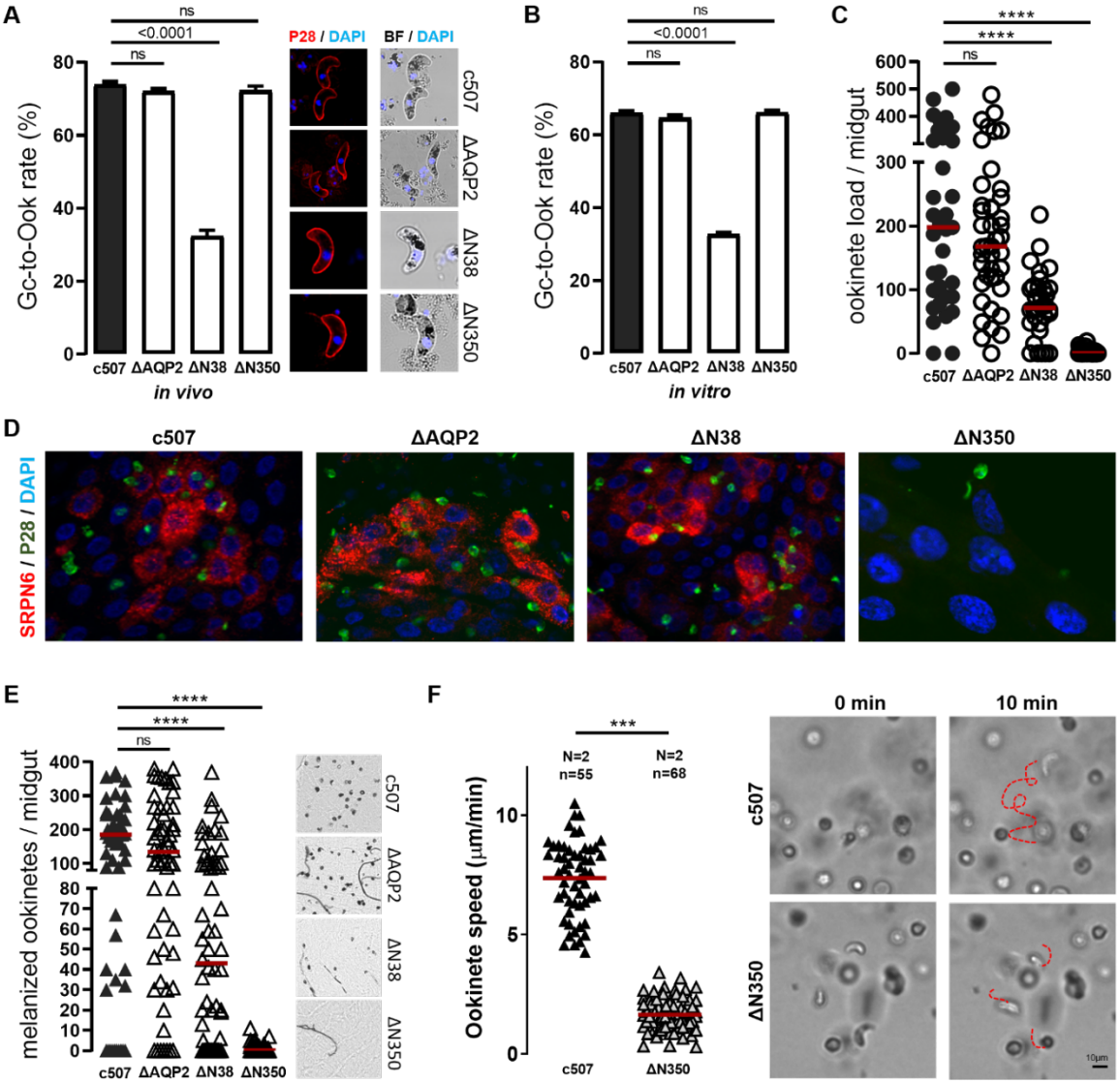

Figure 3.12. *ΔAQP2*, ΔN38 and *ΔN350* ookinete formation, development and mosquito midgut epithelium. *c507* (WT) (control), *ΔAQP2*, *ΔN38* and ΔN35 female gamete conversion to ookinete *in vivo* **(A)** and *in vitro* **(B)** in the *A. coluzzii* midgut. Error bars show SEM, whereas statistical significance was determined with a two-tailed, unpaired Student's *t*-test. Fluorescent microscopy images presented in **(A)** are from confocal sections of WT and mutant ookinetes in the blood bolus of *A. coluzzii* mosquitoes 20-22 hours pbf, stained with the P28 antibody (red) and DAPI (blue). BF is bright field. Images were taken at x400 magnification. **(C)** Load of invading ookinetes in the midguts of *A. coluzzii* mosquitoes, at 24-25 hours pbf. Statistical significance was determined using the Mann Whitney U-test. **(D)** Fluorescence images of ookinete-invaded *A. coluzzii* midgut epithelial cells, at 25-26 hours pbf, stained with SRPN6

antibody (red), P28 antibody (green) and DAPI (blue). Images were taken at X400 magnification. **(E)** Melanised ookinete load in *CTL4*-silenced *A. coluzzii* infected with *c507* (WT), *ΔAQP2*, *ΔN38* and *ΔN350* parasite lines. Red lines indicate median; ns, not significant. All data derived from two individual biological replicates. Statistical significance was determined using Mann Whitney U-test. Representative bright field images indicating melanised ookinetes. **(F)** *ΔN350* and *c507* (WT) (control) velocity during *in vitro* motility assay. Ookinetes were allowed to translocate on MatrigelTM prepared slides and their speed was calculated using time-lapse shooting mode, every 10 sec for a total of 10 min. *c507* (WT) ookinetes were used as reference control. P-values were calculated according to Student's *t*-test; N corresponds to the number of ookinetes, whereas horizontal lines indicate arithmetic mean. The samples were obtained from at least four independent preparations. The speed of individual ookinetes was measured using the manual tracking plugin in the Icy software package (http://icy.bioimageanalysis.org/). Representative images of *c507* (WT) and *ΔN350* mutant ookinetes position in Matrigel, are also shown, before and after 10 min of time-lapse imaging. Red dotted lines indicate the average ookinetes motion profiling. Images were taken using light microscopy, at x400 magnification. Scale bar is 10 μm.

To further support this result, *ΔN350* ookinetes were injected into the haemocoel of *A. coluzzii* mosquitoes to assess if the oocyst defective phenotype could be rescued. Indeed, the defective phenotype of the *ΔN350* ookinetes was rescued when midgut invasion was bypassed (Guttery *et al.*, 2012). Infection establishment was also quantitatively assessed in the mosquito abdomen, as injected ookinetes can rest anywhere in the haemocoel and develop into oocysts (Paskewitz & Shi, 2006). Upon dissection, many of the recovered oocysts were also observed to be floating in the haemolymph. *P. berghei ΔN350* oocysts were observed in 82% of the injected mosquito midguts that were dissected, and the median infection intensity was determined to be 11.00 ± 1.29 compared to 13.50 ± 1.86 found for the WT control parasites. Following 21-days post ookinete haemocoel injections, salivary gland sporozoites were found to be 2,907 ± 132 for the *ΔN350* parasite line compared to the 3,087 ± 174 sporozoites found for the WT (control) parasite line (**Figure 3.13**).

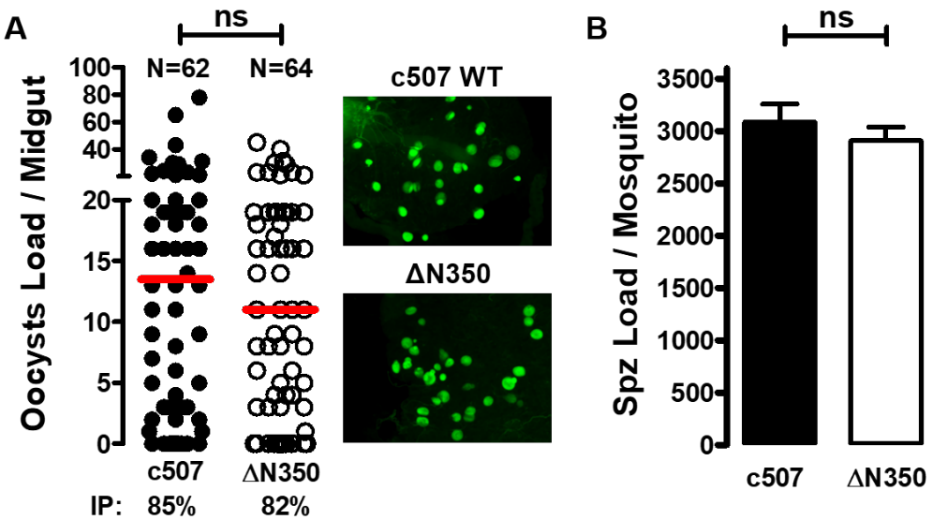

Figure 3.13. *ΔN350* midgut oocyst and salivary gland sporozoite numbers following direct injections of mutant or WT (control) ookinetes in *A. coluzzii* haemocoel. (A) Each dot represents the number of *ΔN350* or *c507* (WT) (control) oocysts on an individual mosquito and the median is indicated with a red line (N = number of midguts examined). Oocyst load was determined by counting parasites developed all over the mosquito abdomen area. All parasite phenotypes were evaluated following two biological experiments. Infection prevalence (IP) was calculated as the percentage of midguts that were infected with at least one oocyst. Median number of oocysts were compared using the Mann Whitney U-test. Representative images of *ΔN350* or *c507* (WT) infected *A. coluzzii* midguts at day-8 pbf, indicating the constitutively *GFP*-expressing oocysts. **(B)** Salivary gland *ΔN350* and *c507* (WT) control sporozoite load in *A. coluzzii* mosquitoes, at day-21 pbf. The mean of the pooled data of two batches of 25 homogenised salivary glands collected in two biological replicates is presented. Error bars show standard error.

3.2.7.5 *ΔAQP2*, *ΔN38* and *ΔN350* oocyst development and sporozoite formation

Mutant parasite lines were then assessed for their ability to form oocysts *in vivo*, following infection of *A. coluzzii* mosquitoes (**Figure 3.14, A; Table 3.4**). Oocysts were observed by fluorescence microscopy and carefully enumerated at day-12 pbf. The *ΔAQP2* and *ΔN38* parasite lines were able to establish infection in the mosquito midgut at the oocyst stage, although the latter produced only 34.5% of the total oocyst load recorded for the WT (*ΔN38* median: 5, WT median: 14.5). The prevalence of infection was also lower in *ΔN38* parasites (69%), whilst *ΔAQP2* oocyst infection prevalence (85%) was comparable to the WT (87%). Interestingly, *ΔAQP2* oocyst load was very much alike to the WT with median oocyst density which was found to be

13.0. This observation further supports that the absence of this gene does not bear any severe consequences during ookinete development, oocyst formation or vulnerability to the mosquito immune responses. On the contrary, *ΔN350* parasites were severely compromised in reaching the oocyst stage with median infection intensity and prevalence at 0 and 6%, respectively. These results validate what was previously shown for N350 essentiality in ookinete gliding motility.

Mutant oocysts were then assessed for their ability to mature and form sporozoites (**Figure 3.14, B; Table 3.5**). At day-15 pbf, mosquito midguts were dissected, homogenised and sporozoites were counted using a haemocytometer and light microscopy. Detection of sporozoites in the midgut would require successful nuclear division and oocyst plasma membrane retraction through internal invaginations in order to form the sporoblasts and thus, the sporozoites (Aly *et al.*, 2009). Presence of sporozoites in midguts was observed for the *ΔN38* (9,780 ± 3,080) even though in lower numbers compared to the WT (28,650 ± 3,050), due to their prior developmental defects during gamete fertilisation and/or ookinete development. One would expect that since *ΔAQP2* oocyst load is comparable to the WT, midgut sporozoite numbers should also follow the same pattern. However, *ΔAQP2* oocysts seem to have led to the production of very little sporozoites (401 ± 101) suggesting defects possibly during oocyst maturation. As expected, no *ΔN350* sporozoites were observed.

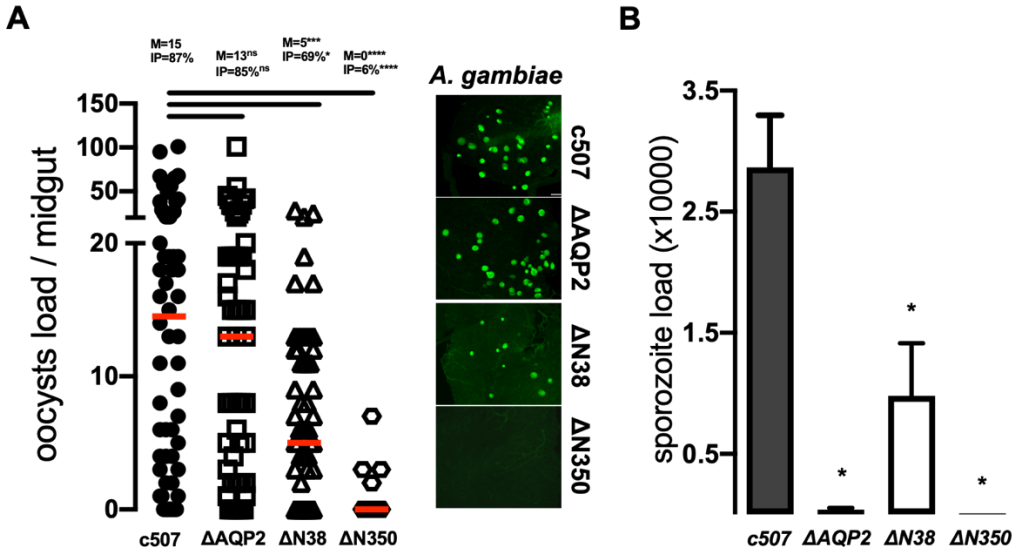

Figure 3.14. *ΔAQP2*, *ΔN38* and *ΔN350* oocyst development and sporozoite formation. (A) *ΔAQP2*, *ΔN38* and *ΔN350* oocyst graphs indicating parasite distribution in the midguts of *A. coluzzii* mosquitoes as counted at day-12 pbf. *c507* (WT) infections were used as control. Data derived from two independent biological

replicates. m corresponds to the median oocyst infection intensities, also shown as a horizontal red line. IP, oocyst infection prevalence; ns, not significant. Statistical analysis was performed using Mann Whitney U-test for infection intensity and Fisher's exact test for infection prevalence. Fluorescent microscopy images of *GFP*-expressing oocysts, representative for each mutant and *c507* (WT) control infection intensity, as recorded in the midguts of *A. coluzzii* mosquitoes. Images were taken at X100 magnification. **(B)** Midgut *ΔAQP2*, *ΔN38*, *ΔN350* and *c507* (WT) control sporozoite numbers in *A. coluzzii* mosquitoes, at day-15 pbf. The mean of the pooled data from two biological replicates is presented. For each replicate, sporozoite numbers were determined from two batches of 25 homogenised midguts using light microscopy. Statistical significance was determined using a two-tailed, unpaired Student's *t*-test. Error bars show standard error.

Table 3.1. *In vivo* and *in vitro* gametocyte-to-ookinete (Gc/Ook) conversion rates of *ΔAQP2*, *ΔN38*, *ΔN350* and control ANKA *c507* (WT) parasite lines in naïve *A. coluzzii* mosquitoes

	Parasite line	Number of experiments	No of midguts / Replicate	Number of Macrogametes	Number of Ookinetes	Fertilisation Rate (%)	Reduction (%)	*p*-value
in vivo	*c507* (WT)	2	10	184	520	73.86		
	ΔAQP2	2	10	222	574	72.11	-2.37	0.0674 (ns)
	ΔN38	2	10	450	225	33.33	-54.85	<0.0001
	ΔN350	2	10	151	380	71.56	-3.11	0.2565 (ns)
in vitro	*c507* (WT)	2	10	274	711	72.18		
	ΔAQP2	2	10	282	788	73.64	+2.02	0.1067 (ns)
	ΔN38	2	10	805	456	36.16	-49.90	<0.0001
	ΔN350	2	10	278	779	73.70	+2.11	0.9343 (ns)

The *in vivo* and *in vitro* gametocyte-to-ookinete (Gc/Ook) conversion rates were calculated as the percentage of P28-positive ookinetes to the total number of the P28-positive macrogametes and ookinetes together. The *in vivo* conversion rates were calculated from suspensions of 10 homogenised midguts, assayed 16-17 hours pbf. Statistical significance was determined using a two-tailed, unpaired Student's *t*-test (ns, non-significant).

Table 3.2. Number of P28-positive *ΔAQP2*, *ΔN38*, *ΔN350* and control ANKA *c507* (WT) ookinetes in the midguts of *A. coluzzii* mosquitoes, at 24-26 hours pbf

Parasite line	Number of experiments	No of midguts	P28+ ookinete range	Infection Intensity		*p*-value	Standard Error	Fold Difference
				Arithmetic mean	Median			
c507 (WT)	2	35	0-500	210.80	198.00		23.01	
ΔAQP2	2	43	0-479	188.40	168.00	0.5946 (ns)	16.89	1.18
ΔN38	2	32	0-218	76.22	71.50	<0.0001	9.08	2.77
ΔN350	2	44	0-19	2.14	0.00	<0.0001	0.59	N/A

P28-positive ookinetes in the mosquito midgut were enumerated at 24-26 hours post mosquito blood feeding using fluorescence microscopy. The fold difference was calculated based on the median number of P28-positive KO ookinetes against WT.

Table 3.3. Melanised *ΔAQP2*, *ΔN38*, *ΔN350* and control ANKA *c507* (WT) ookinetes in *CTL4* knockdown *A. coluzzii* mosquitoes

Parasite line	Number of experiments	No of midguts	Prevalence (%)	Infection Intensity		Ookinete range	*p*-value
				Arithmetic mean	Median		
c507 (WT)	2	60 (50/10)	83.33	162.30	185.50	0-389	
ΔAQP2	2	57 (50/7)	87.72	151.00	134.00	0-380	0.5466 (ns)
ΔN38	2	62 (44/18)	70.97	71.26	43.00	0-370	<0.0001
ΔN350	2	77 (17/60)	22.08	0.71	0.00	0-11	<0.0001

The table shows the number of *ΔAQP2*, *ΔN38*, *ΔN350* and control WT melanised parasites in two independent biological replicates, in the midguts of *CTL4*-silenced *A. coluzzii* mosquitoes, 6 days pbf. The total number of midguts is indicated in the third column, as the ratio between the number of infected midguts to the number of uninfected midguts. Prevalence shows the percentage of midguts with at least one melanised parasite. Midguts with zero parasites were also considered for calculation of the mean and median of the parasite densities. Statistical significance was determined using the Mann Whitney U-test.

Table 3.4. *ΔAQP2*, *ΔN38, ΔN350* and control ANKA *c507* (WT) oocyst load in naive *A. coluzzii* mosquito midguts, at day-12 pbf

Parasite line	Number of experiments	Number of midguts	Prevalence (%)	*p*-value	Infection Intensity				
					Arithmetic mean	Median	Parasite range	*p*-value	Fold change
c507 (WT)	2	60 (52/8)	86.67		19.88	14.50	0-101		
ΔAQP2	2	54 (46/8)	85.19	>0.9999	16.17	13.00	0-101	0.5642	-1.22
ΔN38	2	56 (39/17)	69.64	0.0407	6.88	5.00	0-28	0.0003	-2.89
ΔN350	2	65 (4/61)	6.15	<0.0001	0.23	0.00	0-7	<0.0001	>19.88

ΔAQP2, *ΔN38, ΔN350* and WT parasite infections of naive *A. coluzzii* mosquitoes was assessed 12-days pbf. Equal numbers of *ΔAQP2*, *ΔN38, ΔN350* or Pb*c507* (WT) infected midguts from independent biological replicates (indicated in the second column) were pooled for each group. The total number of midguts is indicated in the third column, as the ratio between the number of infected midguts to the number of uninfected midguts. Prevalence shows the percentage of midguts with at least one oocyst. Midguts with zero parasites were also considered for calculation of the arithmetic mean and median of parasite densities (number per midgut). Fold differences (tenth column) between *ΔAQP2*, *ΔN38, ΔN350* and WT oocyst densities were computed using the median values. Statistical significance of the oocyst load was determined using the Mann Whitney U-test, whereas statistical significance of the prevalence percentages was assessed by Fisher's exact test.

Table 3.5. Midgut sporozoite numbers of the *P. berghei ΔAQP2*, *ΔN38*, *ΔN350* and control ANKA *c507* (WT) parasite lines in naive *A. coluzzii* mosquitoes

Parasite line	Number of experiments	Mean	Range	SEM	*p*-value	Infectivity to mice (21dpi)
c507 (WT)	2	2,865.00	2,560.00-3,170.00	305.00		6/6
ΔAQP2	2	40.10	30.00-50.20	10.10	0.0489	0/7
ΔN38	2	978.00	670.00-1,286.00	308.00	0.0112	0/6
ΔN350	2	10.00	10.00-10.00	0.00	0.0115	0/6

The table reports *ΔAQP2*, *ΔN38*, *ΔN350* or ANKA *c507* (WT) midgut (oocyst) sporozoite numbers from two biological replicates of naive *A. coluzzii* infections. For each replicate, sporozoite numbers were determined from two batches of 25 homogenised midguts at day-15 post infection. SEM represents the standard error from the mean. Statistical significance was determined using a two-tailed, unpaired Student's *t*-test. Infectivity to mice was assayed by allowing infected mosquitoes to feed on Balb/C mice on day-21 of infection. Parasitaemia of mice was assayed by Giemsa-stained thin blood smears from day-5 onwards.

3.2.7.6 *ΔAQP2* oocyst development and nuclear division

Upon closer examination, an additional distinct phenotype of the *ΔAQP2* oocysts was detected. Specifically, a defective phenotype was identified with regards to either the mitotic endoreplication events taking place in the developing oocyst or the sporoblasts development and the subsequent sporozoite formation.

From day-12 to day-16 post infection, WT oocysts dramatically increased in size (see below) and about 85-90% of those had either sporulated with mature sporozoites arranged in an array pattern inside the mature oocyst or appeared to be already ruptured with sporozoites egressing from them. In contrast, about 98% of the *ΔAQP2* oocysts were completely void of sporozoites at day-16 post infection, yet, exhibiting similar morphology with those observed at day-12 post infection (**Figure 3.15, A**). Specifically, day-16 *ΔAQP2* oocysts lacked the characteristic DNA-staining pattern of mature oocysts where the haploid nuclei of the fully formed sporozoites are distinct, highly organised and aligned close to the oocysts' periphery. Although some DNA could be observed in *ΔAQP2* oocysts, its arrangement was disorganised, and its content appeared slightly lesser than that of the WT oocysts. Interestingly, the morphological structure of the mutant oocysts remained as such even at day-20 pbf (**Figure 3.15, C**). This steady maturation phase also explains the fact that very few sporozoites were detected in the preparations of homogenised *ΔAQP2* midguts at day-15 pbf; 100 ± 31 *ΔAQP2* sporozoites/midgut compared to the 1023 ± 118 WT (control) sporozoites/midgut infected *A. coluzzii* mosquitoes (**Figure 3.15, D**).

The abnormal development of the *ΔAQP2* oocysts can be further validated by the invariable oocyst load in the midguts of *A. coluzzii* at day-16, 18 and 20 post infection, indicating that none or very few oocysts have been indeed ruptured in order for sporozoites to be released into the mosquito haemocoel. On the other hand, the number of WT oocysts has been gradually decreasing from day-16 pbf onwards, reaching zero infection intensity levels at day-20 pbf. Interestingly, all of the *ΔAQP2* oocysts were GFP-positive at day-16 and day-18 pbf, but over time there was a drastic loss on the number of GFP-positive oocysts. By day-20 pbf, 70% of *ΔAQP2* oocysts had lost GFP fluorescence and hence were no longer viable. This loss of GFP also coincided with the observation of some degenerating oocysts (**Figure 3.15, B**).

Nevertheless, the genome organisation of the *ΔAQP2* oocysts was clearly different from that of the tight and small nucleus characteristic of the tetraploid ookinete

indicating that endomitosis had been at the very least initiated in the mutant oocysts. The few sporoblasts observed, also confirm that nucleus movement close to the oocyst's periphery as well as oocyst membrane retraction occurred up to a certain point and therefore, the developmental inhibition occurred just before sporozoite production. However, further investigation of other characteristic traits of the mature oocysts' morphology such as microtubule appearance, mitochondria development, inner and outer sporoblastoid folding, was not carried out.

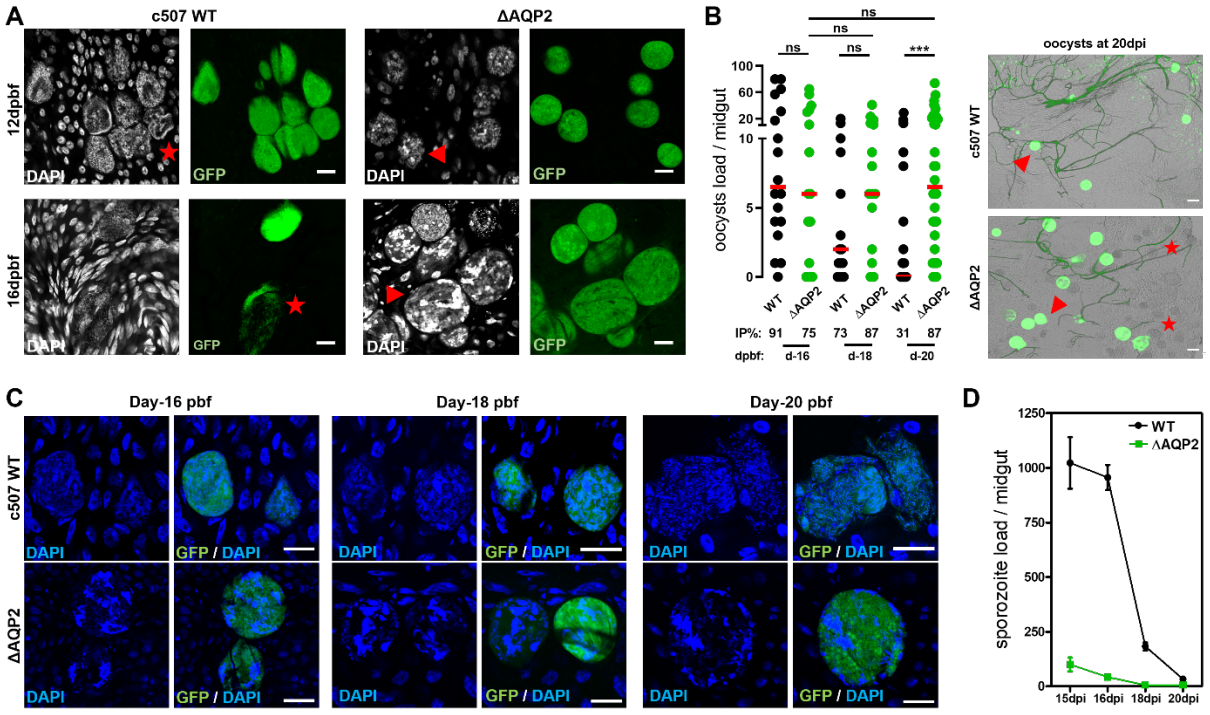

Figure 3.15. *ΔAQP2* oocyst development. (A) Fluorescent microscopy images of *ΔAQP2* and *c507* (WT) (control) *GFP*-expressing oocysts at day-12 and day-16 post infection, from the midguts of *A. coluzzii* mosquitoes. Mature oocysts with the haploid nuclei of formed sporozoites are distinct, highly organised and aligned on the oocyst's periphery, and are indicated with an asterisk, whereas immature oocysts with disorganised genome content are indicated with an arrowhead. DNA was visualised by DAPI (white) staining. Images were taken at x400 magnification. Scale bar is 20 µm. **(B)** *ΔAQP2* oocyst load at 16, 18 and 20-days pbf in *A. coluzzii* mosquitoes. The median oocyst infection intensity for each condition is also shown in horizontal red lines. IP; oocyst infection prevalence calculated as the percentage of midguts that appeared to have at least one oocyst. Mosquito infection with the *c507* (WT) line served as a control. Data derived from two individual biological replicates and statistical significance was determined using the Mann Whitney U-test. ns, non-

significant. Fluorescence microscopy images of *GFP*-expressing (green) oocysts following infection with the *ΔAQP2* or WT control parasite lines. Arrowheads indicate GFP(+) oocysts, whereas asterisks show GFP(-) oocysts. WT control and *ΔAQP2* parasites express GFP in most oocysts at day-15 post infection, whereas by day-20 most of the *ΔAQP2* oocysts have lost their GFP fluorescence and thus appear transparent. Images were taken at x200 magnification. Scale bar is 30 μm. **(C)** Nuclear division progress of *ΔAQP2* and WT oocysts at day-16, day-18 and day-20 pbf in *A. coluzzii* mosquitoes. Oocysts are GFP (green) positive as a result of the constitutive *eGFP* expression in the *c507* (WT) parental line. DNA was visualised by DAPI (blue) in order to observe the sporoblast and genome content distribution of each oocyst. Images were taken at x400 magnification. Scale bar is 20 μm. **(D)** Midgut sporozoite load in *ΔAQP2* and *c507* (WT) (control) infected *A. coluzzii* mosquitoes at 15, 16, 18 and 20-days pbf. The mean of the pooled data from two biological replicates is presented. The number of sporozoites was calculated from suspensions of 20 homogenised midguts, assayed in two batches of ten. Error bars show standard error.

It is generally accepted that oocyst size is heterogeneous, and the developmental rate of the individual oocyst is asynchronous (Ponnudurai *et al.*, 1989). However, *ΔAQP2* oocysts displayed a clear shift towards larger size compared to the WT, especially from day-12 post mosquito infection onwards. Specifically, the mean size of WT and *ΔAQP2* oocysts was similar at day-12 post infection at 42.79 ± 0.81μm and 39.68 ± 1.12 μm, respectively, whereas at day-15 post infection the average size of WT and *ΔAQP2* oocysts were 40.50 ± 1.09 μm and 50.50 ± 1.20 μm, respectively. The size difference was even more striking at day-20 post infection where WT oocyst size was 44.01 ± 1.70 μm, compared to the 66.81 ± 1.16 μm size of the *ΔAQP2* oocysts. However, this dramatic increase reached a plateau by day-20 pbf where the size of the mutant oocysts does not noticeably differ from day-17 (62.92 ± 1.69 μm) or day-18 post infection (65.58 ± 1.71 μm) (**Figure 3.16; Table 3.6**). These results suggest that up to a specific size, *ΔAQP2* oocyst size does not radically increase further. To conclude, it is clear that even if the complete maturation of *ΔAQP2* oocysts was inhibited prior to sporozoite formation, they kept increasing in size rapidly suggesting that water and nutrients uptake or secretion was possibly continued with a different rate compared to the WT. The fact that no further increase was observed in their size might also be due to what has been previously observed; day-20 oocysts seem to lose their GFP fluorescence and thus are no longer viable.

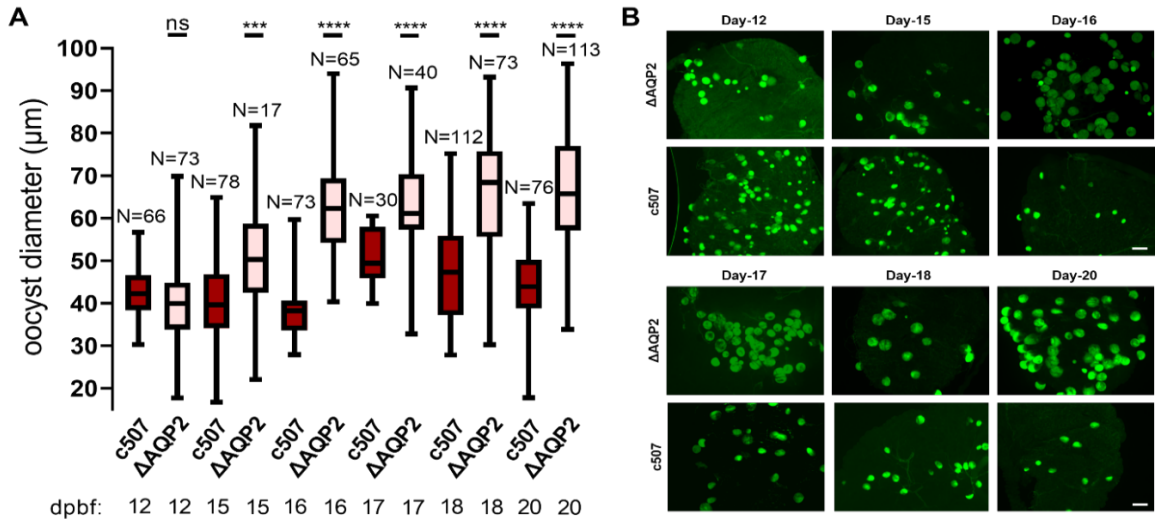

Figure 3.16. *ΔAQP2* oocyst size progression. (A) Box plot of the diameter measurements of *ΔAQP2* (pink) and *c507* (WT) control (red) oocysts at day-12, day-15, day-16, day-17, day-18 and day-20 post infection. Upper and lower whiskers represent the largest and smallest oocyst diameter, respectively. Horizontal line in each box indicates mean and whiskers show SEM. Data derived from two individual biological replicates. N is the total number of oocysts analysed, whereas statistical significance was determined using the unpaired Student's *t*-test. Oocyst size measurement was recorded randomly from about 20 midguts of each condition. **(B)** Fluorescent images of *ΔAQP2* and *c507* (WT) (control) oocysts, showing the progression in size at day-12, day-15, day-16, day-17, day-18 and day-20 post infection, respectively. Oocysts are GFP (green) positive as a result of the constitutive *eGFP* expression in the *Pbc507* (WT) reference line. Images were taken at x100 magnification. Scale bar is 80 µm.

3.2.7.7 *ΔAQP2*, *ΔN38* and *ΔN350* transmission to the host

The ability of the mutant parasites to establish infection in the next vertebrate host upon mosquito bite was assessed. At day-21 post infection, mosquitoes were allowed to feed on mice which were then monitored for consequent infection. Successful transmission would be indicated by the observation of asexual blood stage parasites. Interestingly, transmission appeared to be unsuccessful following bites by all *ΔAQP2*, *ΔN38* and *ΔN350* infected mosquitoes (**Table 3.5**). Therefore, the substantial reduction in the number of *ΔAQP2*, *ΔN38* and *ΔN350* midgut oocysts and subsequently midgut oocyst sporozoites translated to a complete blockage in the rodent malaria transmission. In conclusion, all three genes are essential in order for *P. berghei* parasites to be able to complete their lifecycle in their mosquito vector.

3.2.7.8 Analysis of new *ΔAQP2*, *ΔN38* and *ΔN350 P. berghei* clones

To validate the proposed function and thus the essentiality of the AQP2, N38 and N350 *P. berghei* genes, mosquito infections with a different clonal KO population for each gene were performed. The new *ΔAQP2*, *ΔN38*, and *ΔN350* clones were also generated using the ANKA *c507 GFP*-expressing genetic background line. Consistent with the previous analysed clonal populations, all three mutant parasite lines exhibited normal development in mouse blood stages (**Figure 3.17, A**). Going a step further, the macrogametocyte-to-ookinete conversion rates of the *ΔAQP2* and *ΔN350* parasites in the *A. coluzzii* midgut lumen were comparable to the *c507* (WT) parental line, indicating that no developmental defects are accompanying these parasites during the gametocyte-to-ookinete transition. However, macrogametes lacking expression of *N38* displayed a significant reduction ($P<0.0001$) in their ability to form ookinetes compared to the WT, ranging from 26% to 52% (average 41%) in *ΔN38* and 56% to 92% (average 73%) in WT parasites (**Figure 3.17, B; Table 3.7**). These results confirm what was previously observed for the ΔN38 parasites.

Following *A. coluzzii* mosquito infections, *ΔAQP2* parasites rendered similar infection intensity and prevalence to the WT control (*ΔAQP2* median: 11; *ΔAQP2* prevalence: 73%; WT median: 13; WT prevalence: 75%), whereas a dramatic reduction in the number of oocysts was observed for the *ΔN38* and *ΔN350* mutant parasites (*ΔN38* median: 3; *ΔN350* median: 0) (**Table 3.17, C; Table 3.8**). Midgut sporozoite counting at day-15 pbf revealed low *ΔAQP2* sporozoite load, compared to what was expected based on the high number of oocysts previously determined. The reduction in the number of *ΔN38* and *ΔN350* oocysts further affected the total midgut sporozoite load at day-15 pbf (**Figure 3.17, D; Table 3.9**).

To further validate that the observed elimination of the *ΔN350* parasites at the oocyst stage was due to the previous identified impaired ookinete motility, the motility of the mutant ookinetes was assessed by monitoring their Matrigel *in vitro* translocation speed. *ΔN350* mutant and WT ookinetes exhibited a significant variation ($p<0.0001$) as to their gliding motile behaviour; the average velocity of WT and *ΔN350* ookinetes was determined to be 7.63 ± 1.47 and 1.66 ± 0.75 μm/min, respectively (**Figure 3.18, A**). Therefore, this assay establishes once more that ookinetes lacking expression of *N350* display motility defects, which subsequently affect their ability to invade the mosquito midgut epithelium and eventually develop into oocysts.

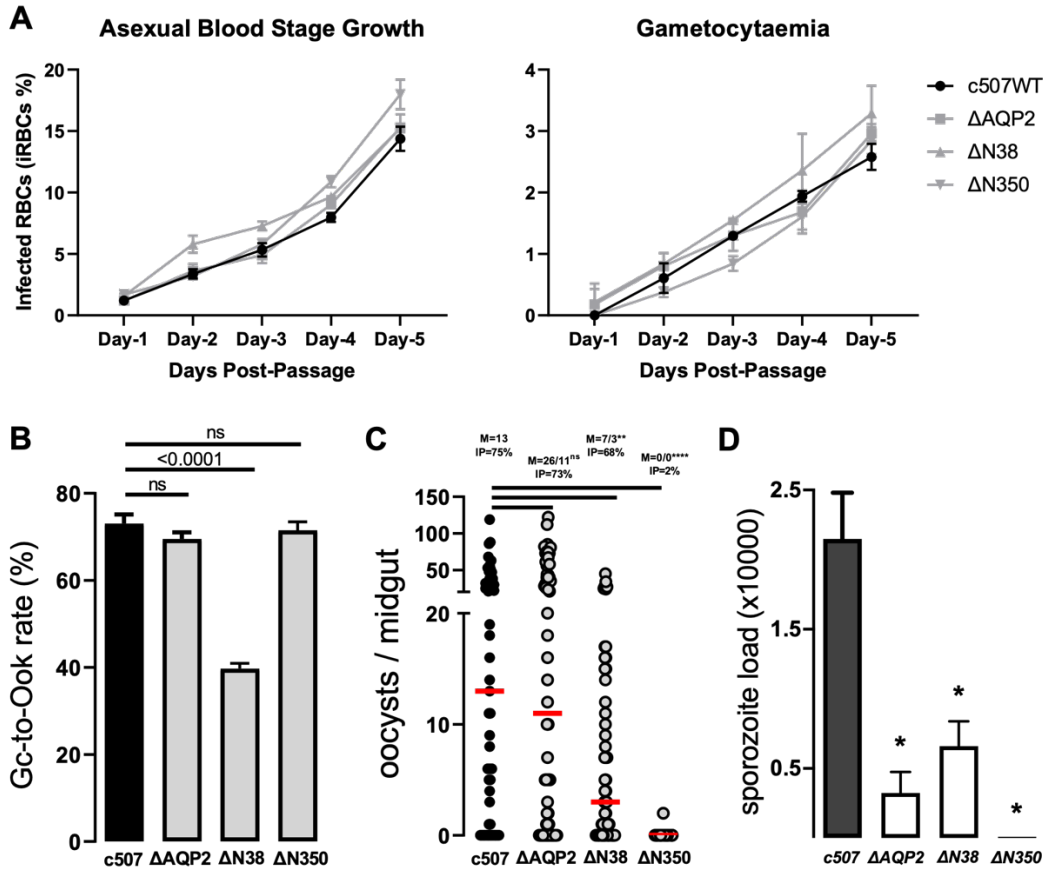

Figure 3.17. Phenotypic analysis of new *ΔAQP2*, *ΔN38* and *ΔN350 P. berghei* clonal populations. (A) ABS growth and gametocyte production of the *Δ*AQP2, *ΔN38* and *ΔN350* mutant parasite lines at day-1, day-2, day-3, day-4 and day-5 post infection. The *P. berghei c507* (WT) line was used as positive control. Mice were infected with the same number of parasite-infected RBCs and each group was consisted from five CD1 mice. Data are presented as mean with SEM. Data derived from two individual biological replicates. **(B)** *ΔAQP2*, *ΔN38*, *ΔN350* and *c507* (WT) (control) *in vivo* macrogamete-to-ookinete conversion rates as determined in the *A. coluzzii* midguts at 16-17 hours pbf. Error bars show SEM, whereas statistical significance was determined with a two-tailed, unpaired Student's *t*-test. **(C)** Oocyst load of the *ΔAQP2*, *ΔN38*, *ΔN350* and *c507* (WT) control parasites in the midguts of infected *A. coluzzii* mosquitoes at day-8 pbf. The presented data derived from two individual biological replicates (n). The median number (M) for each line is indicated by a horizontal red line and samples with significant Mann Whitney U P-values ($P<0.05$) are labelled with an asterisk. Infection prevalence corresponds to the percentage of the infected midguts that appeared to have at least one oocyst. Data have been previously reported in the MRes thesis of Tanguy Rene Balthazar Besson (2019). **(D)** Midgut *ΔAQP2*, *ΔN38*, *ΔN350* and *c507* (WT) sporozoite numbers in *A.*

coluzzii mosquitoes, at day-15 pbf. The mean of the pooled data from two biological replicates is presented. For each replicate, sporozoite numbers were determined from two batches of 25 homogenised midguts. Statistical significance was determined using a two-tailed, unpaired Student's *t*-test. Error bars show standard error from the mean.

Last but not least, the defective phenotype of *ΔAQP2* oocysts to produce sporozoites was further investigated. *ΔAQP2*-infected *A. coluzzii* midguts were dissected at day-12 post infection and stained against their DNA, in order to monitor the mitotic endoreplications and sporozoite formation within the developing oocyst (**Figure 3.18, B**). The genome organisation of the mutant KO oocysts was clearly different from that of the WT i.e. only very few sporoblasts were observed within the *ΔAQP2* oocysts and sporozoites were not readily distributed close to the oocyst periphery.

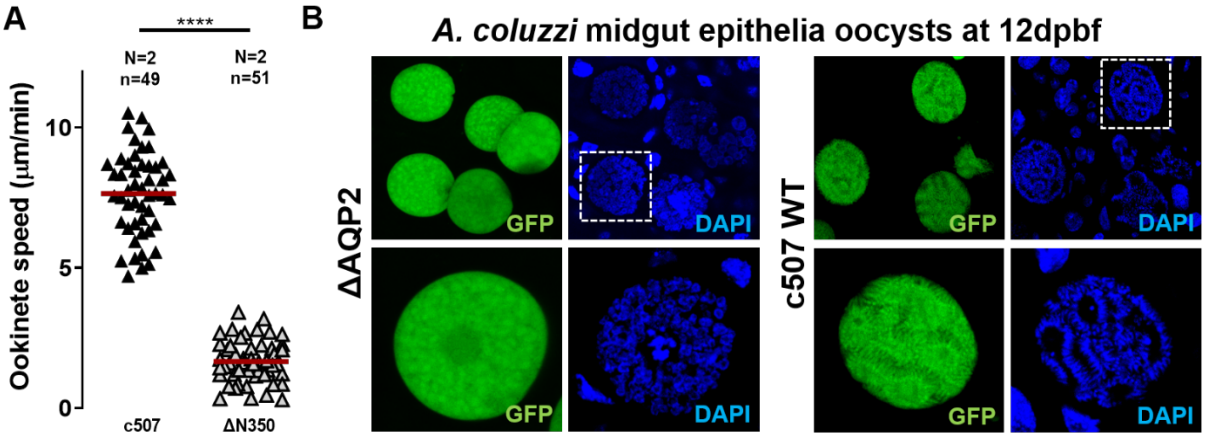

Figure 3.18. Functional characterisation of *P. berghei* AQP2 and N350, following analysis of different KO clonal populations. (A) *ΔN350* and *c507* (WT) (control) velocity during *in vitro* motility assay. Ookinetes were allowed to translocate on MatrigelTM prepared slides and their speed was calculated using time-lapse shooting mode, every 10 sec for a total of 10 min. *c507* (WT) ookinetes were used as reference control. P-values were calculated according to Student's *t*-test. N corresponds to the number of ookinetes, whereas horizontal lines indicate the arithmetic mean of the speed. The samples were obtained from at least four independent slide preparations. The speed of individual ookinetes was measured using the manual tracking plugin in the Icy software package. **(B)** Fluorescent microscopy images of *ΔAQP2* and *c507* (WT) (control) *GFP*-expressing oocysts in the midguts of *A. coluzzii* mosquitoes, at day-12 post infection. DNA was visualised by DAPI (blue) staining in order to observe the sporoblast and genome content and distribution of each oocyst. Images were taken at x400 magnification. Scale bar is 10 μm.

Table 3.6. Oocyst size of the *P. berghei* ΔAQP2 and control *ANKA c507* (WT) parasite lines at day-12, day-15, day-16, day-17, day-18, day-20 post mosquito blood feeding

Parasite line	Days Post-Infection	Number of oocysts measured	Range (μm)	Mean	SEM	*p*-value
c507 (WT)	12	66	30.24-56.70	42.79	0.81	
ΔAQP2	12	73	17.71-69.86	39.68	1.11	0.0287
c507 (WT)	15	78	16.70-64.89	40.50	1.09	
ΔAQP2	15	112	22.08-81.80	50.50	1.21	<0.0001
c507 (WT)	16	73	27.90-59.66	38.11	0.68	
ΔAQP2	16	65	40.28-93.95	62.09	1.38	<0.0001
c507 (WT)	17	17	39.92-60.50	50.08	1.67	
ΔAQP2	17	36	32.79-90.68	62.92	1.69	<0.0001
c507 (WT)	18	30	27.77-75.19	47.41	2.27	
ΔAQP2	18	76	30.22-93.21	65.45	1.68	<0.0001
c507 (WT)	20	40	17.78-63.45	44.01	1.70	
ΔAQP2	20	113	33.82-96.36	66.81	1.16	<0.0001

The table reports the size of *ΔAQP2* and ANKA *c507* (WT) midgut oocysts at day-12, day-15, day-16, day-17, day-18 and day-20 post mosquito infection. About 20 midguts were collected for each parasite line at each time point, and oocyst size measurement was recorded randomly across all midgut tissues. Data derived from two individual biological replicates. Statistical significance was determined using the unpaired Student's *t*-test

Table 3.7. *In vivo* macrogametocyte-to-ookinete (Gc/Ook) conversion rates of *P. berghei ΔAQP2*, *ΔN38*, *ΔN350* different clonal populations and control ANKA *c507* (WT) parasite lines in naïve *A. coluzzii* mosquitoes

Parasite line	Number of experiments	No of midguts / Replicate	Number of Macrogametes	Number of Ookinetes	Fertilisation Rate (%)	Reduction (%)	*p*-value
c507 (WT)	2	10	238	566	70.40		
ΔAQP2	2	10	202	437	68.39	2.86	0.1970 (ns)
ΔN38	2	10	504	305	37.70	46.45	<0.0001 (****)
ΔN350	2	10	156	383	71.06	-1.47	0.6017 (ns)

The *in vivo* macrogametocyte-to-ookinete (Gc/Ook) conversion rates were calculated as the percentage of P28-positive ookinetes to the total number of the P28-positive macrogametes and ookinetes together. Rates were calculated from suspensions of 10 homogenised midguts and assayed 16-17 hours pbf. Statistical significance was determined using a two-tailed, unpaired Student's *t*-test (ns, non-significant).

Table 3.8. Oocyst load of *P. berghei ΔAQP2*, *ΔN38, ΔN350* different clonal populations and control ANKA *c507* (WT), in naive *A. coluzzii* mosquito midguts, following 12 days of infection

Parasite line	Number of experiments	Number of midguts	Prevalence (%)	*p*-value	Infection Intensity				Fold change
					Arithmetic mean	Median	Parasite range	*p*-value	
c507 (WT)	2	57 (43/14)	75.44		21.82	13.00	0-119		
ΔAQP2	2	60 (44/16)	73.33	0.8348 (ns)	25.96	11.00	0-122	0.8921 (ns)	1.18
ΔN38	2	59 (40/19)	67.79	0.4138 (ns)	7.37	3.00	0-45	0.0019 (**)	4.33
ΔN350	2	64 (1/63)	1.56	<0.0001 (****)	0.03	0.00	0-2	<0.0001 (****)	N/A

ΔAQP2, *ΔN38, ΔN350* and WT parasite infections of naive *A. coluzzii* mosquitoes was assessed 8-days pbf. Equal numbers of *ΔAQP2*, *ΔN38, ΔN350* or Pb*c507* (WT) infected midguts from independent biological replicates (indicated in the second column) were pooled for each group. The total number of midguts is indicated in the third column, as the ratio between the number of infected midguts to the number of uninfected midguts. Prevalence shows the percentage of midguts with at least one oocyst. Midguts with zero parasites were also considered for calculation of the arithmetic mean and median of parasite densities (number per midgut). Fold differences (tenth column) between *ΔAQP2*, *ΔN38, ΔN350* and WT oocyst densities were computed using the median values. Statistical significance of the oocyst load was determined using the Mann Whitney U-test, whereas statistical significance of the prevalence percentages was assessed by Fisher's exact test. Data have been previously reported in the MRes thesis of Tanguy Rene Balthazar Besson (2019).

Table 3.9. Midgut sporozoite numbers of *P. berghei ΔAQP2*, *ΔN38*, *ΔN350* different clonal populations and control ANKA *c507* (WT) parasite lines in naive *A. coluzzii* mosquitoes

Parasite line	Number of experiments	Mean	Range	SEM	*p*-value
c507 (WT)	2	2,149.00	1,914.00-2,383.00	234.00	
ΔAQP2	2	324.00	217.00-431.00	107.00	0.0194
ΔN38	2	659.00	533.00-786.00	126.50	0.0306
ΔN350	2	10.00	10.00-10.00	0.00	0.0118

The table reports *ΔAQP2*, *ΔN38*, *ΔN350* or ANKA *c507* (WT) midgut (oocyst) sporozoite numbers from two biological replicates of naive *A. coluzzii* infections. For each replicate, sporozoite numbers were determined from two batches of 25 homogenised midguts at day-15 post infection. SEM represents the standard error from the mean. Statistical significance was determined using a two-tailed, unpaired Student's *t*-test.

3.2.8 Implication of the mosquito complement-like system on *ΔAQP2*, *ΔN38* and *ΔN350* oocyst development

An interesting question arising from the study of the three mutants was whether a mosquito elicited immune response could be held responsible for the phenotypes observed and if so, to what degree. A powerful way to determine this was to perform RNAi experiments against LRIM1, followed by mosquito infections with the three mutants and the *c507* (WT) parasite line which served as a positive control. Midguts were then collected at day-11 pbf and oocysts were enumerated.

Interestingly, oocyst formation in the *ΔN350* mutant parasites was not recovered following LRIM1 silencing indicating that the N350 gene function is essential for parasite development prior to the mosquito immune responses triggered following *Plasmodium* infection. The *ΔN38* line however, no longer showed a diminished oocyst load compared to the WT with a median infection intensity of 4.0 in ds*LacZ*-injected (63.0% infection prevalence) and 79.0 in *LRIM1*-silenced (92.0% infection prevalence) *ΔN38*-infected mosquitoes and, 11.0 in ds*LacZ*-injected (87.0% infection prevalence) and 96.0 in *LRIM1*-silenced (91.0% infection prevalence) WT-infected mosquitoes. Nevertheless, even though increased *ΔN38* mutant parasite numbers were observed in the absence of LRIM1, their levels fail to reach anywhere near that of the WT confirming that the mutant phenotype is attributed to both the mosquito immune responses and the previously shown gametocyte-to-ookinete conversion defects. Following *LRIM1*-silencing, the *ΔAQP2* line was again not significantly different ($p=0.8554$) compared to the WT with *ΔAQP2* median oocyst load of 9.5 in ds*LacZ*-injected (80% infection prevalence) and 102.5 in *LRIM1*-silenced (94% infection prevalence) mosquitoes (**Figure 3.19, A; Table 3.10**). These data suggest that the complement-like pathway, mainly hamper the development of the *ΔN38* parasites since *LRIM1*-silencing lead to a dramatic increase in the number of *ΔN38* oocysts. Since *LRIM1*-silencing did not lead to rescue of the *ΔN350* parasite line phenotype at the oocyst stage, these data validate what is known regarding the function of the complement-like system following ookinete formation and midgut traversal as well as that complement activity is not observed in mosquito compartments other than the haemolymph (Blandin *et al*., 2004; Povelones *et al*., 2009).

Due to the significant increase ($p<0.0001$) in the *ΔAQP2* and *ΔN38* oocyst numbers, I then went to investigate whether complement-like pathway silencing had an impact

also on the number of sporozoites formed. To do so, *LRIM1*-silenced and ds*LacZ*-injected mosquitoes were dissected at day-15 pbf and midguts were homogenised prior to sporozoite enumeration. The *ΔN350* parasite line was completely impaired from sporozoite formation both in the ds*LacZ*-injected mosquitoes and after silencing of the complement-like system. A small number of sporozoites were detected in ds*LacZ*-injected *ΔN38* infected mosquitoes (480.80 ± 70.10), with a 7-fold higher number in *LRIM1*-silenced *A. coluzzii* mosquitoes infected with the same parasite line (3,449.00 ± 355.90). Similarly, an 8-fold increase in the number of oocysts was observed for the *ΔAQP2* parasites following *LRIM1*-silencing (828.70 ± 434.50) compared to the ds*LacZ*-injected control mosquitoes (100.30 ± 62.30). However, *ΔAQP2* sporozoite counts were much lower compared to the ds*LRIM1*-silenced WT infected mosquitoes (16,190.00 ± 1,733.00), despite the similar oocyst load in both ds*LacZ*-injected and *LRIM1*-silenced mosquitoes (**Figure 3.19, B; Table 3.11**). As previously mentioned, this is attributed to the delayed development and possibly the abnormal nuclear division of the *ΔAQP2* oocysts.

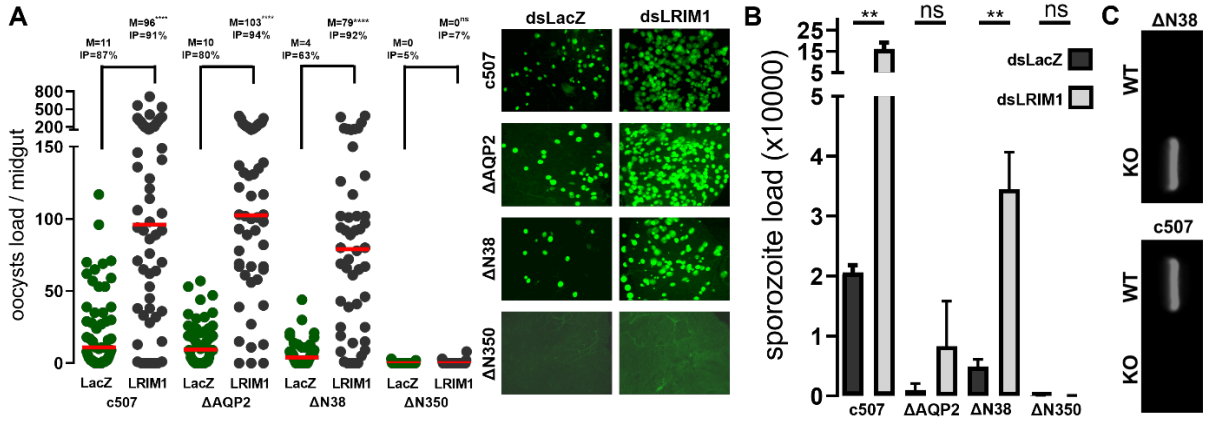

Figure 3.19. Effect of *LRIM1*-silencing on *ΔAQP2*, *ΔN38* and *ΔN350* oocyst and sporozoite numbers in *A. coluzzii* midguts. (A) *ΔAQP2*, *ΔN38* and *ΔN350* oocyst load in the midguts of *LRIM1*-silenced *A. coluzzii* mosquitoes, at day-12 post infection. ds*LacZ*-injected mosquitoes were used as controls. M corresponds to the median oocyst infection intensities, also shown in horizontal red line for each condition. IP; infection prevalence meaning the percentage of the mosquito midguts that were infected with at least one oocyst. Data derived from two independent biological replicates where for each biological replicate oocyst load was determined from a minimum of 30 midguts per mosquito group. Statistical significance was determined using the Mann Whitney U-test where ns, non-significant. Representative fluorescent

images of *ΔAQP2*, *ΔN38*, *ΔN350* and *c507* (WT) (control) infected midguts of ds*LacZ*-injected and *LRIM1*-silenced *A. coluzzii,* at day-12 post infection. Images were taken at X100 magnification. **(B)** Sporozoite numbers of *ΔAQP2*, *ΔN38*, *ΔN350* and *c507* (WT) (control) *P. berghei* lines as determined in the midguts of ds*LacZ*-injected and *LRIM1*-silenced *A. coluzzii* mosquitoes. Data derived from two biological replicates. For each biological replicate sporozoite load was determined from a minimum of 20 midguts per mosquito group. Statistical significance was calculated using a two-tailed, unpaired Student's *t*-test. Error bars show SEM. **(C)** PCR genotypic analysis of the *ΔN38* KO or WT locus on blood stage parasites of the *ΔN38* and WT parasite lines following transmission from *LRIM1*-silenced *A. coluzzii* mosquitoes. The set of genotypic analysis primers used was GT+GW1 for the KO locus and QCR1+QCR2 for the WT locus. Images are representative from two sets of replicates.

The ability of the mutant parasites to be transmitted to a vertebrate host upon *LRIM1*-silenced and control ds*LacZ*-injected *A. coluzzii* mosquito bites and thus, complete parasite lifecycle was assessed. At day-21 post infection, mosquitoes were allowed to feed on mice which were then monitored for infection. Interestingly, transmission appeared to be successful in all mice following bites from the *ΔN38*-infected *LRIM1*-silenced mosquitoes, but in none of the mice bitten by the *ΔAQP2* and *ΔN350*-infected *LRIM1*-silenced mosquitoes. PCR analysis on gDNA extracted from blood stage parasites from the positive mice, confirmed that parasites encompassed the *ΔN38* locus and that there was no contamination with the WT locus that was absent from all the mice (**Figure 3.19, C**). None of the mice used got infected after bite-back experiments using ds*LacZ*-injected mosquitoes infected with *ΔAQP2*, *ΔN38* or *ΔN350* parasites. These data suggest that only the *ΔN38* parasites are fully rescued when silencing key components of the complement-like system. Despite the slight increase in the number of midgut *ΔAQP2* sporozoites found in *LRIM1*-silenced mosquitoes, it was not enough to rescue the parasite lifecycle suggesting that other developmental impairments might be responsible for their reduced infection capacity.

Table 3.10. Effect of *LRIM1*-silencing on *ΔAQP2*, *ΔN38*, *ΔN350* and control ANKA *c507* (WT) infections in *A. coluzzii* mosquitoes

Parasite line	dsRNA	Number of exp.	Midguts number	Prevalence (%)	*p*-value	Infection Intensity				
						Arithmetic mean	Median	Parasite range	Fold Change	*p*-value
c507 (WT)	*LacZ*	2	54 (47/7)	87.04		23.54	11.00	0-117		
	LRIM1		56 (51/5)	91.07	0.5551 (ns)	146.7	96.00	0-713	8.73	<0.0001
ΔAQP2	*LacZ*	2	56 (45/11)	80.36		13.96	9.50	0-57		
	LRIM1		52 (49/3)	94.23	0.04 (*)	124.80	102.50	0-384	10.79	<0.0001
ΔN38	*LacZ*	2	51 (32/19)	62.74		6.37	4.00	0-44		
	LRIM1		48 (44/4)	91.67	<0.0007 (***)	88.83	79.00	0-386	19.75	<0.0001
ΔN350	*LacZ*	2	57 (3/54)	5.26		0.11	0.00	0-3		
	LRIM1		60 (4/56)	6.67	>0.999 (ns)	0.25	0.00	0-8	N/A	0.7945 (ns)

ΔAQP2, *ΔN38*, *ΔN350* and control WT parasite infections of *LRIM1*-silenced *A. coluzzii* mosquitoes was assessed at day-12 pbf. Infection of ds*LacZ*-injected mosquitoes were used as control. Number of midguts is shown as the ratio between the number of infected midguts to the number of uninfected midguts. Statistical significance for the median oocyst load was determined using the Mann Whitney U-test, whereas statistical significance of the prevalence percentages was assessed by Fisher's exact test (ns, non-significant). Infectivity to mice was assayed by allowing infected mosquitoes to feed on Balb/C mice on day-21 of infection. Parasitaemia of mice was assayed by Giemsa-stained thin blood smears from day-5 onwards.

Table 3.11. Midgut sporozoite numbers of *ΔAQP2*, *ΔN38*, *ΔN350* and control ANKA *c507* (WT) *P. berghei* in ds*LacZ* (control) and ds*LRIM1*-injected *A. coluzzii* mosquitoes

Parasite line	dsRNA	Number of experiments	Mean	Range	SEM	*p*-value	Infectivity to mice (21dpi)
c507 (WT)	*LacZ*	2	2,060.00	1,980.00-2,200.00	70.24		6/6
	LRIM1		16,190.00	13,960.00-19,960.00	1,733.00	0.0012	5/5
ΔAQP2	*LacZ*	2	103.00	38.00-225.00	62.33		0/6
	LRIM1		828.70	367.00-1,697.00	434.50	0.1724	0/7
ΔN38	*LacZ*	2	488.00	348.00-565.00	70.12		0/5
	LRIM1		3,449.00	3,042.00-4,158.00	355.9	0.0012	6/6
ΔN350	*LacZ*	2	4.67	0.00-14.00	4.67		0/6
	LRIM1		3.33	0.00-10.00	3.33	0.8276	0/7

The table reports *ΔAQP2*, *ΔN38*, *ΔN350* or ANKA *c507* (WT) midgut (oocyst) sporozoite numbers from two biological replicates of ds*LacZ*-injected and *LRIM1*-silenced *A. coluzzii* infections. For each replicate, sporozoite numbers were determined from two batches of 15 homogenised midguts at day-15 post infection. SEM represents the standard error from the mean. Statistical significance was determined using the unpaired Student's *t*-test

3.2.9 Generation of *P. berghei AQP2-3HA*, *N38-3HA* and *N350-3HA* transgenic lines: A tool for protein assays

3.2.9.1 C-terminal 3xHA tagging of the endogenous AQP2, N38 and N350 loci

In order to facilitate *Pb*AQP2, *Pb*N38 and *Pb*N350 protein expression studies, transgenic *AQP2-3HA*, *N38-3HA* and *N350-3HA* lines were generated using the *c507* genetic background line. 3HA tagging of AQP2, N38 and N350 was facilitated by replacement of the native 3'UTR region of the endogenous genes with a 3xHA-tagged counterpart. The sub-cloned *AQP2*, *N38* and *N350* targeting sequences were cloned (in absence of their TAG stop codon) in-frame with a triple 3HA-tag epitope held on a gene targeting vector, which was introduced into the locus by single homologous recombination (**Figure 3.20, A**). Vectors were supplied by the PlasmoGEM resource with the following PlasmoGEM ID codes; PbGEM-066039 for *AQP2-3HA*, PbGEM-058364 for *N38-3HA* and PbGEM-012712 for *N350-3HA*. Successful integration of the 3HA-tagging vectors in *c507 P. berghei* parasites was detected by genotypic analysis PCR on gDNA obtained from blood stages of the mixed population following transfection and one round of pyrimethamine selection (**Figure 3.20, B**).

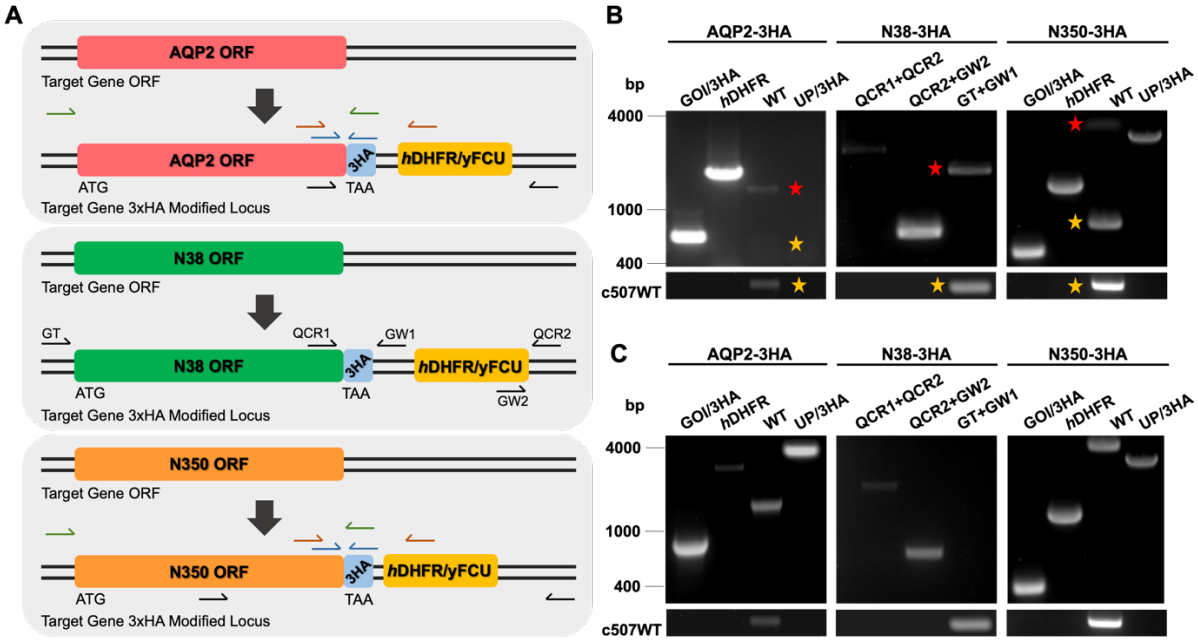

Figure 3.20. Generation of *P. berghei AQP2-3HA*, *N38-3HA* and *N350-3HA* transgenic lines. (A) Schematic representation of the C-terminal 3HA-tagging strategy of *AQP2*, *N38* and *N350*. 3HA-tagging was facilitated by replacing part of the 3'UTR of each gene with a 3HA-tagged counterpart, while the ORF of each gene remained unaffected. The gene targeting construct holds the final part of the *AQP2*,

N38 and *N350* 3'UTR region, sub-cloned in-frame with the 3HA-tag (blue). The tagging vector was introduced into the native genomic locus by single homologous recombination following linearisation of the PlasmoGEM vectors by NotI. Homologous recombination thus, resulted in replacement of the native stop codon and 3' UTR of *AQP2*, *N38* and *N350* with a C-terminally 3HA-tagged version. Downstream of the 3HA-fused construct, the *h*DHFR-TS/yFCU pyrimethamine resistance cassette (yellow) was also integrated into the genome. **(B-C)** Genotypic analysis of the transfectant populations. gDNA was collected from parasites that survived one round of pyrimethamine selection **(B)** and later, from those who established infection following dilution cloning **(C)** and genotyped by diagnostic PCR. The signal initially observed for both the WT (yellow asterisks) and mutant (red asterisks) locus, indicates mixed WT/transgenic parasite population. However, the WT parasites that managed to survive the first round of drug selection, possibly through episomal contamination, were completely eliminated following dilution cloning. Successful isolation of the clonal transgenic populations is demonstrated by the detection of the 3HA-tagged locus in all clonal populations, but not in the WT locus. The combination of the GT/GW1 and GW2/QCR2 primers (Gomes *et al*., 2015) were used to analyse the *N38-3HA* transgenic locus and were designed to map the integration site following homologous recombination, whereas the QCR1/QCR2 primer combination detects only the unmodified form of the gene. The PlasmoGEM provided GW, QCR1, QCR2 and GT primers were not conclusive for the *AQP2-3HA* and *N350-3HA* locus, so custom primers were designed for detection of the integrated construct; specific for the integrated drug selection cassette (*h*DHFR; orange), the integrated region between the gene of interest and the 3HA sequence (GOI/3HA; blue), the integrated region between an upstream region of the gene of interest and the 3HA sequence (up/3HA; green) and the WT genome (WT; black) upstream and downstream of the integrated cassette. The latter set of primers (named WT) is expected to give bands for both the WT and the mutant loci. However, due to the integration of the cassette in the genome of the transgenic parasites, the expected size of the PCR product is expected to be higher (red asterisks) compared to the unmodified locus of the WT parasites (yellow asterisks). gDNA from the *c507* (WT) parasite line served as quality control. Images are representative for all clonal populations isolated.

To obtain single clones, successive dilutions of the mixed population (limited dilution cloning) was performed under pyrimethamine treatment. Following mouse infection

establishment, successful isolation of clonal mutant populations was verified by PCR where a clear lack of WT genome indicated success (**Figure 3.20, C**). Four (I, II,III, VI) pure tagged clones for the *Pb*AQP2 locus, two (II, V) clones of the *Pb*N38 tagged locus and two (III, IV) clones for the *Pb*N350 tagged locus were obtained. From these, one clone per transgenic line was selected in order to investigate the expression pattern of the respective protein during parasite development.

3.2.9.2 Assessing the functionality of the *PbAQP2-3HA*, *PbN38-3HA* and *PbN350-3HA* transgenic lines

To confirm that the functionality of the HA-tag does not interfere with the proteins function, the 3HA-transgenic lines were used to infect *A. coluzzii* mosquitoes prior to midgut oocyst and sporozoite count at day-9 and 15 pbf, respectively (**Figure 3.21**).

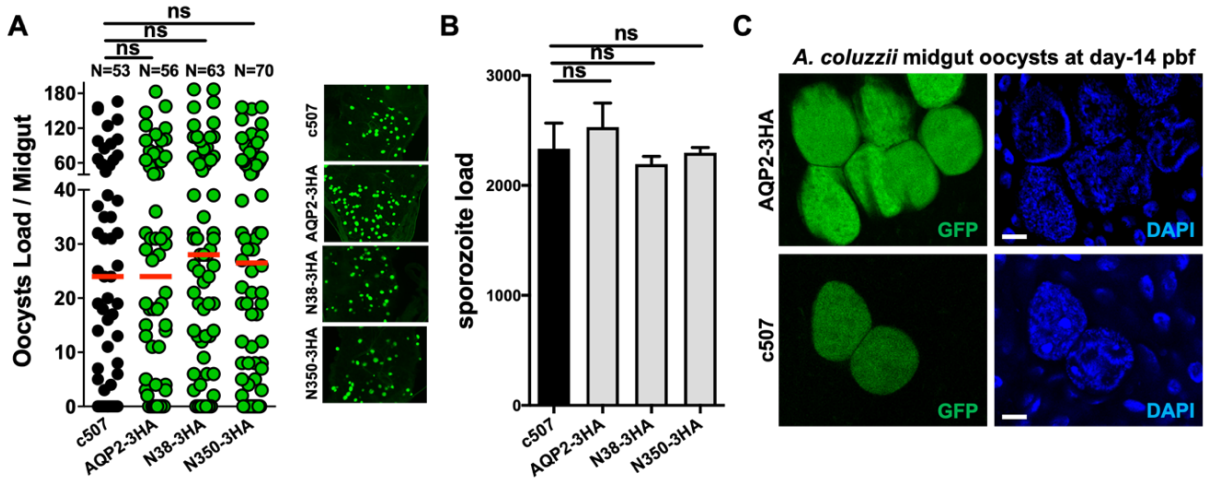

Figure 3.21. Phenotypic analysis of the *PbAQP2-3HA*, *PbN38-3HA* and *PbN350-3HA* transgenic lines. (A) Oocyst load for the HA-tagged parasite lines in the midguts of infected *A. coluzzii* mosquitoes at day-9 pbf. Infection with the *P. berghei* ANKA *c507* (WT) line served as a control. The presented data derived from two biological replicates where the number of midguts analysed in total is shown (N). Red lines indicate the median oocyst intensity and samples with significant Mann Whitney U P-values ($P<0.05$) are labelled with an asterisk. ns, non-significant. Fluorescent microscopy images of *GFP*-expressing oocysts in the midguts of *A. coluzzii* mosquitoes, representative for each parasite line. Images were taken at X200 magnification. **(B)** Midgut *PbAQP2-3HA*, *PbN38-3HA* and *PbN350-3HA* and *c507* (WT) sporozoite numbers in *A. coluzzii* mosquitoes, as determined at day-15 pbf. The mean of the pooled data from two biological replicates is presented. Error bars show standard error. **(C)** Fluorescent microscopy images of *AQP2-3HA* and *c507* (WT)

(control) *GFP*-expressing oocysts in the midguts of *A. coluzzii* mosquitoes, at day-15 pbf. DNA was visualised following DAPI (blue) staining. Scale bar is 5 μm.

All transgenic parasites formed oocyst numbers similar to the WT (*PbAQP2-3HA* median:24; *PbN38-3HA* median: 24; *PbN350-3HA* median: 28, *Pbc507*WT median: 26) (**Figure 3.21, A**). Since the defective phenotype of parasites lacking expression of *AQP2* is only observed after oocyst formation, during oocyst maturation and sporozoite development, the *PbAQP2-3HA* midgut sporozoite load was also investigated at day-15 pbf. Presence of *AQP2-3HA* sporozoites in the midguts of *A. coluzzii* mosquitoes was detected at similar levels to the WT (**Figure 3.21, B**). The morphology of the oocysts was also similar to that of the WT, with sporulation centres fully formed and sporozoites localised close to the oocysts' periphery (**Figure 3.21, C**). Development of the *PbN38-3HA* and *PbN350-3HA* parasite lines was also assessed up to the midgut sporozoite stage where it was confirmed that both lines form sporozoite numbers similar to the WT (2194 ± 71 and 2298 ± 47, respectively) (**Figure 3.21, B**). Together these findings demonstrate the successful generation of fully functional *PbAQP2-3HA*, *PbN38-3HA* and *PbN350-3HA* lines.

3.2.9.3 *P. berghei* AQP2, N38 and N350 expression pattern

To investigate the expression pattern of *P. berghei AQP2*, *N38* and *N350* at the protein level, western blot assays were performed on whole protein extracts of *AQP2-3HA*, *N38-3HA* and *N350-3HA* MBS, ABS, purified non-activated and activated gametocytes and purified *in vitro* cultivated ookinetes, using an anti-HA antibody. The results showed that *AQP2* is highly expressed in non-activated and activated gametocytes, whereas no band was detected in extracts derived from MBS, ABS, ookinetes or midgut sporozoites. Expression of *AQP2* in salivary gland sporozoites should be also investigated since transcripts were detected in salivary gland sporozoites at day-21 pbf. Protein migrated in SDS-PAGE gels at around 75kDa, matching with the combined size of the protein monomer (70.1kDa) with the HA-tag (3.27kDa). Similar to *AQP2*, *N38* expression starts in the non-activated gametocytes, continues in activated gametocytes and reaches maximum levels during ookinete development. Therefore, its expression in MBS derives from its presence in the blood stage gametocytes rather in the ABS. A clear band of approximately 37kDa matches the combined size of the protein monomer (30.4kDa) with the HA-tag (3.27kDa), however, a slightly lower band of approximately 25kDa suggests that N38 in ookinetes

might have undergone either alternative splicing or post-translational modifications, following proteases activity. Comparable to N38, N350 is abundant in all stages starting from non-activated gametocytes to ookinetes. Additionally, the absence of a band in ABS suggests that its expression in MBS derived from its presence in the blood stage non-activated gametocytes. Lastly, the expected size of the band was calculated to be around 125kDa which corresponds to the molecular weight of the N350 monomer (121.9kDa) together with the HA-tag (3.2kDa). The ˜90kDa band observed in the non-activated gametocytes sample might suggest that the protein has been processed to a smaller fraction at this stage (**Figure 3.22**).

Under non-reducing conditions, each protein-specific band was observed exclusively at the size of the expected monomer. This suggests that the *Pb*AQP2, *Pb*N38 and *Pb*N350 proteins do not form homodimers or heterodimers. The specificity of the western blot was verified by the absence of signal in the *c507* (WT) protein samples.

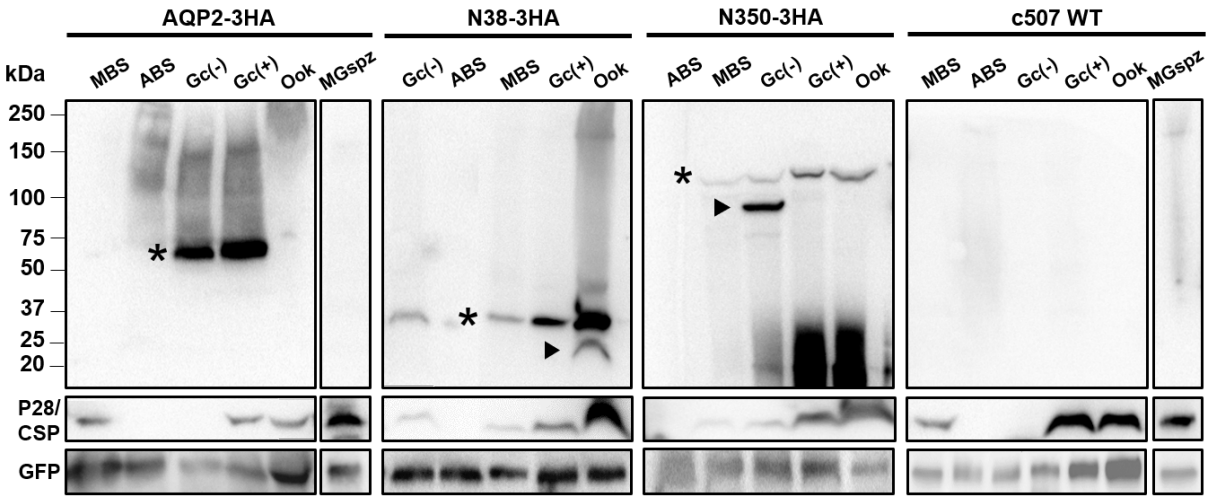

Figure 3.22. Expression of *P. berghei AQP2*, *N38* and *N350* following 3HA-tagging of their C-terminal. Anti-HA western blot analysis of the *AQP2-3HA*, *N38-3HA* and *N350-3HA* protein products which are found to migrate in between the 50kDa-75kDa, 25kDa-37kDa and 100kDa-150kDa marker, respectively (black asterisks indicate monomers; arrowhead indicates potential alternative expression or cleaved products of *N38* and *N350*). Probing against P28/CSP and GFP served as stage-specific and loading controls, respectively. Protein extracts from *c507* (WT) parasites served as negative control of the HA specificity. MBS; Mixed Blood Stages, ABS; Asexual Blood Stages, Gc(-); non-activated gametocytes, Gc(+) activated gametocytes, Ook; purified ookinetes; MGspz: midgut sporozoites. The western blot

analysis of the N38/HA MBS, Gc(+) and Ook samples has been previously reported in the MRes thesis of Tanguy Rene Balthazar Besson (2019).

3.2.10 Summary

This chapter has outlined the following (**Figure 3.23**):

- The viable use of the STM approach to perform high-throughput reverse genetic screening of *P. berghei* mutants during their development in *A. gambiae*.
- Identification of new *Plasmodium* candidate genes; *AQP2*, *N38* and *N350*, found to be essential for parasites to complete their lifecycle in *A. coluzzii* mosquitoes.
- *P. berghei AQP2* is highly transcribed in gametocytes, ookinetes and salivary gland sporozoites, however, it was found to be translated only in gametocytes. It is important for sporogonic development in the developing oocyst.
- *P. berghei N350* and *N38* are highly transcribed and expressed in both non-activated and activated gametocytes, and ookinetes. N38 seems to be involved in the gametocyte-to-ookinete developmental transition, whereas N350 is important for ookinetes gliding motility prior to mosquito midgut invasion.
- Silencing key components of the mosquito complement-like system results in a radical increase in *ΔPbAQP2* and *ΔPbN38* infection intensity and prevalence, as well as transmission rescue of the *ΔPbN38* parasites back to the rodent host.

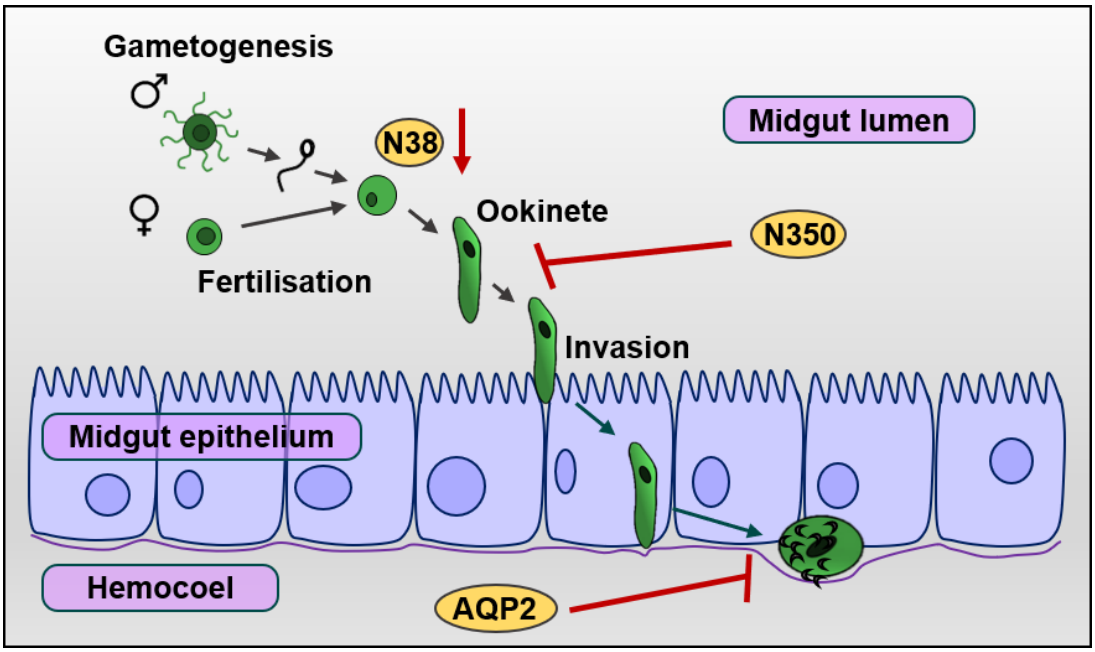

Figure 3.23. Proposed model of the function of *P. berghei* N38, N350 and AQP2 proteins, during parasite development in *A. coluzzii*. Of these, N38 appear to be involved in gametocyte-to-ookinete developmental transition, while N350 plays an

essential role in ookinete motility and AQP2 is important for oocyst maturation and sporozoite formation. Disruption of any of these genes lead to transmission blockage.

3.3 Discussion

3.3.1 High-Throughput functional screening of *P. berghei* barcoded mutants

Despite the extensive research efforts on functionally characterising *Plasmodium* genes that are highly transcribed during the asexual lifecycle in the vertebrate host, mechanisms and molecules involved during development in the mosquito vector remain poorly understood. Here, a high-throughput functional profiling approach of *P. berghei* genes previously found to be highly upregulated within the first 24 hours of mosquito blood feeding (Akinosoglou *et al.*, 2015) is reported.

PlasmoGEM barcoded vectors can be used to perform functional screens of *Plasmodium* genes with regards to their importance in the parasite lifecycle, either in the human host or in the mosquito vector. Similarly to what has been previously suggested for studying *P. berghei* genes essential for blood stage development (Gomes *et al.*, 2015; Schwach *et al.*, 2015; Bushell *et al.*, 2017), an optimised approach of the STM methodology was adapted in order to generate pools of barcoded mutants for genes that are highly upregulated during the initial stages of *Anopheles* mosquito infections. This enabled the generation of six pools of ˜30 KO mutants; each one of them carrying its unique barcode. Following *A. coluzzii* infection, mosquito sample collection at specific time-points matching with the distinct developmental stages of the parasite lifecycle was carried out, prior to gDNA extraction and barcode sequencing. From there, the abundance of each barcode was determined in order to later inform us about the magnitude of the corresponding mutant. In this way, we were able to track the developmental progress of the multiple barcoded mutants and identify potential function of the disrupted locus during all the distinct stages of the parasite in the mosquito vector.

It is possible that following parasites ingestion within the mosquito midgut lumen, cross-fertilisation events between the individual mutants may lead to heterozygosity and thus to genetic complementation of the KO locus. To avoid allele-dosage effects leading to controversial results, the transcriptional silencing of the paternal DNA during zygote and ookinete formation (Ukegbu *et al.*, 2015) was taken advantage and, introduced the *Δhap2* line as the reference line for generating the various pools of the barcoded mutants. Hap2 is a male specific gamete factor that when disrupted, male

gametes are unable to fuse with the female macrogametes (Hirai *et al.*, 2008; Liu *et al.*, 2008; Blagborough *et al.*, 2013a). However, the specific protein-protein interactions needed for the fusion of the macrogametes and microgametes membrane have not yet been identified. Hence, through this specific set-up, identification of female gametocyte specific molecules that directly interact with the microgamete surface protein *hap2* could be pointed-out. From ookinete midgut invasion onwards, where both paternal and maternal transcriptomes are active, more genes important for parasite development or interaction with its mosquito vector could be detected.

As we primarily aimed at validating the suggested STM high-throughput reverse genetic screening method for studying *P. berghei* mosquito stages, analysis of the first pool of barcoded mutants was solely carried out. This pool consisted of thirty-two transgenic parasite lines; twenty of those have been previously characterised and therefore their stage dynamics were more or less predictable, whereas ten of those were still novel and uncharacterised. Two lines of evidence support our conclusion that fitness measurements based on barcode counting can be applied for studying *Plasmodium* mosquito stages: (1) phenotype consistency between the derived data and the current literature regarding some of the KO mutant parasite lines such as; *ΔPBANKA_111920* (*Δc43*) (Ukegbu *et al.*, 2020) which seems to have undergone dramatic losses at the oocyst stages, *ΔPBANKA_083040* (*ΔG2*) which reached almost zero abundance at the salivary gland sporozoite stage and *ΔPBANKA_100220* (*ΔP36p*) previously known to be important during the sporozoite hepatic stage (van Dijk *et al.*, 2005) and did not show any losses during mosquito development; (2) mutant lines of three novel genes (*AQP2*, *N38*, *N350*) that displayed drastic abundance reduction either at the oocyst or the sporozoite stages, appeared to have suffered exactly the same bottlenecks after generating their analogous single KO lines. Some KOs appeared to have different dynamics of what was initially expected, maybe due to unknown so far interactions with other mutant parasites.

The scale of barseq screens in *P. berghei* is currently restricted by the complexity of the parasite pools that can be generated, which in turn is limited both by the transfection efficiency and the relatively large differences in recombination rates of different PlasmoGEM vectors. As a result of such heterogeneity, screening pools of mutants poses the risk of losing genotypes that are either generated in small numbers due to less efficient recombination rates of their specific-target locus or because they

have a reduced fitness during blood stage development. Nevertheless, it has been previously shown that by simultaneously co-transfecting multiple individual vectors, it is feasible to generate pool cocktails starting from ˜48 (Gomes *et al.*, 2015) up to ˜100 (Bushell *et al.*, 2017) barcoded mutants. Previous *P. berghei* transcriptomic analysis in *A. gambiae* mosquitoes revealed ˜1640 genes that exhibited statistically significant differential regulation during mosquito stages (Akinosoglou *et al.*, 2015). Therefore, by taking advantage of this current high-throughput methodology, functional screening of these genes can be completed in less time and with minimum costs and animal usage.

Further experimental support for scrutinising the concept of pleiotropic functions of *Plasmodium* genes requires the development of a scalable, inducible and conditional KO system. This will allow systematic identification of essential gene functions at multiple lifecycle stages. This specifically applies for genes such as the *PBANKA_111920* (*c43*), previously shown to be expressed during both the ookinete and sporozoite stages. When knocked out, mutant parasites are eliminated at the oocyst stage due to clearance by the complement-like system (Ukegbu *et al.*, 2020). This bottleneck seems to be carried on to the sporozoite stage and therefore, dynamic changes beyond oocyst development cannot be further investigated.

The use of vector pools to phenotype mixtures of mutants is particularly suited to *P. berghei* where a library of cloned mutants would be, otherwise, of limited value i.e. there is an absence of an *in vitro* culture system for blood stages and therefore each cloned mutant has to be generated and propagated in mice. In marked contrast, the human malaria parasite *P. falciparum* has an efficient culture system for blood stages and the CRISPR-Cas9 system is currently being used successfully to transfect linear DNA in *P. falciparum* (Ghorbal *et al.*, 2014). If this method increases recombination rates significantly, it raises the exciting prospect of generating also large numbers of barcoded *P. falciparum* mutants that could then be pooled for genetic barseq screening. Already a library of 38,000 mutants has been generated using transposon mutagenesis, leading to the identification of 2680 genes essential for optimal growth of asexual blood stages *in vitro* (Zhang *et al.*, 2018). Furthermore, a group at the University of Copenhagen suggested a way to dissect *P. falciparum* fitness costs associated with drug resistance (Nag *et al*., 2017).

In the mosquito, *Plasmodium* faces multiple physical barriers (i.e. peritrophic matrix, midgut epithelium, salivary glands epithelium) as well as attacks from the innate

immune system, all resulting in substantial population losses. Such *Plasmodium* bottlenecks have been shown to take place during the gametocyte-to-ookinete, ookinete-to-oocyst and oocyst sporozoite-to-salivary gland sporozoite developmental transition. The RNAi technology in mosquitoes (Blandin *et al.*, 2002) has revealed different *Plasmodium* genes that are associated with parasite survival despite the mosquito immune responses (Ramphul *et al.*, 2015; Canepa *et al.*, 2016; Ukegbu *et al.*, 2020), parasite survival despite the cellular responses taking place at the place and time of ookinete midgut traversal (Vlachou *et al*., 2005; Oliveira *et al*., 2012), or protein-protein interactions between parasite and mosquito tissues (Vega-Rodriguez *et al.*, 2014). For these reasons, silencing mosquito key components prior to infection with the pool of KO mutants could reveal multiple mosquito-parasite protein-protein interactions crucial for the developmental progress of the latter.

3.3.2 Identification of three novel *Plasmodium* genes important for *Plasmodium* development in *A. coluzzii*

The high-throughput reverse genetics screening revealed three novel *Plasmodium* genes that are important for parasite development in the mosquito; *AQP2*, *N38* and *N350*. Bioinformatic analysis showed that all genes are highly conserved among human *Plasmodium spp.* in addition to a 90-95% conservation in their amino acid sequences with the rodent malaria parasite *P. yoelii.* Well-preserved positions of their multiple transmembrane domains across their full length, which especially in the case of AQP2 are predicted to constitute the individual pores of the channel, might also indicate similar roles of the proteins across the *Plasmodium* genus. *P. berghei AQP2* was found to be highly transcribed in the activated gametocytes, ookinetes and in lower levels in the salivary gland sporozoites. *P. berghei N38* and *N350* are specifically transcribed in gametocytes and ookinetes. Western blot analysis showed that *AQP2* is exclusively expressed in blood stage gametocytes and gametes following ingestion in the mosquito midgut, whereas *N38* and *N350* expression starts in blood stage gametocytes and continues until ookinete development. As mentioned, *PbAQP2* transcripts seem to reappear in the salivary gland sporozoites, however, its expression and a potential role of the protein at this stage has not been further investigated.

Aquaporin-2 is essential for *P. berghei* sporozoite development

One of the genes found to be important in parasites survival in *A. coluzzii* mosquitoes was *AQP2*, a protein belonging to the aquaporins family. Generally, aquaporins are

integral membrane proteins that serve as channels in the transfer of water and possibly small solutes across the membrane. The AQP channel is formed by an hourglass structure with six transmembrane alpha helical domains connected by five extramembrane loops. The NPA motif is in the centre of the pore and forms a ring (Jung *et al.*, 1994; Gonen & Walz, 2006; Jung *et al.*, 2006). This ring functions as the primary filter of the channel and regulates the flow of water through the channel. The directionality of water and solute diffusion was found to be determined by the prevailing osmotic and chemical gradients (Laforenza *et al.*, 2016). Due to these properties, aquaporins are known to be implicated in a vast array of functions from motility to osmotic regulation thus making them an attractive target for drug development.

It has been shown that both *P. falciparum* and *P. berghei* encode two aquaporin proteins; the aquaglyceroporin AQP1 (PBANKA_0915600; PF3D7_1132800) and the putative aquaporin AQP2 (PBANKA_1427100, PF3D7_0810400), both located on the parasites plasma membrane where they facilitate the passage of glycerol, water, urea, small polyols or carbonyl compounds through their amphipathic pores (Beitz *et al.*, 2004; Promeneur *et al.*, 2007; Lian *et al.*, 2009; Kenthirapalan *et al.*, 2012). Since malaria parasites undergo drastic osmotic changes during tissue migration, the function of their AQPs is thought to be of crucial importance to complete their lifecycle.

Whilst extensive research efforts have been made to characterise *P. falciparum* and *P. berghei* AQP1, there has been little work on AQP2 aside from its inclusion in transcriptomic and proteomic analysis (Hall *et al.*, 2005; Otto *et al.*, 2014). There are currently conflicting reports concerning the fitness cost during parasites blood stage development upon aquaporin deletion; Promeneur *et al.* report that genetic ablation of *P. berghei AQP1* results in deficiency in glycerol acquisition which then affects the parasites intraerythrocytic growth, intrahepatocytic replication, merozoites infectivity and phospholipid synthesis (Promeneur *et al.*, 2007; Promeneur *et al.*, 2018). Kenthirapalan *et al.* report that disruption of *AQP1* does not affect the parasites fitness during blood stages development (Kenthirapalan *et al.*, 2012). It has only been reported once that *PbAQP1* is expressed during sporozoite development, however, whether its deletion affects parasites lifecycle in the mosquito vector has not been further investigated (Promeneur *et al.*, 2018). Here, the homologue of *P. berghei AQP1*, *AQP2*, has been newly characterised. *P. berghei AQP2* is highly transcribed in gametocytes, ookinetes and salivary gland sporozoites, but it seems to be exclusively

translated in non-activated gametocytes and gametes. *AQP2* deletion has a profound effect on the progression of sporogony in the developing oocyst.

AQP2 encodes a medium size putative aquaporin, with the aquaporin-like domain spanning across the C-terminal of the protein. Protein sequence alignment showed a highly conserved C-terminal among all *Plasmodium spp.*, as opposed to the N-terminus which has not been robustly predicted to have sequence or structurally similarities with any other so far characterised proteins. Since there has been little work on experimentally characterising the function of *PbAQP2,* the prediction that it encodes an aquaporin-like protein comes only from *in silico* analysis. Only the N-terminal region of *Pf*AQP2 showed high confidence similarities to the yeast ATPase subunits, whereas *Pb*AQP2 did not. Since aquaporins have been previously shown to be involved in the passive transport of water and uncharged solutes (Carbrey & Agre, 2009), this possibly points to the loss of this function for *PbAQP2*. However, long N-terminal sequences of unknown function have been reported previously in known yeast aquaporins (Fischer *et al.*, 2009). All these uncertainties regarding the N-terminal end of AQP2 possibly indicates that the conserved function of the protein is to mediate the passage of molecules across membranes through its C-terminus, where any additional domains might rather play a supportive role with no catalytic significance. Other structural homologues of *Plasmodium* AQP2, human aquaporin 5 (Horsefield *et al.*, 2008) and *Pichia pastoris* Aqy1, have been shown to exclusively function as water channels (Boury-Jamot *et al.*, 2006; Fischer *et al.*, 2009) suggesting that this function is possibly shared between all its homologues.

P. berghei ΔAQP2 oocyst numbers in *A. coluzzii* mosquitoes were determined to be comparable to that of the WT, however, a 70-fold decrease on the sporozoite numbers was observed at day-15 post infection. This reduction in parasite numbers was also carried on to later stages, eventually resulting in transmission blockade. Interestingly, this study has highlighted an apparent paradox between *AQP2* expression and function. Whilst the gene was found to be expressed exclusively in gametocytes, its disruption did not lead to any impairments during the early developmental processes with comparable exflagellation and gametocyte-to-ookinete conversion rates to that reported for the WT. Expression was not identified during the oocyst sporozoite development and yet it is this stage that the KO of *AQP2* directly affects, preventing normal nuclear division within developing oocysts and sporozoite production. This

indirect effect is possibly related to the lack of *AQP2* at earlier stages; for example, by impairing metabolism or nutrient import that may be later required for sporogony progression i.e. since aquaporins are responsible for water transportation across the parasite membrane, and the developing oocyst's need for water is of great importance in order to complete the multiple mitotic endoreplications occurring prior to sporozoite formation, metabolism energy could be insufficient and thus, oocysts cannot further develop. Nevertheless, AQP2 is important for sporozoite maturation inside the oocyst and thus, the major bottleneck during *ΔAQP2* development is clearly that of the oocyst-to-sporozoite developmental transition. The question of how *ΔAQP2* oocysts escape the ookinete-to-oocyst checkpoint and make it to a relatively advanced developmental stage, whilst others are lost during early oocyst development, remains to be explored. It might indeed point to a less strict cell cycle control in plasmodia than in any other organisms. This asynchrony between expression and stage-specific function has been also observed for the *P. berghei* LAP3 and LAP4 proteins, both expressed in crystalloid formations during ookinete development. Disruption of these genes prevents formation of the crystalloids, increases oocyst growth and blocks sporogony (Saeed *et al.*, 2015; 2018; 2019).

The differentiating oocyst is a spherical or ovoid structure and is surrounded by a thick capsule. The differentiating material within the oocyst is known as the sporoblastoid body, which is surrounded by a thin trilaminar plasma membrane called the outer sporoblastoid membrane. Large sporoblastoid nuclei result from the growth and repeated division of the original zygote nucleus, whereas the onset of sporozoite development is marked by the changes in these sporoblastoid nuclei accompanied by the formation of fragments of a new cytoplasmic membrane. Large nuclei around the periphery of the sporoblastoid become flattened and come close to the outer sporoblastoid membrane while at the same time electron opaque nuclear material appears at the periphery of the nucleus, taking the form of fibers. These fibers later merge at the site of the nuclear envelope in close proximity with membrane fragments of the sporoblastoid outer membrane and following the appearance of a row of microtubules close to the newly differentiated membrane regions, the transfer of cytoplasmic components and the elongation of the fibers, fully formed sporozoites are produced (detailed description in Vanderberg & Rhodin, 1967). Mutant oocysts for *AQP2*, while at first seems to have undergone sporoblastoid formation and initial mitotic DNA synthesis with their distinct nucleus to have moved close to the oocysts'

periphery, do not further indicate any sign of microtubule arrangement and/or membrane folding. The steady development of the *ΔAQP2* oocysts remained as such even after 20-days pbf where from that point onwards oocysts started losing their GFP fluorescence and hence, were no longer viable. It has been previously shown that whilst oocysts lacking the tandem repeat region (*ΔRep*) of CSP are normally formed, their sporozoite development is defective resulting in the concomitant loss of their plasmalemma integrity (Ferguson *et al.*, 2014). Therefore, the lack of AQP2 might result in abnormal osmotic regulation in the developing oocyst and consequently to the degeneration of their plasma membrane and eventually their death. However, the images obtained at this stage do not inform us further about the series of events and thus, electron microscopy of *ΔAQP2* oocysts could give us a better insight on the events occur and on the function of this gene at this critical stage.

Previous studies have shown that *PbAQP1*-null parasites are viable, however, they proliferate more slowly than the WT parasites, possibly due to the ablation of glycerol and water transport (Promeneur *et al*., 2007). Inside the RBCs, the malaria parasites reside within a PVM so that the uptake of glycerol and water from the host into the parasite occurs across both the erythrocyte plasma membrane and the PVM. *AQP9*, a highly expressed aquaglyceroporin found in mouse erythrocytes, has been shown to be part of the major pathway of glycerol and water transportation within the RBCs (Liu *et al.*, 2007). It can be suggested that following *AQP9* expression, glycerol and water molecules cross the PVM, through pores within the membrane, in order to later gain entry into the parasite. Therefore, even in the absence of *AQP1*, parasites found alternative ways to absorb necessary for their development molecules from their immediate environment. This may explain the ability of *AQP1*-null parasites to survive despite their slow growth (Promeneur *et al.*, 2007; 2018). This is in stark contrast to what has been observed for *AQP2*-null parasites, where not only do oocysts fail to mature and produce sporozoites, but they also undergo progressive elimination.

The substantial 2-fold difference in size between the WT and mutant *ΔAQP2* oocysts indicates a continuous enlargement of the mutant oocysts, despite the abnormal nuclear division and subsequent impairment in sporozoite production. This is possibly due to the absence of a regulatory factor which could monitor water and possibly other essential compounds taken up and/or secreted by the developing oocysts. Along these lines, the exact function of this putative membrane pore remains unclear but could be

investigated in a similar manner to AQP1. Briefly, whether AQP2 mediates transportation of glycerol, water or other compounds can be studied by either using yeast or *Xenopus* oocytes (Hansen *et al.*, 2002; Zeuthen *et al.*, 2006; Song *et al.*, 2012). Several other methods have been also developed to follow the movement of water through biological membranes. Changes in cell volume can be recorded by optical, electrical and tracer methods, whereas the intracellular water exchange time and the permeability of the cell membrane can be assessed by influx or efflux techniques using deuterated or tritiated water (Pfeuffer *et al.*, 1998; Promeneur *et al.*, 2018) or diffusion properties (Pfeuffer *et al.*, 1998). However, while the permeability properties for water, glycerol and ammonia have been often investigated in *Plasmodium*-infected erythrocytes and hepatocytes (Zanner *et al.*, 1990; Beitz *et al.*, 2004; Zeuthen *et al.*, 2006; Mauritz *et al.*, 2009; Promeneur *et al.*, 2018), there is no information available regarding *Plasmodium* mosquito stages.

Much research has indicated that aquaporins play a key role in tolerating osmotic stress in *Plasmodium* parasites (Beitz, 2005; Hansen *et al.*, 2002). It is therefore possible that in non-optimal growth conditions, for example at different temperatures or humidity levels, the *AQP2* mutant parasites might appear to have different developmental progression compared to WT. Future experiments where the lifecycle of the mutant parasites is assessed under a less favourable external environment could lead to interesting findings about the function of this protein. In a previous study where the AQP1 function was investigated by generating a *P. berghei* KO line, which again was tested using optimal conditions, reported normal growth during blood stages development (Kenthirapalan *et al.*, 2012). However, the phenotypic screen assessed only one aspect of parasite development (parasite numbers) and overlooked other more subtle differences. Reports in yeast have previously demonstrated that some gene deletions, whilst not causing an overt mutant phenotype, can exert an effect on the intracellular concentration of metabolites (Raamsdonk *et al.*, 2001). Particularly, since *AQP2* encodes a water and/or glycerol channel, its absence is expected to result in a completely different constitution of the parasite metabolome. Therefore, analysis of the KO metabolomic profile can help to reveal its phenotype and therefore function.

***Pb*N38 is important for gametocyte-to-ookinete developmental transition**

The *ΔN38 P. berghei* line also suffers substantial losses following *A. coluzzii* infection. Mutant parasites showed normal development in the rodent host and up to the

exflagellation process of the male gametocytes in the mosquito vector, however, they displayed significant decline ($p<0.0001$) during the gametocyte-to-ookinete developmental transition. Whether this is due to defects that govern gametes membrane fusion and fertilisation or to developmental defects of the ookinetes, has not been investigated. Nonetheless, this reduction seems to have also affected subsequent developmental stages as mutant oocyst numbers were significantly lower ($p=0.0003$) compared to the WT. This impairment finally affected their capacity for transmission to the next mammalian host.

PbN38 is highly transcribed during gametocytes and ookinete stages, where RT-PCR analysis showed sexual development specific transcripts for both rodent and human malaria parasites. Both *Pb*N38 and *Pf*N38 genes have 12 introns however during RT-PCR multiple size bands were revealed only for the *P. berghei* homologue. Specifically, multiple size bands were identified in the range of 450bp-1Kbp (**Appendix 10**); lengths found to match both the expected size of an intronless transcript as well as transcript-products of multiple differential splicing events i.e. primers were designed to map in two separate exons that are five introns apart from each other.

Ookinete development requires a capable number of fertile male and female gametes that are able to fertilise and further mature into a zygote. As a result, a defect in any of these steps could result in a markedly reduced number of ookinetes as observed for *ΔN38* parasites. In the first case of gametocyte activation, successful exflagellation was observed with rates comparable to those of the WT. Even though not quantified, female fertility also appeared unaffected; the surface protein P28 was detected on the female gametocyte periphery as expected following female gametocyte activation and parasite emergence from the RBC (Paton *et al.*, 1993). Thus, defect in ookinete formation could be traced in two events: the inability of fertilisation to occur either from defects in one or both gametes (e.g. macrogamete release of the exflagellation centre, membranes fusion) and the inability of the zygote to successfully mature into the motile ookinete (e.g. meiotic DNA inhibition, cytokinesis inhibition). Nevertheless, *ΔN38* gametes formed ookinetes which were then able to traverse the mosquito midgut.

The new genes described in this thesis to be involved in gametocyte-to-ookinete development, constitute an exciting addition to the long list of genes previously described to play a key role in this developmental stage (van Dijk *et al.*, 2001; Tewari *et al.*, 2005; Reininger *et al.*, 2005; von Besser *et al.*, 2006; Liu *et al.*, 2008; van Dijk

et al., 2010; Ukegbu *et al.*, 2017b). These data suggest that multiple genes function in an orchestrated manner in order for *Plasmodium* gametocytes to successfully fuse, pass through the zygote stage and eventually develop into the motile ookinetes.

N350 is important for *P. berghei* ookinete gliding motility

P. berghei and *P. falciparum N350* is a gene highly expressed during the midgut stages of parasite development in the mosquito vector. *P. berghei* mutant parasites lacking expression of *N350* cannot reach the oocyst stage due to gliding motility defects accompanying the parasite at the ookinete stage, inhibiting them from reaching the mosquito midgut epithelium. *In vitro* motility assay showed that *ΔN350* ookinetes move at one third of the speed determined for the WT parasites. Other genes such as *CTRP* (Dessens *et al.*, 1999; Yuda *et al.*, 1999) and *c53* (unpublished data, with the permission of Dr. Valerie Ukegbu, Imperial College London) have also been found to be important for ookinete gliding motility suggesting a multifactorial motility machinery in *Plasmodium* ookinetes. In all cases, gene expression is critical for ookinete motility and midgut invasion, and therefore infections of melanotic refractory or *CTL4*-silenced *A. gambiae* mosquitoes completely abolishes the presence of melanised KO ookinetes (Dessens *et al.*, 2001). The function of *P. falciparum N350* has not been further investigated, however, the conserved sequence and structural modelling prediction amongst all *Plasmodium spp* suggests a well-established function of this gene during *Plasmodium* development.

It has been shown that CTRP has six integrin I region-like domains through which it physically interacts with the basal lamina components laminin and collagen IV (Arrighi & Hurd, 2002) and seven fully redundant thrombospondin-like domains (Ramakrishnan *et al.*, 2011). Despite the fourteen transmembrane domains of N350, domain prediction using *in silico* analysis was not conclusive. This together with the fact that N350 homologues could not be strongly identified might suggest a non-conserved function of N350 among the apicomplexa phylum. Nonetheless, physical interaction of N350 with other molecules affecting the motility and/or invasion machinery of the parasites might explain this phenotype.

Despite the motility defects accompanying the *Δ350* ookinetes, some parasites were detected in the midgut epithelium of naïve and *CTL4*-silenced *A. coluzzii* mosquitoes. A possible explanation for this observation would be that ookinetes formed in close proximity to the apical side of the mosquito midgut epithelium do not have to go

through a long distance in order to gain access into the gut epithelium and thus manage to successfully complete their traversal through it. Those ookinetes that are for example formed in the middle of the midgut lumen need to cover a longer distance towards the midgut epithelium and when taking into consideration the toxic and thick environment of the blood bolus, this renders them incapable of reaching the midgut epithelial cells in the end. This indication also suggests that N350 has a very conserved function during ookinete motility and beyond that, its absence does not interfere with parasite developmental progression i.e. KO parasites, once near the midgut epithelium, can breach the PM and traverse the mosquito midgut epithelium.

The successful rescue of the *ΔN350* transmission blockade following *ΔN350* ookinete haemocoel injections, similarly to Δ*CTRP* (Nacer *et al.*, 2008), highly suggests that N350 is foremost a component of the ookinete motility/invasion machinery. Nevertheless, it would be interesting to see whether haemocoel injections of other mutant lines, known to be associated with basal lamina components, can be rescued.

***LRIM1*-silencing rescues *ΔN38* parasites transmission, but does not restore *ΔN350* oocyst formation and *ΔAQP2* sporozoites production**

I then sought to investigate whether AQP2, N38 and N350 facilitate for the parasite specific protein-protein interactions with the mosquito complement-like system by silencing *LRIM1* in mosquitoes, a major parasite antagonist, prior to infecting them with the *ΔAQP2*, *ΔN38* and *ΔN350* mutant parasites. As expected, *ΔN350* parasites were not rescued at the oocyst stage validating our previous findings that these parasites are eliminated prior to midgut traversal and confrontation with the mosquito haemolymph components. On the other hand, a significant increase ($p<0.0001$) on the oocyst numbers in *LRIM1*-silenced mosquitoes compared to control *LacZ*-dsRNA injected mosquitoes was observed for both the *ΔAQP2* and *ΔN38* parasite lines, albeit at levels significantly lower ($p=0.8554$ and $p=0.0928$, respectively) than the ones observed for the WT parasites. This observation could possibly confirm the existence of intrinsic defects responsible for the phenotype rather than specific interactions between mutant parasites and the mosquito immune system. It is possible that impaired parasites are killed faster than the WT parasites and that in the absence of an efficient immune system activity, some of these parasites are able to survive. These data correlate well with the hypothesis that mosquito immunity sets the base level at

which vector–parasite interactions occur and that the parasite has to overcome defence mechanisms that are already in place (Sinden *et al.*, 2004).

The increase observed in *ΔN38* oocyst numbers following *LRIM1*-silencing indicates that interactions with the complement-like pathway possibly play an important role in the survival of this mutant line following midgut traversal. Both the gametocyte-to-ookinete developmental transition and innate immune interactions, therefore, likely play a part in the clearance of the *N38* mutant parasites prior to oocyst formation. Other proteins are also known to function both in protecting parasites against the mosquito complement-like system and facilitating normal developmental progression in the mosquito vector. *P. berghei* P47 is one such example, having been implicated in both protection from the complement-like response as well as in *in vivo* and *in vitro* female gametocyte fertility (van Dijk *et al.*, 2010; Ukegbu *et al.*, 2017b). It is therefore possible that similar to P47, N38 plays a dual role in both ookinete production and survival despite the robust complement-mediated attacks.

Even if both *ΔAQP2* oocyst and sporozoite load drastically increased following *LRIM1*-silencing, transmission to the mammalian host was abolished. This possibly points to the fact that either the number of sporozoites produced is not yet enough to guarantee transmission back to the rodent host, that maturation of the midgut sporozoites and translocation into the salivary glands lumen is delayed or that sporozoites suffer severe developmental impairments that render them unable to establish infection in the mammalian host liver (e.g. motility). Bite back experiments at later time-points could lead to successful transmission of the mutant parasites, whereas in order to assess the infection capacity of the mutant sporozoites, direct subcutaneous inoculation of midgut or salivary gland sporozoites should be administrated to mice and monitored for asexual blood stages growth.

AQP2, N38 and N350 as candidates for malaria elimination interventions

The importance of identifying new genes critical for *Plasmodium* parasites survival is to first gain basic knowledge on the parasite-mosquito interactions leading to malaria transmission and then, to evaluate them as targets for malaria elimination interventions. The previously identified gametocyte specific P230 and P48/45 proteins are essential during *in vitro* fertilisation (van Dijk *et al.*, 2001; van Dijk *et al.*, 2010) and are currently under consideration as clinical candidate TBV antigens (Acquah *et al.*, 2019; Singh *et al*., 2019). Since the use of genes with a key role in parasite fertilisation

has been so far proven promising for TBV trials, further work should aim to further characterise the role of N38 in this process. Additionally, N350, whose function takes place prior to midgut invasion, should be further explored for such opportunities. Despite the function of AQP2 during oocyst development and maturation, its gametocyte-specific expression also puts it in the list with the TBV candidate targets.

It is widely accepted that to achieve eradication and long-term control, it will be necessary to use interventions that inhibit the transmission of parasites from humans to mosquitoes. Mosquito genetic control that aims to reduce the harmful impact of pest and vector populations through the dissemination of specific desirable traits is considered as one of the currently most encouraging options. In the spirit of ongoing experiments, it is possible to generate genetically modified mosquitoes which will be designed to express specific blocking nanobodies against the parasite AQP2, N38 or N350 proteins. Nanobodies are single-domain antibodies which due to their only one fragment and small size could be expressed in organisms lacking an adaptive immune system (Hamers-Casterman *et al.*, 1993). If such an intervention proves to be efficient in blocking parasite transmission, it could be also programmed to propagate throughout a population using gene drive technologies (Burt *et al.*, 2003). In the case of transmission blockage through AQP2-antibody mediated disruption, it should be noted that *T. brucei* has been previously shown to tolerate the loss of all three of its aquaporins, despite the glycerol uptake disruption (Jeacock *et al.*, 2017). However, since glycerol is a great carbon source for *Plasmodium* parasites metabolism during mosquito stages, such a loss could prove lethal. Given the fact that *P. berghei* AQP2 is essential for the initiation of sporogony in the developing oocyst, TB interventions against it may indeed prove encouraging.

Western blot analysis revealed that *P. berghei AQP2*, *N38* and *N350* expression starts in the blood stage gametocytes and continues during activation in the mosquito midgut lumen. An elimination strategy that aims to reduce the permissiveness of gametocytes in the host blood as well of gametes in the vector midgut could be proved promising i.e. cumulative effect that reduces the gametocytaemia levels in the host (number of gametocytes that have the potential to establish infection in the mosquito vector) and the gamete fertilisation capacity in the mosquito midgut lumen that previously escaped clearance in the human host. Similar to the robust immune responses identified against antigens on the surface of erythrocytes infected with asexual stage parasites

(Chan *et al.*, 2014), there is also plenty of scientific evidence that proves the existence of various robust natural immune responses against antigens on the surface of gametocyte infected RBCs (reviewed in Baird *et al.*, 1991; de Jong *et al*., 2020). Therefore, the localisation of the aforementioned proteins and whether they are accessible by antibodies while still encapsulated in the RBC membrane, still needs to be further investigated. Nevertheless, such a blood stage and transmission blocking vaccine combination strategy that targets the same parasite lifecycle stage but in the two individual hosts could indeed constitute an effective intervention.

This chapter, therefore, identifies three novel *P. berghei* genes that play fundamental roles in the lifecycle of the malaria parasite while in its *Anopheles* mosquito vector. It is shown that all three genes are important for infection establishment in the mosquito midgut and that deletion of any of these genes ultimately leads to transmission blockade. These findings provide fundamental insights into the biology of the malaria parasites and identify potential targets for antimalaria therapy.

CHAPTER 4. PHENOTYPIC AND FUNCTIONAL CHARACTERISATION OF *PLASMODIUM* GENES ESSENTIAL FOR RODENT MALARIA TRANSMISSION

4.1 Introduction

Plasmodium ookinete-to-oocyst developmental transition in the mosquito midgut is characterised by dramatic parasite losses, resulting in limited numbers of parasites able to complete their lifecycle in the vector (Sinden *et al.*, 2007). Most of these parasite losses occur during the ookinete-to-oocyst transition (Garver *et al.*, 2013; Smith *et al.*, 2014) and specifically, upon ookinete exit at the midgut sub-epithelial space. Ookinete traversal of the mosquito midgut epithelium leads to activation of the JNK signalling pathway which later induces apoptosis in the invaded cells. At the same time, induction of the HPX2 and NOX5 effectors potentiates nitration of the ookinetes that are henceforth marked for elimination by reactions of the mosquito complement-like system (Oliveira *et al.*, 2012; Garver *et al.*, 2013). The complement-like system involves the complement factor-3 like protein TEP1 that circulates in the haemolymph together with a complex of two leucine rich repeat proteins, LRIM1 and APL1C (Fraiture *et al.*, 2009; Povelones *et al.*, 2009). Upon parasite recognition, $TEP1_{CUT}$ is released from the complex and attacks the ookinete surface by triggering *in situ* assembly of a TEP1 convertase, which locally processes more $TEP1_{CUT}$ molecules that bind to the ookinete surface causing lysis or melanisation (Blandin *et al.*, 2004). Hence, the success of *Plasmodium* infection and transmission at this stage balances on a knife-edge, making disease control interventions such as transmission blocking drugs, vaccines and effector-producing GM mosquitoes an attractive goal.

The *Plasmodium* genome sequencing project (Carlton *et al.*, 2002; Gardner *et al.*, 2002) has facilitated one of the fastest-growing fields of malarial functional genomics with genome-wide surveys conducted both at the transcriptome and proteome levels. The generation of the first *P. berghei* and *P. falciparum* KO lines, that took place more than twenty years ago (Ménard & Janse, 1997; Sultan *et al.*, 1997; Crabb *et al.*, 1997; Dessens *et al.*, 1999), set the foundations for reverse genetic studies. Gene targeting studies have identified a number of proteins expressed during ookinete stages and potentially implicated in parasite-vector interactions, involving membrane-bound or secreted proteins. The major ookinete surface proteins *Pb*s25 and *Pb*s28 are known to be localised on the ookinete surface (Tomas *et al.*, 2001), whereas microneme molecules such as CTRP (Dessens *et al.*, 1999; Yuda *et al.*, 1999), CelTOS (Kariu *et*

al., 2006), chitinase (Dessens *et al.*, 2001) and SOAP (Dessens *et al.*, 2003) as well as members of the LAPS (Raine *et al.*, 2007) and PPLP protein families (Kadota *et al.*, 2004; Ecker *et al.*, 2007) are secreted. Yet, disruption of only a few of these genes hinder malaria transmission, the majority of which being implicated in the ookinete molecular motor machinery.

Over the last years, a lot of effort has been made to unravel some of the mechanisms underlying the interactions between the *Plasmodium* parasite and the mosquito immune system. The characterisation of *P. falciparum Pf*s47 as a key player in parasite evasion of the mosquito complement-like responses has shed light on the mechanisms parasites employ to endure the mosquito immune responses, especially those of the complement-like system. GPI-anchored *Pf*s47 is shown to interfere with activation of the JNK signalling and in this way, helps ookinetes to escape nitration and subsequent complement-mediated attack (Molina-Cruz *et al.*, 2013; Ramphul *et al.*, 2015). Interestingly, the immune evasion function of *Pf*s47 is allele dependent, meaning that different alleles allow survival in mosquitoes from different geographical locations (Molina-Cruz & Barillas-Mury, 2014; 2015). This function is shared by its orthologue in the rodent malaria parasite *P. berghei* (Ukegbu *et al.*, 2017b), in addition to playing a role in gamete fertilisation (van Dijk *et al.*, 2010; Ukegbu *et al.*, 2017b).

Previous transcriptomic profiling studies of field *P. falciparum* isolates in midguts of *A. coluzzii* and *A. arabiensis* mosquitoes and of *A. coluzzii* mosquito midguts infected with a laboratory *P. berghei* strain, identified hundreds of genes exhibiting conserved and differential expression during gametocyte to oocyst development (Akinosoglou *et al.*, 2015). Several of them, encoding putatively secreted or membrane-associated proteins, were made part of a screen to identify genes that function during parasite infection of the mosquito midgut. Of those, *Plasmodium c43* encodes a GPI anchored protein with two conserved cysteines close to its C-terminal (Ukegbu *et al*, 2020) that was shown to be highly conserved among the different *Plasmodium spp.* It has been found to be localised on the surface of mosquito stages of malaria parasites and its function seems to be related with ookinetes protections against the robust mosquito immune system responses. Its disruption in *P. berghei* parasites inhibits mosquito infection and abolishes transmission (Ukegbu *et al*., 2020). *Plasmodium P47* encodes a GPI-anchored protein which belongs to the 6-cys protein family and is needed for the *in vitro* fertilisation of *P. berghei* parasites and *P. falciparum* ookinete protection

against responses of the mosquito innate immune system (Thompson *et al.*, 2001; van Dijk *et al.*, 2010; Arredondo *et al.*, 2012; Ukegbu *et al.*, 2017b). Lastly, *c01* encodes a putatively secreted polypeptide and *c57* a putatively membrane-associated protein and were found to be highly conserved in the different *Plasmodium spp*. The host laboratory had preliminary evidence that they are essential for parasite development and transmission, since their absence is associated with a reduced ability of the parasites to form ookinetes and develop into oocysts (unpublished data, with the permission of Dr. Valerie Ukegbu, Imperial College London). Here, continuation of the work on the phenotypic and functional analysis of *P. berghei c43* (Ukegbu *et al.*, 2020), *P47* (Ukegbu *et al.*, 2017b), *c01* and *c57* is reported.

4.2 Results

4.2.1 Developmental profiling of *P. berghei* and *P. falciparum c01*, *c43*, *P47* and *c57* transcriptional activity

The stage-specific transcriptional activity of *P. berghei* and *P. falciparum c01*, *c43*, *P47* and *c57* was investigated by carrying out RT-PCR (**Figure 4.1**). To investigate the transcription pattern of *P. berghei* genes, cDNA was isolated from midguts and salivary glands of *A. coluzzii* mosquitoes previously fed on *P. berghei* infected mice and purified *in vitro* parasite stages collected after 1 hour and 24 hours of incubation in ookinete culture medium. In this assay, the *P. berghei* line ANKA *c507* (WT) that constitutively expresses *GFP*, as well as the ANKA 2.33 NGP were used as controls. For *P. falciparum* analysis, *A. coluzzii* midguts and salivary glands were collected following infection with the NF54 parasite line via an optimised SMFA, whereas the ABS and gametocyte *in vitro* stages were purified from the culturing flasks.

RT-PCR analysis revealed that transcripts of the *P. berghei c01*, *c43*, *c57* and *P47* genes were present at 24 hours pbf in the midguts of infected *A. coluzzii* mosquitoes as well as in purified *in vitro* ookinetes. Since transcription of the genes was not identified in the NGP cDNA sample, it can be concluded that transcripts observed in mosquito midguts at 24 hours pbf did not derive from the parasite earlier asexual blood stages that persist in the blood bolus but mainly from ookinetes formed afterwards. Furthermore, *c01*, *P47* and *c57* transcripts were detected in infected *A. coluzzii* midguts at 1 hour pbf and in purified activated gametocytes. This, together with the fact that no transcripts were detected in the cDNA sample derived from the NGP *P. berghei* strain, suggests that *c01*, *P47* and *c57* transcription starts upon gametocyte

activation and zygote formation. Additionally, the RT-PCR results revealed low levels of *c43* transcription in MBS and purified gametocytes, which together with the absence of transcripts in the NGP MBS cDNA sample, indicates that *c43* transcription possibly begins in gametocytes and peaks at the ookinete stage. No *c43* transcripts were detected in mature oocysts at day-15 pbf but strong transcription of the gene was observed again in salivary gland sporozoites at day-21 pbf.

RT-PCR analysis of *P. falciparum* cDNA samples revealed transcripts of *c43* and *P47* at 1 hour and 24 hours pbf of *A. coluzzii* mosquitoes, as well as in purified activated gametocytes. The fact that no *c43* and *P47* transcripts were detected in *in vitro* cultured ABS parasites indicates that both genes transcription begins in gametocytes and peaks later in zygotes and ookinetes. Furthermore, *c43* transcripts were not detected in oocysts at day-10 post mosquito blood feeding but reappeared in mosquito salivary glands, indicative of *c43* re-transcription at this transmittable stage (Ukegbu *et al.*, 2020). These data together indicate that *c43* exhibits similar transcription pattern between the rodent and human orthologues starting in activated gametocytes, peaking in ookinetes, pausing in oocysts and midgut sporozoites, and starting again in salivary gland sporozoites. Similarly, *P. falciparum c01* and *c57* are highly transcribed at 1 hour and 24 hours pbf of *A. coluzzii* mosquitoes, as well as in purified activated gametocytes. Transcripts for both genes were also detected in the ABS, possibly indicating that their transcription has already started during the asexual proliferation of the parasite. However, due to the inconsistent RT-PCR results, as regards to the transcription pattern of the stage-specific controls *Pfs16* and *Pfs25* which might indicate some contamination of the ABS sample by gametocytes (**Figure 4.1**), final conclusion about the transcription of *Pfc01* and *Pfc57* during asexual development of the parasite cannot be drawn. Nevertheless, it is certain that both genes are highly transcribed during the initial stages of parasite infection in the mosquito midgut.

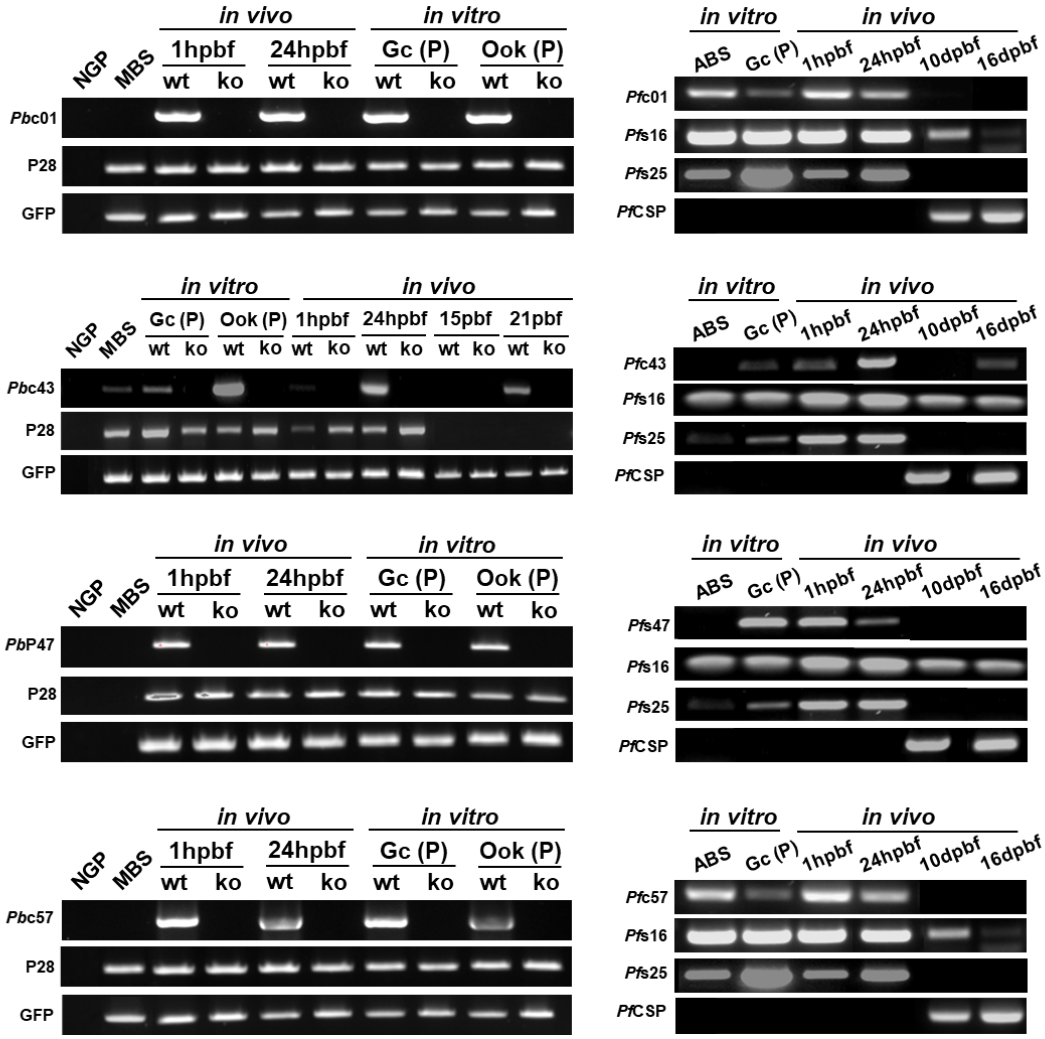

Figure 4.1. Transcription profiling of *P. berghei c01*, *c43*, *P47* and *c57*. RT-PCR analysis of *P. berghei* and *P. falciparum c01*, *c43*, *P47* and *c57* transcripts in infected *A. coluzzii* midguts and in purified *in vitro* parasite populations. Genes encoding the female/zygote sexual stage protein, P28, and the constitutively expressed gene, *eGFP*, served as both stage-specific and loading controls for *P. berghei* cDNA. cDNA samples derived from the KO parasite populations, served as negative controls for the primers specificity. The reduced ability of the *P. berghei ΔP47* gametocytes to form ookinetes *in vitro,* was overcome after mixing multiple *ΔP47* ookinete cultures together, prior to ookinete purification and RNA extraction. Additionally, *P. berghei Δc43* midgut and salivary gland sporozoites were obtained from *LRIM1*-silenced *A. coluzzii* mosquitoes at day-15 and day-21 pbf, respectively. Gametocyte expressed gene *Pfs16* and *Pfs25*, and sporozoite-expressed gene *PfCSP* served as both stage-specific and loading controls for *P. falciparum* cDNA. *Pfs16* transcripts are expected to be found at the gametocyte and sporozoite stages, whereas little transcription is expected during the parasite asexual developmental cycle (Moelans *et al*., 1991; Lobo

et al., 1994; Niederwieser *et al*., 2000). *Pfs25* expression commences only after fertilisation, however several studies report transcription in blood-stage gametocytes and less, in asexual parasites (Niederwieser *et al*., 2000). However, the presence of intense PCR bands at this stage for both genes might indicate some contamination of the samples with blood stage gametocytes. Two sets of RNA samples have been used for the transcriptional analysis of the aforementioned genes; one set to analyse the transcription pattern of *Pfc*43 and *Pf*P47, and one more for the transcriptional analysis of *Pfc*01 and *Pfc*57. For the transcriptional analysis of *Pfs16*, *Pfs25* and *PfCSP*, the same PCR reaction was performed between the two sets, further explaining their identical transcription pattern. Data regarding the *P. berghei* and *P. falciparum c43* have been previously reported in (Ukegbu *et al*., 2020). MBS, mixed blood stages; ABS, asexual blood stages; NGP, 2.33 non-gametocyte producing strain; 1 hour pbf (hpbf), 1 hour pbf; 24hpbf, 24 hours pbf; 10 days pbf (dpbf), 10 days pbf; 15dpbf, 15 days pbf; 16dpbf, 16 days pbf; 21dpbf, 21 days pbf; Gc (P), purified activated gametocytes; Ook (P), purified ookinetes.

4.2.2 Phenotypic and functional characterisation of c43

4.2.2.1 Phenotypic characterisation of *P. berghei Δc43* parasites

To functionally characterise the *P. berghei* gene, a mutant KO parasite was generated in the ANKA *c507* (WT) paternal parasite line, that constitutively expresses *GFP*. Phenotypic characterisation of *P. berghei* parasites that lack expression of *c43* (*Δc43*/green) showed that they exhibit normal development in mouse blood stages, male gametocyte activation, macrogamete-to-ookinete developmental transition, ookinete motility while still in the mosquito midgut lumen and, ookinete invasion and traversal through the mosquito midgut epithelium. However, no oocysts were detected *in A. coluzzii* midguts at 3, 5, 7 or 10 days pbf, indicating complete abolishment of oocyst formation. Thus, oocyst and salivary gland sporozoites were never observed and transmission to mice following mosquito bite-back was abolished. However, silencing of the complement-like system restored ookinete-to-oocyst transition. Nonetheless, the rescued *Δc43* oocysts in *LRIM1*- or *TEP1*-silenced mosquitoes were defective in producing any sporozoites and thus, transmission back to the rodent host remained nonexistent (Ukegbu *et al.*, 2020).

The findings from (Ukegbu *et al*., 2020) are in disagreement with those previously reported, which showed that *ΔPSOP25* (*Δc43*) parasites exhibit reduced ookinete

conversion rates and defective ookinete maturation (Zheng *et al.*, 2017). To investigate this further, a new *Δc43* parasite line was generated to be further characterised. The new *P. berghei Δc43*/red parasite line was generated by Dr. Ana-Rita Gomes in the host laboratory (Ukegbu *et al.*, 2020) using the same disruption vector (PbGEM-042760) as the one used by the authors of the previous study (Zheng *et al.*, 2017) and in the *1804cl1 P. berghei* line that constitutively expresses *mCherry*.

Phenotypic analysis showed that the macrogamete-to-ookinete conversion rate determined for the *Δc43*/red parasites (78.33 ± 0.17, 80.50 ± 0.50) is comparable to the WT (77.32 ± 0.35, 80.88 ± 0.24) both *in vitro* and *in vivo* in *A. coluzzii* infections, respectively (**Figure 4.2, A**). These ookinetes are morphologically normal as indicated by Giemsa-staining as well as by immunofluorescence assay (**Figure 4.2, B**). Going a step further, their ability to invade the *A. coluzzii* midgut epithelium was tested by imaging *Δc43*/red-infected midgut epithelia at 25 hours pbf, a time that coincides with ookinete midgut traversal. Indeed, the mutant *Δc43*/red parasites were able to invade and later traverse the midgut epithelium of the *A. coluzzii* mosquitoes at levels comparable to the WT (**Figure 4.2, C**). However, despite the normal development of the *Δc43*/red parasites up to this point, oocyst development was completely abolished at day-10 pbf (**Figure 4.2, D**). This also lead to the production of zero midgut oocyst sporozoites and therefore, to transmission blockage (**Figure 4.2, E**).

Since the vector of choice in the previous studies was *A. stephensi,* infection of *A. stephensi* Nijmegen strain mosquitoes with both the *Δc43*/red and *Δc43*/green parasites was performed prior to macrogamete-to-ookinete conversion rate and oocyst count. Importantly, the macrogamete-to-ookinete *in vivo* conversion rates of the two mutant parasites lines was similar to the WT (*Δc43*/red mean: 78.45 ± 0.05, *Δc43*/green mean: 80.55 ± 1.80, WT mean: 79.22 ± 2.02) (**Figure 4.2, F**). Following oocyst formation, the number of mutant parasites was significantly reduced ($p<0.0001$) compared to the WT but did not drop down to zero (*Δc43*/red median: 7.5, *Δc43*/green median: 6, WT median: 142.5) (**Figure 4.2, G**). The reduced number of *Δc43* oocysts formed further affected the number of midgut sporozoites produced (*Δc43*/red mean: 253.3 ± 13.34, *Δc43*/green mean: 319.5 ± 25.50, WT mean: 45,905 ± 6,778), as determined at day-15 pbf (**Figure 4.2, H**). The number of *Δc43*/red and *Δc43*/green oocysts and midgut sporozoites was not zero as initially observed following *A. coluzzii*

infections (Ukegbu *et al.*, 2020), possibly due the high susceptibility of the *A. stephensi* strain to *Plasmodium* infection (Feldmann *et al.*, 1989).

In conclusion, these results validate the phenotype observed by (Ukegbu *et al.*, 2020); that *Δc43 P. berghei* parasites form numericaly and morphologically normal ookinetes that are able to invade the moquito midgut epithelium, but are eliminated upon exitting into the sub-epithelial space of the basal side of the midgut from reactions of the complement system thus, abolishing oocyst formation.

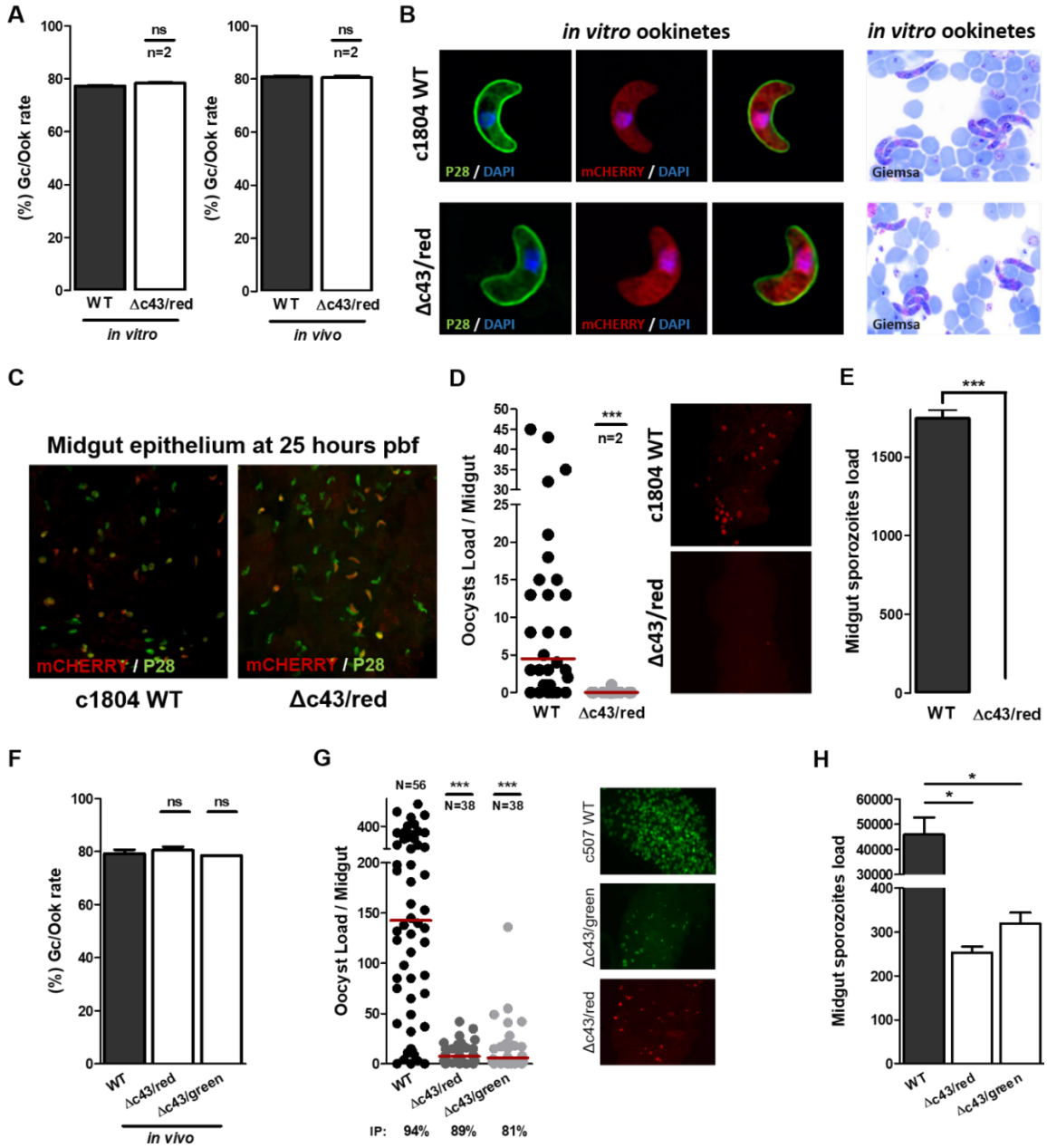

Figure 4.2. Phenotypic characterisation of *Δc43*/red in *A. coluzzii* and *A. stephensi*. (A) Female gametocyte to ookinete conversion rate *in vitro* (left), and *in vivo* in the *A. coluzzii* midgut (middle left) of *P. berghei* c1804 (WT) and mutant

Δc43/red lines. Error bars indicate SEM. Statistical significance was determined with a two-tailed, unpaired Student's *t*-test (ns, non-significant). Data derived from two individual biological replicates (n). **(B)** Representative images of *in vitro* produced WT and *Δc43*/red ookinetes that have been either stained with an antibody against their P28 surface protein (green) (left panel) or with Giemsa-stain (right panel). DNA was stained with DAPI. The constitutively expressed *mCherry* is in red. **(C)** WT and *Δc43*/red ookinetes while traversing the *A. coluzzii* midgut epithelium at 25 hours pbf. Ookinetes have been stained with an antibody specific to their P28 surface protein (green), whereas mCherry is in red. **(D)** *Δc43*/red oocyst graphs indicating distribution in *A. coluzzii* midguts as counted 10 days post infection. Infection with the *P. berghei* c1804 (WT) line was used as control. Data derived from two individual biological replicates (n). Red lines indicate the median oocyst number of each parasite line. Statistical analysis was performed with Mann Whitney U-test. Representative fluorescent microscopy images of *Δc43*/red and WT *mCherry*-expressing oocysts in *A. coluzzii* midguts, at X100 magnification. **(E)** Midgut *Δc43*/red and c1804 WT sporozoite numbers in *A. coluzzii* mosquitoes, at day-15 pbf. The mean of the pooled data from two biological replicates is presented. For each replicate, sporozoite numbers were determined from two batches of 25 homogenised midguts using light microscopy. Error bars show standard error. Statistical analysis was performed using a two-tailed, unpaired Student's *t*-test. **(F)** Gametocyte-to-ookinete conversion rate in the midgut bolus of *c507* (WT), *Δc43*/green and *Δc43*/red *P. berghei* lines in *A. stephensi* mosquitoes. Data derived from two biological replicates, where statistical significance was determined with a two-tailed, unpaired Student's *t*-test (ns, non-significant). **(G)** *Δc43*/green and *Δc43*/red oocyst loads in the midguts of *A. stephensi* mosquitoes, at day-10 pbf. Infection with the *c507* (WT) parasite line served as a control. The median oocyst number is indicated by the red horizontal lines. Infection prevalence corresponds to the percentage of the infected midguts that appeared to have at least one oocyst. Data derived from two individual biological replicates, where N is the number of midguts dissected prior to oocyst count. Statistical significance was determined using the Mann Whitney U-test. Representative fluorescent images of *Δc43*/green, *Δc43*/red and *c507* (WT) oocysts in the midguts of infected *A. stephensi* mosquitoes. Images were taken at x100 magnification. **(H)** Sporozoite numbers of the *Δc43*/red and *Δc43*/green *P. berghei* lines in the midguts of *A. stephensi* mosquitoes 15 days pbf. The *c507* (WT) parasite line served as a control. Statistical analysis was

performed using a two-tailed, unpaired Student's *t*-test. All data presented in (Figure 3.7, A-H) have been previously reported in (Ukegbu *et al.*, 2020).

4.2.2.2 Morphological analysis of *P. berghei Δc43* oocysts

The *Δc43/red* and *Δc43/green* oocysts formed in the midguts of *A. stephensi* mosquitoes were notably smaller and with an abnormal morphology compared to the WT. This phenotype was also previously observed, when the restored *Δc43* oocysts formed in the midguts of *LRIM1*-silenced *A. coluzzii* mosquitoes were morphologically different compared to the WT, in regards to both their size and the DNA distribution in them. Also, these oocysts were shown to produce very few sporozoites, a phenotype that eventually leads to transmission abolishment (Ukegbu *et al.*, 2020). To investigate this defective phenotype, monitoring of the *Δc43/green* (from now refferred to as *Δc43*) oocyst size and morphology at various time points was carried out. At day-14 and day-16 pbf the average *Δc43* oocyst diameter was 20.1 and 17.3 μm compared to 27.4 and 31.7 μm of *c507* (WT) oocysts, respectively (**Figure 4.3, A; Table 4.1**).

In contrast to the normal morphology of the WT oocysts, fluorescent imaging of day-14 *Δc43* oocysts revealed notable structural deviations. Based on their size and DNA distribution following staining with DAPI, they can be categorised in three types; Type 1 (normal size oocysts displaying a large, digitated endomitotic nucleus and containing fully formed sporozoites), Type 2 (small oocysts displaying a digitated endomitotic nucleus but with no observable sporozoites) and Type 3 (small oocysts with no DNA staining, indicating death or progress of cell death). For the WT control, Type 1 oocysts dominated (90%) with oocysts displaying either large mature sporoblasts or sporozoites close to the periphery of the oocysts. A smaller proportion of Type 2 (7%) oocysts were also identified, for which a large number of foci of a large, highly lobed nucleus but in which no sporoblasts or sporozoites were observable. Lastly, a very small number (3%) of sick or dying Type 3 oocysts were identified in the WT cohort. Fluorescent imaging of *Δc43* oocysts revealed that mature, sporulated Type 1 oocysts were almost completely absent from this cohort (2%). Whilst 6% of the *Δc43* oocysts were of Type 2, displaying a small size with a digitated nucleus, the number of nuclear lobe foci were substantially fewer compared to that observed for WT oocysts. The majority of *Δc43* oocysts were of Type 3 (92%); small size with no DNA content indicating either death or termination of development at the very initial steps of the mitotic endoreplication (**Figure 4.3, B-C**). Importantly, for the majority of the oocysts,

the abnormality in development was distinguishable already from day-5 post infection onwards, indicating that the defective phenotype appeared soon after oocyst formation and long before sporozoite production. This might be due to either deficiency in the DNA endoreplication mechanism, oocyst elimination by the mosquito late phase immune responses or due to deficiencies in uptaking nutrients needed.

Whether the abnormal morphology of the *Δc43* oocysts is either due to the attack of the mosquito innate immunity or due to the incapability of the mutant oocysts to uptake important nutrients for their development was then examined. To do so, LITAF, an *Anopheles* specific LPS-induced TNFα transcription factor which is believed to be implicated in the late phase of immunity against the developing oocyst (Smith *et al.*, 2012), was knocked down prior to mosquito feed with the *Δc43* parasites. The results indicated that not only do oocysts have the characteristic abnormal morphology, but also the deficient oocyst phenotype was not recovered i.e similarly to what is known when *LRIM1* is silenced (data not shown). Examination of whether the provision of more nutrients could enhance oocyst development was then investigated. To do so, *Δc43*-infected mosquitoes, were submitted to a second blood feeding just 3 days later. Nevertheless, similar to before, no further increase on the size of the oocysts was observed suggesting that the defective phenotype is due to molecular defects rather than, lack of nutrients or attacks by the late immune responses (data not shown).

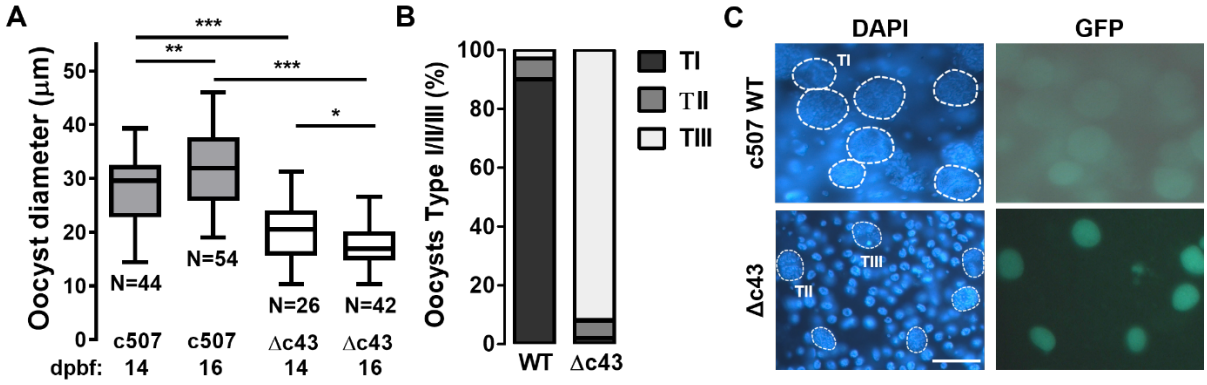

Figure 4.3. Morphological analysis of *Δc43* oocysts in *LRIM1*-silenced *A. coluzzii* mosquitoes. (A) Box plot of diameter measurements of *Δc43* and *c507* (WT) oocysts at day-14 and day-16 pbf. Upper and lower whiskers represent the largest and smallest oocyst diameter, respectively. Horizontal line in each box indicates mean of two individual biological replicates and whiskers show SEM. N is number of oocysts. Statistical significance was carried out using a two-tailed, unpaired Student's *t*-test. **(B)** Graphs showing the proportions of Type 1 (TI; oocysts displaying a large, digitated

endomitotic nucleus and containing fully formed sporozoites), Type 2 (TII; small oocysts displaying a digitated endomitotic nucleus but with no observable sporozoites) and Type 3 (TIII; small oocysts with no DNA staining, indicating death or progress of cell death) WT and *Δc43* oocysts, in the midguts of *LRIM1*-silenced mosquitoes at day-14 post mosquito blood feeding. **(C)** Representative images of rescued *Δc43* oocysts in *LRIM1*-silenced *A. coluzzii* mosquitoes showing variable morphology and smaller size compared to the control *c507* (WT) oocysts. Scale bar is 30 μm. The data presented in this figure have been previously reported in (Ukegbu *et al*., 2020).

Table 4.1. Oocyst size of the *P. berghei Δc43* and control *ANKA c507* (WT) parasite lines at day-14 and day-16 pbf, in the midguts of *LRIM1*-silenced *A. coluzzii* mosquitoes

Parasite line	Days Post-Infection	Number of oocysts measured	Range (μm)	Mean	SEM	*p*-value
c507 (WT)	14	44	14.40-39.30	27.44	1.03	
Δc43	14	26	10.30-31.30	20.50	1.12	0.0052
WT	16	54	19.00-46.00	31.74	1.08	
Δc43	16	42	9.28-26.60	16.90	0.58	0.0150

The table reports the size of *Δc43* and ANKA *c507* (WT) oocysts in the midguts of *LRIM1*-silenced *A. coluzzii* mosquitoes, at day-14 and day-16 pbf. About 20 midguts were collected for each parasite line at each time point, and oocyst size measurement was recorded randomly across all midgut tissues. Data derived from two individual biological replicates. Statistical significance was determined using the unpaired Student's *t*-test

4.2.2.3 *P. falciparum* c43 protein expression and sub-cellular localisation

Previous work has shown that *P. berghei c43* is highly expressed on the ookinete and sporozoite surface (Ukegbu *et al.*, 2020). In order to experimentally investigate the expression pattern and potential membrane-anchoring capacity of *P. falciparum* c43, I carried out western blot and immunofluorescence assays. A rabbit polyclonal antibody against a codon-optimised coding fragment of *P. falciparum c43* (amino acids 25-481) expressed in *E. coli* cells and lacking the predicted signal peptide and C-terminal transmembrane domain was previously raised by H. Yassine and used here to examine the *Pfc*43 protein expression and localisation.

To initially examine the affinity and specificity of this antibody, the *Pb(Pfc43) P. berghei* line in which the *P. berghei c43* locus was replaced by its *P. falciparum* orthologue (**Figure 4.4, A**), was generated by Dr. Valerie Ukegbu in the host laboratory. PCR genotypic analysis confirmed successful modification of the endogenous *Pbc43* genomic locus (**Figure 4.4, B**), whereas qRT-PCR and RT-PCR analysis confirmed that *Pfc43* is transcribed in *in vitro* cultured *P. berghei* ookinetes and at levels similar to the *Pbc43* endogenous locus (**Figure 4.4, C**). Western blot analysis of total protein extracts prepared from purified *in vitro* cultured *Pb(Pfc43)* ookinetes revealed a strong band of approximately 60kDa, corresponding to the predicted molecular weight of the deduced *Pfc*43 protein (**Figure 4.4, D**). This band was absent from *c507* (WT) and *Δc43* protein extracts confirming the specificity of the α-*Pfc*43 antibody. Under strong reducing conditions, the 65 kDa of Pbc43 was resolved in a single 37-kDa band, whereas under nonreducing conditions both the 60-65 kDa and 37 kDa band could be detected, confirming what was previously found that *Pbc*43 forms homodimer upon disulphide bonding of the conserved pair of cysteine residues (Ukegbu *et al*., 2020). Noteworthy, in contrast to what was observed with the *Pbc*43 protein, the results did not show dimerisation of the ectopically expressed *Pfc*43 protein (**Figure 4.4, D**).

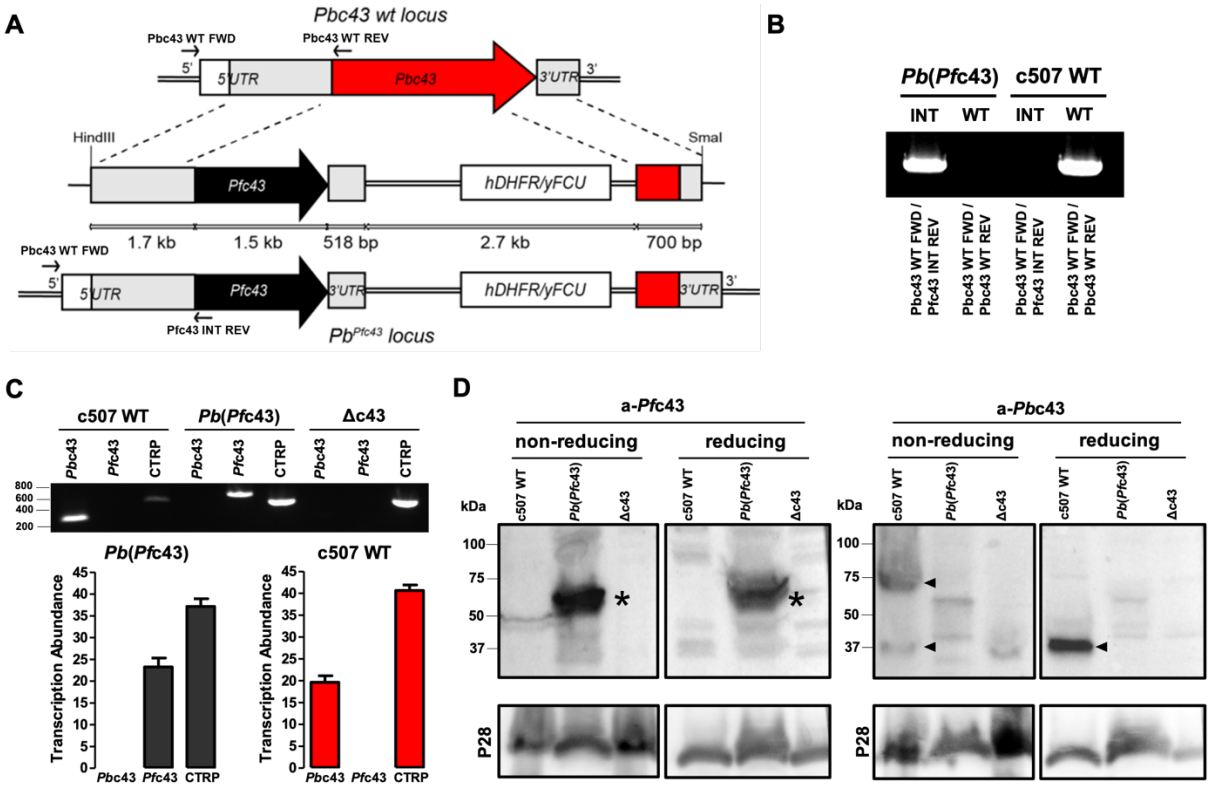

Figure 4.4. Generation and phenotypic analysis of *Pb(Pfc43)*. (A) Schematic diagram of the endogenous *Pbc*43 locus, targeting construct and resulting transgenic *Pb(Pfc43)* locus. Arrows *Pbc*43 WT FWD, *Pbc43* WT REV and *Pfc43* INT REV indicate binding sites for primers used in diagnostic PCR. The transgenic line was generated by Dr. Valerie Ukegbu, whereas the figure was adapted from (Ukegbu *et al.*, 2020). **(B)** Diagnostic PCR on *Pb(Pfc43)* blood stage parasites, to determine integration of the *Pfc*43 targeting construct into the endogenous *Pbc*43 locus. The *Pbc43* WT FWD and *Pfc43* INT REV primers were used to detect integration, whereas the *Pbc43* WT FWD and *Pbc43* WT REV primers that bind to the endogenous *Pbc*43 locus, were used to confirm absence of the endogenous gene in the *Pb(Pfc43)* transgenic line. The *c507* (WT) parasite served as a control. **(C)** RT-PCR (top panel) and qRT-PCR (bottom panel) analysis of purified *in vitro* ookinetes to confirm expression of *Pfc43* in the *Pb(Pfc43)* transgenic line. Amplifications of *Pbc43* and *ctrp* during RT-PCR were used as positive control for the endogenous locus and stage-specific control, respectively. Images are representative of two individual biological replicates. During qRT-PCR, the transcription abundance of *Pfc43*, *Pbc43* and *ctrp* was normalised against the constitutive expressed *eGFP*. *CTRP* was used as a stage-specific control, whereas the *c507* (WT) line was used to compare the transcription levels of the endogenous *Pbc43* gene and the *Pfc43* transgene. Data derived from two

individual biological replicates. **(D)** Western blot analysis under reducing and non-reducing conditions of whole *c507* (WT), *Δc43* and *Pb(Pfc43)* parasite cell lysates using the α-*Pbc*43 and α-*Pfc*43 antibodies. *Pfc*43 protein bands are indicated with asterisks, whereas *Pbc*43 bands are indicated with arrowheads. For the detection of *Pbc*43, a rabbit polyclonal antibody against the codon-optimised fragment of the protein was raised by H. Yassine. The fragment lacking both the signal peptide and the C-terminal hydrophobic domain (amino acids 22-327) was expressed in *E. coli* cells. The ANKA *c507* line that constitutively expresses *GFP* (Janse *et al.*, 2006a) and the *P. berghei Δc43* line that lacks expression of *c43* and constitutively expresses *GFP*, were used as positive and negative control, respectively. P28 was used as a loading control. Data have been previously reported in (Ukegbu *et al.*, 2020).

The same α-*Pfc*43 antibody was used to investigate the expression pattern and sub-cellular localisation of *P*fc43 in *P. falciparum* NF54 parasites. Western blot analysis showed the *Pfc*43 protein to be abundant in the midgut and salivary gland sporozoites but was absent in non-activated purified gametocytes (**Figure 4.5**). The expected size of the *P. falciparum* c43 protein is around 60kDa, however intense bands in the salivary gland and midgut sporozoite samples appear also on a different size of about ~45kDa. Strong reacting bands of about 20 kDa have been also observed in the midgut sporozoite sample. A possible conclusion is that the bands of lower molecular weight represent specific binding, and that they are breakdown products of the next strongest band of 60kDa. The reacting bands of about 75 kDa in the midgut and salivary gland sporozoite samples have not been investigated further. Due to the lack of a successful method to *in vitro* cultivate *P. falciparum* ookinetes, the expression of the protein at this stage was not investigated. Similar to what was also previously observed, under non-reducing conditions, *Pfc*43 does not form dimers.

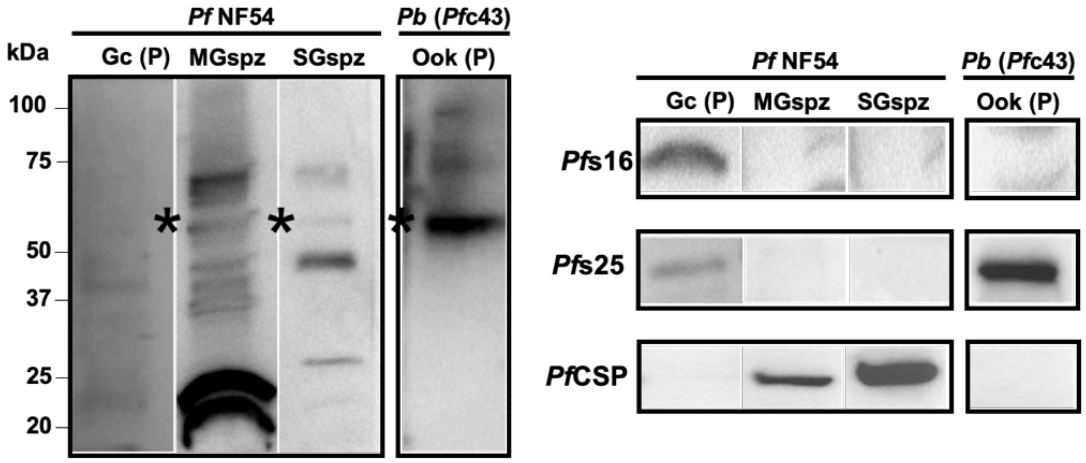

Figure 4.5. *Pfc*43 protein expression pattern. Western blot analysis of *Pfc*43 in protein extracts of purified non-activated gametocytes, midgut and salivary gland sporozoites using the a-*Pfc*43 antibody. The *P. falciparum* NF54 parasite line was used for *A. coluzzii* mosquito infections. Protein extract from the *P. berghei Pb(Pfc43)* transgenic line was used as positive control. Probing with the a-*Pfs*16, a-*Pfs*25 and a-*Pf*CSP antibodies served as stage-specific controls. *Pfc*43 protein bands, at 60kDa, are indicated with asterisks. Gc (P), non-activated purified gametocytes; MGspz, midgut sporozoites; SGspz, salivary gland sporozoites; Ook; *in vitro* ookinetes.

To examine the sub-cellular localisation of *Pfc*43, the a-*Pfc*43 antibody was used in immunofluorescence assays. The results showed that *Pfc*43 prominently localises on the surface of female gametocytes or early stage zygotes found in the *A. coluzzii* blood bolus at 1 hour pbf, as well as on the surface of ookinetes while traversing the mosquito midgut epithelia at 30 hours pbf, and early-oocysts found in the midgut wall of *A. coluzzii* mosquitoes following 2 days of infection. *Pfc*43 has been also maintained on the surface of sporozoites found in both the developing midgut oocysts and in the salivary glands at 10 and 16 days pbf, respectively (**Figure 4.6**). No staining with the α-*Pfc*43 antibody was observed in *in vitro* cultured ABS or blood stage gametocytes, suggesting that *de novo* expression of the protein starts after gamete fertilisation.

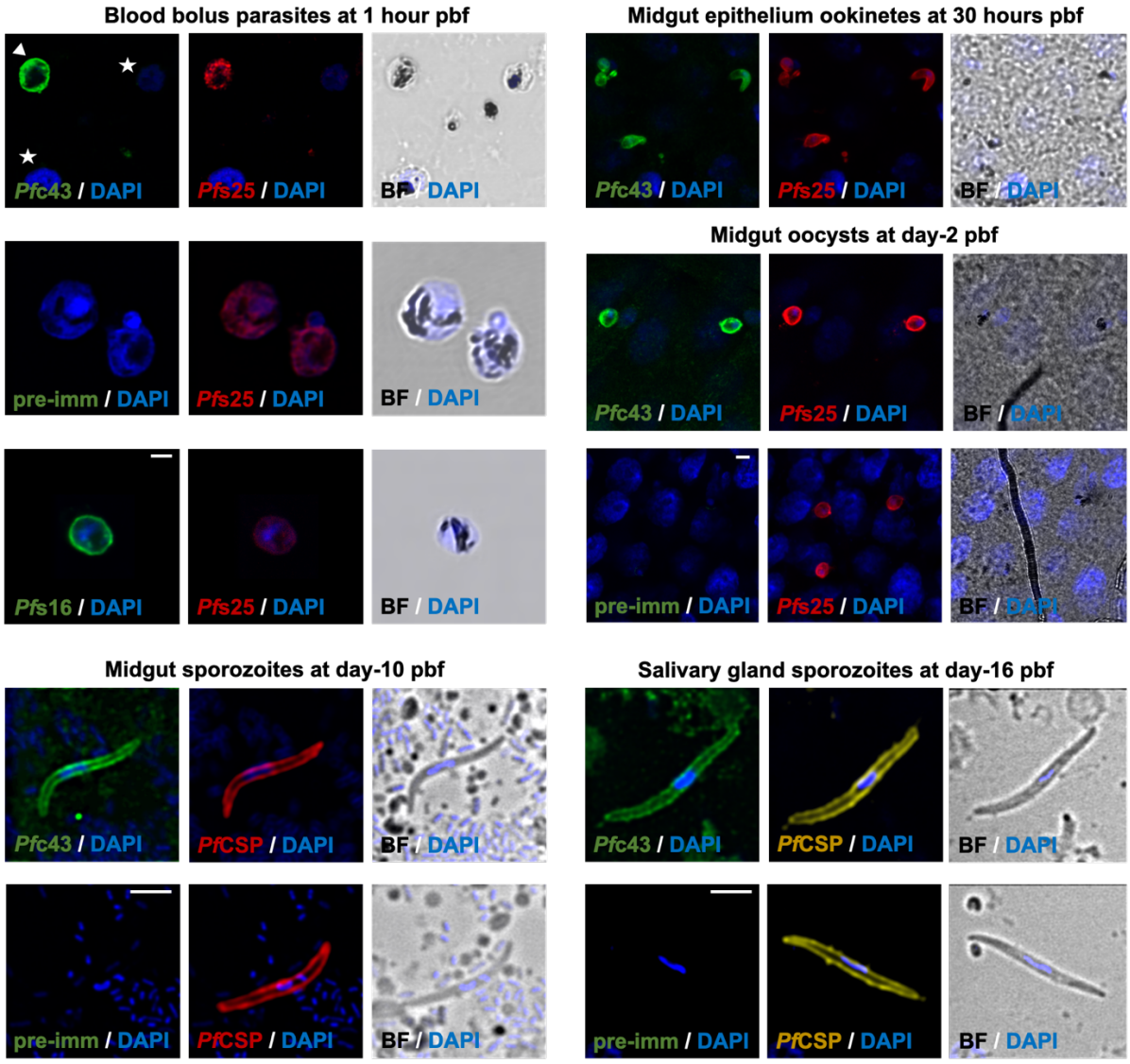

Figure 4.6. *P. falciparum c43* sub-cellular localisation. Immunofluorescence assays of activated gametocytes or zygotes (arrowhead) and rings (asterisks) found in the blood bolus of *A. coluzzii* mosquitoes at 1 hour pbf, ookinetes while traversing the mosquito midgut epithelium at 30 hours pbf, early-oocysts in the midgut wall at day-2 pbf, and midgut and salivary gland sporozoites at day-10 and day-16 pbf, respectively. Parasites were stained with the a-*Pfc*43 antibody and the female gamete/zygote and ookinete a-*Pfs*25 (red) or sporozoite a-*Pf*CSP (red; yellow) antibodies, whereas staining against the gametocyte specific protein *Pfs*16 was used to confirm parasite integrity. Staining with pre-immune serum was used as a negative control. DNA was stained with DAPI. Images were taken from confocal sections of fixed parasites and midguts, at X630 magnification BF is bright field. Scale bars length correspond to 5 µm. Data have been previously reported in (Ukegbu *et al.*, 2020).

4.2.2.4 Investigation of a conserved function between *Pb*c43 and *Pf*c43

Next, we investigated whether the *P. falciparum* orthologue of c43 can complement the function of its *P. berghei* orthologue suggesting a conserved function of this protein. To do so, naïve *A. coluzzii* mosquitoes were infected with the *Pb(Pfc43)* parasite line prior to midgut oocyst count. Infections with *c507* (WT) and *Δc43* parasites served as positive and negative controls, respectively. The results showed that the *Pb(Pfc43)* line exhibited an intermediate phenotype compared to *c507* (WT) and *Δc43* parasites, in both infection prevalence and intensity (*Pb(Pfc43)* median: 1.0, *Pb(Pfc43)* prevalence: 62.22%; *Δc43* median: 0.0, *Δc43* prevalence: 0.0%; *c507* (WT) median: 15.0, *c507* (WT) prevalence: 85.71%) (**Figure 4.7, A; Table 4.2**). Compared to the *c507* (WT) oocysts, *Pb(Pfc43)* oocysts looked morphologically variable and smaller in size, however this was not further measured and formally analysed. In fact, their morphology was more similar to the *Δc43* oocysts formed in the midguts of *LRIM1*-silenced *A. coluzzii* (Ukegbu *et al.,* 2020). Going a step further, the number of midgut oocyst sporozoites were counted following 15 days pbf. The number of *Pb(Pfc43)* sporozoites (320.00 ± 31.00) produced was very small compared to the WT (2,430.00 ± 444.50), but was significantly higher (p=0.0319) when compared to the *Δc43* line (0.00 ± 0.00) (**Figure 4.7, B; Table 4.3**).

Whether the defective phenotype of the *Pb(Pfc43)* parasite line could be rescued upon *LRIM1*-silencing was then assessed. Indeed, the number of *Pb(Pfc43)* oocysts produced in *LRIM1*-silenced (median: 6.5) mosquitoes was significanty higher (p=0.0004) compared to the number of oocysts produced in the ds*LacZ*-injected mosquitoes (median: 1.0) (**Figure 4.7, C; Table 4.4**), yet oocysts remained small and morphologically variable. Similarly, the number of oocyst sporozoites produced in the midgut of the complement-silenced mosquitoes was 3-fold higher compared to the number produced in the control mosquitoes but still significantly smaller (p=0.0005) compared to the WT sporozoites produced in the mosquitoes of the same immune background (**Figure 4.7, D; Table 4.5**). All these results suggest that *Pf*c43 can only partially complement the function of its *P. berghei* orthologue.

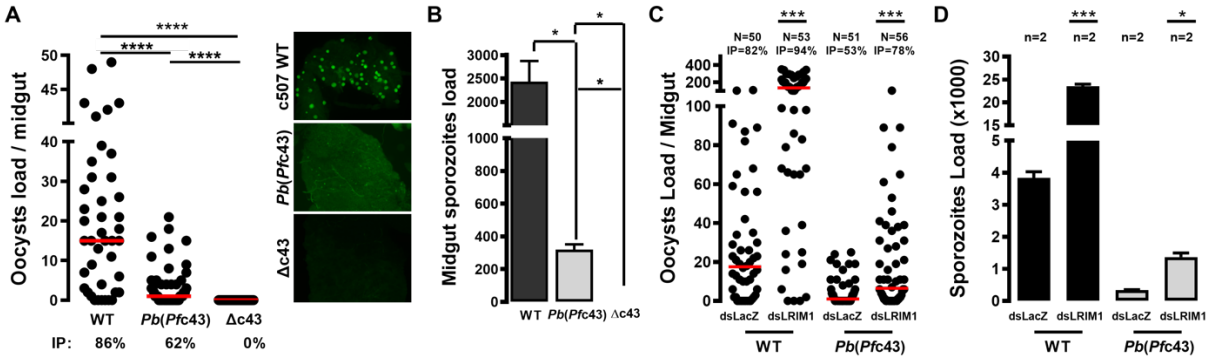

Figure 4.7. Phenotypic analysis of *P. berghei Pb(Pfc43)* parasites in *A. coluzzii*. **(A)** Oocyst density in naïve *A. coluzzii* mosquitoes infected with the *Pb(Pfc43)* transgenic line. The *c507* (WT) and *Δc43* parasites served as controls. Red horizontal lines indicate median, whereas infection prevalence (IP) corresponds to the percentage of midguts that were infected with at least one oocyst. Representative fluorescent images of the oocyst density in the midguts of naïve *A. coluzzii* mosquitoes infected with the *Pb(Pfc43)*, *c507* (WT) and *Δc43* parasite lines, at day-7 pbf. Statistical significance of the oocyst load was determined using the Mann Whitney U-test. Although these experiments have been previously performed by Dr. Valerie Ukegbu and are reported in (Ukegbu *et al.*, 2020), they were repeated by myself to confirm the phenotype observed. **(B)** Midgut sporozoite load in naïve *Pb(Pfc43)*-infected *A. coluzzii* mosquitoes as determined at day-15 pbf. Infection with the *c507* (WT) and *Δc43* parasites lines served as control. For each replicate, sporozoite numbers were determined from two batches of 25 homogenised midguts using light microscopy. Statistical significance was determined using a two-tailed, unpaired Student's *t*-test. Error bars show standard error from the mean. **(C)** Oocyst density in ds*LacZ*-injected and *LRIM1*-silenced *A. coluzzii* mosquitoes infected with the *Pb(Pfc43)* transgenic line. Infection with the *c507* (WT) parasite line served as a control to assess the knockdown efficiency. Red horizontal lines indicate median whereas, N corresponds to the number of midguts collected and IP, to infection prevalence. Representative fluorescent images of the oocyst density in the midguts of ds*LacZ*-injected and complement-silenced *A. coluzzii* mosquitoes infected with the *Pb(Pfc43)* and *c507* (WT) parasite lines, at day-7 pbf. Statistical significance was carried out using the Mann Whitney U-test. The first replicate of this set of experiments has been previously reported in (Ukegbu *et al.*, 2020), however, it was afterwards repeated in order to increase the data robustness. **(D)** Midgut sporozoite load in ds*LacZ*-injected and *LRIM1*-silenced *Pb(Pfc43)*-infected *A. coluzzii* mosquitoes as

determined at day-15 pbf. Infection with the *c507* (WT) parasites line served as a control. For each replicate, sporozoite numbers were determined from two batches of 25 homogenised midguts using light microscopy. Error bars show standard error from the mean, where n corresponds to the number of replicates performed. All data derived from two individual biological replicates. Statistical significance was determined using a two-tailed, unpaired Student's *t*-test.

Table 4.2. *P. berghei Pb(Pfc43)*, *Δc43* and control ANKA *c507* (WT) oocyst load in naive *A. coluzzii* infections, at day-7 pbf

Parasite line	Number of experiments	Number of midguts	Prevalence (%)	*p*-value[1]	p-value[2]	Infection Intensity				
						Arithmetic mean	Median	Parasite range	*p*-value[1]	*p*-value[2]
c507 (WT)	2	42 (36/6)	85.71			18.40	15.00	0-49		
Pb(Pfc43)	2	45 (28/27)	62.22	0.0005		3.78	1.00	0-21	<0.0001	
Δc43	2	35 (0/35)	0.00	<0.0001	<0.0001	0.00	0.00	0-0	<0.0001	<0.0001

Pb(Pfc43), *Δc43* and control ANKA *c507* (WT) infections of naive *A. gambiae* mosquitoes was assessed 7 days pbf. Number of midguts is shown as the ratio between the number of infected midguts to the number of uninfected midguts. Statistical significance of the oocyst load was determined using the Mann Whitney U-test. Statistical significance of the prevalence percentages was assessed by Fisher's exact test (ns, non-significant). *P*-value[1] corresponds to the statistical significance between the WT and transgenic parasites lines, whereas *p*-value[2] corresponds to the statitistical analysis between the *Pb(Pfc43)* and *Δc43* parasites. Although these experiments have been previously performed by Dr. Valerie Ukegbu and are reported in (Ukegbu *et al.*, 2020), they were repeated by myself to confirm the phenotype observed.

Table 4.3. Midgut sporozoite numbers of the *P. berghei Pb(Pfc43)*, *Δc43* and control ANKA *c507* (WT) parasite lines in naive *A. coluzzii* mosquitoes at day-15 pbf

Parasite line	Number of experiments	Mean	Range	SEM	*p*-value[1]	*p*-value[2]
c507 (WT)	2	2,430.00	1,985.00-2,874.00	444.5		
Pb(Pfc43)	2	320.00	289.00-351.00	31.00	0.0418	
Δc43	2	0.00	0.00-0.00	0.00	0.0319	0.0467

The table reports the midgut (oocyst) sporozoite numbers of the *Pb(Pfc43)*, *Δc43* or ANKA *c507* (WT) parasite lines, from two biological replicates of naive *A. coluzzii* infections. For each replicate, sporozoite numbers were determined from two batches of 25 homogenised midguts, at day-15 post infection. SEM represents the standard error from the mean. *P*-value[1] corresponds to the statistical significance between the WT and transgenic parasites lines, whereas *p*-value[2] corresponds to the statitistical analysis between the *Pb(Pfc43)* and *Δc43* parasites.

Table 4.4. Effect of *LRIM1*-silencing on *P. berghei Pb(Pfc43)* and control ANKA *c507* (WT) infections in *A. coluzzii* mosquitoes

Parasite line	dsRNA	Number of exp.	Midguts number	Prevalence (%)	*p*-value	Infection Intensity		Parasite range	Fold Change	*p*-value
						Arithmetic mean	Median			
c507 (WT)	*LacZ*	2	50 (41/9)	82.00		27.40	17.50	0-109		
	LRIM1		53 (50/3)	94.33	0.0673	145.80	135.00	0-350	7.71	<0.0001
Pb(Pfc43)	*LacZ*	2	51 (27/24)	52.94		4.82	1.00	0-25		
	LRIM1		53 (43/13)	76.79	0.01442	19.46	6.50	0-102	6.50	0.0007

P. berghei Pb(Pfc43) and WT parasite infections of *LRIM1*-silenced *A. coluzzii* mosquitoes was assessed at day-7 pbf. Infection of ds*LacZ*-injected mosquitoes were used as control. Number of midguts is shown as the ratio between the number of infected midguts to the number of uninfected midguts. Data derived from two individual biological replicates as indicated in the third column. Statistical significance for the median oocyst load was determined using the Mann Whitney U-test, whereas statistical significance of the prevalence percentages was assessed by Fisher's exact test (ns, non-significant). The first replicate of this set of experiments has been previously reported in (Ukegbu *et al.*, 2020), however, it was afterwards repeated in order to increase the data robustness.

Table 4.5. Midgut sporozoite numbers of *P. berghei Pb(Pfc43)* and control ANKA *c507* (WT) in ds*LacZ* (control) and ds*LRIM1*-injected *A. coluzzii* mosquitoes

Parasite line	dsRNA	Number of experiments	Mean	Range	SEM	*p*-value[1]	*p*-value[2]
c507 (WT)	*LacZ*	2	13,836.00	13,638.00-14,034.00	198.00		
	LRIM1		23,504.00	23,013.60-23,995.20	490.80	0.0007	
Pb(Pfc43)	*LacZ*	2	346.85	337.48-356.23	9.37		0.0032
	LRIM1		456.41	443.68-469.13	12.72	0.0145	0.0005

The table reports *Pb(Pfc43)* or ANKA *c507* (WT) midgut (oocyst) sporozoite numbers from two biological replicates of ds*LacZ*-injected and *LRIM1*-silenced *A. coluzzii* infections. For each replicate, sporozoite numbers were determined from two batches of 25 homogenised midguts, at day-15 post infection. SEM represents the standard error from the mean. *P*-value[1] corresponds to the statistical significance between the parasite load in *dsLacZ*-injected and *LRIM1*-silenced mosquitoes for each line, whereas *p*-value[2] corresponds to the statitistical analysis between the WT and *Pb(Pfc43)* parasites in mosquitoes of the same immune background.

4.2.2.5 Antibody-mediated transmission-blocking assays

c43 seems to have an important role during *Plasmodium* development in the mosquito vector, both in protecting parasites from the robust attacks of the mosquito immune system and in fascilitating sporozoite production in the midgut oocysts. Therefore, we sought to examine whether targeting *P. berghei* and *P. falciparum* c43, using antibodies generated against each of the respective orthologous proteins, could reduce parasite infectivity and malaria transmission potential.

The transmission blocking efficacy of α-*Pbc*43 antibodies against *P. berghei* parasites was tested following addition of multiple concentrations of α-*Pbc*43 antibody to blood drawn from infected mice and mosquito blood feeding via an optimised SMFA. The antibody used was raised against a 301 amino acid (amino acids 22-331, -SP/TM) protein fragment of the native *Pbc43* gene sequence, previously expressed in Sf9 insect cells. UPC10 antibodies (purified IgG2a from murine myeloma, clone UPC10) (Blagborough *et al*., 2009) at concentrations of 50, 100 and 250 µg/mL were used as a negative control and to compare the transmission inhibition activity of the a-*Pbc*43 antibody. Mosquitoes treated with the a-*Pbc*43 antibody displayed a median oocyst intensity of 11.5, 6.0 and 6.0 compared to those treated with UPC10 antibodies, where the median infection intensity was 18.5, 21.0 and 17.0 at 50, 100 and 250 µg/mL antibody concentrations, respectively (**Figure 4.8, A; Table 4.6**). At 100 µg/mL, the inhibition of oocyst intensity was 72.7% and the inhibition of infection prevalence was 35.5%, whereas these values increased to 90.3% and 65.6% at 250 µg/mL, respectively, suggesting a concentration-dependent transmission blocking activity.

The transmission blocking efficacy of α-*Pfc*43 antibodies against *P. falciparum* malaria was examined via an optimised SMFA, where purified IgG antibodies were added to the *in vitro* cultured gametocytaemic blood at final concentrations of 0, 50, 125 and 250 µg/mL prior to mosquitoes blood feeding (Habtewold *et al.*, 2019). Following oocyst count at day-7 pbf, the results revealed a substantial inhibition of both infection intensity and prevalence in an antibody concentration-dependent manner (**Figure 4.8, B; Table 4.7**). At 125 and 250 µg/mL of antibody concentration, the total inhibition in infection intensity determined was 57.1% and 76.2%, whereas the overall inhibition in infection prevalence was 37.3% and 35.6%, respectively.

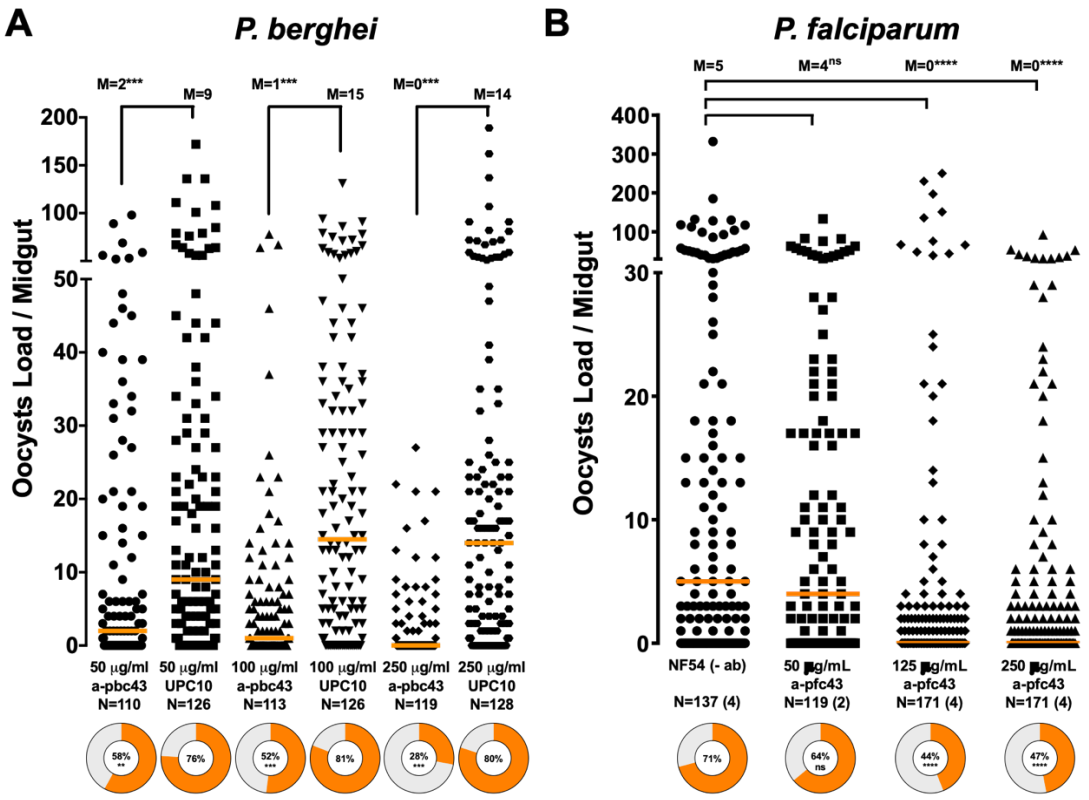

Figure 4.8. Transmission blocking efficacies of anti-c43 antibodies on *P. berghei* (A) and *P. falciparum* (B) infections of *A. coluzzii* mosquitoes, shown as dot plots of oocyst number distribution. The α-*Pbc*43 and α-*Pfc*43 antibodies were provided through SMFAs at concentrations of 50 µg/mL, 100 µg/mL and 250 µg/mL, and 50 µg/mL, 125 µg/mL and 250 µg/mL, respectively, and compared with UPC10 antibodies and no antibodies that were used as negative controls for *P. berghei* and *P. falciparum* respectively. Individual data points represent oocyst numbers from individual mosquitoes at day-7 and day-10 post mosquito blood feeding, respectively. M corresponds to the median oocyst load, also shown in horizontal orange lines. N, number of midguts; ns, not significant. The number of replicates performed for each condition is indicated in the parenthesis next to the number of midguts analysed. The orange area of the pie charts indicates the prevalence of infection. Statistical analysis was performed with the Mann Whitney U-test for infection intensity and Fisher's exact test for infection prevalence. This set of figures has been reported before in (Ukegbu *et al.*, 2020). TBV experiments using the a-*Pbc*43 antibody were performed by Dr. Fiona Angrisano and Dr. Andrew Blagborough. TBV experimental procedures using the a-*Pfc*43 antibody were partially assisted by Dr. Sofia Tapanelli.

It has been shown that targeting different epitopes of a protein can have profound differences in their blocking activity and therefore, can improve the efficacy as vaccine candidates. The identified transmission-blocking epitope may also provide the basis for evaluating the functionality of the targeted protein as well as to scrutinize its action mechanism (Bustamante *et al.*, 2000; Armistead *et al.*, 2014). Therefore, another a-*Pfc*43 peptide antibody (amino acids 372-386), called a-*Pfc*43^{P2}, that specifically targets the region of the *P. falciparum* orthologue gene between the two conserved cysteine residues and the predicted GPI-anchor at the C-terminal region, was raised in order to be assessed for its transmission blocking activity. Prior to the TBV experiments, this antibody was validated for its specificity by performing IFAs. Subsequently, similarly to what was previously performed, multiple concentrations of the antibody were included in infected blood which was later used for SMFA of *A. coluzzii* mosquitoes with *P. falciparum*. Following oocyst count, the results showed that the peptide antibody a-*Pfc*43^{P2} conferred a significant transmission blocking activity ($p=0.0002$ and $p=0.0085$) at the concentration of 125 µg/mL and 250 µg/mL, respectively, similar to what has been previously observed for the full-length antibody. Additionally, a gradual decrease on the infection prevalence was observed at a concentration-dependent manner, however this was not statistically significant for the concentrations of 50 µg/mL and 125 µg/mL, used. Additionally, the infection intensity did not drop following antibody addition (**Appendix 11**). These data suggest that the region of the c43 protein where antibodies bind is not critical to block transmission nor the functionality of the protein.

Table 4.6. Evaluation of the a-*Pb*c43 transmission blocking efficacy in SMFA

Number of experiments	a-*Pb*c43 ab concentrations	Number of midguts	Prevalence (%)	*p*-value	Infection Intensity		Parasite range	*p*-value
					Arithmetic mean	Median		
R1, R2, R3	apbc43 50µg/mL	64/46	58.18		12.05	2.00	0-98	0.0010 (***)
	UPC10 50µg/mL	96/30	76.19	0.0035	21.85	9.00	0-172	
	apbc43 100µg/mL	59/54	52.21		6.25	1.00	0-78	<0.0001 (***)
	UPC10 100µg/mL	102/24	80.95	<0.0001	22.92	14.50	0-131	
	apbc43 250µg/mL	33/86	27.73		2.28	0.00	0-27	<0.0001 (***)
	UPC10 250µg/mL	103/25	80.47	<0.0001	23.67	14.00	0-189	
R1	apbc43 50µg/mL	24/13	64.86		24.27	21.00	0-98	0.0429 (*)
	UPC10 50µg/mL	20/6	76.92	0.4059	46.27	40.00	0-172	
	apbc43 100µg/mL	21/21	50.00		8.59	0.50	0-78	<0.0001 (***)
	UPC10 100µg/mL	33/2	94.29	<0.0001	43.31	42.00	0-131	
	apbc43 250µg/mL	3/29	9.37		0.50	0.00	0-8	<0.0001 (***)
	UPC10 250µg/mL	37/8	82.22	<0.0001	34.40	23.00	0-189	
R2	apbc43 50µg/mL	20/15	57.14		5.11	1.00	0-48	0.0068 (**)
	UPC10 50µg/mL	34/16	68.00	0.3630	19.04	10.50	0-136	
	apbc43 100µg/mL	28/22	56.00		5.08	1.50	0-64	0.0004 (***)
	UPC10 100µg/mL	37/13	74.00	0.0928	17.22	12.00	0-86	
	apbc43 250µg/mL	19/31	38.00		3.48	0.00	0-22	<0.0001 (***)
	UPC10 250µg/mL	34/9	79.07	<0.0001	20.81	9.00	0-162	
R3	apbc43 50µg/mL	20/18	52.63		6.53	2.00	0-40	0.0052 (**)
	UPC10 50µg/mL	42/8	84.00	0.0020	11.96	6.0	0-79	
	apbc43 100µg/mL	10/11	47.61		4.33	0.00	0-23	0.0067 (**)
	UPC10 100µg/mL	32/9	78.05	0.0222	12.46	8.00	0-44	
	apbc43 250µg/mL	11/26	29.73		2.19	0.00	0-27	<0.0001 (***)
	UPC10 250µg/mL	32/8	80.00	<0.0001	14.63	7.00	0-70	

Oocyst data at day-10 post *A. coluzzii* blood feeding from *P. berghei* SMFA's using the α-*Pb*c43 antibody. *P. berghei* SMFA's with UPC10 antibodies served as a control. *P*-values for infection prevalence were calculated using the Fisher's exact test and *P*-values for infection intensities on the basis of the median number of oocysts was calculated using the Mann Whitney U-test. Experimental procedures were performed by F. Angrisano and A. Blagborough and data have been also reported in (Ukegbu *et al.*, 2020).

Table 4.7. Evaluation of the a-*Pfc*43 transmission blocking efficacy in SMFA

a-*Pfc*43 ab concentrations	Number of experiments	Number of midguts	Prevalence (%)	*p*-value	Infection intensity			
					Arithmetic mean	Median	Parasite range	*p*-value
NF54(-)	4	97/40	71.00		22.05	5.00	0-332	
NF54(50µg/µL)	2	76/43	64.00	0.2843	13.73	4.00	0-133	0.2926 (ns)
NF54(125µg/µL)	4	76/95	44.00	<0.0001	9.45	0.00	0-250	<0.0001 (***)
NF54(250µg/µL)	4	78/93	46.00	<0.0001	5.25	0.00	0-92	<0.0001 (***)
NF54(-)	R1	25/3	89.29		71.29	47.00	0-332	
NF54(125µg/µL)		13/15	46.43	0.0013	34.82	0.00	0-230	0.0019 (**)
NF54(250µg/µL)		12/14	46.15	0.0010	8.731	0.00	0-92	<0.0001 (***)
NF54(-)	R2	20/8	68.00		4.56	2.00	0-18	
NF54(125µg/µL)		27/19	52.50	0.3250	2.03	1.00	0-52	0.0586 (ns)
NF54(250µg/µL)		18/22	45.00	0.0468	1.68	0.00	0-45	0.0180 (*)
NF54 (-)	R4	22/18	55.00		7.27	2.00	0-53	
NF54 (50µg/µl)		44/32	57.89	0.8444	11.64	2.00	0-133	0.5938 (ns)
NF54 (125µg/µL)		22/27	44.89	0.3974	10.00	0.00	0-250	0.2272 (ns)
NF54 (250µg/µL)		21/37	36.21	0.0971	4.57	0.00	0-53	0.0698 (ns)
NF54(-)	R5	33/11	75.00		14.09	6.50	0-58	
NF54(50µg/µL)		32/11	74.00	1.0000	17.42	9.00	0-83	0.5907 (ns)
NF54(125µg/µL)		20/34	37.00	0.0002	1.31	0.00	0-21	<0.0001 (***)
NF54(250µg/µL)		27/20	57.00	0.1207	7.19	1.00	0-42	0.0190 (*)

Oocyst data at day-7 post *A. coluzzii* mosquitoes blood feeding from *P. falciparum* SMFAs using the α-*Pfc*43 antibody. *P*-values for infection prevalence were calculated using the Fisher's exact test, whereas *P*-values for infection intensities on the basis of the median number of oocysts was calculated using the Mann Whitney U-test. Experimental procedures were assisted by Dr. Sofia Tapanelli and data have been also reported in (Ukegbu *et al.*, 2020).

4.2.3 Phenotypic and functional characterisation of P47

4.2.3.1 *P. berghei* P47 protein expression and sub-cellular localisation

A rabbit polyclonal antibody against the *P. berghei* P47 coding region lacking the signal peptide and the C-terminal hydrophobic domain (amino acids 30–412) was raised for western blot and immunofluorescence assays. In these assays, the ANKA *c507 P. berghei* line that constitutively expresses *GFP* but is otherwise WT (Janse *et al.*, 2006a) and the *ΔP47* line whose the endogenous *P47* gene has been deleted and also expresses *GFP* throughout the parasite lifecycle (van Dijk *et al.*, 2010) were used. The results showed that the P47 protein can be detected, in almost equal abundance, in non-activated and activated female gametocytes and *in vitro* cultured ookinetes of the WT parasite line, whereas it was absent from gametocytes and ookinetes of the mutant KO parasite line (**Figure 4.9, A**) (Ukegbu *et al*., 2017b). To further investigate its sub-cellular localisation, membrane fractionations were conducted using purified WT and *ΔP47 in vitro* gametocyte samples. Localisation experiments in purified *in vitro* ookinetes were not performed, due to the severely affected capacity for fertilisation of the *ΔP47* line (van Dijk *et al.*, 2010). Samples collected as previously described, were subjected to western blot analysis. The results showed that P47 was not present in the cytosolic fraction released after ookinete hypotonic lysis but was detected in the Triton X-100 fraction, where membrane-bound proteins are expected to be located. Under both non-reducing and reducing conditions P47 appears as a monomer (~40kDa) **(Figure 4.9, B)**. These data reveal that P47 is a membrane-bound protein, also supported by the predicted GPI-anchor.

The same antibody was used to further investigate the sub-cellular localisation of P47 in *in vivo* and *in vitro P. berghei* parasites. In immunofluorescence assays, P47 was found to be localised on the surface of *in vitro* female activated gametocytes and of ookinetes in the blood bolus of *A. coluzzii* mosquitoes at 17-18 hours after mosquito blood feeding (**Figure 4.9, C**). Additionally, the distribution of the protein was very similar to that of the female gamete and ookinete surface protein, P28 (Sidén-Kiamos *et al.*, 2000). A similar surface distribution was detected in ookinetes while traversing the mosquito midgut epithelium at 24 hours pbf (**Figure 4.9, C**). Therefore, *P. berghei* P47 is located on the surface of both gametocytes and ookinetes (Ukegbu *et al*., 2017b). No difference between permeabilised and non-permeabilised *in vitro* ookinetes and gametocytes was observed, further supporting the previous findings that P47 is exclusively found on the parasite surface.

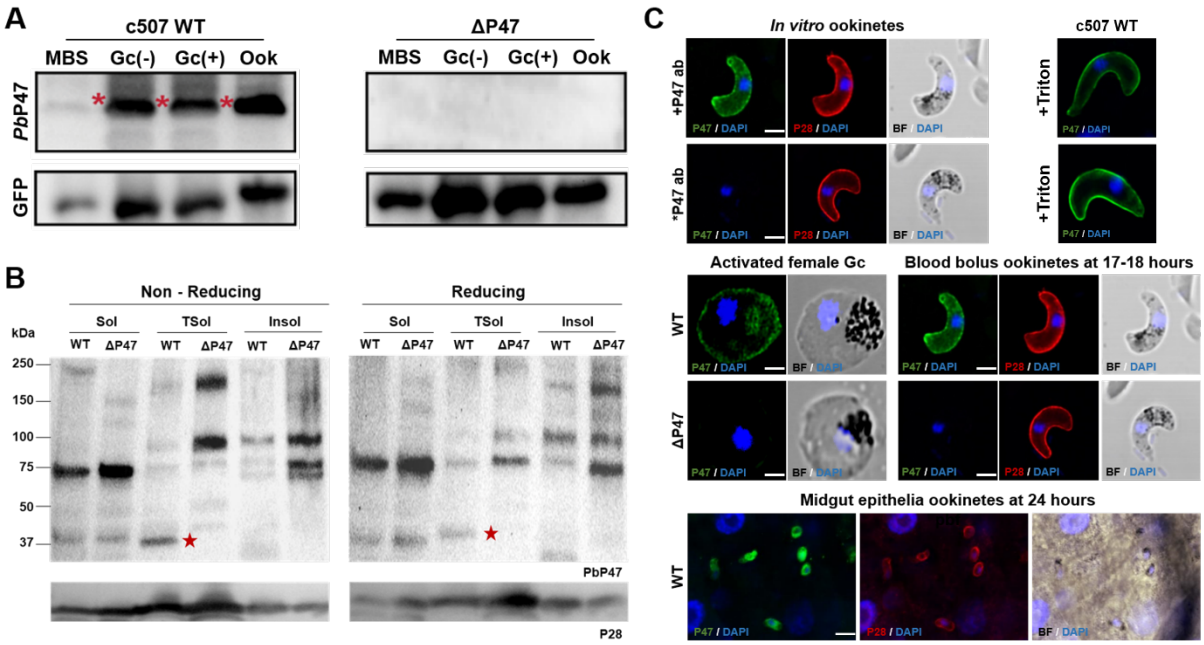

Figure 4.9. Expression analysis of the *P. berghei* P47 protein. (A) Western blot analysis of protein extracts of ANKA *c507* (WT) and *ΔP47* parasites using the *Pb*P47 and GFP (loading control) antibodies. P47 monomers (˜40kDa) are indicated with red asterisks. MBS, purified mixed blood stages; Gc (−), non-activated gametocytes; Gc (+), activated gametocytes; Ook, *in vitro* produced ookinetes following 24 hours of activation. The experiment was carried out by Dr. Valerie Ukegbu, whereas the figure was adapted from (Ukegbu *et al.*, 2017b). **(B)** Western blot analysis of *P. berghei in vitro* gametocyte fractionation protein samples under reducing and non-reducing conditions. Red asterisks indicate P47 monomers (~40kDa) under both non-reducing and reducing conditions. *ΔP47* gametocyte protein extracts were used as control for non-specific signal. Antibody against the female gametocytes P28 surface protein was also used as stage-specific control and also to assess the purity of the samples. **(C)** Immunofluorescence assays of WT *in vitro* ookinetes (top panel), WT and *ΔP47* activated female gametocytes (middle left panel) and ookinetes in the blood bolus of *A. coluzzii* mosquitoes at 17-18 hours pbf (middle right panel) and WT ookinetes while traversing the mosquito midgut epithelium at 24 hours pbf (bottom panel). Parasites were stained with the a-P47 (green) and a-P28 (red) antibodies. DNA was stained with DAPI. BF is bright field. The *ΔP47* parasite line was used as a negative control for gametocyte and blood bolus ookinete imaging, and non-primary antibody staining was used as a control for *in vitro* produced ookinetes (-P47 ab). Images were taken from confocal sections of fixed parasites and midguts at X630 magnification. Scale bar is 5 µm for the *in vitro* ookinetes, activated female gametocytes and blood bolus ookinetes,

whereas for invading ookinetes through the mosquito midgut epithelium the scalebar is 20 µm. The activated female gametocyte immunofluorescence assay was performed by Dr. Valerie Ukegbu, whereas the presented data have been previously reported in (Ukegbu *et al.* 2017b).

4.2.3.2 Effect of P47 deletion on *P. berghei* midgut infection establishment

The expression of *P47* during the sexual stages of the parasite indicates a potential function of the protein during either the developmental transition of gametocytes into ookinetes or during the ookinetes journey through the midgut epithelium. In order to assess the essentiality of the gene at these stages, the *ΔP47* line that constitutively expresses *GFP* (van Dijk *et al.*, 2010) was used to infect *A. coluzzii* mosquitoes prior to oocysts enumeration. At the same time, infection of complement silenced mosquitoes as well as of ds*LacZ*-injected control mosquitoes was carried out.

The results showed that the median infection intensity of the *ΔP47* line in the three sets of naïve *A. coluzzii* mosquito infections was 0.00, whereas only 19% of the midguts were found to be infected with at least one oocyst (**Figure 4.10, A**). Similar results were obtained in ds*LacZ*-injected (control) mosquitoes, confirming that this is not an effect of injury that is known to activate mosquito immunity (Nsango *et al.*, 2013). Only 8% and 16% of the midguts assessed harboured any oocysts. However, when *LRIM1* or *TEP1* were silenced, a large number of morphologically normal *ΔP47* oocysts were observed with median intensities of 22.0 and 36.5, respectively. The infection prevalence also increased from 8% and 16% in ds*LacZ*-injected controls to 96% in *LRIM1* and 89% in *TEP1*-knockdown mosquitoes, respectively. Parallel infections with the parental WT *P. berghei* line were also carried out as control to the gene silencing experiments. The results showed median infection intensities of 200.0 (92% infection prevalence) in *LRIM1*- and 397.0 (100% infection prevalence) in *TEP1*-silenced mosquitoes. Ds*LacZ*-injected controls showed median infection intensities of 13.0 (87% infection prevalence) and 26.0 (85% infection prevalence), respectively (**Figure 4.10, B; Table 4.8**). These data suggest that *P. berghei* P47 seems to be important for parasites to survive the robust immune responses, agreeing with what was previously shown for its *P. falciparum* orthologue (Molina-Cruz *et al.*, 2013).

Additionally, midgut and salivary gland sporozoite quantification was carried out in ds*LacZ*-injected and *LRIM1*-silenced *A. coluzzii* mosquitoes at day-15 and day-21 post mosquito blood feeding, respectively. The results revealed a very small number of

ΔP47 sporozoites in the midguts of ds*LacZ*-injected control mosquitoes, which dropped down to zero levels later in the salivary glands. However, approximately 100-fold increase in *ΔP47* sporozoite numbers was recorded in the midguts of *LRIM1* knockdown mosquitoes at day-15 pbf, where about half of these reached the salivary glands at day-21 post infection. Only *ΔP47* sporozoites from *LRIM1*-silenced *A. coluzzii* mosquitoes could be readily transmitted to all mice during bite back experiments, whereas none of the mice used to blood feed ds*LacZ*-injected *ΔP47* infected mosquitoes produced ABS parasites (Ukegbu *et al.*, 2017b).

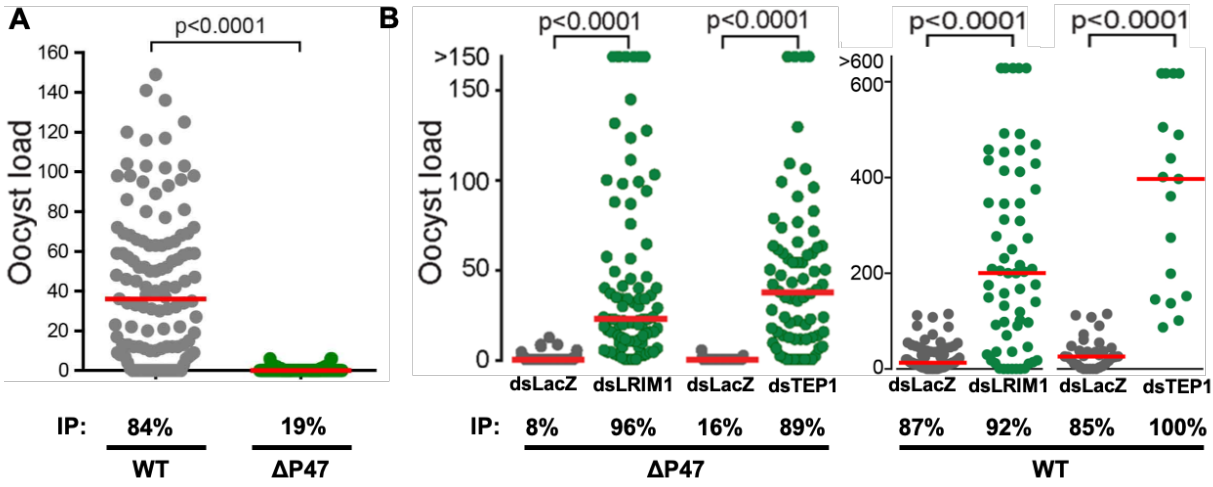

Figure 4.10. Phenotypic analysis of the *P. berghei ΔP47* parasite line in *A. coluzzii* mosquito infections. *ΔP47* oocyst load in the midguts of naïve **(A)**, *dsLacZ*-injected and *LRIM1*-silences **(B)** *A. coluzzii* mosquitoes at day-8 pbf. The median number of oocysts of three individual biological replicates is shown with a red line. The infection prevalence (IP; percentage of midguts harbouring at least one oocyst) is shown. Statistical significance was determined with the Mann Whitney U-test. Experimental procedures were performed by Dr. Valerie Ukegbu, Dr. Chrysanthi Taxiarchi and myself, whereas figure was adapted from (Ukegbu *et al.*, 2017b).

4.2.3.3 Monitoring the developmental progress of *P. berghei ΔP47* ookinetes

As previously suggested, mutant KO parasites are possibly eliminated by reactions of the complement-like system taking place at the basal side of the midgut epithelium that directly interacts with the haemolymph components. To better monitor the developmental progress of *ΔP47* ookinetes being formed in the midgut lumen, successful invasion and traversal through the mosquito midgut epithelium was investigated prior to examination of their potential to establish midgut infection.

A. coluzzii midguts infected with the *P. berghei ΔP47* or control ANKA *c507* (WT) parasite lines were dissected at 25 hours pbf in order to be later stained against the parasite ookinete surface protein, P28. The aim of this experiment was to confirm that *ΔP47* ookinetes developing in the mosquito midgut lumen are able to invade the midgut epithelium. Indeed, a large number of P28-positive *ΔP47* ookinetes were detected (**Figure 4.11, A; Table 4.9**), however the median number determined was 1.94-fold lower compared to the WT control. GFP imaging of the ookinetes - since the transgenic line constitutively expresses *GFP* - revealed that most of the *ΔP47* mutant ookinetes, previously found to be positive for P28, were GFP-negative. More importantly, the ratio of dead ookinetes (GFP-/P28+) against the total number of invading ookinetes (GFP-/P28+ and GFP+/P28+) for *ΔP47* parasites was empirically higher when compared to the WT (**Figure 4.11, B**). It has been previously shown that GFP fluorescence is rapidly depleted in dead ookinetes but continue to express P28 (Blandin *et al.*, 2004). Hence these results confirm that *ΔP47* ookinetes successfully invade the mosquito midgut epithelium but are killed upon traversal.

Going a step further, to investigate whether *ΔP47* ookinetes are killed during or immediately after midgut epithelium traversal, ds*CTL4*- and ds*LacZ*-injected (control) mosquitoes were infected with the *ΔP47* or WT parasites. *CTL4*-silencing results in an increased ookinete melanisation activity, immediately after ookinetes traverse the mosquito midgut epithelium (Osta *et al.*, 2004a) (**Figure 4.11, C; Table 4.10**).

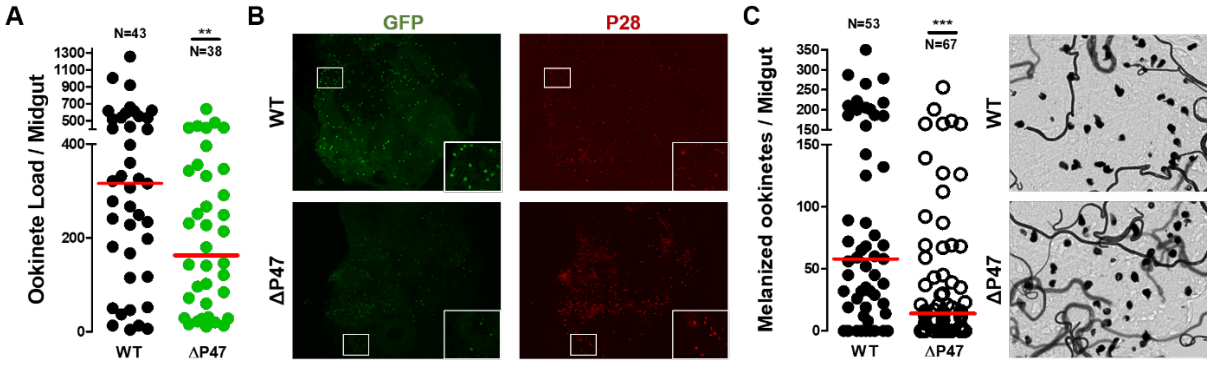

Figure 4.11. *ΔP47* ookinete development through *A. coluzzii* midgut epithelium. **(A)** Load of *ΔP47* invaded ookinetes in the midguts of *A. coluzzii* mosquitoes, at 25 hours pbf. Red lines show the median ookinete load, where N is the total number of midguts used for counting out of three individual infections. Statistical significance was determined using the Mann Whitney U-test. These data have been previously reported in (Ukegbu *et al.*, 2017b). **(B)** Fluorescence microscopy of *ΔP47* and ANKA *c507* (WT)

ookinetes stained with P28 antibody in the *A. coluzzii* midgut epithelium 25 hours pbf. Images are taken at 100x magnification. **(C)** Load of melanised *ΔP47* and ANKA *c507* (WT) ookinetes in the midguts of *CTL4*-silenced mosquitoes. Red lines show the median ookinete load, where N is the total number of midguts collected from three individual replicates. Light microscopy images (100x magnification) of melanised parasites in *CTL4*-silenced *A. coluzzii* mosquito midguts. Although these data have been previously collected by C. Taxiarchi and reported in (Ukegbu *et al.*, 2017b), I had to repeat the experiment in order to validate the observed phenotype.

The next question asked was whether the development of the *ΔP47* parasites stops due to developmental impairments at the very early oocyst stage or due to reactions provoked by haemolymph-derived complement factors immediately after midgut traversal. To decipher which of the above hypotheses is valid, the infection intensity of *ΔP47* and ANKA *c507* (WT) infected *A. coluzzii* mosquitoes was closely monitored from 24 hours pbf, a time that coincides with ookinete traversal of the mosquito midgut epithelium, to 5 days pbf, when mid-mature oocysts are presented on the basal lamina of the midgut wall. The median numbers of WT and *ΔP47* invading ookinetes in *A. coluzzii* infected midguts dissected at 24 hours pbf were 316 and 180, respectively. The median oocyst intensity determined in midguts dissected at day-3 pbf were 112 and 0, respectively, whereas the analogous data for midguts dissected at day-5 pbf were 60.5 and 0.0, respectively (**Figure 4.12**). These results indicate that *ΔP47* parasites are indeed killed due to reactions of the complement-like system.

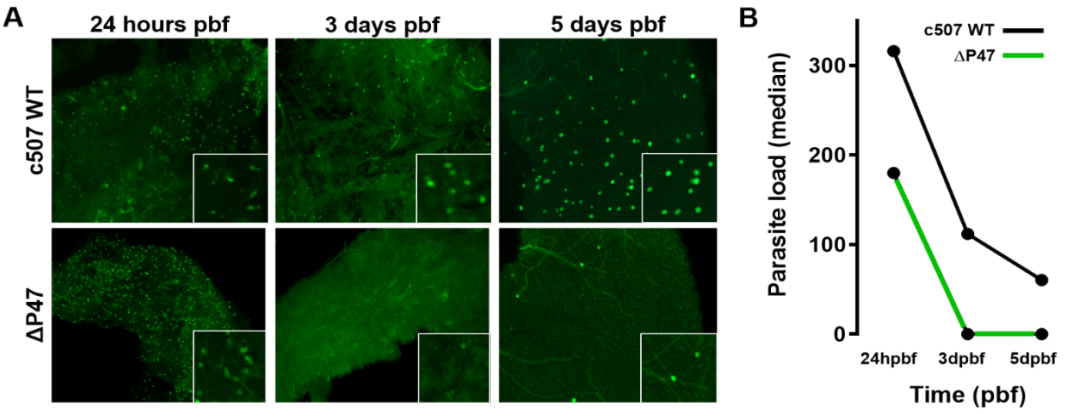

Figure 4.12. *ΔP47* parasite load in *A. coluzzii* midgut epithelia. (A) Fluorescence images of *ΔP47* (green line) and WT (black line) ookinetes and oocysts in the midguts of *A. coluzzii* midgut epithelia at 24 hours, 3 days and 5 days pbf. Both parasite lines constitutively express *GFP*. Images are representative of two sets of experiments and were taken at X100 magnification. **(B)** *ΔP47* and WT parasite loads after infection of

A. coluzzii at 24 hours (ookinetes), day-3 and day-5 (oocysts) pbf. The median value of the pooled data from two replicates was used for each presented condition.

To investigate whether the mechanism responsible for the elimination of the *ΔP47* parasites is the complement pathway, midgut epithelia of naïve mosquitoes infected with *ΔP47* or WT control parasites were dissected at 28–30 hours pbf and stained against the parasite surface protein P28 and the mosquito complement molecule TEP1. Whilst P28 is found in all ookinetes, TEP1 marks ookinetes that are either dead or in the process of being killed (Blandin *et al.*, 2004). From four independent biological replicates, a total of 6,476 (29 midguts) and 22,895 (37 midguts) *ΔP47* and WT ookinetes, respectively, were analysed. The results revealed that the fraction of TEP1-stained *ΔP47* ookinetes (91.8% ± 4.4%) was significantly higher ($p<0.0001$) than the fraction of TEP1-stained WT ookinetes (77.8% ± 8.4%) **(Figure 4.13; Table 4.11**). These data indicate that either the lack of P47 leads to an exaggerated TEP1-binding on the ookinete surface thus leading to their killing, or that *ΔP47* ookinetes are defective and undergo cell death thus attracting TEP1 molecules on their surface.

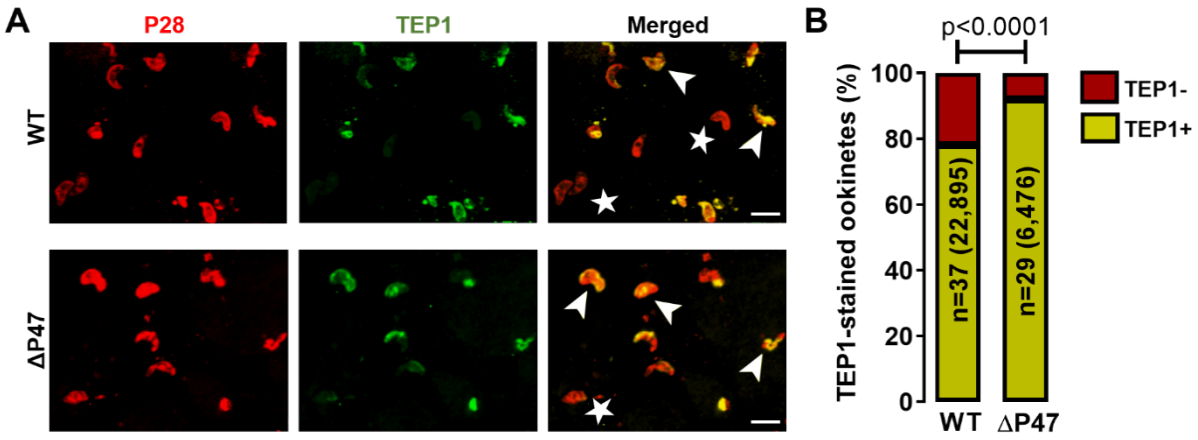

Figure 4.13. TEP1-mediated killing of *P. berghei ΔP47* ookinetes. (A) *ΔP47* and *c507* (WT) ookinetes in *A. coluzzii* midgut epithelia at 28-30 hours pbf stained with a-TEP1 (red) and a-P28 (green) antibodies. Ookinetes stained for both TEP1 and P28 (arrowheads) indicates that are either dead or marked for killing, while P28 single stained ookinetes (asterisks) are considered to be alive. Images were taken at X400 magnification. Scale bar is 20 µm. **(B)** Percentage of *ΔP47* and *c507* (WT) ookinetes stained for both TEP1 and P28 (yellow) or stained for P28 only (green), where n represents the total number of midguts analysed in four biological replicates with the total number of ookinetes examined for each parasite line in the parenthesis. A subset of these data has been previously reported in (Ukegbu *et al.*, 2017b).

Table 4.8. Effect of *LRIM1*-silencing on *ΔP47* infections in *A. coluzzii* mosquitoes

Parasite line	dsRNA	Number of exp.	Midguts number	Prevalence (%)	*p*-value	Infection Intensity		Parasite range	Fold Change	*p*-value
						Arithmetic mean	Median			
ΔP47	*LacZ*	4	131 (21/110)	16.03		0.52	0.0	0-12		
	LRIM1		91 (86/5)	94.50	<0.0001	49.50	22.0	0-505	22.0	<0.0001
ΔP47	*LacZ*	3	95 (8/87)	8.42		0.14	0.0	0-5		
	TEP1		74 (66/8)	89.19	0.0364	46.60	36.5	0-261	36.5	<0.0001
c507 (WT)	*LacZ*	4	81 (71/11)	87.65		23.70	13.0	0-115		
	LRIM1		62 (57/5)	91.94	0.4241	238.10	200.0	0-900	15.4	<0.0001
c507 (WT)	*LacZ*	2	33 (28/5)	84.85		33.70	26.0	0-115		
	TEP1		17 (17/0)	100	0.1520	397.50	397.0	87-910	15.3	<0.0001

ΔP47 and control WT parasite infections of *LRIM1*-silenced *A. coluzzii* mosquitoes was assessed at day-10 pbf. Infection of ds*LacZ*-injected mosquitoes was used as control. Number of midguts is shown as the ratio between the number of infected midguts to the number of uninfected midguts. Statistical significance was determined using the Mann Whitney U-test, whereas statistical significance of the prevalence percentages was assessed by Fisher's exact test (ns, non-significant). Experimental procedures were performed by Dr. Valerie Ukegbu, Dr. Chrysanthi Taxiarchi and myself, whereas table was adapted from (Ukegbu *et al.*, 2017b).

Table 4.9. Number of P28-positive *ΔP47* and control ANKA *c507* (WT) ookinetes in *A. coluzzii* mosquitoes, at 25 hours pbf

Parasite line	Number of experiments	No of midguts	P28+ ookinete range	Infection Intensity		*p*-value	Standard Error	Fold Difference
				Arithmetic mean	Median			
c507 (WT)	3	41	4-1256	354.1	316.0		44.10	
ΔP47	3	38	11-639	202.2	163.0	<0.0001	26.88	1.94

P28-positive ookinetes in the mosquito midgut were enumerated at 25 hours post mosquito blood feeding using fluorescence microscopy. The fold difference was calculated based on the median number of P28-positive KO ookinetes against WT. A subset of these data has been previously reported in (Ukegbu *et al.*, 2017b).

Table 4.10. Melanised *ΔP47* and control ANKA *c507* (WT) ookinetes in *CTL4* knockdown *A. coluzzii* mosquitoes

Parasite line	Number of experiments	No of midguts	Prevalence (%)	Infection Intensity		Ookinete range	*p*-value
				Arithmetic mean	Median		
c507 (WT)	3	53 (44/9)	83.01	90.06	58.0	0-350	
ΔP47	3	67(49/18)	73.13	40.19	14.0	0-256	0.0004

The table shows the number of *ΔP47* and control WT melanised parasites in three independent biological replicates, in the midguts of *CTL4*-silenced *A. coluzzii* mosquitoes, 6 days pbf. The total number of midguts is indicated in the third column, as the ratio between the number of infected midguts to the number of uninfected midguts. Prevalence shows the percentage of midguts with at least one melanised parasite. Midguts with zero parasites were also considered for calculation of the mean and median of the parasite densities. Statistical significance was determined using the Mann Whitney U-test. Although these data have been previously collected by C. Taxiarchi and reported in (Ukegbu *et al.*, 2017b), I had to repeat the experiment in order to validate the observed phenotype.

Table 4.11. Number of TEP1-positive *ΔP47* and control ANKA *c507* (WT) ookinetes in the midguts of *A. coluzzii* mosquitoes

Parasite line	Number of experiments	No of midguts	TEP1+/P28+ ookinetes	TEP1-/P28+ ookinetes	Total No of ookinetes	Ookinete percentage (%)	Standard Error	*p*-value
c507 (WT)	4	37	17,809	5,086	22,895	77.8	8.4	
ΔP47	4	29	5,948	528	6,476	91.8	4.4	<0.0001

TEP1/P28-positive *ΔP47* and WT ookinetes were enumerated at 28-30 hours pbf in the midgut of *A. coluzzii*, using fluorescence microscopy. The ookinete percentage (%) was calculated as the ratio of the TEP1+/P28+ ookinetes to the total number of ookinetes counted (stained for both TEP1+/P28+ and single P28+). Statistical significance was determined with a two-tailed, unpaired Student's *t*-test (ns, non-significant). These data have been also previously reported in (Ukegbu *et al.*, 2017b).

4.2.3.4 Assessing the capacity of *ΔP47* parasites to form ookinetes

The smaller number of *ΔP47* compared to ANKA *c507* (WT) parasites regarding both the load of ookinetes found to invade the mosquito midgut epithelium and the oocysts determined in *TEP1*- and *LRIM1*-knockdown mosquitoes, pointed to an additional function of *Pb*P47 prior to mosquito midgut invasion, presumably in fertilisation, as shown previously (van Dijk *et al.*, 2010). To confirm this, the gametocyte-to-ookinete conversion rate of *ΔP47* parasites was measured, *in vivo* in the *A. coluzzii* midgut bolus at 17-18 hours pbf and *in vitro* after 24 hours post activation in complete culture medium (**Figure 4.14, A; Table 4.12**). Mosquito infection with the ANKA *c507* (WT) *P. berghei* line served as a control.

A significant 5.5-fold difference ($p<0.0001$) in gametocyte-to-ookinete rate was observed between the two parasites, ranging from 72% to 84% (mean value: 78%) in WT and 9% to 20% (mean value: 13%) in *ΔP47* parasites in a total of three biological replicates. Nevertheless, the *in vivo* gametocyte-to-ookinete rate of the KO parasites was substantially higher than the one observed *in vitro*, where the latter reached almost zero levels, ranging from 0.1% to 0.4% (mean value: 0.3%). These results are also largely in agreement with the 99.9% reduction in the capacity of the *ΔP47* parasites to form ookinetes *in vitro*, previously observed by (van Dijk *et al.*, 2010). In conclusion, *P. berghei* P47 has an important, but not essential role, during gamete fertilisation taking place in the mosquito midgut lumen 15 mins post ingestion.

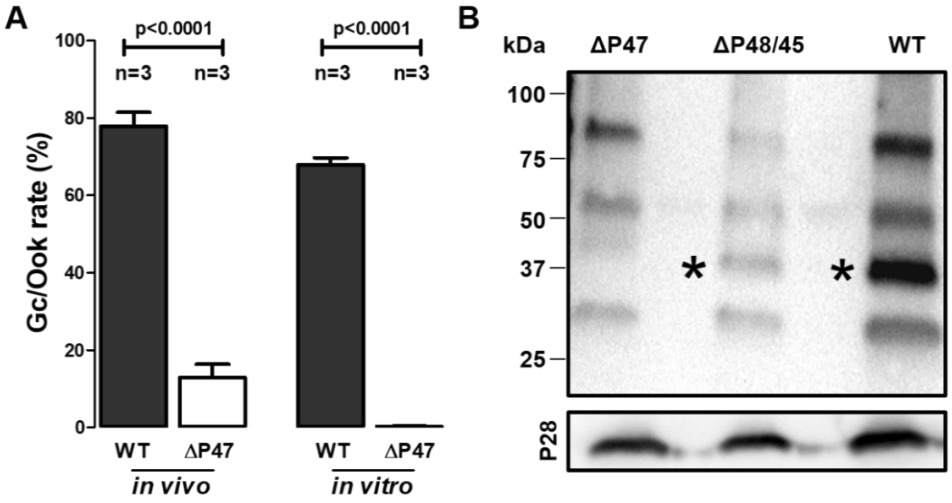

Figure 4.14. Gametocyte-to-ookinete developmental transition of *ΔP47* parasites. (A) *In vivo* and *in vitro* gametocyte-to-ookinete (Gc/Ook) conversion rates of *ΔP47* and control ANKA *c507* (WT) parasites. Error bars show standard error, whereas n corresponds to the number of replicates performed. Statistical significance

was determined using a two-tailed, unpaired Student's *t*-test. Data have been previously reported in (Ukegbu *et al.*, 2017b). **(B)** Western blot assay on whole protein extracts of *ΔP48/45* and ANKA *c507* (WT) *in vitro* ookinetes. Asterisks indicate P47 monomers (~40kDa) under non-reducing conditions. *ΔP47* ookinete protein extracts were used as control for non-specific signal. Antibody against the female gametocytes P28 surface protein was also used as stage-specific control.

It has been previously reported that in *P. falciparum ΔP48/45* mutants, the P230 protein cannot be retained on the surface of the parasites (Eksi *et al.*, 2006), a result that may indicate that tethering of P230 to the surface of the male gamete is mediated by P48/45. To examine whether this is true for *P. berghei* P47, whole protein extracts from *ΔP48/45* purified *in vitro* ookinetes were used in a western blot assay where the abundance of P47 was examined. The results showed that in the absence of P48/45, *P47* is normally expressed in ookinetes (**Figure 4.14, B**).

4.2.3.5 Analysis of a new *ΔP47 P. berghei* clone

Different clones of KO parasites with regards to the percentage of *PbP47* coding sequence that has been disrupted during homologous recombination and/or to their genetic background, might have different phenotypes when infecting mosquitoes. To validate the proposed function of *P. berghei* P47, phenotypic characterisation and infectivity assessment in ds*LacZ*-injected (control) and *LRIM1*-silenced *A. coluzzii* mosquitoes of a different *ΔP47* line were carried out. The new *ΔP47* parasite line called *ΔP47*/red, was generated by Dr. Ana-Rita Gomes in the host laboratory using the ANKA *1804cl1* reference line that constitutively expresses *mCherry* and a PlasmoGEM disruption vector (PbGEM-343204). Following homologous recombination, 100% of the *ΔP47*/red coding sequence was disrupted, whereas 250bp on the 5' end and 123bp on the 3' end of the gene coding sequence remained on the genome of the initial *ΔP47*/ANKA *c507* line (van Dijk *et al.*, 2010).

To investigate the ability of the *ΔP47*/red gametes to fertilise and form ookinetes *in vivo*, quantification of the gametocyte-to-ookinete conversion rates in the midgut bolus of *A. coluzzii* mosquitoes at 17-18 hours pbf was carried out. Mosquito infection with the ANKA *1804cl1* (WT) *P. berghei* line served as a control. A significant 4.5-fold difference ($p<0.0001$) in the gametocyte-to-ookinete conversion rates was determined for the mutant parasites, ranging from 17.86% to 18.87% (mean value: 18.37%) compared to the WT, ranging from 79.88% to 83.41% (mean value: 81.65%) (**Figure**

4.15, A). Following this, ookinete load of the mutant and WT parasite lines in the midguts of infected *A. coluzzii* mosquitoes was determined at 24-25 hours pbf. The median number of *ΔP47* and WT ookinetes counted was 148 and 219, respectively (**Figure 4.15, B**), confirming once more that the reduced fertilisation capacity of *ΔP47* macrogametes affects the number of ookinetes invading the *A. coluzzii* midgut wall.

To determine whether the *ΔP47*/red line can be fully rescued when silencing the mosquito complement-like pathway, *LRIM1*-silenced and ds*LacZ*-injected *A. coluzzii* mosquitoes were infected and qualitative data of oocysts and midgut and salivary gland sporozoites were collected. Parallel infection with the ANKA *1804cl1* (WT) line served as a control, to confirm sufficient efficiency of *LRIM1*-knockdown. The results showed that the median intensities of infection with the *ΔP47* line significantly increased ($p<0.0001$) from 0.0 (0% prevalence) in ds*LacZ*-injected to 33.0 (86.27% prevalence) in *LRIM1*-silenced mosquitoes (**Figure 4.15, C**), supporting the previous findings that mosquito complement silencing rescues *ΔP47* oocysts survival.

The next question that needed to be answered was whether the mutant KO parasites, following silencing of the mosquito complement-like pathway, are also able to produce sporozoites that can subsequently infect the vertebrate host and thus, complete the transmission cycle. Indeed, midgut and salivary gland sporozoite numbers were significantly higher ($p=0.0009$ and $p=0.03245$, respectively) in the *LRIM1*-silenced *A. coluzzii* mosquitoes (6,150 spz/midgut and 2,388 spz/salivary glands) compared to the ds*LacZ*-injected control mosquitoes (25 spz/midgut and 77 spz/salivary glands) (**Figure 4.15, D**). Infectivity to mice was assayed by allowing infected mosquitoes to feed on c57BL/6 mice at day-21 pbf. Interestingly, the *ΔP47* sporozoites produced in the *LRIM1*-silenced *A. coluzzii* mosquitoes could be transmitted to all five mice used for producing ABS parasites, whereas transmission of the *ΔP47* sporozoites produced in the ds*LacZ*-injected mosquitoes was completed abolished. PCR analysis on gDNA extracted from blood stage parasites from the infected mice confirmed that parasites encompassed the *ΔP47* locus (**Figure 4.15, E**).

In conclusion, all these data confirm that different *ΔP47* parasite clones have similar defective phenotypes in regard to their fertility capacity and infection intensity in *A. coluzzii* mosquitoes. Only when silencing components of the mosquito complement-like system mutant parasites complete their lifecycle and hence, can successfully be transmitted back to the next mammalian host (Ukegbu *et al.*, 2017b).

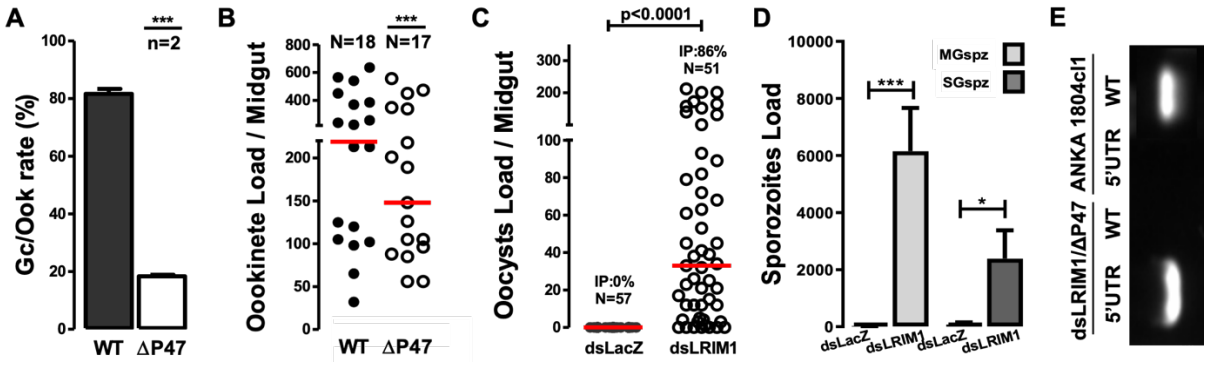

Figure 4.15. Phenotypic analysis of the *P. berghei ΔP47*/red parasite line in *A. coluzzii* infections. (A) *In vivo* gametocyte-to-ookinete (Gc/Ook) conversion rates of *ΔP47* and WT parasites, in the blood bolus of infected *A. coluzzii* at 17-18 hours pbf. Number of replicates (N), infection prevalence (IP) and standard error are shown. Statistical significance was determined with a two-tailed, unpaired Student's *t*-test. **(B)** *ΔP47* and WT ookinete loads in the midguts of *A. coluzzii* mosquitoes, at 24-25 hours pbf. Red lines show the median ookinete load, where n is the total number of midguts collected for the two individual biological replicates performed. Statistical significance was determined using the Mann Whitney U-test. **(C)** Effect of *LRIM1*-silencing and ds*LacZ*-injections (control) on the *ΔP47* oocyst load. The median number of oocysts is shown with a red line, where N is the total number of midguts used for oocyst counting. For each of the two biological replicates, oocyst load was determined from a minimum of 25 midguts per mosquito group. Statistical significance was determined using the Mann Whitney U-test. **(D)** Midgut and salivary gland *ΔP47* sporozoite load in infected ds*LacZ*-injected and *LRIM1*-silenced mosquitoes. The mean of the pooled data from two individual biological replicates is presented. The number of sporozoites was calculated from suspensions of 20 homogenised midguts/salivary glands, assayed in two batches of ten at day-15 pbf for midgut sporozoites and at day-21 pbf for salivary gland sporozoites. Statistical significance was determined using a two-tailed, unpaired Student's t-test. Error bars show standard error. **(E)** PCR genotypic analysis of the *ΔP47* KO locus on blood stage parasites following transmission from *LRIM1*-silenced *A. coluzzii* mosquitoes. gDNA from ANKA *1804cl1* WT parasites was used as control for the set of primers that map to the WT locus.

Table 4.12. *In vivo* and *in vitro* gametocyte-to-ookinete (Gc/Ook) conversion rates of *ΔP47* and control ANKA *c507* (WT) parasite lines in naïve *A. coluzzii* mosquitoes

	Parasite line	Number of experiments	No of midguts / Replicate	Number of Macrogametes	Number of Ookinetes	Fertilisation Rate (%)	Reduction (%)	*p*-value
in vivo	*c507* (WT)	2	10	72	319	81.65		
	ΔP47	2	10	504	117	18.87	80.99	0.0025
in vitro	*c507* (WT)	3	10	948	1574	62.41		
	ΔP47	3	10	1652	35	2.07	96.69	<0.0001

The *in vivo* and *in vitro* gametocyte-to-ookinete (Gc/Ook) conversion rates were calculated as the percentage of P28-positive ookinetes to the total number of the P28-positive macrogametes and ookinetes. The *in vivo* conversion rates were calculated from suspensions of 10 homogenised midguts, assayed 16-17 hours pbf. Statistical significance was determined using a two-tailed, unpaired Student's *t*-test (ns, non-significant). Data have been previously reported in (Ukegbu *et al.*, 2017b).

4.2.4 Phenotypic characterisation of *P. berghei c01* and *c57*

P. berghei c01 and *c57* were found to be highly transcribed at the ookinete stage (Akinosoglou *et al.*, 2015). Bioinformatic analysis revealed that *c01* encodes a putatively secreted polypeptide and *c57* encodes a putatively membrane-associated protein (unpublished data, with the permission of Dr. Valerie Ukegbu, Imperial College London). Analysis from (Yeoh *et al.*, 2017) indicated that *c01* is also highly transcribed in female gametocytes and *c57* is upregulated in male gametocytes. Preliminary data showed that disruption of these genes leads to a reduced ability of the mutant parasites to form ookinetes which is later mirrored in the reduced number of oocysts produced on the mosquito midguts as well as on the transmission blockage observed (unpublished data, with the permission of Dr. Valerie Ukegbu, Imperial College London). Here, I investigated whether the function of these proteins is exclusively dependent on the female or male alleles carried by the parasite, as previously also suggested by their transcriptional profiling in (Yeoh *et al*., 2017). Additionally, whether silencing of the complement system could rescue transmission of the KO mutant parasites was assessed. The *P. berghei Δc01* and *Δc57* parasite lines used were generated by Dr. Valerie Ukegbu and Dr. Chrysanthi Taxiarchi.

4.2.4.1 Sex-specific complementation of *Δc01* and *Δc57* by genetic crossing

A powerful way of determining if a *P. berghei* gene is required in the early or only during the late stages of mosquito infection, is to perform genetic complementation experiments with sex-specific *P. berghei* mutants (Raine *et al.*, 2007). If both female and male derived alleles can rescue the mutant phenotype, the associated gene product is not required until after both the male and female genomes become available for transcription in the developing zygote. In contrast, if only the female- or male-derived allele is capable of rescuing the KO phenotype, the gene product must be present pre-fertilisation or very early post-fertilisation.

Genetic crosses between *Δc01* and *Δc57* parasites with either of the *P. berghei* transgenic lines which are unable to produce fertile female (*ΔP47* or Δ*nek4*) or male (Δ*hap2* or Δ*map2*) gametes (Khan *et al.*, 2005; Reininger *et al.*, 2005; Tewari *et al.*, 2005; Mair *et al.*, 2006; von Besser *et al.*, 2006) yielded oocysts of normal morphology and numbers (**Figure 4.16; Table 4.13**). This leads to the conclusion that the functional copy of *Pbc01* and *Pbc57* are not exclusively inherited from the male neither

the female gamete, a result inconsistent with the observed *c01* female-biased and *c57* male-biased gametocyte transcription pattern (Yeoh *et al.*, 2017).

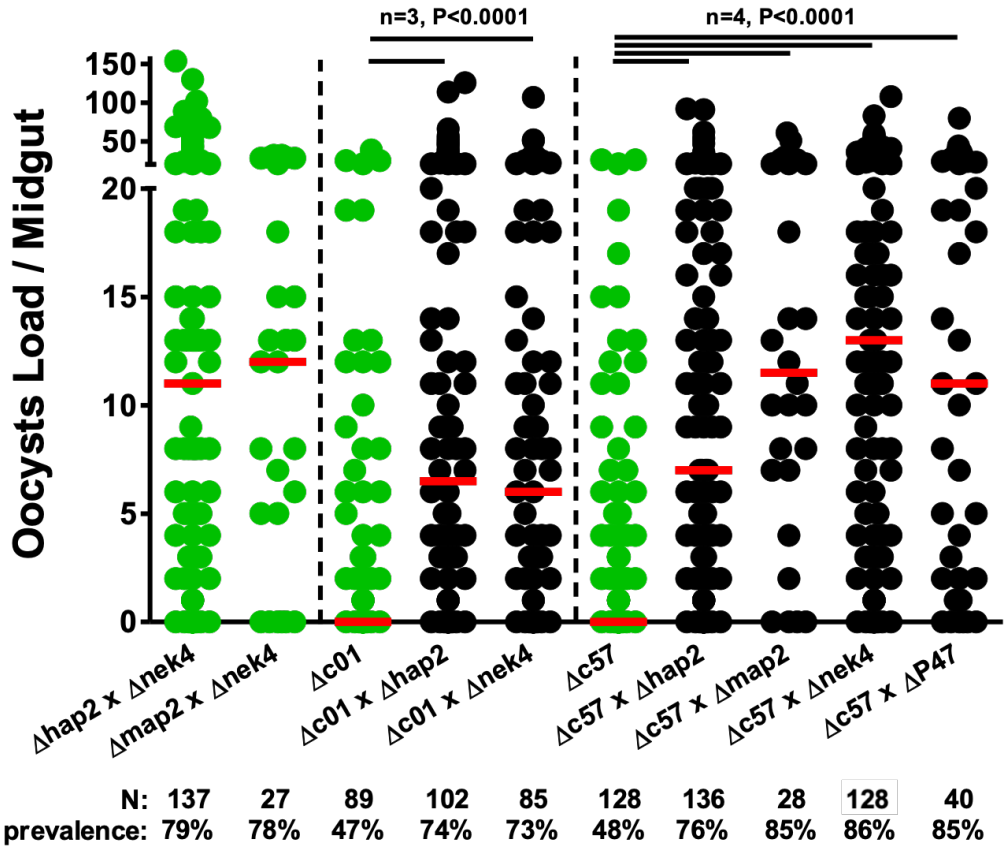

Figure 4.16. Genetic crosses of *Δc01* and *Δc57* parasites with *P. berghei* male and female deficient lines. Oocyst numbers following crosses between *Δc01* or *Δc57* and various female (*ΔP47* or Δ*nek4*) or male (Δ*hap2* or Δ*map2*) mutant lines. Red lines indicate median oocyst load, whereas n corresponds to the number of replicates performed for each set of mutant line. N corresponds to the total number of midguts collected and prevalence is the percentage of midguts that were infected with at least one oocyst. Statistical significance was determined using the Mann Whitney U-test.

4.2.4.2 *Δc01* and *Δc57* development following complement silencing

Since *Δc01* and *Δc57* parasites undergo a substantial reduction at the oocyst stage when infecting *A. coluzzii* mosquitoes, I went on to investigate whether silencing of the mosquito complement-like system could lead to an increased number of live mutant oocysts. To do so, *LRIM1*-silenced and ds*LacZ*-injected (control) mosquitoes were infected with *Δc01* and *Δc57* parasites and oocyst numbers were counted at day-8 pbf. Parallel infections with the parental WT *P. berghei* line were also carried out as a control to the gene silencing experiments (data not shown). The median intensities of

infection with the *Δc01* and *ΔPbc57* in ds*LacZ*-injected mosquitoes was 0 (prevalence 43%) and 1 (prevalence 57%), respectively. On the other hand, the median intensities of infection with the *Δc01* and *Δc57* parasite lines in *LRIM1*-silenced *A. coluzzii* mosquitoes was 13.5 (prevalence 76%) and 8 (prevalence 75%), respectively (**Figure 4.17, A; Table 4.14**). The results, once again, undoubtedly show that the average infection intensity increased significantly ($p<0.0001$) for both mutant lines when infected in *LRIM1*-silenced compared to ds*LacZ*-injected mosquitoes.

The results described above raised the question of whether the mutant oocysts were also capable of producing viable sporozoites to complete the transmission cycle. It has been previously shown that silencing complement components might have different effects on whether transmission to the rodent host is fully rescued; *ΔP47* parasite development (Ukegbu *et al.*, 2017b) is fully rescued, whereas *Δc43* parasites produce sporozoite empty oocysts resulting in transmission abolishment (Ukegbu *et al.*, 2020).

Δc01 and *Δc57* midgut and salivary gland sporozoite numbers were counted at day-15 and day-21 pbf, respectively. The mean number of midgut and salivary gland sporozoites counted in infected ds*LacZ*-injected mosquitoes was 244 (±58) / 73 (±33) for *Δc01* and 356 (±135) / 66 (±37) for *Δc57,* whereas the analogous numbers in *LRIM1*-silenced mosquitoes were 1347 (±637) / 625 (±188) and 1708 (±592) / 507 (±143), respectively (**Figure 4.17, B; Table 4.15**). These results strongly indicate that by suppressing the mosquito complement-like pathway, rescue of the KO phenotype at the oocyst stage can be achieved which ultimately leads to sporozoite formation and migration to the salivary glands.

The infectivity of *Δc01* and *Δc57* sporozoites was assessed by allowing infected mosquitoes to feed on c57/BL6 mice in bite-back experiments (mosquito-to-mouse transmission) and monitoring their parasitaemia for 14 consecutive days following mosquito feed. *Δc01* sporozoites of *LRIM1*-silenced *A. coluzzii* could be readily transmitted to five out of six mice used producing all ABS parasites, whereas two out of six mice were found positive after they got bitten by ds*LacZ*-injected mosquitoes. None of the nine mice used was infected after bite-back experiments using ds*LacZ*-injected mosquitoes infected with *Δc57* parasites, which is consistent with previous data showing that the majority of *Δc57* parasites could not reach the mosquito salivary glands. All eight mice used during bite-back experiments of *Δc57* infected *LRIM1*-silenced mosquitoes were positive by the end of day-14 post-inoculation. Finally, PCR

analysis on gDNA extracted from blood stage parasites from the infected mice confirmed the absence of the *c01* and *c57* genes in the genome (**Figure 4.17, C**).

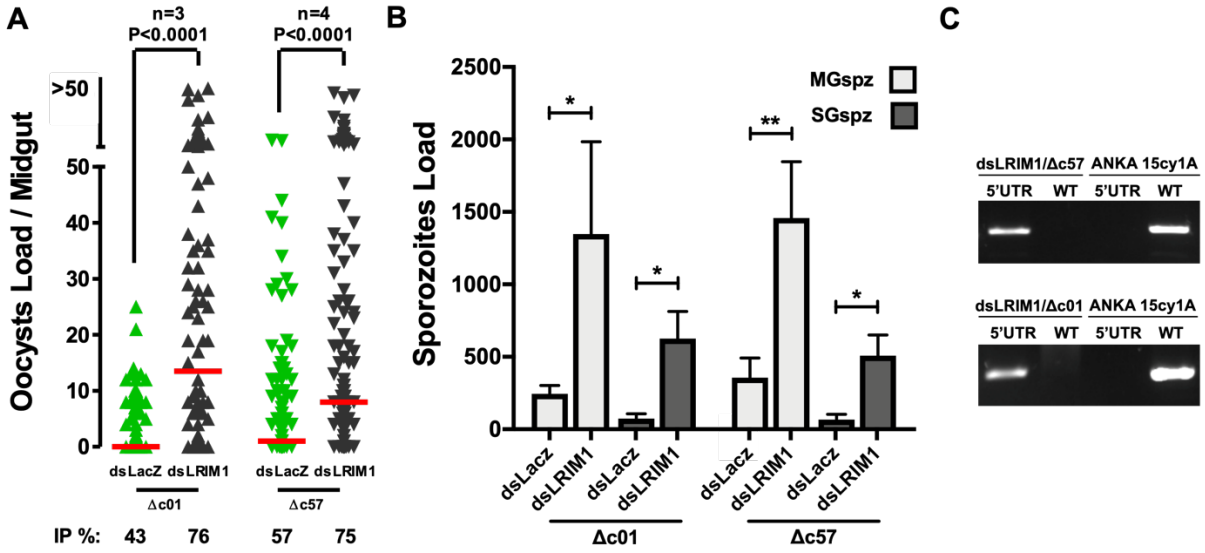

Figure 4.17. Effect of *LRIM1*-silencing on *Δc01* and *Δc57* parasites development. **(A)** Effect of ds*LacZ* injections (control) and *LRIM1*-silencing on the KO oocyst development. The median number is shown with a red line, where n is the number of replicates performed and N, the total number of midguts harboured. Statistical significance was determined using the Mann Whitney U-test. **(B)** Midgut and salivary gland sporozoite numbers in *Δc01* (left panel) and *Δc57* (right panel) infected ds*LacZ*-injected and *LRIM1*-silenced mosquitoes. The mean of the pooled data from three and four individual biological replicates is presented, respectively. Statistical significance was determined using a two-tailed, unpaired Student's t-test. Error bars show standard error. **(C)** PCR genotypic analysis of the *Δc01* and *Δc57* KO or WT locus on blood stage parasites following transmission from ds*LacZ*–injected and *LRIM1*-silenced *A. coluzzii* for *Δc01* and *LRIM1*-silenced mosquitoes for *Δc57* parasites.

Table 4.13. Genetic crosses between *Δc01* and *Δc57* with female or male gamete deficient mutants

Genetic Crosses	Number of experiments	Number of midguts	Prevalence (%)	Infection Intensity		Parasite range	*p*-value
				Arithmetic mean	Median		
Δ*hap2* (♀) x Δ*nek4* (♂)	4	137 (108/29)	78.83	19.47	11.00	0-154	
Δ*map2* (♀) x Δ*nek4* (♂)	4	27 (21/6)	77.88	12.93	12.00	0-32	
Δc01	3	89 (42/47)	47.19	3.64	0.00	0-39	
Δc01 x Δ*hap2* (♀)	3	102 (75/27)	73.53	14.36	6.50	0-126	<0.0001
Δc01 x Δ*nek4* (♂)	3	85 (62/23)	72.94	11.34	6.00	0-107	<0.0001
Δc57	4	128 (62/66)	48.44	2.91	0.00	0-26	
Δc57 x Δ*hap2* (♀)	4	136 (104/32)	76.47	11.95	7.00	0-92	<0.0001
Δc57 x Δ*map2* (♀)	4	28 (24/4)	85.71	15.43	11.50	0-61	<0.0001
Δc57 x Δ*nek4* (♂)	4	128 (111/17)	86.05	17.57	13.00	0-108	<0.0001
Δc57 x *ΔP47* (♂)	4	40 (34/6)	85.00	15.18	11.00	0-80	<0.0001

The table reports on the outcome of *A. coluzzii* infections with *P. berghei* progeny derived from crosses between *Δc01* and *Δc57* with mutants that are either female (Δ*nek4*) or male (Δ*hap2*) gamete deficient. The total number of midguts is indicated in the third column, as the ratio between the number of infected midguts to the number of uninfected midguts. The results from three to four independent experiments are shown, respectively. Crosses between Δ*hap2*/Δ*nek4* and Δ*map2*/Δ*nek4* were used as positive controls. Infections were performed by directly feeding mosquitoes on mice that were previously co-infected with the two lines. P-values were calculated using the Mann Whitney U-test.

Table 4.14. Effect of *LRIM1*-silencing on *Δc01* and *Δc57* infections in *A. coluzzii* mosquitoes

Parasite line	dsRNA	Number of exp.	Midguts number	Prevalence (%)	*p*-value	Infection Intensity		Parasite range	Fold Change	*p*-value
						Arithmetic mean	Median			
Δc01	*LacZ*	3	97 (42/55)	43.30		2.93	0.00	0-25		
	LRIM1		90 (68/22)	75.56	0.0541	33.51	13.50	0-218	<13.50	<0.0001
Δc57	*LacZ*	4	134 (77/57)	57.47		6.43	1.00	0-69		
	LRIM1		124 (93/31)	75.00	0.0214	26.17	8.00	0-205	8.00	<0.0001

Δc01 and *Δc57* parasite infections of *LRIM1*-silenced *A. coluzzii* mosquitoes was assessed at day-12 pbf. Infection of ds*LacZ*-injected mosquitoes were used as control. Number of midguts is shown as the ratio between the number of infected midguts to the number of uninfected midguts. Statistical significance for the median oocyst load was determined using the Mann Whitney U-test, whereas statistical significance of the prevalence percentages was assessed by Fisher's exact test (ns, non-significant). Infectivity to mice was assayed by allowing infected mosquitoes to feed on Balb/C mice on day-21 of infection. Parasitaemia of mice was assayed by Giemsa-stained thin blood smears from day-5 onwards.

Table 4.15. Midgut and salivary gland sporozoite numbers of *Δc01* and *Δc57 P. berghei* in ds*LacZ* (control) and ds*LRIM1*-injected *A. coluzzii* mosquitoes

Parasite line	dsRNA	Number of experiments	Midgut Sporozoites		*p*-value	Salivary glands sporozoites		*p*-value	Infectivity to mice (21dpi)
			Mean	SEM		Mean	SEM		
Δc01	*LacZ*	3	244.24	57.88		73.50	33.55		2/6
	LRIM1		1,346.72	637.39	0.0135	625.01	188.05	0.0447	5/6
Δc57	*LacZ*	4	356.01	135.11		65.93	36.80		0-9
	LRIM1		1,707.72	592.30	0.0020	507.50	143.26	0.0245	8/8

The table reports *Δc01* or *Δc57* midgut (oocyst) sporozoite numbers from three and four biological replicates of ds*LacZ*-injected and *LRIM1*-silenced *A. coluzzii* infections, respectively. For each replicate, sporozoite numbers were determined from two batches of 15 homogenised midguts at day-15 post infection. SEM represents the standard error from the mean. Statistical significance was determined using a two-tailed, unpaired Student's t-test. Infectivity to mice was assayed by allowing infected mosquitoes to feed on c57BL/6 mice on day 21 of infection. Parasitaemia of mice was assayed by Giemsa-stained thin blood smears on day 5, 8, 10, 13 and 15 post-inoculation.

4.2.5 Summary

- *P. berghei* c43 is essential for sporogonic development in the developing oocyst. *Δc43* oocysts are morphologically variable and remain smaller in size compared to the WT oocysts, at the same timepoint.
- *P. falciparum c43* is an ookinete and sporozoite specific protein, localised on the parasite surface. At first glance, genetic complementation of *Pfc*43 in *P. berghei* suggests that *P. berghei* and *P. falciparum* c43 do not share the same function.
- Antibodies against the *P. berghei* or *P. falciparum c43* interfere with parasite immune evasion when ingested with the infectious bloodmeal, and drastically reduce the prevalence and intensity of infection.
- *P. berghei P47* is expressed on the surface of female gametocytes and ookinetes and it serves distinct functions in promoting gametocyte-to-ookinete development as well as protecting ookinetes from the mosquito complement-like responses.
- Parasites lacking *c01* or *c57* undergo a substantial reduction at the oocyst stage, unless silencing key factors of the complement-like system.

4.3 Discussion

4.3.1 Characterisation of the *P. berghei c43*, P47, c01 and c57 proteins

Within about 24 hours inside the mosquito, *Plasmodium* parasites must fertilise to form ookinetes which then have to invade and traverse the midgut cell wall in order to establish a successful infection, marked by the development of oocysts between the midgut epithelium and basal lamina on the midgut periphery. Following that, oocysts mature so that sporozoites are produced and released into the haemocoel prior to migration into the salivary gland lumen. In addition to the developmental progression of the parasite within its mosquito vector, parasites must successfully survive the mosquito effective antiplasmodial immune responses mounted acutely especially immediately after ookinete traversal through the mosquito midgut epithelium into the sub-epithelial space (Blandin *et al.*, 2004; Osta *et al.*, 2004a; Vlachou *et al.*, 2006).

So far, the mechanisms underpinning gamete fertilisation, ookinete traversal of the mosquito midgut epithelium and parasite evasion from reactions of the complement-like system have not been fully elucidated. In this chapter, characterisation of four *Plasmodium* genes for which preliminary evidence supported to have an essential role during parasite development in the mosquito vector i.e. parasites lacking expression of any of these genes have a compromised ability to form oocysts, is described.

4.3.1.1 Characterisation of the ookinete and sporozoite protein c43

Plasmodium c43 is a membrane bound protein found on the surface of ookinetes and sporozoites and is required for ookinetes to evade the mosquito complement-like system responses as well as for oocysts sporogonic development. Disruption of *P. berghei* c43 triggers robust complement activation and ookinete elimination upon mosquito midgut traversal resulting in transmission abolishment. Silencing the complement-like system restores ookinete-to-oocyst transition, however further maturation of the developing oocyst does not take place (Ukegbu *et al.*, 2020).

c43 was firstly named as POS8 and was shown to have a critical role during ookinete-mediated midgut invasion as well as in subsequent oocyst development (Kaneko *et al.*, 2015). A later study by Zheng *et al.* reported the gene as being critical during ookinete maturation, designating it as *PSOP25* (Zheng *et al.*, 2017). Data presented in (Ukegbu *et al*., 2020) show c43 to have no role during ookinete maturation or mosquito midgut invasion since KO ookinetes look morphologically normal and are able to invade the mosquito midgut epithelial cells at a rate similar to the WT (Ukegbu *et al*., 2020). In further agreement with this, phenotypic analysis of an additional clone (*Δc43/red*) described in this chapter revealed the same exactly phenotype. To match the vector of choice in the previous studies (Kaneko *et al*., 2015; Zheng *et al*., 2017), infections were performed using also *A. stephensi* mosquitoes. Indeed, *Δc43/red* parasites were able to form ookinetes which were then able to invade the mosquito midgut epithelium at a rate similar to the WT. Following ookinete traversal though, a dramatic reduction in the number of oocysts was observed but did not reach zero as shown in *A. gambiae* mosquitoes. This is consistent with findings by Kaneko *et al*. (Kaneko *et al*., 2015) as well as with the general understanding that the *A. stephensi* mosquitoes are high susceptible to parasite infections (Feldmann *et al*., 1989) due to their less robust immune responses compared to *A. coluzzii*.

The *Δc43* oocysts that developed in the *A. stephensi* mosquitoes were morphologically different compared to the WT and, produced only a very small amount of sporozoites which though are unable to establish infection back to the rodent host. These findings are consistent with the morphology of the *Δc43* oocysts developed in complement silenced *A. coluzzii* mosquitoes (Ukegbu *et al*., 2020). It can be suggested that the abnormal morphology of the *Δc43* oocysts could be related to the inhibition of DNA replication in the early stages of infection, which could further explain why the oocysts

appear to be of empty sporoblasts. The small oocyst size as well as the inability to complete sporulation carries the hallmarks of cell cycle arrest. Therefore, these observations suggest that *P. berghei c43* is further involved in oocyst maturation and sporozoite formation, possibly during the mitotic endoreplications. It has been previously shown that two GPI-anchored proteins of *T. brucei* and *S. cerevisiae* are also important for cell cycle progression; GPI8, a GPI-anchored protein found on *T. brucei* surface was found to be essential in cell cycle progression in bloodstream *Trypanosomes* (Lillico *et al.*, 2003) and GPI7, a GPI-anchored protein on *S. cerevisiae* surface, was found to be involved in cell separation after cytokinesis (Fujita *et al.*, 2004). These data together suggest that GPI-anchored proteins of the cell surface might be involved in cell cycle progression, either as signalling molecules or by modulating factors needed during the DNA replication process.

P. berghei and *P. falciparum c43* was found to be expressed on the surface of ookinetes and midgut and salivary gland sporozoites (Ukegbu *et al*., 2020) however, transcriptional analysis showed transcripts to only be present in ookinetes and salivary gland sporozoites, but not in sporozoites when still in the developing midgut oocysts at day-15 pbf and day-11 pbf, respectively. It could be suggested that c43 is indeed *de novo* expressed at the salivary gland sporozoites, even though the transcription pattern detected does not support this conclusion. One could say that the c43 protein is stable (possibly due to stable folding patterns facilitated by the two conserved cysteines on the C-terminal of the protein) and thus can be maintained for long periods on the parasite surface. Another explanation would be that c43 mRNA is assembled with other proteins into quiescent messenger ribonucleoprotein particles (mRNPSs) and in this way stored for translation at a later time (Buchan & Parker, 2009). A model suggests that this type of translational control helps the parasite to always be ready to respond to external stimuli (Parker *et al.*, 2007). For instance, it has been shown that *Plasmodium* uses RNA-binding proteins such as DOZI, CITH and ALBA family proteins to impose translational repression and mRNA stabilisation on transcripts of female gametocytes (; Paton *et al.*, 1993; Mair *et al.*, 2006; Mair *et al.*, 2010; Guerreiro *et al.*, 2014; Painter *et al.*, 2017; Painter *et al.*, 2018). Presence of the protein during all these stages has been shown to be related with more than one functions.

Genetic complementation of *P. berghei c43* with its *P. falciparum* orthologue led to the production of some oocysts, which were though morphologically different compared

to the WT and did not yield a large amount of sporozoites. The number of oocysts produced were more comparable to those of the *Δc43* line, but still significantly lower ($p<0.0001$) compared to the WT. Hence, these data show a non-conserved function of c43 between its *P. berghei* and *P. falciparum* orthologues as well as point to a unique function of *P. berghei c43* with regards to its function during oocyst sporulation and sporozoites production. Before finalising our conclusion though, other factors should be further investigated such as the correct folding of the *P. falciparum* c43 protein as well as its stability in a *Plasmodium* species that it is not normally its compatible environment. Once could suggest that since the two proteins share a poor protein sequence similarity in addition to an extra amino acid insertion found in the N-terminal of the *Pfc*43 coding sequence, it is difficult to maintain a conserved function. Whether this domain replaces the function of a protein homodimer, as *Pb*c43 was found to form, is not yet known.

4.3.1.2 Characterisation of the female gametocyte specific protein P47

P. falciparum P47, initially described by the lab of Carolina Barillas-Mury (Molina-Cruz *et al.*, 2013), is the first protein found to be important for the parasite to survive the robust mosquito innate immune responses. A model has been already proposed for the function of the *P. falciparum* gametocyte surface protein P47 in preventing parasite elimination by mediating suppression of the JNK signalling in *A. gambiae* invaded midgut cells (Molina-Cruz *et al.*, 2013; Ramphul *et al.*, 2015). JNK signalling is thought to trigger apoptosis of the invaded cells through activation of effector caspases. It also induces the production of HPX2 and NOX5, which together potentiate nitration of ookinetes marking them for destruction by reactions of the mosquito complement-like system (Oliveira *et al.*, 2012). Disruption of the JNK pathway, by silencing activators of this cascade, greatly enhances infection (Garver *et al.*, 2013). Therefore, P47 suppresses activation of the JNK pathway and at the same time inhibits ookinete nitration and subsequent elimination by reactions of the complement-like system (Molina-Cruz *et al.*, 2013; Ramphul *et al.*, 2015).

P. berghei P47 is a GPI-anchored protein which was shown to be highly expressed on the surface of female gametocytes and ookinetes. Here, a dual function of this protein has been demonstrated during the early stages of *A. gambiae* infection in promoting both gametocyte-to-ookinete development in the midgut lumen, presumably in female gamete fertility as previously reported *in vitro* (van Dijk *et al.*, 2010) and ookinete-to-

oocyst developmental transition by mediating ookinete protection from the mosquito immune responses (Ukegbu *et al.*, 2017b). Whilst the former function is non-essential *in vivo*, even if its disruption is accountable for a great reduction in the number of ookinetes formed, the latter is crucial since its disruption completely abolishes transmission. The exact role of *P. berghei* P47 in fertilisation remains to be determined. However, it is possible that *Pfs*47 also shares a similar function during fertilisation *in vivo* (Canepa *et al*., 2018). This cannot be further tested *in vitro* as *P. falciparum* ookinete culturing methods are not yet feasible.

The higher *in vivo* conversion rates of *ΔP47* gametes compared to the previously determined *in vitro* rates (van Dijk *et al.*, 2010) can be possibly explained by the presence of bacteria and bacteria metabolites in the midgut lumen, which are otherwise absent in the *in vitro* ookinete culture environment. It is so far known that midgut microbiota act against *Plasmodium* and prime the mosquito for infection (Dong *et al.*, 2009), however a positive effect can be suggested at this instance.

P. berghei parasites that lack expression of *P47* do not make it to the oocyst stage due to the ookinetes clearance by the mosquito complement-like system, once the traverse the mosquito midgut epithelium. However, this phenotype can be averted by silencing key factors of the mosquito complement-like system, such as LRIM1 and TEP1. Following complement silencing, not only is oocyst formation restored but also transmission back to the rodent host is fully rescued (Ukegbu *et al.*, 2017b). However, whether the *P. berghei* P47 functions similarly to its *P. falciparum* orthologue in suppressing the JNK pathway, has not been fully understood.

It can be suggested that when a major surface protein such as P47 is missing, the ookinete surface may be recognised by the mosquito innate immune system as foreign and trigger nitration followed by TEP1 attack. This is also in agreement with previous data showing that the presence of P47 on the ookinete surface is required for its own survival (Ukegbu *et al.*, 2017b) as well as by the positive evolutionary selection observed in these genes (Conway *et al.*, 2001; Escalante *et al.*, 2001; Anthony *et al*., 2007; Molina-Cruz *et al.*, 2015). This function might also be extended to other stage specific 6-cysteine containing proteins such as the gametocyte-specific P48/45 and P230 that are known to be important for the *in vitro* fertilisation of the female and male gametes (van Dijk *et al*., 2001; 2010) as well as the sporozoite-specific P52 and P36 that are known to be important in the development of the parasitophorous vacuole in

liver stages by protecting sporozoites from the vertebrate immunity (Ishino *et al.*, 2005; Annoura *et al.*, 2014). Together all these data could suggest that members of the gametocyte specific 6-cysteine-containing proteins may have specifically evolved to function in interactions with the hosts' immune system.

4.3.1.3 Characterisation of the gametocyte and ookinete proteins *c01* and *c57*

The initial functional characterisation of *c01* and *c57* has led to the identification of two genes with essential roles in the rodent malaria transmission. Their absence has been shown to result in a mildly compromised ability of the parasites to form oocysts which further leads to transmission abolishment (unpublished data, with the permission of Dr. Valerie Ukegbu, Imperial College London). This chapter outlines that following silencing of the mosquito complement-like system, oocyst and sporozoite formation is restored allowing the KO mutant parasites to complete their lifecycle in the mosquito vector. The mechanism underlying the survival of the KO ookinetes following silencing of components of the complement-like system, has not been further investigated.

When silencing *A. coluzzii* complement-like system, *P. berghei Δc01* and *Δc57* parasites are able to develop into oocysts which later give rise to sporozoites that can be readily transmitted to the rodent host, following the mosquito's next bloodmeal. This result confirms what was previously suggested, that these proteins are important for ookinetes to survive the innate immune responses occurring immediately after parasite traversal through the midgut epithelial cells. However, whether these proteins contribute to the survival of the parasites at the oocyst stage, when the late phase of immunity takes place, has not been further investigated. Expression of the proteins at this stage could, indeed, point to a related factor. The late phase of immunity takes place during oocyst development and mainly involves components of the *Ag*STAT-A pathway, that limit *Plasmodium* infection by either inducing NOS expression (Gupta *et al.*, 2009) or other components including the Lipopolysaccharide-Induced Tumor Necrosis Factor (LITAF) (Smith *et al.*, 2012) and evokin (Ramirez *et al.*, 2015). Therefore, by investigating whether a protein known to be important for parasites to survive the complement-like system responses is also needed for parasite survival against the late phase of immunity, could give us a better insight into the mechanisms underlying the interactions of *Plasmodium* parasites with the mosquito innate immune system during its different developmental stages. So far, none of the *Plasmodium* molecules have been found to play such a dual role.

Work from Zheng and co-workers already showed that following production of an antibody that targets the full length of the *P. berghei* c57 protein, previously produced in the *E. coli* expression system, *c57* was found to be highly expressed on the surface of ookinetes but not in gametocytes or schizonts. Additional TBV experiments where mice were immunised with the recombinant protein prior to *A. stephensi* mosquito infection showed a significant reduction both in the oocyst density and infection prevalence (Zheng *et al.*, 2016). Similar work should be carried out in order to investigate the cellular localisation and essentiality of *P. berghei* c01. Following that, generation of polyclonal antibodies that are specific for their *P. falciparum* orthologues could give us useful insights into the expression and function of these proteins in the human malaria parasite, with the potential to further assess them as TBV antigens.

4.3.2 Conserved function of c01, c43, P47 and c57 among species could enhance the use of *P. berghei* as a good malaria model system

P. berghei is widely used as a rodent model for the study of malaria. Apart from the technical advantages that it offers such as safety during handling, *in vitro* culturing and ability for *in vitro* culturing and infection establishment in *A. gambiae* mosquitoes*,* it has similar biology as well as conserved interaction pattern with the human malaria parasite *P. falciparum,* during development in *Anopheles* mosquitoes (Waters & Janse, 2004; Mendes *et al.*, 2008; Prugnolle *et al.*, 2008). Therefore, the characterisation of *P. berghei* genes could give us useful and accurate information about their *P. falciparum* orthologues.

Data presented in this chapter as well as data previously reported in (Ukegbu *et al*., 2020) show that *P. falciparum* and *P. berghei c43* have similar expression patterns and localisation on the parasite surface. It has been also shown that when replacing the *P. berghei c43* with its *P. falciparum* orthologue, *P. berghei* parasites have a more moderated phenotype compared to the complete abolishment of *P. berghei Δc43* parasites at the oocyst stage i.e. *Pf*c43 partially rescues the absence of *Pb*c43. This might be either due to the non-conserved function of the two proteins or to the different molecular structure of the proteins, possibly needed for efficient protein-protein interactions; *Pf*c43 has an extra domain in its C-terminal which might not be correctly folded when in *P. berghei*. Additionally, both *P. berghei* and *P. falciparum* P47 have been shown to be critical for parasites to survive the mosquito immune responses. Unless silencing key components of the complement system, knockouts lacking any

of these proteins were substantially impaired in their capability to form oocysts, which in both cases eventually led to transmission abolishment. As previously mentioned, *Pf*s47 is involved in suppressing the JNK pathway of the invaded mosquito midgut cells, important for activation of the complement-like system as well as for marking the invaded ookinetes for TEP1-mediated killing (Molina-Cruz *et al.*, 2013; Ramphul *et al.*, 2015). However, a similar function of *P. berghei* P47 has not been solely identified. Nevertheless, generation of mutant KO *P. falciparum* lines for these genes would be critical in characterising them further. Especially now that the CRISPR-Cas9 methodology is widely used for generating mutant *P. falciparum* parasites (Ghorbal *et al.*, 2014; Lee *et al.*, 2014; Wagner *et al.*, 2014), characterisation of *P. falciparum* genes that seem to be essential for *P. berghei* development is plausible.

4.3.3 c43, P47, c01 and c57 as potential TBV candidates

TBVs are considered a high-priority research area, given its potential as an important tool during the malaria elimination strategy. The limited number of TBV candidates investigated to date demands increasing efforts in TBV antigen discovery. *Plasmodium* genes expressed during the early stages of mosquito infection constitute the most promising TBV candidates (Vermeulen *et al.*, 1985). Additionally, an optimal TBV target protein would be localised at the parasitic cell surface, conserved across all five human malaria species and, the function and structure of such a target would be known thereby allowing rational selection of immunologically vulnerable domains. Antibodies that have been found to specifically bind to multiple TBV targets have confirmed co-localisation with proteins located on the surface of the male gametes plasma membrane (P230, P48/45) (van Dijk *et al.*, 2001; van Schaijk *et al.*, 2006) or female gametes and ookinetes (P28/25) (Sidén-Kiamos *et al.*, 2000).

Based on findings presented in this chapter for *c43* and *P47* as well as from previous expression analysis studies for *c57* (Zheng *et al.*, 2016), all genes are predominantly expressed during gametogenesis and ookinete development. IFA analysis confirmed their expression on the parasite surface, a key parameter for making them suitable TBV candidates. Zheng *et al*., have showed that following immunisation of mice with a recombinant full length *Pb*c57 protein and *A. stephensi* mosquito infection with a *P. berghei* WT parasite line, a dramatic reduction in both the number of oocysts and total number of infected midguts was observed. Incubation of *in vitro* ookinete cultures with multiple concentrations of the full length antibody also showed significant reduction in

the number of ookinetes produced (Zheng *et al.*, 2016). This finding is in further agreement with what was described for *Pbc*57 and its role in ookinete development, during gametocyte-to-ookinete transition or ookinete maturation (unpublished data, with the permission of Dr. Valerie Ukegbu, Imperial College London).

Here, it has been demonstrated that antibody-mediated targeting of *P. berghei* or *P. falciparum c43* prior to *A. coluzzii* feeding via a SMFA results in a significant transmission-blocking efficacy ($p<0.0001$) in a dose-depended manner. It is important to note that in the presence of 125 μg/mL and 250 μg/mL a-*Pbc*43 or a-*Pfc*43 antibodies the infection prevalence was not dramatically reduced (52.21% and 27.72% in the presence of 125 μg/mL and 250 μg/mL a-*Pbc*43 antibody compared to the 80.95% and 80.47% in the presence of the UPC10 control antibodies, respectively and 44.00% and 46.00% in the presence of 125 μg/mL and 250 μg/mL a-*Pfc*43 antibody compared to the 71.00% in the control sample) (Ukegbu *et al.*, 2020). However, a successful TBV candidate should aim to reduce except from the infection intensity also the infection prevalence; if the infection prevalence remains high and the infection intensity is reduced down to 1-2 oocysts per midgut, transmission blockage in the area would not be achieved since one only oocyst is able to produce thousands of sporozoites which are still capable of infecting multiple mammalian hosts. Therefore, better designed antibodies targeting the full length of the protein or more antibodies that target critical epitopes for the protein should be further tested in order to achieve more predominant results.

Since *P. berghei* and *P. falciparum* c43 is expressed on the ookinete and sporozoite surface, it constitutes a potential TBV candidate that could be effective both in the human body, during the early liver stages of parasite infection, and in the mosquito vector. Regarding the latter and considering that the mosquito midgut is a harsh and highly proteolytic environment, antibodies targeting c43 during ookinete development in the mosquito midgut lumen would have to be of high titer and high avidity in order to survive for an extended period of time and efficiently influence the final steps of midgut invasion. It is therefore important that this caveat be factored in when testing TBVs targeting ookinete antigens. Beyond that, it would be interesting to examine whether silencing of the complement system would lead to the same levels of reduction in infection intensity and prevalence, as previously observed following TBV experiments against *Pfs*47 (Canepa *et al.*, 2018). Given that c43 also facilitates

Plasmodium survival against the robust immune attacks, by suppressing this eliminating factor we would expect the relative infection levels to be the same. Lastly, additional studies could be carried out in order to examine the transmission blocking efficacy of antibodies targeting *P. vivax* c43, as yet an uncharacterised protein.

Based on the dual role of P47 during gametocyte-to-ookinete developmental transition as well as parasite evasion of the mosquito innate immune responses, one would expect that it would constitue a strong candidate for transmission blocking interventions. Indeed, a recent study has shown that antibodies binding a 52 amino acid region of *Pf*s47 confer a strong transmission blocking activity against the laboratory *P. falciparum* strains in *A. gambiae* mosquitoes (Canepa *et al.*, 2018). In the same study, antibodies binding different regions of the protein showed either weak or no transmission blocking activity, consistent with an earlier study which reported that none of the three tested monoclonal antibodies against *Pf*s47 could affect *P. falciparum* infections in *A stephensi* (van Schaijk *et al.*, 2006). These findings agree with the general understanding that antibodies binding different regions of a targeted protein can have profound differences in their blocking activity, especially when antibodies have a primarily neutralising function (Armistead *et al.*, 2014; Canepa *et al.*, 2018; Singh *et al.*, 2019). Indeed, a second polyclonal α-*Pb*c43 antibody, raised against a codon optimised *Pbc43* gene fragment, did not confer any transmission blocking activity against *P. berghei* parasites despite producing strong signals in western blot analysis and immunofluorescence assays (Ukegbu *et al*., 2020). Similarly, the peptide antibody a-*Pf*c43^{P2}, which targets a small conserved region close to the cysteine residues of the C-terminal of *Pf*c43, did not lead to strong inhibition of oocyst formation despite the specificity determined in western blot and immunofluorescence assay analyses (Ukegbu *et al.*, 2020).

Notwithstanding their exact function in parasite immune evasion c01, c43, P47 and c57 constitute good targets for the development of novel interventions that aim to block malaria transmission in the mosquito vector. The idea is that the presence of such specific antibodies will interfere with the proteins function and as such, will make ookinetes susceptible to the complement-like responses triggered at the time of midgut traversal. One such approach is TBVs that aim to boost the generation of antibodies in the human serum, which when ingested by mosquitoes together with gametocytes will interfere with the proteins function and block further development. Several putative

TBVs are currently being investigated at a pre-clinical stage including those targeting the gametocyte and ookinete specific proteins *Pf*s230, *Pf*s48/45 and *Pf*s25 (Chaturvedi *et al.*, 2016). Another more ambitious approach is the generation of genetically modified mosquitoes that express single-chain antibodies or nanobodies against the specific surface proteins. When expressed in the mosquito, these antibodies are expected to specifically bind to the proteins and in this way confer refractoriness to infection leading to malaria transmission blockage (Isaacs *et al.*, 2011; Gantz *et al.*, 2015;). Such genetic features can be spread within wild mosquito populations in a super-Mendelian fashion via means of gene drive (e.g. CRISPR/Cas9) and can lead to sustainable local malaria elimination (Hamond *et al.*, 2016; Hammond & Galizi, 2017; Carballar-Lejarazú & James, 2017).

CHAPTER 5. CHARACTERISATION OF THE IMPACT OF THE MOSQUITO COMPLEMENT-LIKE RESPONSES ON SHAPING THE TRANSMITTED MALARIA PARASITE POPULATIONS

5.1 Introduction

Malaria transmission requires the *Plasmodium* parasite to complete an intricate replicative cycle in the mosquito, which involves transition through several developmental stages and interactions with the mosquito midgut and salivary gland tissues as well as haemolymph components. These mosquito parts act either as physical barriers to *Plasmodium* development or as activity sites of the mosquito innate immunity and, are largely responsible for the parasite population dramatic losses. The greatest parasite population bottleneck occurs during the ookinete-to-oocyst developmental transition, which coincides with the ookinete traversal of the mosquito midgut epithelium (Vlachou *et al.*, 2006). It has been estimated that over 80% of the *P. berghei* ookinetes cannot make it through to the oocyst stage (Levashina *et al.*, 2001; Osta *et al.*, 2004b). These losses are largely associated with the mammal complement activity (Lensen *et al.*, 1997), transmission blocking antibodies and cytokines ingested during mosquito bloodmeal (Sinden, 2010; Sutherland, 2009), the mosquito intestinal microbial flora (Dong *et al.*, 2009; Meister *et al.*, 2009) and most effectively the mosquito innate immunity (Levashina *et al.*, 2001; Osta *et al.*, 2004b).

In the mosquito midgut lumen, immune responses largely involve the antibacterial NF-κB signalling pathway Imd. After mosquito blood-meal, midgut bacterial levels and associated immune stimuli increase dramatically causing enhanced Imd responses (Dong *et al.*, 2009; Meister *et al.*, 2009). These responses are known to have an indirect impact on parasite infection. Direct parasite recognition by components of the Imd pathway has also been shown, but the mechanisms involved are yet unknown (Garver *et al.*, 2012). During ookinete traversal, activation of the JNK pathway triggers a nitration reaction with two important outcomes: apoptosis of the invaded cells and ookinete marking for destruction by the mosquito complement-like pathway (Garver *et al.*, 2013). Guided by LRIM1 and APLI1C, a complex of two leucine-rich repeat proteins, the complement factor-3 like protein TEP1 plays a key role in the elimination of the parasites by orchestrating their lysis or melanisation (Levashina *et al.*, 2001). This reaction occurs right after TEP1 binding to the ookinete surface, as soon as they make it to the basal sub-epithelial space of the midgut (Blandin *et al.*, 2004). These

reactions are assisted by actin-mediated cellular responses triggered by the invaded cells (Schlegelmilch & Vlachou, 2013; Shiao *et al.*, 2006).

Despite the major losses during the early stages of infection, some parasites survive the robust attacks of the mosquito immune system and manage to complete their transmission cycle suggesting that *Plasmodium* parasites have developed mechanisms to either evade or endure the *Anopheles* innate immunity. Indeed, it has been previously shown that *P. falciparum* P47, a surface protein of gametocytes and ookinetes, is involved in the suppression of JNK signalling in the invaded *A. gambiae* midgut epithelial cells and thus inhibit parasite nitration and subsequent clearance by the complement-like system (Molina-Cruz *et al.*, 2013; Ramphul *et al.*, 2015). Interestingly, KO lines cannot reach the oocyst stage unless key factors of the complement like pathway, such as TEP1 and LRIM1, are silenced. This function *Pf*s47 is shared by its *P. berghei* homologue which protects ookinetes from complement-like reactions, in addition to playing an important role in gamete fertilisation (Ukegbu *et al.*, 2017b). *P. berghei* c43 has been also shown to facilitate ookinete immune evasion, by an unknown yet mechanism. Similarly to P47, only when silencing key components of the complement system Δc43 oocyst formation is restored (Ukegbu *et al.*, 2020).

Previous *in vivo* transcriptional profiling studies using both laboratory *P. berghei* and field *P. falciparum* populations in *A. gambiae* and *A. arabiensis* mosquitoes during the critical gametocyte-to-ookinete-to-oocyst developmental transition stages, identified a number of additional *Plasmodium* genes that are expressed during the midgut and specifically at the ookinete stages and thus, thought to assist parasites in evading or tolerating the mosquito complement reactions (Akinosoglou *et al.*, 2015). From these, six genes encoding membrane-bound or secreted proteins were selected for a comparative functional characterisation. *P47* and its homologue *P48/45* are female and male gametocyte specific genes, respectively, belonging to the 6-cys protein family which is known to be important for cell-to-cell interactions. Specifically, they have been previously shown to be important for gametes *in vitro* fertilisation (van Dijk *et al.*, 2001; van Dijk *et al.*, 2010), with *P. berghei* P47 to be also involved during gametes *in vivo* fertilisation in the mosquito midgut lumen (Ukegbu *et al.*, 2017b). *c43* encodes a GPI anchored protein with two conserved cysteines close to its C-terminal and, it is localised on the ookinete and sporozoite surface. Previous work in the lab showed that it is needed for both ookinetes evasion from the mosquito complement-

like responses and oocysts sporogonic development (Ukegbu *et al.*, 2020). Additionally, *PIMMS2* encodes an ookinete specific protein with structural similarities to the subtilisin-like protein family which was shown to be important for ookinete invasion in the *A. gambiae* midgut epithelium (Ukegbu *et al.*, 2017a). The *ΔPIMMS2* parasite line has been chosen to be used due to the inability of the parasite to traverse the mosquito midgut epithelium and thus, to directly face the components of the complement system circulating in the mosquito haemolymph. Lastly, *c01* and *c57* are highly transcribed at the ookinete stages (Akinosoglou *et al.*, 2015) and they encode a putatively secreted and a membrane-bound protein, respectively (**Figure 5.1**).

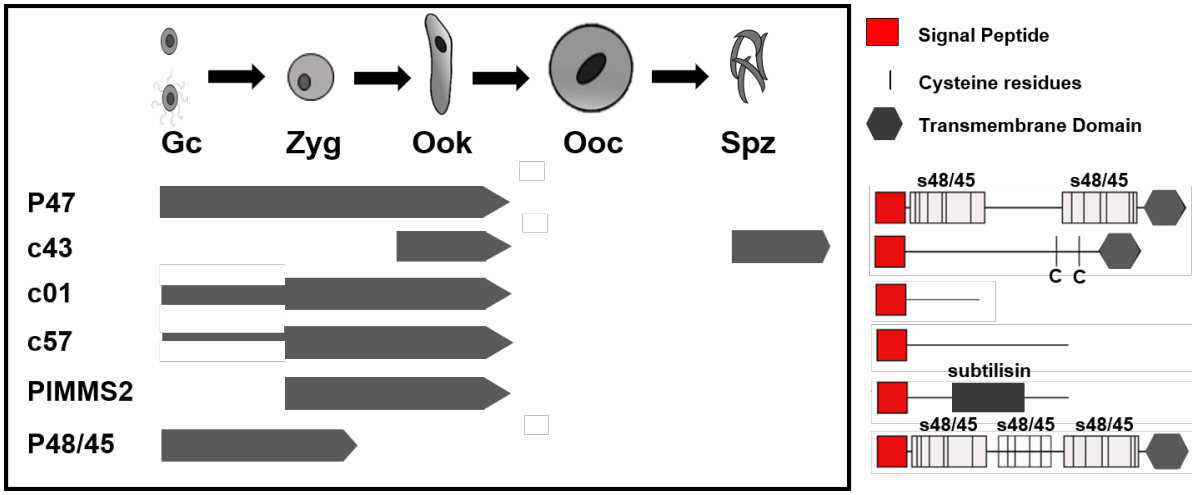

Figure 5.1. *P. berghei P47*, *c43*, *c01*, *c57*, *PIMMS2* and *P48/45* transcription pattern and schematic protein models. The transcription pattern of *P47* (van Dijk *et al.*, 2010), *c43* (Ukegbu *et al.*, 2020), *c01*, *c57*, *PIMMS2* (Ukegbu *et al.*, 2017a) and *P48/45* (van Dijk *et al.*, 2001) (left panel) is shown during different distinct stages of parasite development in the mosquito vector. The schematic protein models (right panel) of all genes were generated by *in silico* sequence analysis of their amino acid sequences. The predicted signal peptide (SP; red squares), GPI-anchored transmembrane domain (TM; blue hexagons), subtilisin-like domain for PIMMS2 and the characteristic 6-cys family s48/45 domains for the proteins P47 and P48/45, are shown. The conserved cysteine residues of P47, c43 and P48/45 are also shown. The length of each gene model is proportional to its length of amino acids.

It has been already shown that *c01*, *c43*, *P47*, *c57* and *P48/45* disruption leads to ookinetes that traverse the mosquito midgut epithelium but are eliminated from complement reactions upon reaching the basal sub-epithelial space. When genes encoding key components of the complement-like system are silenced, such as *LRIM1*

or *TEP1*, oocyst formation is restored (Ukegbu *et al.*, 2020; Ukegbu *et al.*, 2020; Giorgalli *et al.*, unpublished). A key hypothesis that I set to investigate was whether such ookinete surface proteins have a role in assisting parasites to endure the complement system attacks. According to this hypothesis, the lack of any of these proteins would lead to modifications of the ookinete surface to the extent that they are susceptible to the responses triggered by the complement-like system. Because some of these proteins have already been shown to have developmental (e.g. P47, c43) or other physiological functions (e.g. PIMMS2), a related hypothesis is that mutant parasites exhibit compromised fitness which makes them susceptible to reactions of the complement system. Therefore, by performing a comparative analysis of *P. berghei* lines lacking *c01*, *c43*, *P47*, *c57*, *P48/45* or *PIMMS2*, I set to elucidate the impact of *Plasmodium* immunity-mediated bottleneck observed in the mosquito midgut and, to investigate the model supporting that specific parasite proteins mediate parasite evasion or endurance of the complement responses.

5.2 Results

5.2.1 Comparative analysis of mutant *P. berghei* lines in *A. coluzzii* infections

Plasmodium genes expressed during the critical stage of gametocyte-to-ookinete-to-oocyst transition are either essential for the parasite morphological and physiological development or are potential modulators of the mosquito anti-*Plasmodium* mounted immune responses. It has been already shown that *P. berghei* parasites lacking expression of *c01*, *c43* (Ukegbu *et al.*, 2020), *P47* (Ukegbu *et al.*, 2017b), *c57*, *P48/45* (van Dijk *et al.*, 2001; van Dijk *et al.*, 2010) and *PIMMS2* (Ukegbu *et al.*, 2017a) undergo dramatic losses at the oocyst stages. Here, a comparative analysis of their ability to form oocysts is presented (**Figure 5.2; Table 5.1**).

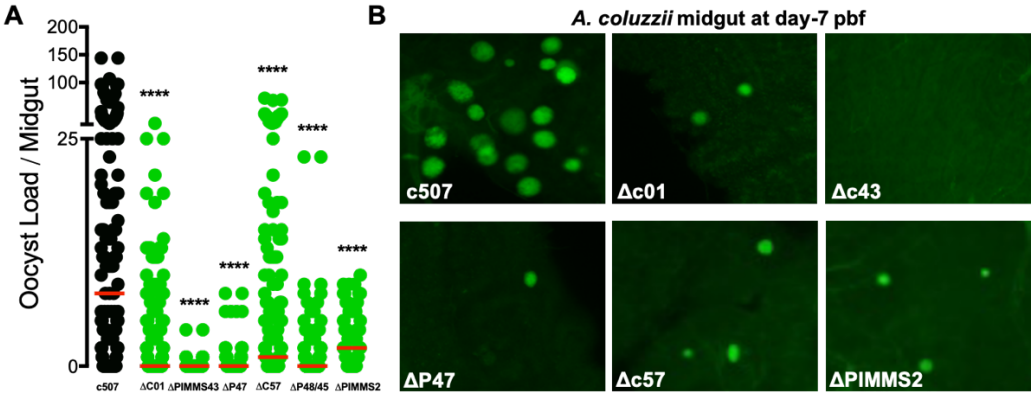

Figure 5.2. Phenotypic analysis of the *Δc01*, *Δc43*, *ΔP47*, *Δc57*, *ΔP48/45*, *ΔPIMMS2 P. berghei* parasite lines in *A. coluzzii* mosquitoes. (A) Oocyst load of

the *Δc01*, *Δc43*, *ΔP47*, *Δc57*, *ΔP48/45* and *ΔPIMMS2* parasite lines in the midguts of infected *A. coluzzii* mosquitoes at day-7 pbf. Infection with the *P. berghei* the ANKA *c507* (WT) line served as a control. The presented data derived from four biological replicates (n). Red lines indicate the median oocyst intensity. Statistical significance was calculated using the Mann Whitney U-test (P>0.0001). Infection prevalence (IP) corresponds to the percentage of the infected midguts that appeared to have at least one oocyst. **(B)** Fluorescent microscopy images of *GFP*-expressing oocysts, representative for the infection intensity of each mutant and WT parasite lines in the midguts of *A. coluzzii* mosquitoes. Images were taken at X200 magnification.

It has been previously shown that *P. berghei ΔP47* and *ΔP48/45* mutant parasites while producing normal numbers of mature gametocytes during their blood stage development, go through 99.9% reduction in their *in vitro* (van Dijk *et al.*, 2001; van Dijk *et al.*, 2010) and *in vivo* (Ukegbu *et al.*, 2017b) fertilisation capacity. On the contrary, disruption of c43 does not influence the ability of *P. berghei* gametes to fertilise (Ukegbu *et al.*, 2020). To comparatively investigate the ability of the *P. berghei Δc01*, *Δc43, ΔP47, Δc57*, *ΔPIMMS2* and *ΔP48/45* gametes to successfully fuse and form ookinetes *in vivo*, measurement of their gametocyte-to-ookinete conversion rates in the *A. coluzzii* midgut bolus at 17-18 hours pbf were assessed. The *in vivo* fertilisation capacity of the *ΔPIMMS2* parasites was examined for the first time here, whereas mosquito infection with the ANKA *c507* (WT) *P. berghei* line served as a control. The mutant lines lacking expression of *c43* and *PIMMS2* appeared to have gametocyte-to-ookinete conversion rates similar to the WT, ranging from 78% to 83% (mean value 80%) in *Δc43*, 80% to 82% (mean value 81%) in *ΔPIMMS2* and 80% to 87% (mean value 84%) in WT. However, a significant 5-fold and 14-fold difference ($p<0.0001$) in the gametocyte-to-ookinete conversion rate was observed for the *ΔP47* and *ΔP48/45* lines ranging from 14% to 18% (mean value 16%) in *ΔP47* and 3% to 7% (mean value 6%) in *ΔP48/45* parasites. These results, also, partially confirm what was previously observed during *in vitro* fertilisation i.e. even if reduced conversion rates were determined *in vivo*, these values are noticeably higher compared to the 0.1% conversion rate determined *in vitro* for the two lines (van Dijk *et al*., 2010). Less dramatic reduction was observed in the fertilisation rates of the *Δc01* and *Δc57* lines ranging from 53% to 62% (mean value 56%) in *Δc01* and 45% to 50% (mean value 47%) in *Δc57* parasites (**Figure 5.3, A; Table 5.2**).

Despite the reduced fertilisation capacity of some mutant parasite lines, the previous results confirmed that all mutant *P. berghei* parasites are able to more or less produce ookinetes. Going a step further, to investigate whether oocysts elimination is related to ookinete related defects occurred before, during or immediately after midgut epithelium traversal, the ookinete load of the mutants and WT parasite lines found on *A. coluzzii* midgut epithelium was determined. Mosquito midguts were dissected at 25-26 hours pbf, a time that coincides with ookinete midgut epithelium traversal, and ookinetes were visualised after staining with an antibody against their P28 surface protein (Sidén-Kiamos *et al.*, 2000). The median number of WT, *Δc01*, *Δc43*, *ΔP47*, *Δc57*, *ΔP48/45* and *ΔPIMMS2* invading ookinetes was 333, 282, 298, 180, 258, 15 and 332, respectively (**Figure 5.3, B; Table 5.3**). It is thus clear that the reduced gametocyte-to-ookinete conversion rate of *Δc01*, *Δc57*, *ΔP47* and *ΔP48/45* parasites affected the total number of ookinetes invaded the midgut epithelium.

Additionally to the P28-positive ookinete counting, staining of SRPN6, a malaria parasite invasion marker in mosquitoes (Abraham *et al.*, 2005), was also performed in order to confirm successful ookinete invasion of the midgut epithelial cells. As illustrated by the images, all mutant and WT invading ookinetes are in close proximity or within SRPN6-positive cells suggesting that they are all able to successfully enter the mosquito midgut epithelial cells (**Figure 5.3, C**). To conclude, these results confirm that *Δc01*, *Δc43*, *ΔP47*, *Δc57*, *ΔP48/45* and *ΔPIMMS2* ookinetes are capable of invading the mosquito midgut epithelium. Furthermore, the number of invading ookinetes is relative to the number of ookinetes initially formed in the midgut lumen, which varies due to the different fertilisation capacity of each mutant parasite line.

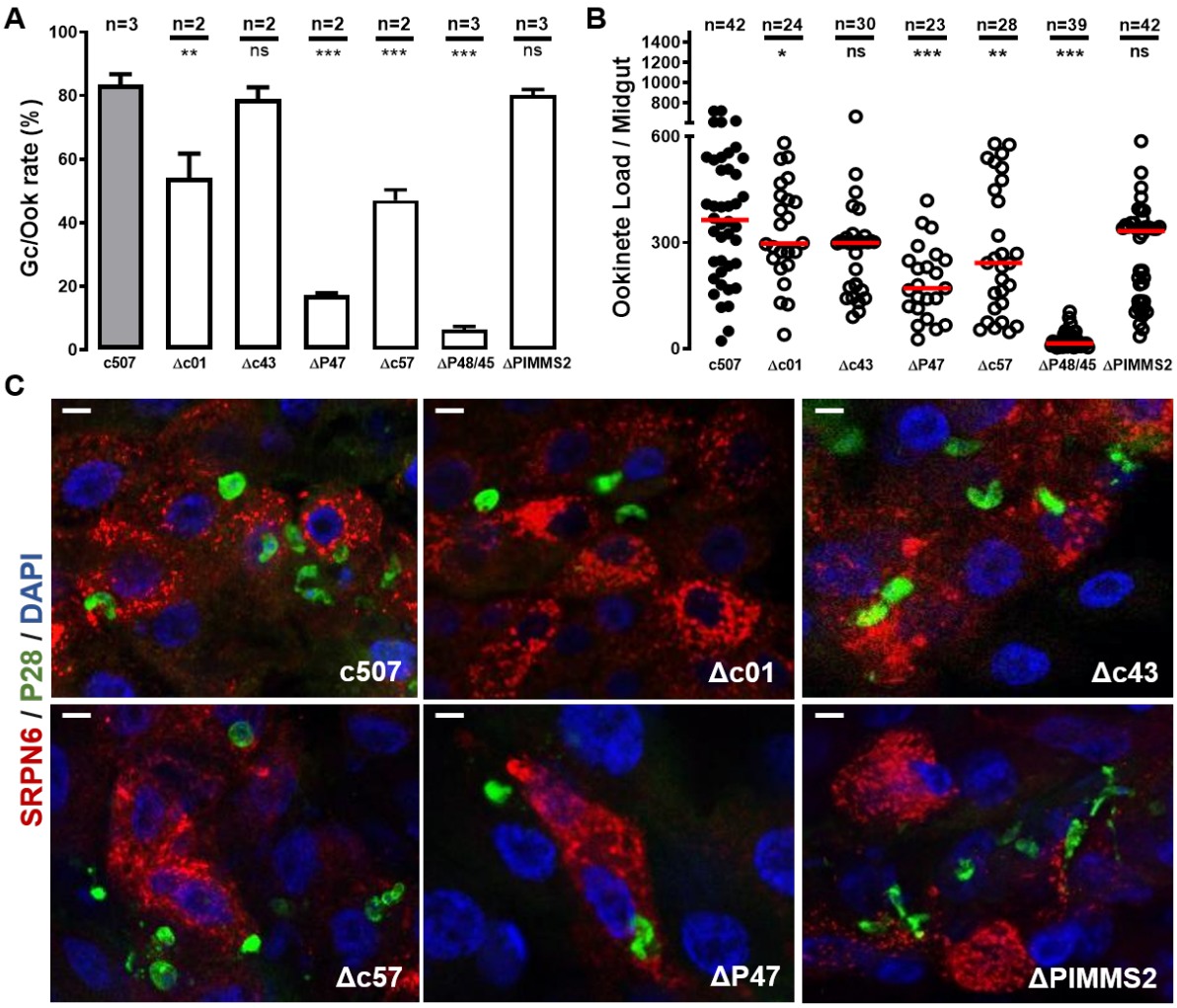

Figure 5.3. *Δc01*, *Δc43*, *ΔP47*, *Δc57*, *ΔP48/45* and *ΔPIMMS2* parasite development in the mosquito midgut lumen and traversal of the mosquito midgut epithelium. **(A)** *In vivo* gametocyte-to-ookinete (Gc/Ook) conversion rates of mutant *P. berghei* lines in the midgut lumen of *A. coluzzii* mosquitoes. Mosquito infection with the *P. berghei c507* (WT) line served as a control. The number of biological replicates (n) and standard error are shown. Statistical significance was determined with a two-tailed, unpaired Student's *t*-test. **(B)** Load of invading ookinetes in the midguts of *A. coluzzii* mosquitoes at 24-25 hours pbf. Red lines show the median ookinete load; n is the total number of midguts examined. Statistical significance was determined using the Mann Whitney U-test. **(C)** Fluorescent images of ookinete-invaded *A. coluzzii* midgut epithelial cells stained with the SRPN6 antibody (red), at 25-26 hours pbf. Ookinetes are stained with the P28 antibody (green), whereas DAPI (blue) was used to stain the ookinetes and the midgut epithelium cells nuclei. Images were taken at X400 magnification. Representative image of the *ΔP48/45* invading ookinetes are not shown due to the small number of ookinetes found in the midgut. Scale bar is 20 μm.

Table 5.1. *P. berghei Δc01*, *Δc43*, *ΔP47*, *Δc57*, *ΔP48/45*, *ΔPIMMS2* and control ANKA *c507* (WT) oocyst load in naive *A. coluzzii* infections at day-7 pbf

Parasite line	Number of experiments	Number of midguts	Prevalence (%)	*p*-value	Infection Intensity		Parasite range	*p*-value
					Arithmetic mean	Median		
c507 (WT)	4	151 (113/38)	74.83		19.66	8.00	0-144	
Δc01	4	145 (68/77)	46.90	<0.0001	3.58	0.00	0-27	<0.0001
Δc43	4	166 (0/166)	0.00	<0.0001	0.00	0.00	0-0	<0.0001
ΔP47	4	165 (37/128)	22.42	<0.0001	0.49	0.00	0-8	<0.0001
Δc57	4	166 (101/65)	60.84	0.0084	6.96	1.00	0-72	<0.0001
ΔP48/45	4	166 (53/113)	31.93	<0.0001	1.17	0.00	0-23	<0.0001
ΔPIMMS2	4	101 (68/33)	67.33	0.2018	2.49	2.00	0-10	<0.0001

Δc01, *Δc43*, *ΔP47*, *Δc57*, *ΔP48/45*, *ΔPIMMS2* and WT parasite infections of naive *A. gambiae* mosquitoes was assessed 7-8 days pbf. Number of midguts is shown as the ratio between the number of infected midguts to the number of uninfected midguts. Statistical significance of the oocyst load was determined using the Mann Whitney U-test. Statistical significance of the prevalence percentages was assessed by Fisher's exact test (ns, non-significant).

Table 5.2. *In vivo* gametocyte-to-ookinete (Gc/Ook) conversion rates of *Δc01*, *Δc43*, *ΔP47*, *Δc57*, *ΔP48/45*, *ΔPIMMS2* and control ANKA *c507* (WT) parasite lines in naïve *A. coluzzii* mosquitoes

Parasite line	Number of experiments	No of midguts / Replicate	Number of Macrogametes	Number of Ookinetes	Fertilisation Rate (%)	Reduction (%)	*p*-value
c507 (WT)	3	10	1136	3303	83.49		
Δc01	2	10	934	1056	56.16	32.74	<0.0001
Δc43	2	10	219	620	79.73	4.50	0.2136
ΔP47	2	10	1735	305	16.42	80.33	<0.0001
Δc57	2	10	1154	1192	47.47	43.15	<0.0001
ΔP48/45	3	10	694	34	5.66	93.23	<0.0001
ΔPIMMS2	3	10	265	611	80.72	3.32	0.9803

The *in vivo* gametocyte-to-ookinete (Gc/Ook) conversion rates were calculated as the percentage of P28-positive ookinetes to the total number of the P28-positive macrogametes and ookinetes together. The conversion rates were calculated from suspensions of 10 homogenised midguts, assayed 16-17 hours pbf. Statistical significance was determined with a two-tailed, unpaired Student's *t*-test (ns, non-significant).

Table 5.3. Number of P28-positive *Δc01*, *Δc43*, *ΔP47*, *Δc57*, *ΔP48/45*, *ΔPIMMS2* and control ANKA *c507* (WT) ookinetes in the midguts of *A. coluzzii* mosquitoes

Parasite line	Number of experiments	No of midguts	P28+ ookinete range	Infection Intensity		*p*-value	Standard Error	Fold Change
				Arithmetic mean	Median			
c507 (WT)	3	42	22-700	371.40	364.50		27.66	
Δc01	2	24	40-542	329.10	297.50	0.2345	28.61	0.82
Δc43	2	30	90-575	277.60	339.50	0.0032	22.76	0.93
ΔP47	2	23	27-392	188.10	171.00	<0.0001	21.57	0.47
Δc57	2	28	47-533	277.70	242.50	0.1232	34.69	0.66
ΔP48/45	3	39	3-102	25.00	15.00	<0.0001	3.82	0.04
ΔPIMMS2	3	42	35-552	268.20	332.50	0.0456	20.65	0.91

P28-positive ookinetes in the mosquito midgut were enumerated at 24-26 hours post mosquito blood feeding using fluorescence microscopy. Statistical significance was calculated using a two-tailed, Student's *t*-test (ns, non-significant). The fold difference was calculated based on the median number of P28-positive KO ookinetes against WT.

5.2.2 *Δc01*, *Δc43*, *ΔP47*, *Δc57, ΔP48/45* and *ΔPIMMS2* ookinetes traversal through *A. coluzzii* midgut epithelium

Δc01, *Δc43*, *ΔP47*, *Δc57*, *ΔP48/45* and *ΔPIMMS2* parasites display morphologically normal ookinetes in the mosquito midgut lumen, which are able to successfully enter its midgut epithelium. However, these ookinetes undergo dramatic losses at the oocyst stage with some of them dropping down to zero levels.

Going a step further, to establish that the mutant KO ookinetes are killed immediately after midgut epithelium traversal, infection of *CTL4*-silenced and control ds*LacZ*-injected mosquitoes with the mutant parasite lines was performed. Reducing *A. coluzzii CTL4* levels leads to melanisation of all complement-targeted ookinetes, in this way providing a powerful assay to assess successful midgut traversal (Osta *et al.*, 2004a). Since this reaction occurs immediately after ookinetes have traversed the midgut epithelium, this method can be used to readily visualise the dead ookinetes. Mosquito infection with the ANKA *c507* (WT) *P. berghei* line served as a control.

The results revealed that *Δc01*, *Δc43*, *ΔP47*, *Δc57* and *ΔP48/45* ookinetes undergo melanisation as soon as they traverse the mosquito midgut epithelial wall. Most intriguingly, however, only a tiny fraction of *ΔPIMMS2* ookinetes were able to traverse the midgut epithelium and reach the haemolymph before undergoing melanisation (**Figure 5.4; Table 5.4**). The number of *Δc01*, *Δc43*, *ΔP47*, *Δc57* and *ΔP48/45* and WT melanised ookinetes that infected the same batch of *CTL4*-knockdown mosquitoes was analogous to the number of P28-positive ookinetes counted for each line during invasion assays, and largely depend on the fertilisation capacity of each line. The median number of *ΔPIMMS2* melanised ookinetes counted was only 7 ± 1.45 ookinetes per mosquito, compared to the WT median which was determined to be 65 ± 12.9 ookinetes per mosquito. Considering that the number of *ΔPIMMS2* P28-positive ookinetes previously determined in *A. coluzzii* midguts at 24 hours pbf was similar to that of the WT, this indication clearly shows that ookinetes lacking expression of *PIMMS2* are incapable of reaching the basal side of the cell, presumably due to developmental defects occurring before exiting the midgut epithelium. These data also let us to conclude that *Δc01*, *Δc43*, *ΔP47*, *Δc57* and *ΔP48/45* ookinetes are capable of successfully entering and later traversing the mosquito midgut epithelial cells. No melanised ookinetes were observed in the midguts of infected ds*LacZ*-injected *A. coluzzii*, further supporting the function of CTL4 (Osta *et al.*, 2004a).

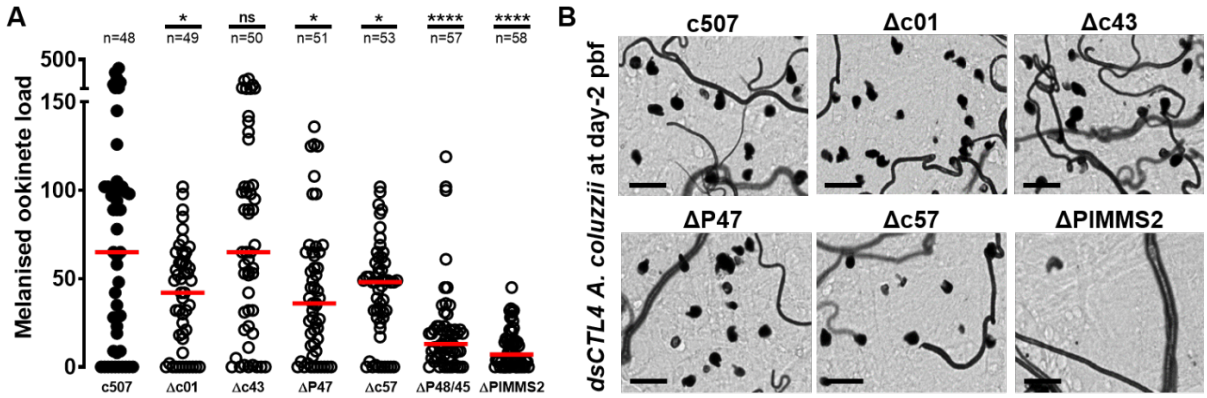

Figure 5.4. *Δc01*, *Δc43*, *ΔP47*, *Δc57*, *ΔP48/45* and *ΔPIMMS2* infections in *CTL4*-silenced *A. coluzzii* mosquitoes. (A) Graph indicating the number of mutants and WT (control) parasites counted in the individual midguts of previously *CTL4*-silenced *A. coluzzii* mosquitoes, 2 days pbf. Horizontal red bars indicate the median, where n is the number of midguts examined. The presented data derived from two individual biological replicates. Two-tailed P-values by Mann Whitney U-test are also shown. **(B)** Light microscopy images illustrate melanised *Δc01*, *Δc43*, *ΔP47*, *Δc57* and *ΔPIMMS2* *P. berghei* ookinetes in *CTL4*-silenced *A. coluzzii* mosquito midguts at day-2 pbf. Images were taken at X100 magnification. Scale bar is 40 μm.

5.2.3 The implication of *A. coluzzii* complement-like system in *Δc01*, *Δc43*, *ΔP47*, *Δc57*, *ΔP48/45* and *ΔPIMMS2* ookinetes elimination

P. berghei Δc01, *Δc43*, *ΔP47*, *Δc57*, *ΔP48/45* and *ΔPIMMS2* parasites display morphologically normal ookinetes which are able to successfully invade the *A. coluzzii* midgut epithelium. Apart *ΔPIMMS2* parasites, all other mutant ookinetes are capable of traversing the midgut wall and make their way to its basal side. These ookinetes though undergo dramatic losses at the oocyst stage, with some of them dropping down to zero levels. When silencing key components of the complement system, oocyst development is restored (Ukegbu *et al.*, 2017b; Ukegbu *et al.*, 2020; Giorgalli *et al.*, unpublished). Thus, parasites clearance is associated with the mosquito immune responses taking at the basal side of the mosquito midgut epithelium.

To comparatively investigate the complement activity during the elimination of the mutant ookinetes right after midgut traversal, the TEP1 activity on the basal side of the midgut wall was quantified. Specifically, midgut epithelia of naïve mosquitoes infected with the *Δc01*, *Δc43*, *ΔP47*, *Δc57*, *ΔP48/45*, *ΔPIMMS2* and WT (control) parasites were dissected at 28 - 30 hours pbf, a time-point that coincides with ookinetes midgut

traversal through the mosquito midgut epithelium, and stained with antibodies against the mosquito haemolymph-derived protein TEP1 (Blandin *et al.*, 2004) and the parasite P28 surface protein (Sidén-Kiamos *et al.*, 2000). Whilst both live and dead ookinetes exhibit P28 on their surface, TEP1 marks only ookinetes that are lead to death by either lysis or melanisation (Blandin *et al.*, 2004). Thus, differentiation between all (P28+/TEP1- and P28+/TEP1+) and dead (P28+/TEP1+) ookinetes can be obtained (Povelones *et al.*, 2009). Several independent biological replicate infections were carried-out where a total of 6916 (23 midguts) *Δc01*, 7829 (23 midguts) *Δc43*, 8641 (37 midguts) *ΔP47*, 6309 (22 midguts) *Δc57*, 532 (25 midguts) *ΔP48/45*, 3242 (15 midguts) *ΔPIMMS2* and 44329 (47 midguts) WT (control) ookinetes were analysed. The results showed that the proportion of TEP1-marked *Δc43* (mean value 88.15% ± 5.17%) and *ΔP47* (mean value 91.27% ± 3.91%) (Ukegbu *et al.*, 2017b; Ukegbu *et al.*, 2020) was significantly higher ($p<0.0001$) than the proportion of TEP1-stained WT control ookinetes (mean value 79.85% ± 5.73%), whereas the proportion of TEP1-marked *Δc01* (mean value 81.02% ± 5.17%), *Δc57* (mean value 79.98% ± 8.11%) and *ΔP48/45* (mean value 69.88% ± 9.76%) was slightly higher but yet, not significantly different to the WT parasites. Only 14.29% ± 4.50% of the *ΔPIMMS2* ookinetes were found to be targeted by the TEP1 antibody (**Figure 5.5, A; Table 5.5**). These data suggest that similar levels of TEP1-binding constitute to the elimination of the *Δc01*, *Δc43*, *ΔP47*, *Δc57*, *ΔP48/45* ookinetes immediately after midgut traversal. Therefore *Δc01*, *Δc43*, *ΔP47*, *Δc57* and *ΔP48/45* ookinetes survival is largely dependent on the complement-like responses, but some developmental defects may also accompany their elimination. Interestingly, *ΔPIMMS2* ookinetes were not highly marked by TEP1-binding. Together with previous findings indicated that *ΔPIMMS2* ookinetes are able to invade the *A. coluzzii* midgut epithelium, this let us conclude that the reduced TEP1-mediated killing is related with the fact that mutant ookinete development is terminated before parasite exposure to haemolymph components.

It has been previously shown that when silencing the mosquito complement-like system, the number of some of the live mutant oocysts dramatically increase (Ukegbu *et al.*, 2017b; Ukegbu *et al.*, 2020). To comparatively investigate the impact of the complement system in eliminating the different mutant lines, *LRIM1*-silenced and ds*LacZ*-injected (control) mosquitoes were infected with all mutant parasite lines prior to oocyst count at day-7 pbf. Parallel infection with the parental WT *P. berghei* line was carried out as a control to the gene silencing effect. The median intensities of

infection with the *Δc01*, *Δc43*, *ΔP47*, *Δc57*, *ΔP48/45*, *ΔPIMMS2* and WT in ds*LacZ*-injected mosquitoes were 1 (prevalence 52%), 0 (prevalence 3%), 0 (prevalence 62%), 1 (prevalence 58%), 0 (prevalence 33%), 2 (prevalence 69%) and 15 (prevalence 84%), respectively. The median intensities of infection with the *Δc01*, *Δc43*, *ΔP47*, *Δc57*, *ΔP48/45*, *ΔPIMMS2* and WT in *LRIM1*-silenced mosquitoes were 28 (prevalence 87%), 64 (prevalence 83%), 49 (prevalence 86%), 9 (prevalence 75%), 3 (prevalence 68%), 28 (prevalence 90%) and 125 (prevalence 90%), respectively (**Figure 5.6, A; Table 5.6**). These results clearly show that in all cases, when silencing the complement-like system, oocyst formation is restored. The difference in fold change between the infection intensity in *dsLacZ* and *dsLRIM1*-injected mosquitoes varies between different mutant lines, possibly due to other developmental defects accompanying the mutants (**Figure 5.6, B**).

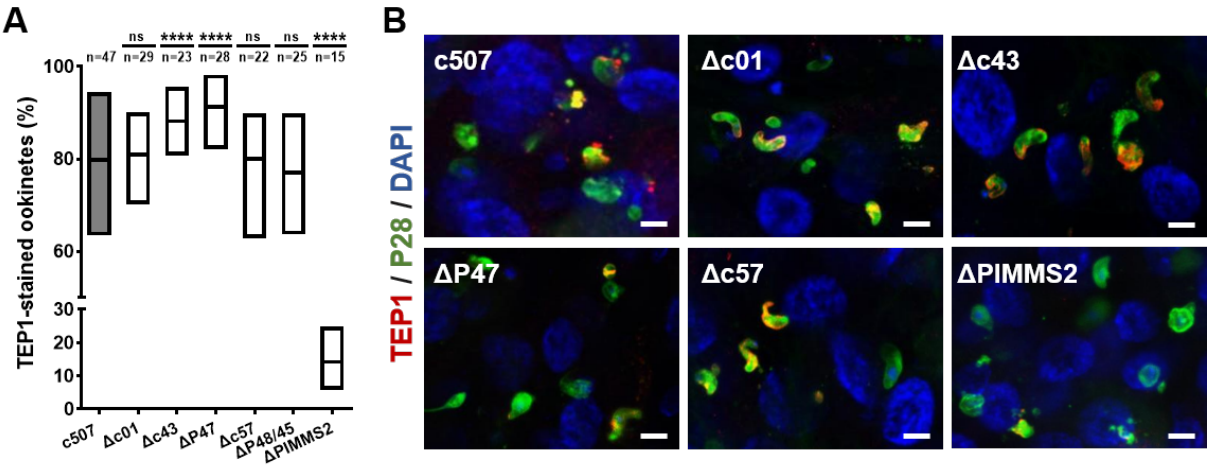

Figure 5.5. TEP1-mediated elimination of *Δc01*, *Δc43*, *ΔP47 Δc57*, *ΔP48/45* and *ΔPIMMS2 P. berghei* ookinetes right after midgut traversal. (A) Box plots showing the percentage of *Δc01*, *Δc43*, *ΔP47 Δc57*, *ΔP48/45* and *ΔPIMMS2* ookinetes that were positive for both TEP1 and P28 (TEP1+/P28+) antibody staining, out of the total P28 (P28+) stained ookinetes. Mosquito infection with the *c507* (WT) line served as a control. The median number, the 50% percentile (box) and the range of double-stained ookinetes are shown. Data derived from at least two independent biological replicates, where n is the total number of midguts dissected for counting. Statistical significance was determined using a two-tailed, unpaired Student's *t*-test (ns, non-significant) **(B)** Fluorescent images of KO and WT *P. berghei* ookinetes in *A. coluzzii* midgut epithelia at 28-30 hours pbf, stained with either both TEP1 and P28 antibodies (red/green), or just with the P28 antibody (green). Fluorescence images are representative of two sets of experiments and were taken at X400 magnification. Scale bar is 20 μm.

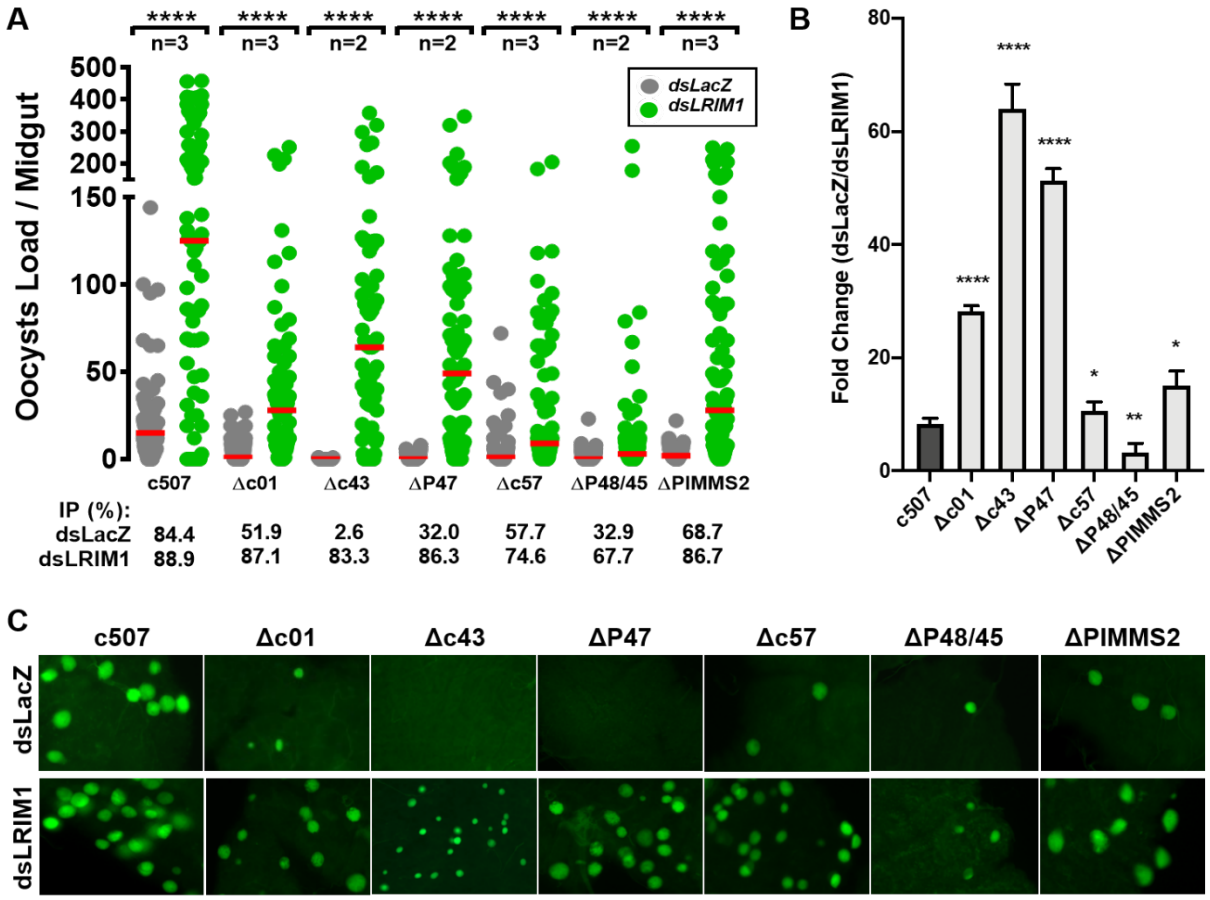

Figure 5.6. Phenotypic analysis of *Δc01*, *Δc43*, *ΔP47*, *ΔPbc57*, *ΔP48/45* and *ΔPIMMS2 P. berghei* parasite lines in *A. coluzzii* infections when silencing the mosquito complement-like system. (A) Effect of ds*LacZ* injections (control) (grey) and *LRIM1*-silencing (green) on the oocyst load of the mutant parasite lines in *A. coluzzii* infections. Mosquito infection with the *P. berghei c507* (WT) parasites served as a control. The dots represent the number of oocysts counted in the individual mosquito midguts. Red lines indicate the median oocyst intensity. For each biological replicate (n), oocyst load was determined from approximately 30 midguts per mosquito group. Infection prevalence corresponds to the percentage of the infected midguts that appeared to have at least one oocyst. Statistical significance was determined using the Mann Whitney U-test. **(B)** Fold change based on the median oocyst intensity in infected *LRIM1*-silenced and ds*LacZ*-injected *A. coluzzii* midguts. The mean fold change calculated for all biological replicates performed, is presented. Error bars show standard error. Statistical significance was determined using a two-tailed, unpaired Student's *t*-test. **(C)** Representative fluorescent images of oocysts in ds*LacZ*-injected and *LRIM1*-silenced mosquito midguts infected with the various KO mutants or WT parasites. Images were taken at X200 magnification. Scale bar is 20 μm.

Table 5.4. Melanised *Δc01*, *Δc43*, *ΔP47*, *Δc57*, *ΔP48/45*, *ΔPIMMS2* and control ANKA *c507* (WT) ookinetes in *CTL4* knockdown *A. coluzzii* mosquitoes

Parasite line	Number of experiments	No of midguts Total (replicate)	No of midguts with melanised ookinetes Total (replicates)	Infection Intensity		Ookinete range	*p*-value
				Arithmetic mean	Median		
c507 (WT)	2	48 (22,26)	38 (18, 20)	81.90	65.00	0-398	
Δc01	2	49 (24,25)	39 (19, 20)	40.10	42.00	0-102	0.0212
Δc43	2	50 (26, 24)	44 (23, 21)	76.34	65.00	0-269	0.7889
ΔP47	2	51 (24, 27)	42 (21, 21)	41.69	36.00	0-136	0.0428
Δc57	2	53 (26, 27)	45 (22, 23)	42.49	48.00	0-102	0.0437
ΔP48/45	2	57 (28, 29)	48 (25, 23)	19.79	13.00	0-119	<0.0001
ΔPIMMS2	2	58 (28, 30)	44 (19, 25)	10.34	7.00	0-45	<0.00001

The table shows the number of *Δc01*, *Δc43*, *ΔP47*, *Δc57*, *ΔP48/45*, *ΔPIMMS2* and WT melanised parasites in two independent biological replicates in the midguts of *CTL4*-silenced *A. coluzzii* mosquitoes, 2-3 days pbf. Statistical significance for the median ookinete load was determined using the Mann Whitney U-test (non-parametric test).

Table 5.5. Number of TEP1-positive *Δc01*, *Δc43*, *ΔP47*, *Δc57*, *ΔP48/45*, *ΔPIMMS2* and control ANKA *c507* (WT) ookinetes in the midguts of *A. coluzzii* mosquitoes

Parasite line	Number of experiments	No of midguts	TEP1+/P28+ ookinetes	TEP1-/P28+ ookinetes	Total No of ookinetes	Ookinete percentage (%)	Standard Error	*p*-value
c507 (WT)	3	47	35,054	9,275	44,329	79.85	0.84	
Δc01	3	29	5,673	1,243	6,916	81.02	1.08	0.4131
Δc43	2	23	7,123	706	7,829	88.15	1.11	<0.0001
ΔP47	2	28	7,924	717	8,641	91.27	0.64	<0.0001
Δc57	3	22	5,110	1,199	6,309	79.98	1.73	0.9398
ΔP48/45	3	25	408	124	532	77.07	1.17	0.0560
ΔPIMMS2	3	15	457	2,785	3,242	14.19	1.16	<0.0001

TEP1/P28-positive *Δc01*, *Δc43*, *ΔP47*, *Δc57*, *ΔP48/45*, *ΔPIMMS2* and WT ookinetes were enumerated at 28-30 hours pbf in the midgut of *A. coluzzii*, using fluorescence microscopy. The ookinete percentage (%) was calculated as the ratio of the TEP1+/P28+ ookinetes to the total number of ookinetes counted (stained for both TEP1+/P28+ and single P28+). Statistical significance was determined using a two-tailed, unpaired Student's *t*-test (ns, non-significant).

Table 5.6. Effect of *LRIM1*-silencing on *P. berghei Δc01*, *Δc43*, *ΔP47*, *Δc57*, *ΔP48/45*, *ΔPIMMS2* and control ANKA *c507* (WT) infections in *A. coluzzii* mosquitoes

Parasite line	dsRNA	Number of exp.	Midguts number	Prevalence (%)	*p*-value	Infection Intensity		Parasite range	Fold Change	*p*-value
						Arithmetic mean	Median			
c507 (WT)	*LacZ*	3	77 (65/12)	84.41		20.99	15.00	0-144		
	LRIM1		81 (72/9)	88.89	0.4851	161.7	125.0	0-458	8.33	<0.0001
Δc01	*LacZ*	3	77 (40/37)	51.94		3.96	1.00	0-27		
	LRIM1		70 (61/9)	87.14	<0.0001	43.41	28.00	0-251	28.0	<0.0001
Δc43	*LacZ*	2	77 (2/74)	2.60		0.04	0.00	0-1		
	LRIM1		66 (55/11)	83.33	<0.0001	77.77	64.00	0-358	>64.0	<0.0001
ΔP47	*LacZ*	2	78 (25/53)	32.05		0.92	0.00	0-8		
	LRIM1		73 (63/10)	86.30	<0.0001	66.04	49.00	0-347	49.0	<0.0001
Δc57	*LacZ*	3	71 (41/30)	57.74		5.80	1.00	0-72		
	LRIM1		71 (53/18)	74.65	0.0504	32.21	9.00	0-205	9.0	<0.0001
ΔP48/45	*LacZ*	2	88 (29/59)	32.95		1.10	0.00	0-23		
	LRIM1		74 (50/24)	67.57	<0.0001	14.77	3.00	0-254	>3.0	<0.0001
ΔPIMMS2	*LacZ*	3	96 (66/30)	68.75		2.85	2.00	0-22		
	LRIM1		97 (87/10)	89.70	0.0130	57.18	28.00	0-250	14.0	<0.0001

P. berghei Δc01, *Δc43*, *ΔP47*, *Δc57*, *ΔP48/45*, *ΔPIMMS2* and WT parasite infections of *LRIM1*-silenced *A. coluzzii* mosquitoes was assessed at day-7 pbf. Infection of ds*LacZ*-injected mosquitoes were used as control. Number of midguts is shown as the ratio between the number of infected midguts to the number of uninfected midguts. Statistical significance for the median oocyst load was determined using the Mann Whitney U-test between the *dsLacZ*- and *dsLRIM1*-modified mosquito datasets for each parasite line, whereas statistical significance of the prevalence percentages was assessed by Fisher's exact test (ns, non-significant). Fold change was calculated based on the median oocyst intensity (some of the datasets (*Δc43*, *ΔP48/45* and *ΔPIMMS2*) follow the normal distribution pattern as determined by the D'Agostino and Pearson normality test, however, since the number of non-homogenous groups is more than the homogenous groups, the median oocyst intensity was used to determine the fold change between the *dsLacZ*- and *dsLRIM1*-injected infection intensities).

5.2.4 Experimental selection of mutant alleles in *P. berghei* KO populations following serial passages through *A. coluzzii* mosquitoes

The next question to consider was to identify what makes these mutant ookinetes susceptible to the complement-like system. One thing that all these genes have in common is that they are all associated with developmental processes occurring during midgut infection and that their KO leads to loss of parasite fitness. It is known that such genes are under strong selection pressure that removes deleterious gene alterations from the population. Failing that, it could be that specific interactions of these proteins with components of the mosquito immune system might facilitate parasite immune evasion and eventually, survival and completion of their lifecycle within the mosquito vector. Hence, these genes might function similarly to P47 - previously found to suppress JNK signalling within the invaded midgut epithelial cells, and in this way inhibiting parasite clearance by the complement (Molina-Cruz *et al.*, 2013).

I went to examine whether the mosquito complement-like system acts as this filtering mechanism. To do so, a continuous artificial short-term selection pressure was employed on multiple *P. berghei* mutant parasites, with the aim to identify potential removal of specific mutant alleles. Briefly, I mixed all six *Δc01*, *Δc43*, *ΔP47*, *Δc57*, *ΔP4845* and *ΔPIMMS2* mutant parasite lines in a single mouse and performed serial mouse-to-mosquito-to-mouse transmission cycles through either ds*LacZ*-injected (control) or complement-silenced *A. coluzzii* mosquitoes. These mosquito immune backgrounds were selected so as to achieve different levels of selection pressure affecting parasite survival; when in *LRIM1*-silenced mosquitoes, the selection pressure is minimised and thus most of the ookinetes successfully develop into oocysts, whereas in ds*LacZ*-injected mosquitoes the immune system threshold is higher and still capable of efficiently killing about 80% of the ingested parasite population (Blandin *et al.*, 2004; Osta *et al.*, 2004b). Subsequently, the infected mice of each transmission cycle were used to infect the next batch of the same group of dsRNA-injected mosquitoes and this cycle of serial mouse-to-mosquito-to-mouse infections was continued for a total of five times (**Figure 5.7, A**). Following mosquitoes next bloodmeal uptake and development of ABS in the recipient rodent host, blood was collected and gDNA was extracted. The frequency of the WT and KO alleles in the population was then monitored by qRT-PCR, using gDNA from extracted blood stage parasites as a template and primers that were specifically designed to map either on the WT or KO allele of each gene of interest (**Table 2.7**). Specifically, the

WT-specific primers were designed to map on the coding sequence of the gene of interest, whereas the KO specific primers were designed to map on the integration side between the KO cassette and the parasite unmodified genome (**Figure 5.7, B**).

Each loci abundance analysis was determined as follows; since all transgenic parasites were generated on the *c507* background line, *eGFP* was used to normalise the Ct values for each KO and WT locus determined with qRT-PCR. Following, the abundance of each allele (WT or KO) was calculated as the percentage out of the total number of alleles presented in the population i.e. the sum of all WT and KO locus abundance values together was considered to be 100% from which the abundance of the individual WT and KO alleles was then calculated. To compare whether the abundance of each WT and KO allele changes following each transmission cycle, I compared the frequency of each alleles to the initial abundance determined in the input parasite population (parasite population collected from mice used during the first mosquito infection which includes ABS and gametocytes). The calculations were performed for each replicate and for each mouse-to-mosquito-to-mouse transmission cycle, given the fact that parasites successfully transmitted back to the rodent host.

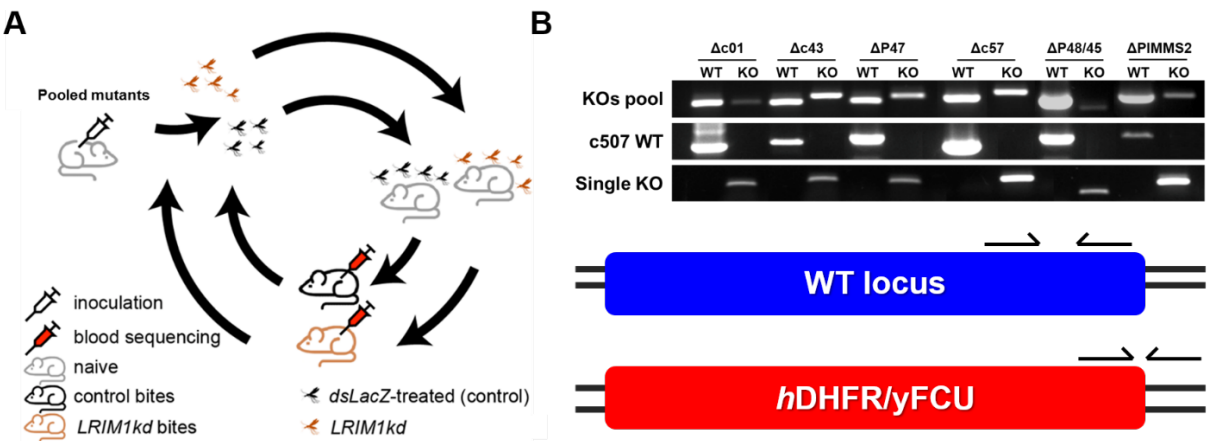

Figure 5.7. Experimental design of *P. berghei* mutants selection through *A. coluzzii* mosquitoes. (A) Experimental design of the mutant *P. berghei* parasites pool serial passaging through *LRIM1*-silenced and ds*LacZ*-injected *A. coluzzii* mosquitoes. The *Δc01*, *Δc43*, *ΔP47*, *Δc57*, *ΔP48/45* and *ΔPIMMS2* mutant parasites were mixed in a single mouse, which was used to feed complement-silenced and control ds*LacZ*-injected *A. coluzzii* mosquitoes. At day-21 pbf, the two groups of dsRNA-injected mosquitoes were allowed to individually feed on anaesthetised mice whose parasitaemia was monitored regularly following the recipient of potentially infective sporozoites. The infected mice were afterwards used to infect the next batch of the

same group of dsRNA-injected mosquitoes and this cycle of serial infections was repeated from mouse-to-mosquito-to-mouse for a total of five times. In every cycle infected blood was collected from the individual mice and gDNA extraction was performed prior to monitoring of the WT and KO alleles in the population via qRT-PCR. **(B)** PCR genotypic analysis of the *Pbc01*, *Pbc43*, *PbP47*, *Pbc57*, *PbP48/45* and *PbPIMMS2* KO and WT locus, on blood stage parasites prior to infection of the *LRIM1*-silenced and ds*LacZ*-injected (control) *A. coluzzii* mosquitoes (input population). Analysis of the WT or single KO locus served as a control as well as to show the specificity of each set of primers used later for monitoring the alleles abundance in the population. WT primers have been designed to amplify an arbitrary region of the gene, whereas KO primers were designed to map the junction between the replacement cassette (*h*DHFR/yFCU) and the WT genome. gDNA, gDNA; KOs, pooled gDNA sample extracted from all mutants that were used to infect the first batch of complement-silenced and ds*LacZ*-injected mosquitoes; KO, single KO gDNA sample extracted individually from blood stages of each mutant.

Given that 6 different KO mutants were included in the input parasite population introduced to the *A. coluzzii* mosquitoes, each KO allele is expected to be present at a rate of 2.78% in the alleles population (assuming that each mutant line is equally represented in the gametocyte stages since none of the them have any defects during gametocyte development and equal amounts of infected RBCs from each mutant line were introduced in the mice used for the first mosquito infection). Therefore, the WT allele for a specific locus is expected to be present at a rate of 13.88% i.e. the KO allele is carried only by the analogous mutant parasite, whereas the WT allele for the same locus is carried by all the other mutant parasites that are KO for a different allele. This would mean that following fertilisation in the mosquito midgut lumen, about 71.4% of the diploid zygotes would be heterozygous for two different KO alleles, whereas only 28.6% of the diploid zygotes would be homozygous for one specific KO allele (**Appendix 12**). Therefore, the ideal abundance threshold for each allele would be to be set by its frequency in the initial gametocyte input population i.e. since all parasite mosquito stages derive from them. However, a SMFA using purified gametocytes was not carried out in order to infect the *A. coluzzii* mosquitoes as any manipulation of the gametocytes prior to mosquito feed would significantly reduce their capacity for establishing a successful infection. Additionally, gametocyte-specific primers for the WT or KO alleles could not be designed for the input population qRT-PCR analysis.

Additional to the alleles frequency monitoring, quantitative data of the infection during oocyst development were collected for each transmission cycle. The median number of oocysts enumerated in the *LRIM1*-silenced mosquitoes of the first transmission cycle was significantly higher (p<0.0001) compared to the ds*LacZ*-injected control (**Figure 5.8, A**). Midgut infection establishment in the control mosquitoes was observed for one of the two replicates and not for more than one transmission cycles, whereas the *LRIM1*-silenced mosquitoes permitted parasites to establish midgut infection during all transmission cycles and for both replicates. For this reason, data for more transmission cycles were not recorded for the *dsLacZ*-injected mosquitoes.

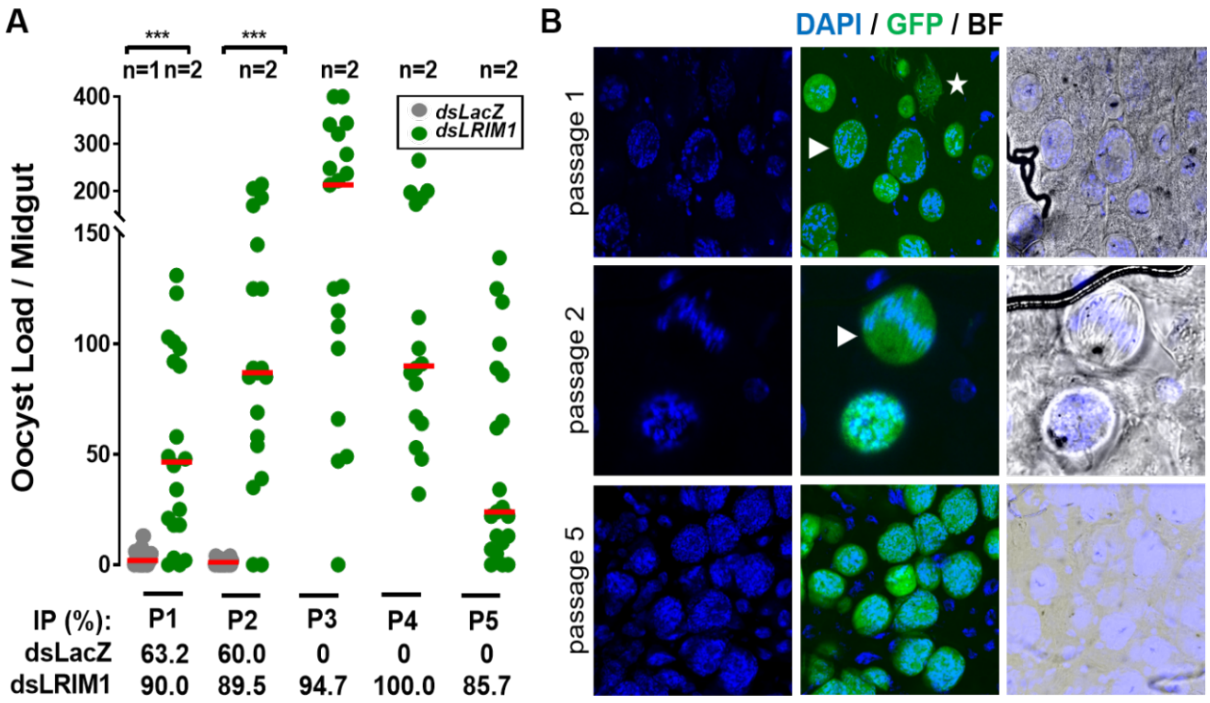

Figure 5.8. Infection intensity and oocysts morphology during serial passaging of the *P. berghei* pool of barcoded mutants. (A) Number of oocysts counted in the midguts of *LRIM1*-silenced and ds*LacZ*-injected (control) *A. coluzzii* mosquitoes at day-11 pbf, following infection with the pool of *P. berghei* mutants. Oocysts intensity and prevalence was monitored for every transmission cycle and for two individual biological replicates (n). Transmission through the ds*LacZ*-injected mosquitoes was completely eliminated following two mouse-to-mosquito-to-mouse transmission cycles in the first replicate, whereas no transmission was observed following one transmission cycle in the second replicate. Median number is indicated by a horizontal red line and samples with significant Mann Whitney U P-values (P<0.05) are labelled with an asterisk. Infection prevalence (IP) corresponds to the percentage of the

midguts that appeared to have at least one oocyst. P1-5; midgut oocyst load in ds*LacZ*-injected or *LRIM1*-silenced *A. coluzzii* mosquitoes following one, two, three and four mouse-to-mosquito-to-mouse transmission cycles. Note that the parasite population that passed through the ds*LacZ*-injected (control) mosquitoes were not able to establish midgut infection for more than two mouse-to-mosquito-to-mouse transmission cycles. **(B)** Representative fluorescent images of 11-days old oocysts in *A. coluzzii* midguts infected with the pool of six mutants, following one, two and four mouse-to-mosquito-to-mouse transmission cycles. Oocysts with abnormal morphology and DNA distribution are indicated with an arrowhead, whereas oocysts whose sporogony was completed to a high degree with mature sporozoites readily observed close to the oocyst's periphery are indicated with an asterisk. *GFP*-expressing parasites appear green, where DNA was stained with DAPI (blue). Images were taken at X400 magnification.

DNA staining of *LRIM1*-silenced *A. coluzzii* midguts at day-12 pbf, a time point that coincides with sporozoite formation within the developing oocyst, revealed that most of the oocysts of the first transmission cycle were not uniform in size, shape or sporulation progression. In fact, only 25-30% of the oocysts displayed a large, digitated endomitotic nucleus and contained fully formed sporozoites. The majority of them displayed either a large digitated endomitotic nucleus with no observable sporozoites or they were highly vacuolated with a paused mitotic division and a sick appearance indicating death or progress of cell death. It is unknown which genotypic combination is responsible for each oocyst morphological phenotype. It has been previously shown that the developing oocyst of the single KO parasite lines, except *Δc43*, do not display any morphological abnormalities. This let us conclude that the abnormal DNA distribution observed in the oocysts developed following simultaneous infection with the six mutants is due to heterozygosis of two different KO alleles rather than complete lack of a specific gene. It has not been further investigated whether the unusual oocysts progressively mature and eventually form sporozoites but since transmission back to the rodent host was observed, it is assumed that infectious sporozoites were eventually produced. Nevertheless, following four transmission cycles, the number of mutant alleles in the population was reduced and the developing oocyst became similar to that of the WT - presumably due to the loss of most of the KO alleles and the reduction in the different allele combinations within the population (**Figure 5.8, B**).

As previously mentioned, transmission through the ds*LacZ*-injected mosquitoes was observed during the first transmission cycle for one of the two replicates and only for one of the three mice used during bite back experiments. Transmission was completely blocked during the first transmission cycle of the second replicate, possibly due to biological variations of the mosquitoes and mice used at the time. Nevertheless, analysis of the infected blood sample collected following the first transmission cycle through the ds*LacZ*-injected mosquitoes of the first replicate showed a massive reduction in the abundance of almost all KO alleles. Going further into detail, the *c01* KO allele was the mutant allele with the highest abundance, covering about 18% of the total WT and KO alleles population. The relative abundance of all other mutant alleles was calculated to be less than 0.05% (**Figure 5.9**). Following mosquito initial infection with mice that have been previously infected with similar amounts of mutant parasites and given the fact that no WT parasites were used, the diploid zygotes formed following fertilisation in the midgut lumen are mainly heterozygotes for two of their KO loci, or in less abundant, homozygotes for one KO locus. Therefore, these values indicate that the *c01* KO heterozygotes were primarily responsible for the successful passage of the pooled parasite population through the ds*LacZ*-injected mosquitoes. In further agreement, the same parasite line was found to be occasionally transmitted back to the rodent host through naïve or ds*LacZ*-injected mosquitoes.

Conversely, the immunocompromised mosquitoes permitted mutants to pass through with various and reducing frequencies during both replicates and for all transmission cycles. Except the *c57* KO allele which was completely eliminated following one and two transmission cycles in replicate one and two, respectively, all other mutant alleles maintained themselves in the population even after three infection cycles. Surprisingly, the *PIMMS2* KO and *P48/45* KO alleles managed to maintain themselves in the population at very low frequencies (relative abundance 0.0005% and 0.0009%, respectively) until the end of the experiment (**Figure 5.9, A**). Nevertheless, even in the immunocompromised mosquitoes, all KO alleles underwent drastic reduction in their relative abundance. The only difference observed when compared to the infection of the ds*LacZ*-injected mosquitoes, which resulted in a complete transmission blockage, is that the KO alleles in the immunocompromised mosquitoes managed to maintain themselves in the population for longer periods (**Figure 5.9, B**). Subsequent crosses in the midgut lumen eventually resulted in the generation of WT parasites i.e. reduction

of the KO alleles in the population results in a respective increase in the number of WT alleles, which were then able to continue multiple transmission cycles.

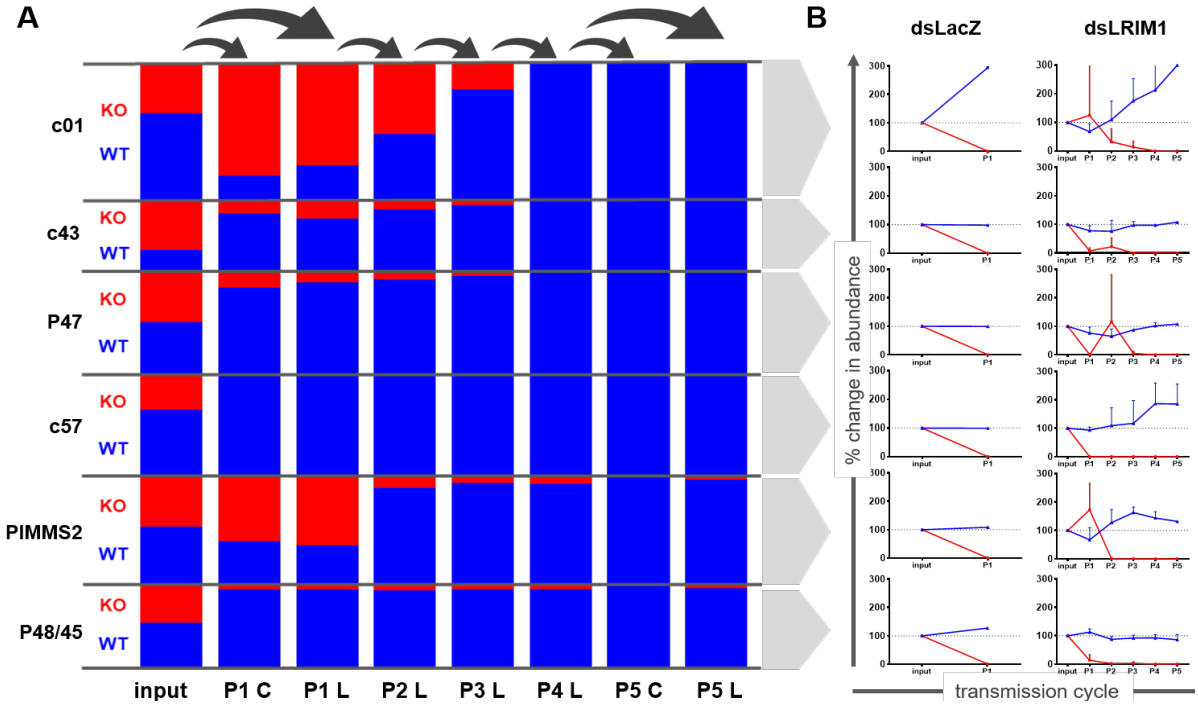

Figure 5.9. Experimental selection of the *P. berghei* pool of barcoded mutants through ds*LacZ*-injected and complement silenced *A. coluzzii* mosquitoes. (A) Relative abundance (y-axis) of *c01*, *c43*, *P47*, *c57*, *P48/45* and *PIMMS2* KO and WT locus on blood stage parasites following serial transmission cycles (x-axis) through ds*LacZ*- and ds*LRIM1*-injected *A. coluzzii* mosquitoes, as assayed by quantitative RT-PCR. The graphs show in different colours the percent (%) abundance of the KO and WT locus for each gene, as determined out of the total parasite population that successfully transmitted from the dsRNA-injected mosquitoes to the mice. The percent (%) abundance of the individual locus shown on each graph corresponds to the average of at least two values, derived from the blood sample analysis of individual mice used during the same transmission cycle. In total, five sequential mosquito-to-mouse-to-mosquito transmission cycles have been performed and the presented data derived from two individual biological replicates. The introduced to the parasite genome, *eGFP* gene was used as reference. In the first replicate and during the first transmission cycle, parasites used for infecting the ds*LacZ*-injected group of mosquitoes were competent to complete their lifecycle and transmit back to the mice, however they were eliminated during their second transmission cycle and thus, were unable to transmit to the mice for a second time. On the other hand, parasites were

not transmitted following their first passage through the ds*LacZ*-injected mosquitoes in replicate two. After four transmission cycles, parasites that have been so far exclusively being transmitted through *LRIM1*-silenced *A. coluzzii* were used to infect ds*LacZ*-injected mosquitoes. The aim of this infection was to assess whether the resulted parasite population was able to establish infection, also, in non-immunocompromised mosquitoes in contrast with their initial incapability of infecting the same group of mosquitoes. Input; initial parasite population that was used to infect the mosquitoes of the first mouse-to-mosquito-to-mouse transmission cycle, P1 C; parasite population derived following one mouse-to-mosquito-to-mouse transmission cycle through ds*LacZ*-injected *A. coluzzii* mosquitoes, P1-5 L; parasite population derived following one, two, three and four mouse-to-mosquito-to-mouse transmission cycles through ds*LRIM1*-injected *A. coluzzii* mosquitoes, respectively, P5 C; parasite population derived following three mouse-to-mosquito-to-mouse transmission cycles through *LRIM1*-silenced *A. coluzzii* mosquitoes, prior to a final transmission cycle through ds*LacZ*-injected mosquitoes. **(B)** Change (y-axis) in the relative abundance of the WT and KO alleles of *P. berghei c01*, *c43*, *P47*, *c57*, *P48/45* and *PIMMS2* following serial mouse-to-mosquito-to-mouse transmission passaging (x-axis). Each graph represents each gene, where the blue line indicates the change in the abundance of its respective WT allele (blue) and the red line shows the change in the abundance of its respective KO allele (red). The WT and KO abundance values determined for the input population were considered as the absolute value and based on each locus relative abundance determined at each transmission cycle, the % increase or decrease was calculated. Data regarding the blood stage parasite population that passed through the ds*LacZ*-injected mosquitoes derived from one biological replicate and only for one mouse-to-mosquito-to-mouse transmission cycle, whereas data regarding the abundance values of blood stage parasites that passed through the complement silenced mosquitoes derived from two individual biological replicates and for five transmission cycles. Error bars show standard error.

Following four serial transmission cycles through *LRIM1*-silenced *A. coluzzii* mosquitoes and almost complete replacement of the *c01*, *c57*, *c43* and *P47* KO alleles with their respective WT, the resulted modified parasite population was used to infect ds*LacZ*-injected mosquitoes and see whether parasite development could this time lead to a successful infection of the rodent host. Indeed, the parasite population in the presence of an unaffected complement-like system was able to infect both the ds*LacZ*-

injected *A. coluzzii* mosquitoes and the next rodent host. Quantification of the alleles abundance showed a complete loss of all KO alleles, indicating the complete elimination of all mutant parasites (**Figure 5.9, A**). Since the *PIMMS2* and *P48/45* KO alleles managed to maintain themselves in the population after four transmission cycles through the immunocompromised mosquitoes, even at very low frequencies, it can be evidently suggested that the complement system is the responsible mechanism for clearing out all the rest of the KO alleles.

All these results make us conclude that the mosquito complement-like system indeed acts as a ‘‘sieve’’ removing parasites carrying deleterious, loss-of-fitness mutations or those that have been damaged by upstream immune responses. The population is stabilised on a particular non-extreme and uniform genotypic and phenotypic background in a way that can guarantee its maintenance, even at low frequencies, for prolonged periods of time. The robustness of the approach used is also enhanced by the fact that the data obtained validate what has been already known; none of the KO parasites are competent to survive the robust mosquito immune responses unless silencing key components of the mosquito complement-like system. Notably, the overall outcome of this experiment as well as the fact that the individual results were robust between both replicates performed, allow us to strongly accept the previously described hypothesis.

5.2.5 Complement molecules mRNA recruitment in the midguts with high activity of TEP1-mediated killing

Analysis of *A. coluzzii* midgut transcriptional responses to infection with *Δc01*, *Δc43*, *ΔP47* and *Δc57* compared to *c507* (WT) *P. berghei* parasites by RNAseq, identified a large number of differentially regulated genes at 24 hours pbf (Ukegbu *et al.*, 2020; Giorgalli *et al.*, unpublished). Most of them were found to be involved in systemic immune responses of the complement-like system and downstream effector reactions. Among those, *TEP1*, *LRIM1* and *APL1C* were found to be downregulated. When considered together with the increased complement activity observed in the basal side of the midgut epithelium following invasion of the mutant ookinetes, these data could point to a negative feedback mechanism whose aim is to downregulate this self-damaging innate immune response. However, since most of these genes are thought to be largely expressed in haemocytes and fat body cells it is more likely that midgut infection by the mutant KO ookinetes causes mobilisation of haemocytes from the

haemolymph, which later attach to the midgut tissues causing a temporal depletion of the relevant transcripts (Frolet *et al.*, 2006; Smith *et al.*, 2015; Castillo *et al.*, 2017).

To examine this hypothesis, the abundance of *TEP1*, *LRIM1* and *APL1C* transcripts was quantified in the midgut and whole body (excluding legs, wings and heads) of *A. coluzzii* mosquitoes that were previously infected with one of the mutant or control *c507* (WT) parasites, at 24 hours pbf. The results revealed a striking difference in the transcript abundance of all three genes between midgut and whole mosquitoes (**Figure 5.10, A**). Specifically, the relative transcript abundance of *TEP1*, *LRIM1* and *APL1C* following infections with the mutant parasites compared to the WT control was notably lower in the midgut compare to the whole mosquitoes.

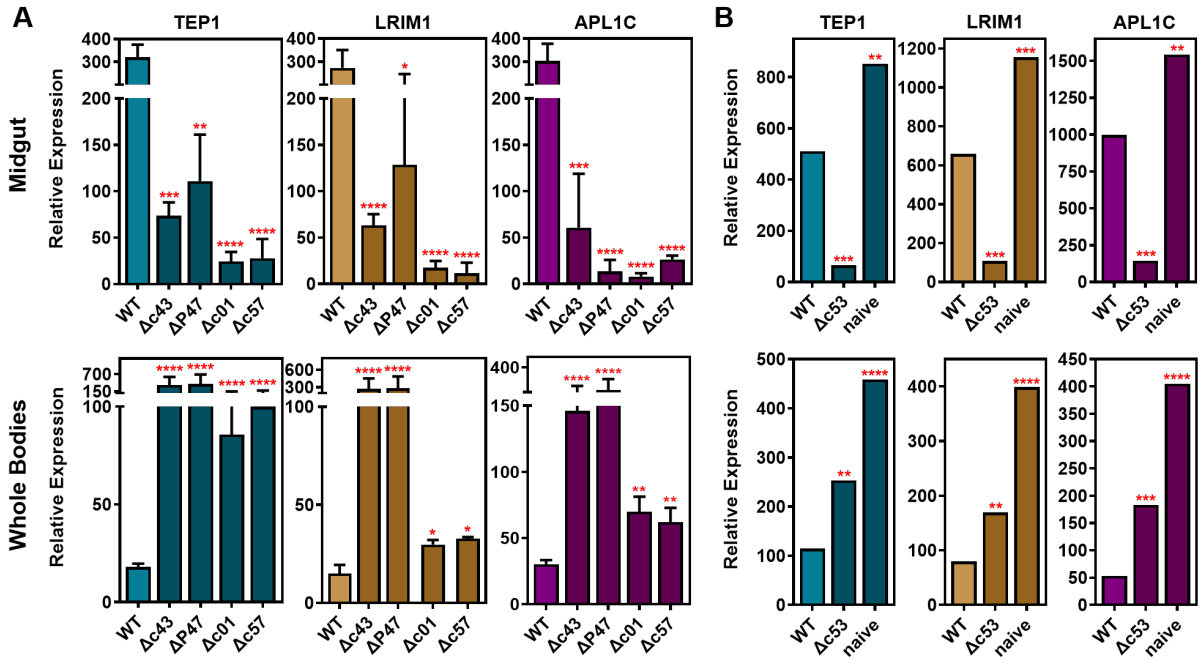

Figure 5.10. Complement-like system transcripts abundance in mosquito tissues upon infection. Relative abundance of *TEP1*, *LRIM1* and *APL1C* transcripts in the midgut and whole body of *A. coluzzii* mosquitoes infected with the *c507* (WT), *Δc01*, *Δc43*, *ΔP47* or *Δc57* **(A)** parasite lines, measured by qRT- PCR at 24 hours pbf. Mosquito blood feeding on mice infected with *Δc53* parasites or noninfected mice were used as controls **(B)**. Whole body refers to mosquito tissues after the removal of wings, legs and head. Data derived from two independent replicates in (A) and one replicate in (B), normalised to the abundance of mosquito *S7* transcripts and referenced to data obtained at 1 hour pbf that was used as baseline. Error bars indicate SEM. One-way ANOVA test was performed between the relative expression value of the KO-infected mosquito samples and the WT-infected mosquito samples. Data regarding the *TEP1*,

LRIM1 and *APL1C* transcripts abundance in mosquito samples infected with Δc43 and WT parasites are reported in (Ukegbu *et al.*, 2020).

A. coluzzii infections with the *Δc53* parasite line and mosquitoes fed on noninfected mice served as additional controls (**Figure 5.10, B**). Ookinetes lacking expression of *c53* are shown to be immotile and unable to traverse the mosquito midgut epithelium (unpublished data, with the permission of Dr. Valerie Ukegbu, Imperial College London). Thus, since mutant ookinetes do not reach the basal side of the midgut epithelium, low complement activity would be expected. Surprisingly, following infection with the *Δc53* parasites resulted in low levels of *TEP1*, *LRIM1* and *TEP1* mRNA transcripts in the midgut area and high levels in the whole body. On the contrary, mosquitoes that were let to blood feed on non-infected mice appeared to have much higher abundance of *TEP1*, *LRIM1* and *TEP1* mRNA transcripts both in their midgut and whole body, compared to the WT-infected mosquitoes. The immune genes abundance in the midguts and whole bodies of mosquitoes that have been fed on non-infected mice is on a similar pattern in relation to the WT-parasites infected mice, for both mosquito compartments i.e. transcription is higher for all genes and in both compartments of mosquitoes fed on non-infected mice compared to those fed on WT-parasites infected mice, meaning that there is not a specific regulation. All these data corroborate our hypothesis that ookinetes lacking *c01*, *c43*, *P47* or *c57* trigger a massive mobilisation and differentiation of the haemocytes in the mosquito midgut area, needed for fast translation of the preserved mRNA and rapid response to the pathogen-associated stimuli. It can be further suggested that haemocyte mobilisation is not triggered from ookinetes that have already traversed the mosquito midgut epithelium, but from signals already initiated while in the midgut lumen.

5.2.6 *P. berghei* PIMMS2 essentiality during ookinete midgut traversal

As previously highlighted, most of the *ΔPIMMS2* ookinetes are unable to reach the mosquito midgut sub-epithelial space on its basal side. Thus, ookinetes lacking expression of *PIMMS2* do not face the mosquito haemolymph components and thus are not eliminated by molecules found in the mosquito circulatory system including those of the complement-like system. In other words, these data suggest that PIMMS2 is probably involved in ookinete exit of the mosquito midgut epithelial cells. To confirm the position in the midgut epithelium cell that *ΔPIMMS2* ookinete development is terminated, immunofluorescence assays were performed using phalloidin staining on

ΔPIMMS2 infected *A. coluzzii* midgut epithelia 26 hours pbf (**Figure 5.11**). Phalloidin specifically binds to F-actin, a major constituent of all muscle cells that surround the outward midgut basal surface of *Anopheles* mosquitoes (Schlegelmilch & Vlachou, 2013). Using phalloidin staining, I was thus able to distinguish the apical side of the cell which is adjacent to the midgut lumen and on the opposite side its basal part which faces the basement membrane and outwardly the mosquito haemolymph. Following fluorescent imaging and events enumeration, 95% of the *ΔPIMMS2* ookinetes were found to be accumulated on the apical side of the cell, whereas about 5% of the ookinetes were neighbouring to the basal side. The latter were presumably located within the extensive network of crypts formed by invaginations of the basal plasma membrane known as the basal labyrinth. Quantitative data were only collected from 10-15 fields of view; therefore, the data are not presented. To satisfactory quantify this difference, further data should be collected.

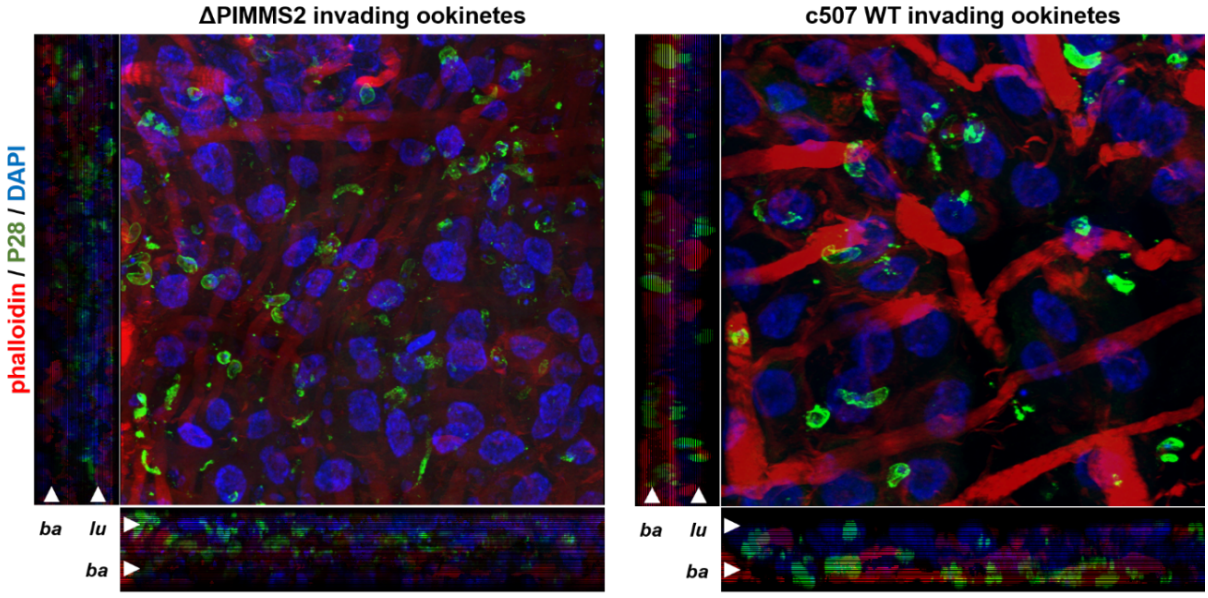

Figure 5.11. *ΔPIMMS2* ookinete traversal through the *A. coluzzii* midgut epithelium. Fluorescence images of *A. coluzzii* midgut epithelia infected with *ΔPIMMS2* (left panel) and WT ookinetes at 26 hours pbf, stained with a fluorescently labelled phalloidin compound (red). Phalloidin was used to visualise the midgut basal side as it specifically stains filamentous actin, a major constituent of all muscle cells that surround the outward midgut basal surface of mosquitoes. Ookinetes were stained with the P28 antibody (green), whereas DAPI (blue) was used to stain the ookinetes and the midgut epithelium cells nuclei. Orthogonal sections show ookinetes that have either emerged from the midgut cells basal side and thus, appear to be

localised in close proximity to the stained-filamentous actin or have been trapped within the cells and are found to be accumulated at a distance from the midgut basal side. Fluorescence images of *A. coluzzii* midguts are representative of two sets of experiments and were taken at X400 magnification. lu = lumen; ba = basal lamina.

5.2.7 Role of the complement-like system during cellular responses

5.2.7.1 Effect of *LRIM1*-silencing on the number of invading ookinetes

Our current understanding of the function of PIMMS2 is that it is probably involved in the ookinete midgut egress. This implies that the majority of the invading-ookinetes who lack expression of *PIMMS2* are restricted to the interior of the midgut cells and thus, are unable to successfully traverse the midgut wall. The question asked was why *ΔPIMMS2* oocyst load increases when silencing the complement like system. Since gamete fertilisation and ookinete midgut traversal are the only two processes taking place before oocyst formation, it could be hypothesised that silencing of the complement-like system increases the capacity of the parasites for fertilisation and/or the number of ookinetes traversing the mosquito midgut epithelium.

The first hypothesis would require complement-mediated parasite killing to occur in the midgut lumen which is against the general understanding that the complement-like responses take place in the haemolymph. For this purpose, measurement of the gametocyte-to-ookinete conversion rate in non-treated, ds*LacZ*-injected and *LRIM1*-silenced *A. coluzzii* midgut bolus at 17-18 hours pbf was assessed. *LRIM1*-silencing did not affect the gametocyte-to-ookinete conversion rate (82.36% ± 1.46%) which remained similar to that recorded in control ds*LacZ*-injected and in non-treated mosquitoes (Ukegbu *et al.*, 2017b) (**Figure 5.12, A; Table 5.7**). These data thus falsified the initial hypothesis and affirmed that complement-like responses do not influence events occurring in mosquito compartments other than the haemolymph.

Whether complement silencing leads to alterations in the susceptibility of the midgut epithelium to ookinete invasion was then assessed. To do so, the number of ookinetes invading the midgut epithelium of non-treated, ds*LacZ*-injected (control) and *LRIM1*-silenced *A. coluzzii* mosquitoes at 25-26 hours pbf was recorded following staining of the ookinetes with an antibody targeting their P28 surface protein. The median number of WT ookinetes counted was 521.5 (± 45.41) in non-treated, 508.00 (± 52.78) in ds*LacZ*-injected and 815.8 (± 62.91) in *LRIM1*-silenced mosquitoes (**Figure 5.12, B; Table 5.8**) revealing that, the number of ookinetes able to invade the mosquito midgut

epithelium of *LRIM1*-silenced mosquitoes is significantly higher (p<0.0001). To assess whether this effect is *LRIM1*-silencing specific or other components of the complement-like system might be also involved, the median number of the invading ookinetes was recorded following *TEP1*-silencing. The median number of WT ookinetes determined was 508.00 (± 52.78) in ds*LacZ*-injected and 812.8 (± 70.25) in *TEP1*-silenced mosquitoes suggesting otherwise (**Figure 5.12, B; Table 5.8**).

To better understand the rate by which ookinetes are invading the midgut epithelium of the *A. coluzzii* mosquitoes with the different immune backgrounds, the number of WT invading ookinetes was tracked at multiple time-points starting from 18 to 22 and from 22 to 26 hours pbf. As expected, the median number of invading ookinetes at all time-points was similar between the non-treated and the ds*LacZ*-injected mosquitoes, whereas a 2-fold increase was observed in the number of ookinetes found in the epithelial cells of *LRIM1*- and *TEP1*-silenced mosquitoes. These data suggest that the large number of invading ookinetes previously observed at 25-26 hours pbf, is due to a process that have started earlier on (**Figure 5.12, C; Table 5.9**).

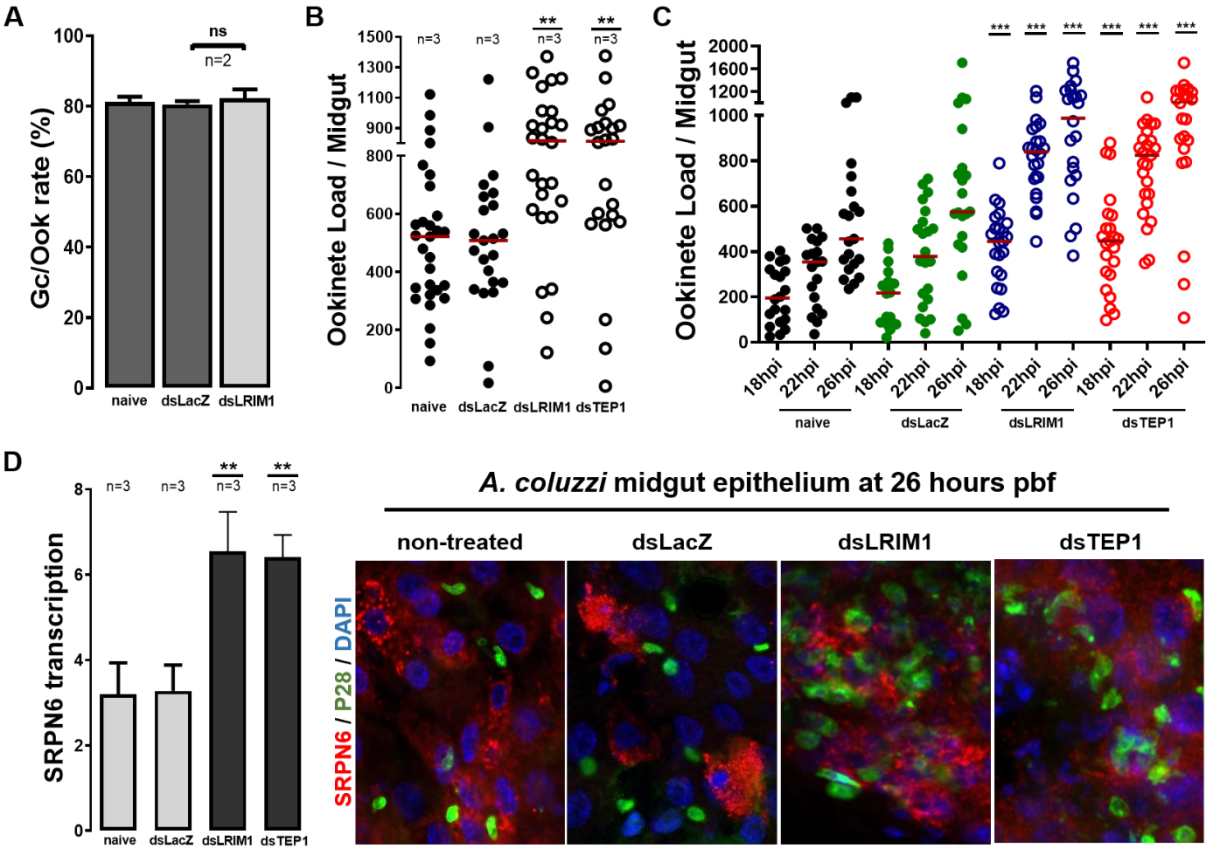

Figure 5.12. Effect of *LRIM1*-silencing on ookinete developmental progress in the *A. coluzzii* midgut lumen and epithelium. (A) *In vivo* gametocyte to-ookinete

(Gc/Ook) conversion rates of the *c507* (WT) parasite line in the midgut blood bolus of non-treated (control), ds*LacZ*-injected (control) and *LRIM1*-silenced infected *A. coluzzii* at 17-18 hours pbf. Number of replicates (n) and standard error are shown. Statistical significance was determined using a two-tailed, unpaired Student's *t*-test. **(B)** Load of WT invaded ookinetes in the midguts of non-treated, ds*LacZ*-injected, *LRIM1*- and *TEP1*-silenced *A. coluzzii* mosquitoes, at 25-26 hours pbf. Ookinetes were counted following staining with an antibody against their P28-surface protein. Data derived from three individual biological replicates (n). Red lines indicate median load. Statistical significance was determined using the Mann Whitney U-test between the ds*LacZ*/ds*LRIM1* and ds*LacZ*/ds*TEP1* datasets, respectively. **(C)** Ookinete load in the midguts of non-treated, ds*LacZ*-injected, *LRIM1*-silenced and *TEP1*-silenced *A. coluzzii* mosquitoes at 18 hours, 22 hours and 26 hours pbf. Ookinetes were counted following staining with an antibody against the P28 surface protein. The *c507* (WT) parasite line was used for mosquito infection. The median number of ookinetes is shown with a red line. For each of the two replicates, ookinete load was determined from a minimum of 15 midguts per mosquito immune background. Statistical significance was determined using the Mann Whitney U-test between the ds*LacZ*/ds*LRIM1* and ds*LacZ*/ds*TEP1* datasets, respectively. **(D)** *SRPN6* transcription levels following infection of naïve, ds*LacZ*-injected, *LRIM1*-silenced and *TEP1*-depleted *A. coluzzii* mosquitoes, at 25-26 hours pbf, as determined by qRT-PCR. Mosquito infection was performed using the *c507* parasite line. Data were normalised to e*GFP* expression and calibrated to the average of all replicates performed. RNA samples from three individual biological replicates were collected. Statistical significance was determined using a two-tailed, unpaired Student's *t*-test between the ds*LacZ*/ds*LRIM1* and ds*LacZ*/ds*TEP1* datasets, respectively. Representative fluorescence images of ookinetes invading the midgut epithelium of non-treated, ds*LacZ*-injected, *LRIM1*-silenced and *TEP1*-silenced *A. coluzzii*, at 25-26 hours pbf. Staining was performed using antibodies against SRPN6 (red), P28 (green) and DAPI (blue). Images were taken at X400 magnification.

qRT-PCR on midgut samples derived from either non-treated, *dsLacZ*-injected (control) or *LRIM1*- and *TEP1*-silenced infected *A. coluzzii* mosquitoes at 25-26 hours pbf was performed to assess the transcription pattern of *SRPN6*. *SRPN6* transcription was detected to be increased by 2.05 and 2.00 times in *LRIM1*-silenced and 1.95 and 2.01 times in *TEP1*-silenced compared to non-treated and ds*LacZ*-injected

mosquitoes, respectively. This increase was further reflected in the number of SRPN6-positive midgut epithelial cells found in close proximity with invading ookinetes in the complement silenced mosquitoes compared to the control (**Figure 5.12, D**).

To conclude, silencing of the complement-like system leads to cellular alterations of the mosquito midgut epithelium that allows higher number of ookinetes to invade, traverse and reach the basal sub-epithelial space in order to develop into oocysts.

5.2.7.2 Actin-hood formation following *LRIM1*-silencing

While migrating intracellularly, *Plasmodium* ookinetes are in direct contact with the cytoplasm of the invaded cells without being surrounded by a parasitophorous vacuole (Meis *et al.*, 1989). The damage inflicted to the invaded cell is irreversible and ultimately leads to apoptosis (Han *et al.*, 2000; Baton & Ranford-Cartwright, 2004; Vlachou *et al.*, 2004). The cell alters morphologically with a substantial loss of microvilli and protrudes towards the apical side of the epithelium (Han *et al.*, 2000; Vlachou *et al.*, 2004). While protrusion of the cell appears to be mediated by a purse-string mechanism at the basal side of the dying cell (Han *et al.*, 2000), the surrounding area undergoes a series of cellular responses to seal the invaded area including neighbouring cells becoming elongated and extending lamellipodia towards the protruding cell. A lamellipodia-like structure extended by the invaded cell itself towards migrating parasites was observed to also cover ookinetes tightly, like a 'hood' while emerging from the epithelium into the sub-epithelial space. It has been shown that this hood is rich in filamentous actin (F-actin) (Schlegelmilch & Vlachou, 2013).

As described above, *ΔPIMMS2* oocyst load increases following *LRIM1*-silencing despite the impairment of mutant parasites to traverse the mosquito midgut epithelium. I wanted to investigate a potential link between the hood formation, which would indicate successful traversal of the *ΔPIMMS2* ookinetes, and the complement-like system. To do so, midgut epithelia from *P. berghei* WT and *ΔPIMMS2* infected ds*LacZ*-injected (control) and *LRIM1*-silenced *A. coluzzii*, were dissected at 25-26 hours after the blood-meal, a period that corresponds to midgut invasion.

Careful examination of serial confocal sections showed that about 90-95% of the WT ookinetes, in both ds*LacZ*- and ds*LRIM1*-injected mosquitoes, appeared to be exiting the epithelium and be in a close proximity with a thin but well-defined layer of actin filaments. Some parasites were completely engulfed in F-actin, while others displayed

phalloidin staining mostly at one pole. The 5-10% of ookinetes that appeared to not be surrounded by actin filaments might be due to the fact that have either been trapped within the midgut epithelium cell or have not yet exited. On the other hand, *ΔPIMMS2*-infected epithelia of ds*LacZ*-injected *A. coluzzii* mosquitoes did not show any hood formation, not even at a close proximity to the few ookinetes found on the basal side of the epithelium. Since this hood is built only around ookinetes that reach the sub-epithelia space, this outcome confirms what was previously shown regarding the function of PIMMS2. Notably, only after *LRIM1*-silencing, about 80% of the ookinetes were found to be associated with actin filaments. Even more surprising, a massive increase on the number of *ΔPIMMS2* ookinetes that were located close to the basal side of the midgut epithelium was observed. Of them, about 40-50% were found to be surrounded by actin filaments and lysed i.e. P28 traits were found around the ookinetes (**Figure 5.13**). Quantitative data were only collected from 10-15 fields of view; therefore, the data are not presented. To satisfactory quantify this difference though, further data should be collected for each condition tested. Nevertheless, these results suggest that the complement-like system could have an additional role in regulating the cellular responses of the ookinete invaded epithelial cells induced at the time and place of ookinete traversal of the mosquito midgut epithelium.

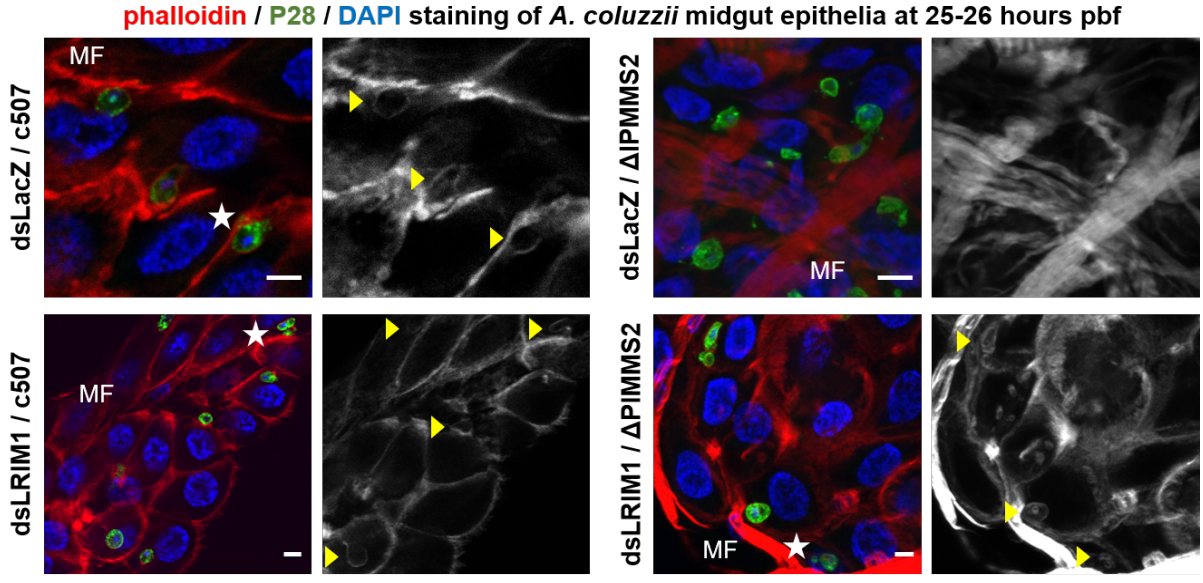

Figure 5.13. Effect of *LRIM1*-silencing on the actin-hood formation. Fluorescence images of WT and ΔIMMS2 ookinetes while exiting the midgut epithelium of ds*LacZ*-injected and *LRIM1*-silenced *A. coluzzii* mosquitoes, at 25-26 hours pbf. WT ookinetes in the epithelial cells of both ds*LacZ*- and ds*LRIM1*-injected mosquitoes and *ΔPIMMS2* ookinetes in the epithelial cells of *LRIM1*-silenced mosquitoes are surrounded by actin

hood structure (yellow arrowheads) while exiting the epithelium. *ΔPIMMS2* ookinetes in the epithelium of ds*LacZ*-injected infected mosquitoes are non-hooded, as no actin filaments can be detected around them. All confocal sections have been captured close to the basal side of the midgut epithelium, where the muscle fibers (MF) are indicated in red. Note the signs of lysis (white asterisks) and the thick ring-shaped F-actin hood. Staining was performed using phalloidin (red) against the filamentous actin of the muscle cells and the hood, P28 (green) and DAPI (blue). The images on the right present the single phalloidin channel where the actin-hoods surrounding each ookinete are clearly indicated (yellow arrowheads). Images were taken at X400 magnification and are representative of all midguts and field views observed for each condition. Scale bar corresponds to 20 μm.

Table 5.7. *In vivo* gametocyte-to-ookinete (Gc/Ook) conversion rates of ANKA *c507* (WT) parasites in naïve, ds*LacZ*-injected and *LRIM1*-silenced *A. coluzzii* mosquitoes

Parasite line	Immune Background	Number of experiments	No of midguts / Replicate	Number of Macrogametes	Number of Ookinetes	Fertilisation Rate (%)	Reduction (%)	*p*-value
c507 (WT)	naïve	2	10	176	655	78.82		
	ds*LacZ*	2	10	125	515	83.06	105.38	0.6900 (ns)
	ds*LRIM1*	2	10	159	652	80.39	101.99	0.5135 (ns)

The *in vivo* gametocyte-to-ookinete (Gc/Ook) conversion rates were calculated as the percentage of P28-positive ookinetes to the total number of the P28-positive macrogametes and ookinetes together. The conversion rates were calculated from suspensions of 10 homogenised midguts, assayed 17-18 hours pbf. Statistical significance was determined with a two-tailed, unpaired Student's *t*-test (ns, non-significant) between the naïve/ds*LacZ* and ds*LacZ*/ds*LRIM1* datasets.

Table 5.8. Number of P28-positive ANKA *c507* (WT) ookinetes in the midguts of naïve, ds*LacZ*-injected and *LRIM1*-silenced *A. coluzzii* mosquitoes

Parasite line	Immune Background	Number of experiments	No of midguts	P28+ ookinete range	Infection Intensity		*p*-value	Standard Error	Fold Change
					Arithmetic mean	Median			
c507 (WT)	naïve	3	29	93-1028	510.8	521.5		45.41	
	ds*LacZ*	3	23	17-1203	513.6	508.0		52.78	1.00
	ds*LRIM1*	3	26	122-1249	795.6	815.8	0.0009 (***)	62.91	1.56
	ds*TEP1*	3	22	6-1369	739.7	812.8	0.0046 (***)	70.25	1.56

P28-positive ookinetes in the mosquito midgut were enumerated at 25-26 hours post mosquito blood feeding using fluorescence microscopy. Data derived from three individual biological replicates. Standard error corresponds to the standard error of means. Statistical significance was calculated using a two-tailed, Student's *t*-test (ns, non-significant). The fold difference was calculated based on the median number of P28-positive ookinetes found in the midgut epithelium of ds*LacZ*-injected mosquitoes, respectively.

Table 5.9. Number of P28-positive ANKA *c507* (WT) ookinetes in the midguts of naïve, ds*LacZ*, *dsLRIM1* and *dsTEP1*-injected *A. coluzzii* mosquitoes at 18, 22 and 26 hours post infection

Parasite line	Immune Background	Time Point (hours pbf)	No of midguts	P28+ ookinete range	Infection Intensity		*p*-value	Standard Error	Fold Change
					Arithmetic mean	Median			
c507 (WT)	naïve	18	20	25-403	206.4	195.0		28.12	
		22	19	35-502	306.1	354.0		34.37	
		26	21	235-1101	544.3	456.0		58.91	
c507 (WT)	ds*LacZ*	18	20	21-436	197.4	217.0	0.9551 (ns)	27.66	
		22	22	39-721	381.0	378.5	>0.9999 (ns)	45.67	
		26	22	51-1567	641.5	574.0	0.4639 (ns)	80.77	
c507 (WT)	ds*LRIM1*	18	23	125-790	419.8	445.0	0.0549 (ns)	35.29	2.05
		22	24	444-1213	817.7	840.0	<0.0001 (***)	35.10	2.22
		26	22	382-1709	981.6	988.5	<0.0001 (***)	73.83	1.72
c507 (WT)	ds*TEP1*	18	23	98-880	441.1	446.0	0.0085 (**)	45.12	2.05
		22	25	349-1101	767.9	825.0	0.0155 (*)	39.31	2.18
		26	23	108-1810	970.9	1002.0	<0.0001 (***)	73.52	1.75

P28-positive ookinetes in the midguts of naïve, ds*LacZ*-injected, *LRIM1*-silenced and *TEP1*-silenced mosquitoes were enumerated at 18, 22 and 26 hours post mosquito blood feeding using fluorescence microscopy. Data derived from two individual biological replicates. Standard error corresponds to the standard error of means. The fold difference was calculated based on the median number of P28-positive ookinetes found in the midgut epithelium of ds*LacZ*-injected mosquitoes at each time point, respectively.

5.2.8 Summary

This chapter has outlined the following (**Figure 5.14**):

- *A. coluzzii* complement-like system acts as a filter removing parasites carrying deleterious, loss-of-fitness mutations or damaged by upstream immune responses. When silencing the complement-like system, mutant parasites pass through with various and reducing frequencies for longer periods.
- Mosquitoes infected with *P. berghei Δc01*, *Δc43*, *ΔP47*, *Δc57* parasites were found to have high levels of *TEP1*, *LRIM1* and *APL1C* transcripts on the basal side of their midgut wall, possibly due to the high activity of the complement-like system in eliminating the mutant ookinetes once they traverse the midgut epithelium.
- *P. berghei ΔPIMMS2* ookinetes are able to invade *A. coluzzii* midgut epithelium but are later trapped within the epithelial cells. Thus, PIMMS2 facilitates ookinete egress of the mosquito midgut epithelium.
- The complement-like system seems to have an additional role in regulating the cellular responses triggered by the invaded midgut epithelial cells, at the time of ookinete midgut traversal. When silenced, ookinetes invasion rates increases.

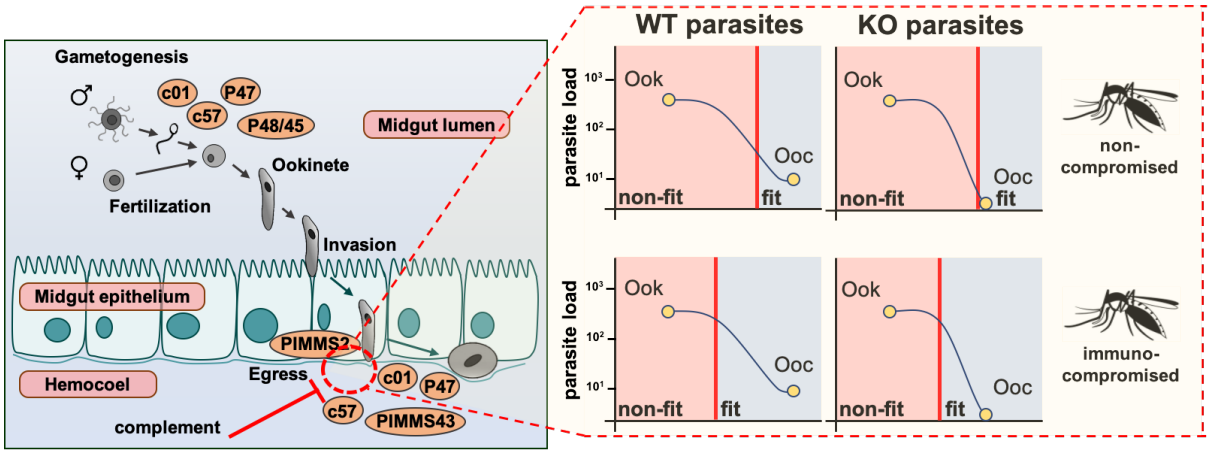

Figure 5.14. Proposed model of the function of the mosquito complement-like system in shaping the ingested parasite population. It has been previously shown that about 80% of the WT *P. berghei* ookinetes is eliminated by complement reactions, possibly due to the fact that some of them have fitness levels that do not pass the threshold set by the mosquito complement-like system (Levashina *et al.*, 2001; Osta *et al.*, 2004). KO parasites have lower fitness levels (compared to the WT) and when ingested in the non-compromised mosquitoes undergo a drastic reduction at the oocyst stage. For example, *P. berghei* c01, c43, P47, c57, P48/45 and PIMMS2 have important roles during parasite development in the mosquito vector (left panel). Mutant

parasites lacking expression of any of these genes form ookinetes that are able to reach the sub-epithelial space of the mosquito midgut epithelium. However, these mutant parasites have compromised fitness which makes them susceptible (non-fit) to reactions of the complement-like system that take place on the basal side of the mosquito midgut. When key components of the complement-like system are silenced, more KO parasites are able to survive (fit) and make it to the oocyst stage. The red line on the right panel of the figure indicates the threshold set by the mosquito complement-like system. Parasite in the red-colour area are those who are non-fit enough and therefore eliminated by the mosquito complement-like system, whereas parasites in the blue-coloured area are those who are fit enough to survive despite the robust attacks of the mosquito complement-like system.

5.3 Discussion

The immune system of the African mosquito *A. gambiae* comprises a robust barrier to infection by the malaria parasite *Plasmodium*. Soon after entering into the mosquito via a bloodmeal, parasites are sequentially attacked by an array of immune responses, each having an impact on the effective parasite population size (Levashina *et al.*, 2001; Sinden *et al.*, 2007). The majority of parasite losses are recorded when ookinetes traverse the mosquito midgut epithelium and encounter the mosquito complement-like system (Blandin *et al.*, 2004; Osta *et al.*, 2004a; Vlachou *et al.*, 2006). Nonetheless, some parasites manage to escape the robust immune responses triggered by the mosquito vector and successfully continue their transmission cycle.

A lot of effort has been made in order to scrutinise the underlying mechanism by which the complement-like system eliminates *Plasmodium* infection. Despite the fact that the major components of this pathway have been well characterised (Clayton *et al.*, 2014; Povelones *et al.*, 2016), it is yet unknown how these molecules are activated and later on triggered towards *Plasmodium* elimination. In the same line of thinking, it is also not yet clear why some parasites survive despite the robust mosquito immune responses i.e. whether specific *Plasmodium* genes have essential functions in parasite immune evasion or that loss-of-function of any of these genes bears a fitness cost that exceeds a certain threshold required for recognition and clearance by the complement.

P47 is the first protein found so far to be important for the parasite to survive the robust immune responses (Molina-Cruz *et al.*, 2013). It has been shown that *P. falciparum* P47 is somehow involved in the suppression of JNK signalling, in this way inhibiting

parasite clearance by the complement system. KO lines cannot reach the oocyst stage, unless silencing key factors of the complement-like pathway (Ramphul *et al.*, 2015; Molina-Cruz *et al.*, 2017). It has been also recently revealed that the *P. berghei* orthologue has a similar function in protecting ookinetes from complement reactions, in addition to playing an important role in gamete fertilisation (Ukegbu *et al.*, 2017b).

Therefore, the question derived was whether more proteins could function similarly to P47 in protecting ookinetes from complement-like responses. To investigate this, several previously identified genes including *PbP47* (van Dijk *et al.*, 2010; Ukegbu *et al.*, 2017b), *Pbc43* (Ukegbu *et al.*, 2020), *PbPIMMS2* (Ukegbu *et al.*, 2017a), *PbP48/45* (van Dijk *et al.*, 2001; van Dijk *et al.*, 2010), *Pbc01* and *Pbc57*, were selected for further comparative phenotypic characterisation.

5.3.1 Comparative functional and phenotypic analysis of *P. berghei* Δc01, Δc43, ΔP47, Δc57, ΔP48/45 and ΔPIMMS2 parasites in *A. coluzzii*

The ability of the mutant parasites to develop into ookinetes was first simultaneously examined. Data confirmed what has been previously observed for *P. berghei* c01 and c57 (unpublished data, with the permission of Dr. Valerie Ukegbu, Imperial College London); that similarly to P47 and P48/45 (van Dijk *et al.*, 2010; Ukegbu *et al.*, 2017b), c01 and c57 are involved in the gametocyte-to-ookinete conversion process, possibly during gamete fertilisation or ookinete development. On the contrary, c43 and PIMMS2 do not seem to play a role in this process. Other genes found to be important during *P. berghei* gamete fertilisation include P230, a male fertility factor which similarly to P47 and P48/45 belongs to the 6-cystein family of proteins (van Dijk *et al.*, 2001; van Dijk *et al.*, 2010), HAP2, a male fertility factor important during gametes membrane fusion (von Besser *et al.*, 2006; Liu *et al.*, 2008), MAP2, a male fertility factor found to be involved during gamete exflagellation (Billker *et al.*, 1997; Tewari *et al.*, 2005; Tewari *et al.*, 2010), NEK4, a female fertility factor needed for zygote genome replication (Reininger *et al.*, 2005) and PPM1, a metallo-dependent protein phosphatase with an important role during male gametocytes exflagellation (Guttery *et al.*, 2014). The diversity in both the function and structure of these proteins suggests that *Plasmodium* gamete fertilisation and ookinete development is a complex procedure which is regulated by multiple membrane associated as well as secreted factors. However, whether specific protein-protein interactions or upstream signalling pathways are triggered by these proteins still remains unknown.

The comparative ability of the mutant ookinetes to successfully traverse the mosquito midgut epithelium and reach the sub-epithelial space was then investigated. Following staining of *Δc01*, *Δc43*, *ΔP47*, *Δc57*, *ΔP48/45* and *ΔPIMMS2*-infected mosquito midgut epithelium with an antibody targeting the SRPN6 invasion marker of *A. coluzzii* mosquitoes*,* it was revealed that all mutant parasites are able to invade the mosquito midgut epithelium at a rate comparable to their gametocyte-to-ookinete conversion ability. However, following mosquito *CTL4*-silencing and infection with *Δc01*, *Δc43*, *ΔP47*, *Δc57*, *ΔP48/45* and *ΔPIMMS2* parasites, it was revealed that *P. berghei* ookinetes lacking expression of *PIMMS2* were unable to exit the mosquito midgut epithelium and thus, reach the basal side of the midgut wall. All other mutant parasites were able to complete their traversal though the mosquito midgut epithelial cells, at a rate comparable to the number of ookinetes previously formed in the midgut lumen.

Going a step further, to verify an already known phenotype regarding the ability of the mutant parasites to establish successful infection in the mosquito midgut (Ukegbu *et al.*, 2017a; 2017b; 2019; van Dijk *et al.*, 2001; 2010), their ability to form oocysts was comparatively investigated. As shown, oocyst development for all mutants was notably reduced. Responsible for this elimination was the complement-like system, also shown by the increased TEP1-activity observed on the surface of the traversed ookinetes. Importantly though, when silencing key components of the complement-like system oocyst formation was recovered for all mutant parasites. The observation that the mutant oocyst numbers were inferior to the WT oocyst numbers in *LRIM1*-silenced mosquitoes and that TEP1 did not mark all of the traversed ookinetes suggest that other immune responses are also involved in the killing of the mutant ookinetes. Indeed, it has been previously shown that some dead ookinetes in the midgut epithelium are not bound by TEP1, indicating alternative means employed by the mosquito to kill *Plasmodium* ookinetes (Blandin *et al.*, 2004). Other mosquito immune factors such as fibrinogen-related proteins (FREPs or FBNs) and LRRD7, members of the FREP and LRRD PRR families, respectively, have been shown to also be important for *Plasmodium* midgut infection (Dong *et al.*, 2006; 2009). Of these, FBN9 is shown to co-localise with ookinetes probably mediating their death (Dong *et al.*, 2009). Nonetheless, all the above scenarios suggest that the bait proteins somehow interfere with the mosquito innate immune responses and in this way promote ookinete survival. Alternatively, they may confer a fitness advantage to the surviving ookinetes and thus are not highly marked by subsequent destruction mechanisms.

The data previously presented indicate that apart from P47, other gametocyte specific 6-cysteine-containing proteins (Annoura *et al.*, 2014), such as P48/45 and P230, may also play a pivotal role in protecting *P. berghei* ookinetes against the complement-like pathway. Here, it is shown that *P. berghei* parasites lacking expression of *P48/45* undergo dramatic reduction at the oocyst stage following infection of *A. gambiae* mosquitoes. Silencing key factors of the complement-like system restores oocyst development. However, the relative increase in the number of *P. berghei ΔP48/45* oocysts formed after complement silencing is not as dramatic (compared to the WT or other mutant parasites), due to severe fertilisation defects accompanying the KO parasites. Importantly, the *in vivo* gametocyte-to-ookinete conversion rate of *ΔP48/45* parasites was similar to the *in vitro* (van Dijk *et al*., 2010), in contrast with the 20% increase observed between the *in vitro* and *in vivo* experiments of *ΔP47* parasites (van Dijk *et al.*, 2010; Ukegbu *et al.*, 2017b). It has been shown that *P. falciparum* P230, a protein also involved in the process of *in vitro* fertilisation, forms a complex with P48/45 at the surface of gametocytes and gametes (Kumar & Wizel, 1992; Kocken *et al.*, 1993; Eksi *et al.*, 2006). In the absence of P48/45, P230 cannot be retained on the gamete surface (Eksi *et al.*, 2006). Thus, the fact that *ΔP48/45* parasites *in vitro* fertilisation rate is not increased following parasite ingestion into the mosquito midgut lumen, might be related to cumulative defects caused by lack of both proteins.

P. berghei c43, P47 and P48/45 are GPI-anchored membrane-bound proteins (van Dijk *et al.*, 2001; van Dijk *et al.*, 2010; Ukegbu *et al.*, 2017b; Ukegbu *et al.*, 2020), *Pb*PIMMS2 is a surface protein with structural similarities to the subtilisin-like proteins (Ukegbu *et al.*, 2017a), *Pb*c57 is putative membrane-associated protein, whereas *Pb*c01 is a putative secreted polypeptide. Unless silencing key-components of the mosquito complement-like system (Blandin *et al.*, 2002; Osta *et al.*, 2004a) parasites lacking expression of any of these genes are notably decreased before reaching the oocyst stage. Therefore, these proteins somehow facilitate resistance to or endurance of mosquito innate immune reactions. If indeed specific molecular interactions exist between the parasite and its mosquito vector, it could be suggested that ookinete evasion of the complement responses is mainly facilitated by the parasite surface composition and the direct physical interactions between these proteins and components of the mosquito complement-like system. In the same line of thinking, the absence of conserved domains among these proteins could point to alternative mechanisms that *Plasmodium* parasites use to avoid recognition by the mosquito

immune system, possibly to more effectively avoid the multiple immune responses as well as potential resistance development by the latter.

The fold-change in the number of oocysts determined in *LRIM1*-silenced compared to *dsLacZ*-injected *A. coluzzii* mosquitoes varied between the individual mutants. If we assume that the levels of *LRIM1*-silencing were similar in all mosquitoes prior to parasite infection, this variation can be possibly explained due to other developmental defects accompanying the parasites that do not allow their progression into the next stage. For example, *ΔP47* and *ΔP48/45* parasites suffer a dramatic bottleneck already at the gametocyte-to-ookinete transition which results in a smaller number of ookinetes formed and have the potential to further develop into oocysts. Additionally, *ΔPIMMS2* ookinetes are incapable of exiting the mosquito midgut epithelial cells and this susceptibility affects their total outcome number on the basal side of the midgut wall. On the contrary, *Δc43* parasites that seem to not have any developmental defects prior to oocyst formation (Ukegbu *et al*., 2002), have the highest fold-change value between *dsLacZ*-injected and *LRIM1*-silenced mosquitoes i.e. since there are no losses associated with developmental defects of the parasite during the gametocyte-to-ookinete-to-oocyst transition, a maximum number of ookinetes are present in the basal side of the midgut wall which unless they are cleared by the complement-like system, they can make it to the oocyst stage. The ˜8 fold-change determined for the WT oocyst load between the two sets of mosquitoes further confirm that about 80% of the ookinetes cannot make it to the oocyst stage due to reactions of the complement-like system (Blandin *et al.*, 2004; Osta *et al.*, 2004b; Vlachou *et al.*, 2006).

5.3.2 The complement-like system actively removes undesirable genotypes with negative effects from the population

The next question asked was what then makes these mutant ookinetes susceptible to the complement-like system. Whilst WT ookinete elimination rates can vary between different infections suggesting some level of stochasticity, the discoveries that several *P. falciparum* and *P. berghei* proteins promote ookinete resistance to this response (Molina-Cruz *et al.*, 2013; Ramphul *et al.*, 2015; Ukegbu *et al.*, 2017b; Ukegbu *et al.*, 2020) support the idea of specific mosquito-parasite interactions that eventually greatly affect the infection outcome. It is possible that all the proteins encoded by these genes are exposed to the vector environment and therefore, interact with it. However, the fact that *Δc01*, *Δc43*, *ΔP47*, *Δc57*, *ΔP48/45* and *ΔPIMMS2* survive only after

silencing components of the complement-like system, suggests a more generic function of the mosquito complement-like system, possibly in eliminating parasites that do not exceed a certain threshold required for recognition and clearance. Nonetheless, one thing that these genes have in common is that they are all associated with developmental processes occurred during midgut infection and that their KO leads to loss of parasite fitness. It is known that such genes with deleterious or loss-of-fitness mutations must be removed from the population.

Whilst doing direct experiments to understand the molecular mechanisms underlying parasite removal from the population is difficult with the current experimental systems, the role and impact of the mosquito complement system as a clearance mechanism was tested. The experimental set up designed to assess this characteristic of the complement system included the serial passage from mouse-to-mosquito-to-mouse of a pool of six different mutant parasite lines for a total of five transmission cycles. Through this short-term passaging, I was seeking to investigate whether the mosquito complement system indeed shapes the transmitted parasite population by monitoring the allele content of the parasite population at each transmission cycle with qRT-PCR analysis. The results indicated that already in the second mouse-to-mosquito-to-mouse transmission cycle through ds*LacZ*-injected mosquitoes, the complement-like system removed all mutant alleles from the population and blocked transmission. On the contrary, the *LRIM1*-injected mosquitoes permitted mutants to pass through with various frequencies for all transmission cycles. More specifically, all *c01*, *c43*, *P47*, *c57*, *P48/45* and *PIMMS2* KO alleles were present in the population for all first four transmission cycles, whereas beyond that the WT alleles of *c01*, *c43*, *P47* and *c57* prevailed instead and only the *PIMMS2* and *P48/45* KO alleles managed pass through the fifth transmission cycle. Nevertheless, these findings propose that only in the absence of the mosquito complement-like pathway, parasites that carry deleterious alleles can be maintained in the population from generation to generation.

It is of great interest that the *c43* KO alleles were not completely eliminated following serial passages in *LRIM1*-silenced mosquitoes i.e. identified in transmission cycles one, two, three of Replicate 1 and transmission cycles one and two of Replicate 2. However, previous data showed that parasites lacking expression of *c43* are not able to transmit back to the rodent host even after infection of *LRIM1*-silenced *A. coluzzii* mosquitoes (Ukegbu *et al.*, 2020). This discrepancy can be possibly explained by the

ability of the *c43* KO allele to mask itself with a WT allele through heterozygosity, in order to avoid clearance by the complement system. In this way, the complement-like system does not target the parasite for elimination and thus, if maintained through heterozygosity for many generations, could lead to innovations that can be transmitted on their own when conditions are favourable e.g. another mosquito population, resistance development. However, the allele dosage effect of a specific locus during the *Plasmodium* lifecycle in its mosquito vector has not been yet scrutinized. Another theory could support that, WT ookinetes lead the way for the *c43* KO homozygotes in order for the latter to successfully traverse the mosquito midgut epithelium, before being targeted by the JNK pathway for TEP1-mediated elimination. This hypothesis could also point to a synergistic relationship between different parasites of a different fitness level. However, the question of how this communication is accomplished, is still unknown; especially when it comes to mosquito stages.

Despite the successful transmission of some *P. berghei* mutants through the *LRIM1*-silenced *A. coluzzii* mosquitoes for multiple transmission cycles, it seems that the complement system still has an adverse effect in eliminating certain KO alleles. This can be explained by the fact that the knockdown efficiency of *LRIM1* is not absolute, especially following *Plasmodium* infection and upregulation of the complement-like system. It has been previously shown that LRIM1 protein abundance is eliminated following *LRIM1*-silencing via RNAi (Povelones *et al.*, 2009), however, monitoring of the protein levels after *Plasmodium* infection was not carried out. Nevertheless, preliminary data on the transcription levels of *LRIM1* in *LRIM1*-silenced *P. berghei* infected *A. coluzzii* mosquitoes after 26 hours of infection, indicated a 30-fold increase in the abundance of *LRIM1* compared to *LRIM1*-silenced mosquitoes prior to mosquito infection (**Appendix 13**). Therefore, by using transgenic *LRIM1*-KO mosquitoes, whose complement-like system threshold is expected to be zero, I could examine whether the absence of immunity pressure could result in a longer sustainability of the mutant alleles. Nonetheless, other mechanisms of parasite elimination might also be involved in mutant alleles clearance, either these include cellular responses (Vlachou *et al.*, 2005) or other humoral reaction components such as FREPs, FBNs or LRRD7 proteins (Dong *et al.*, 2006; Dong *et al.*, 2009).

The *A. gambiae*/*P. berghei* model system used to carry out the selection experiments, is a system that has been widely used to characterise the *Anopheles* innate immune

responses (Levashina *et al.*, 2001; Christophides *et al.*, 2002; Osta *et al.*, 2004a). However, *A. gambiae* does not constitute the natural vector of *P. berghei* and therefore, due to the lack of a common evolution pathway, the *A. gambiae* vector competence for *P. berghei* infection is assumed to be lower compared to if these two organisms had a coevolutionary history i.e. the low vector competence of *A. gambiae* could be because of the fact that *P. berghei* is not well adapted to this vector, and the frequency and intensity of contacts between the parasite and the mosquito have not yet determined the level of coadaptation. On the other hand, *P. falciparum* and *A. gambiae* share a coevolutionary history and thus parasites have possibly better adapted to evade the mosquito responses. Therefore, studies that aim to scrutinise the interactions between the mosquito innate immune system and malaria parasites should be carried out with caution. For example, one problem using *A. gambiae/P. berghei* to model mosquito immunity to *P. falciparum* is that for many reasons including the strikingly different infection intensities, mosquito immune responses to the rodent and human parasite are both qualitatively and quantitatively different (Tahar *et al.*, 2002; Dong *et al.*, 2006). Additionally, so far, most immune effectors that have been identified in the laboratory model such as LRIM1, CTL4, CTLMA4, TEP1 and SRPN2 have not been shown to somehow influence *P. falciparum* infections in sympatric infections (Cohuet *et al.*, 2006; Michel *et al.*, 2006). In accordance with this, preliminary data have shown that the elimination of *P. falciparum* isolates of the African origin NF54 parasites in the West Africa strain of *A. coluzzii* is not facilitated by TEP1-mediated killing, as no TEP1 activity was detected on the surface of the invading ookinetes (**Appendix 14**). In conclusion, the hypothesis that the complement-like system actively removes parasites that carry mutations associated with parasite fitness cost might not be universal for all *Anopheles*/*Plasmodium* combinations. Whether the two organisms had a common evolutionary framework in similar geographic regions is though, of major importance.

The findings described let us conclude that the mosquito complement-like system has a catalytic role in shaping the ingested parasite populations by removing parasites carrying deleterious, loss-of-fitness mutations, or damaged by upstream immune responses. In other words, the complement-like system removes all mutant alleles that are associated with parasite fitness cost. This, in combination with directional selection of P47 and possibly others, provides a powerful evolutionary framework for the shaping of the parasite populations transmitted in any given settings.

It is important to point out that the experimental procedure carried out here was only for a short period of time and does not fully reflect the evolutionary time scale in which the natural selection normally takes place. The artificial selection window that was given here was an approximation to what would be expected in the field, given that specific mutations on the specific alleles do not offer a fitness advantage to the parasites. An additional population genetics approach to assess the diversification and genetic structure of these genes would inform us further on the selection mechanism that underlies the removal or continuance of such alleles in the population.

5.3.3 *P. berghei* PIMMS2 role during ookinete midgut traversal

PIMMS2 is an ookinete-specific protein exhibiting structural similarities to subtilisin-like proteins and has been shown to be involved in ookinete midgut invasion (Ukegbu *et al.*, 2017a). Ookinetes lacking expression of *PIMMS2* are trapped within the midgut epithelial cells and thus, are unable to exit to the sub-epithelial space. Previously characterised subtilisin-like proteins in *Plasmodium* include SUB1, SUB2, and SUB3 (Le Roch *et al.*, 2004). *P. falciparum* SUB1 and SUB2 are known to play an important role in merozoite invasion of erythrocytes as well as in merozoite egress from erythrocytes (Harris *et al.*, 2005; Green *et al.*, 2006; Guttery *et al.*, 2012; Tawk *et al.*, 2013; Child *et al.*, 2013; Giganti *et al.*, 2014). *P. berghei* SUB2 is found in ookinetes and it has been suggested to play a role in modifying the cytoskeletal network of the invaded mosquito midgut cells (Han *et al.*, 2000). Pace *et al.* recently showed that the *P. berghei* orthologue of SUB1, plays an important role in male gamete egress by enzymatically processing SERA3 and thus, promoting male microgamete activation (Pino *et al.*, 2017; Pace *et al.*, 2019). These findings could point to a conserved machinery between subtilisin-like proteins in order for *Plasmodium* parasites to egress and continue their lifecycle in both their mammalian host and mosquito vector. However, the fact that PIMMS2 absence does not interfere with ookinete midgut invasion but affects its development only during egress from the epithelial cells, suggests that different mechanisms are involved in these distinguished processes.

A suggested mechanism for the function of *P. berghei* PIMMS2 could be that it is needed in order to interact with a member of the *A. gambiae* serpin protein family (Suwanchaichinda & Kanost, 2009). Serpins are serine protease inhibitors that regulate insect-specific innate immune responses by inhibiting other endogenous proteases. For example, knockdown of SRPN2 strongly interferes with the invasion of

A. gambiae midguts by the rodent malaria parasite *P. berghei* (Michel *et al.*, 2005), whereas *A. gambiae* SRPN10 is induced by *P. berghei* infection and possibly regulates apoptosis of the invaded midgut cells (Danielli *et al.*, 2003; 2005). Additionally, *SRPN6* is specifically expressed in midgut cells that have been invaded by *Plasmodium* ookinetes and in circulating and attached haemocytes. When knocked-down, parasites appear to have a delayed progress in their clearance via lysis (Abraham *et al.*, 2005). Therefore, *ΔPIMMS2* infection of *SRPN*-depleted *A. gambiae* mosquitoes could reveal key interactions between the *Plasmodium* serine protease PIMMS2 with substrates of the mosquito serine protease inhibitors that are responsible for ookinetes successful midgut traversal.

5.3.4 Implication of the complement-like system during anti-*Plasmodium* cellular responses in *A. coluzzii*

P. berghei ΔPIMMS2 ookinetes are able to invade the mosquito midgut epithelium but are incapable to later egress from the epithelial cell and reach the midgut basal lamina in order to further develop into oocysts. However, the number of the mutant oocysts formed following complement silencing was significantly higher ($p<0.0001$) compared to the control infections. The question asked was what then causes this increase in the number of *ΔPIMMS2* oocysts since, the defect accompanying the KO parasites occurs before complement attack. As shown, the *Plasmodium* gamete fertilisation capacity is not affected by reactions of the mosquito complement-like system (Ukegbu *et al.*, 2017b) hence the number of ookinetes initially formed in the midgut lumen of *LRIM1*-silenced and ds*LacZ*-injected (control) mosquitoes does not vary. However, monitoring of the number of invading ookinetes while traversing the mosquito midgut epithelium at 26-28 hours post mosquito blood feeding revealed that more parasites are capable in gaining access to the midgut epithelial cells of *LRIM1*-silenced compared to ds*LacZ*-injected (control) infected *A. coluzzii* mosquitoes.

The data from this chapter suggest that, complement silencing might result in changes of the midgut susceptibility to ookinete invasion. Specifically, the complement-like responses might be involved in limiting the number of ookinetes invading the midgut epithelium, for example through reorganisation of the actin cytoskeleton, with the aim to balance the budding-off events of the invaded apoptotic cells with midgut integrity and therefore, mosquito survival. Thus, silencing the complement responses leads to an uncontrolled rate of invasion events. Indeed, previous evidence indicates a link

between the humoral and cellular responses which culminate with ookinete killing and possibly mosquito survival. Hood formation of the invaded midgut cells, an actin-based membranous structure which surrounds ookinetes as they exit the epithelial cell layer, believed to also support parasite lysis (Schlegelmilch & Vlachou, 2013; Vlachou *et al.*, 2004) and has been shown to be associated with the function of the WASP protein, an *A. gambiae* actin polymerisation promoter (Schlegelmilch & Vlachou, 2013). Furthermore, CLIPA7, a negative regulator of melanisation in *A. gambiae* (Osta *et al.*, 2004a), shares an integrin interaction domain on its C-terminal end. Since integrin signalling triggers cytoskeleton reorganisation of the invaded midgut epithelial cells (Juliano, 2002) this could suggest an additional link between the two responses.

The idea of a potential functional link between the humoral and cellular immune responses derived from the observation of Elrod-Erickson *et al.* that *Drosophila* Imd mutants exhibit defects in the humoral immune responses as well in phagocytosis blockage (Elrod-Erickson *et al.*, 2000). However, recent work from Castillo and co-workers has shown that in *A. gambiae,* contact of haemocytes with the nitrated midgut basal surface, at the time of ookinete midgut traversal, triggers the release of specific haemocyte-derived microvesicles (HdMv). These HdMv, by possibly delivering some critical immunity factor(s), are able to promote activation of the TEP1 effector protein (Castillo *et al.*, 2017) suggesting that the cellular responses are necessary for activating the humoral responses during *Plasmodium* infection of *A. gambiae*. At the same time, work from Kamarredine and co-workers on the Apolipophorin-II/I genes, two lipid carrier proteins important for both mosquito egg and *Plasmodium* development (Vlachou *et al.*, 2005; Lambrechts *et al.* 2005; Mendes *et al.*, 2008; Rono *et al.*, 2010), revealed a negative correlation with the TEP1-mediated immune responses triggered during mosquito systemic infections (Kamareddine *et al.*, 2016). Their work provides novel insights into the functional interplay between lipid metabolism and humoral responses and at the same time, points to a wider network that interconnects the multiple branches of the mosquito immune responses.

The fold-change in the number of invading ookinetes was much smaller (2-fold) compared to the fold-change in the number of oocysts (10-fold), determined between ds*LacZ*-injected and *LRIM1*-silenced mosquitoes. Assuming that the epithelium has a maximum capacity in the number of ookinetes that can invade i.e. other mechanisms initiated by the midgut epithelial cells are possibly triggered in order to somehow stop

more ookinetes from invading, as a self-protection mechanism of the mosquito, this observation confirms the importance of the complement-like system. A secondary role of the complement system can be suggested, possibly to support the cellular responses triggered by the invaded cells at the time of ookinete midgut traversal.

LRIM1 has been shown to be also involved in hood-linked parasite killing suggesting that the formation of the hood and the complement initiation on the parasites may indeed cooperate towards parasite killing (Schlegelmilch & Vlachou, 2013). This is also in in agreement with previous observations presented in this chapter where *ΔPIMMS2* invading ookinetes in the midguts of *LRIM1*-silenced *A. coluzzii* mosquitoes appeared to be surrounded by a hood-like structure. Since similar hood-like structures were not observed around *ΔPIMMS2* invading ookinetes through the midgut epithelium of ds*LacZ*-injected mosquitoes (control), these findings indeed point to a successful traversal of the mutant ookinetes that unless silencing the complement-like system it would not be visible. Whether these parasites are already dead or in the process of being killed has not been further investigated.

CHAPTER 6: CONCLUDING REMARKS AND FUTURE PERSPECTIVES

Mosquito midgut stages of the malaria parasites offer an attractive system to study host-parasite interactions and are an ideal target for blocking malaria transmission since due to the high activity of the mosquito innate immune system against these stages, parasite numbers drop dramatically. Previous work has profiled the developmental transcriptomes of the rodent *P. berghei* and human *P. falciparum* parasites during their development in the midguts of *A. gambiae* mosquitoes and highlighted genes putatively involved in parasite development and/or host-parasite interactions (Akinosoglou *et al.*, 2015). Based on these findings, this project initially aimed to use the STM methodology in order to simultaneously phenotype pools of individually tagged *P. berghei* mutants, of genes previously found to be highly upregulated in midgut stages (Akinosoglou *et al.*, 2015). The second goal of this project was to provide a detailed phenotypic and functional characterisation of genes previously found to be crucial for *Plasmodium* infection establishment in the mosquito midgut as well as to define the molecular mechanisms underlying the *Plasmodium* immunity mediated bottleneck that takes place in the mosquito midgut against parasites lacking expression of such genes.

The STM methodology has been extensively used in bacterial pathogens to identify virulence genes, by parallel phenotyping pools of individually tagged mutants (Mazurkiewicz *et al.*, 2006). The properties of the STM approach have previously enabled large scale genetic screens of *P. berghei* mutants during their blood stage development, resulting in a dramatic reduction in workload as well as in a sharp decrease of the animal usage (Gomes *et al.*, 2015; Bushell *et al.*, 2017). Therefore, by creating pools of barcoded *P. berghei* mutant parasites, we went to identify novel *Plasmodium* genes with essential role during the gametocyte-to-ookinete-to-oocyst-to-sporozoite developmental transition in the *Anopheles* mosquitoes. Analysis of the first pool of mutants revealed three novel genes; *AQP2*, *N38* and *N350*. All genes were found to be highly transcribed in gametocytes and ookinetes and, have important roles in gamete development or fertilisation, ookinete motility and invasion and during oocyst development and sporozoites production. Once specific integration vectors are available for the entire genome of *P. berghei*, it will be possible to create larger pools of mutants which can then be combined into even more complex superpools, to empower truly genome-wide screens of parasite growth and differentiation using only

a fraction of the number of rodents required today to study much smaller gene sets. Ideally, barcoded PlasmoGEM vectors targeting genes of the human malaria parasite would enable us to investigate both genes that have crucial role during field parasite development in the mosquito vector as well as to investigate conserved functions of the different homologues between species. In this way we could better evaluate the use of the rodent malaria parasite as a model organism too.

Much still remains to fully understand the molecular basis of *Plasmodium* survival in the mosquito midgut, specifically with regards to their survival despite the robust reactions of the mosquito complement-like system. Here, there is clear evidence that the mosquito complement-like system acts as a filter removing parasites that carry mutations which reduce their fitness levels required to overcome the immune threshold set by the complement system. Recent findings suggest the existence of the mosquito midgut "Pfs47 receptor", which following interaction with the *Plasmodium* ookinete facilitates its survival despite the robust mosquito immune responses (Molina-Cruz *et al.*, 2020). Together with other findings, this evidence further supports the "lock-and-key" theory in which a parasite expressing a compatible haplotype of a specific protein, "the key," is able to evade the mosquito immune system by interacting with a mosquito specific receptor, "the lock". Different haplotypes of both "the key" and "the lock" exist in different continents. In other words, this theory matches that of disruptive selection of the mosquito followed by directional selection of parasite alleles. Therefore, it would be interesting to carry out bioinformatic analysis of all genes shown in this thesis to play a role in parasite survival despite the mosquito immune attacks, in order to identify any genetic structure that may have between different continents or even in different regions of the same continent. This will give us more information on the selection pressure that has been applied on these genes and thus, on the alternative mechanisms the parasites evolved to overcome the mosquito immune barrier. Importantly, the two proposed selection mechanisms do not contradict with each other but rather, a combination of both would provide a powerful evolutionary framework for the shaping of the transmitted parasite populations.

This thesis has outlined several genes that have been identified to have critical functions in *Plasmodium* transmission biology; genes that are expressed in gametocytes and play roles in gamete development or fertilisation, genes expressed *de novo* in zygotes or ookinetes with roles in ookinete motility or invasion and, genes

that are expressed in ookinetes and are involved in parasite survival against the mosquito complement-like responses. Since all the identified genes are critical for *Plasmodium* transmission, transmission blocking interventions against them could be proved promising. Due to the high level of conservation in genome organisation and individual gene content between the rodent and human malaria parasites, there is good reason to believe that the results presented in this thesis can be relevant to transmission of human malaria parasites. It will therefore guide the generation of transgenic parasites that will help to elucidate the roles of genes in the human malaria parasite and could potentially lead to the identification of new targets toward novel malaria control approaches. One such approach is the development of TBVs, aiming to block the sexual development of the malaria parasite during its mosquito stages. Additionally, in the spirit of ongoing experiments to genetically modify mosquitoes in order to eradicate malaria, it might be possible to generate genetically modified mosquitoes expressing single-chain antibodies or nanobodies which bind these proteins, conferring refractoriness to infection and leading to malaria transmission blocking (Isaacs *et al.*, 2011; Gantz *et al.*, 2015). Gene drives are ideally suited for spreading such genetic elements within field mosquito population as the short generation time of insects allows them to spread to fixation very quickly even if released from a low initial frequency (Burt, 2003; Hammond & Galizi, 2017).

REFERENCES

Abraham, E. G., Pinto, S. B., Ghosh, A., Vanlandingham, D. L., Budd, A., Higgs, S., Kafatos, F. C., Jacobs-Lorena, M., & Michel, K. (2005). An immune-responsive serpin, SRPN6, mediates mosquito defense against malaria parasites. *Proc Natl Acad Sci USA*. 102, 16327–16332

Acquah, K., Adjah, J., Williamson, K. C., & Amoah, L. E. (2019). Transmission-blocking vaccines: old friends and new prospects. *Inf and Immu*. 87, e00775-18

Adepoju, P. (2019). RTS,S malaria vaccine pilots in three African countries. *Lancet*. 393, 1685

Agaisse, H., & Perrimon, N. (2004). The roles of JAK/STAT signalling in Drosophila immune responses. *Immunol Rev*. 198, 72-82

Agre, P., King, L. S., Yasui, M., Guggino, W. B., Ottersen, O. P., Fujiyoshi, Y., Engel, A., & Nielsen, S. (2002). Aquaporin water channels - From atomic structure to clinical medicine. *J Physiol*. 542, 3-16

Aikawa, M., Carter, R., Ito, Y., & Nijhout, M. M. (1984). New observations on gametogenesis, fertilisation, and zygote transformation in *Plasmodium* gallinaceum. *J Protoz*. 31, 403–413

Akaki, M., & Dvorak, J. A. (2006). A chemotactic response facilitates mosquito salivary gland infection by malaria sporozoites. *J Exp Biol*. 208, 3211-3218

Akinosoglou, K. A., Bushell, E. S. C., Ukegbu, C. V., Schlegelmilch, T., Cho, J. S., Redmond, S., Sala, K. A., Christophides, G. K., & Vlachou, D. (2015). Characterisation of *Plasmodium* developmental transcriptomes in *Anopheles gambiae* midgut reveals novel regulators of malaria transmission. *Cell Microbiol*. 17, 254–268

Alano, P. (1991). *Plasmodium* sexual stage antigens. *Parasitol Today*. 7, 199–203

Alonso, P. L., Sacarlal, J., Aponte, J. J., Leach, A., Macete, E., Aide, P., *et al.*, & Ballou, W. R. (2005). Duration of protection with RTS,S/AS02A malaria vaccine in prevention of *Plasmodium falciparum* disease in Mozambican children: Single-blind extended follow-up of a randomised controlled trial. *Lancet*. 366, 2012-2018

Alonso, P. L., Sacarlal, J., Aponte, J. J., Leach, A., Macete, E., Milman, J., & Cohen, J. (2004). Efficacy of the RTS,S/AS02A vaccine against *Plasmodium falciparum* infection and disease in young African children: Randomised controlled trial. *Lancet*. 364, 1411-1420

Aly, A. S. I., & Matuschewski, K. (2005). A malarial cysteine protease is necessary for *Plasmodium* sporozoite egress from oocysts. *J Exp Med*. 202, 225-230

Aly, A., Vaughan, A. M., & Kappe, S. H. I. (2009). Malaria Parasite Development in the Mosquito and Infection of the Mammalian Host. *Annu Rev Micobiol*. 63, 195-221

Amino, R., Thiberge, S., Blazquez, S., Baldacci, P., Renaud, O., Shorte, S., & Ménard, R. (2007). Imaging malaria sporozoites in the dermis of the mammalian host. *Nat Protocols*. 2, 1705–1712

An, C., Budd, A., Kanost, M. R., & Michel, K. (2011). Characterisation of a regulatory

unit that controls melanisation and lonengivity. *Cell Mol Life Sci.* 68, 1929-1939

Angrisano, F., Sala, K. A., Da, D. F., Liu, Y., Pei, J., Grishin, V., Snell, W. J., & Blagborough, A. M. (2017). Targeting the Conserved Fusion Loop of HAP2 Inhibits the Transmission of *Plasmodium berghei* and *falciparum*. *Cell Reports*. 21, 2868-2878

Annoura, T., Van Schaijk, B. C. L., Ploemen, I. H. J., Sajid, M., Lin, J. W., Vos, M. W., *et al*., & Khan, S. M. (2014). Two *Plasmodium* 6-Cys family-related proteins have distinct and critical roles in liver-stage development. *FASEB J*. 28, 2158–2170

Anthony, T. G., Polley, S. D., Vogler, A. P., & Conway, D. J. (2007). Evidence of non-neutral polymorphism in *Plasmodium falciparum* gamete surface protein genes Pfs47 and Pfs48/45. *Mol Biochem Parasitol*. 156, 117-123

Apio, B., Nalunkuma, A., Okello, D., Riley, E., & Egwang, T. G. (2000). Human IgG subclass antibodies to the 19 kilodalton carboxy terminal fragment of *Plasmodium Falciparum* merozoite surface protein 1 (MSP119) and predominance of the MAD20 allelic type of MSP1 in Uganda. *East African Medical J*. 77, 189-193

Arai, M., Mitsuke, H., Ikeda, M., Xia, J. X., Kikuchi, T., Satake, M., & Shimizu, T. (2004). ConPred II: A consensus prediction method for obtaining transmembrane topology models with high reliability. *Nucleic Acids Res*. 32, 390-393

Arbouzova, N. I., & Zeidler, M. P. (2006). JAK/STAT signalling in Drosophila: insights into conserved regulatory and cellular functions. *Development*. 133, 2605-16

Ariey, F., Witkowski, B., Amaratunga, C., Beghain, J., Langlois, A.-C., Khim, N., *et al.*, & Ménard, D. (2014). A molecular marker of artemisinin-resistant *Plasmodium falciparum* malaria. *Nature*. 505, 50-55

Armistead, J. S., Morlais, I., Mathias, D. K., Jardim, J. G., Joy, J., Fridman, A., *et al.*, & Dinglasana, R. R. (2014). Antibodies to a single, conserved epitope in *Anopheles* APN1 inhibit universal transmission of *Plasmodium falciparum* and *Plasmodium vivax* malaria. *Infect Immun*. 82, 818-829

Arredondo, S. A., Cai, M., Takayama, Y., MacDonald, N. J., Anderson, D. E., Aravind, L., Marius Clore, G., & Miller, L. H. (2012). Structure of the *Plasmodium* 6-cysteine s48/45 domain. *Proc Natl Acad Sci USA.* 109, 6692–6697.

Arredondo, S. A., & Kappe, S. H. I. (2017). The s48/45 six-cysteine proteins: mediators of interaction throughout the *Plasmodium* lifecycle. *Int J Parasitol*. 47, 409-423

Arrighi, R. B. G., & Hurd, H. (2002). The role of *Plasmodium berghei* ookinete proteins in binding to basal lamina components and transformation into oocysts. *Int J Parasitol*. 32, 91-98

Arrighi, R. B. G., Lycett, G., Mahairaki, V., Sidén-Kiamos, I., & Louis, C. (2005). Laminin and the malaria parasite's journey through the mosquito midgut. *J Exp Biol*. 208, 2497-2502

Ashley, E. A., Dhorda, M., Fairhurst, R. M., Amaratunga, C., Lim, P., Suon, S., *et al.*, White, N. J., & Tracking Resistance to Artemisimin Collaboration (TRAC) (2014). Spread of artemisinin resistance in *Plasmodium falciparum* malaria. *N Engl J Med*. 37, 411-423

Avril, M., Bernabeu, M., Benjamin, M., Brazier, A. J., & Smith, J. D. (2016). Interaction

between endothelial protein C receptor and intercellular adhesion molecule 1 to mediate binding of *Plasmodium falciparum*-infected erythrocytes to endothelial cells. *MBio*. 7, 615-616

Avril, M., Gamain, B., Lépolard, C., Viaud, N., Scherf, A., & Gysin, J. (2006). Characterisation of anti-var2CSA-PfEMP1 cytoadhesion inhibitory mouse monoclonal antibodies. *Microbes Infect*. 8, 2863-2871

Bahia, A. C., Dong, Y., Blumberg, B. J., Mlambo, G., Tripathi, A., Benmarzouk-Hidalgo, O. J., Chandra, R., & Dimopoulos, G. (2014). Exploring *Anopheles* gut bacteria for *Plasmodium* blocking activity. *Environ Microbiol*. 16, 2980-2994

Bahia, A. C., Kubota, M. S., Tempone, A. J., Araújo, H. R. C., Guedes, B. A. M., Orfanó, A. S., *et al*., & Traub-Csekö, Y. M. (2011). The JAK/STAT pathway controls *Plasmodium vivax* load in early stages of *Anopheles* aquasalis infection. *PLoS Negl Trop Dis*. 11, e1317

Bahl, A., Brunk, B., Crabtree, J., Fraunholz, M. J., Gajria, B., Grant, G. R., *et al.*, & Whetzel, P. (2003). PlasmoDB: The *Plasmodium* genome resource. A database integrating experimental and computational data. *Nucleic Acids Res*. 31, 212-215

Baird, J. K., Jones, T. R., Danudrigo, E. W., Annis, B. A., Bangs, M. J., Basri, H., Purnomo, R., & Masbar, S. (1991). Age-dependent acquires protection against *Plasmodium falciparum* in people having two years exposure to hyperendemic malaria. *Am J Trop Med Hyg.* 45, 65-76

Bando, H., Okado, K., Guelbeogo, W. M., Badolo, A., Aonuma, H., Nelson, B., Fukumoto, S., Xuan, X., Sagnon, N., & Kanuka, H. (2013). Intra-specific diversity of Serratia marcescens in *Anopheles* mosquito midgut defines *Plasmodium* transmission capacity. *Sci Rep*. 3, 1641

Bannister, L., & Mitchell, G. (2003). The ins, outs and roundabouts of malaria. *Trends Parasitol*. 19, 209–213

Barillas-Mury, C. (2007). CLIP proteases and *Plasmodium* melanisation in *Anopheles gambiae*. *Trends Parasitol*. 23, 297-299

Barillas-Mury, C., Han, Y. S., Seeley, D., & Kafatos, F. C. (1999). *Anopheles gambiae* Ag-STAT, a new insect member of the STAT family, is activated in response to bacterial infection. *EMBO J*. 18, 959-967

Bartholomay, C., Mayhew, G. F., Fuchs, J. F., Rocheleau, T. A., Erickson, S. M., Aliota, M. T., & Christensen, B. M. (2007). Profiling infection responses in the haemocytes of the mosquito, *Aedes aegypti*. *Insect Mol Biol*. 16, 761–776

Baruch, D. I., Pasloske, B. L., Singh, H. B., Bi, X., Ma, X. C., Feldman, M., Tarashi, T. F., & Howard, R. J. (1995). Cloning the *P. falciparum* gene encoding PfEMP1, a malarial variant antigen and adherence receptor on the surface of parasitised human erythrocytes. *Cell*. 82, 77-87

Basir, R., Rahiman, S. S. F., Hasballah, K., Chong, W. C., Talib, H., Yam, M. F., Jabbarzare, M., Tie, T. H., Othmanm F., Moklas, M. A. M., Abdulah, W. O., & Ahmad, Z. (2012). *Plasmodium berghei* ANKA infection in ICR mice as a model of cerebral malaria. *Iranian J Parasitol.* 7, 62-74

Baton, L. A., Robertson, A., Warr, E., Strand, M. R., & Dimopoulos, G. (2009).

Genome-wide transcriptomic profiling of *Anopheles gambiae* haemocytes reveals pathogen-specific signatures upon bacterial challenge and *Plasmodium berghei* infection. *BMC Genomics*. 10, 257-270

Baton, L. A., & Ranford-Cartwright, L. C. (2004). *Plasmodium falciparum* ookinete invasion of the midgut epithelium of *Anopheles stephensi* is consistent with the Time Bomb model. *Parasitology*. 129, 663-676

Baum, J., Papenfuss, A. T., Baum, B., Speed, T. P., & Cowman, A. F. (2006). Regulation of apicomplexan actin-based motility. *Nature Reviews Microbiology*. 4, 621-628

Baxter, R. H. G., Chang, C., Chelliah, Y., Blandin, S., Levashina, E. A., & Deisenhofer, J. (2007). Structural basis for conserved complement factor-like function in the antimalarial protein TEP1. *Proc Natl Acad Sci USA.* 104, 11615-11620

Beare, N. A. V, Taylor, T. E., Harding, S. P., Lewallen, S., & Molyneux, M. E. (2006). Malarial retinopathy: A newly established diagnostic sign in severe malaria. *American Journal of Tropical Medicine and Hygiene*. 75, 790–797

Beeson, J. G., Chan, J. A., & Fowkes, F. J. I. (2013). PfEMP1 as a target of human immunity and a vaccine candidate against malaria. *Expert Review of Vaccines*.12, 105-108

Beitz, E., Pavlovic-Djuranovic, S., Yasui, M., Agre, P., & Schultz, J. E. (2004). Molecular dissection of water and glycerol permeability of the aquaglyceroporin from *Plasmodium falciparum* by mutational analysis. *Proc Natl Acad Sci USA.* 101, 1153-1158

Beitz, E. (2005). Aquaporins from pathogenic protozoan parasites: structure, function and potential for chemotherapy. *Biology of the Cell*. 97, 373-383

Belachew, E. B. (2018). Immune repsonse and evasion mechanismsm of *Plasmodium falciparum* parasites. *J Immunol Res*. 2018, e6529681

Bell, D., Peeling, R. W., & WHO-Regional Office for the Western Specific/TDR (2006). Evaluation of rapid diagnostic tests: Malaria. *Nat Reviews Microbiol*. 4, S34-38

Bell, D., & Winstanley, P. (2004). Current issues in the treatment of uncomplicated malaria in Africa. *British Medical Bulletin*. 71, 29-43

Bendtsen, J. D., Nielsen, H., von Heijne, G., & Brunak, S. (2004). Improved prediction of signal peptides: SignalP 3.0. *Journal of Molecular Biology*. 340, 783-795

Bernardini, F., Galizi, R., Menichelli, M., Papathanos, P. A., Dritsou, V., Marois, E., Crisanti, A., & Windbichler, N. (2014). Site-specific genetic engineering of the *Anopheles gambiae* Y chromosome. *Proc Natl Acad Sci USA.* 111, 7600-7605

Bignami, A., Bastiannelli, G. (1890). Osservazioni suile febbri malariche estive-autunnali. *la Riforma Medica.* 232, 1334–1335

Billker, O., Shaw, M. K., Margos, G., & Sinden, R. E. (1997). The roles of temperature, pH and mosquito factors as triggers of male and female gametogenesis of *Plasmodium berghei in vitro*. *Parasitology.* 11, 1–7

Billker, O, Lindo, V., Panico, M., Etienne, A. E., Paxton, T., Dell, A., Rogers, M., Sinden, R. E., & Morris, H. R. (1998). Identification of xanthurenic acid as the

putative inducer of malaria development in the mosquito. *Nature*. 392, 289–292

Billker, O., Miller, A. J., & Sinden, R. E. (2000). Determination of mosquito blood-meal pH in situ by ion-selective microelectrode measurement: Implications for the regulation of malarial gametogenesis. *Parasitology*. 120, 547-551

Billker, O., Dechamps, S., Tewari, R., Wenig, G., Franke-Fayard, B., & Brinkmann, V. (2004). Calcium and a calcium-dependent protein kinase regulate gamete formation and mosquito transmission in a malaria parasite. *Cell*. 117, 503–514

Bisi, D. C., & Lampe, D. J. (2011). Secretion of an anti-*Plasmodium* effector proteins from a natural pantoea agglomerans isolate by using PelB and HlyA secretion signals. *App Environm Microbiol*. 77, 4669-4675

Blagborough, A. M., & Sinden, R. E. (2009). *P. berghei* HAP2 induces strong malaria transmission-blocking immunity *in vivo* and *in vitro*. *Vaccine*. 27, 5187-5194

Blagborough, A. M., Delves, M. J., Butcher, G., & Sinden, R. E. (2013a). Assessing transmission blockade in *Plasmodium* spp. *Methods Mol Biol*. 923, 557-600

Blagborough, A. M., Churcher, T. S., Upton, L. M., Ghani, A. C., Gething, P. W., & Sinden, R. E. (2013b). Transmission-blocking interventions eliminate malaria from laboratory populations. *Nat Commun.* 4, 1812

Blandin, S., Moita, L. F., Köcher, T., Wilm, M., Kafatos, F. C., & Levashina, E. A. (2002). Reverse genetics in the mosquito *Anopheles gambiae*: Targeted disruption of the defensin gene. *EMBO Rep*. 3, 852–856

Blandin, S., Shiao, S. H., Moita, L. F., Janse, C. J., Waters, A. P., Kafatos, F. C., & Levashina, E. A. (2004). Complement-like protein TEP1 is a determinant of vectorial capacity in the malaria vector *A. gambiae*. *Cell*. 116(5), 661–670

Blandin, S., Marois, E., & Levashina, E. A. (2008). Antimalarial responses in *Anopheles gambiae*: From a complement-like protein to a complement-like pathway. *Cell Host Microbe*. 3, 364-374

Boëte, C. (2005). Malaria parasites in mosquitoes: Laboratory models, evolutionary temptation and the real world. *Trends Parasitol*. 21, 445-447

Boisson, B., Jacques, J. C., Choumet, V., Martin, E., Xu, J., Vernick, K., & Bourgouin, C. (2006). Gene silencing in mosquito salivary glands by RNAi. *FEBS Letters*. 580, 1988-1992

Bongio, N. J., & Lampe, D. J. (2015). Inhibition of *Plasmodium berghei* development in mosquitoes by effector proteins secreted from Asaia sp. Bacteria using a novel native secretion signal. *PLoS One*. 10, 30143541

Bourtzis, K., Dobson, S. L., Xi, Z., Rasgon, J. L., Calvitti, M., Moreira, L. A., *et al*., & Gilles, J. R. L. (2014). Harnessing mosquito-Wolbachia symbiosis for vector and disease control. *Acta Tropica*. 132, S150-163

Boury-Jamot, M., Sougrat, R., Tailhardat, M., le Varlet, B. Le, Bonté, F., Dumas, M., & Verbavatz, J. M. (2006). Expression and function of aquaporins in human skin: Is aquaporin-3 just a glycerol transporter? *Biochimica et Biophysica Acta - Biomembranes*. 1758, 1034-1042

Bousema, T., & Drakeley, C. J. (2011). Epidemiology and infectivity of *Plasmodium*

falciparum and *Plasmodium vivax* gametocytes in relation to malaria control and elimination. *Clin Microbiol Rev*. 24, 377-410

Bousema, J. T., Drakeley, C. J., & Sauerwein, R. W. (2006). Sexual-stage antibody responses to P. *falciparum* in endemic populations. *Curr Mol Med*. 6, 223–229

Bracchi-Ricard, V., Barik, S., Delvecchio, C., Doerig, C., Chakrabarti, R., & Chakrabarti, D. (2015). PfPK6, a novel cyclin-dependent kinase/mitogen-activated protein kinase-related protein kinase from *Plasmodium falciparum*. *Biochem J*. 347, 255-263

Braks, J. A. M., Franke-Fayard, B., Kroeze, H., Janse, C. J., & Waters, A. P. (2006). Development and application of a positive - Negative selectable marker system for use in reverse genetics in *Plasmodium*. *Nucleic Acids Res*. 14, e39

Brancucci, N. M. B., Bertschi, N. L., Zhu, L., Niederwieser, I., Chin, W. H., Wampfler, R., Freynmond, C., Rottmann, M., Felger, I., Bozdech, Z., & Voss, T. S. (2014). Heterochromatin protein 1 secures survival and transmission of malaria parasites. *Cell Host Microbe*. 16, 165-176

Brazier, A. J., Avril, M., Bernabeu, M., Benjamin, M., & Smith, J. D. (2017). Pathogenicity determinants of the human malaria parasite *Plasmodium falciparum* have ancient origins. *Host-Microbe Biol.* 2, e00348-16

Brett, D., Pospisil, H., Valcárcel, J., Reich, J., & Bork, P. (2002). Alternative splicing and genome complexity. *Nat Genetics*. 30, 29-30

Broadbent, K. M., Broadbent, J. C., Ribacke, U., Wirth, D., Rinn, J. L., & Sabeti, P. C. (2015). Strand-specific RNA sequencing in *Plasmodium falciparum* malaria identifies developmentally regulated long non-coding RNA and circular RNA. *BMC Genomics*. 16, 454-476

Bruce-Chwatt, L. J. (1987). Malaria and its control: Present situation and future prospects. *Ann Rev Public Health*. 8, 75-110

Bruce-Chwatt, L. J., Wernsdorfer, W., & McGregor, I. (1988). History of malaria from prehistory to erradication. *Malaria Princ Practice Malariol*. 36, 7-15

Bruce, M. C., Alano, P., Duthie, S., & Carter, R. (1990). Commitment of the malaria parasite *Plasmodium falciparum* to sexual and asexual development. *Parasitology*. 100, 191-200

Brugat, T., Reid, A. J., Lin, J. W., Cunningham, D., Tumwine, I., Kushinga, G., *et al*., & Langhorne, J. (2017). Antibody-independent mechanisms regulate the establishment of chronic *Plasmodium* infection. *Nat Microbiol*. 2, 16276-16298

Bubik, M. F., Willer, E. A., Bihari, P., Jurgenliemk, G., Ammer, H., Krombach, F. Zahler, S., Vollmar, A. M., & Fürst, R. (2012). A novel approach to prevent endothelial hyperpermeability: the *Crataegus* extract WS(R) 1442 targets the cAMP/Rap1 pathway. *Mol Cell Cardiol.* 52, 196–205

Buchan, J. R., & Parker, R. (2009). Eukaryotic stress granules: The ins and outs of translation. *Mol Cell*. 36, 932-941

Buckling, A., Ranford-Cartwright, L. C., Miles, A., & Read, A. (1999). Chloroquine increases *P. falciparum* gametocytogenesis *in vitro*. *Parasitology*. 118, 339-346

Bulet, P., Hetru, C., Dimarcq, J. L., & Hoffmann, D. (1999). Antimicrobial peptides in insects; structure and function. *Dev Comp Immunol*. 23, 329-44

Bull, P. C., & Abdi, A. I. (2016). The role of PfEMP1 as targets of naturally acquired immunity to childhood malaria: Vaccine prospects. *Parasitology*. 143, 171-186

Burda, P. C., Roelli, M. A., Schaffner, M., Khan, S. M., Janse, C. J., & Heussler, V. T. (2015). A *Plasmodium* phospholipase is involved in disruption of the liver stage parasitophorous vacuole membrane. *PLoS Path*. 11, e1004760

Burt, A. (2003). Site-specific selfish genes as tools for the control and genetic engineering of natural populations. *Proc Biol Sci.* 270, 921-928

Bushell, E. S. C., Ecker, A., Schlegelmilch, T., Goulding, D., Dougan, G., Sinden, R. E., Christophides, G. K., Kafatos, F. C., & Vlachou, D. (2009). Paternal effect of the nuclear formin-like protein MISFIT on *Plasmodium* development in the mosquito vector. *PLoS Path*. 5, e1000539

Bushell, E. S. C., Gomes, A. R., Sanderson, T., Anar, B., Girling, G., Herd, C., *et al.*, & Billker, O. (2017). Functional profiling of a *Plasmodium* genome reveals an abundance of essential genes. *Cell*. 170, 260-272

Bustamante, P. J., Woodruff, D. C., Oh, J., Keister, D. B., Muratova, O., & Williamson, K. C. (2000). Differential ability of specific regions of *Plasmodium falciparum* sexual-stage antigen, Pfs230, to induce malaria transmission-blocking immunity. *Parasit Immunol*. 22, 373-380

Bryant, W. B., & Michel, K. (2014). Blood feeding induces haemocyte proliferation and activation in the African malaria mosquito, *Anopheles gambiae* Giles. *J Exp Biol*. 217, 1238–1245

Cáceres, J. F., & Kornblihtt, A. R. (2002). Alternative splicing: Multiple control mechanisms and involvement in human disease. *Trends Gen*. 18, 186-193

Calvanese, L., Pellegrini-Calace, M., & Oliva, R. (2013). *In silico* study of human aquaporin AQP11 and AQP12 channels. *Protein Sci*. 22, 455-466

Canepa, G. E., Molina-Cruz, A., & Barillas-Mury, C. (2016). Molecular analysis of Pfs47-mediated *Plasmodium* evasion of mosquito immunity. *PLoS*. 11, e0168279

Canepa, G. E., Molina-Cruz, A., Yenkoidiok-Douti, L., Calvo, E., Williams, A. E., Burkhardt, M., *et al*., & Barillas-Mury, C. (2018). Antibody targeting of a specific region of Pfs47 blocks *Plasmodium falciparum* malaria transmission. *Npj Vaccines*. 3, 26

Canning, E. U., & Sinden, R. E. (1973). The organisation of the ookinete and observations on nuclear division in oocysts of *P. berghei*. *Parasitology*. 67, 29–40

Carballar-Lejarazú, R., & James, A. A. (2017). Population modification of Anopheline species to control malaria transmission. *Pathog Glob Health*. 111, 424-435

Carbrey, J. M., & Agre, P. (2009). Discovery of the aquaporins and development of the field. *Handbook of Exp Pharmacol*. 190, 3-28

Carlton, J. M., Hayton, K., Cravo, P. V., & Walliker, D. (2001). Of mice and malaria mutants: Unravelling the genetics of drug resistance using rodent malaria models. *Trends Parasitol.* 17, 236-242

Carlton, J. M., Angiuoli, S. V., Suh, B. B., Kooij, T. W., Pertea, M., Silva, J. C., *et al*., & Carucci, D. J. (2002). Genome sequence and comparative analysis of the model rodent malaria parasite *Plasmodium yoelii yoelii*. *Nature*. 419, 512-519

Carlton, J. M., Adams, J. H., Silva, J. C., Bidwell, S. L., Lorenzi, H., Caler, E., *et al*., & Fraser-Liggett, C. M. (2008). Comparative genomics of the neglected human malaria parasite *Plasmodium vivax*. *Nature*. 455, 757-763

Carruthers, V. B., & Tomley, F. M. (2010). Receptor-ligand interaction and invasion: Microneme proteins in apicomplexans. *Subcell Biochem*. 47, 33–45

Carter, R., & Chen, D. H. (1976). Malaria transmission blocked by immunisation with gametes of the malaria parasite. *Nature*. 263**,** 57-60

Carter, R., Coulson, A., Bhatti, S., Taylor, B. J., & Elliott, J. F. (1995). Predicted disulphide-bonded structures for three uniquely related proteins of *Plasmodium falciparum*, Pfs230, Pfs48 45 and Pf12. *Mol Bioch Paras*. 71, 203-210

Carter, R., Mendis, K. N., Miller, L. H., Molineaux, L., & Saul, A. (2000). Malaria transmission-blocking vaccines - how can their development be supported? *Nature Med*. 6, 241-244

Carter, R. (2001). Transmission blocking malaria vaccines. *Vaccine*. 19, 2309-2314

Carter, V., Nacer, A. M., Sinden, R. E., & Hurd, H. (2007). Minimum requirements for ookinete to oocyst transformation in *Plasmodium*. *Int J Parasitol*. 37, 1221-1232

Carvalho, D. O., McKemey, A. R., Garziera, L., Lacroix, R., Donnelly, C. A., Alphey, L., Malavasi, A., & Capurro, M. L. (2015). Suppression of a field population of *Aedes aegypti i*n Brazil by sustained release of transgenic male mosquitoes. *PLoS Negl Trop Dis*. 9, e0003864

Carvalho, T. G., & Ménard, R. (2005). Manipulating the *Plasmodium* genome. *Curr Issues Mol Biol*. 7, 39-55

Castillo, J. C., Robertson, A. E., & Strand, M. R. (2006). Characterisation of haemocytes from the mosquitoes *Anopheles gambiae* and *Aedes aegypti*. *Insect Biochem Mol Biol*. 36, 891-903

Castillo, J. C., Brown, M. R., & Strand, M. R. (2011). Blood feeding and insulin-like peptide 3 stimulate proliferation of haemocytes in the mosquito *Aedes aegypti. PLoS Path*. 7, e1002274

Castillo, J. C., Ferreira, A. B. B., Trisnadi, N., & Barillas-Mury, C. (2017). Activation of mosquito complement antiplasmodial response requires cellular immunity. *Science Immunol*. 2, eaal1505

Catteruccia, F., Nolan, T., Loukeris, T. G., Blass, C., Savakis, C., Kafatos, F. C., & Crisanti, A. (2000). Stable germline transformation of the malaria mosquito *Anopheles stephensi*. *Nature*. 405, 959-962

Catteruccia, F., Nolan, T., Blass, C., Muller, H. M., Crisanti, A., Kafatos, F. C., & Loukeris, T. G. (2002). Toward *Anopheles* transformation: Minos element activity in anopheline cells and embryos. *Proc Natl Acad Sci USA*. 97, 2157-2162

Champer, J., Buchman, A., & Akbari, O. S. (2016). Engineering gene drives to manipulate the fate of wild populations. *Nature Rev Gen*. 17, 146-159

Chandler, C. I. R., Whitty, C. J. M, & Ansah, E. K. (2010). How can malaria rapid diagnostic tests achieve their potential? A qualitative study of a trial at health facilities in Ghana. *Malar J.* 9, 95-110

Chaturvedi, N., Bharti, P. K., Tiwari, A., & Singh, N. (2016). Strategies & recent development of transmission-blocking vaccines against *Plasmodium falciparum*. *Indian J Med Res*. 143, 696-711

Chakravorty, S. J., Hughes, K. R., & Craig, A. G. (2008). Host response to cytoadherence in *Plasmodium falciparum*. *Biochem Soc. Trans*. 36, 221–228

Chan, J. A., Fowkes, F. J. I., & Beeson, J. G. (2014). Surface antigens of *Plasmodium falciparum*-infected erythrocytes as immune targets and malaria vaccine candidates. *Cell Mol Life Sci*. 71, 66433-66457

Child, M. A., Harris, P. K., Collins, C. R., Withers-Martinez, C., Yeoh, S., & Blackman, M. J. (2013). Molecular determinants for subcellular trafficking of the malarial sheddase PfSUB2. *Traffic.* 14, 1053–1064

Christophides, G. K, Zdobnov, E., Barillas-Mury, C., Blandin, S., Blass, C., Brey, P. T., Danielli, A., Dimopoulos, G., Hetru, C., *et al*., & Kafatos, F. C. (2002). Immunity genes and gene families in *Anopheles gambiae*. *Science*. 298, 159–165

Christophides, G. K, Vlachou, D., & Kafatos, F. C. (2004). Comparative and functional genomics of the innate immune system in the malaria vector *Anopheles gambiae*. *Immunol Rev*. 198, 127–148

Chu, T., Lingelbach, K., & Przyborski, J. M. (2011). Genetic evidence strongly support an essential role for PfPV1 in intra-erythrocytic growth of *Plasmodium falciparum*. *PLoS One*. 6, e18396

Churcher, T. S., Dawes, E. J., Sinden, R. E., Christophides, G. K., Koella, J. C., & Bašanez, M. G. (2010). Population biology of malaria within the mosquito: Density-dependent processes and potential implications for transmission-blocking interventions. *Malaria J*. 9, 311-322

Clark I. A., & Cowden W. B. (2003). The pathophysiology of *Plasmodium falciparum* malaria. *Pharmacol Ther*. 99, 221–60

Claudianos, C., Dessens, J. T., Trueman, H. E., Arai, M., Mendoza, J., Butcher, G. A., Crompton, T., & Sinden, R. E. (2002). A malaria scavenger receptor-like protein essential for parasite development. *Mol Microbiol*. 45, 1473-1484

Clayton, A. M., Dong, Y., & Dimopoulos, G. (2014). The *Anopheles* innate immune system in the defense against malaria infection. *J Inn Imm*. 6, 169–181

Coggins, S. A., Estévez-Lao, T. Y., & Hillyer, J. F. (2012). Increased survivorship following bacterial infection by the mosquito *Aedes aegypti* as compared to *Anopheles gambiae* correlates with increased transcriptional induction of antimicrobial peptides. *Dev Comp Imm*. 37, 390-401

Cohuet, A., Osta, M. A., Morlais, I., Awono-Ambene, P. H., Michel, K., Simard, F., Christophides, G. K., Fontenille, D., & Kafatos, F. C. (2006). *Anopheles* and *Plasmodium*: From laboratory models to natural systems in the field. *EMBO Reports*. 7, 1285-1289

Coleman, B. I., Skillman, K. M., Jiang, R. H. Y., Childs, L. M., Atenhofen, L. M., Ganter,

M., Leung, Y., Goldowitz, I., *et al*., & Duraisingh, M. T. (2014). A *Plasmodium falciparum* Histone Deacetylase regulates antigenic variation and gametocyte conversion. *Cell Host Microbe*. 16, 177-186

Collins, W. E. (2012). *Plasmodium malariae*: A malaria parasite of monkeys and humans. *Annual Review of Entomology*. 57, 107–121

Conway, D. J., Machado, R. L. D., Singh, B., Dessert, P., Mikes, Z. S., Povoa, M. M., Oduola, A. M. J., & Roper, C. (2001). Extreme geographical fixation of variation in the *Plasmodium falciparum* gamete surface protein gene Pfs48/45 compared with microsatellite loci. *Mol Biochem Parasitol*. 115, 145-156

Corby-Harris, V., Drexler, A., de Jong, L. W., Antonova, Y., Pakpour, N., Ziegler, R., Ramberg, F., Lewis, E. E., Brown, J. M., Luckhart, S., & Riehle, M. A. (2010). Activation of Akt signalling reduces the prevalence and intensity of malaria parasite infection and lifespan in *A. stephensi* mosquitoes. *PLoS Path*. 6, e100103

Cowman, A. F. & Crabb, B. S. (2006). Invasion of red blood cells by malaria parasites. *Cell*. 124 , 755–766

Crabb, B. S., Cooke, B. M., Reeder, J. C., Waller, R. F., Caruana, S. R., Davern, K. M., Wickham, M. E., Brown, G. V., Coppel, R. L., & Cowman, A. F. (1997). Targeted gene disruption shows that knobs enable malaria-infected red cells to cytoadhere under physiological shear stress. *Cell*. 89, 287-296

Craig V., J., Adams, M. D., Myers, E. W., Li, P. W., Mural, R. J., Sutton, G. G., *et al*., & Zhu, X. (2001). The sequence of the human genome. *Science*. 291, 1304-1351

Craig, M. H., Bredenkamp, B. L., Williams, V. C. H., Rossouw, E. J., Kelly, V. J., Kleinschmidt, I., Martineau, A., & Henry, G. F. J. (2002). Field and laboratory comparative evaluation of ten rapid malaria diagnostic tests. *Trans R Soc Trop Med Hyg.* 96, 258-265

Craig, A. G., Grau, G. E., Janse, C. J., Kazura, J. W., Milner, D., Barnwell, J. W., Turner, G., Langhorne, J. & Participants of the Hinxton Retreat meeting on animal models for research on severe malaria. (2012). The role of animal models for research on severe malaria. *PLoS Path*. 8, 1002401

Crompton, P. D., Moebius, S., Protugal, S., Waisberg, M., Hart, G., Garver, L. S., Miller, L. H., Barillas-Mury, C., & Pierce, S. K. (2010) Malaria immunity in man and mosquito: insights into unsolved mysteries of a deadly infectious disease. *Annual Review of Immunology*. 32, 157-187

Crotti, E., Damiani, C., Pajoro, M., Gonella, E., Rizzi, A., Ricci, I., *et al.*, & Daffonchio, D. (2009). Asaia, a versatile acetic acid bacterial symbiont, capable of cross-colonising insects of phylogenetically distant genera and orders. *Environm Microbiol*. 11, 3252-3264

Currà, C., Gessmann, R., Pace, T., Picci, L., Peruzzi, G., Varamogianni-Mamatsi, V., *et al*., & Sidén-Kiamos, I. (2016). Release of *Plasmodium* sporozoites requires proteins with histone-fold dimerisation domains. *Nat Commun*. 7, 13846-13855

Curtis, C. F., Pates, H. V., Takken, W., Maxwell, C. A., Myamba, J., Priestman, A., Akinpelu, O., Yayo, A. M., & Hu, J. T. (1999). Biological problems with the replacement of a vector population by *Plasmodium*-refractory mosquitoes. *Parassitologia*. 41, 479-481

Curtis, C. F., Maxwell, C. A., Magesa, S. M., Rwegoshora, R. T., & Wilkes, T. J. (2007). Insecticide-treated bed-nets for malaria mosquito control. *J Am Mosq Control Assoc*. 22, 501-506

Daily, J. P., Scanfeld, D., Pochet, N., le Roch, K., Plouffe, D., Kamal, M., Sarr, O., Mboup, S., Ndir, O., *et al*., & Regev, A. (2007). Distinct physiological states of *Plasmodium falciparum* in malaria-infected patients. *Nature*. 450, 1091-1095

Damiani, C., Ricci, I., Crotti, E., Rossi, P., Rizzi, A., Scuppa, P., Capone, A., Ulissi, U., Epis, S., Cenghi, M., *et al*., & Favia, G. (2010). Mosquito-bacteria symbiosis: The case of *Anopheles gambiae* and Asaia. *Microb Ecol*. 60, 644-654

Danielli, A., Barillas-Mury, C., Kumar, S., Kafatos, F. C., & Loukeris, T. G. (2005). Overexpression and altered nucleocytoplasmic distribution of *Anopheles* ovalbumin-like SRPN10 serpins in *Plasmodium*-infected midgut cells. *Cell Microbiol*. 7, 181–190

Danielli, A., Kafatos, F. C., & Loukeris, T. G. (2003). Cloning and characterisation of four *Anopheles gambiae* serpin isoforms, differentially induced in the midgut by *Plasmodium berghei* invasion. *J Biol Chem.* 278, 4184-4193

Dari, F. D., Churcher, T. S., Yerbanga, R.S., Yaméogo, B., Sangaré, I., Oedraogo, J. B., Sinder, R. E., Blagborough, A. M., & Cohuet, A. (2014). Experimental study of the relationship between *Plasmodium* gametocyte density and infection success in mosquitoes; implications for the evaluation of malaria transmission-reducing interventions. *Exp Parasitol.* 149, 74-83

Das, S., Manna, S., Saha, B., Hati, A. K., & Roy, S. (2018). Novel pfkelch13 Gene Polymorphism Associates With Artemisinin Resistance in Eastern India. *Clin Infect Dis*. 69, 1144-1152

Dawes, E. J., Churcher, T. S., Zhuang, S., Sinden, R. E., & Bašez, M. G. (2009). *Anopheles* mortality is both age- and *Plasmodium*-density dependent: Implications for malaria transmission. *Malar J*. 8, 228-244

de Freece, C., Damiani, C., Valzano, M., D'Amelio, S., Cappelli, A., Ricci, I., & Favia, G. (2014). Detection and isolation of the α-proteobacterium Asaia in Culex mosquitoes. *Med Vet Entomol*. 28, 438-442

de Jong, R. M., Tebeje, S. K., Meerstein-Kessel, L., Tadesse, F. G., Jore, M. M., Stone, W. J., & Bousema, T. (2020). Immunity against sexual stage *Plasmodium falciparum* and *Plasmodium vivax* parasites. *Immunol Rev.* 293, 190-215

de Koning-Ward, T. F., Fidock, D. A., Thathy, V., Ménard, R., van Spaendonk, R. M. L., Waters, A. P., & Janse, C. J. (2000). The selectable marker human dihydrofolate reductase enables sequential genetic manipulation of the *Plasmodium berghei* genome. *Mol Biochem Parasitol*. 106, 199-212

de Koning-Ward, T. F., Janse, C. J., & Waters, A. P. (2002). The development of genetic tools for dissecting the biology of malaria parasites. *Annu Micobiol*. 54, 157-185

de Koning-Ward, T. F., Olivieri, A., Bertuccini, L., Hood, A., Silvestrini, F., Charvalias, K., *et al*., & Ranford-Cartwright, L. C. (2008). The role of osmiophilic bodies and Pfg377 expression in female gametocyte emergence and mosquito infectivity in the human malaria parasite *Plasmodium falciparum*. *Mol Microbiol*. 67, 278-290

de Oca, M. M., Engwerda, C., & Haque, A. (2013). *Plasmodium berghei* infection of C57BL/6J mice: A model of severe malaria. *Methods Mol Biol*. 1031, 203-213

Dearsly, A. L., Sinden, R. E., & Self, I. A. (1990). Sexual development in malarial parasites: gametocyte production, fertility and infectivity to the mosquito vector. *Parasitology.* 3, 359–68

Deligianni, E., Morgan, R. N., Bertuccini, L., Wirth, C. C., Silmon de Monerri, N. C., Spanos, L., Blackman, M. J., Louis, C., Pradel, G., & Sidén-Kiamos, I. (2013). A perforin-like protein mediates disruption of the erythrocyte membrane during egress of *Plasmodium berghei* male gametocytes. *Cell Microbiol*. 15, 1438-1455

Dessens, J. T., Beetsma, A. L., Dimopoulos, G., Wengelnik, K., Crisanti, A., Kafatos, F. C., & Sinden, R. E. (1999). CTRP is essential for mosquito infection by malaria ookinetes. *EMBO J*. 18, 6221–6227

Dessens, J. T., Mendoza, J., Claudianos, C., Vinetz, J. M., Khater, E., Hassard, S., Ranawaka, G. R., & Sinden, R. E. (2001). Knockout of the rodent malaria parasite PbCHT1 reduces infectivity to mosquitoes. *Infect Immun*. 69, 4041–4047

Dessens, J. T., Sidén-Kiamos, I., Mendoza, J., Mahairaki, V., Khater, E., Vlachou, D., Xu, X. J., Kafatos, F. C., Louis, C., Dimopoulos, G., & Sinden, R. E. (2003). SOAP, a novel malaria ookinete protein involved in mosquito midgut invasion and oocyst development. *Mol Microbiol*. 49, 319–329

Dimopoulos, G., Seeley, D., Wolf, A., & Kafatos, F. C. (1998). Malaria infection of the mosquito *Anopheles gambiae* activates immune-responsive genes during critical transition stages of the parasite lifecycle. *EMBO J*. 17, 6115-6123

Dimopoulos, G., Casavant, T. L., Chang, S., Scheetz, T., Roberts, C., Donohue, M., Donohue, M., Schultz, J., *et al.*, & Kafatos, F. C. (2002a). *Anopheles gambiae* pilot gene discovery project: Identification of mosquito innate immunity genes from expressed sequence tags generated from immune-competent cell lines. *Proc Natl Acad Sci USA*. 97, 6619-6624

Dimopoulos, G., Christophides, G. K., Meister, S., Schultz, J., White, K. P., Barillas-Mury, C., & Kafatos, F. C. (2002b). Genome expression analysis of *Anopheles gambiae*: Responses to injury, bacterial challenge, and malaria infection. *Proc Natl Acad Sci USA*. 10, 8814-8819

Dinglasan, R. R., Fields, I., Shahabuddin, M., Azad, A. F., & Sacci, J. B. (2003). Monoclonal antibody MG96 completely blocks *Plasmodium yoelii* development in *Anopheles stephensi*. *Infect Immun*. 71, 6995-7001

Dinglasan, R. R., Kalume, D. E., Kanzok, S. M., Ghosh, A. K., Muratova, O., Pandey, A., & Jacobs-Lorena, M. (2007). Disruption of *Plasmodium falciparum* development by antibodies against a conserved mosquito midgut antigen. *Proc Natl Acad Sci USA.* 104, 13461–13466

Dinglasan, R. R., & Jacobs-Lorena, M. (2008). Flipping the paradigm on malaria transmission-blocking vaccines. *Trends Parasitol*. 24, 364–370

Dinko, B., Pradel, G. (2016). Immune evasion by P. *falciparum* parasites: converting a host protection mechanism for tits benefit. *J Immunol Res*. 2018, e6529681

Dong, Y., Aguilar, R., Xi, Z., Warr, E., Mongin, E., & Dimopoulos, G. (2006). *Anopheles*

gambiae immune responses to human and rodent *Plasmodium* parasite species. *PLoS Path*. 2, 513–525

Dong, Y., Manfredini, F., & Dimopoulos, G. (2009). Implication of the mosquito midgut microbiota in the defense against malaria parasites. *PLoS Path*. 5, e1000423

Dong, Y., Das, S., Cirimotich, C., Souza-Neto, J. A., McLean, K. J., & Dimopoulos, G. (2011). Engineered *Anopheles* immunity to *Plasmodium* infection. *PLoS Path*. 7, e1002458

Dong, Y., Cirimotich, C. M., Pike, A., Chandra, R., & Dimopoulos, G. (2012). *Anopheles* NF-κB-regulated splicing factors direct pathogen-specific repertoires of the pattern recognition receptor AgDscam. *Cell Host Mic*. 12, 521–530

Doolan, D. L., Hedstrom, R. C., Gardner, M. J., Sedegah, M., Wang, H., Gramzinski, R. A., Margalith, M., Hobart, P. & Hoffman, S. L. (1998). DNA vaccination as an approach to malaria control: current status and strategies. *Curr Top Microbiol Immunol*. 226, 37–56

Doolan, D. L., Southwood, S., Freilich, D. A., Sidney, J., Graber, N. L., Shatney, L., Bebris, L., Florens, L., *et al*., & Sette, A. (2003). Identification of *Plasmodium falciparum* antigens by antigenic analysis of genomic and proteomic data. *Proc Natl Acad Sci USA.* 100, 9952-9957

Douglas, A. D., Williams, A. R., Illingworth, J. J., Kamuyu, G., Biswas, S., Goodman, A. L., *et al.*, & Draper, S. J. (2011). The blood stage malaria antigen PfRH5 is susceptible to vaccine-inducible cross-strain neutralising antibody. *Nat Commun*. 20, 601-620

Douglas, R. G., Amino, R., Sinnis, P., & Frischknecht, F. (2015). Active migration and passive transport of malaria parasites. *Trends Parasitol.* 31, 357-362

Doumbo, O. K., Niaré, K., Healy, S. A., Sagara, I., & Duffy, P. E. (2018). Malaria transmission-blocking vaccines: Present status and future perspectives. *Towards malaria elimination - A leap forward.* DOI: 10.5772/intechopen.77241

Drakeley, C. J., Bousema, J. T., Akim, N. I., Teelen, K., Roeffen, W., Lensen, A. H., Bolmer, M., Eling, W., & Sauerwein, R. W. (2006). Transmission-reducing immunity is inversely related to age in *Plasmodium falciparum* gametocyte carriers. *Parasite Immunol*. 28, 185–190

Drexler, A., Nuss, A., Hauck, E., Glennon, E., Cheung, K., Brown, M., & Luckhart, S. (2012). Human IGF1 extends lifespan and enhances resistance to *Plasmodium falciparum* infection in the malaria vector A. *stephensi*. *J Exp Biol*. 216, 208-217

Druilhe, P., Tall, A., & Sokhna, C. (2005). Worms can worsen malaria: Towards a new means to roll back malaria? *Trends Parasitol*. 21, 359-362

Dubois, D. J., & Soldati-Favre, D. (2019). Biogenesis and secretion of micronemes in *Toxoplasma gondii*. *Cell Microbiol.* 5, e13018

Dubremetz, J. F., Garcia-Reguet, N., Conseil, V., & Fourmaux, M. N. (1998). Apical organelles and host-cell invasion by Apicomplexa. *Int J Parasitol.* 28, 1007-1013

Ecker, A., Pinto, S. B., Baker, K. W., Kafatos, F. C., & Sinden, R. E. (2007). *Plasmodium berghei*: *Plasmodium* perforin-like protein 5 is required for mosquito

midgut invasion in *Anopheles stephensi*. *Exp Parasitol*. 116, 504–508

Ecker, A., Bushell, E. S. C., Tewari, R., & Sinden, R. E. (2008). Reverse genetics screen identifies six proteins important for malaria development in the mosquito. *Mol Microbiol*. 70, 209–220

Egan, T. J., & Kaschula, C. H. (2007). Strategies to reverse drug resistance in malaria. *Curr Opin Infect Dis*. 20, 598-604

Eksi, S., Czesny, B., van Gemert, G. J., Sauerwein, R. W., Eling, W., & Williamson, K. C. (2006). Malaria transmission-blocking antigen, Pfs230, mediates human red blood cell binding to exflagellating male parasites and oocyst production. *Mol Microbiol*. 61, 991–998

Eksi, S., Morahan, B. J., Haile, Y., Furuya, T., Jiang, H., Ali, O., Xu, H., Kiattibutr, K., Suri, A., *et al*., & Williamson, K. C. (2012). *Plasmodium falciparum* gametocyte development 1 (Pfgdv1) and gametocytogenesis early gene identification and commitment to sexual development. *PLoS Path.* 8, e1002964

Eldering, M., Morlais, I., Van Gemert, G. J., van de Vegte-Bolmer, M., Graumans, W., Siebelink-Stoter, R., Vos, M., & Sauerwein, R. W. (2016). Variation in susceptibility of African *Plasmodium falciparum* malaria parasites to TEP1 mediated killing in *Anopheles gambiae* mosquitoes. *Sci Rep*. 6, 20440-20447

Elrod-Erickson, M., Mishra, S., & Schneider, D. (2000). Interactions between the cellular and humoral immune responses in Drosophila. *Curr Biol*. 10, 781-784

Epis, S., Gaibani, P., Ulissi, U., Chouaia, B., Ricci, I., Damiani, C., Sambri, V., Castelli, F., Buelli, F., Daffonchio, D., Bandi, C., & Favia, G. (2012). Do mosquito-associated bacteria of the genus Asaia circulate in humans? *Eur J Clin Microbiol Infect Dis*. 31, 1137-1140

Epstein, J. E., Tewari, K., Lyke, K. E., Sim, B. K. L., Billingsley, P. F., Laurens, M. B., Gunasekera, A., *et al*., & Hoffman, S. L. (2011). Live attenuated malaria vaccine designed to protect through hepatic CD8+ T cell immunity. *Science*. 334, 475-480

Epstein, J. E., Paolino, K. M., Richie, T. L., Sedegah, M., Singer, A., Ruben, A. J., Chakravarty, S., Stafford, A., *et al*., & Hoffman, S. L. (2017). Protection against *Plasmodium falciparum* malaria by PfSPZ vaccine. *JCI Insight*. 2, e89154

Escalante, A. A., Grebert, H. M., Chaiyaroj, S. C., Magris, M., Biswas, S., Nahlen, B. L., & Lal, A. A. (2001). Polymorphism in the gene encoding the apical membrane antigen-1 (AMA-1) of *Plasmodium falciparum*. X. Asembo Bay Cohort Project. *Mol Biochem Parasitol*. 113, 279-287

Fang, W., Vega-Rodríguez, J., Ghosh, A. K., Jacobs-Lorena, M., Kang, A., & Leger, R. J. St. (2011). Development of transgenic fungi that kill human malaria parasites in mosquitoes. *Science*. 331, 1074-1077

Fang, H., Klages, N., Baechler, B., Hillner, E., Yu, L., Pardo, M., Choudhary, J., & Brochet, M. (2017). Multiple short windows of calcium-dependent protein kinase 4 activity coordinate distinct cell cycle events during *Plasmodium* gametogenesis. *eLife*. 10, e26524

Farrance, C. E., Rhee, A., Jones, R. M., Musiychuk, K., Shamloul, M., Sharma, S., *et al*., & Yusibov, V. (2011). A plant-produced Pfs230 vaccine candidate blocks

transmission of *Plasmodium falciparum*. *Clin Vaccine Immunol*. 18, 1352-1357

Favia, G., Ricci, I., Damiani, C., Raddadi, N., Crotti, E., Marzorati, M., Rizzi, A., Urso, R., Brusetti, L., Borin, A., *et al.*, & Daffonchio, D. (2007). Bacteria of the genus Asaia stably associate with *Anopheles stephensi*, an Asian malarial mosquito vector. *Proc Natl Acad Sci USA*. 104, 9047-9051

Feldmann, A. M., & Ponnudurai, T. (1989). Selection of A. *stephensi* for refractoriness and susceptibility to *Plasmodium falciparum*. *Med Vet Entomol*. 3, 41-52

Ferguson, D. J. P., Balaban, A. E., Patzewitz, E. M., Wall, R. J., Hopp, C. S., Poulin, B., Mohmmed, A., Malhotra, P., Coppi, A., Sinnis, P., & Tewari, R. (2014). The repeat region of the circumsporozoite protein is critical for sporozoites formation and maturation in *Plasmodium*. *PLoS One*. 9, e113923

Fidock, D. A., & Wellems, T. E. (2002). Transformation with human dihydrofolate reductase renders malaria parasites insensitive to WR99210 but does not affect the intrinsic activity of proguanil. *Proc Natl Acad Sci USA*. 94, 10931-10936

Filarsky, M., Fraschka, S. A., Niederwieser, I., Brancucci, N. M. B., Carrington, E., Carrió, E., Moes, S., Jenoe, P., Bartfai, R., & Voss, T. S. (2018). GDV1 induces sexual commitment of malaria parasites by antagonising HP1-dependent gene silencing. *Science*. 359, 1259-1263

Fischer, G., Kosinska-Eriksson, U., Aponte-Santamaría, C., Palmgren, M., Geijer, C., Hedfalk, K., Hohmann, S., de Groot, B. L., Neutze, R., & Lindkvist-Petersson, K. (2009). Crystal structure of a yeast aquaporin at 1.15 Å reveals a novel gating mechanism. *PLoS Biol*. 7, e1000130

Fraiture, M., Baxter, R. H. G., Steinert, S., Chelliah, Y., Frolet, C., Quispe-Tintaya, W., Hoffmann, J. A., Blandin, S., & Levashina, E. (2009). Two mosquito LRR proteins function as complement control factors in the TEP1-mediated killing of *Plasmodium*. *Cell Host Microbe*. 5, 273–284

Fried, M., & Duffy, P. E. (2015). Designing a VAR2CSA-based vaccine to prevent placental malaria. *Vaccine*. 33, 7483-7488

Frischknecht, F. Baldacci, P., Martin, B., Zimmer, C., Thiberge, S., Olivo-Marin, J. C., Shorte, S. L., & Ménard, R. (2004). Imaging movement of malaria parasites during transmission by *Anopheles* mosquitoes*. Cell. Microbiol.* 6, 687–694

Frischknecht, F., & Matuschewski, K. (2017). *Plasmodium* sporozoite biology. *Cold Spring Harb Pespect Med*. 7, a025478

Frolet, C., Thoma, M., Blandin, S., Hoffmann, J. A., & Levashina, E. A. (2006). Boosting NF-κB-dependent basal immunity of *Anopheles gambiae* aborts development of *Plasmodium berghei*. *Immunity*. 25, 677-685

Fujita, M., Yoko-o, T., Okamoto, M., & Jigami, Y. (2004). GPI7 involved in glycosylphosphatidylinositol biosynthesis is essential for yeast cell separation. *J Biol Chem*. 279, 51869–51879

Galizi, R., Doyle, L. A., Menichelli, M., Bernardini, F., Deredec, A., Burt, A., Stoddard, B. L., Windbichler, N., & Crisanti, A. (2014). A synthetic sex ratio distortion system for the control of the human malaria mosquito. *Nat Commun*. 5, 3977-3985

Gantz, V. M., Jasinskiene, N., Tatarenkova, O., Fazekas, A., Macias, V. M., Bier, E.,

& James, A. A. (2015). Highly efficient Cas9-mediated gene drive for population modification of the malaria vector mosquito A. *stephensi*. *Proc Natl Acad Sci USA*. 112, e6736-6743

Gardner, M. J., Hall, N., Fung, E., White, O., Berriman, M., Hyman, R. W., Carlton, J. M., Pain, A., Nelson, K. E., *et al*., & Barrell, B. (2002). Genome sequence of the human malaria parasite *Plasmodium falciparum*. *Nature*. 419, 498–511

Garver, L. S., Dong, Y., & Dimopoulos, G. (2009). Caspar controls resistance to *Plasmodium falciparum* in diverse anopheline species. *PLoS Path*. 5, e1000335

Garver, L. S., Bahia, A. C., Das, S., Souza-Neto, J. A., Shiao, J., Dong, Y., & Dimopoulos, G. (2012). *Anopheles* Imd pathway factors and effectors in infection intensity-dependent anti-*Plasmodium* action. *PLoS Path*. 8, 7–9

Garver, L., de Almeida-Oliveira, G., & Barillas-Mury, C. (2013). The JNK pathway is a key mediator of *A. gambiae* antiplasmodial immunity. *PLoS Path*. 9, e1003622

Gerloff, D. L., Creasey, A., Maslau, S., & Carter, R. (2005). Structural models for the protein family characterised by gamete surface protein Pfs230 of *Plasmodium falciparum*. *Proc Natl Acad Sci USA.* 102, 13598-13603

Ghanchi, N. K., Mårtensson, A., Ursing, J., Jafri, S., Bereczky, S., Hussain, R., & Beg, M. (2010). Genetic diversity among *Plasmodium falciparum* field isolates in Pakistan measured with PCR genotyping of the merozoite surface protein 1 and 2. *Malar J*. 9, 1-7

Ghorbal, M., Gorman, M., MacPherson, C. R., Martins, R. M., Scherf, A., & Lopez-Rubio, J. J. (2014). Genome editing in the human malaria parasite *Plasmodium falciparum* using the CRISPR-Cas9 system. *Nature Biotech*. 32, 819-821

Ghosh, A. K., Ribolla, P. E. M., & Jacobs-Lorena, M. (2001). Targeting *Plasmodium* ligands on mosquito salivary glands and midgut with a phage display peptide library. *Proc Natl Acad Sci USA*. 98, 13278–13281

Ghosh, A. K., Devenport, M., Jethwaney, D., Kalume, D. E., Pandey, A., Anderson, V. E., & Jacobs-Lorena, M. (2009). Malaria parasite invasion of the mosquito salivary gland requires interaction between the *Plasmodium* TRAP and the *Anopheles* saglin proteins. *PLoS Path*. 5, e1000265

Ghosh, A. K., Coppens, I., Gardsvoll, H., Ploug, M., & Jacobs-Lorena, M. (2011a). *Plasmodium* ookinetes coopt mammalian plasminogen to invade the mosquito midgut. *Proc Natl Acad Sci USA.* 108, 17153–17158

Ghosh, A. K., & Jacobs-Lorena, M. (2011b). Surface-expressed enolases of *Plasmodium* and other pathogens. *Mem Inst Oswaldo Cruz*. 106, 85–90

Giganti, D., Bouillon, A., Tawk, L., Robert, F., Martinez, M., Crublet, E., Weber, P., Girard-Blanc, C., Petres, S., *et al*., & Barale, J. C. (2014). A novel *Plasmodium*-specific prodomain fold regulates the malaria drug target SUB1 subtilase. *Nat Commun*. 10, 4833-4844

Ginsburg, H. (2006). Progress in *in silico* functional genomics: the malaria Metabolic Pathways database. *Trends Parasitol*. 22, 238-240

Golenser, J., Waknine, J. H., Krugliak, M., Hunt, N. H., & Grau, G. (2006). Current perspectives on the mechanism of action of artemisinins. *Parasitol*. 36, 1427-1441

Gomes, A. R., Bushell, E. S. C., Schwach, F., Girling, G., Anar, B., Quail, M. A., Herd, C., Modrzynska, K., Rayner, J. C., & Billker, O. (2015). A genome-scale vector resource enables high-throughput reverse genetic screening in a malaria parasite. *Cell Host Microbe*. 17, 404-413

Gonen, T., & Walz, T. (2006). The structure of aquaporins. *Rev Biophys*. 39, 361-396

González-Lázaro, M., Dinglasan, R. R., Hernández-Hernández, F. de la C., Rodríguez, M. H., Laclaustra, M., Jacobs-Lorena, M., & Flores-Romo, L. (2009). *Anopheles gambiae* Croquemort SCRBQ2, expression profile in the mosquito and its potential interaction with the malaria parasite *Plasmodium berghei*. *Insect Biochem Mol Biol*. 39, 395-402

Goodman, A. L., Forbes, E. K., Williams, A. R., Douglas, A. D., de Cassan, S. C., Bauza, K., Biswas, S., Dicks, M. D. J., Llewellyn, D., Moore, A. C., *et al*., & Draper, S. J. (2013). The utility of *Plasmodium berghei* as a rodent model for anti-merozoite malaria vaccine assessment. *Sci Rep*. 3, 1706-1719

Goonewardene, R., Daily, J., Kaslow, D., Sullivan, T. J., Duffy, P. E., Carter, R., Mendis, K., & Wirth, D. (2006). Transfection of the malaria parasite and expression of firefly luciferase. *Proc Natl Acad Sci USA*. 90, 5234-5236

Gotz, P. (1986) Encapsulation in arthropods. I*mmunity in Invertebrates*. pp153-170

Goulielmaki, E., Sidén-Kiamos, I., & Loukeris, T.G. (2014). Functional characterisation of *Anopheles* matrix metalloprotease 1 reveals its agonistic role during sporogonic development of malaria parasites. *Infect. Immun*. 82, 4865-4877

Graham, L. A., Flannery, A. R., & Stevens, T. H. (2003). Structure and assembly of the yeast v-ATPase. *J Bioenerg Biomembr.* 35, 301-312

Grassi, B. (1898). Rapporti tra la malaria e peculiari insetti (zanzaroni e zanzare palustri). *R. C. Accad. Lincei*. 7, 163–177

Graves, P. M., Burkot, T. R., Carter, R., Cattani, J. A., Lagog, M., Parker, J., Brabin, B. J., Gibson, F. D., Bradley, D. J., & Alpers, M. P. (1988). Measurement of malarial infectivity of human populations to mosquitoes in the Madang area, Papua New Guinea. *Parasitology.* 96, 251–263

Green, J. L., Hinds, L., Grainger, M., Knuepfer, E., & Holder, A. A. (2006). *Plasmodium* thrombospondin related apical merozoite protein (PTRAMP) is shed from the surface of merozoites by PfSUB2 upon invasion of erythrocytes. *Mol Biochem Parasitology*. 150, 114–117

Greenwood, B. M., Fidock, D. A., Kyle, D. E., Kappe, S. H. I., Alonso, P. L., Collins, F. H., & Duffy, P. E. (2008). Malaria: progress, perils, and prospects for eradication. *J Clin Invest*. 118, 1266-1276

Griffin, J., Hollingsworth, T. D., Okell, L., Churcher, T. S., White, M., Hinsley, W., Bousema, T., Drakeley, C. J., Ferguson, N. M., Basáñez, M. G., & Ghani, A. C. (2010). Reducing *Plasmodium falciparum* malaria transmission in Africa: A model-based evaluation of intervention strategies. *PLoS Medicine*. 7, e1000324

Griffin, J. T., Bhatt, S., Sinka, M. E., Gething, P. W., Lynch, M., Patouillard, E., Shutes, E., Newman, R. D., Alonso, P., Cibulskis, R. E., & Ghani, A. C. (2016). Potential for reduction of burden and local elimination of malaria by reducing *Plasmodium*

falciparum malaria transmission: A mathematical modelling study. *Lancet Infect Dis*. 16, 465-472

Guerreiro, A., Deligianni, E., Santos, J. M., Silva, P. A. G. C., Louis, C., Pain, A., Janse, C. J., Franke-Fayard, B., Carret, C. K., Sidén-Kiamos, I., & Mair. G. R. (2014). Genome-wide RIP-Chip analysis of translational repressor-bound mRNAs in the *Plasmodium* gametocyte. *Genome Biol*. 15, 493-506

Gupta, L., Molina-Cruz, A., Kumar, S., Rodrigues, J., Dixit, R., Zamora, R. E., & Barillas-Mury, C. (2009). The STAT pathway mediates late-phase immunity against *Plasmodium* in the mosquito *A. gambiae*. *Cell Host Microbe*. 5, 498-507

Guttery, D. S., Poulin, B., Ferguson, D. J. P., Szöor, B., Wickstead, B., Carroll, P. L., Ramakrishnan, C., *et al.*, & Tewari, R. (2012). A unique protein phosphatase with Kelch-Like domains (PPKL) in *Plasmodium* modulates ookinete differentiation, motility and invasion. *PLoS Path*. 8, e1002948

Guttery, D. S., Poulin, B., Ramaprasad, A., Wall, R. J., Ferguson, D. J. P., Brady, D., Patzewitz, E. M., Whipple, S., *et al*., & Tewari, R. (2014). Genome-wide functional analysis of *Plasmodium* protein phosphatases reveals key regulators of parasite development and differentiation. *Cell Host Microbe*. 16, 128-140

Gwadz, R. W. (1976). Successful immunisation against the sexual stages of *Plasmodium gallinaceum*. *Science*. 193**,** 1150-1151

Habtewold, T., Povelones, M., Blagborough, A. M., & Christophides, G. K. (2008). Transmission-blocking immunity in the malaria non-vector mosquito *Anopheles* quadriannulatus species A. *PLoS Path*. 4, e1000070

Habtewold, T., Tapanelli, S., Masters, E. K. G., Hoermann, A., Windbichler, N., & Christophides, G. K. (2019). Streamlined SMFA and mosquito dark-feeding regime significantly improve malaria transmission-blocking assay robustness and sensitivity. *Malar J*. 18, 24-35

Hall, T. A. (1999). BioEdit: a user-friendly biological sequence alignment editor and analysis program for Windows 95/98/ NT. *Nucl Acids Symp*. DOI: 10.14601-1499

Hall, N., Karras, M., Raine, J. D., Carlton, J. M., Kooij, T. W. A., Berriman, M., Florens, L., Janssen, C. S., Pain, A., Christophides, G. K., *et al.*, & Sinden, R. E. (2005). A comprehensive survey of the *Plasmodium* lifecycle by genomic, transcriptomic, and proteomic analyses. *Science*. 307, 82–86

Hamers-Casterman, C., Atarhouch, T., Muyldermans, S., Robinson, G., Hammers, C., Songa, E. B., Bendahman, N., & Hammers, R. (1993). Naturally occurring antibodies devoid of light chains. *Nature*. 363, 446-448

Hamilton, W. L., Claessens, A., Otto, D. T., Kekre, M., Fairhurst, R. M., Rayner, J. C., & Kwiatkowski, D. (2017). Extreme mutation bias and high AT content in *Plasmodium falciparum. Nucleic Acids Res.* 45, 1889–1901

Hammond, A. M., Galizi, R., Kyrou, K., Simoni, A., Siniscalchi, C., Katsanos, Gribble, M., Baker, D., Marois, E., Russell, S., Burt, A., Windbichler, N., Crisanti, A., & Nolan, T. (2016). A CRISPR-Cas9 gene drive system targeting female reproduction in the malaria mosquito vector *Anopheles gambiae*. *Nature Biotech*. 34, 78-83

Hammond, A. M., & Galizi, R. (2017). Gene drives to fight malaria: current state and future directions. *Pathog Glob Health*. 111, 412-423

Han, Y. S., Thompson, J., Kafatos, F. C., & Barillas-Mury, C. (2000). MC8 - Molecular interactions between *Anopheles stephensi* midgut cells and *Plasmodium berghei*: The time bomb theory of ookinete invasion. *Embo J*. 95, 28–29

Han, Y. S., & Barillas-Mury, C. (2002). Implications of time bomb model of ookinete invasion of midgut cells. *Insect Biochem Mol Biol.* 32, 1311–1316

Hansen, M., Kun, J. F. J., Schultz, J. E., & Beitz, E. (2002). A single, bi-functional aquaglyceroporin in blood stage *Plasmodium falciparum* malaria parasites. *J Biol Chem*. 15, 4874-4882

Harris, P. K., Yeoh, S., Dluzewski, A. R., O'Donnell, R. A., Withers-Martinez, C., Hackett, F., Bannister, L. H., Mitchell, G. H., & Blackman, M. J. (2005). Molecular identification of a malaria merozoite surface sheddase. *PLoS Path*. 1, 241–251

Haynes, J. D., Diggs, C. L., Hines, F. A., & Desjardins, R. E. (1976) Culture of human malaria parasites *Plasmodium falciparum*. *Nature.* 263, 767-769

Heddini, A. (2002). Malaria pathogenesis: A jigsaw with an increasing number of pieces. *Int J Parasitol*. 32, 1587-1598

Hedfalk, K., Pettersson, N., Öberg, F., Hohmann, S., & Gordon, E. (2008). Production, characterisation and crystallisation of the *Plasmodium falciparum* aquaporin. *Protein Expr Purif*. 59, 69-78

Hensel, M., Shea, J. E., Gleeson, C., Jones, M. D., Dalton, E., & Holden, D. W. (1995). Simultaneous identification of bacterial virulence genes by negative selection. *Science*. 269, 400-403

Herrera, S., Perlaza, B. L., Bonelo, A., & Arévalo-Herrera, M. (2002). Aotus monkeys: Their great value for anti-malaria vaccines and drug testing. *Int J Parasitol*. 32, 1625–1635

Hill, D. R., Baird, J. K., Parise, M. E., Lewis, L. S., Ryan, E. T., & Magill, A. J. (2006). Primaquine: Report from CDC expert meeting on malaria chemoprophylaxis I. *Am J Trop Med Hyg.* 75, 402–15

Hillyer, J. F., Schmidt, S. L., Fuchs, J. F., Boyle, J. P., & Christensen, B. M. (2005). Age-associated mortality in immune challenged mosquitoes (*Aedes aegypti*) correlates with a decrease in haemocyte numbers. *Cell Microbiol*. 7, 39-51

Hillyer, J. F., Barreau, C., & Vernick, K. D. (2007). Efficiency of salivary gland invasion by malaria sporozoites is controlled by rapid sporozoite destruction in the mosquito haemocoel. *Int J Parasitol*. 37, 673-681

Hirai, M., Arai, M., Kawai, S., & Matsuoka, H. (2006). PbGCbeta is essential for *Plasmodium* ookinete motility to invade midgut cell and for successful completion of parasite lifecycle in mosquitoes. *J Biochem*. 140, 747–757

Hirai, M., Arai, M., Mori, T., Miyagishima, S., Kawai, S., Kita, K., Kuroiwa, T., Terenius, O., & Matsuoka, H. (2008). Male fertility of malaria parasites is determined by GCS1, a plant-type reproduction factor. *Curr Biol*. 18, 607-613

Hisaeda, H., Stowers, A. W., Tsuboi, T., Collins, W. E., Sattabongkot, J. S.,

Suwanabun, N., Torii, M., & Kaslow, D. C. (2000). Antibodies to malaria vaccine candidates Pvs25 and Pvs28 completely block the ability of *Plasmodium vivax* to infect mosquitoes. *Infect Immun*. 68, 6618-6623

Hoffman, S. L., Goh, L. M. L., Luke, T. C., Schneider, I., Le, T. P., Doolan, D. L., Sacci, J., de la Vega, P., Dowler, M., *et al*., & Richie, T. L. (2002). Protection of humans against malaria by immunisation with radiation-attenuated *Plasmodium falciparum* sporozoites. *J Infect Dis.* 185, 1155-1164

Holder, A. A., Blackman, M. J., Burghaus, P. A., Chappel, J. A., Ling, I. T., McCallum-Deighton, N., & Shai, S. (1992). A malaria merozoite surface protein (MSP1)-structure, processing and function. *Mem Inst Oswaldo Cruz*. 87, 37-42

Holt, R. A, Subramanian, G. M., Halpern, A., Sutton, G., Charlab, R., Nusskern, D. R., Wincker, P., Clark, A. G., *et al.*, & Hoffman, S. L. (2002). The genome sequence of the malaria mosquito *Anopheles gambiae*. *Science*. 298, 129–149

Horsefield, R., Norden, K., Fellert, M., Backmark, A., Tornroth-Horsefield, S., Terwisscha van Scheltinga, A. C., Kvassman, J., Kjellbom, P., Johanson, U., & Neutze, R. (2008). High-resolution X-ray structure of human aquaporin 5. *Proc Natl Acad Sci.* 105, 13327-13332

Hub, J. S., & de Groot, B. L. (2008). Mechanism of selectivity in aquaporins and aquaglyceroporins. *Proc Natl Acad Sci.* 105, 1198-1203

Huff, C. G., Marchbank, D., & Shiroishi, T. (1958). Changes in infectiousness of gametocytes. Analysis of the possible causative factors. *Exp Parasitol*. 7**,** 399-417

Hviid, L., Lavstsen, T., & Jensen, A. T. (2018). A vaccine targeted specifically to prevent cerebral malaria – is there hope? *Expert Rev Vaccines*. 17, 565-567

Hyde, J. E. (2007). Drug-resistant malaria - An insight. *FEBS Journal*. 274, 4688-4698

Ikadai, H., Shaw-Saliba, K., Kanzok, S. M., McLean, K. J., Tanaka, T. Q., Cao, J., Williamson, K. C., & Jacobs-Lorena, M. (2013). Transposon mutagenesis identifies genes essential for *P. falciparum* gametocytogenesis. *Proc Natl Acad Sci USA.* 110, 1676-1684

Isaacs, A. T., Li, F., Jasinskiene, N., Chen, X., Nirmala, X., Marinotti, O., Vinetz, J. M., & James, A. A. (2011). Engineered resistance to *Plasmodium falciparum* development in transgenic *Anopheles stephensi*. *PLoS Path*. 7, e1002017

Ishino, T., Chinzei, Y., & Yuda, M. (2005). A *Plasmodium* sporozoite protein with a membrane attack complex domain is required for breaching the liver sinusoidal cell layer prior to hepatocyte infection. *Cell Microbiol*. 7, 199-208

Ishino, T., Orito, Y., Chinzei, Y., & Yuda, M. (2006). A calcium-dependent protein kinase regulates *Plasmodium* ookinete access to the midgut epithelial cell. *Mol Microbiol*. *59*, 1175–1184

Ishizuka, A. S., Lyke, K. E., DeZure, A., Berry, A. A., Richie, T. L., Mendoza, F. H., Enama, M. E., Gordon, I. J., Chang, L. J., Sarwar, U. N., Zephir, K. L., Holman, L. A., *et al*., & Seder, R. A. (2016). Protection against malaria at 1 year and immune correlates following PfSPZ vaccination. *Nature Med*. 22, 614-623

Ito, J., Ghosh, A., Moreira, L. A., Wimmer, E. A., & Jacobs-Lorena, M. (2002).

Transgenic anopheline mosquitoes impaired in transmission of a malaria parasite. *Nature*. 417, 452-455

Itsara, L. S., Zhou, Y., Do, J., Dungel, S., Fishbaugher, M. E., Betz, W. W., Nguyen, T., Navarro, M. J., Flannery, E. L., Vaughan, A. M., Kappe, S. H. I., & Ghosh, A. K. (2018). PfCap380 as a marker for *Plasmodium falciparum* oocyst development *in vivo* and *in vitro*. *Malar J*. 17, 135-148

Janeway, C. A., & Medzhitov, R. (2002). Innate immune recognition. *Annu Rev Immunol.* 20, 197–216.

Janse, C. J., van der Klooster, P. F. J., van der Kaay, H. J., van der Ploeg, M., & Overdulve, J. P. (1986). Rapid repeated DNA replication during microgametogenesis and DNA synthesis in young zygotes of *Plasmodium berghei*. *Trans R Soc Trop Med Hyg.* 80, 154–157

Janse, C. J., & Waters, A. P. (1995). *Plasmodium berghei*: The application of cultivation and purification techniques to molecular studies of malaria parasites. *Parasitology Today*. 11, 138–143

Janse, C. J., Franke-Fayard, B., Mair, G. R., Ramesar, J., Thiel, C., Engelmann, S., Matuschewski, K., van Gemert, G. J., Sauerwein, R. W., & Waters, A. P. (2006a). High efficiency transfection of *Plasmodium berghei* facilitates novel selection procedures. *Mol Biochem Parasitol*. 145, 60–70

Janse, C. J, Ramesar, J., & Waters, A. P. (2006b). High-efficiency transfection and drug selection of genetically transformed blood stages of the rodent malaria parasite *Plasmodium berghei*. *Nature Protocols*. 1, 346–356

Janssen, C. S., Barrett, M. P., Lawson, D., Quail, M. A., Harris, D., Bowman, S., Philips, R. S., & Turner, C. M. R. (2001). Gene discovery in *Plasmodium* chabaudi by genome survey sequencing. *Mol Biochem Parasitol*. 113, 251-260

Jaramillo-Gutierrez, G., Molina-Cruz, A., Kumar, S., & Barillas-Mury, C. (2010). The *Anopheles gambiae* oxidation resistance 1 (OXR1) gene regulates expression of enzymes that detoxify reactive oxygen species. *PLoS One*. 5, e11168

Jeacock, L., Baker, N., Wiedemar, N., Mäser, P., & Horn, D. (2017). Aquaglyceroporin-null trypanosomes display glycerol transport defects and respiratory-inhibitor sensitivity. *PLoS Path*. 13, e1006307

Jenkins, N. (2007). *Plasmodium falciparum* intercellular adhesion molecule-1-based cytoadherence-related signalling in human endothelial cells. *J of Infectious Diseases* 196, 321–327

Jinek, M., Chylinski, K., Fonfara, I., Hauer, M., Doudna, J. A., & Charpentier, E. (2012). A programmable dual-RNA–guided DNA endonuclease in adaptive bacterial immunity. *Science*. 337, 816–821

Jones, S., Grignard, L., Nebie, I., Chilongola, J., Dodoo, D., Sauerwein, R., Theisen, M., Roeffen, W., Singh, S. K., *et al*., & Singh, R. K. (2015). Naturally acquired antibody responses to recombinant Pfs230 and Pfs48/45 transmission blocking vaccine candidates. *J Infect.* 71, 117–127

Josling, G. A., Venezia, J., Orchard, L., Russell, T. J., Painter, H. J., & Llinas, M. (2019) Regulation of sexual differentiation is linked to invasion in malaria parasites.

BioRxiv. DOI: 10.1101/533877

Jung, J. S., Preston, G. M., Smith, B. L., Guggino, W. B., & Agre, P. (1994). Molecular structure of the water channel through aquaporin CHIP. The hourglass model. *J Biol Chem*. 269, 14648-14654

Jung, J. S., Bhat, R. V., Preston, G. M., Guggino, W. B., & Agre, P. (2006). Molecular characterisation of an aquaporin cDNA from brain: candidate osmoreceptor and regulator of water balance. *Proc Natl Acad Sci USA.* 91, 13052-13056

Juliano, R. L. (2002). Signal transduction by cell adhesion receptors and the cytoskeleton : Functions of integrins, cadherins, selectins, and immunoglobulin-superfamily members. *Annu Rev Pharmacol Toxicol*. 42, 283-323

Kadota, K., Ishino, T., Matsuyama, T., Chinzei, Y., & Yuda, M. (2004). Essential role of membrane-attack protein in malarial transmission to mosquito host. *Proc Natl Acad Sci USA*. 101, 16310–16315

Kaestli, M., Cockburn, I. A., Cortes, A., Baea, K., Rowe, J. A., & Beck, H. P. (2006). Virulence of malaria is associated with differential expression of *P. falciparum* var gene subgroups in a case-control study. *J Infect Dis.* 193, 1567-1574

Kafsack, B. F., Rovira-Graells, N., Clark, T. G., Bancells, C., Crowley, V. M., Campino, S. G., Williams A. E., Drought, L. G., Kwiatkowski, D. P., Baker, D. A., Cortes, A., & Llinas, M. (2014). A transcriptional switch underlies commitment to sexual development in malaria parasites. *Nature.* 507, 248– 252

Kaiser, K., Camargo, N., Coppens, I., Morrisey, J. M., Vaidya, A. B., & Kappe, S. H. I. (2004). A member of a conserved *Plasmodium* protein family with membrane-attack complex/perforin (MACPF)-like domains localises to the micronemes of sporozoites. *Mol Biochem Parasitol*. 133, 15-26

Kajla, M. K., Shi, L., Li, B., Luckhart, S., Li, J., & Paskewitz, S. M. (2011). A new role for an old antimicrobial: Lysozyme c-1 can function to protect malaria parasites in *Anopheles* mosquitoes. *PLoS One*. 6, e19649

Kamareddine, L., Nakhleh, J., & Osta, M. A. (2016). Functional interaction between apolipophorins and complement regulate the mosquito immune response to systemic infections. *J Innate Immun*. 8, 314-326

Kaneko, I., Iwanaga, S., Kato, T., Kobayashi, I., & Yuda, M. (2015). Genome-wide identification of the target genes of AP2-O, a *Plasmodium* AP2-family transcription factor. *PLoS Path*. 11, e1004905

Kappe, S., Bruderer, T., Gantt, S., Fujioka, H., Nussenzweig, V., & Ménard, R. (1999). Conservation of a gliding motility and cell invasion machinery in Apicomplexan parasites. *J Cell Biol*. 147, 937-944

Kariu, T., Ishino, T., Yano, K., Chinzei, Y., & Yuda, M. (2006). CelTOS, a novel malarial protein that mediates transmission to mosquito and vertebrate hosts. *Mol Microbiol*. 59, 1369–1379

Kawamoto, F., Alejo-Blanco, R., Fleck, S. L., Kawamoto, Y., & Sinden, R. E. (1990). Possible roles of Ca2+ and cGMP as mediators of the exflagellation of *P. berghei* and *Plasmodium falciparum*. *Mol Biochem Parasitol*. 42, 101-108

Kelemen, O., Convertini, P., Zhang, Z., Wen, Y., Shen, M., Falaleeva, M., & Stamm,

S. (2013). Function of alternative splicing. *Gene*. 514, 1-30

Kelley, L. A., Mezulis, S., Yates, C. M., Wass, M. N., & Sternberg, M. J. E. (2015). The Phyre2 web portal for protein modeling, prediction and analysis. *Nature Protocols*. 10, 845-858

Kenthirapalan, S., Waters, A. P., Matuschewski, K., & Kooij, T. W. A. (2012). Flow cytometry-assisted isolation of recombinant *P. berghei* parasites exemplified by functional analysis of aquaglyceroporin. *Int J Parasitol*. 42, 1185-1192

Khan, S. M., Franke-Fayard, B., Mair, G. R., Lasonder, E., Janse, C. J., Mann, M., & Waters, A. P. (2005). Proteome analysis of separated male and female gametocytes reveals novel sex-specific *Plasmodium* biology. *Cell*, 121, 675–687

Khater, E. I., Sinden, R. E., & Dessens, J. T. (2004). A malaria membrane skeletal protein is essential for normal morphogenesis, motility, and infectivity of sporozoites. *J Cell Biol*. 167, 425-432

Kim, W., Koo, H., Richman, A. M., Seeley, D., Vizioli, J., Klocko, A. D., & O'brochta, D. A. (2009). Ectopic expression of a cecropin transgene in the human malaria vector mosquito *Anopheles gambiae* (Diptera: Culicidae): effects on susceptibility to *Plasmodium*. *J Med Entomol*. 41, 447-455

Klug, D., & Frischknecht, F. (2017). Motility precedes egress of malaria parasites from oocysts. *eLife*. 6, e19157

Knapp, B., Nau, U., Hundt, E., & Kupper, H. A. (1991). Demonstration of alternative splicing of a pre-mRNA expressed in the blood stage form of *Plasmodium falciparum*. *J Biol Chem*. 266, 7148-7154

Kocken, C. H., Jansen, J., Kaan, A. M., Beckers, P. J., Ponnudurai, T., Kaslow, D. C., Konings, R. N., & Schoenmakers, J. G. (1993). Cloning and expression of the gene coding for the transmission blocking target antigen Pfs48/45 of *Plasmodium falciparum*. *Mol Biochem Parasitol*. 61, 59–68

Kotsyfakis, M., Ehret-Sabatier, L., Sidén-Kiamos, I., Mendoza, J., Sinden, R. E., & Louis, C. (2005). *Plasmodium berghei* ookinetes bind to *Anopheles gambiae* and Drosophila melanogaster annexins. *Mol Microbiol*. 57, 171–179

Kumar, N., & Wizel, B. (1992). Further characterisation of interactions between gamete surface antigens of P. *falciparum*. *Mol Biochem Parasitol*. *53*, 113–120

Kumar, S., Gupta, L., Han, Y. S., & Barillas-Mury, C. (2004). Inducible peroxidases mediate nitration of *Anopheles* midgut cells undergoing apoptosis in response to *Plasmodium* invasion. *J Biol Chem*. 279, 53475-53482

Kumar, S., & Barillas-Mury, C. (2005). Ookinete-induced midgut peroxidases detonate the time bomb in anopheline mosquitoes. *Insect Biochem Mol Biol*. 35, 721-727

Kumar, S., Stecher, G., Li, M., Knyaz, C., & Tamura, K. (2018). MEGA X: Molecular evolutionary genetics analysis across computing platforms. *Mol Biol Evol*. 35, 1547-1549

Kyrou, K., Hammond, A. M., Galizi, R., Kranjc, N., Burt, A., Beaghton, A. K., Nolan, T., & Crisanti, A. (2018). A CRISPR–Cas9 gene drive targeting doublesex causes complete population suppression in caged *Anopheles gambiae* mosquitoes. *Nat Biotech.* 36, 1062–1066

LaCount, D. J., Vignali, M., Chettier, R., Phansalkar, A., Bell, R., Hesselberth, J. R., Shoenfeld, L. W., Ota, I., Sahasrabudhe, S., Kurschner, C., Fields, S., & Hughes, R. E. (2005). A protein interaction network of the malaria parasite *Plasmodium falciparum*. *Nature*. 438, 103-107

Laforenza, U., Bottino, C., & Gastaldi, G. (2016). Mammalian aquaglyceroporin function in metabolism. *Biochim Biophys Acta.* 1858, 1-11

Lal, K., Prieto, J. H., Bromley, E., Sanderson, S. J., Yates, J. R., Wastling, J. M., Tomley, F. M., & Sinder, R. E. (2009a). Characterisation of *Plasmodium* invasive organelles; an ookinete microneme proteome. *Proteomics*. 9, 1142–1151

Lal, K., Delves, M. J., Bromley, E., Wastling, J. M., Tomley, F. M., & Sinden, R. E. (2009b). *Plasmodium* male development gene-1 (mdv-1) is important for female sexual development and identifies a polarised plasma membrane during zygote development. *Int J Parasitol*. 39, 755-761

Lamacchia, M., Clayton, J. R., Wang-Sattler, R., Steinmetz, L. M., Levashina, E. A., & Blandin, S. (2013). Silencing of genes and alleles by RNAi in *Anopheles gambiae*. *Methods Molr Biol*. 923, 161-176

Lambrechts, L., Halbert, J., Durand, P., Gouagna, L. C., & Koella, J. C. (2005). Host genotype by parasite genotype interactions underlying the resistance of anopheline mosquitoes to *Plasmodium falciparum*. *Malar J*. 4, 11-19

Lang-Unnasch, N., & Murphy, A. D. (1998). Metabolic changes of the parasite during the transition from the human to the mosquito. *Annu Rev Micobiol*. 52, 561-590

Langreth, S. G., & Peterson, E. (1985). Pathogenicity, stability, and immunogenicity of a knobless clone of *Plasmodium falciparum* in Colombian owl monkeys. *Infect Immun*. 47, 760-766

Langridge, G. C., Phan, M. D., Turner, D. J., Perkins, T. T., Parts, L., Haase, J., Charles, I., Maskell, D. J., *et al.*, & Turner, A. K. (2009). Simultaneous assay of every Salmonella Typhi gene using one million transposon mutants. *Genome Research*. 19, 2308-2316

Lasonder, E., Janse, C. J., van Gemert, G. J., Mair, G. R., Vermunt, A. M. W., Douradinha, B. G., van Noort, V., *et al*., & Stunnenberg, H. G. (2008). Proteomic profiling of *Plasmodium* sporozoite maturation identifies new proteins essential for parasite development and infectivity. *PLoS Path*. 4, e10000195

Lavazec, C., Boudin, C., Lacroix, R., Bonnet, S., Diop, A., Thiberge, S., Boisson, B., Tahar, R., & Bourgouin, C. (2007). Carboxypeptidases B of *Anopheles gambiae* as targets for a *Plasmodium*, *falciparum* transmission-blocking vaccine. *Infect Immun*. 75, 1635–164

Lavine, M. D., & Strand, M. R. (2002). Insect haemocytes and their role in immunity. *Insect Biochem Mol Biol*, 32, 1295–1309

Le Roch, K. G., Johnson, J. R., Florens, L., Zhou, Y., Santrosyan, A., Grainger, M., *et al*., & Winzeler, E. A. (2004). Global analysis of transcript and protein levels across the *Plasmodium falciparum* lifecycle. *Genome Research.* 14, 2308–2318

Le, B. V., Williams, M., Logarajah, S., & Baxter, R. H. G. (2012). Molecular basis for genetic resistance of *Anopheles gambiae* to *Plasmodium*: Structural analysis of

TEP1 susceptible and resistant alleles. *PLoS Path*. *8*, e1002958

Lee, M. Cs., & Fidock, D. A. (2014). CRISPR-mediated genome editing of *Plasmodium falciparum* malaria parasites. *Genome Medicine*. 6, 63-67

Lee, R. S., Waters, A. P., & Brewer, J. M. (2018). A cryptic cycle in haematopoietic niches promotes initiation of malaria transmission and evasion of chemotherapy. *Nat Commun*. 9, 1689-1897

Leitner, W. W., Bergmann-Leitner, E. S., & Angov, E. (2010). Comparison of *P. berghei* challenge models for the evaluation of pre-erythrocytic malaria vaccines and their effect on perceived vaccine efficacy. *Malar J*. 9, 145-157

Lensen, A. H., Bolmer-van de Vegte, M., van Gemert, G. J., Eling, W. M., & Sauerwein, R. W. (1997). Leukocytes in a *P. falciparum*-infected bloodmeal reduce transmission of malaria to mosquitoes. *Infect Immun*, 65, 3834–3837

Levashina, E. A., Moita, L. F., Blandin, S., Vriend, G., Lagueux, M., & Kafatos, F. C. (2001). Conserved role of a complement-like protein in phagocytosis revealed by dsRNA KO in cultured cells of the mosquito, *A. gambiae*. *Cell*. 104, 709–718

Lian, L. Y., Al-Helal, M., Roslaini, A. M., Fisher, N., Bray, P. G., Ward, S. A., & Biagini, G. A. (2009). Glycerol: An unexpected major metabolite of energy metabolism by the human malaria parasite. *Malar J*. 8, 38-42

Lillico, S., Field, M. C., Blundell, P., Coombs, G. H., & Mottram, J. C. (2003). Essential roles for GPI-anchored proteins in African trypanosomes revealed using mutants deficient in GPI8. *Mol Biol Cell*. 14, 1182–1194

Lin, J., Reid, A. J., Cunningham, D., Böhme, U., Tumwine, I., Keller-Mclaughlin, S., Sanders, M. J., Berriman, M., & Langhorne, J. (2018). Genomic and transcriptomic comparisons of closely related malaria parasites differing in virulence and sequestration pattern. *Wellcome Open Research*. 3, 142-162

Liu, Y., Promeneur, D., Rojek, A., Kumar, N., Frøkiær, J., Nielsen, S., King, L. S., Agre, P., & Carbrey, J. (2007). AQP9 is the major pathway for glycerol uptake by mouse erythrocytes, with implications for malarial virulence. *Proc Natl Acad Sci USA.* 104, 12560-12564

Liu, Y., Tewari, R., Ning, J., Blagborough, A. M., Garbom, S., Pei, J., Grishin, N. V., Steele, R. E., Sinden, R. E., Snell, W. J., & Billker, O. (2008). The conserved plant sterility gene *HAP2* functions after attachment of fusogenic membranes in *Chlamydomonas* and *Plasmodium* gametes. *Genes Develop*. 22, 1051–1068

Lobo, C. A., Kinings, R. N. H., & Kumar, N. (1994). Expression of early gametocyte-stage antigens Pfg27 and Pfs16 in synchronized gametocytes and non-gametocyte oroducing clones of *P. falciparum*. *Mol Bioch Parasitol*. 68, 151-154

López, R., Garcia, J., Puentes, A., Curtidor, H., Ocampo, M., Vera, R., Rodriguez, L. E., Suarez, J., Urquiza, M., *et al*., & Patarroyo, M. E. (2003). Identification of specific Hep *G2* cell binding regions in *P. falciparum* sporozoite-threonine-asparagine-rich protein (STARP). *Vaccine*. 21, 2404-2411

Luckhart, S., Vodovotz, Y., Cui, L., & Rosenberg, R. (2002). The mosquito *Anopheles stephensi* limits malaria parasite development with inducible synthesis of nitric oxide. *Proc Natl Acad Sci USA.* 95, 5700-5705

Luckhart, S., & Riehle, M. A. (2007). The insulin signalling cascade from nematodes to mammals: Insights into innate immunity of *Anopheles* mosquitoes to malaria parasite infection. *Dev Comp Immunol.* 31, 647-656

Luplertlop, N., Surasombatpattana, P., Patramool, S., Dumas, E., Wasinpiyamongkol, L., Saune, L., Hamel, R., *et al*., & Missé, D. (2011). Induction of a peptide with activity against a broad spectrum of pathogens in the *Aedes aegypti* salivary gland, following infection with Dengue virus. *PLoS Path*. 13, e1001252

Lyke, K. E., Ishizuka, A. S., Berry, A. A., Chakravarty, S., DeZure, A., Enama, M. E., James, E. R., *et al*., & Seder, R. A. (2017). Attenuated PfSPZ vaccine induces strain-transcending T cells and durable protection against heterologous controlled human malaria infection. *Proc Natl Acad Sci USA*. 114, 2711-2716

Mabaso, M. L. H., Sharp, B., & Lengeler, C. (2004). Historical review of malarial control in southern African with emphasis on the use of indoor residual house-spraying. *Trop Med Int Health.* 9, 846-856

Mackinnon, M. J., & Read, A. F. (1999). Selection for high and low virulence in the malaria parasite *Plasmodium* chabaudi. *Proc Biol Sci*. 266, 741–748

Mahairaki, V., Voyatzi, T., Sidén-Kiamos, I., & Louis, C. (2005). The *A. gambiae* gamma1 laminin directly binds the *Plasmodium berghei* circumsporozoite - and *TRAP*-related protein. *Mol Biochem Parasitol*. 140, 119-121

Mair, G. R., Braks, J. A. M., Garver, L. S., Wiegant, J. C. A. G., Hall, N., Dirks, R. W., Khan, S. M., Dimopoulos, G., Janse, C. J., & Waters, A. P. (2006). Regulation of sexual development of *Plasmodium* by translational repression. *Science.* 313, 667–669

Mair, G. R., Lasonder, E., Garver, L. S., Franke-Fayard, B., Carret, C. K., Wiegant, J. C. A. G., Dirks, R. W., Dimopoulos, G., Janse, C. J., & Waters, A. P. (2010). Universal features of post-transcriptional gene regulation are critical for *Plasmodium* zygote development. *PLoS Path.* 6, e1000767

Malkin, E., Hu, J., Li, Z., Chen, Z., Bi, X., Reed, Z., Dubovsky, F., Liu, J., Wang, Q., Pan, X., *et al*., & Cao, Z. (2008). A Phase 1 trial of PfCP2.9: An AMA1/MSP1 chimeric recombinant protein vaccine for *Plasmodium falciparum* malaria. *Vaccine*. 26, 6864-6873

Mani, R., Onge, R. P., Hartman, J. L., Giaever, G., & Roth, F. P. (2008). Defining genetic interaction. *Proc Natl Acad Sci USA*. 105, 3461-3466

Marin-Mogollon, C., Salman, A. M., Koolen, K. M. J., Bolscher, J. M., van Pul, A. F. A. J., Miyazaki, S., Imai, T., *et al*., & Khan, S. M. (2019). A *P. falciparum* NF54 reporter line expressing mCherry-luciferase in gametocytes, sporozoites, and liver-stages. *Front Cell Infect Microbiol*. 9, 96-107

Marinotti, O., Jasinskiene, N., Fazekas, A., Scaife, S., Fu, G., Mattingly, S. T., Chow, K., Brown, D. M., Alphey, L., & James, A. A. (2013). Development of a population suppression strain of the human malaria vector mosquito, *Anopheles stephensi*. *Malar J*. 12, 142-152

Marti, M., Good, R. T., Rug, M., Knuepfer, E., & Cowman, A. F. (2004). Targeting virulence and remodeling proteins to the host. *Science*. 306, 1930-1933

Martin, W. J., Finerty, J., & Rosenthal, A. (1971). Isolation of *Plasmodium berghei* (malaria) parasites by ammonium chloride lysis of infected erythrocytes. *Nature New Biology*. 233, 260-261

Mathias, D. K., Pastrana-Mena, R., Ranucci, E., Tao, D., Ferruti, P., Ortega, C., Staples, G. O., Zaia, J., Takashina, E., Tsuboi, T., Borg, N. A., Verotta, L., & Dinglasan, R. R. (2013). A small molecule glycosaminoglycan mimetic blocks *Plasmodium* invasion of the mosquito midgut. *PLoS Path*. 9, e1003757

Matuschewski, K., Ross, J., Brown, S. M., Kaiser, K., Nussenzweig, V., & Kappe, S. H. I. (2002). Infectivity-associated changes in the transcriptional repertoire of the malaria parasite sporozoite stage. *J Biol Chem*. 277, 41948-41953

Matuschewski, K. (2006). Getting infectious: Formation and maturation of *Plasmodium* sporozoites in the *Anopheles* vector. *Cell Microbiol*. 8, 1547–1556

Matuschewski, K., & Mueller, A. K. (2007). Vaccines against malaria - An update. *FEBS Journal*. 366, 2806-2814

Mauritz, J. M. A., Esposito, A., Ginsburg, H., Kaminski, C. F., Tiffert, T., & Lew, V. L. (2009). The homeostasis of *Plasmodium falciparum*-infected red blood cells. *PLoS Computational Biology*. 5, e1000339

Mayengue, P. I., Ndounga, M., Malonga, F. V., Bitemo, M., & Ntoumi, F. (2011). Genetic polymorphism of merozoite surface protein-1 and merozoite surface protein-2 in *P. falciparum* isolates from Brazzaville, Republic of Congo. *Malar J*. 10, 276-283

Mazurkiewicz, P., Tang, C. M., Boone, C., & Holden, D. W. (2006). Signature-tagged mutagenesis: Barcoding mutants for genome-wide screens. *Nature Reviews Genetics*. 7, 929-939

McPherson, J. D., Marra, M., Hillier, L. D., Waterston, R. H., Chinwalla, A., Wallis, J., Sekhon, M., Wylie, K., Mardis, E. R., Wilson, R. K., *et al*., & Lehrach, H. (2001). A physical map of the human genome. *Nature*. 409, 934-941

Meis, J. F., Pool, G., van Gemert, G. J., Lensen, A. H., Ponnudurai, T., & Meuwissen, J. H. (1989). *Plasmodium falciparum* ookinetes migrate intercellularly through *Anopheles stephensi* midgut epithelium. *Parasitol Res*. 76, 13-19

Meister, M., Hetru, J. A., & Hoffmann, J. A. (2000). The antimicrobial host defense of Drosophila. *Curr Top Microbiol Immunol.* 248, 17-36

Meister, S., Koutsos, A. C., & Christophides, G. K. (2004). The *Plasmodium* parasite - a “new” challenge for insect innate immunity. *Int J Parasitol*. 34, 1473–1482

Meister, S., Kanzok, S. M., Zheng, X. l., Luna, C., Li, T. R., Hoa, N. T., Clayton, J. T., White, K. P., Kafatos, F. C., Christophides, G. K., & Zheng, L. (2005). Immune signalling pathways regulating bacterial and malaria parasite infection of the mosquito *A. gambiae*. *Proc Natl Acad Sci USA.* 102, 11420-11425

Meister, S., Agianian, B., Turlure, F., Relógio, A., Morlais, I., Kafatos, F. C., & Christophides, G. K. (2009). *A. gambiae* PGRPLC-mediated defense against bacteria modulates infections with malaria parasites. *PLoS Path*. 5, e100542

Ménard, R., & Janse, C. J. (1997). Gene targeting in parasites. *Methods.* 13, 148-157

Ménard, R., Sultan, A. A., Cortes, C., Altszuler, R., van Dijk, M. R., Janse, C. J., Waters, A. P., Nussenzweig, R. S., & Nussenzweig, V. (1997). Circumsporozoite protein is required for development of malaria sporozoites in mosquitoes. *Nature*. 385, 336-340

Ménard, R., Tavares, J., Cockburn, I. A., Markus, M., Zavala, F., & Amino, R. (2013). Looking under the skin: the first steps in malarial infection and immunity. *Nature Rev Microbiol.* 11, 701–712

Mendes, A. M., Schlegelmilch, T., Cohuet, A., Awono-Ambene, P., de Iorio, M., Fontenille, D., Christophides, G. K., Kafatos, F. C., & Vlachou, D. (2008). Conserved mosquito/parasite interactions affect development of *Plasmodium falciparum* in Africa. *PLoS Path*. 4, e1000069

Mendis, K., Rietveld, A., Warsame, M., Bosman, A., Greenwood, B., & Wernsdorfer, W. H. (2009). From malaria control to eradication: The WHO perspective. *Trop Med Int Health.* 14, 802-809

Mendis, K. N., Munesinghe, Y. D., de Silva, Y. N., Keragalla, I., & Carter, R. (1987). Malaria transmission-blocking immunity induced by natural infections of *Plasmodium vivax* in humans. *Infect Immun*. 55, 369–72

Meredith, J. M., Basu, S., Nimmo, D. D., Larget-Thiery, I., Warr, E. L., Underhill, A., McArthur, C. C., Carter, V., Hurd, H., Bourgouin, C., & Eggleston, P. (2011). Site-specific integration and expression of an anti-malarial gene in transgenic *A. gambiae* significantly reduces *Plasmodium* infections. *PLoS One*. 6, e14587

Michel, K., Budd, A., Pinto, S., Gibson, T. J., & Kafatos, F. C. (2005). *Anopheles gambiae* SRPN2 facilitates midgut invasion by the malaria parasite *Plasmodium berghei*. *EMBO Rep*. 6, 891-897

Michel, K., Suwanchaichinda, C., Morlais, I., Lambrechts, L., Cohuet, A., Awono-Ambene, P. H., Simard, F., Fontenille, D., Kanost, M. R., & Kafatos, F. C. (2006). Increased melanising activity in *A. gambiae* does not affect development of *P. falciparum*. *Proc Natl Acad Sci USA.* 6, e14587

Mikolajczak, S. A., Silva-Rivera, H., Peng, X., Tarun, A. S., Camargo, N., Jacobs-Lorena, V., *et al.*, & Kappe, S. H. I. (2008). Distinct malaria parasite sporozoites reveal transcriptional changes that cause differential tissue infection competence in the mosquito vector and mammalian host. *Mol Cell Biol.* 28, 6196-61207

Miller, L., & Greenwood, B. (2002). A shadow over Africa. *Science*. 298, 121-122

Minard, G., Tran, F. H., Raharimalala, F. N., Hellard, E., Ravelonandro, P., Mavingui, P., & Moro, C. V. (2013). Prevalence, genomic and metabolic profiles of Acinetobacter and Asaia associated with field-caught *Aedes albopictus* from Madagascar. *FEMS Microbiol Ecol*. 83, 63-73

Mita, T., Tanabe, K., & Kita, K. (2009). Spread and evolution of *Plasmodium falciparum* drug resistance. *Parasitol Int*. 58, 201-209

Mitri, C., Jacques, J. C., Thiery, I., Riehle, M. M., Xu, J., Bischoff, E., Morlais, I., Nsango, S. E., Vernick, K. D., & Bourgouin, C. (2009). Fine pathogen discrimination within the APL1 gene family protects *A. gambiae* against human and rodent malaria species. *PLoS Path*. 5, e1000576

Mitri, C., Bischoff, E., Takashima, E., Williams, M., Eiglmeier, K., Pain, A., Guelbeogo, W. M., Gneme, A., Brito-Favallo, E., *et al.*, & Vernick, K. D. (2015). An evolution-based screen for genetic differentiation between *Anopheles* sister taxa enriches for detection of functional immune factors. *PLoS Path*. 12, e1005836

Marin-Mogollon, C., van de Vegte-Bolmer, M., van Gemert, G. J., van Paul, F. J. A., Ramesar, J., Othman, A. S., *et al*., & Shahid, M. K. (2018). The *P. falciparum* male gametocyte protein P230p, a paralog of P230, is vital for ookinete formation and mosquito transmission. *Sci Rep*. 8, 7061

Moelans, I. I. M. D., Klaassen, C. H. W., Kaslow, D. C., Konings, R. N. H., & Schoenmakers, J. G. G. (1991). Minimal variation in Pfs16, a novel protein located in the membrane of gametes and sporozoites of *Plasmodium falciparum*. *Mol Biochem Parasitol*. 46, 311-313

Mohammed, H., Mindaye, T., Belayneh, M., Kassa, M., Assefa, A., Tadesse, M., Woyessa, A., Mengesha, T., & Kebede, A. (2015). Genetic diversity of *Plasmodium falciparum* isolates based on MSP-1 and MSP-2 genes from Kolla-Shele area, Arbaminch Zuria District, southwest Ethiopia. *Malar J*. 14, 73-80

Molina-Cruz, A., de Jong, R. J., Ortega, C., Haile, A., Abban, E., Rodrigues, J., Jaramillo-Gutierrez, G., & Barillas-Mury, C. (2012). Some strains of {*Plasmodium*} *falciparum*, a human malaria parasite, evade the complement-like system of *Anopheles gambiae* mosquitoes. *Proc Natl Acad Sci USA*. 109, 1957-1962

Molina-Cruz, A., Garver, L. S., Alabaster, A., Bangiolo, L., Haile, A., Winikor, J., Ortega, C., van Shaijk, B. C. L., Sauerwein, R. W., Taylor-Salmon, E., & Barillas-Mury, C. (2013). The human malaria parasite Pfs47 gene mediates evasion of the mosquito immune system. *Science.* 340, 984–987

Molina-Cruz, A., & Barillas-Mury, C. (2014). The remarkable journey of adaptation of the *Plasmodium falciparum* malaria parasite to New World anopheline mosquitoes. *Mem Inst Oswaldo Cruz.* 109, 662-667

Molina-Cruz, A., Canepa, G. E., Kamath, N., Pavlovic, N. V., Mu, J., Ramphul, U. N., Ramirez, J. L., & Barillas-Mury, C. (2015). *Plasmodium* evasion of mosquito immunity and global transmission: The lock-and-key theory. *Proc Natl Acad Sci USA*. 112, 15178–15183

Molina-Cruz, A., Canepa, G. E., & Barillas-Mury, C. (2017). *Plasmodium* P47 : a key gene for malaria transmission by mosquitoes. *Curr Opin Microbiol*. 40, 168–174

Molina-Cruz, A., Canepa G. E., Alves e Silva, T. L., Williams A. E., Nagyal, S., Yenkoidiok-Douti, L., Nagata, B. M., Calvo, E., Andersen, J., Boulanger, M. J., & Barillas-Mury, C. (2020). *P. falciparum* evades immunity of anopheline mosquitoes by interacting with a Pfs47 midgut receptor. *Proc Natl Acad Sci USA*. 117, 2597-2605

Moon, R. W., Taylor, C. J., Bex, C., Schepers, R., Goulding, D., Janse, C. J., & Billker, O. (2009). A cyclic GMP signalling module that regulates gliding motility in a malaria parasite. *PLoS Path*. 5, e1000599

Moreira, L. A., Ito, J., Ghosh, A., Devenport, M., Zieler, H., Abraham, E. G., Crisanti, A., Nolan, T., Catteruccia, F., & Jacobs-Lorena, M. (2002). Bee venom phospholipase inhibits malaria parasite development in transgenic mosquitoes. *J*

Biol Chem. 25, 40839-40843

Moreira, C. K., Naissant, B., Coppi, A., Bennett, B. L., Aime, E., Franke-Fayard, B., Janse, C. J., Coppens, I., Sinnis, P., & Templeton, T. J. (2016). The *Plasmodium* PHIST and RESA-like protein families of human and rodent malaria parasites. *PLoS One*. 11, e0152510

Moret, Y., & Siva-Jothy, M. (2003). Adaptive innate immunity? Responsive-mode prophylaxis in the mealworm beetle, Tenebrio molitor. *Proc Biol.* 270, 2475-2480

Mueller, A. K., Labaled, M., Kappe, S. H. I., & Matuschewski, K. (2005). Genetically modified *Plasmodium* parasites as a protective experimental malaria vaccine. *Nature*. 433, 164-167

Muhia, D. K., Swales, C. A., Eckstein-Ludwig, U., Saran, S., Polley, S. D., Kelly, J. M., Schaap, P., Krishna, S., & Baker, D. A. (2003). Multiple splice variants encode a novel adenylyl cyclase of possible plastid origin expressed in the sexual stage of the malaria parasite *Plasmodium falciparum*. *J Biol Chem*. 278, 22014-22022

Murata, K., Mitsuoka, K., Hirai, T., Walz, T., Agre, P., Heymannm B. J., Engel, A., & Fujiyoshi, Y. (2000). Structural determinants of water permeation through aquaporin-1. *Nature*. 276, 31515-31520

Nacer, A., Walker, K., & Hurd, H. (2008). Localisation of laminin within *Plasmodium berghei* oocysts and the midgut epithelial cells of *Anopheles stephensi*. *Parasit Vectors*. 22, 33-48

Nag, S., Dalgaard, M. D., Kofoed, P. E., Ursing, J., Crespo, M., O'Brien Andersen, L., Aarestrup, F. M., Lund, O., & Alifrangis, M. (2017). High throughput resistance profiling of *Plasmodium falciparum* infections based on custom dual indexing and Illumina next generation sequencing-technology. *Sci Rep*. 7, 2398-2411

Nagasawa, H., Procell, P. M., Atkinson, C. T., Campbell, G. H., Collins, W. E., & Aikawa, M. (1987). Localisation of circumsporozoite protein of *Plasmodium* ovale in midgut oocysts. *Infect Immun*.55, 2928-2932

Nakhleh, J., Christophides, G. K., & Osta, M. A. (2017). The serine protease homolog CLIPA14 modulates the intensity of the immune response in the mosquito *Anopheles gambiae*. *J Biol Chem*. 292, 18217-18226

Neveu, G., Dupuy, F., Ladli, M., Barbieri, D., Naissant, B., Richard, C., Martins, R. M., Lopez-Rubio, J. J., Bachmann, A., Verdier, F., & Lavazec, C. (2018). *Plasmodium falciparum* gametocyte-infected erythrocytes do not adhere to human primary erythroblasts. *Sci Rep.* 8, 17886

Ngufor, C., N'Guessan, R., Fagbohoun, J., Odjo, A., Malone, D., Akogbeto, M., & Rowland, M. (2014). Olyset Duo® (a pyriproxyfen and permethrin mixture net): An experimental hut trial against pyrethroid resistant *Anopheles gambiae* and Culex quinquefasciatus in southern Benin. *PLoS One*. 9, e93603

Ni, J. Q., Zhou, R., Czech, B., Liu, L. P., Holderbaum, L., Yang-Zhou, D., Shim, H, S., Tao, R., Handler, D., *et al.*, & Perrimon, N. (2011). A genome-scale shRNA resource for transgenic RNAi in Drosophila. *Nat Methods*. 8, 405-407

Niederwieser, I., Felger, I., & Beck, H. P. (2000). *Plasmodium falciparum*: Expression of gametocyte-specific genes in monolayer cultures and malaria-positive blood

samples. *Exp Parasitol*. 95, 163-169

Nsango, S. E., Pompon, J., Xie, T., Rademacher, A., Fraiture, M., Thoma, M., Awono-Ambene, P. H., Moyou, R. S., Morlais, I., & Levashina, E. A. (2013). AP-1/Fos-TGase2 axis mediates wounding-induced *P. falciparum* killing in *Anopheles gambiae*. *J Biol Chem*. 288, 16145-16154

Nunes, J. K., Woods, C., Carter, T., Raphael, T., Morin, M. J., Diallo, D., Leboulleux, D., Jain, S., Loucq, C., Kaslow, D. C., & Birkett, A. J. (2014). Development of a transmission-blocking malaria vaccine: Progress, challenges, and the path forward. *Vaccine*. 32, 5531-5539

Nussenzweig, R. S., Vanderberg, J., Most, H., & Orton, C. (1967). Protective immunity produced by the injection of X-irradiated sporozoites of *Plasmodium berghei*. *Nature*. 134, 1183-1190

Oaks S. C. Jr., Mitchell V. S., Pearson, G. W. & Carpenter, C. C. J. (1991). Malaria: Obstacles and Opportunities. *National Academy Press*. Retrieved from https://www.ncbi.nlm.nih.gov/pubmed/25121285

Okulate, M. A., Kalume, D., Reddy, R., Kristiansen, T., Bhattacharyya, M., Chaerkady, R., Pandey, A., & Kumar, N. (2007). Identification and molecular characterisation of a novel protein Saglin as a target of monoclonal antibodies affecting salivary gland infectivity of *Plasmodium* sporozoites. *Insect Mol Biol*. 16, 711-722

Oliveira, G., Lieberman, J., & Barillas-Mury, C. (2012). Epithelial nitration by a peroxidase/NOX5 system mediates antiplasmodial immunity. *Science.* 335, 856–859

Olivieri, A., Bertuccini, L., Deligianni, E., Franke-Fayard, B., Currà, C., Sidén-Kiamos, I., Hanssen, E., Grasso, F., Superti, F., Pace, T., Fratini, F., Janse, C. J., & Ponzi, M. (2015). Distinct properties of the egress-related osmiophilic bodies in male and female gametocytes of the rodent malaria parasite *Plasmodium berghei*. *Cell Microbiol*. 17, 355-368

Olszewski, K. L., Morrisey, J. M., Wilinski, D., Burns, J. M., Vaidaya, A. B., Rabinowitz, J. D., & Llinas, M. (2009). Host-parasite interactions reveales by *Plasmodium falciparum* metabolomics. *Cell Host Microbiome.* 5, 191-199

Olszewski, K. L., & Llinás, M. (2011). Central carbon metabolism of *Plasmodium* parasites. *Mol Biochem Parasitol*. 175, 95-103

Omasits, U., Ahrens, C. H., Müller, S., & Wollscheid, B. (2014). Protter: Interactive protein feature visualisation and integration with experimental proteomic data. *Bioinformatics*. 30, 884-886

Onwujekwe, O., Uzochukwu, B., Dike, N., Okoli, C., Eze, S., & Chukwuogo, O. (2009). Are there geographic and socio-economic differences in incidence, burden and prevention of malaria? A study in southeast Nigeria. *Int J Equity Health.* 8, 45-52

Osta, M. A., Christophides, G. K., & Kafatos, F. C. (2004a). Effects of mosquito genes on *Plasmodium* development. *Science.* 303, 2030–2032

Osta, M. A., Christophides, G. K., Vlachou, D., & Kafatos, F. C. (2004b). Innate immunity in the malaria vector *Anopheles gambiae*: comparative and functional genomics. *J Exp Biol*. 207, 2551–2563

Otto, T. D., Böhme, U., Jackson, A. P., Hunt, M., Franke-Fayard, B., Hoeijmakers, W. A. M., *et al*., & Janse, C. J. (2014). A comprehensive evaluation of rodent malaria parasite genomes and gene expression. *BMC Medicine*. 12, 86-102

Ouédraogo, A. L., Roeffen, W., Luty, A. J. F., de Vlas, S. J., Nebie, I., Ilboudo-Sanogo, E., Cuzin-Ouattara, N., Teleen, K., *et al.*, & Sauerwein, R. (2011). Naturally acquired immune responses to *P. falciparum* sexual stage antigens Pfs48/45 and Pfs230 in an area of seasonal transmission. *Infect Immun*. 79, 4957–64

Ouédraogo, A. L., Eckhoff, P. A., Luty, A. J. F., Roeffen, W., Sauerwein, R. W., Bousema, R., & Wenger, E. A. (2018). Modeling the impact of *Plasmodium falciparum* sexual stage immunity on the composition and dynamics of the human infectious reservoir for malaria in natural settings. *PLos Path*. 14, e1007034

Outchkourov, N. S., Roeffen, W., Kaan, A., Jansen, J., Luty, A., Schuiffel, D., van Gemert, G. J., van de Vegte-Bolmer, M., Sauerwein, R. W., & Stunnenberg, H. G. (2008). Correctly folded Pfs48/45 protein of *Plasmodium falciparum* elicits malaria transmission-blocking immunity in mice. *Proc Natl Acad Sci USA.* 293, 190-215

Pace, T., Grasso, F., Camarda, G., Suarez, C., Blackman, M. J., Ponzi, M., & Olivieri, A. (2019). The *Plasmodium berghei* serine protease PbSUB1 plays an important role in male gamete egress. *Cell Microbiol*. 21, e13028

Pain, A., Bohme, U., Berry, A. E., Mungall, K., Finn, R. D., Jackson, A. P., Mourier, T., Mistry, J., Pasini, E. M., *et al*., & Berriman, M. (2008). The genome of the simian and human malaria parasite *Plasmodium malariae*. *Nature*. 455, 799-803

Painter, H. J., Carrasquilla, M., & Llinas, M. (2017). Capturing in vivo RNA transcriptional dynamics from the malaria parasite *P. falciparum*. *Genome Res*. 27, 6074–6086

Painter, H. J., Neo, C. C., Aswathy, S., Istvan, A., Storey, J. D., & Llinás, M. (2018). Real-time in vivo global transcriptional dynamics during *Plasmodium falciparum* blood stage development. *Nat Comm*. 9, 2656-2668

Pakpour, N., Corby-Harris, V., Green, G. P., Smithers, H. M., Cheung, K. W., Riehle, M. A., & Luckhart, S. (2012). Ingested human insulin inhibits the mosquito NF-κB-dependent immune response to *P. falciparum*. *Infect Immun*. 80, 2141-2149

Parker, R., & Sheth, U. (2007). P-bodies and the control of mRNA translation and degradation. *Mol Cell*. 25, 635-646

Paskewitz, S. M., & Shi, L. (2006). Bypassing the midgut results in development of *Plasmodium berghei* oocysts in a refractory strain of *Anopheles gambiae* (Diptera: Culicidae). *J Med Entomol.* 42, 712-715

Pasvol, G. (2001). Cell-cell interaction in the pathogenesis of severe *falciparum* malaria. *Clin Med.* 6, 495–500.

Pasvol, G. (2005). The treatment of complicated and severe malaria. *British Medical Bulletin*. 75–76, 29–47

Patankar, S., Munasinghe, A., Shoaibi, A., Cummings, L. M., & Wirth, D. F. (2013). Serial analysis of gene expression in *Plasmodium falciparum* reveals the global expression profile of erythrocytic stages and the presence of anti-sense transcripts in the malarial parasite. *Mol Biol Cell.* 12, 3114-3125

Pates, H., & Curtis, C. (2004). Mosquito behavior and vector control. *Annu Rev Entomol.* 50, 53-70

Paton, M. G., Barker, G. C., Matsuoka, H., Ramesar, J., Janse, C. J., Waters, A. P., & Sinden, R. E. (1993). Structure and expression of a post-transcriptionally regulated malaria gene encoding a surface protein from the sexual stages of *Plasmodium berghei*. *Mol Biochem Parasitol*. 59, 263-275

Perkins, S. L., & Schall, J. J. (2002). A molecular phylogeny of malarial parasites recovered from cytochrome b gene sequences. *J Parasitol.* 88, 972-978

Pfander, C., Anar, B., Schwach, F., Otto, T. D., Brochet, M., Volkmann, K., Quail, M. A., Pain, A., Rosen, B., Skarnes, W., Rayner, J. C., & Billker, O. (2011). A scalable pipeline for highly effective genetic modification of a malaria parasite. *Nature Methods*. 8, 1078-1082

Pfeuffer, J., Bröer, S., Bröer, A., Lechte, M., Flögel, U., & Leibfritz, D. (1998). Expression of aquaporins in Xenopus laevis oocytes and glial cells as detected by diffusion-weighted 1H NMR spectroscopy and photometric swelling assay. *Biochim Biophys Acta.* 1448, 27-36

Pham, L. N., Dionne, M.S., Shirasu-Hiza, M., & Schneider, D. (2007). A specific primed immune response in Drosophila is phagocytosis dependent. *PLoS Path*. 3, e26

Philip, N., Vaikkinen, H. J., Tetley, L., & Waters, A. P. (2012). A unique Kelch domain phosphatase in *Plasmodium* regulates ookinete morphology, motility and invasion. *PLoS One*. *7,* e44617

Phillips, R. S., Brannan, L. R., Balmer, P., & Neuville, P. (1997). Antigenic variation during malaria infection--the contribution from the murine parasite *Plasmodium* chabaudi. *Parasite Immunol*, 19, 427–434

Pimenta, P. F., Touray, M., & Miller, L. (1994). The journey of malaria sporozoites in the mosquito salivary gland. *J Eukaryot Microbiol.* 41, 608-624

Pino, P., Caldelari, R., Mukherjee, B., Vahokoski, J., Klages, N., Maco, B., Collins, C. R., Blackman, M. J., Kursula, I., Heussler, V., Brochet, M., & Soldati-Favre, D. (2017). A multistage antimalarial targets the plasmepsins IX and X essential for invasion and egress. *Science*. 358, 522-528

Pinto, S. B., Kafatos, F. C., & Michel, K. (2008). The parasite invasion marker SRPN6 reduces sporozoite numbers in salivary glands of *Anopheles gambiae*. *Cell Microbiol*. 10, 891-898

Ponnudurai, T., Lensen, A. H. W., Leeuwenberg, A. D. E. M., & Meuwissen, J. H. E. T. (1982). Cultivation of fertile Plasmodium falciparum gametocytes in semi-automated systems. 1. Static cultures. *Trans R Soc Trop Med Hyg*. 76, 812–818

Ponnudurai, T., Lensen, A. H. W., van Gemert, G. J. A., Bensink, M. P. E., Bolmer, M., & Meuwissen, J. H. E. (1989). Sporozoite load of mosquitoes infected with *Plasmodium falciparum. Trans R Soc Trop Med Hyg.* 89, 67–70

Povelones, M., Waterhouse, R. M., Kafatos, F. C., & Christophides, G. K. (2009). Leucine-rich repeat protein complex activates mosquito complement in defense against *Plasmodium* parasites. *Science.* 324, 258–261

Povelones, M., Bhagavatula, L., Yassine, H., Tan, L. A., Upton, L. M., Osta, M. A., &

Christophides, G. K. (2013). The CLIP-Domain Serine Protease Homolog *SPCLIP1* Regulates Complement Recruitment to Microbial Surfaces in the Malaria Mosquito *Anopheles gambiae*. *PLoS Path*. 9, e1003623

Povelones, M., Osta, M. A., & Christophides, G. K. (2016). The Complement System of Malaria Vector Mosquitoes. *Adv Ins Phys.* 51, 223-242

Pradel, G., & Frevert, U. (2001). Malaria sporozoites activel enter and pass through rat Kupffer cells prior to hepatocyte invasions. *Hepatology*. 33, 1154-1165

Pradel, G., Hayton, K., Aravind, L., Iyer, L. M., Abrahamsen, M. S., Bonawitz, A., Mejia, C., & Templeton, T. J. (2004). A multidomain adhesion protein family expressed in *P. falciparum* is essential for transmission to the mosquito. *J Exp Med.* 199, 1533-1544

Pradel, G. (2007). Proteins of the malaria parasite sexual stages: Expression, function and potential for transmission blocking strategies. *Parasitology*. 134, 1911-1929

Prieto, J. H., Koncarevic, S., Park, S. K., Yates, J., & Becker, K. (2014). Large-scale differential proteome analysis in *Plasmodium falciparum* under drug treatment. *Methods Mol Biol*. 1201, 269-279

Promeneur, D., Liu, Y., Maciel, J., Agre, P., King, L. S., & Kumar, N. (2007). Aquaglyceroporin PbAQP during intraerythrocytic development of the malaria parasite *Plasmodium berghei*. *Proc Natl Acad Sci USA.* 104, 2211-2216

Promeneur, D., Mlambo, G., Agre, P., & Coppens, I. (2018). Aquaglyceroporin PbAQP is required for efficient progression through the liver stage of *Plasmodium* infection. *Sci Rep*. 8, 655-666

Prugnolle, F., McGee, K., Keebler, J., & Awadalla, P. (2008). Selection shapes malaria genomes and drives divergence between pathogens infecting hominids versus rodents. *BMC Evol Biol*. 8, 223-232

Quevillon, E., Silventoinen, V., Pillai, S., Harte, N., Mulder, N., Apweiler, R., & Lopez, R. (2005). InterProScan: Protein domains identifier. *Nucleic Acids*. 33, 116-120

Raamsdonk, L. M., Teusink, B., Broadhurst, D., Zhang, N., Hayes, A., Walsh, M. C., Berden, J. A., Brindle, K. M., Kell, D. B., Rowland, J. J., Westerhoff, H. V., van Dam, K., & Oliver, S. G. (2001). A functional genomics strategy that uses metabolome data to reveal the phenotype of silent mutations. *Nat Biot.* 19, 45-50

Raibaud, A., Brahimi, K., Roth, C. W., Brey, P. T., & Faust, D. M. (2006). Differential gene expression in the ookinete stage of the malaria parasite *Plasmodium berghei*. *Mol Biochem Parasitol*. 150, 107-113

Raine, J. D., Ecker, A., Mendoza, J., Tewari, R., Stanway, R. R., & Sinden, R. E. (2007). Female inheritance of Malarial lap genes is essential for mosquito transmission. *PLoS Path*. 3, e30

Ramakrishnan, C., Dessens, J. T., Armson, R., Pinto, S. B., Talman, A. M., Blagborough, A. M., & Sinden, R. E. (2011). Vital functions of the malarial ookinete protein, CTRP, reside in the A domains. *Int J Parasitol*. 41, 1029-1039

Ramirez, J. L., Garver, L. S., Brayner, F. A., Alves, L. C., Rodrigues, J., Molina-Cruz, A., & Barillas-Mury, C. (2014). The role of haemocytes in *Anopheles gambiae* antiplasmodial immunity. *J Inn Immun.* 6, 119–128

Ramirez, J. L., Oliveira, G., Calvo, E., Dalli, J., Colas, R. A., Serhan, C. N., Ribeiro, J. M., & Barillas-Mury, C. (2015). A mosquito lipoxin/lipocalin complex mediates innate immune priming in *Anopheles gambiae*. *Nat Commun*. 6, 7403-7410

Ramphul, U. N., Garver, L. S., Molina-Cruz, A., Canepa, G. E., & Barillas-Mury, C. (2015). *Plasmodium falciparum* evades mosquito immunity by disrupting JNK-mediated apoptosis of invaded cells. *Proc Natl Acad Sci USA.* 112, 1273–1280

Ranford-Cartwright, L. C., Balfe, P., Carter, R., & Walliker, D. (1991). Genetic hybrids of *Plasmodium falciparum* identified by amplification of genomic DNA from single oocysts. *Mol Biochem Parasitol*. 49, 239–244

Regules, J. A., Cicatelli, S. B., Bennett, J. W., Paolino, K. M., Twomey, P. S., Moon, J. E., *et al*., & Vakemans, J. (2016). Fractional third and fourth dose of RTS,S/AS01 malaria candidate vaccine: A phase 2a controlled human malaria parasite infection and immunogenicity study. *J Infect Dis.* 214, 762-771

Reininger, L., Billker, O., Tewari, R., Mukhopadhyay, A., Fennell, C., Dorin-Semblat, D., Doerig, C., Goldring, D., Harmse, L., Ranford-Cartwright, L., Packer, J., & Doerig, c. (2005). A NIMA-related protein kinase is essential for completion of the sexual cycle of malaria parasites. *J Biol Chem*. 280, 31957–31964

Reininger, L., Tewari, R., Fennell, C., Holland, Z., Goldring, D., Ranford-Cartwright, L., Billker, O., & Doerig, C. (2009). An essential role for the *Plasmodium* Nek-2 Nima-related protein kinase in the sexual development of malaria parasites. *J Biol Chem*. 284, 20858–20868

Rener, J., Graves, P. M., Carter, R., Williams, J. L., & Burkot, T. R. (1983). Target antigens in transmission-blocking immunity on gametes of *Plasmodium falciparum*. *J Exp Med*. 158, 976-981

Richman, A. M., Bulet, P., Hetru, C., Barillas-Mury, C., Hoffmann, J. A., & Kafatos, F. C. (1996). Inducible immune factors of the vector mosquito Anopheles gambiae: biochemical purification of a defensin antibacterial peptide and molecular cloning of preprodefensin cDNA. *Insect Mol Biol*. 5, 203–210

Rieckmann, K. H., Carson, P. E., Beaudoin, R. L., Cassells, J. S., & Sell, K. W. (1974). Sporozoite induced immunity in man against an ethiopian strain of *Plasmodium falciparum*. *Trans R Soc Trop Med Hyg.* 68, 258-259

Riehle, M. M., Markianos, K., Niaré, O., Xu, J., Li, J., Touré, A. M., Podiougou, F., Diawara, S., *et al*., & Vernick, K. D. (2006). Natural malaria infection in *Anopheles gambiae* is regulated by a single genomic control region. *Science*. 312, 577-579

Riehle, M. M., Xu, J., Lazzaro, B. P., Rottschaefer, S. M., Coulibaly, B., Sacko, M., Niare, O., Morlais, I., Traore, S. F., & Vernick, K. D. (2008). *Anopheles gambiae* APL1 is a family of variable LRR proteins required for *REL1*-mediated protection from themalaria parasite, *Plasmodium berghei*. *PLoS One*. 3, e3672

Rodrigues, J., Brayner, F. A., Alves, L. C., Dixit, R., & Barillas-Mury, C. (2010). Haemocyte differentiation mediates innate immune memory in *Anopheles gambiae* mosquitoes. *Science*. 329, 1353-1355

Rodriguez, M. H., & de la Hernández-Hernández, F. C. (2004). Insect-malaria parasites interactions: The salivary gland. *Insect Biochem Mol Biol*. 34, 615-624

Rodríguez, M. H., Martínez-Barnetche, J., Alvarado-Delgado, A., Batista, C., Argotte-Ramos, S., Hernández-Martínez, S., Gonzalez-Ceron, L., Torres, J. A., Margos, G., & Rodríguez, M. H. (2007). The surface protein Pvs25 of *Plasmodium vivax* ookinetes interacts with calreticulin on the midgut apical surface of the malaria vector *Anopheles albimanus*. *Mol Biochem Parasitol*. 153, 167–177

Rogan, W. J., & Chen, A. (2005). Health risks and benefits of bis(4-chlorophenyl)-1,1,1-trichloroethane (DDT). *Lancet*. 366, 763-773

Rono, M. K., Whitten, M. M. A., Oulad-Abdelghani, M., Levashina, E. A., & Marois, E. (2010). The major yolk protein vitellogenin interferes with the anti-*Plasmodium* response in the malaria mosquito *Anopheles gambiae*. *PLoS Biology*. 8, e100434

Ross, R. (1897). On some peculiar pigmented cells found in two mosquitos fed on malarial blood. *Br Med J*. 2, 1786-1788

Roth, O., Sadd, B. M., Schmid-Hempel, P., & Kurtz, J. (2009). Strain-specific priming of resistance in the red flour beetle, *Tribolium castaneum*. *Proc Sci.* 276, 145-151

Rowe, J. A., Claessens, A., Corrigan, R. A., & Arman, M. (2009). Adhesion of *Plasmodium falciparum*-infected erythrocytes to human cells: Molecular mechanisms and therapeutic implications. *Expert Rev Mol Med.* 11, e16

RTS,S Clinical Trials Partnership. (2014). Efficacy and safety of the RTS,S/AS01 malaria vaccine during 18 Months after vaccination: a Phase 3 randomized, controlled trial in children and young infants at 11 African sites. *PLoS Med*. 11, e1001685

RTS,S Clinical Trials Partnership. (2015). Efficacy and safety of RTS,S/AS01 malaria vaccine with or without a booster dose in infants and children in Africa: Final results of a phase 3, individually randomised, controlled trial. *Lancet*. 386, 31-45

Sachs, J., & Malaney, P. (2002). The economic and social burden of malaria. *Nature*. 415, 680-685

Sadasivaiah, S., Tozan, Y., & Breman, J. G. (2007). Dichlorodiphenyltrichloroethane (DDT) for indoor residual spraying in Africa: How can it be used for malaria control? *Am J Trop Med Hyg.* 77, 249-263

Sadd, B. M., & Schmid-Hempel, P. (2006). Insect immunity shows specificity in protection upon secondary pathogen exposure. *Curr Biol*. 16, 1206-1210

Saeed, S., Tremp, A. Z., & Dessens J. T. (2015). Biogenesis of the crystalloid organelle in *Plasmodium* involves mucrotubule-dependent vesicle transport and assembly. *Int J Parasitol*. 45, 537-547

Saeed, S., Tremp, A. Z., & Dessens J. T. (2018). The *Plasmodium* LAP complex affects crystalloid biogenesis and oocyst cell division. *Int Parasitol*. 48, 1073-1078

Saeed, S., Lau, C. I., Tremp, A. Z., Crompton, T., & Dessens, J. T. (2019). Dysregulated gene expression in oocysts of *P. berghei* LAP mutants. *Mol Biochem Parasitol*. 229, 1-5

Saenz, F. E., Balu, B., Smith, J., Mendonca, S. R., & Adams, J. H. (2008). The transmembrane isoform of *Plasmodium falciparum* MAEBL is essential for the invasion of *Anopheles* salivary glands. *PLoS One*. 3, e2287

Saitou, N., & Nei, M. (1987). The neighbor-joining method: a new method for reconstructing phylogenetic trees. *Mol Biol Evol.* 4, 406-425

Sakamoto, H., Thiberge, S., Akerman, S., Janse, C. J., Carvalho, T. G., & Ménard, R. (2005). Towards systematic identification of *Plasmodium* essential genes by transposon shuttle mutagenesis. *Nucleic Acids Research*. 10, e174

Sam-Yellowe, T. Y., Florens, L., Wang, T., Raine, J. D., Carucci, D. J., Sinden, R. E., & Yates, J. R. (2004). Proteome analysis of rhoptry-enriched fractions isolated from *Plasmodium* merozoites. *J Proteome Res.* 3, 995-1001

Sambrook, J., & W Russell, D. (2001). Molecular Cloning: A Laboratory Manual. *Cold Spring Harbor Laboratory Press,* Cold Spring Harbor, New York, USA

Sarov, M., Schneider, S., Pozniakovski, A., Roguev, A., Ernst, S., Zhang, Y., Haymanm A, A., & Stewart, A. F. (2006). A recombineering pipeline for functional genomics applied to *Caenorhabditis elegans*. *Nature Methods*. 3, 839-844

Sasaki, H., Sekiguchi, H., Sugiyama, M., & Ikadai, H. (2017). *Plasmodium berghei* Cap93, a novel oocyst capsule-associated protein, plays a role in sporozoite development. *Parasit Vectors*. 10, 399-408

Sauerwein, R. W., & Bousema, T. (2015). Transmission blocking malaria vaccines: Assays and candidates in clinical development. *Vaccine*. 33, 7476–7482

Saul, A. (2007). Mosquito stage, transmission blocking vaccines for malaria. *Cur Opin Infecti Dis*. 5, 476–481

Saxena, A., Wu, Y., & Garboczi, D. N. (2007). *Plasmodium* P25 and P28 surface proteins: potential transmission-blocking vaccines. *Eukaryotic Cell*. 6, 1260–1265

Schlegelmilch, T., & Vlachou, D. (2013). Cell analysis of mosquito midgut invasion: the defensive role of the actin-based hood. *Pathog Glob Health*. 107, 480–492

Schmid-Hempel, P. (2004). Evolutionary ecology of insect immune defenses. *Ann Rev Entomol*. 50, 5029-5051

Schnitger, A. K. D., Yassine, H., Kafatos, F. C., & Osta, M. A. (2009). Two C-type lectins cooperate to defend *Anopheles gambiae* against Gram-negative bacteria. *J Biol Chem*. 284, 17616–17624

Schofield L, & Hackett F. (1993). Signal transduction in host cells by a glycophosphatidylinositol toxin of malaria parasites. *J Exp Med*. 177, 145–53

Scholz, S. M., Simon, N., Lavazec, C., Dude, M. A., Templeton, T. J., & Pradel, G. (2008). PfCCp proteins of *Plasmodium falciparum*: Gametocyte-specific expression and role in complement-mediated inhibition of exflagellation. *Int J Parasitol*. 38, 327–340

Schwartz, A., & Koella, J. C. (2009). Melanisation of *Plasmodium falciparum* and C-25 Sephadex Beads by Field-Caught *Anopheles gambiae* (Diptera: Culicidae) from Southern Tanzania. *J Med Entomol.* 39, 84-88

Schwach, F., Bushell, E. S. C., Gomes, A. R., Anar, B., Girling, G., Herd, C., Rayner, J. C., & Billker, O. (2015). PlasmoGEM, a database supporting a community resource for large-scale experimental genetics in malaria parasites. *Nucleic Acids Res*. 43, 1176-1182

Seder, R. A., Chang, L. J., Enama, M. E., Zephir, K. L., Sarwar, U. N., Gordon, I. J., Holman, L. A., James, E. R., Billingsley, P. F., *et al*., & Hoffman, S. L. (2013). Protection against malaria by intravenous immunisation with a nonreplicating sporozoite vaccine. *Science*. 341, 1359-1365

Sherman I. W., Eda S., & Winograd E. (2003). Cytoadherence and sequestration in *Plasmodium falciparum*: defining the ties that bind. *Microbes Infect*. 5, 897–909

Sherrard-Smith, E., Sala, K. A., Betancourt, M., Upton, L. M., Angrisano, F., Morin, M. J., Ghani, A. C., Churcher, T., S. & Blagborough, A. M. (2018). Synergy in anti-malarial pre-erythrocytic and transmission-blocking antibodies is achieved by reducing parasite density. *eLife*. 7, e35213

Shiao, S. H., Whitten, M. M. A., Zachary, D., Hoffmann, J. A., & Levashina, E. A. (2006). Fz2 and Cdc42 mediate melanisation and actin polymerisation but are dispensable for *Plasmodium* killing in the midgut. *PLoS Path*. *2*, 1152–1164

Sidén-Kiamos, I., Vlachou, D., Margos, G., Beetsma., A., Waters, A. P., Sinden, R. E., & Louis, C. (2000). Distinct roles for pbs21 and pbs25 in the *in vitro* ookinete to oocyst transformation of *Plasmodium berghei*. *J Cell Sci*. 113, 3419–342

Sidén-Kiamos, I., Ecker, A., Nybäck, S., Louis, C., Sinden, R. E., & Billker, O. (2006). *Plasmodium berghei* calcium-dependent protein kinase 3 is required for ookinete gliding motility and mosquito midgut invasion. *Mol Microbiol.* 60, 1355–1363

Sidén-Kiamos, I., Pace, T., Klonizakis, A., Nardini, M., Garcia, C. R. S., & Currà, C. (2018). Identification of *P. berghei* Oocyst Rupture Protein 2 (ORP2) domains involved in sporozoite egress from the oocyst. *Int J Parasitol*. 48, 1127-1136

Sievers, F., Wilm, A., Dineen, D., Gibson, T. J., Karplus, K., Li, W., Lopez, R., McWilliam, H., Remmert, M., Söding, J., Thompson, J. D., & Higgins, D. G. (2011). Fast, scalable generation of high-quality protein multiple sequence alignments using Clustal Omega. *Mol Syst Biol.* 7, 539-545

Silvestrini, F., Alano, P., & Williams, J. L. (2000). Commitment to the production of male and female gametocytes in the human malaria parasite *Plasmodium falciparum*. *Parasitology*. 121, 465-471

Sinden, R. E. (1974). Excystment by sporozoites of malaria parasites. *Nature*. 252, 314-321

Sinden, R. E. & Strong, K. (1978). An ultrastructural study of the development of P*. falciparum* in *A. gambiae*. *Trans R Soc Trop Med Hyg*. 72, 477-491

Sinden, R. E. (1982). Gametocytogenesis of *Plasmodium falciparum in vitro*: an electron microscopic study. *Parasitology*. 84, 1-11

Sinden, R. E., & Hartley, R. H. (1985). Identification of the meiotic division of malarial parasites. *J Protoz*. 32, 742–744

Sinden, R. E. (1991). Mitosis and meiosis in malarial parasites. *Acta Leid*. 60, 19–27

Sinden, R. E. (1996). Infection of mosquitoes with rodent malaria. *Mol Biol Ins Disease Vectors*. 28, 67-91

Sinden, R. E. (1998). Gametocytes and development. *Paras Vectors.* 10, 216-228

Sinden, R., E., Butcher, G. A., & Beetsma, A. L. (2002). Maintenance of the *Plasmodium berghei* lifecycle. *Method Mol Med*. 72, 25-40

Sinden, R. E., Alavi, Y., & Raine, J. D. (2004). Mosquito-malaria interactions: A reappraisal of the concepts of susceptibility and refractoriness. *Insect Biochem Mol Biol*. 34, 625-629

Sinden, R. E., Dawes, E. J., Alavi, Y., Waldock, J., Finney, O., Mendoza, J., Butcher, G. A., Andrews, L., Hill, A. V., Gilbert, S. C., & Basáñez, M. G. (2007). Progression of *Plasmodium berghei* through *Anopheles stephensi* is density-dependent. *PLoS Path*. 3, 2005–2016

Sinden, R. E. (2010). A biologist's perspective on malaria vaccine development. *Human Vaccines*. 6, 3–11

Sinden, R. E., (2017). Developing transmission-blocking strategies for malaria control. *PLoS Path*. 13, 1553-7366

Singh, N., Preiser, P., Rénia, L., Balu, B., Barnwell, J., Blair, P., Jarra, W., Voza, T., Landau, I., & Adams, J. H. (2004). Conservation and developmental control of alternative splicing in maebl among malaria parasites. *J Mol Biol.* 343, 589-599

Singh, B., & Daneshvar, C. (2013). Human infections and detection of *Plasmodium malariae*. *Clin Microbiol Rev*. 26, 165–184

Singh, S. K., Thrane, S., Chourasia, B. K., Teelen, K., Graumans, W., Stoter, R., van Gemert, G. J., van de Vegte-Bolmer, M., *et al*., & Theisen, M. (2019). Pfs230 and Pfs48/45 fusion proteins elicit strong transmission-blocking antibody responses against *Plasmodium falciparum*. *Front Immunol*. 10, 1256-1268

Sinha, A., Hughes, K. R., Modrzynska, K. K., Otto, T. D., Pfander, C., Dickens, N. J., Religa, A. A., *et al*., & Waters, A. P. (2014). A cascade of DNA-binding proteins for sexual commitment and development in *Plasmodium*. *Nature*. 507, 253-257

Skarnes, W. C., Rosen, B., West, A. P., Koutsourakis, M., Bushell, W., Iyer, V., Mujika, A. O., Thomas, A., *et al*., & Bradley, A. (2011). A conditional knockout resource for the genome-wide study of mouse gene function. *Nature*. 474, 337-342

Smith, A. M. M., Heisler, L. E., Mellor, J., Kaper, F., Thompson, M. J., Chee, M., Roth, F. P., Giaever, G., & Nislow, C. (2009). Quantitative phenotyping via deep barcode sequencing. *Genome Research*. 19, 1836–1842

Smith, R. C., Eappen, A. G., Radtke, A. J., & Jacobs-Lorena, M. (2012). Regulation of anti-*Plasmodium* immunity by a LITAF-like transcription factor in the malaria vector *Anopheles gambiae*. *PLoS Path*. 8, e1002965

Smith, R. C., Vega-Rodríguez, J., & Jacobs-Lorena, M. (2014). The *Plasmodium* bottleneck: Malaria parasite losses in the mosquito vector. *Mem Do Inst Osw Cruz*. 109, 644–661

Smith, R. C., Barillas-Mury, C., & Jacobs-Lorena, M. (2015). Haemocyte differentiation mediates the mosquito late-phase immune response against *Plasmodium* in *Anopheles gambiae*. *Proc Natl Acad Sci USA.* 112, 3412-3420

Smith, T. G., Walliker, D., & Ranford-Cartwright, L. (2002). Sexual differentiation and sex determination in the Apicomplexa. *Trends Parasitol.* 18, 315-323

Song, J., Almasalmeh, A., Krenc, D., & Beitz, E. (2012). Molar concentrations of sorbitol and polyethylene glycol inhibit the aquaglyceroporin but not that of *E. coli*: Involvement of the channel vestibules. *Biochim Biophy Acta.* 1818, 1218-1224

Spaccapelo, R., Naitza, S., Robson, K. J., & Crisanti, A. (1997). Thrombospondin-related adhesive protein (*TRAP*) of *Plasmodium berghei* and parasite motility. *Lancet*. 350, 335-339

Srinivasan, P., Fujioka, H., & Jacobs-Lorena, M. (2008). PbCap380, a novel oocyst capsule protein, is essential for malaria parasite survival in the mosquito. *Cell Microbiol*. 10, 1304-1312

Stone, W. J., Dantzler, K. W., Nilsson, S. K., Drakeley, C. J., Marti, M., Bousema, T., & Rijpma, S. R. (2016). Naturally acquired immunity to sexual stage P. *falciparum* parasites. *Parasitology*. 143,187–98

Stone, W. J., Campo, J. J., Ouedraogo, A. L., Meerstein-Kessel, L., Morlais, I., Da, D., Cohuet, A., *et al*., &, Jore, M. M. (2018). Unravelling the immune signature of *P. falciparum* transmission-reducing immunity. *Nat Commun*. 9, 558-572

Strand, M. R. (2008a). Haemocytes and their role in immunity. *Ins Immun.* 32, 25-47

Strand, M. R. (2008b). The insect cellular immune response. *Ins Sci*. 15, 1-14

Sui, H., Han, B. G., Lee, J. K., Walian, P., & Jap, B. K. (2001). Structural basis of water-specific transport through the AQP1 water channel. *Nature*. 414, 872-878

Sultan, A. A., Thathy, V., Frevert, U., Robson, K. J. H., Crisanti, A., Nussenzweig, V., Nussenzweig, R. S., & Ménard, R. (1997). TRAP is necessary for gliding motility and infectivity of *Plasmodium* sporozoites. *Cell*. 90, 511-522

Sutherland, C. J. (2009). Surface antigens of *Plasmodium falciparum* gametocytes - A new class of transmission-blocking vaccine targets? *Mol Biochem Parasitol.* 166, 93-98

Suwanchaichinda, C., & Kanost, M. R. (2009). The serpin gene family in *Anopheles gambiae*. *Gene*. 442, 47-54

Tachibana, M., Miura, K., Takashima, E., Morita, M., Nagaoka, H., Zhou, L., Long, C. A., King, C. R., Torii, M., Tsuboi, T., & Ishino, T. (2019). Identification of domains within Pfs230 that elicit transmission blocking antibody responses. *Vaccine*. 37, 1799-1806

Tadesse, F. G*.,* Meerstein-Kessel, L*.,* Goncalves, B. P*.,* Drakeley, C*.,* Ranford-Cartwright, L. & Bousema, T. (2019). Gametocyte sex ratio: the key to understanding *P. falciparum* transmission? *Trends Parasitol.* 35*,* 226–238

Tahar, R., Boudin, C., Thiery, I., & Bourgouin, C. (2002). Immune response of *Anopheles gambiae* to the early sporogonic stages of the human malaria parasite *Plasmodium falciparum*. *EMBO J*. 21, 6673-6680

Talman, A. M., Paul, R. E. L., Sokhna, C. S., Domarle, O., Ariey, F., Trape, J. F., & Robert, V. (2004). Influence of chemotherapy on the *Plasmodium* gametocyte sex ratio of mice and humans. *Am J Trop Med Hyg*. 71, 739-744

Taniguchi, T., Miyauchi, E., Nakamura, S., Hirai, M., Suzue, K., Imai, T., Nomura, T.,

Handa, T., Okada, H., *et al.*, & Hisaeda, H. (2015). *Plasmodium berghei* ANKA causes intestinal malaria associated with dysbiosis. *Sci Rep*. 6, 17248-17256

Tawk, L., Lacroix, C., Gueirard, P., Kent, R., Gorgette, O., Thiberge, S., Mercereau-Puijalon, O., Ménard,, R., & Barale, J. C. (2013). A key role for *Plasmodium* subtilisin-like SUB1 protease in egress of malaria parasites from host hepatocytes. *J Biol Chem*. 288, 33336–33346

Teixeira, M. M., Almeida, I. C., & Gazzinelli, R. T. (2002). Introduction: Innate recognition of bacteria and protozoan parasites. *Microb Infect.* 4, 883–886

Tembo, D. L., Nyoni, B., Murikoli, R. V., Mukaka, M., Milner, D. A., Berriman, M., Rogerson, S. J., Taylor, T. E., Molyneux, M. E., Mandala, W. L., Craig, A. C., & Montgomery, J. (2014). Differential PfEMP1 expression is associated with cerebral malaria pathology. *PLoS Path*. 10, e1004537

Templeton, T. J., & Kaslow, D. C. (1999). Identification of additional members define a *Plasmodium falciparum* gene superfamily which includes Pfs48/45 and Pfs230. *Mol Biochem Parasitol*. 101, 223-227

Tewari, R., Spaccapelo, R., Bistoni, F., Holder, A. A., & Crisanti, A. (2002). Function of region I and II adhesive motifs of *Plasmodium falciparum* circumsporozoite protein in sporozoite motility and infectivity. *J Biol Chem*. 277, 47613-47618

Tewari, R., Dorin, D., Moon, R., Doerig, C., & Billker, O. (2005). An atypical mitogen-activated protein kinase controls cytokinesis and flagellar motility during male gamete formation in a malaria parasite. *Mol Microbiol*. 58, 1253-1263

Tewari, R., Straschil, U., Bateman, A., Böhme, U., Cherevach, I., Gong, P., Pain, A., & Billker, O. (2010). The systematic functional analysis of *Plasmodium* protein kinases identifies essential regulators of mosquito transmission. *Cell Host Microbe.* 8, 377–387

Thomas, D. D., Donnelly, C., Wood, R., & Alphey, L. (2000). Insect population control using a dominant, repressible, lethal genetic system. *Science*. 287, 2474-2476

Thompson, J., Janse, C. J., & Waters, A. P. (2001). Comparative genomics in *Plasmodium*: a tool for the identification of genes and functional analysis. *Mol Biochem Parasitol*. 118, 147–154

Thompson, J. D., Gibson, T. J., & Higgins, D. G. (2003). Multiple Sequence Alignment Using ClustalW and ClustalX. *Curr Protoc Bioinformatics*. 2, 23-35

Tomas, A. M., Margos, G., Dimopoulos, G., van Lin, L. H. M., de Koning-Ward, T. F., Sinha, R., Lupetti, P., Beetsma, A. L., *et al*., & Sinden, R. E. (2001). P25 and P28 proteins of the malaria ookinete surface have multiple and partially redundant functions. *EMBO J*. 20, 3975–3983

Trager, W., & Jensen, J. B. (1976). Human malaria parasites in continuous culture. *Science.* 193, 673–675

Tremp, A. Z., Khater, E. I., & Dessens, J. T. (2008). IMC1b is a putative membrane skeleton protein involved in cell shape, mechanical strength, motility, and infectivity of malaria ookinetes. *J Biol Chem*. 283, 27604–27611

Tremp, A. Z., Carter, V., Saeed, S., & Dessens, J. T. (2013). Morphogenesis of *Plasmodium* zoites is uncoupled from tensile strength. *Mol Microbiol*. 89, 552-564

Trueman, H. E., Raine, J. D., Florens, L., Dessens, J. T., Mendoza, J., Johnson, J., Waller, C. C., Delrieu, I., Holder, A. A., Carucci, D. J., Yates, J. R., & Sinden, R. E. (2006). Functional characterisation of an LCCL–Lectin domain containing protein family in *Plasmodium berghei*. *J Parasitol*. 90, 1062-1071

Turner, L., Lavstsen, T., Berger, S. S., Wang, C., Petersen, J. E. V., Avril, M., Brazier, A., Freeth, J., Jespersen, J. S., Nielsen, M. A., Magistrado, P., Lusingu, J., Smith, J. D., Higgins, M. K., & Theander, T. G. (2013). Severe malaria is associated with parasite binding to endothelial protein C receptor. *Nature*. 498, 502-505

Ukegbu, C. V., Cho, J. S., Christophides, G. K., & Vlachou, D. (2015). Transcriptional silencing and activation of paternal DNA during *Plasmodium berghei* zygotic development and transformation to oocyst. *Cell Microbiol*. 17, 1230-1240

Ukegbu, C. V., Akinosoglou, K. A., Christophides, G. K., & Vlachou, D. (2017a). *Plasmodium berghei* PIMMS2 promotes ookinete invasion of the *Anopheles gambiae* mosquito midgut. *Infect Immun*. 85, e00139-17

Ukegbu, C. V., Giorgalli, M., Yassine, H., Ramirez, J. L., Taxiarchi, C., Barillas-Mury, C., Christophides, G. K. & Vlachou, D. (2017b). *Plasmodium berghei* P47 is essential for ookinete protection from the *Anopheles gambiae* complement-like response, *Sci Rep.* 7, 6026-6037

Ukegbu, C. V., Giorgalli, M., Tapanelli, S., Rona L. P. D., Jaye A., Wyer, C., Angrisano, F., Blagborough, A. M., Christophides, G. K., & Vlachou, D. (2020). *Plasmodium* PIMMS43 is required for ookinete evasion of the mosquito complement-like response and sporogonic development. *Proc Natl Acad Sci USA.* 117, 7363-7373

van der Wel, A., Tomás, A., Kocken, C. H. M., Malhotra, P., Janse, C. J., Waters, A. P., & Thomas, A. W. (1997). Transfection of the primate malaria parasite *Plasmodium malariae* using entirely heterologous constructs. *J Exp Med*. 185, 1499–1503

van Dijk, M. R., Waters, A. P., & Janse, C. J. (1995). Stable transfection of malaria parasite blood stages. *Science*. 268, 1358-1362

van Dijk, M. R., Janse, C. J., & Waters, A. P. (1996). Expression of a *Plasmodium* gene introduced into subtelomeric regions of *Plasmodium berghei* chromosomes. *Science*. 271, 662-665

van Dijk, M. R., Janse, C. J., Thompson, J., Waters, A. P., Braks, J. A. M., Dodemont, H. J., Stunnenberg, H. G., van Gemert, G. J., Sauerqein, R. W., & Eling, W. (2001). A Central Role for P48/45 in Malaria Parasite Male Gamete Fertility. *Cell*. 104, 153–164

van Dijk, M. R., Douradinha, B., Franke-Fayard, B., Heussler, V., van Dooren, M. W., van Schaijk, B., van Gemert, G. J., Sauerwein, R. W., Mota, M. M., Waters, A. P., & Janse, C. J. (2005). Genetically attenuated, P36p-deficient malarial sporozoites induce protective immunity and apoptosis of infected liver cells. *Proc Natl Acad Sci USA.* 102, 12194-12199

van Dijk, M. R, van Schaijk, B., Khan, S. M., van Dooren, M. W., Ramesar, J., Kaczanowski, S., van Gemert, G. J., Stunnenberg, H. G., Eling, W. M., Sauerwein, R. W., Waters, A. P., & Janse, C. J. (2010). Three members of the 6-cys protein family of *Plasmodium* play a role in fertility. *PLoS Pathog*. 6, 1–13

van Dooren, G. G., Su, V., D'Ombrain, M. C., & McFadden, G. I. (2002). Processing of an apicoplast leader sequence in *Plasmodium falciparum* and the identification of a putative leader cleavage enzyme. *J Biol Chem*. 277, 23612-23619

van Schaijk, B., van Dijk, M. R., van de Vegte-Bolmer, M., van Gemert, G. J., van Dooren, M. W., Eksi, S., Roeffen, W. E. G., Janse, C. J., Waters, A. P., & Sauerwein, R. W. (2006). Pfs47, paralog of the male fertility factor Pfs48/45, is a female specific surface protein in *Plasmodium falciparum*. *Mol Biochem Parasitol*. 149, 216–222

Vanderberg, J., & Rhodin, J. (1967). Differentiation of nuclear and cytoplasmic fine structure during sporogonic development of *P. berghei*. *Cell Biol*. 32, C7-10

Vaughan, A. M., Mikolajczak, S. A., Camargo, N., Lakshmanan, V., Kennedy, M., Lindner, S. E., Miller, J. L., Hume, J. C. C., & Kappe, S. H. I. (2012). A transgenic *Plasmodium falciparum* NF54 strain that expresses GFP-luciferase throughout the parasite lifecycle. *Mol Biochem Parasitol*. 186, 143–147

Vega-Rodriguez, J., Ghosh, A. K., Kanzok, S. M., Dinglasan, R. R., Wang, S., Bongio, N. J., Kalume, D. E., Miura, K., Long, C. A., Pandey, A., & Jacobs-Lorena, M. (2014). Multiple pathways for *Plasmodium* ookinete invasion of the mosquito midgut. *Proc Natl Acad Sci USA*. 111, e492-500

Venkatesan, M., Amaratunga, C., Campino, S., Auburn, S., Koch, O., Lim, P., Uk, S., Socheat, D., Kwiatkowski, D. P., Fairhurst, R. M., & Plowe, C. V. (2012). Using CF11 cellulose columns to inexpensively and effectively remove human DNA from Plasmodium falciparum-infected whole blood samples. *Malaria J.* 11, 41-48

Vermeulen, A. N., Ponnudurai, T., Beckers, P. J., Verhave, J. P., Smits, M. A., & Meuwissen, J. H. (1985). Sequential expression of antigens on sexual stages of *Plasmodium falciparum* accessible to transmission-blocking antibodies in the mosquito. *J Exp Med*. 162, 1460–1476

Villarino, N. F., LeCleir, G. R., Denny, J. E., Dearth, S. P., Harding, C. L., Sloan, S. S., Gribble, J. L., Campagna, S. R., Wilhelm, S. W., & Schmidt, N. W. (2016). Composition of the gut microbiota modulates the severity of malaria. *Proc Natl Acad Sci USA.* 113, 2235-2240

Vizioli, J., Bulet, P., Charlet, M., Lowenberger, C., Blass, C., Müller, H. M., Dimopoulos, G., Hoffman, J., Kafatos, F. C., & Richman, A. (2000). Cloning and analysis of a cecropin gene from the malaria vector mosquito, *Anopheles gambiae*. *Insect Mol Biol.* 9, 75-84

Vizioli, J., Richman, A. D., Uttenweiler-Joseph, S., Blass, C., & Bulet, P. (2001). The defensin peptide of the malaria vector mosquito *A. gambiae*: Antimicrobial activities and expression in adult mosquitoes. *Insect Bioche Mol Biol*. 31, 241-248

Vizioli, J., Bulet, P., Hoffmann, J. A., Kafatos, F. C., Muller, H. M., & Dimopoulos, G. (2002). Gambicin: A novel immune responsive antimicrobial peptide from the malaria vector *Anopheles gambiae*. *Proc Natl Acad Sci.* 98, 12630-12635

Vlachou, D., Lycett, G., Sidén-Kiamos, I., Blass, C., Sinden, R. E., & Louis, C. (2001). *Anopheles gambiae* laminin interacts with the P25 surface protein of *Plasmodium berghei* ookinetes. *Mol Biochem Parasitol*. 112, 229-237

Vlachou, D., Zimmermann, T., Cantera, R., Janse, C. J., Waters, A. P., & Kafatos, F.

C. (2004). Real-time, *in vivo* analysis of malaria ookinete locomotion and mosquito midgut invasion. *Cell Microbiol*. 6, 671–685

Vlachou, D., Schlegelmilch, T., Christophides, G. K., & Kafatos, F. C. (2005). Functional genomic analysis of midgut epithelial responses in *Anopheles* during *Plasmodium* invasion. *Curr Biol*. 15, 1185–1195

Vlachou, D., Schlegelmilch, T., Runn, E., Mendes, A., & Kafatos, F. C. (2006). The developmental migration of *Plasmodium* in mosquitoes. *Curr Opin Genet Dev*. 16, 384-391

Volkman, S. K., Barry, A. E., Lyons, E. J., Nielsen, K. M., Thomas, S. M., Choi, M., Thakore, S. S., Day, K. P., Wirth, D. F., & Hartl, D. L. (2001). Recent origin of *Plasmodium falciparum* from a single progenitor. *Science*. 293, 482-484

Volkmann, K., Pfander, C., Burstroem, C., Ahras, M., Goulding, D., Rayner, J. C., Frischknecht, F., Billker, O., & Brochet, M. (2012). The alveolin IMC1h is required for normal ookinete and sporozoite motility behaviour and host colonisation in *Plasmodium berghei*. *PLoS One*. 7, e41409

Volz, J., Osta, M. A., Kafatos, F. C., & Müller, H. M. (2005). The roles of two clip domain serine protease in innate immune responses of the malaria vector *Anopheles gambiae*. *J Biol Chem*. 280, 40161-40168

Volz, J., Müller, H. M., Zdanowicz, A., Kafatos, F. C., & Osta, M. A. (2006). A genetic module regulates the melanisation response of *Anopheles* to *Plasmodium*. *Cell Microbiol*. 8, 1392-13405

von Besser, K., Frank, A. C., Johnson, M. A., & Preuss, D. (2006). Arabidopsis HAP2 (GCS1) is a sperm-specific gene required for pollen tube guidance and fertilisation. *Development*. 133, 4761-4769

Wagner, J. C., Platt, R. J., Goldfless, S. J., Zhang, F., & Niles, J. C. (2014). Efficient CRISPR-Cas9-mediated genome editing in *Plasmodium falciparum*. *Nature Methods*. 11, 915-918

Wang, J., Huang, L., Li, J., Fan, Q., Long, Y., Li, Y., & Zhou, B. (2010). Artemisinin directly targets malarial mitochondria through its specific mitochondrial activation. *PLoS One*. 5, e9582

Wang, Q., Fujioka, H., & Nussenzweig, V. (2005). Exit of *Plasmodium* sporozoites from oocysts is an active process that involves the circumsporozoite protein. *PLoS Path*. 1, e9

Wang, S., Ghosh, A. K., Bongio, N., Stebbings, K. A., Lampe, D. J., & Jacobs-Lorena, M. (2012). Fighting malaria with engineered symbiotic bacteria from vector mosquitoes. *Proc Natl Acad Sci USA.* 109, 12734-12739

Wang, S., Dos-Santos, A. L. A., Huang, W., Liu, K. C., Oshaghi, M. A., Wei, G., Agre, P., & Jacobs-Lorena, M. (2017). Driving mosquito refractoriness to *Plasmodium falciparum* with engineered symbiotic bacteria. *Science.* 357, 1399-1402

Wang, X., Mu, J., Li, G., Chen, P., Guo, X., Fu, L., Chen, L., Su, X., & Wellems, T. E. (2005). Decreased prevalence of the *Plasmodium falciparum* chloroquine resistance transporter 76T marker associated with cessation of chloroquine use against *Plasmodium falciparum* malaria in Hainan, People's Republic of China.

Am J Trop Med Hyg. 72, 410-414

Ward, P., Equinet, L., Packer, J., & Doerig, C. (2004). Protein kinases of the human malaria parasite *Plasmodium falciparum*: The kinome of a divergent eukaryote. *BMC Genomics*. 5, 79-93

Warimwe, G. M., Keane, T. M., Fegan, G., Musyoki, J. N., Newton, C. R., Pain, A., Berriman, M., March, K., & Bull, P. C. (2009). *P. falciparum* var gene expression is modified by host immunity. *Proc Natl Acad Sci USA.* 106, 21801-21806

Wassmer, S. C., Cianciolo, G. J., Combes, V., & Grau, G. E. (2006). LMP-420, a new therapeutic approach for cerebral malaria? *Med Sci*. 22, 343–345

Waterhouse, R. M., Kriventseva, E. V., Meister, S., Xi, Z., Alvarez, K. S., Bartholomay, L. C., Barillas-Mury, C., Bian, G., Blandin, S., *et al*., & Christophides, G. K. (2007). Evolutionary dynamics of immune-related genes and pathways in disease-vector mosquitoes. *Science*. 316, 1738-1743

Waters, A. P., Thomas, A. W., van Dijk, M. R., & Janse, C. J. (1997). Transfection of malaria parasites. *Methods.* 13, 134-147

Waters, A. P. (2002). Orthology between the genomes of *Plasmodium falciparum* and rodent malaria parasites: possible practical applications. *Philos Trans R Soc Lond B Biol Sci.* 357, 55–63

Waters, A. P., & Janse, C. J. (2004). Malaria parasites: Genomes and molecular biology. *Caister Acad Press*. Leiden University Medical Centre, The Netherlands

Weatherall, D. J., Miller, L. H., Baruch, D. I., Marsh, K., Doumbo, O. K., Casals-Pascual, C., & Roberts, D. J. (2002). Malaria and the red cell. *Med Microbiol Immunol.* 201, 593-598

Weathersby, A. B. (1952). The role of the stolviach wall in the exogenous development of *Plasmodium* galllnaceum as studied by means of haelviocoel injections of susceptible and refractory mosquitoes. *J Infect Dis.* 91, 198-205

Weathersby, A. B. (1954). The ectopic development of malaria oocysts. *Exp Parasitol. 3*, 538–543

White, N. J. (2008). *Plasmodium malariae*: The fifth human malaria parasite. *Clin Infect Dis*. 46, 172–173

Whitten, M., Shiao, S. H., & Levashina, E. A. (2006). Mosquito midguts and malaria: Cell biology, compartmentalisation and immunology. *Par Immunol*. 28, 121–130

WHO | Global vector control response [Internet]. WHO. [cited 2017 Sep 29]. Available from: http://www.who.int/malaria/areas/vector_control/global-vector-control

WHO | World malaria report 2019 [Internet]. WHO [cited 2019 Dec 4]. Available from: https://www.who.int/publications-detail/world-malaria-report-2019

WHO | A global brief on vector-borne diseases [Internet]. WHO. [cited 2017 Sep 29]. Available from: http://www.who.int/campaigns/world-health-day/2014/global-brief

Wilke, A. B. B., & Marrelli, M. T. (2015). Paratransgenesis: A promising new strategy for mosquito vector control. *Parasit Vectors*. 8, 342-351

Williams, M., Contet, A., Hou, C. F. D., Levashina, E. A., & Baxter, R. H. G. (2019). *Anopheles gambiae* TEP1 forms a complex with the coiled-coil domain of *LRIM1*/*APL1C* following a conformational change in the thioester domain. *PloS One*. 14, e0218203

Williamson, K. C. (2003). Pfs230: From malaria transmission-blocking vaccine candidate toward function. *Parasit Immunol*,.25, 351–359

Windbichler, N., Papathanos, P. A., Catteruccia, F., Ranson, H., Burt, A., & Crisanti, A. (2007). Homing endonuclease mediated gene targeting in *Anopheles gambiae* cells and embryos. *Nucleic Acids Res.* 35, 5922-5933

Winzeler, E. A., Shoemaker, D. D., Astromoff, A., Liang, H., Anderson, K., Andre, B., Bangham, R., Benito, R., Boeke, J. D., Bussey, H., *et al.*, & Davis, R. W. (1999). Functional characterisation of the Saccharomyces cerevisiae genome by gene deletion and parallel analysis. *Science*. 285, 901-906

Wirth, C. C., Glushakova, S., Scheuermayer, M., Repnik, U., Garg, S., Schaack, D., Kachman, M. M., *et al*., & Pradel, G. (2014). Perforin-like protein PPLP2 permeabilises the red blood cell membrane during egress of *Plasmodium falciparum* gametocytes. *Cell Microbiol*. 16, 709-733

Wirth, C. C., Bennink, S., Scheuermayer, M., Fisher, R., & Pradel, G. (2015). Perforin-like protein PPLP4 is crucial for mosquito midgut infection by *Plasmodium falciparum*. *Mol Bio Par.* 201, 90-99

Wise de Valdez, M. R., Nimmo, D., Betz, J., Gong, H. F., James, A. A., Alphey, L., & Black, W. C. (2011). Genetic elimination of Dengue vector mosquitoes. *Proc Natl Acad Sci USA.* 108, 4772-4775

Withers-Martinez, C., Suarez, C., Fulle, S., Kher, S., Penzo, M., Ebejer, J. P., Koussis, K., Hackett, F., Jirgensons, A., Finn, P., & Blackman, M. J. (2012). *Plasmodium* subtilisin-like protease 1 (SUB1): Insights into the active-site structure, specificity and function of a pan-malaria drug target. *Int J Parasitol.* 42, 597–612

Wongsrichanalai, C., Barcus, M. J., Muth, S., Sutamihardja, A., & Wernsdorfer, W. H. (2007). A review of malaria diagnostic tools: microscopy and rapid diagnostic test (RDT). *Am J Trop Med Hyg*. 77, 119–27

Wu, Y., Kirkman, L. A., & Wellems, T. E. (1996). Transformation of *Plasmodium falciparum* malaria parasites by homologous integration of plasmids that confer resistance to pyrimethamine. *Proc Natl Acad Sci USA*. 93, 1130-1134

Xu, W. Y., Wang, X. X., Qi, J., Duan, J. H. & Huang, F. S. (2010). *Plasmodium yoelii:* influence of immune modulators on the development of the liver stage. *Exp Parasitol.* 126, 254–258

Yassine, H., & Osta, M. (2010). *A. gambiae* innate immunity. *Cell Microbiol*. 12, 1-9

Yassine, H., Kamareddine, L., Chamat, S., Christophides, G. K., & Osta, M. a. (2014). A serine protease homolog negatively regulates TEP1 consumption in systemic infections of the malaria vector *Anopheles gambiae*. *J Inn Immun.* 6, 806–818

Yeoh, S., O'Donnell, R., Koussis, K., Dluzewski, A., Ansell, K., Osborne, S., Hackett, F., Withers-Martinez, C., Mitchell, G. H., *et al*., & Blackman, M. J. (2007). Subcellular discharge of a serine protease mediates release of invasive malaria

parasites from host erythrocytes. *Cell*. 131, 1072–1083

Yeoh, L. M., Goodman, C. D., Mollard, V., McFadden, G. I., & Ralph, S. A. (2017). Comparative transcriptomics of female and male gametocytes in *Plasmodium berghei* and the evolution of sex in alveolates. *BMC Genomics*. 18, 734-750

Yeoh, L. M., Lee, V. V., McFadden, G. I., & Ralph, S. A. (2019). Alternative splicing in apicomplexan parasites. *MBio*. 10, e02866-18

Yilmaz, B., Portugal, S., Tran, T. M., Gozzelino, R., Ramos, S., Gomes, J., Regalado, A., Cowan, P. J., *et al*., & Soares, M. P. (2014). Gut microbiota elicits a protective immune response against malaria transmission. *Cell*. 159, 1277-1289

Yoeli, M., Hargreaves, B., Carter, R., & Walliker, D. (1975). Sudden increase in virulence in a strain of *P. berghei yoelii. Ann Trop Med Parasitol.* 69, 173-178

Yoshida, S., Ioka, D., Matsuoka, H., Endo, H., & Ishii, A. (2001). Bacteria expressing single-chain immunotoxin inhibit malaria parasite development in mosquitoes. *Mol Biochem Parasitol*. 113, 89-96

Yoshida, S., Shimada, Y., Kondoh, D., Kouzuma, Y., Ghosh, A. K., Jacobs-Lorena, M., & Sinden, R. E. (2007). Haemolytic C-type lectin CEL-III from sea cucumber expressed in transgenic mosquitoes impairs malaria parasite development. *PLoS Path*. 3, e192

Young, J. A., Fivelman, Q. L., Blair, P. L., de La Vega, P., le Roch, K. G., Zhou, Y., Carucci, D. J., Baker, D. A., & Winzeler, E. A. (2005). The *Plasmodium falciparum* sexual development transcriptome: A microarray analysis using ontology-based pattern identification. *Mol Biochem Parasitol*. 143, 67-79

Yuda, M., Sakaida, H., & Chinzei, Y. (1999). Targeted disruption of the *Plasmodium berghei CTRP* gene reveals its essential role in malaria infection of the vector mosquito. *J Exp Med.* 190, 1711-1716

Yuda, M., Yano, K., Tsuboi, T., Torii, M., & Chinzei, Y. (2001). Von Willebrand factor A domain-related protein, a novel microneme protein of the malaria ookinete conserved throughout *Plasmodium* parasites. *Mol Biochem Parasitol*. 116, 65–72

Yuda, M., Iwanaga, S., Kaneko, I. & Kato, T. (2015). Global transcriptional repression: an initial and essential step for *Plasmodium* sexual development. *Proc Natl Acad Sci USA.* 112, 12824–12829

Zanner, M. A., Galey, W. R., Scaletti, J. V., Brahm, J., & Vander Jagt, D. L. (1990). Water and urea transport in human erythrocytes infected with the malaria parasite *Plasmodium falciparum*. *Mol Biochem Parasitol*. 40, 269-278

Zeuthen, T., Wu, B., Pavlovic-Djuranovic, S., Holm, L. M., Uzcategui, N. L., Duszenko, M., Kun, J. F. J., Schultz, J. E., & Beitz, E. (2006). Ammonia permeability of the aquaglyceroporins from *Plasmodium falciparum*, Toxoplasma gondii and *Trypansoma brucei*. *Mol Microbiol*. 40, 269-278

Zhang, C., Li, Z., Cui, H., Jiang, Y., Yang, Z., Wang, X., Gao, H., Liu, C., Zhang, S., Su, X. Z., & Yuan, J. (2017). Systematic CRISPR-Cas9-mediated modifications of *Plasmodium yoelii* ApiAP2 genes reveal functional insights into parasite development. *MBio.* 8, e01986-17

Zhang, M., Wang, C., Otto, T. D., Oberstaller, J., Liao, X., Adapa, S. R., Udenze, K.,

Bronner, I. F., Csandra, D., Mayho, M., Brown, J., Swanson, J., Rayner, J. C., Jiang, R., & Adams, J. H. (2018). Uncovering the essential genes of the human malaria parasite Plasmodium *falciparum* by saturation mutagenesis. *Science*. 360, eaap7847

Zheng, W., Kou, X., Du, Y., Liu, F., Yu, C., Tsuboi, T., Fan, Q., Luo, E., Cao, Y., & Cui, L. (2016). Identification of three ookinete-specific genes and evaluation of their transmission-blocking potentials in *Plasmodium berghei*. *Vaccine*. 34, 2570-2578

Zheng, W., Liu, F., He, Y., Liu, Q., Humphreys, G. B., Tsuboi, T., Fan, Q., Luo, E., Cao, Y., & Cui, L. (2017). Functional characterisation of *Plasmodium berghei* PSOP25 during ookinete development and as a malaria transmission-blocking vaccine candidate. *Parasit Vectors.* 10, 8-19

Zieler, H, Nawrocki, J. P., & Shahabuddin, M. (1999). *Plasmodium gallinaceum* ookinetes adhere specifically to the midgut epithelium of *Aedes aegypti* by interaction with a carbohydrate ligand. *Exp Biol*. 202, 485–495

Zieler, H, & Dvorak, J. A. (2000). Invasion *in vitro* of mosquito midgut cells by the malaria parasite proceeds by a conserved mechanism and results in death of the invaded midgut cells. *Proc Natl Acad Sci USA*. 97, 11516–11521

Zieler, H., Keister, D., Dvorak, J. A., & Ribeiro, J. M. (2001). A snake venom phospholipase A 2 blocks malaria parasite development in the mosquito by inhibiting ookinete association with the midgut surface. *Exp Biol*. 204, 4157-4167

Zug, R., & Hammerstein, P. (2012). Still a host of hosts for Wolbachia: Data suggest that 40% of terrestrial arthropod species are infected. *PLoS One*. 7, e38544

APPENDICIES

APPENDIX 1:

SPRINGER NATURE LICENSE
TERMS AND CONDITIONS

Apr 12, 2020

This Agreement between Imperial College London -- Maria Giorgalli ("You") and Springer Nature ("Springer Nature") consists of your license details and the terms and conditions provided by Springer Nature and Copyright Clearance Center.

License Number	4806460475062
License date	Apr 12, 2020
Licensed Content Publisher	Springer Nature
Licensed Content Publication	Nature Reviews Microbiology
Licensed Content Title	Looking under the skin: the first steps in malarial infection and immunity
Licensed Content Author	R. Ménard, J. Tavares, I. Cockburn, M. Markus, F. Zavala, R. Amino
Licensed Content Date	Sep 16, 2013
Type of Use	Thesis/Dissertation
Requestor type	academic/university or research institute
Portion	figures/tables/illustrations
Number of figures/tables/illustrations	1
Format	print and electronic

Appendix 1. Permission to reproduce figures from (Menard *et al.*, 2013).

APPENDIX 2:

THE COMPANY OF BIOLOGISTS LICENSE TERMS AND CONDITIONS

Apr 12, 2020

This Agreement between Imperial College London -- Maria Giorgalli ("You") and The Company of Biologists ("The Company of Biologists") consists of your license details and the terms and conditions provided by The Journal of Experimental Biology and Copyright Clearance Center.

License Number	1028035-1
License date	Apr 12, 2020
Licensed Content Publisher	The Company of Biologists
Licensed Content Publication	The Journal of Experimental Biology
Licensed Content Title	Innate immunity in the malaria vector Anopheles gambiae: comparative and functional genomics
Licensed Content Author	M. A. Osta, G. K. Christophides, D. Vlachou, F. C. Kafatos
Licensed Content Date	April 29, 2004
Licensed Content Pages	13
Start Page	2551
End Page	2563
Type of Use	reuse in a thesis/dissertation
Portion	figures/tables/illustrations
Number of figures/tables/illustrations	1
Format	both print and electronic

Appendix 2: Permission to reproduce figures from (Osta *et al.*, 2004b).

APPENDIX 3:

EMBO PRESS
TERMS AND CONDITIONS

Apr 13, 2020

This Agreement between Imperial College London -- Maria Giorgalli ("You") and EMBO Press ("EMBO Press") consists of your license details and the terms and conditions provided by EMBO Press and Copyright Clearance Center.

License Number	600010998
License date	Apr 13, 2020
Licensed Content Publisher	EMBO Press
Licensed Content Publication	EMBO Journal
Licensed Content Title	Molecular interactions between Anopheles stephensi midgut cells and Plasmodium berghei: the time bomb theory of ookinete invasion of mosquitoes
Licensed Content Author	Y. S. Han, J. Thompson, F. C. Kafatos, C. Barillas-Mury
Licensed Content Date	Nov 15, 2000
Licensed Content Pages	10
Start Page	6030
End Page	6040
Type of Use	reuse in a thesis/dissertation
Portion	figures/tables/illustrations
Number of figures/tables/illustrations	1
Format	both print and electronic

Appendix 3: Permission to reproduce figures from (Han *et al.*, 2000).

APPENDIX 4:

ELSEVIER LICENSE
TERMS AND CONDITIONS

Apr 12, 2020

This Agreement between Imperial College London -- Maria Giorgalli ("You") and Elsevier ("Elsevier") consists of your license details and the terms and conditions provided by Elsevier and Copyright Clearance Center.

License Number	4806441221452
License date	Apr 12, 2020
Licensed Content Publisher	Elsevier
Licensed Content Publication	Elsevier Books
Licensed Content Title	Advances in Insect Physiology
Licensed Content Author	M. Povelones,M.A. Osta,G.K. Christophides
Licensed Content Date	Jan 1, 2016
Licensed Content Pages	20
Start Page	223
End Page	242
Type of Use	reuse in a thesis/dissertation
Portion	figures/tables/illustrations
Number of figures/tables/illustrations	1
Format	both print and electronic

Appendix 4. Permission to reproduce figures from (Povelones *et al.*, 2016).

APPENDIX 5:

Gene ID	PlasmoGEM ID	Description
PBANKA_111920	PbGEM-042760	conserved protein, unknown function (c43)
PBANKA_145770	PbGEM-080757	conserved protein, unknown function (c57)
PBANKA_135960	PbGEM-061442	6-cysteine protein (P48/45)
PBANKA_011110	PbGEM-533195	6-cysteine protein (P12p)
PBANKA_030610	PbGEM-533427	6-cysteine protein (P230)
PBANKA_110760	PbGEM-265060	6-cysteine protein (P38)
PBANKA_100220	PbGEM-292744	6-cysteine protein (P36p)
PBANKA_135970	PbGEM-343204	6-cysteine protein (P47)
PBANKA_100210	PbGEM-333419	6-cysteine protein (P36)
PBANKA_030600	PbGEM-328491	6-cysteine protein (P230p)
PBANKA_080810	PbGEM-283762	6-cysteine protein (B9)
PBANKA_100260	PbGEM-292800	6-cysteine protein (P41)
PBANKA_142590	PbGEM-065839	conserved protein, unknown function
PBANKA_081070	PbGEM-090719	subpellicular microtubule protein (SPM1)>c81
PBANKA_083040	PbGEM-027375	G2 protein
PBANKA_103780	PbGEM-097822	secreted ookinete adhesive protein (SOAP)
PBANKA_110690	PbGEM-098495	conserved protein, unknown function (PIMMS2)
PBANKA_122540	PbGEM-050063	gamete release protein (GAMER)
PBANKA_135380	PbGEM-108229	conserved protein, unknown function (c53)
PBANKA_060390	PbGEM-017530	HAD domain ookinete protein (HADO)
PBANKA_072090	PbGEM-089969	conserved protein, unknown function (c72)
PBANKA_133810	PbGEM-252084	conserved protein, unknown function (N38)
PBANKA_091910	PbGEM-289441	parasitophorous vacuolar protein 1 (PV1)
PBANKA_142710	PbGEM-321755	aquaporin, putative (AQP2)
PBANKA_114540	PbGEM-101239	*Plasmodium* exported protein (PHIST)
PBANKA_134980	PbGEM-107890	TRAP
PBANKA_041350	PbGEM-121274	Conserved protein, unknown function (N350)
PBANKA_100240-tag	PbGEM-034607	DPAP3 - tag barcode compatible
PBANKA_145120-tag	PbGEM-324931	P25 alpha - tag barcode compatible
PBANKA_051490-tag	PbGEM-015553	P28 - tag barcode compatible
PBANKA_030600-tag	PbGEM-226060	P230p - tag barcode compatible
PBANKA_041040-tag	PbGEM-012298	Gsk3 - tag barcode compatible

Appendix 5. Identification numbers (ID), PlasmoGEM vector IDs and description name of the genes included in the first pool of the high-throughput reverse genetics screen. Some genes were targeted for disruption while others were just tagged and used as controls. Genes included in the first pool were chosen by Dr. Dina Vlachou and are based on findings previously reported in (Akinosoglou *et al.*, 2015).

APPENDIX 6:

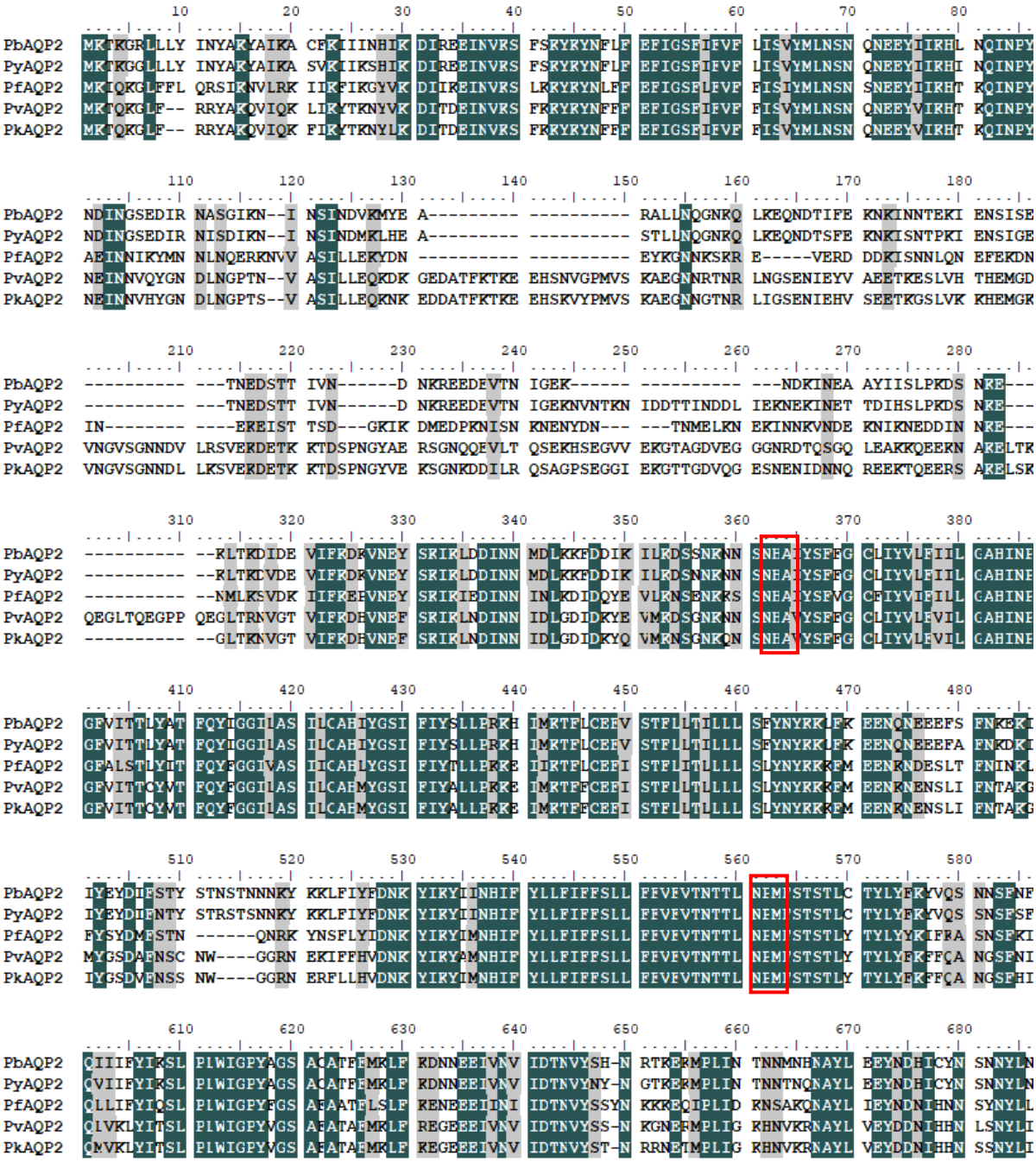

Appendix 6. Multiple sequence alignment of AQP2 *P. berghei* (*Pb*AQP2), *P. yoelii yoelii* (*Py*AQP2), *P. falciparum* (*Pf*AQP2), *P. vivax* (*Pv*AQP2) and *P. malariae* (*Pk*AQP2) proteins as performed by ClustalW and visualised by Bioedit Sequence Alignment Editor. Coloured blocks indicate identical (green) or moderately (grey) conserved amino acid residues among all *spp.* The two conserved NPA and NPM motifs are also indicated in red boxes.

APPENDIX 7:

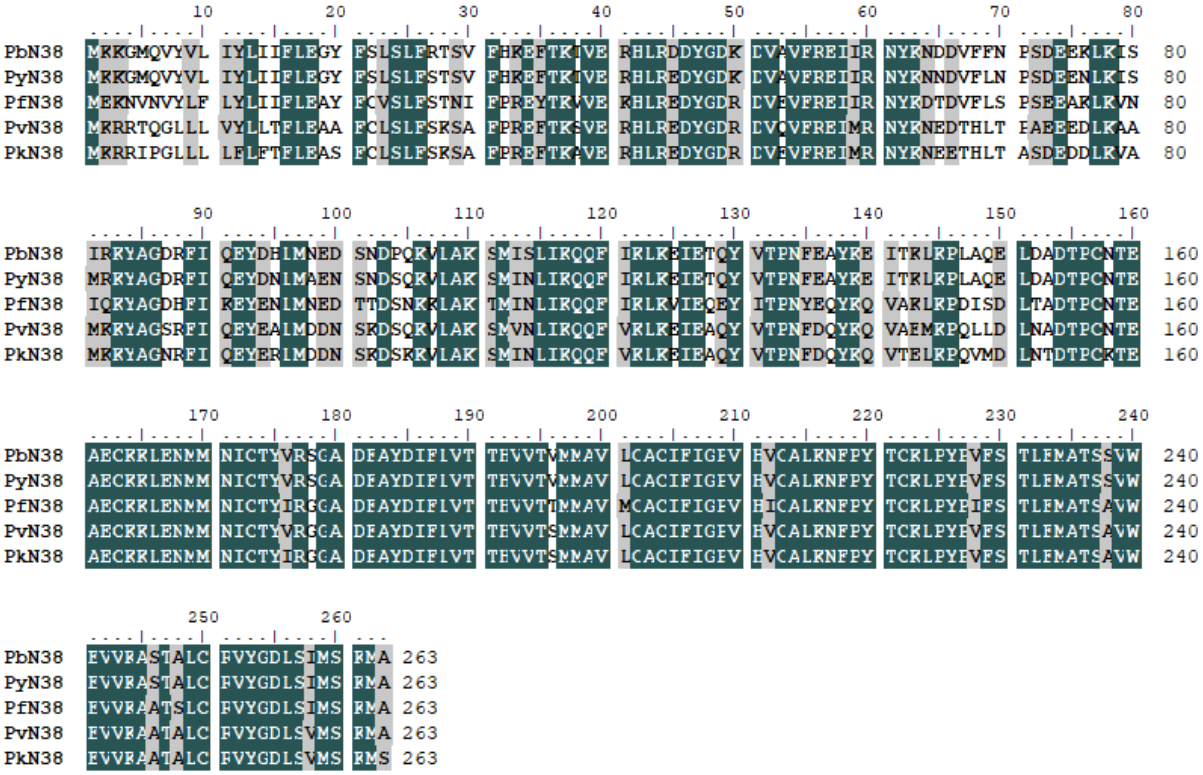

Appendix 7. Multiple sequence alignment of N38 *P. berghei* (*Pb*N38), *P. yoelii yoelii* (*Py*N38), *P. falciparum* (*Pf*N38), *P. vivax* (*Pv*N38) and *P. malariae* (*Pk*N38) proteins as performed by ClustalW and visualised by Bioedit Sequence Alignment Editor. Coloured blocks indicate identical (green) or moderately (grey) conserved amino acid residues among all *spp.*

APPENDIX 8:

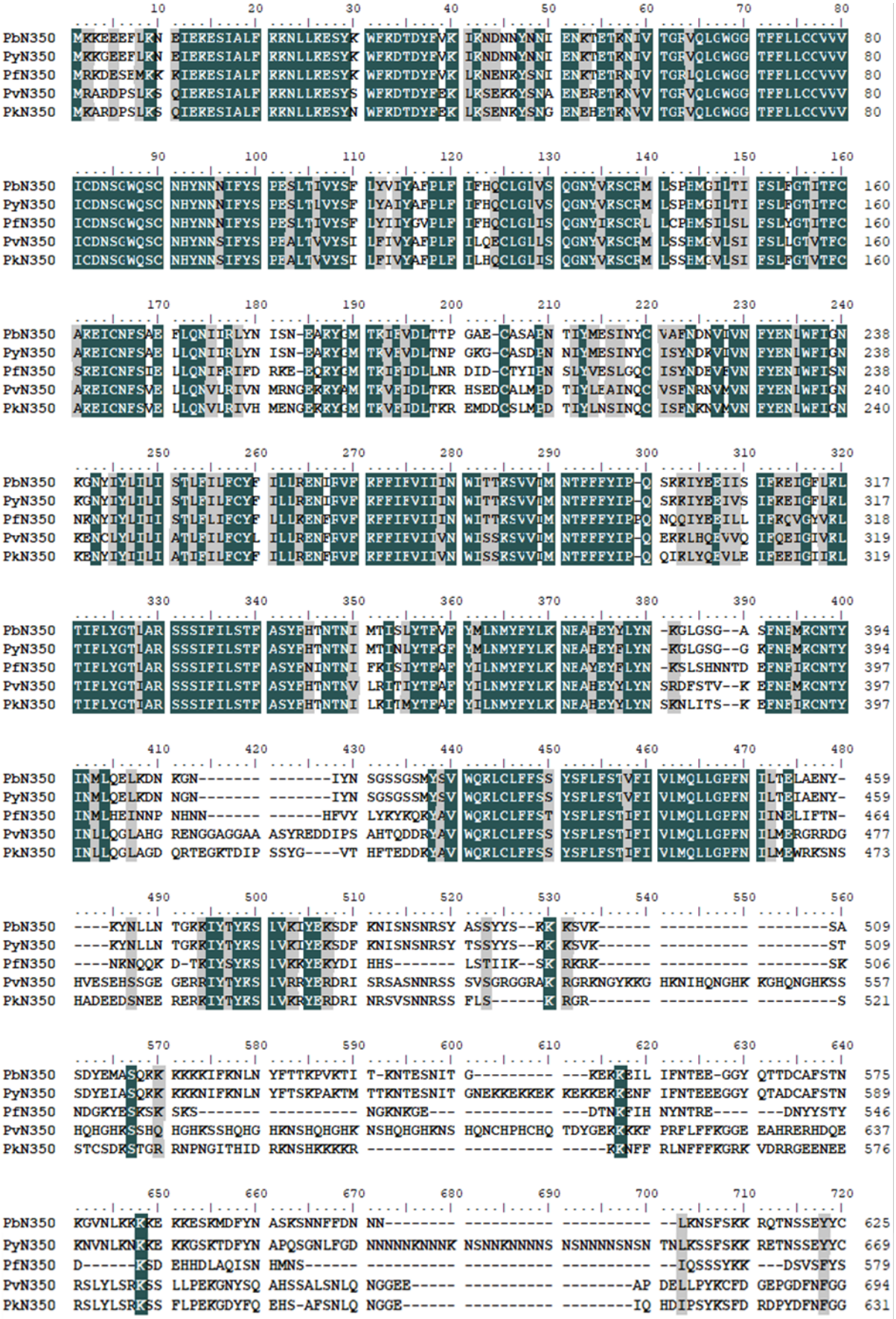

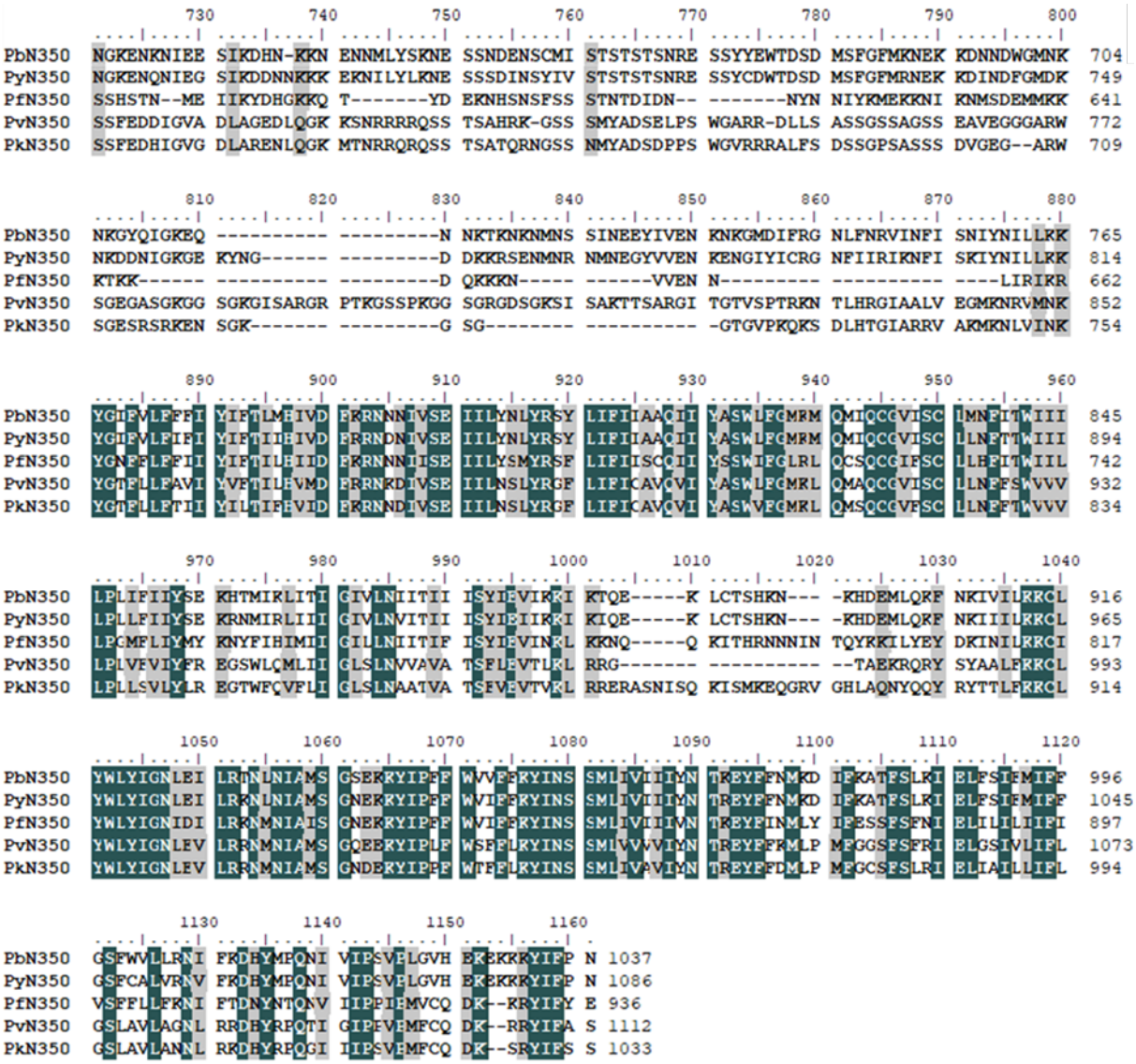

Appendix 8. Multiple sequence alignment of N350 *P. berghei* (*Pb*N350), *P. yoelii yoelii* (*Py*N350), *P. falciparum* (*Pf*N350), *P. vivax* (*Pv*N350) and *P. malariae* (*Pk*N350) proteins as performed by ClustalW and visualised by Bioedit Sequence Alignment Editor. Coloured blocks indicate identical (green) or moderately (grey) conserved amino acid residues among all *spp.*

APPENDIX 9:

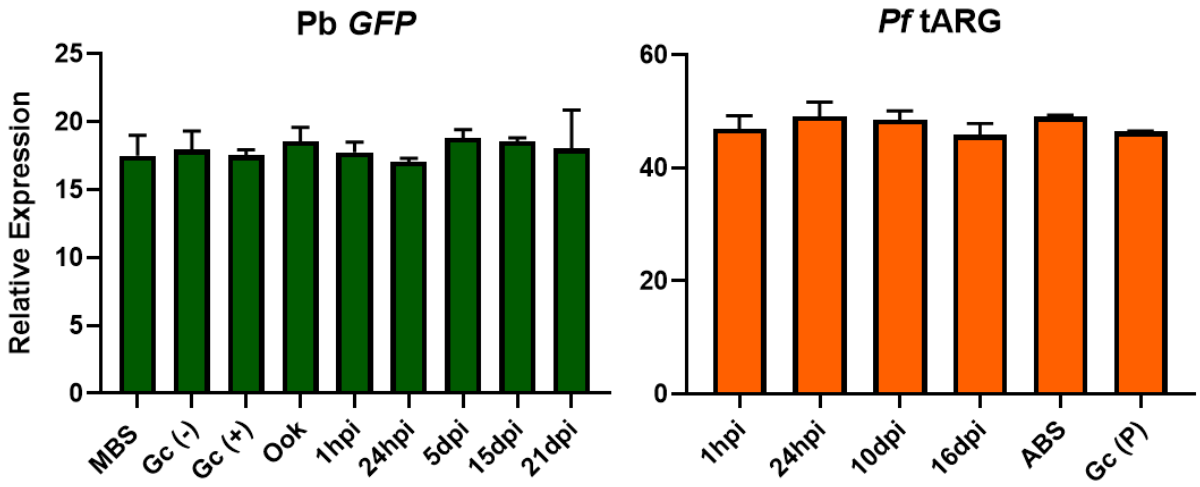

Appendix 9. Transcription profiling of *P. berghei eGFP* and *P. falciparum tARG housekeeping genes.* Relative abundance of *eGFP* (*Pb* GFP) and *arg-tRNA ligase* (*Pf tARG*) transcripts in *P. berghei* and *P. falciparum*-infected *A. coluzzii* midguts and salivary glands as well as in *in vitro* purified samples, as determined by qRT-PCR. The *P. berghei* ANKA *c507* that constitutively expresses *GFP* but is otherwise WT, and the *P. falciparum* NF54 WT lines were used. Transcription values have been normalised against the constitutive expressed *actin* gene. The average expression and standard errors of two independent biological replicates (different batches of mosquitoes fed on different blood sources) are shown. Statistical significance was calculated using one-way ANOVA test and was determined to be non-significant for all samples. MBS; Mixed Blood Stages, Gc (-); Non-activated Gametocytes, Gc (+); Activated Gametocytes, Ook; Ookinetes, hpi; hours post infection, dpi; days post infection, ABS; Asexual Blood Stages.

APPENDIX 10:

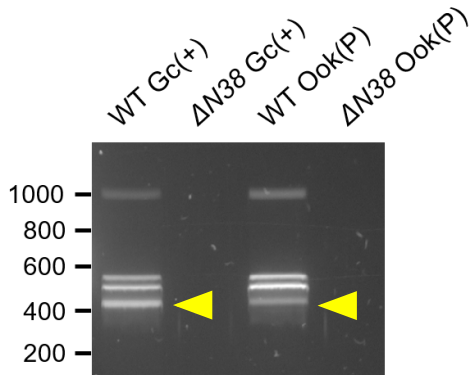

Appendix 10: Alternative splicing products of *P. berghei N38.* RT-PCR analysis of *P. berghei N38* alternative transcripts in activated gametocytes and *in vitro* ookinetes. The intronless product is expected to localise at about 470bp length (yellow arrowheads). The primers have been designed to map in two separate exons that are five introns apart from each other and therefore, alternative spliced transcripts are found between 400bp-1000bp length. Samples from *P. berghei ΔN38* activated gametocytes and *in vitro* ookinetes were used as a negative control for the primers specificity. Gc (+); Activated Gametocytes, Ook (P); *in vitro* Purified Ookinetes.

APPENDIX 11:

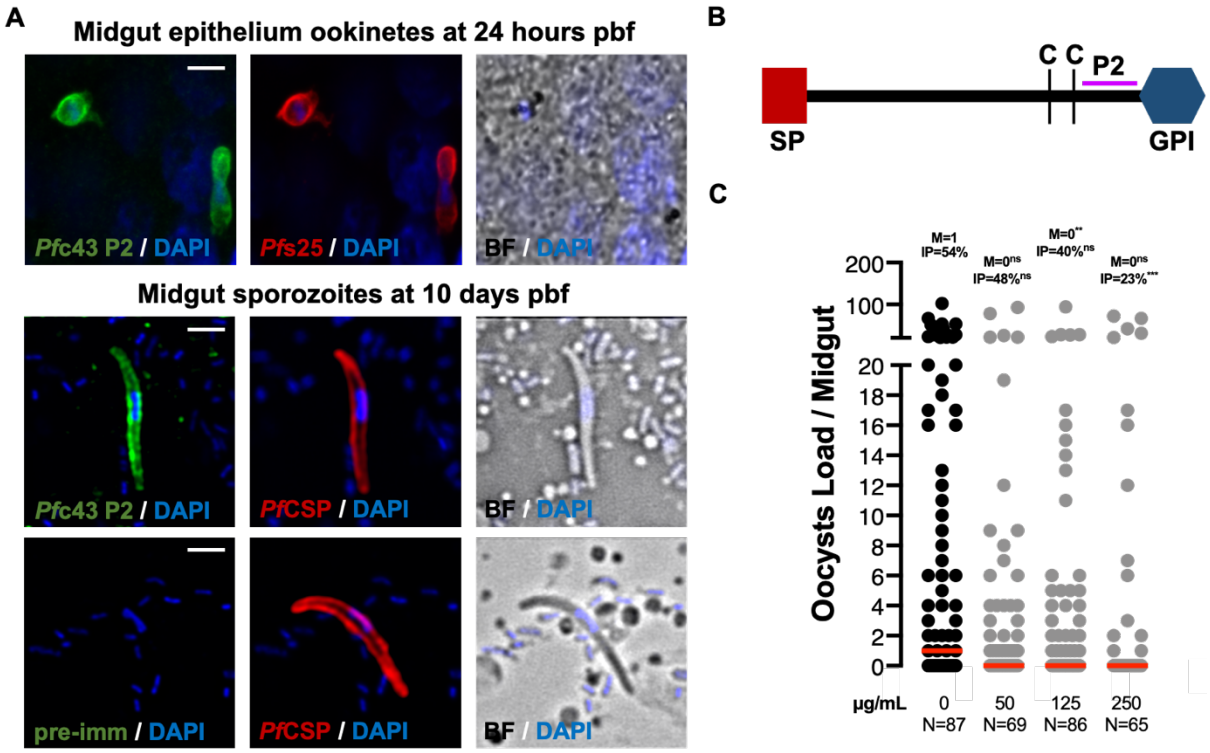

Appendix 11. Transmission blocking efficacy of a-*Pfc*43^{P2}. (A) Immunofluorescence assays of *P. falciparum* ookinetes while traversing the mosquito midgut epithelium at 24 hours pbf and midgut sporozoites at day-10 pbf. Parasites were stained with the a-*Pfc*43^{P2} antibody and the ookinete specific a-*Pfs*25 (red) or sporozoite a-*PfCSP* (red) antibodies. Staining with pre-immune (pre-imm) serum was used as a negative control. DNA was stained with DAPI. Scale bars correspond to 5 µm. **(B)** Schematic representation of the *P. falciparum c43* gene and the targeting epitope of the a-Pfc43^{P2} antibody (amino acids 372-386). The two conserved cysteine residues, the signal peptide and the transmembrane domain / GPI anchor are also shown. **(C)** Transmission blocking efficacy of the a-*Pfc*43^{P2} antibody following *P. falciparum* infection of *A. coluzzii* mosquitoes, shown as dot plots of oocyst number distribution. The α-Pfc43 P2 antibody was provided through SMFAs at concentrations of 50, 125 and 250 µg/mL and compared with no antibodies condition that was used as negative control. M corresponds to the median oocyst infection intensities, also shown as horizontal red lines. IP, oocyst infection prevalence; N, number of midguts analysed. Data derived from two biological replicates, whereas statistical analysis was performed with Mann Whitney U-test. TBV experiments using the a-*Pfc*43 P2 antibody were assisted by Dr. Sofia Tapanelli.

APPENDIX 12:

A

Alleles	KO (provided from the corresponding KO parasite)	WT (provided from all other KO parasites)
c01	2.78%	13.88%
c43	2.78%	13.88%
P47	2.78%	13.88%
c57	2.78%	13.88%
P48/45	2.78%	13.88%
PIMMS2	2.78%	13.88%

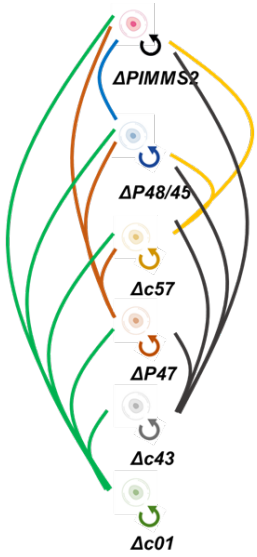

B

♀ \ ♂	Δc01	Δc43	ΔP47	Δc57	ΔP48/45	ΔPIMMS2
Δc01	c01ko c01ko / c01ko c01ko	c01ko c01wt / c43wt c43ko	c01ko c01wt / P47wt P47ko	c01ko c01wt / c57wt c57ko	c01ko c01wt / P4845wt P4845ko	c01ko c01wt / PIMMS2wt PIMMS2ko
Δc43		c43ko c43ko / c43ko c43ko	c43ko c43wt / P47wt P47ko	c43ko c43wt / c57wt c57ko	c43ko c43wt / P4845wt P4845ko	c43ko c43wt / PIMMS2wt PIMMS2ko
ΔP47			P47ko P47ko / P47ko P47ko	P47ko P47wt / c57wt c57ko	P47ko P47wt / P4845wt P4845ko	P47ko P47wt / PIMMS2wt PIMMS2ko
Δc57				c57ko c57ko / c57ko c57ko	c57ko c57wt / P4845wt P4845ko	c57ko c57wt / PIMMS2wt PIMMS2ko
ΔP48/45					P4845ko P4845ko / P4845ko P4845ko	P4845ko P4845wt / PIMMS2wt PIMMS2ko
ΔPIMMS2						PIMMS2ko PIMMS2ko / PIMMS2ko PIMMS2ko

Appendix 12. *P. berghei* c01, c43, P47, c57, P48/45 and PIMMS2 KO and WT alleles estimated frequencies in the gametocyte pool of barcoded mutants, following fertilisation in the mosquito midgut lumen. (A) Diagram indicating the estimated frequency of each allele for each locus in the population, assuming that each mutant line is equally represented in the gametocyte stages. The potential combinations of the different KO gametes following fertilisation are indicated on the left panel. **(B)** Diagram explaining the zygotes (heterozygotes (green table cells) / homozygotes (purple table sets) for each KO and their crosses) expected to be formed in the mosquito midgut lumen following fertilisation. In total, 15 different heterozygous combinations and 6 different homozygous combinations are expected.

APPENDIX 13:

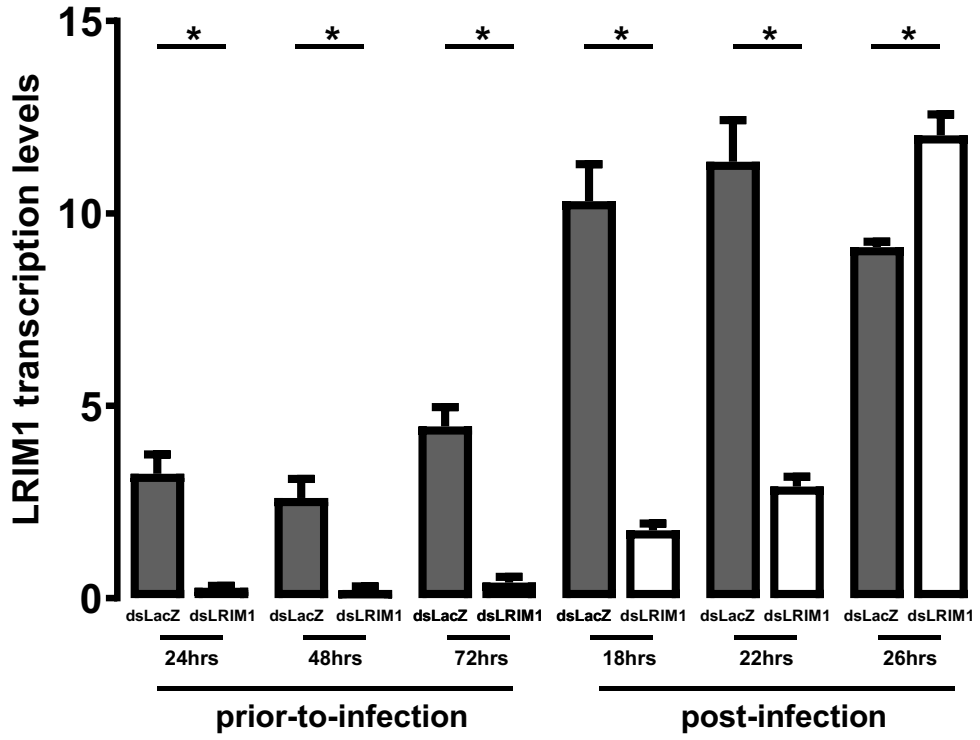

Appendix 13. Transcription levels of *LRIM1* in *LRIM1*-silenced *A. coluzzii* mosquitoes, before and after *P. berghei* infection. Level of *LRIM1* gene transcription in whole *A. coluzzii* mosquitoes injected with ds*LacZ* (control) or ds*LRIM1* at 24, 48 and 72 hours prior to infection and 18, 22 and 26 hours post infection with the *c507* (WT) *P. berghei* line. Transcription levels of *LRIM1* were normalised against the ribosomal *S7* gene expression. The data derived from qRT RT-PCR analysis of samples collected in two biological replicates. Statistical significance was determined using a two-tailed, unpaired Student's *t*-test.

APPENDIX 14:

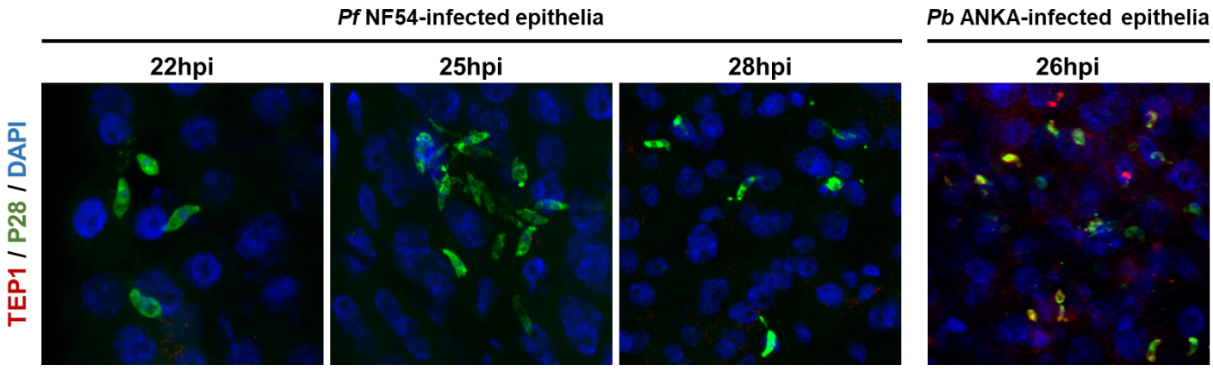

Appendix 14. TEP1-staining of *P. falciparum* NF54 isolates right after midgut traversal in *A. coluzzii* mosquitoes. Fluorescent images of the *P. falciparum* NF54 and *P. berghei* ANKA *c507* (WT) (positive control) ookinetes in *A. coluzzii* whole midgut epithelia at multiple time-points pbf, stained with both TEP1 (red) and *Pf*s25 or *Pb*P28 (green) antibodies, respectively. Ookinetes stained for both TEP1 and P28 (yellow) indicate that are either dead or marked for killing, while P28 single stained ookinetes (green) are considered alive; *P28* (green) is abundantly expressed on the ookinete surface. Fluorescence images of *A. coluzzii* midguts are representative of two sets of experiments and were taken at X400 magnification.

‘‘For since the creation of the world
His invisible attributes,
His eternal power and divine nature,
have been clearly seen,
being understood through what has been made,
so that they are without excuse’’

Romans 1:20